EFFECTS OF DEFORMATION PROPERTIES ON THE BOND OF REINFORCING BARS

By
Michael L. Tholen
David Darwin

A Report on Research Sponsored by

THE NATIONAL SCIENCE FOUNDATION
Research Grants No. MSS-9021066 and CMS-9402563

THE U.S. DEPARTMENT OF TRANSPORTATION
FEDERAL HIGHWAY ADMINISTRATION

THE CIVIL ENGINEERING RESEARCH FOUNDATION
Contract No. 91-N6002

THE REINFORCED CONCRETE RESEARCH COUNCIL
Project 56

Structural Engineering and Engineering Materials
SM Report No. 42
October 1996

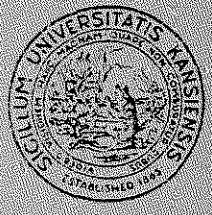

THE UNIVERSITY OF KANSAS CENTER FOR RESEARCH, INC.
2291 Irving Hill Drive - Campus West, Lawrence, Kansas 66045

EFFECTS OF DEFORMATION PROPERTIES ON THE BOND OF REINFORCING BARS

By
Michael L. Tholen
David Darwin

A Report on Research Sponsored by

THE NATIONAL SCIENCE FOUNDATION
Research Grants No. MSS-9021066 and CMS-9402563

THE U.S. DEPARTMENT OF TRANSPORTATION
FEDERAL HIGHWAY ADMINISTRATION

THE CIVIL ENGINEERING RESEARCH FOUNDATION
Contract No. 91-N6002

THE REINFORCED CONCRETE RESEARCH COUNCIL
Project 56

Structural Engineering and Engineering Materials
SM Report No. 42

UNIVERSITY OF KANSAS CENTER FOR RESEARCH, INC.
LAWRENCE, KANSAS
October 1996

ABSTRACT

The effects of deformation properties on the bond of steel reinforcing bars to concrete are studied to develop guidelines for commercially produced high relative rib area deformation patterns and accurate equations to predict bond strength. The fundamental behavior of bond is studied using finite element analysis.

Beam-end tests are used to investigate the effects of bar size, relative rib area, and the ratio of rib width (measured parallel to the longitudinal axis of the bar) to center-to-center rib spacing on bond strength. 139 specimens containing bars with relative rib areas, R_r, ranging from 0.05 to 0.28 were tested both with and without transverse stirrups confining the test bar. Bond strength is not affected by R_r for bars not confined by transverse stirrups, but increases as bar size and R_r increase for bars confined by transverse stirrups. Bond strength decreases when the ratio of rib width to center-to-center rib spacing is greater than 0.45.

Splice tests are used to investigate the effects of bar size, relative rib area, epoxy coating, and the amount of transverse reinforcement confining the bars on splice strength. Thirty tests of beams containing No. 5 and No. 11 (16 and 36 mm) bars are combined with sixty-three previously reported tests of beams containing No. 8 (25 mm) bars. The combined results include tests for bars with R_r ranging from 0.065 to 0.140. The results show that splice strength is unaffected by R_r for splices not confined by transverse reinforcement, but increases as bar size and R_r increase for splices confined by transverse reinforcement. Under all conditions of confinement, epoxy coating has a less detrimental effect on the splice strength of high relative rib area bars than on the splice strength of conventional bars. Accurate splice strength equations, that account for the effects of bar size, relative rib area, and epoxy coating on bond strength, are combined with a reliability-based strength reduction factor

TABLE OF CONTENTS

LIST OF SYMBOLS

A_b = bar area, in $in.^2$

A_{tr} = area of each stirrup or tie crossing the potential plane of splitting adjacent to the reinforcement being developed or spliced, in $in.^2$

a = average vertical distance between the top and bottom LVDTs used to measure rotation, in in.

b = intercepts of the best-fit lines relating $T_s/f'_c{}^{1/4}$ to NA_{tr}/n in Figs. 3.6 and 3.7 or beam width, in in.

C/U = relative bond strength of epoxy-coated bar to uncoated bar

c = $c_m + 0.5d_b$ or cohesion, in ksi

c_b = bottom cover of reinforcing bars, in in.

c_M = maximum value of c_s or c_b ($c_M/c_m \leq 3.5$), in in.

c_m = minimum value of c_s or c_b ($c_M/c_m \leq 3.5$), in in.

c_s = $\min(c_{si} + 0.25 \text{ in.}, c_{so})$ or $\min(c_{si}, c_{so})$, in in.

c_{si} = one-half of clear spacing between bars, in in.

c_{so} = side cover of reinforcing bars, in in.

d = beam effective depth, in in.

d_b = nominal bar diameter, in in.

d_s = nominal stirrup diameter, in in.

E = modulus of elasticity, in ksi

f'_c = concrete compressive strength, in psi; $f'_c{}^{1/2}$ and $f'_c{}^{1/4}$ in psi

f_s = steel stress at failure, in psi

f'_t = concrete tensile strength, in psi

f_y = yield strength of bars being spliced or developed, in psi

f_{yt} = yield strength of transverse reinforcement, in psi

G_c = fracture energy of concrete, in lb/in.

h = beam depth, in in.

K_{tr} = $35.3\ t_r t_d A_{tr}/sn$, term representing the effect of transverse reinforcement on bond strength. $K_{tr}(conv.) = 34.5\ (0.72d_b + 0.28)A_{tr}/sn$ for conventional reinforcement (average $R_r = 0.0727$). $K_{tr}(new) = 53\ (0.72d_b + 0.28)A_{tr}/sn$ for new reinforcement (average $R_r = 0.1275$)

= $A_{tr}f_{yt}/(1500\ sn)$ in the expressions for ACI 318-95

k_n = normal stiffness of interface elements, kips/in.

k_{sy}, k_{sz} = shear stiffnesses of interface elements, kips/in.

l = beam length, in ft

l_c = length of constant moment region, in ft

l_d = development or splice length, in in.

l_{db} = basic development length, in in.

l_s = splice length, in in.

M = slope of the modified relationship in Eq. 3.2

$M_{Rr = 0.075}$ = value of M at $R_r = 0.075$

M_u = moment at splice failure, in kip-in.

m = slopes of the best-fit lines relating $T_s/f'_c{}^{1/4}$ to NA_{tr}/n in Figs. 3.6 and 3.7

N = number of transverse reinforcing bars (stirrups or ties) crossing l_d

n = number of bars being developed or spliced along the plane of splitting

P = total applied load at splice failure, in kips

R_r = ratio of projected rib area normal to bar axis to the product of the nominal bar perimeter and the center-to-center rib spacing

s = spacing of transverse reinforcement, in in.

T_b = total force in a bar at splice failure, in lb

T_c = concrete contribution to total force in a bar at splice failure, in lb

T_s = confining steel contribution to total force in a bar at splice failure, in lb

t_d = $0.72\ d_b + 0.28$, term representing the effect of bar size on T_s

t_r = $9.6\ R_r + 0.28$, term representing the effect of relative rib area on T_s

U = average ultimate bond force per unit length of the bar, in lb/in.

W_r = ratio of rib width (measured parallel to the longitudinal axis of the bar) to center-to-center rib spacing

w_1 = crack width at which tensile strength of concrete drops to zero, in psi

Δ_b = deflection of the bottom LVDT used to measure rotation, in in.

Δ_t = deflection of the top LVDT used to measure rotation, in in.

α = reinforcement location factor or parameter used to maintain numerical stability in finite element analysis

β = coating factor

ϕ = reliability-based strength reduction factor

μ = coefficient of friction

θ = rotation, rad.

ρ = reinforcement ratio

ρ_b = balanced reinforcement ratio

σ = stress, in psi

σ_n = normal stress, in ksi

σ_s = shear stress, in ksi

σ_{sy}, σ_{sz} = mutually perpendicular shear stresses, in ksi

LIST OF TABLES

LIST OF FIGURES

CHAPTER 1: INTRODUCTION

1.1 General

The tensile strength of concrete is much lower than the compressive strength and is usually neglected in design. For this reason, reinforcing steel must be added to resist any tensile forces in a member that can arise from axial loading or bending. If the member is to act as intended, there must be adequate bond developed so that stresses can be transferred between the concrete and reinforcement.

Reinforcing steel originally consisted of smooth bars. The bond strength of these bars was provided by friction and chemical adhesion between the steel and concrete. Both of these contributions to bond strength are very weak which necessitated the use of end hooks to properly anchor the bars. With the introduction of deformed bars, bond strength was greatly improved by the addition of a mechanical interlock component to bond strength provided by bearing of the ribs on the surrounding concrete. This eliminated the need for end hooks in most cases. Another advantage of deformed bars is that bond is provided along the entire length of the bar instead of only at the ends, as is the case for hooked smooth bars. This helps enforce strain compatibility between the steel and concrete along the length of the member, which is one of the primary assumptions on which the design of reinforced concrete is based. True strain compatibility would require perfect bond, but the improved bond of deformed bars makes this assumption nearly correct.

To ensure that the strength of a bar is developed, an adequate splice or development length must be provided. An accurate equation to predict splice and development lengths is needed to ensure safety without compromising the cost of

the structure due to overly conservative requirements. If bond strength can be improved, the cost of the structure can be reduced while maintaining safety.

The current study extends previous research at the University of Kansas to develop deformation patterns with improved bond characteristics. This report presents the results of tests to evaluate improved deformation patterns and investigate the effects of deformation properties on bond strength. The test results are used to develop accurate equations to predict splice and development length which take into account the effects of deformation properties on bond strength. In addition to the experimental work, the finite element method is used to study bond between reinforcing bars and concrete. The results of a study to investigate the economic and practical construction benefits produced in actual structures through the use of new design equations for bars with improved bond characteristics is also presented.

1.2 Previous Work

1.2.1 Deformation Properties

The earliest investigation into the bond strength of deformed bars was reported by Abrams (1913). In that study, smooth and deformed bars were tested using beam and pullout specimens. Deformed bars were reported to produce higher bond strengths than smooth bars. However, because Abrams was interested in studying bond over a wide range of slip, most of the specimens were reinforced against bursting, and he doubted whether the high ultimate bond strengths were useful because of the excessive amount of slip which accompanied them. A round bar with 0.082 in. (2.1 mm) deep threads spaced 0.125 in. (3.2

mm) on center was also tested. This bar produced substantially higher bond forces at low slips and at ultimate than the commercially produced bars tested.

In the 1940s, Clark (1946, 1949) investigated the bond performance of 17 deformation patterns in use at the time of the study, using mostly pullout and some beam specimens. The bars were rated based on the bond stresses developed at predetermined values of slip. Clark observed that the rating increased as the ratio of shearing area (bar perimeter times the distance between deformations) to the bearing area (projected rib area normal to the bar axis) of the deformations decreased. The relationship between shearing and bearing areas is currently expressed as the inverse ratio, known as relative rib area, R_r. As shown in Fig. 1.1, relative rib area is defined as the projected rib area normal to the bar axis (bearing area) divided by the product of the nominal bar perimeter and the center-to-center rib spacing (shearing area). The work by Clark over 45 years ago is the basis for the current deformation requirements for minimum rib height and maximum spacing given in ASTM A 615/A 615M, A 616/A 616M, A 617/A 617M, and A 706/A 706M. Clark also recommended that the ratio of shearing to bearing area be limited to a maximum of 10 ($R_r = 0.10$) and if possible 5 or 6 ($R_r = 0.20$ or 0.17). These recommendations were not included in the ASTM requirements, and as a result, values of R_r for deformed bars currently in use in the U. S. are much lower than Clark's recommendations, typically ranging from 0.06 to 0.08.

Rehm (1957, 1961) reported that, if the ratio of rib spacing to height is greater than 10 and the rib face angle (the angle between the face of the rib and the longitudinal axis of the bar) is greater than 40°, the concrete in front of the ribs crushes, forming a wedge with a lower effective face angle, which then causes

splitting of the surrounding concrete. This observation was supported by Lutz and Gergely (1967) and Skorobogatov and Edwards (1979). Lutz and Gergely (1967) reported that crushing of the concrete in front of the ribs occurs when the rib face angle is greater than about 40°. They also observed that no crushing and greater slip occurs when the rib face angle is less than 30°. Skorobogatov and Edwards (1979) found that rib face angles of 48.5° and 57.8° do not affect the maximum bond stress, because the face angle is flattened by the crushed concrete in front of the ribs.

Losberg and Olsson (1979) found that traditional pullout tests are not useful in studying the bond performance of deformed bars because the failure does not normally involve splitting. Their tests of three different deformation patterns showed substantially different results for pullout tests than for beam tests. They also observed that transverse ribs (ribs oriented perpendicular to the longitudinal axis of the bar) cause slightly less splitting than inclined ribs.

Soretz and Holzenbein (1979) studied the effects of rib height and spacing using bars with the same rib bearing area per unit length but with varying rib heights. They found no difference in bond strength up to a slip of 0.039 in. (1 mm), but above 0.039 in. (1 mm) of slip, the pattern with the smallest rib height showed 20% lower bond strength. The pattern with the largest rib height produced the strongest splitting effect. Soretz and Holzenbein (1979) also studied the effects of rib inclination angle (the angle between the rib and the longitudinal axis of the bar) and rib face angle. They found that bond strength increases slightly the closer the rib inclination angle is to 90° and that rib face angles between 45° and 90° have no effect on bond strength.

Darwin and Graham (1993a, 1993b) used beam-end specimens to study the effects of rib height and spacing on bond strength. Beam-end specimens more closely replicate the state of stress in a beam than pullout specimens. In a pullout specimen, the bar is placed in tension while the surrounding concrete is placed in compression by bearing of the reaction plate. In a beam-end specimen, the bar and surrounding concrete are simultaneously placed in tension. Darwin and Graham used specially machined 1 in. (25 mm) diameter bars with rib heights of 0.050, 0.075, and 0.100 in. (1.27, 1.91, and 2.54 mm) with center-to-center spacings adjusted to give relative rib areas of 0.05, 0.10, and 0.20 for each rib height. They observed that the bond force-slip relationship is a function of relative rib area, independent of the combination of rib height and spacing used to obtain a value of R_r and that the initial stiffness of the bond force-slip curves increases as R_r increases. For low confinement (low cover and no transverse stirrups), bond strength is independent of deformation pattern. However, when additional confinement is provided, by including transverse stirrups or increasing the cover and lead length (length of concrete before the bonded length of the bar), bond strength increases as R_r increases.

1.2.2 Epoxy Coating

The first study of the effects of epoxy coating on the bond strength of deformed bars was conducted by Mathey and Clifton (1976) using pullout specimens. They reported that bars with a coating thickness of 25 mils (0.635 mm) produced unsatisfactory performance. However, for the bars tested with coating thicknesses ranging from 1 to 11 mils (0.025 to 0.279 mm), the average bond strength of the coated bars was only 6% lower than that of uncoated bars.

Treece and Jirsa (1987, 1989) studied the effects of epoxy coating using splice beams in which there was no transverse reinforcement in the splice region. Their tests included ten No. 6 (19 mm) and eleven No. 11 (36 mm) bar specimens. Twelve of the specimens contained epoxy-coated bars. Only four of the specimens contained bottom-cast splices; the rest were top-cast. Four of the No. 6 (19 mm) bar specimens had covers less than or equal to the maximum size of the coarse aggregate. Their tests produced an average ratio of coated to uncoated bar splice strength, C/U, of 0.67. The deformation pattern used by Treece and Jirsa (1987, 1989) (an X-pattern) is no longer used for epoxy-coated bars due to difficulty in applying the coating. The results of these tests are the basis for the current ACI 318 (1995) and AASHTO (1992) development length modification factors for epoxy-coated bars. These factors are 1.5 for bars with cover less than three bar diameters ($3d_b$) or clear spacing between bars less than $6d_b$ and 1.20 for all other bars, with a maximum limit of 1.7 for the product of the epoxy coating and top-bar factors in ACI 318 (1995) and 1.5, 1.15 and 1.7 using the same criteria in AASHTO (1992).

Choi, Hadje-Ghaffari, Darwin and McCabe (1990a, 1991) used beam-end and splice specimens to study the bond strength of No. 5, No. 6, No. 8 and No. 11 (16, 19, 25, and 36 mm) epoxy-coated bars with three different deformation patterns. Coating thicknesses ranged from 3 to 17 mils (0.08 to 0.43 mm). Their tests produced an average C/U of 0.82 for the fifteen splice tests conducted. They observed that coating thickness has little effect on the reduction in bond strength caused by epoxy coating for No. 6 (19 mm) and larger bars. For smaller bars, C/U drops with increasing coating thickness. Epoxy coating was found to be less detrimental to the bond strength of the bars with higher relative rib areas. Choi et

al. (1990a, 1991) also observed that the reduction in bond strength caused by epoxy coating increases with increasing bar size.

Hamad and Jirsa (1990, 1993) tested twelve splice specimens with top-cast bars. Their tests included four specimens with No. 6 (19 mm) bar splices and eight with No. 11 (36 mm) bar splices. Hamad and Jirsa combined the results of their tests and results from Treece and Jirsa (1989), Choi et al. (1990a) and DeVries, Moehle and Hester (1991) and concluded that the reduction in splice strength caused by epoxy coating decreases when transverse reinforcement is added around the splice. The combined test results gave C/U ratios of 0.74 for specimens without transverse reinforcement and 0.80 to 0.85 with transverse reinforcement for No. 11 (36 mm) bars and C/U ratios of 0.67 and 0.74, respectively, for No. 6 (19 mm) bars. In contrast to Choi et al. (1990a, 1991), Hamad and Jirsa (1990, 1993) observed that the reduction in splice strength caused by epoxy coating decreases with increasing bar size.

Hester, Salamizavaregh, Darwin and McCabe (1991, 1993) tested 65 beam and slab splice specimens containing No. 6 and No. 8 (19 and 25 mm) bars. Their tests produced an average C/U ratio of 0.74. They analyzed their tests along with 48 splice test results from earlier studies, including Treece and Jirsa (1987, 1989), Choi et al. (1990a, 1991), and Hamad and Jirsa (1990, 1993). In contrast to Hamad and Jirsa (1990, 1993), they concluded that the percentage decrease in splice strength caused by epoxy-coating is independent of the degree of transverse reinforcement.

In a recent study by Idun and Darwin (1995), beam splice specimens were used to evaluate the bond strength of conventional and high relative rib area No. 8 (25 mm) bars. They observed that epoxy coating was less detrimental to the

splice strength of high relative rib area bars than previously tested conventional bars, which agrees with the observations of Choi et al. (1990a, 1991).

1.2.3 Design Equations

Design equations for development and splice length have been developed based on empirical relationships obtained from experimental data. The design equations used in the 1963 ACI Building Code were based on studies by Mathey and Watstein (1961) and Ferguson and Thompson (1962). These equations were derived from an expression describing the average ultimate bond force per unit length of the bar, U, (in pounds per inch) given as

$$U = 35\sqrt{f'_c} \tag{1.1}$$

where f'_c = the concrete compressive strength in psi. The development length, l_d, can then be obtained by setting $U = A_b f_y / l_d$, where A_b = the area of the bar in in.^{2} and f_y = the yield strength of the bar in psi, and solving Eq. 1.1 for l_d to obtain

$$l_d = \frac{0.028 A_b f_y}{\sqrt{f'_c}} \tag{1.2}$$

Design equations for development and splice length were significantly changed in the 1989 ACI Building Code (ACI 318-89) based on the recommendations of ACI Committee 408, Bond and Development of Reinforcement. In these equations, the development length, l_d, is computed by multiplying the basic development length, l_{db}, by applicable factors from sections 12.2.3 through 12.2.5 of the Code. The basic development length, l_{db}, is given as

$0.04\,A_b f_y / \sqrt{f'_c}$ for No. 11 (36 mm) and smaller bars, $0.085\,f_y / \sqrt{f'_c}$ for No. 14 (43 mm) bars and $0.125\,f_y / \sqrt{f'_c}$ for No. 18 (57 mm) bars. A maximum limit of 100 psi is placed on $\sqrt{f'_c}$ because there is not sufficient experimental data to justify a reduction in splice length for concrete strengths above 10,000 psi (69 MPa). To account for the effects of cover, clear spacing between bars and transverse reinforcement on bond strength, l_{db} is multiplied by a modification factor. The factor is 1.0 for bars satisfying one of four conditions: 1) bars in beams or columns satisfying the minimum specified cover of Code section 7.7.1, transverse reinforcement satisfying minimum tie or stirrup requirements of Code sections 7.10.5 or 11.5.4 and 11.5.5.3, respectively, and clear spacing not less than $3d_b$; 2) bars in beams or columns with minimum specified cover of Code section 7.7.1 and enclosed within transverse reinforcement, A_{tr}, not less than $d_b sn/40$, where s = spacing of stirrups or ties in in., and n = number of bars in a layer being spliced or developed at a critical section; 3) bars in the inner layer of slab or wall reinforcement and with clear spacing not less than $3d_b$; or 4) any bars with cover of not less than $2d_b$ and with clear spacing of not less than $3d_b$. For bars with cover of d_b or less or with clear spacing of $2d_b$ or less, l_{db} is multiplied by 2.0. In cases not meeting the previous criteria, l_{db} is multiplied by 1.4. For No. 11 (36 mm) and smaller bars with clear spacing not less than $5d_b$ and side cover not less than $2.5d_b$, an additional multiplier of 0.85 is allowed. The factors just described may be multiplied by 0.75 for reinforcement enclosed within a spiral or closely spaced ties or stirrups meeting the requirements of Code section 12.2.3.5. The basic development length multiplied by the appropriate factors must be greater than $0.03\,d_b f_y / \sqrt{f'_c}$. In most cases, the splice length is calculated by multiplying l_d by 1.3, except when the area of reinforcement provided is at least

twice that required by analysis and not more than 50% of the reinforcement is spliced within the splice length, in which case l_d is multiplied by 1.0. A strength reduction factor, ϕ, is not used with development or splice lengths because the basic development length equations already include an allowance for understrength.

The 1995 ACI Building Code (ACI 318-95) design equations for development and splice length are based on an analysis of previous experimental data by Orangun, Jirsa and Breen (1975, 1977) and recommendations by ACI Committee 408. Changes in the Code were proposed to simplify the calculation of development and splice lengths. Many designers felt that the criteria in ACI 318-89 were overly complex to apply, because every bar being spliced in a structure had to be classified into one of the three categories. In addition, in some cases, the ACI 318-89 equations required longer development lengths than necessary (ACI Committee 318 1994).

Under ACI 318-95, development lengths may be calculated using simplified equations given in a table found in Code section 12.2.2 or a more detailed expression given in Code section 12.2.3. The equations in the table for bars in normal weight concrete become $l_d / d_b = \alpha\beta f_y / (25 \sqrt{f'_c})$ for No. 6 (19 mm) and smaller bars and $l_d / d_b = \alpha\beta f_y / (20 \sqrt{f'_c})$ for No. 7 (22 mm) and larger bars, if one of two sets of criteria are satisfied. The first set requires clear spacing between bars of not less than d_b, cover not less than d_b, and stirrups or ties throughout l_d not less than the Code minimum. The second set requires clear spacing between bars of not less than $2d_b$ and cover not less than d_b. For cases not meeting either set of criteria, $l_d / d_b = 3 \alpha\beta f_y / (50 \sqrt{f'_c})$ for No. 6 (19 mm) and smaller bars and $l_d / d_b = 3 \alpha\beta f_y / (40 \sqrt{f'_c})$ for No. 7 (22 mm) and larger

bars. The reinforcement location factor, α, is equal to 1.3 for bars with more than 12 in. (305 mm) of fresh concrete below the bar, and 1.0 for all other bars. The coating factor, β, is equal to 1.5 for epoxy-coated bars with cover less than $3d_b$ or clear spacing less than $6d_b$, 1.2 for all other epoxy-coated bars, and 1.0 for uncoated bars.

The more detailed expression found in Code section 12.2.3 is given as

$$\frac{l_d}{d_b} = \frac{3}{40}\frac{\alpha\beta f_y}{\sqrt{f'_c}\left(\frac{c + K_{tr}}{d_b}\right)} \tag{1.3}$$

where c = the smaller of the distance from the center of the bar to the nearest concrete surface or half the center-to-center bar spacing in in., $K_{tr} = A_{tr}f_{yt}/(1500sn)$ = the transverse reinforcement index, A_{tr} = the total area of transverse reinforcement within the spacing s that crosses the potential plane of splitting in $in.^2$, f_{yt} = the specified yield strength of the transverse reinforcement in psi, s = the maximum center-to-center spacing of transverse reinforcement within l_d in in., and n = the number of bars being developed or spliced along the plane of splitting. The criterion for the 1.0 and 1.3 multipliers for determining splice lengths are the same as in ACI 318-89.

A recent study by Idun and Darwin (1995) extended previous work by Darwin, McCabe, Idun and Schoenekase (1992a, 1992b) to include the effects of transverse reinforcement on splice and development length and corrected the database of test results used by Darwin et al. (1992a, 1992b) (which had inadvertently included some top and side-cast bar test results) to include only bottom-cast bars. Idun and Darwin (1995) developed equations for the bond

strength of bars with and without transverse reinforcement. Four equations were developed which reflected the increase in bond strength as R_r increases for bars with transverse reinforcement. A major observation of Idun and Darwin (1995) was that $f'_c{}^{1/4}$ better represents the effect of concrete strength on bond strength than $f'_c{}^{1/2}$, which has traditionally been used. LRFD concepts and Monte Carlo techniques were applied to the bond strength equations to determine reliability based strength reduction (ϕ) factors for splice/development length. In their analysis, the majority of the data were from splice tests. Assuming that the equations developed for splice length would be conservative for calculating development length, Idun and Darwin (1995) used the same equations for both development and splice lengths. For bars without transverse reinforcement, the expression for development/splice lengths was given as

$$l_d = \frac{A_b\left[\frac{f_y}{\phi_d f_c'^{1/4}} - 2280\left(0.082\frac{C_M}{C_m} + 0.918\right)\right]}{63(C_m + 0.5d_b)\left(0.082\frac{C_M}{C_m} + 0.918\right)} \qquad (1.4)$$

where A_b = the area of the bar being spliced or developed in $in.^2$, f_y = the yield strength of the bar being spliced or developed in psi, $\phi_d = 0.85$ = the strength reduction factor, f'_c = the concrete compressive strength in psi, C_m and C_M = the minimum and maximum of C_s or C_b in in., C_s = the minimum of half the center-to-center bar spacing + 0.25 in. or the side cover in in., C_b = the bottom cover in in., and d_b = the nominal bar diameter in in. For bars with transverse reinforcement, the expressions for development/splice lengths were given as

$$l_d = \frac{A_b\left[\frac{f_y}{\phi_d f_c'^{1/4}} - 2280\left(0.082\frac{C_M}{C_m} + 0.918\right)\right] - c_1}{63(C_m + 0.5d_b)\left(0.082\frac{C_M}{C_m} + 0.918\right) + c_2\frac{A_{tr}}{sn}} \quad (1.5)$$

where A_{tr} = the area of each stirrup or tie crossing the potential plane of splitting adjacent to the reinforcement being developed or spliced in in.^{2}, s = the center-to-center spacing of the transverse reinforcement in in., and n = the number of bars being developed or spliced along the plane of splitting. c_1 and c_2 are constants that depend on the relative rib area of the spliced or developed bar. For conventional reinforcement (R_r = 0.065 to 0.085), c_1 = 202 and c_2 = 2187. For high relative rib area bars, c_1 = 471, 531, and 533 and c_2 = 2413, 2791, and 3399 for R_r = 0.101, 0.119, and 0.140, respectively. Improved versions of Eqs. 1.4 and 1.5, presented by Darwin, Zuo, Tholen and Idun (1995a, 1996a), are discussed in Chapter 3.

Recently, Esfahani and Rangan (1996) have developed equations to predict splice strength in normal and high strength concrete. However, these equations cannot be solved directly for splice length.

1.2.4 Finite Element Bond Analysis

The first published nonlinear finite element model for concrete was reported by Ngo and Scordelis (1967). Their work used what is known as a discrete crack model. In this model the nodes of adjacent elements were decoupled when the stress exceeded the tensile strength of the concrete, f'_t. It was assumed that no stress could be carried across the crack once the tensile strength was exceeded.

Rashid (1968) modeled cracking of concrete at the material level. Like Ngo and Scordelis (1967), cracks were assumed to form once the tensile stress exceeded tensile strength of the concrete. Instead of splitting the nodes, cracking was modeled by introducing an orthotropic constitutive matrix with zero strength normal to the crack plane. This model has become known as the smeared crack model.

Hillerborg, Modeer and Petersson (1976) developed a discrete crack representation known as the fictitious crack model. Cracks were assumed to initiate when stresses exceeded the tensile strength of the concrete. However, in the fictitious crack model, the tensile strength across the crack was not assumed to drop immediately to zero, but decreased as the width of the crack increased. This method of modeling cracking in concrete more closely represents the actual behavior, because, even after small cracks have initiated, some tensile stress can be transferred across the crack due to interlock of the aggregate and bridging of cracks around pieces of aggregate. As shown in Fig. 1.2, a simple linear decrease in stress carrying capacity, from the tensile strength at zero crack width to zero at a crack width of w_1 or greater, can be assumed to represent the stress-crack width relationship. The fracture energy, G_c, defined as the energy absorbed per unit crack area in opening the crack from zero width to or beyond w_1, can be calculated from

$$G_c = \int_0^{w_1} \sigma \, dw \tag{1.6}$$

which is equivalent to the area under the stress-displacement curve. If a simple linear decrease is assumed, $G_c = f'_t \, w_1/2$.

A study of the bond-slip behavior of a tension-pull specimen was conducted by Ingraffea, Gerstle, Gergely and Saouma (1984). The effects of concrete crushing and longitudinal splitting were neglected and only the effects of radially propagating secondary cracks were considered. Cracks in the model were propagated by inserting interface elements into the finite element mesh perpendicular to the principal tensile stress. These interface elements were capable of modeling mixed-mode fracture where both normal and shear softening occurs across a crack in the process zone.

Keuser and Mehlhorn (1987) studied various approaches to modeling bond between reinforcing steel and concrete using interface elements. Among their observations were that the behavior of the elements and the quality of results were mainly influenced by the displacement functions of the elements, the density of the finite element mesh, and the bond stress-slip relationship assumed. They concluded that the bond stress-slip relation cannot be modeled adequately by a general function which neglects local influences on bond behavior and that a realistic model requires consideration of the influence of transverse pressure on longitudinal cracking, secondary cracks (small cracks radiating out from the bar due to stress concentrations at the ribs) and the deterioration of bond near tension cracks in the concrete surrounding the bar.

A study of the individual components that contribute to bond slip was conducted by Rots (1989), including the effects of elastic deformation and secondary and longitudinal cracking. Rots (1989) found that the inclusion of longitudinal cracking was essential to accurately model bond slip. He concluded that a model aimed at explaining the fundamentals of bond must include the

individual components contributing to bond slip rather than lumping them together into an interface slip relationship.

Choi, Darwin and McCabe (1990b) used a 3-dimensional finite element model of a beam-end specimen to study the bond of reinforcing steel to concrete. Their model consisted of three substructures, the first of which was a 3-dimensional exterior concrete substructure that cracked along a predefined vertical crack plane. The other two substructures were 2-dimensional models consisting of a refined model of the concrete surrounding the reinforcing bar and a reinforcing bar substructure in which the ribs of the bar were explicitly modeled. The refined concrete and reinforcing bar substructures were connected using special link elements to model the steel-concrete interface. The analysis was conducted using a two step process. In the first step, the exterior concrete substructure was loaded by applying lateral displacements at the nodes where the reinforcing bar substructure was located. This step was used to obtain the clamping force of the concrete as a function of lateral displacement. This force-displacement relationship was used in the second step of the analysis to define nonlinear spring elements which were attached to the refined concrete substructure to represent the confinement provided by the concrete. The reinforcing steel and refined concrete substructure were then analyzed together by applying displacements to the end of the bar to obtain the bond force-slip relationship and the maximum bond force.

The method developed by Choi et al. (1990b) was extended by Hadje-Ghaffari, Darwin and McCabe (1991) to study the effects of bar size, cover and lead length with improved boundary conditions that better matched those of the experimental specimen. This study showed that an increase in the lateral force

provided by the concrete, and therefore an increase in bond strength resulted from increases in cover, lead length, or bar size.

Gerstle and Xie (1992) extended the fictitious crack model developed by Hillerborg et al. (1976) to include mixed-mode fracture in their study of the behavior of a centrally notched plate and a single-notched shear beam. In their analysis, the tangential stiffness of the crack elements was initially set to a very large value to prevent shear displacement across the crack face. The tangential stiffness remained constant until the crack width had reached the point where normal stresses could no longer be transferred across the crack face. At this point the tangential stiffness was set to zero.

The modeling method developed by Choi et al. (1990b) to study bond in a beam-end specimen and later extended by Hadje-Ghaffari et al. (1991) was the basis for a study by Brown, Darwin and McCabe (1993). They improved the models by combining the three substructures used previously into a single 3-dimensional model in which both concrete cracking and bar slip were represented. The models were used to study the effects of deformation height and face angle, concrete cover, lead length, embedded length, and confinement provided by transverse stirrups. The reinforcing bar in the model was square, with deformations explicitly modeled on only one face. Brown et al. (1993) found that steel-concrete interaction could be accurately represented with interface elements only on the compression faces of the ribs. Their study of the effect of rib height on bond strength showed that an increase in rib height resulted in a decrease in slip but little or no change in the load at failure when transverse reinforcement was not included in the model and that the lateral displacements at the front face of the specimen (crack width) were not dependent on rib height up to the peak

load. They also found that the surface area of the concrete splitting crack and the clamping force provided by the concrete to the steel at the peak load were not proportional to the embedded length (doubling the embedded length resulted in less than a 100% increase in the amount of concrete split or the clamping force at the peak load). They believed that this observation may help explain why bond strength does not increase proportionally with embedded length.

Recently, Yao and Murray (1995) studied bond slip of a tension-pull specimen using a distributed discrete cracking model in which the ribs of the bar were explicitly modeled. Their analysis included the effects of longitudinal and secondary cracking, interface behavior and local crushing of the concrete. Their analysis indicated that longitudinal splitting has an important influence on bond. They concluded that it was necessary to include longitudinal splitting effects to reliably predict bond behavior.

1.3 Discussion

The study currently underway at the University of Kansas is the first major study aimed at improving the bond characteristics of deformed bars since the work reported by Clark (1946, 1949). Intervening studies of bond have focused on evaluating existing deformation patterns or studying the effects of a limited number of parameters affecting bond characteristics, such as rib face angle and inclination, rib height, rib spacing, epoxy coating, casting position, etc. The study at the University of Kansas was begun with the goal of developing new deformation patterns with improved bond characteristics, as well as accurately characterizing the bond performance of both the new and conventional reinforcement, to allow the use of shorter splice and development lengths and,

therefore, provide both economic and practical construction benefits by using less reinforcing steel in a structure and reducing congestion in highly reinforced regions.

Experimental efforts in the study were begun by Darwin and Graham (1993a, 1993b) whose work developed deformation pattern guidelines for prototype commercially produced bars. The deformation patterns for the prototype bars were designed to provide higher relative rib areas than obtained with conventional bars. Based on the results obtained by Darwin and Graham (1993a, 1993b), it was believed that high relative rib area bars could produce substantial savings in splice and development lengths over conventional bars. The study was continued by Idun and Darwin (1995) who tested the first high relative rib area No. 8 (25 mm) bars. Using the results of their study, along with tests of conventional bars performed by other researchers, Idun and Darwin (1995) formulated accurate splice and development length equations which were used as the basis for design equations for conventional and high relative rib area reinforcing bars. The portion of the study presented here is aimed at extending the previous research to gain additional data and investigate other parameters that may affect the bond performance of reinforcing bars.

1.4 Objective and Scope

The major objective of this study is to extend the research started by Darwin and Graham (1993a, 1993b), Brown, Darwin and McCabe (1993) and Idun and Darwin (1995) to improve the bond characteristics of deformed bars. The work includes an evaluation of the bond characteristics of a high strength

threaded bar with an ultra-high relative rib area and an estimate of the reduction in splice length and the cost savings obtainable with high relative rib area bars.

The research started by Darwin and Graham (1993a, 1993b) on the effects of deformation height and spacing is extended to include the effects of bar size. Beam-end specimens are used to study the bond strength of 5/8 and 1 in. (16 and 25 mm) diameter specially machined bars. Beam-end specimens containing 1 in. (25 mm) diameter bars are also used to study the effects of increasing rib width parallel to the longitudinal axis of the bar while maintaining the same center-to-center rib spacing. The ratio of rib width to center-to-center rib spacing is studied because, to achieve high relative rib areas, deformations will probably need to be closer together, along with some increase in rib height, compared to current deformation patterns. This will decrease the amount of concrete between the ribs available to resist bearing of the ribs and may cause bond strength to decrease. The results provide guidelines on rib width and spacing for the design of commercially produced high relative rib area deformation patterns. The key test parameters investigated in this portion of the study are bar size, the ratio of rib width to center-to-center rib spacing, and relative rib area.

The finite element analysis of bond begun by Choi et al. (1990b), and later extended by Hadje-Ghaffari et al. (1991) and Brown et al. (1993), is extended to include finite element models in which the square bar with ribs on one face and the concrete substructure with a single crack plane are replaced by a round bar with circumferential ribs and a concrete substructure with multiple cracking planes. The key parameters of this study are the number of faces used to approximate a round bar, the number of cracking planes modeled, the embedded length of the bar, and the thickness of the concrete cover.

Splice tests of No. 5 and No. 11 (16 and 25 mm) conventional and high relative rib area bars are performed, and the results are analyzed to extend the research by Idun and Darwin (1995). Accurate splice and development length equations are proposed that reflect the effects of bar size and relative rib area on the increase in bond strength due to transverse reinforcement. Bar size, relative rib area, transverse reinforcement, cover and clear spacing, concrete strength and the effects of epoxy coating on high relative rib area bars are investigated.

The evaluation of the bond characteristics of ultra-high relative rib area threaded bars is conducted using beam-end specimens to evaluate the effects of cover, bonded and lead lengths, and transverse reinforcement. Splice tests are performed to investigate the effects of cover, splice length, transverse reinforcement, and the role played by interlocking ribs in the splice region on the splice strength of these bars.

Changes in code equations and deformation requirements will be necessary to implement high relative rib area bars into everyday practice. In addition, some additional expense may be incurred in the production of high relative rib area bars. Therefore, it is appropriate to obtain an estimate of the reduction in splice lengths and the amount of steel that can be saved by using the new bars. To obtain these estimates, a study is conducted on typical structures. Splice length and cost comparisons, based on the amount of steel in the structure, are made using the splice length equations contained in ACI 318-95 and the new equations for both conventional and high relative rib area bars.

CHAPTER 2: BEAM-END TESTS

2.1 General

This chapter describes beam-end tests used to investigate the effects of various deformation properties on the bond performance of reinforcing bars. Three different studies were conducted. The first study investigated the amount of increase in bond strength as bar size increases. The second study investigated the effects increasing rib width, parallel to the longitudinal axis of the bar, while maintaining the same center-to-center rib spacing to provide guidelines on rib width and spacing for commercially produced high relative rib area bars. The third study investigated the bond performance of threaded bars to gain additional information for bars with extremely high relative rib areas. In all three studies, the specimens were tested both with and without transverse reinforcement confining the test bar.

In the bar size study, specimens containing specially machined 5/8 and 1 in. (16 and 25 mm) nominal diameter bars, with relative rib areas of 0.05, 0.10, and 0.20, were tested to examine the effect of bar size on bond strength.

In the rib width study, 1 in. (25 mm) diameter machined bars, with relative rib areas of 0.10 and 0.20, were tested. For each value of relative rib area, the rib width, measured at the top of the rib parallel to the longitudinal axis of the bar, was varied to produce different ratios of rib width to center-to-center rib spacing, W_r. This study was conducted because a decrease in center-to-center rib spacing will probably be necessary for deformation patterns of commercially produced high relative rib area bars, while rib widths will probably be nearly the same as for current deformation patterns. This will lead to a decrease in the amount of concrete between the ribs, which may cause a decrease in bond strength. The results of this study provide

additional guidelines for the design of commercially produced high relative rib area deformation patterns.

In the threaded bar study, 1 in. (25 mm) diameter commercially produced threaded bars, with a relative rib area of 0.284, were tested to gain information for bars with extremely high relative rib areas.

2.2 Experimental Program

The principal parameters in this study are deformation height and spacing, the ratio of rib width to center-to-center spacing, bar size, and confinement provided by transverse stirrups. The study uses beam-end specimens to investigate the effect of these parameters on the bond performance of high-strength 1 in. (25 mm) nominal diameter threaded bars and specially machined bars with 5/8 and 1 in. (16 and 25 mm) nominal diameters.

A total of 139 beam-end specimens were tested. Seventy-two of these specimens were used to compare 5/8 and 1 in. (16 and 25 mm) nominal diameter bars with and without transverse reinforcement. Fifty-five specimens were used to evaluate the effects of the rib width to center-to-spacing ratio, W_r, on the bond strength of bars with and without transverse reinforcement. The remaining twelve specimens were used to study the performance of the threaded bars under various degrees of confinement.

2.2.1 Test Specimens

Two sizes of beam-end specimen were used to evaluate the machined bars. An 18 x 24 x 9 in. (457 x 610 x 229 mm) specimen, shown in Figs. 2.1a and 2.1b, was used to evaluate the 1 in. (25 mm) diameter bars, while a 17 3/4 x 24 x 8 5/8 in.

(451 x 610 x 219 mm) specimen was used to evaluate the 5/8 in. (16 mm) diameter bars. The side cover was 4 in. (102 mm) and the bottom cover was 2 in. (51 mm) for both specimens.

Two specimen sizes were also used for the threaded bars. 18 x 24 x 9 in. (457 x 610 x 229 mm) and 19 x 24 x 9 in. (483 x 610 x 229 mm) specimens were used for bottom covers of 2 and 3 in. (51 and 76 mm), respectively. The differences in height provided the same distance from the top of the specimen, as cast, to the center of the bar for both sizes.

Flexural and shear reinforcement were included in the specimen to force a bond failure. Two No. 6 (19 mm) bars were used as flexural reinforcement and four No. 3 (10 mm) side stirrups were used as shear reinforcement. The No. 6 (19 mm) bars had 1 1/2 in. (38 mm) side and bottom cover for all specimen sizes. The side stirrups were oriented parallel to the sides of the specimen to limit confinement of the test bar. In addition to the side stirrups, three or four transverse stirrups were included in the specimens used to evaluate the effects of transverse reinforcement. As shown in Fig. 2.1b for specimens with a 12 in. (305 mm) bonded length, these stirrups were positioned so that there was a 1/2 in. (13 mm) gap between the test bar and the transverse stirrups to avoid damaging the test bars. Three No. 3 (10 mm) transverse stirrups spaced 2 1/2 in. (64 mm) on center and four No. 3 (10 mm) transverse stirrups spaced 3 in. (76 mm) on center were used in the specimens with bonded lengths of 7 1/2 and 12 in. (191 and 305 mm), respectively. A 7 1/2 in. (191 mm) bonded length and three transverse stirrups were used in the specimens used to compare the 5/8 and 1 in. (16 and 25 mm) diameter bars to prevent yielding of the smaller bars before a bond failure occurred. As shown in Figs. 2.1a and 2.1b, two

transverse No. 5 (16 mm) bars were used to lift the specimen and one No. 5 (16 mm) bar was used to hold the test bar in position during casting.

Two polyvinyl chloride (PVC) bond breaker pipes were used to limit the length of the test bar in contact with the concrete. The first was located at the front of the bonded length and positioned in the specimen to provide either a 1/2 or 4 in. (13 or 102 mm) "lead length". The lead length was used to prevent a cone type failure at the loaded end of the bar. The second bond breaker was located at the end of the bonded length and was attached to the transverse No. 5 (16 mm) bar used to hold the test bar in position. A length of steel conduit was positioned against the end of the test bar and extended out of the unloaded end of the specimen to allow insertion of a linear variable differential transformer (LVDT) to measure slip of the unloaded end of the test bar. Spaces between the PVC pipes and the test bar and the conduit were filled with modeling clay to prevent concrete from entering.

2.2.2 Materials

Reinforcing Steel: The machined bars were fabricated from 110 ksi yield strength ASTM A 311 cold rolled steel. In total, 25 different deformation patterns were fabricated for use in this study. Test bar deformation properties are summarized in Table 2.1. All machined bars had a bamboo pattern and a deformation face angle of 60°.

Eighteen deformation patterns, 9 each for 5/8 and 1 in. (16 and 25 mm) bars, were used to study the effects of bar size. The nine patterns used for the 1 in. (25 mm) nominal diameter bars are shown in Fig. 2.2. These bars had rib heights of 0.050, 0.075 and 0.100 in. (1.27, 1.91 and 2.54 mm). The center-to-center spacings, ranging from 0.263 to 2.200 in. (6.68 to 55.88 mm), were adjusted to provide relative

rib areas of 0.20, 0.10, and 0.05 for each rib height. The nine patterns used for the 5/8 in. (16 mm) nominal diameter bars are shown in Fig. 2.3. These bars also had relative rib areas of 0.05, 0.10, and 0.20 with rib heights and widths equal to 5/8 of the dimensions used for the corresponding 1 in. (25 mm) diameter bars having the same relative rib area. This produced bars with rib heights of 0.031, 0.047, and 0.063 in. (0.79, 1.19 and 1.60 mm) and center-to-center spacings ranging from 0.163 to 1.387 in. (4.14 to 35.23 mm).

Eleven deformation patterns were used for 1 in. (25 mm) nominal diameter bars to evaluate the effects of rib width, for a constant center-to-center rib spacing, on bond strength. Four of the patterns, M11-8, M12-8, M31-8, and M32-8 (Fig. 2.2), were also used in the bar size study. The remaining seven patterns are shown in Fig. 2.4. Five of the eleven patterns had a rib height of 0.05 in. (1.27 mm), with center-to-center spacings of 0.263 and 0.525 in. (6.68 and 13.34 mm), and six had a rib height of 0.10 in. (2.54 mm), with center-to-center spacings of 0.550 and 1.100 in. (13.97 and 27.94 mm). These combinations of rib height and center-to-center spacing produced relative rib areas of 0.20 and 0.10. Rib widths (measured at the top of the ribs) were varied to produce ratios of rib width to center-to-center spacing, W_r, ranging from 0.182 to 0.727.

The threaded bars, shown in Fig. 2.5, were manufactured by Williams Form Engineering Corporation for use as high-strength prestressing bars conforming to ASTM A 722 with a yield strength of 139 ksi (956 MPa). The high strength and threaded deformation pattern of these bars allows a very small center-to-center rib spacing, 0.250 in. (6.35 mm), with an average rib height of 0.065 in. (1.65 mm). This provides a relative rib area of 0.284 which is extremely high for a production bar.

Concrete: Two concrete mixes were used for the specimens. Both mixes were air-entrained, containing Portland cement, 3/4 in. (19 mm) maximum size crushed limestone coarse aggregate, and Kansas River sand. The water-cement ratio for the first mix was 0.41. The water-cement ratio for the second mix was reduced to 0.36, and a water reducing admixture was added to maintain workability. The second mix was chosen to decrease the time required for the concrete to reach the testing strength. The concrete was supplied by a local ready mix plant. All specimens in a group were cast from a single batch of concrete. Strength at time of testing ranged from 4,760 to 5,440 psi (32.8 to 37.5 MPa). Mix proportions and concrete properties are summarized in Table 2.2.

2.2.3 Placement and Curing Procedure

Forms for the specimens were made from 3/4 in. (19 mm) plywood, 2 x 4 studs, and all-thread rods. Joints in the forms were sealed with weatherstrip caulking cord. Joints between the bars, PVC pipe, and conduit and the forms were filled with modeling clay. Most of the specimens were cast in forms made of plywood with a polymeric resin coating that did not require the use of a release agent. Polyurethane was used for protection and a release agent was used on forms that did not have this coating.

Just prior to casting, the bonded lengths of the test bars were cleaned with acetone to remove any foreign material. Concrete was then placed in the forms in two lifts; all specimens received the first lift before any specimen received a second lift. Each lift was vibrated with a 3/4 in. (19 mm) internal vibrator at 5 evenly spaced points, with each successive vibration carried out on alternating sides of the specimen.

After finishing and allowing the concrete to set, a curing compound was applied to the tops of the specimens. They were then covered with plastic sheets and allowed to cure until the concrete strength reached at least 3,500 psi (24.1 MPa). The forms were then stripped, and the specimens were inverted for testing. The specimens were allowed to cure in air at least one day before testing.

Standard 6 x 12 in. (152 x 305 mm) cylinders in steel molds were cast during placement of the concrete and were cured in the same manner as the test specimens. The concrete strength reported for each group is the average of at least three cylinders that were tested immediately following completion of all tests in a group.

2.2.4 Test Procedure

The beam-end specimens were tested in an apparatus developed by Donahey and Darwin (1983, 1985) which has been modified by Brettmann, et al. (1984, 1986) and Darwin and Graham (1993a, 1993b). The current study uses the apparatus in the configuration used by Darwin and Graham (1993a, 1993b), as shown in Fig. 2.6. The compressive force is provided by a reaction plate that bears on the bottom 3 1/2 in. (89 mm) of the front face of the specimen. This places the center of the reaction plate approximately 13 3/4 in. (349 mm) below the center of the bar. This configuration was chosen because it more nearly replicates the state of stress in the concrete in an actual beam than did earlier configurations (Darwin and Graham 1993a, 1993b).

Load was applied to the test bar by two 60-ton hollow-core jacks, powered by an Amsler hydraulic testing machine, at a rate of approximately 6 kips (26.7 kN) per minute. Two 1 in. (25 mm) diameter steel rods instrumented as load cells were used to transfer force from the jacks to two yokes that were attached to the test bar with a wedge-grip assembly. The tensile force in the test bar was counteracted by the

reaction plate at the bottom of the specimen (Fig. 2.6) and a tie-down beam at the back of the specimen. The testing apparatus and the tie-down beam were secured to the structural floor with four steel rods.

Spring-loaded linear variable differential transformers (LVDTs) were used to measure slip of the bar and the crack width on top of the specimen as it was loaded. Loaded end slip was measured with two LVDTs which bore against the front face of the specimen and were attached to an aluminum yoke mounted on the test bar. Unloaded end slip was measured with a single LVDT mounted on the unloaded end of the test bar through the steel conduit. A spring-loaded grip assembly, which contained another LVDT, was mounted on top of the specimen, perpendicular to the test bar, at the center of the bonded length. This assembly measured the change in width of the specimen, caused by crack growth, by bearing against the sides of the specimen. Force in the test bar was recorded from the two rods instrumented as load cells using four strain gages in a full bridge configuration for each rod. LVDT and strain gage readings were collected with a Hewlett-Packard data acquisition system and stored on a computer disk. A complete cycle of readings was taken at approximately 1/2 second intervals for the duration of the test.

Crack patterns were sketched after all tests in a group were completed. Test bars were then removed for use in later specimens. This was done in such a way as to minimize disturbance of the concrete in contact with the bar so that this concrete could be examined.

2.3 Results, Observations and Evaluation

The tests were carried out in 9 groups, numbered 2, 4-9, 10a, and 10b.

Groups 6, 7, 9 and 10a contained 72 specimens that were used to study the effects of bar size on bond strength. Each group consisted of nine 1 in. (25 mm) and nine 5/8 in. (16 mm) diameter bar specimens with the deformation patterns shown in Figs. 2.2 and 2.3, respectively. The specimens in these groups had a 7 1/2 in. (191 mm) bonded length, a 1/2 in. (13 mm) lead length, and 2 in. (51 mm) cover. The bars in Groups 7 and 9 were confined by three No. 3 (9.5 mm) transverse stirrups spaced 2 1/2 in. (64 mm) on center.

Groups 2, 4, 5, 8 and 10b contained 55 specimens that were used to study the effects of rib width on bond strength. Each of these groups consisted of eleven specimens with the deformation patterns shown in Fig. 2.4 and patterns M11-8, M12-8, M31-8 and M32-8 shown in Fig. 2.2. The specimens in these groups had a 12 in. (305 mm) bonded length, a 1/2 in. (13 mm) lead length, and 2 in. (51 mm) cover. The bars in Groups 5, 8 and 10b were confined by four No. 3 (9.5 mm) transverse stirrups spaced 3 in. (76 mm) on center.

Group 4 also included 12 specimens that were used to evaluate bond strength of the threaded bars. These tests consisted of three replicates of four configurations. Three configurations used a 12 in. (305 mm) bonded length and a 1/2 in. (13 mm) lead length with either 1) 2 in. (51 mm) cover with four No. 3 (9.5 mm) transverse stirrups, 2) 2 in. (51 mm) cover without transverse stirrups or 3) 3 in. (76 mm) cover without transverse stirrups. The fourth configuration used an 8 1/2 in. (216 mm) bonded length, a 4 in. (102 mm) lead length, and 3 in. (76 mm) cover without transverse stirrups.

Test variables and results are given in Table 2.3.

2.3.1 Cracking Patterns

Specimens were tested in an inverted position, as shown in Fig. 2.6. The observations in this section refer to the specimens, as tested, with the test bar located at the top.

Bar Size Study: These specimens had a 7 1/2 in. (191 mm) bonded length, a 1/2 in. (13 mm) lead length, and 2 in. (51 mm) cover. During the tests, a crack initiated above the test bars at the loaded end and extended through the top cover. For specimens without transverse stirrups (Fig. 2.7a), this crack continued toward the unloaded end, above the test bar, until it reached the end of the bonded length. It then branched out into two arms that extended toward the sides of the specimen. For specimens with transverse stirrups (Fig. 2.7b), cracking began much like the specimens without transverse stirrups, but many more cracks developed near the peak load. These specimens exhibited greater transverse cracking on the top surface above the test bar and around the No. 6 (19 mm) bar flexural reinforcement as concrete near the front face of the specimen moved forward at the time of bond failure; at failure, major cracks began above the flexural reinforcement at the front face and ran back and toward the center of the top surface, meeting above the test bar. These cracks extended farther along the bonded length as relative rib area increased.

On the front face, two cracking patterns were observed for specimens without transverse stirrups. The first, and most common, was a vertical crack above the test bar through the top cover and two cracks forming an inverted V that ran from the test bar down and toward the sides (Fig. 2.7a). In the second pattern, the cracks below the bar started as a single vertical crack and then split into two cracks that ran down and toward the sides (Fig. 2.7c). In addition to these patterns, major cracks developed around the flexural reinforcement at the time of failure in specimens with transverse

stirrups (Fig. 2.7b). These cracks ran nearly vertically up through the top cover and down the front face until they intercepted the sides of the specimen or the reaction plate. Cracks were also observed through the side cover of the flexural reinforcement.

The sides of the specimens without transverse stirrups generally showed very little cracking. As shown in Fig. 2.7b, the specimens with transverse stirrups showed cracks on the sides which began at the front where cracks on the front face had intercepted the sides. The cracks ran up and toward the back of the specimen a short distance then turned vertically and ran up until they intercepted cracks through the side cover of the flexural reinforcement approximately 2 to 3 in. (51 to 76 mm) from the front face.

Rib Width Study: These specimens had a 12 in. (305 mm) bonded length, a 1/2 in. (13 mm) lead length, and 2 in. (51 mm) cover. The crack patterns observed on specimens without transverse stirrups were similar to those described above for the bar size study specimens (Figs. 2.7a and 2.7c). Crack patterns for specimens with transverse stirrups were also similar to those in the bar size study (Fig. 2.7b), but the amount of cracking decreased as the ratio of rib width to center-to-center spacing increased.

Threaded Bar Study: The specimens with a 12 in. (305 mm) bonded length, a 1/2 in. (13 mm) lead length, and 2 in. (51 mm) cover, with and without transverse stirrups, exhibited cracking patterns similar to those described for the bar size study specimens. The crack patterns for specimens with a 12 in. (305 mm) bonded length, a 1/2 in. (13 mm) lead length, and 3 in. (76 mm) cover differed from the 2 in. (51 mm) cover specimens only on the front face, where all of the specimens with the larger cover cracked vertically above and below the test bar (Fig. 2.7c); the crack below the test bar extended a short distance before branching out into two cracks which ran

down and toward the sides of the specimen. In contrast to all other crack patterns described, the specimens with an 8 1/2 in. (216 mm) bonded length, a 4 in. (102 mm) lead length, and 3 in. (76 mm) cover cracked horizontally across the test bar and flexural reinforcement, as shown in Fig. 2.7d. This crack extended to the back of the bonded length where it slanted upward and intercepted the top of the specimen.

2.3.2 Condition of Concrete Between Ribs

After testing, the concrete cover was removed to allow reuse of the test bars and to observe the condition of the concrete between the ribs. The observations that follow are mainly for the concrete below the test bars because the concrete above the bars was damaged in the removal process. It should also be noted that these observations describe the condition of the concrete after failure and not at the peak load.

Three conditions were observed for the concrete between the ribs:

1. *intact* - Concrete between the ribs showed very few signs of damage, appeared as if the bar had been removed cleanly, and remained attached to the surrounding concrete.
2. *crushed* - Concrete in contact with the loaded face of the ribs appeared to be crushed. Often, small pieces of concrete remained on the bar after it was removed.
3. *sheared* - Concrete between the ribs appeared to be sheared off along the outside perimeter of the ribs. This concrete often remained attached to the bar after the bar was removed. This condition may be the result of rapid loading of the concrete at the unloaded end of the bar as the specimen fails.

Individual specimens often exhibited more than one of these conditions, depending on the location along the bonded length.

Bar Size Study: For specimens without transverse stirrups and a relative rib area of 0.05, crushing was observed along the entire bonded length. As the relative rib area increased to 0.10, crushing was observed near the loaded end, but shearing occurred near the unloaded end of the bonded length. At a relative rib area of 0.20, the concrete along most of the bonded length was sheared, with a few specimens showing crushing very near the loaded end. In general, the 5/8 in. (16 mm) diameter bars showed slightly more shearing than the 1 in. (25 mm) diameter bars with relative rib areas of 0.10 and 0.20.

For specimens with transverse stirrups, the concrete at the loaded end was intact because the front face of the specimen pulled out. The end of the region along the bonded length where the concrete remained intact corresponded to the point where cracks that began on the front face above the No. 6 (19 mm) bars met above the test bar (see Fig. 2.7b). This intact concrete extended approximately 3 1/2 in. (89 mm) along the bonded length for bars with a relative rib area of 0.05. This length increased as the relative rib area increased to include most of the bonded length at a relative rib area of 0.20, indicating that bond failure of the No. 6 (19 mm) bar flexural reinforcement may have occurred prior to reaching the full bond strength of these bars. The rest of the bonded length, for both bar sizes, showed crushing and shearing for relative rib areas of 0.05 and 0.20, respectively. For a relative rib area of 0.10, the rest of the bonded length showed crushing and shearing for the 1 and 5/8 in. (25 and 16 mm) bars, respectively.

Rib Width Study: These specimens showed conditions similar to the bar size study specimens described above, except that the amount of shearing increased as the

ratio of rib width to center-to-center spacing, W_r, increased. The relationship between shearing and W_r was most evident for the specimens with transverse stirrups. As mentioned previously, the amount of cracking also decreased as W_r increased, possibly due to more shearing of the concrete.

Threaded Bar Study: The specimens with 2 in. (51 mm) cover, both with and without transverse stirrups, showed shearing on approximately half of the bonded length at the unloaded end. The concrete on the remainder of the bonded length was intact. The specimens with a 12 in. (305 mm) bonded length, a 1/2 in. (13 mm) lead length, and 3 in. (76 mm) cover displayed a sheared condition on all but about 2 in. (51 mm) near the loaded end, while the specimens with an 8 1/2 in. (216 mm) bonded length, a 4 in. (102 mm) lead length, and 3 in. (76 mm) cover were sheared along the entire bonded length.

In general, the nature of the failure adjacent to the bars appears to be primarily dependent on relative rib area. The lower relative rib area bars generally show crushing near the unloaded end of the bar. These bars have less bearing area to transfer force from the bar to the concrete, resulting in higher bearing stresses and increasing the likelihood of crushing the concrete near the ribs. As relative rib area increases, shearing near the unloaded end begins to dominate. The shearing failure may be caused by rapid loading of the concrete near the unloaded end of the bar after the specimen fails. For high relative rib area bars, more of the force in the bar is transferred to the concrete near the loaded end than for lower relative rib area bars. When bond failure begins near the loaded end, the increase in bond stresses at the unloaded end would be greater for higher relative rib area bars. When the ratio of rib width to center-to-center spacing is increased, less concrete is available to resist this rapid increase in load and shearing becomes more dominant.

2.3.3 Load-Slip Response

To compare the load-slip response of the bars with different deformation patterns, the load versus loaded and unloaded end slip curves for replicates of each combination of test variables were averaged. The load-loaded end slip curves shown in Figs. 2.8a to 2.8o and the load-unloaded end slip curves shown in Figs. 2.9a to 2.9o represent the average of two specimens, except the curves for the rib width study specimens with transverse stirrups and the threaded bar study specimens, which represent the average of three specimens. Individual load versus loaded end slip curves for specimens with transverse reinforcement show that, at failure, the load drops steeply with little increase in slip. This is due to the front face of the specimen, from which the loaded end slip is measured, moving with the bar. This steep drop in load makes the average curves irrelevant after the peak load. For this reason, the load versus loaded end slip curves for specimens with transverse stirrups are truncated after one specimen fails.

For specimens without transverse stirrups, the load-loaded end slip and load-unloaded end slip curves (see Figs. 2.8f and Figs. 2.9f, respectively, for typical curves) initially rise very steeply and then flatten out near the peak load. As shown in Figs. 2.9k to 2.9n, this description also applies to the load-unloaded end slip curves for specimens with transverse stirrups, except for specimens with 12 in. (305 mm) bonded lengths where the curves reach a plateau at around 30 kips (133 kN) and then rise again after significant slip. Load-loaded end slip curves for specimens with transverse stirrups generally drop off quickly soon after the curves begin to flatten out. As expected, the load-unloaded end slip curves are initially much steeper than the load-loaded end slip curves due to the greater slip and elastic deformation of the bar at the loaded end.

Bar Size Study: Average load versus loaded and unloaded end slip curves for the bar size study specimens are presented in Figs. 2.8a to 2.8f and 2.9a to 2.9f, respectively. The load-loaded end slip curves show a significant amount of scatter and no definite trends can be observed, except that the initial stiffness of the load-loaded end slip curves for the 1 in. (25 mm) bars (Figs. 2.8d to 2.8f) is higher than that of the 5/8 in. (16 mm) bars (Figs. 2.8a to 2.8c).

The load-unloaded end slip curves are much more consistent than the load-loaded end slip curves. Unlike the loaded end slip curves, the load-unloaded end slip curves for the 5/8 in. (16 mm) bars (Figs. 2.9a to 2.9c) have about the same initial stiffness as the 1 in. (25 mm) bars (Figs. 2.9d to 2.9f). This may be due in part to larger strains in the bars with a smaller cross-sectional area, which would affect the loaded end slip, but not the unloaded end slip. The load-unloaded end slip curves for bars with the same relative rib area are very similar, regardless of rib height. Bars with relative rib areas of 0.10 and 0.20 produce curves that remain linear up to higher loads and have a much sharper transition after the linear portion than bars with a relative rib area of 0.05, which produce a more rounded curve. For specimens without transverse stirrups, the load-unloaded end slip curves differ mainly in the portion of the curve prior to the peak load, because the peak load is nearly the same for all values of relative rib area. For specimens with transverse stirrups, the load-unloaded end slip curves continue to differ throughout most of the curve, because bond strength increases as relative rib area increases.

Rib Width Study: Average load versus loaded and unloaded end slip curves for the specimens used to investigate the effects of rib width to center-to-center spacing ratio are presented in Figs. 2.8g to 2.8j and 2.9g to 2.9j, respectively. As seen in the bar size study specimens, the initial stiffness of the load-unloaded end slip

curves is independent of the presence of transverse stirrups. The load-loaded end slip curves appear to be initially stiffer for the specimens without transverse stirrups. The load-slip curves also show that for bars with the same rib height and spacing, the initial stiffness is not affected by the ratio of rib width to center-to-center rib spacing, W_r. However, near the peak load, the curves for some bars with high values of W_r differ from the curves for bars with lower values of W_r due to the effect of W_r on bond strength, a point which will be discussed in section 2.3.5.

Four deformation patterns (M11-8, M12-8, M31-8 and M32-8) were used in both the bar size and reduced clear space studies, but with bonded lengths of 7 1/2 and 12 in. (191 and 305 mm), respectively, for the two studies. Load versus loaded and unloaded end slip curves for these specimens are compared in Figs. 2.8k to 2.8n and 2.9k to 2.9n, respectively. The load-loaded end slip curves do not show any definite trends regarding the effect of bonded length on the initial stiffness of the curves. However, a comparison of the load-unloaded end slip curves for the two bonded lengths shows that the initial stiffness is higher for the specimens with a longer bonded length, and both sets of curves show that, as would be expected, specimens with longer bonded lengths produce higher peak loads.

Threaded Bar Study: The load versus loaded and unloaded end slip curves for the specimens used to evaluate the threaded bars are shown in Figs. 2.8o and 2.9o, respectively. The initial stiffness of the load-unloaded end slip curves is very similar for all specimen configurations. The load-loaded end slip curve for specimens with an 8 1/2 in. (216 mm) bonded length, a 4 in. (102 mm) lead length, and 3 in. (76 mm) cover are initially slightly stiffer compared to the rest of the configurations. The stiffness of the load-loaded end slip curve for the specimen with an 8 1/2 in. (216 mm) bonded length, and a 4 in. (102 mm) lead length increases slightly above about

25 kips (11.1 kN). This may be due to movement of part of the front face of the specimen as the load increases. The load-unloaded end slip curve for this configuration reached a plateau at about 36 kips (16.0 kN) and began to rise again after significant slip had occurred. The curves for the specimens with 2 in. (51 mm) cover are similar to those for bars with a relative rib area of 0.20 tested with the same configuration as part of the reduced clear space study.

2.3.4 Load-Crack Width Response

Average load versus crack width curves for replicates of the same combinations of test variables are shown in Figs. 2.10a to 2.10o. As would be expected, these curves are very stiff at low loads, before bond cracks have initiated. Near the peak load, the curves begin to flatten out.

Crack widths measured just prior to and at failure, along with the corresponding loads, are given in Table 2.3 for each specimen. Crack widths just prior to failure are the measurements recorded during the cycle of readings immediately before the cycle that produced the peak load. Crack widths at failure are the measurements recorded during the cycle of readings that produced the peak load. The average difference in loads corresponding to these two crack widths is just 0.02 kips (0.09 kN), with a maximum of 0.26 kips (1.16 kN). The crack widths just prior to the peak load (referred to as "crack width before failure") represent the maximum crack width prior to unstable crack growth as the specimen fails and are used in the observations that follow. Also included in Table 2.3 are the crack widths after completion of the test (referred to as "crack width after failure"), which are the final measurements recorded, after the load had returned to zero.

Bar Size Study: Average load versus crack width curves for the bar size study specimens are presented in Figs. 2.10a to 2.10f. The initial stiffness of these curves is approximately the same for all combinations of test variables. The onset of rapid crack growth occurs at a higher load for specimens with stirrups than for specimens without stirrups, indicating that the stirrups help to restrain crack growth. The load-crack width curves for the 5/8 in. (16 mm) bars specimens without transverse stirrups (Figs. 2.10a to 2.10c) are very similar, except in the region immediately after crack growth begins where crack width increases as relative rib area increases. This trend also appears in the curves for the 5/8 in. (16 mm) bars specimens with transverse stirrups, but does not appear in the curves for 1 in. (25 mm) bar specimens (Figs. 2.10d to 2.10f).

Crack widths before and after failure for the bar size study specimens are plotted versus rib height in Figs. 2.11 and 2.12. As shown in Figs 2.11a and 2.11b, for specimens without and with transverse stirrups, respectively, crack widths before failure do not increase as rib height increases. This observation is important because rib height may need to be increased slightly for high relative rib area production bars. The results for these specimens indicate that, prior to failure, this increase in rib height will not result in larger cracks in the member. Figs. 2.12a and 2.12b, for specimens without and with transverse stirrups, respectively, show that crack widths after failure increase as rib height increases in specimens without transverse stirrups, but remain fairly constant as rib height increases in specimens with transverse stirrups.

Crack widths before and after failure are plotted versus relative rib area in Figs. 2.13 and 2.14, respectively. These figures show that crack widths before failure (Figs. 2.13a and 2.13b for specimens without and with transverse stirrups,

respectively) increase as relative rib area increases. For specimens without transverse stirrups, crack widths before failure average 2.99, 4.95, and 7.30 mils (0.076, 0.126, and 0.185 mm) for relative rib areas of 0.05, 0.10, and 0.20, respectively. For specimens with transverse stirrups, crack widths before failure are more than twice as large as for specimens without transverse stirrups and average 9.41, 10.93, and 15.97 mils (0.239, 0.278, and 0.406 mm) for relative rib areas of 0.05, 0.10, and 0.20, respectively. One specimen without transverse stirrups (labeled 6M31-5N) and two specimens with transverse stirrups (labeled 7M21-5S and 9M21-5S) produced unusually large crack widths before failure. These three specimens contained bars with relative rib areas of 0.20. If the crack widths for these three specimens are removed from the data, the average crack widths before failure for $R_r = 0.20$ drop to 6.60 and 11.27 mils (0.168 and 0.286 mm) for specimens without and with transverse stirrups, respectively, but are still slightly higher than the averages for $R_r = 0.10$. Crack widths after failure (Figs. 2.14a and 2.14b, respectively) are larger at relative rib areas of 0.10 and 0.20 than at 0.05. For specimens without transverse stirrups, crack widths after failure average 0.082, 0.122, and 0.111 in. (2.08, 3.10, and 2.82 mm) for relative rib areas of 0.05, 0.10, and 0.20, respectively. For specimens with transverse stirrups, crack widths after failure average 0.131, 0.179, and 0.181 in. (3.33, 4.55, and 4.60 mm) for relative rib areas of 0.05, 0.10, and 0.20, respectively. These results indicate that an increase in relative rib area produces an increase in the wedging action of the bar on the concrete. This increase in wedging action produces more splitting of the concrete, resulting in larger crack widths as relative rib area increases. The effects of the increase in splitting on bond strength will be discussed in section 2.3.5.

Rib Width Study: Average load versus crack width curves are presented in Figs. 2.10g-2.10j for the specimens used in the rib width study. These figures show that the cracking response is not affected by the ratio of rib width to center-to-center spacing, W_r, until near the peak load, where the crack width at failure increases as W_r decreases. This lower crack width is due to the increase in shearing of the concrete between the ribs as W_r is increased, resulting in less splitting force as the specimen fails.

Comparing the load versus crack width curves for deformation patterns that were used in both the bar size and reduced clear spacing studies (Figs. 2.10k to 2.10n) shows that rapid crack growth begins at lower loads in the specimens with the 7 1/2 in. (191 mm) bonded length. Also, the increase in load following the onset of rapid crack growth is larger in the specimens with the 12 in. (305 mm) bonded length.

Threaded Bar Study: The average load versus crack width curves for the specimens used to evaluate the threaded bars are shown in Fig. 2.10o. The specimens with a bonded length of 8 1/2 in. (216 mm) are not shown because the major splitting cracks formed horizontally and were not detected by the assembly used to measure crack widths. The curve shown for specimens with a 12 in. (305 mm) bonded length and 2 in. (51 mm) cover without transverse stirrups is the average of only two specimens, because the third specimen also developed a horizontal splitting crack. The load-crack width response of the specimens with a 12 in. (305 mm) bonded length, both with and without transverse stirrups, was very similar to the response of specimens tested for the reduced clear space study with a relative rib area of 0.20 and the same bonded length

2.3.5 Bond Strength

The bond strengths obtained for each test specimen and the average bond strengths for groups of similar specimens are presented in Table 2.3. Because concrete strengths range from 4760 to 5440 psi (32.8 to 37.5 MPa), the bond strengths are modified so that the tests can be compared on an equitable basis. The modified bond strengths normalized to a concrete compressive strength of 5000 psi (34.5 MPa) are obtained by multiplying the experimental strength by $(5000/f'_c)^{1/4}$ and are also given in Table 2.3. The modification is based on the assumption that bond strength is proportional to the 1/4 power of the concrete strength which has been shown by Darwin et. al. (1995a, 1996a) to represent the effect of concrete strength better than the 1/2 power which has traditionally been used.

Bar Size Study: The modified bond strengths obtained for the bar size study specimens are plotted versus relative rib area in Figs. 2.15a and 2.15b, where each data point represents the average of two tests. For specimens without transverse stirrups (Fig. 2.15a), the bond strengths for each bar size are independent of the relative rib area, but, as expected, are higher for the larger bars. The 1 in. (25 mm) bars produce average bond strengths of 19.11, 19.62 and 19.80 kips (85.0, 87.3 and 88.1 kN), while the 5/8 in. (16 mm) bars produce strengths of 17.30, 17.49 and 17.55 kips (77.0, 77.8 and 78.1 kN) for relative rib areas of 0.05, 0.10 and 0.20, respectively. Considering all relative rib areas, the 1 in. (25 mm) bars produce an average bond strength of 19.51 kips (86.8 kN), which was 2.1 kips (9.3 kN) higher than the average for the smaller bars.

Bond strengths in all cases are increased significantly when transverse stirrups are added. Unlike specimens without transverse stirrups, the specimens with transverse stirrups (Fig. 2.15b) show a strong dependence of bond strength on relative

rib area (independent of the combination of rib height and spacing used to obtain it). The 1 in. (25 mm) bars produce average bond strengths of 26.33, 28.40 and 28.97 kips (117.1, 126.3 and 128.9 kN), while the 5/8 in. (16 mm) bars produce strengths of 22.21, 24.89 and 25.77 kips (98.8, 110.7 and 114.6 kN), for relative rib areas of 0.05, 0.10 and 0.20, respectively. Considering all relative rib areas, the 1 in. (25 mm) bars produce an average bond strength that is 3.61 kips (16.1 kN) higher than the average for the smaller bars. The average bond strengths show a larger increase in bond strength as relative rib area increases from 0.05 to 0.10 than from 0.10 to 0.20. This may be because the peak loads for specimens containing bars with a relative rib area of 0.20 are governed by the bond strength of the No. 6 (19 mm) bar flexural reinforcement.

Comparing Figs. 2.15a and 2.15b shows that the increase in bond strength due to the addition of transverse stirrups is also dependent on bar size, with the larger bars gaining more than the smaller bars. In these tests, the 1 in. (25 mm) bars gained an average of 1.54 kips (6.9 kN) more bond strength than the smaller bars due to the addition of transverse stirrups (2.31, 1.38 and 0.94 kips (10.3, 6.1 and 4.2 kN) for relative rib areas of 0.05, 0.10 and 0.20, respectively). These results indicate that increases in both relative rib area and bar size produce more splitting, which is translated into a higher stress in the transverse stirrups and an increase in the clamping force applied to the bar. This additional clamping force results in higher bond strengths as relative rib area and bar size increase.

The effects of bar size and relative rib area on bond strength for the beam-end tests are very similar to those for the splice tests presented in Chapter 3. However, while the beam-end tests show a greater increase in bond strength due to transverse stirrups for bars with relative rib areas below 0.10 than above 0.10, the splice test

results show that the increase remains nearly linear for bars with relative rib areas between 0.065 and 0.140.

Rib Width Study: To investigate the effects of rib width to center-to-center spacing ratio, the bond strength of the deformation pattern with the smallest rib width for each of the four combinations of rib height and center-to-center spacing (patterns M11-8, M12-8, M31-8 and M32-8) is treated as a base strength. The relative effect of increased rib width is obtained by dividing the bond strength for each test by the base strength of the specimen cast in the same group. The ratios of test to base bond strength for each specimen are presented in Table 2.4 and plotted versus the ratio of rib width to center-to-center spacing, W_r, in Figs. 2.16a and 2.16b for specimens without and with transverse stirrups, respectively.

For tests without transverse stirrups, the ratios of test to base bond strength remain scattered about 1.0 except for the two tests with the highest W_r (0.727). These two tests had test to base bond strength ratios of 0.94 and 0.85, while the values for the remaining sixteen tests ranged from 0.93 to 1.13 with an average of 1.00. These results show that, in specimens without transverse stirrups, bond strength begins to be affected when W_r is greater than about 0.67, because there is not enough concrete between the ribs to resist bearing of the ribs.

For tests with transverse stirrups, the decrease in the test to base bond strength ratios begins at lower W_r ratios than for tests without transverse stirrups. For all deformation patterns, the addition of transverse stirrups produces an increase in bond strength (see Table 2.4). The increase in bond strength results in a larger force that must be carried by the concrete between the ribs and, therefore, a greater effect on the ratio of test to base bond strength as W_r increases. As shown in Fig. 2.16b, the tests with transverse stirrups show a very gradual decrease in average test to base bond

strength ratios from 1.00 for $W_r = 0.182$ to 0.974 for $W_r = 0.455$. A much sharper decrease occurs for W_r ratios of 0.564 to 0.727 (average values of 0.923 and 0.835, respectively).

The results of the rib width study indicate that bond strength is not substantially reduced if W_r is less than about 0.67 and 0.45 for specimens without and with transverse stirrups, respectively. This information is important in the design of high relative rib area production bars, because the deformations will probably need to be closer together, along with some increase in rib height, compared to conventional deformation patterns. Because high relative rib area bars will be used in situations both with and without transverse reinforcement, it is suggested that W_r be limited to a maximum value of 0.45 for high relative rib area bars.

Threaded Bar Study: The average modified bond strengths for the threaded bar specimens ($R_r = 0.28$) are plotted versus relative rib area in Figs. 2.17 and 2.18 for specimens without and with transverse reinforcement, respectively. For comparison, the tests using deformation patterns M11-8, M12-8, M31-8, and M32-8, which were part of the reduced clear space study and tests from Darwin and Graham (1993a, 1993b) given in Table 2.5, are also shown. All specimens in these figures were tested with a 12 in. (305 mm) bonded length, 2 in. (51 mm) cover and, when included, four No. 3 (10 mm) transverse stirrups spaced 3 in. (76 mm) on center. The results from Darwin and Graham (1993a, 1993b) represent machined bars with deformation patterns identical to those in Fig. 2.2 and include only those tests that used the same specimen configuration as the current study. Each data point represents the average of three tests.

Fig. 2.17 shows that bond strengths are virtually independent of deformation pattern for specimens without transverse reinforcement. The test results from the

current study are in good agreement with the tests by Darwin and Graham (1993a, 1993b) for the same deformation patterns (R_r = 0.10 and 0.20). Considering all tests, the modified bond strengths decrease slightly and average 30.06, 30.30, 28.97 and 28.58 kips (133.7, 134.8, 128.9 and 127.1 kN) for relative rib areas of 0.05, 0.10, 0.20 and 0.28, respectively.

Bond strengths, however, increase for all deformation patterns when transverse stirrups are included. As shown in Fig. 2.18, the amount of the increase depends on the relative rib area of the bars. The machined bars with relative rib areas of 0.05, 0.10 and 0.20 exhibit average increases in bond strength of 18, 44 and 59 percent, respectively, over strengths obtained without transverse stirrups. This percentage increases to 79 percent for the threaded bars (R_r = 0.28). The average bond strengths for machined bars with R_r = 0.10 and 0.20 tested in the current study are higher (14% and 7%, respectively) than those from Darwin and Graham (1993a, 1993b).

The results for the threaded bars and for the machined bars tested by Darwin and Graham (1993a, 1993b), using an 8 1/2 in. (216 mm) bonded length, a 4 in. (102 mm) lead length, and 3 in. (76 mm) cover, are presented in Fig. 2.19. Darwin and Graham (1993a, 1993b) observed a strong relationship between bond strength and relative rib area if there is added confinement provided by concrete. Their tests show increases in bond strength of 47, 56 and 64 percent for relative rib areas of 0.05, 0.10 and 0.20, respectively, over specimens tested with a 12 in. (305 mm) bonded length, 1/2 in. (13 mm) lead length, and 2 in. (51 mm) cover. This trend does not continue for the threaded bars (R_r = 0.28) for which a similar comparison shows only a 55 percent increase. The smaller increase for the threaded bars is probably due to shearing of the concrete along the entire bonded length, as discussed in section 2.3.2.

The increase in bond strength seen with increased concrete confinement appears to be partly due to increased cover but mostly due to increased lead length. This is illustrated by the results for threaded bars with a 12 in. (305 mm) bonded length, a 1/2 in. (13 mm) lead length, and 3 in. (76 mm) cover. These tests produced an average modified bond strength of 32.68 kips (145.4 kN), which is only 14 percent higher than the specimens with 2 in. (51 mm) cover. When the lead length was increased to 4 in. (102 mm), while maintaining a 12 1/2 in. (318 mm) total embedment and 3 in. (76 mm) cover, bond strength increased 36 percent, indicating that the increase in lead length is primarily responsible for the increase in bond strength.

2.4 Summary and Recommendations

Bar Size Study: The test results for the bar size study specimens show that bond strength increases as bar size increases in specimens with and without transverse stirrups. For specimens without transverse stirrups, bond strength is unaffected by relative rib area, but when transverse stirrups are present, bond strength increases as relative rib area increases. The amount of the increase in bond strength due to transverse stirrups increases with bar size. These conclusions are very similar to the conclusions drawn from an analysis of the effects of bar size and relative rib area on the splice strength of commercially produced conventional and high relative rib area bars presented in Chapter 3. The beam-end tests presented in this chapter show a smaller increase in bond strength above a relative rib area of 0.10 than below 0.10. However, this smaller increase in bond strength above a relative rib area of 0.10 is not seen in the splice test results presented in Chapter 3, where bond strength increases nearly linearly for relative rib areas ranging from 0.065 to 0.140.

The results show that the width of the longitudinal splitting crack that accompanies bar slip is not affected by rib height prior to specimen failure. Therefore, rib heights for commercially produced high relative rib area bars do not need to be limited due to concerns about increased crack widths in reinforced concrete members. However, crack widths do increase as relative rib area increases. The increase in crack width is due to the greater wedging action provided by bars with higher relative rib areas, resulting in more splitting of the concrete. This increase in wedging action causes no reduction in the bond strength of bars not confined by transverse stirrups and results in an increase in bond strength for bars that are confined by transverse stirrups.

Rib Width Study: The results of the rib width study indicate that bond strength decreases when the ratio of rib width to center-to-center rib spacing, W_r, is greater than about 0.45 for specimens with transverse stirrups, and about 0.66 for specimens without transverse stirrups. Therefore, in the design of commercially produced high relative rib area bars, rib widths should be limited to no greater than 45% of the center-to-center rib spacing.

Threaded Bar Study: The results of the threaded bar study show that bond strength is unaffected by relative rib area in specimens with 2 in. (51 mm) cover and no transverse stirrups, but continues to increase as relative rib area increases, even up to relative rib areas as high as 0.28, when transverse stirrups are present. Similar results are seen in the splice tests using these bars that are presented in Chapter 4.

CHAPTER 3: SPLICE TESTS

3.1 General

This chapter describes the testing and analysis of splice specimens containing No. 5 and No. 11 (16 and 36 mm) conventional and high relative rib area, R_r, commercially produced bars. The results are combined with tests of No. 8 (25 mm) bars previously performed at the University of Kansas including conventional and high relative rib area bar splice tests reported by Idun and Darwin (1995) and conventional bar splice tests reported by Hester, Salamizavaregh, Darwin and McCabe (1991, 1993). The tests are analyzed to determine the effects of bar size and relative rib area on splice strength. The results of this analysis were used by Darwin, Zuo, Tholen and Idun (1995a, 1996a) to develop a best-fit equation for splice strength using a large data base of splice and development strength test results gathered from the literature and tested across North America. Finally, a reliability-based strength reduction factor developed by Darwin, Idun, Zuo and Tholen (1995b) is applied to the best-fit equation to arrive at a design equation that is applicable to splice and development lengths.

3.2 Experimental Program

A total of 30 splice specimens, cast in 7 groups, numbered 12 through 18, were tested. Each group contained four or six specimens. The main test parameters were bar size, relative rib area, epoxy-coating, and the degree of confinement provided by transverse reinforcement. The specimens included twelve No. 5 (16 mm) and eighteen No. 11 (36 mm) bar tests. The No. 5 (16 mm) bar specimens included two matched pairs of coated and uncoated high relative rib area bar tests without transverse reinforcement and four matched pairs of conventional and high relative rib

area uncoated bar tests with transverse reinforcement. The No. 11 (36 mm) bar tests included twelve specimens with high relative rib area bars; two coated and two uncoated without transverse reinforcement, and eight with transverse reinforcement of which one specimen contained coated bars. The remaining six specimens contained conventional No. 11 (36 mm) bars with transverse reinforcement.

3.2.1 Test Specimens

The specimens used in this study were 13 or 16 ft (4 or 4.9 m) long beams with nominal depths of 15.5 to 16 in. (394 to 406 mm) and nominal widths of 12 or 18 in. (305 or 457 mm). The specimens were tested as simply supported beams with cantilevered ends, as shown in Fig. 3.1, with the splices located at the center of a 4 or 6 ft (1.2 or 1.8 m) long constant moment region. All test bars were bottom-cast and lap spliced at the center of the beam. No. 5 (16 mm) bar splice lengths ranged from 10 to 17 in. (254 to 432 mm) with side covers of 1.5 to 2 in. (38 to 51 mm) and 1.25 in. (32 mm) bottom cover. No. 11 (36 mm) bar splice lengths ranged from 27 to 40 in. (686 to 1016 mm) with side covers of 1.5 to 3 in. (38 to 76 mm) and 2 in. (51 mm) bottom cover. Maximum splice lengths of 17 or 40 in. (432 and 1016 mm) were used for specimens tested with a 4 or 6 ft (1.2 or 1.8 m) constant moment region, respectively, so that the ends of the splices would be at least the depth of the member from a support. No. 3 or No. 4 (9.5 or 13 mm) closed stirrups were used within the splice length for specimens with transverse reinforcement. Additional No. 3 (9.5 mm) stirrups were included in the cantilevered ends to provide shear strength. Continuous No. 4 and No. 6 (13 and 19 mm) bars were used as top reinforcement for specimens containing No. 5 and No. 11 (16 and 36 mm) test bars, respectively. Actual member dimensions are given in Table 3.1.

3.2.2 Materials

Reinforcing Steel: All bars met the requirements of ASTM A 615 except that some of the experimental bars did not contain bar markings. Three conventional and two experimental deformation patterns were tested and are shown in Fig. 3.2. Relative rib areas were measured according to the procedure described in Appendix A. The conventional bars had relative rib areas ranging from 0.070 to 0.082 and included one No. 5 (16 mm) bar designated 5N0 (R_r = 0.082) and two No. 11 (36 mm) bars designated 11B0 and 11N0 (R_r = 0.070 and 0.072, respectively). The experimental No. 5 and No. 11 (16 and 36 mm) bars were designated 5C2 (R_r = 0.109) and 11F3 (R_r = 0.127), respectively. (Note: The first number in the designation indicates bar size, the letter indicates the manufacturer, and the final number is 0 for conventional patterns and non-zero for experimental patterns). All bars with the same designation, including the epoxy-coated bars, were made from a single heat of steel. Test bar properties are given in Table 3.2. The yield strengths reported were determined from tests of three samples of each bar designation. Conventional ASTM Grade 60 bars were used for transverse and top reinforcement.

Epoxy Coating: Only the experimental deformation patterns were tested with epoxy coating. The 5C2 and 11F3 bars were coated by ABC Coating Company, Inc. and Florida Steel Corporation, respectively. The average coating thicknesses for all 5C2 and 11F3 bars tested were 9.9 and 6.3 mils (0.16 and 0.25 mm), respectively.

Coating thickness was measured using a magnetic pull-off gage (Mikrotest III Thickness Gage). Measurements were made at the top of the longitudinal ribs because the small rib spacing of the new deformation patterns made it impossible to measure coating thickness between the transverse ribs where it is traditionally measured. Readings were taken at 10 points within the splice length on both

longitudinal ribs. The coating thicknesses reported in Table 3.2 are average values for all bars tested.

Tan, Darwin, Tholen and Zuo (1996) compared the measured thickness of epoxy coating obtained using this method to that obtained using the method specified in ASTM A 775. Four No. 8 (25 mm) conventional bars were measured using both methods. The overall average coating thicknesses for the ASTM method and the method used in the current study were 7.7 and 8.8 mils (0.20 and 0.22 mm), respectively, with standard deviations of 0.132 and 0.183 mils (0.0034 and 0.0046 mm).

Concrete: Air-entrained concrete was supplied by a local ready-mix plant and contained Type I portland cement, Kansas River sand and 3/4 in. (19 mm) maximum nominal size crushed limestone coarse aggregate. Two mix designs were used; one with a 0.44 water-cement ratio and the other with a 0.36 water-cement ratio and a water reducing admixture to increase workability. Concrete strengths ranged from 4110 to 5250 psi (28 to 36 MPa) at test ages of 6 to 30 days. Mix proportions and concrete properties are given in Table 3.3.

3.2.3 Specimen Fabrication

Formwork: Forms were made from 3/4 in. (19 mm) plywood, 2 × 4 studs, and all-thread rods. The plywood (DriForm 90 No-Oil panels made by Champion International Corporation) was manufactured with a polymeric resin coating that did not require the use of a release agent. All-thread rods were used to hold the forms together. Some of these rods extended through the inside of the forms and were used to hold the reinforcing steel cages in place during casting. Joints in the forms were sealed with flexible caulk or modeling clay to prevent leakage.

Reinforcing Steel Cages: Reinforcing steel cages were assembled in the forms and held together using wire ties. The cages consisted of top and bottom longitudinal reinforcement and transverse stirrups. The bottom bars were two to four No. 5 or No. 11 (16 or 36 mm) test bars spliced at the center of the beam (Fig. 3.3). Four to six wire ties were used to hold the spliced bars in contact. To prevent interlocking of the ribs, spliced bars were positioned so that the longitudinal ribs on one bar were horizontal while the longitudinal ribs on the other bar were vertical. Bar markings were not included within the splice length. The test bars were cleaned with acetone to remove debris once before placing the bars in the forms and again just prior to casting. Two continuous No. 4 and No. 6 (13 and 19 mm) conventional bars were used as top reinforcement for specimens with No. 5 and No. 11 (16 and 36 mm) test bars, respectively. No. 3 (9.5 mm) stirrups were provided outside the constant moment region to prevent shear failure. For splices with transverse reinforcement, No. 3 or No. 4 (9.5 or 13 mm) closed stirrups were equally spaced within the splice length and had the same surface condition (coated or uncoated) as the spliced bars. Transverse No. 8 (25 mm) bars located 4 ft (1.2 m) from the center of the beam were used as lifting bars.

Bottom cover was controlled by supporting the test bars on steel chairs. Side cover was controlled by tying the top and bottom reinforcement to the all-thread rods which extended through the inside of the forms. No chairs or rods were located within 6 in. (152 mm) of the ends of the splice. Covers and bar spacings were measured after the forms had been moved to the casting position and are given in Table 3.1.

Placement and Curing Procedure: Each group of specimens was cast from a single batch of concrete. Concrete was placed in two lifts, each approximately one-

half the depth of the specimen. In the first lift, concrete was placed first in the shear region of all specimens followed by the constant moment region. In the second lift, the placement order was reversed so that the constant moment region of all beams was placed first followed by the shear regions. This placement procedure was followed to ensure that the concrete in the splice region was as uniform as possible between specimens in a group. Each lift was vibrated with a 1 1/2 in. (38 mm) square internal vibrator on alternate sides of the beam at 1 ft (0.3 m) intervals.

After initial set of the concrete, the top surface of the beams was covered with wet burlap and plastic. The burlap was kept wet until the forms were stripped when the concrete strength had reached at least 3000 psi (21 MPa). The beams were then left to cure in air until the concrete reached test strength.

Standard 6 × 12 in. (152 × 305 mm) cylinders were cast in steel molds and cured in the same manner as the test specimens. The concrete strength reported is the average of three or more cylinders tested immediately following completion of all splice tests in a group. All specimens were tested in a single day.

3.2.4 Test Procedure

The specimens were inverted from the casting position and tested as simply supported beams (Fig. 3.1). The beams were supported by pin and roller supports mounted on concrete pedestals. Steel plates, attached to the specimen with a thin layer of high strength gypsum cement (Hydrostone), separated the beam from the supports. Downward loads were applied 6 in. (305 mm) from each end to produce a constant moment region between the supports. Load was applied at each end using two 60-ton hollow-core hydraulic jacks powered by an Amsler hydraulic testing machine. Two 1 1/2 in. (38 mm) diameter steel rods were used to transfer the force

from the jacks to a steel spreader beam mounted across the end of the specimen. The rods were attached to the spreader beam with semi-cylindrical rollers to keep the applied load vertical as the ends of the specimen rotated. The specimens were loaded continuously to failure at about 3 kips (13 kN) per minute at each end.

Spring-loaded linear variable differential transformers (LVDTs) bearing against the bottom of the beam were used to measure deflections at each load point and at the middle of the beam. Load on the beam was measured from each of the four load rods that were instrumented as load cells using four strain gages in a full bridge configuration. Load cell and LVDT readings were acquired using a Hewlett-Packard data acquisition system controlled by a computer and stored on the computer's hard disk.

Following completion of the tests, the concrete cover around the splices was removed so that the concrete-steel interface could be observed.

3.3 Results and Observations

Load-deflection curves for the 30 splice test specimens are shown in Figs. 3.4a-g where the beam deflection is the sum of the average deflection at the load points and the deflection at the middle of the beam.

Beams without transverse stirrups in the splice region failed suddenly soon after reaching the peak load. Beams with stirrups typically exhibited a slight drop in load carrying capacity after reaching the peak load followed by sudden splice failure.

Typical beams after splice failure are shown in Fig. 3.5. The first cracks to form were flexure cracks on the tension face of the specimen in the constant moment region. As the load was increased, dominant flexure cracks formed at both ends of the splice and extended across the width of the beam. Longitudinal cracks began to

form in the splice region near the ultimate load. These cracks ran along the length of the splice above the spliced bars and also formed on the sides of the specimen near the level of the splices.

Loads, moments, and bar stresses at splice failure are given in Table 3.1. In all ten matched pairs of beams with conventional and high relative rib area bars tested with transverse reinforcement, the high R_r bars produced a higher bar stress at splice failure. The difference in stress was greater for the No. 11 (36 mm) bars than for the No. 5 (16 mm) bars. The five specimens tested with epoxy-coated bars produced lower stresses at splice failure than the corresponding specimen with uncoated bars.

Concrete damage at the concrete-steel interface was more extensive near the discontinuous end of the spliced bars for specimens with uncoated bars. For conventional bars, the concrete near the loaded face of the ribs showed progressively more crushing from the continuous to the discontinuous end. For high relative rib area bars, the concrete near the discontinuous end appeared to be sheared off between the ribs. In most cases, this concrete remained attached to the bars. Shearing of the concrete between the ribs was most evident for the 11F3 bars tested with transverse reinforcement. Epoxy-coated bars showed little damage to the concrete between the ribs, and the concrete had a smooth, glassy surface.

3.4 Evaluation of Test Results

The evaluations and analyses that follow include the results of the 30 splice tests described in this chapter along with 53 tests reported by Idun and Darwin (1995) and 10 tests reported by Hester et al. (1991, 1993). The tests reported by Idun and Darwin (1995) and Hester et al. (1991, 1993) were performed at the University of Kansas using specimens and procedures very similar to those used for the beams in

the current study. These specimens were cast with concrete using the same materials and similar mix proportions to those used in the current study, with the exception that 16 of the specimens tested by Idun and Darwin (1995) were cast in concrete containing basalt coarse aggregate. The tests reported by Idun and Darwin (1995) were performed using No. 8 (25 mm) conventional and high relative rib area bars (R_r = 0.065-0.085 and 0.101-0.140, respectively) as part of the overall research project on the effect of deformation pattern on bond strength at the University of Kansas. Specimen properties and test results are given in Table 3.4. The splice tests reported by Hester et al. (1991, 1993) used No. 8 (25 mm) conventional bars with relative rib areas ranging from 0.070 to 0.078 and are given in Table 3.5.

The following analyses are based on the assumption that the total force in a bar at splice failure, T_b, can be expressed as the sum of a concrete contribution, T_c, and a transverse steel contribution, T_s.

3.4.1 Uncoated Bars

The evaluation of the test results for the uncoated high relative rib area bars uses an equation for the concrete contribution, T_c, developed from a statistical analysis performed by Darwin et al. (1995a, 1996a) on the results of 133 splice and development tests of bottom-cast bars without transverse reinforcement. This analysis resulted in an equation for T_c that can be expressed as

$$\frac{T_c}{f_c'^{1/4}} = \frac{A_b f_s}{f_c'^{1/4}} = [63\, l_d (c_m + 0.5\, d_b) + 2130\, A_b]\left(0.1\, \frac{c_M}{c_m} + 0.9\right) \qquad (3.1)$$

in which A_b = bar area, $in.^2$

f_s = steel stress at failure, psi

f'_c = concrete compressive strength, psi; $f'^{1/4}_c$, psi

l_d = development or splice length, in.

c_m, c_M = minimum or maximum value of c_s or c_b ($c_M/c_m \leq 3.5$), in.

c_s = $\min(c_{si} + 0.25 \text{ in.}, c_{so})$, in.

c_{si} = one-half of clear spacing between bars, in.

c_{so}, c_b = side cover or bottom cover of reinforcing bars, in.

d_b = bar diameter, in.

Eq. 3.1 produced test/prediction bond strength ratios ranging from 0.72 to 1.29 with an average of 1.00 and coefficient of variation (COV) of 0.107 for the 133 tests used to develop the expression. An important conclusion by Darwin et al. (1995a, 1996a) was that splice and development strength is better represented by the 1/4 power of the concrete compressive strength than by the square root of the strength which has traditionally been used (ACI 318-95).

Splices Without Transverse Reinforcement: Splice strength in beams without transverse reinforcement is unaffected by relative rib area. This can be seen by comparing the test/prediction ratios for the 12 tests of high R_r bars with those of conventional bars. The average test/prediction ratios, based on Eq. 3.1, are 1.02 and 0.93 for the two tests of 5C2 and 11F3 bars performed in this study, respectively. The eight splice tests of high R_r bars reported by Idun and Darwin (1995) produced an average ratio of 1.01, resulting in an average ratio of 1.00 for the twelve high R_r tests without transverse reinforcement. For comparison, an average ratio of 1.02 was obtained from sixteen tests of conventional bars performed at the University of Kansas [one by Idun and Darwin (1995), eight by Choi et al. (1990a, 1991), and seven by Hester et al. (1991, 1993)]. Because the splice strength of bars not confined

by transverse reinforcement is unaffected by relative rib area, the twelve tests of high R_r bars were included in the tests used to develop Eq. 3.1.

Splices With Transverse Reinforcement: To determine the amount of additional bond strength due to transverse steel, T_s, the concrete contribution, T_c (calculated from Eq. 3.1), is subtracted from the experimentally determined total force in the bar, T_b.

T_s, normalized with respect to $f'_c{}^{1/4}$, has been shown by Darwin et al. (1995a, 1996a) to depend primarily on the "effective transverse reinforcement," NA_{tr}/n, in which N = the number of transverse reinforcing bars (stirrups or ties) crossing l_d; A_{tr} = the area of each stirrup or tie crossing the potential plane of splitting adjacent to the reinforcement being developed or spliced, $in.^2$; and n = the number of bars being developed or spliced along the plane of splitting. The value of n is determined by the smaller of c_b or c_s. If c_b controls, the potential plane of splitting passes through the bottom cover and n = 1. If c_s controls, the potential plane of splitting intersects all of the bars and n = the total number of bars being spliced or developed. It is important to note that T_s does not depend on the yield strength of the transverse reinforcement, f_{yt}. This conclusion is supported by experiments showing that transverse reinforcement rarely yields due to a bond failure (Maeda et al. 1991, Sakurada et al. 1993, Azizinamini et al. 1995).

The values of $T_s/f'_c{}^{1/4}$ are plotted versus NA_{tr}/n in Fig. 3.6 for the No. 5, No. 8, and No. 11 (16, 25, and 36 mm) bar specimens tested in concrete containing limestone coarse aggregate. The test results show that $T_s/f'_c{}^{1/4}$ depends primarily on NA_{tr}/n. However, as was seen in the beam-end specimens tested by Darwin and Graham (1993a, 1993b) and those reported in Chapter 2, it is also affected by bar size and relative rib area. The smallest additional bond strength due to transverse

reinforcement was obtained by the conventional No. 5 (16 mm) bars with $R_r = 0.082$, followed by the new No. 5 (16 mm) bars with $R_r = 0.109$, the conventional No. 8 (25 mm) bars with $R_r = 0.065$ to 0.085, the new No. 8 (25 mm) bars with $R_r = 0.101$, the conventional No. 11 (36 mm) bars with $R_r = 0.070$ and 0.072, the new No. 8 (25 mm) bars with $R_r = 0.140$, and finally the new No. 11 (36 mm) bars with $R_r = 0.127$.

The values of $T_s/f'_c{}^{1/4}$ are plotted versus NA_{tr}/n in Fig. 3.7 for the No. 8 (25 mm) bar specimens tested in concrete containing basalt coarse aggregate. These test results also demonstrate that T_s increases as relative rib area increases. Fig. 3.8, which compares test results for No. 8 (25 mm) bars tested in concrete containing limestone and basalt coarse aggregate, shows that concrete properties can have a significant effect on the additional strength due to transverse reinforcement. The basalt coarse aggregate concrete produced substantially higher values of $T_s/f'_c{}^{1/4}$, even though the compressive strengths of the concretes were the same. For this reason the test results are separated based on the type of coarse aggregate used. The higher strengths may be due to the much higher strength of the basalt coarse aggregate.

3.4.2 Epoxy-Coated Bars

Five matched pairs of specimens with coated and uncoated high relative rib area bars were tested in the current study. Two pairs contained 5C2 bars ($R_r = 0.109$) and three pairs contained 11F3 bars ($R_r = 0.127$), one of which had six No. 3 (9.5 mm) stirrups in the splice region. Idun and Darwin (1995) tested five pairs of coated and uncoated bar specimens with relative rib areas ranging from 0.101 to 0.140. All of these specimens had a cover of less than 3 d_b. Bar stresses at failure and ratios of

coated to uncoated bar splice strength, C/U, for the ten pairs of specimens are given in Table 3.6.

In all cases, the coated bar specimens produced lower stresses at failure than the corresponding uncoated bar specimens. However, the C/U ratios produced by these high relative rib area bars were substantially higher than those obtained in previous studies using conventional bars. Treece and Jirsa (1987, 1989) reported an average C/U ratio of 0.66 for 21 tests of coated and uncoated bars. Their results are the basis for the current development length modification factor of 1.5 for bars with cover less than 3 d_b or clear spacing less than 6 d_b (ACI 318-95, AASHTO Highway 1992). A higher ratio, 0.74, was reported by Hester et al. (1991, 1993) based on a data base containing 113 splice tests of conventional bars. The 20 high relative rib area bar tests produced substantially higher C/U ratios, ranging from 0.817 to 0.945, with an overall average of 0.882. These tests indicate that epoxy coating has a less detrimental effect on the splice strength of high relative rib area bars than conventional bars, resulting in a smaller development length modification factor and significant savings in splice length for epoxy-coated bars.

3.5 Application of Test Results to Design

Figs. 3.6 and 3.7 show that the increase in splice strength due to transverse reinforcement, T_s, depends primarily on the effective transverse reinforcement, NA_{tr}/n, but is also affected by bar size and relative rib area. The results shown in these figures were used to develop two terms, t_r and t_d, which reflect the increase in the effectiveness of the transverse reinforcement as relative rib area and bar size increase, respectively.

The analysis is simplified by approximating the best-fit lines for each group of data in Figs. 3.6 and 3.7 with linear functions that have zero intercepts at $NA_{tr}/n = 0$ and cross the best-fit lines at $NA_{tr}/n = 2.0$. These functions take the form

$$\frac{T_s}{f_c'^{1/4}} = \frac{(2m + b)}{2}\frac{NA_{tr}}{n} = M\frac{NA_{tr}}{n} \qquad (3.2)$$

where m and b are the slope and intercept, respectively, of the best-fit expression and M is the modified slope of the approximate expression. This approximation has the advantage of allowing the relationship between $T_s/f'_c{}^{1/4}$ and NA_{tr}/n to be expressed by a single value, M, which represents the combined effects of relative rib area and bar size. The modified expressions (Eq. 3.2) will be conservative for groups of data with a positive intercept, which is the case for all but one of the high relative rib area bars. Values of m, b, and M are given in Table 3.7 for each group of data.

3.5.1 Effect of Relative Rib Area

To determine the effect of relative rib area on T_s, it is first assumed that changes in T_s due to R_r are independent of bar size and concrete properties. The values of M obtained from Eq. 3.2 are plotted versus R_r in Fig. 3.9 for the data in Figs. 3.6 and 3.7. For the conventional No. 8 and No. 11 (25 and 36 mm) bars, the value of R_r represents a weighted average because a range of values was used in these tests.

For each group of data, based on bar size and concrete type, a best-fit expression for M versus R_r was obtained. This expression was used to determine the value of M at $R_r = 0.075$, midway in the range of conventional bars tested. The values of M were then normalized with respect to M at $R_r = 0.075$ to obtain the factor

$t_r = M/M_{R_r=0.075}$ which represents the relative change in slope of the modified expression due to R_r.

The individual values of t_r, obtained from $M/M_{R_r=0.075}$, are plotted versus R_r in Fig. 3.10. Each data point is weighted based on the number of tests it represents. These values were used to obtain a best-fit expression for t_r as a function of R_r, which was found to be

$$t_r = 9.6\, R_r + 0.28 \tag{3.3}$$

with a coefficient of determination, $r^2 = 0.966$. The strongly linear relationship between t_r and R_r supports the initial assumption that changes in T_s due to R_r are independent of bar size and concrete properties.

3.5.2 Effect of Bar Size

The effect of bar size on T_s was determined by first dividing the values of M, obtained from Eq. 3.2, by the value of t_r from Eq. 3.3. This removes the effect of relative rib area from M and converts the original values of M to values corresponding to bars with $R_r = 0.075$. The values of M/t_r are plotted versus d_b in Fig. 3.11 for specimens cast in concrete containing limestone coarse aggregate. A best-fit analysis was performed to obtain the expression

$$\frac{M}{t_r} = 1189\, d_b + 457 \tag{3.4}$$

with $r^2 = 0.974$.

Assuming that this relationship can be generalized for other concretes, the expression was normalized with respect to M/t_r for $d_b = 1$. The resulting expression represents the effect bar size on T_s and becomes

$$t_d = 0.72\, d_b + 0.28 \tag{3.5}$$

The analysis results in a new expression for the effective transverse reinforcement that includes the effects of bar size and relative rib area on T_s.

$$t_r t_d \frac{NA_{tr}}{n} = (9.6\, R_r + 0.28)(0.72\, d_b + 0.28) \frac{NA_{tr}}{n} \tag{3.6}$$

The values of M, $M_{R_r=0.075}$, t_r, and M/t_r used to develop Eqs. 3.3 - 3.6 are given in Table 3.7.

3.5.3 Increase in Splice Strength

The new expression for the effective transverse reinforcement (Eq. 3.6) and the equation for the concrete contribution (Eq. 3.1) were used by Darwin et al. (1995a, 1996a) in a statistical analysis of 166 splice and development tests containing transverse reinforcement. The best-fit expression obtained for the steel contribution was

$$\frac{T_s}{f_c'^{1/4}} = 2226\,(9.6\, R_r + 0.28)(0.72\, d_b + 0.28) \frac{NA_{tr}}{n} + 66 \tag{3.7a}$$

$$\frac{T_s}{f_c'^{1/4}} = 2226\, t_r\, t_d \frac{NA_{tr}}{n} + 66 \tag{3.7b}$$

with $r^2 = 0.856$. This expression, combined with Eq. 3.1, produced an average test/prediction ratio of 1.01 and a COV of 0.125 for the specimens used to develop the equation.

The average value of R_r for conventional bars was found to be 0.0727 by Darwin et al. (1995a, 1996a). This value was obtained from samples of bars produced by six steel mills, for bar sizes No. 5, No. 6, No. 8, and No. 11, and metric bar sizes No. 20, No. 25, No. 30, and No. 35. Substituting $R_r = 0.0727$ and dropping the final term (66), Eq. 3.7a for conventional bars becomes

$$\frac{T_s}{f_c'^{1/4}} = 2175\,(0.72\,d_b + 0.28)\,\frac{NA_{tr}}{n} \tag{3.8}$$

Eq. 3.7a for high relative rib area bars depends on the value of R_r selected. The bars produced for the overall research project at the University of Kansas have shown that bars with relative rib areas of at least 0.14 can be manufactured using current technology and production methods. However, a minimum value of 0.12 seems more reasonable due to the increasing difficulty of producing bars as R_r increases. In addition, a higher average R_r will have to be maintained to insure a minimum value of 0.12. Assuming that the standard deviation of R_r for the new bars will be one-half of that presently obtained for conventional bars, an average R_r of 0.1275 will be necessary to ensure that no more than 5 percent fall below $R_r = 0.12$ (Darwin et al. 1995a, 1996a). Substituting $R_r = 0.1275$ and dropping the final term (66), Eq. 3.7a for high relative rib area bars becomes

$$\frac{T_s}{f_c'^{1/4}} = 3350\,(0.72\,d_b + 0.28)\,\frac{NA_{tr}}{n} \tag{3.9}$$

where $c = (c_m + 0.5\ d_b)(0.1\ c_M/c_m + 0.9)$ and c_m, c_M, c_s, c_{si}, c_{so}, and c_b are defined following Eq. 3.1

$K_{tr} = K_{tr}(\text{conv.}) = 34.5\ t_d\ A_{tr}/sn = 34.5\ (0.72\ d_b + 0.28)\ A_{tr}/sn$ for conventional bars with average $R_r = 0.0727$

$K_{tr} = K_{tr}(\text{new}) = 53\ t_d\ A_{tr}/sn = 53\ (0.72\ d_b + 0.28)\ A_{tr}/sn$ for high relative rib area bars with average $R_r = 0.1275$

This equation can be conservatively simplified by setting $c_M = c_m$ and dropping the 0.25 in. from the definition of c_s following Eq. 3.1. Eq. 3.13 then becomes

$$\frac{l_d}{d_b} = \frac{\dfrac{f_y}{\beta f_c'^{1/4}} - 1900}{72\left(\dfrac{c + K_{tr}}{d_b}\right)} \tag{3.14}$$

where $c = c_m + 0.5\ d_b$ = smaller of the cover to the center of the bar or one-half of the center-to-center bar spacing. The definitions of K_{tr} following Eq. 3.13 remain unchanged.

An analysis by Darwin et al. (1995a, 1996a) showed that test/prediction ratios, using Eq. 3.10 as the predicted strength, were consistently below 1.0 for tests with $(c + K_{tr})/d_b > 4$. This indicates that the bars in these tests were so heavily confined that a pullout failure, rather than a splitting failure, was governing the bond strength. Darwin et al. (1995a, 1996a) also found that especially low strengths were exhibited by specimens with $l_d/d_b < 16$. Therefore, an upper limit of 4 must be placed on $(c + K_{tr})/d_b$ and a lower limit of 16 must be placed on l_d/d_b when Eqs. 3.13 and 3.14 are used in design.

An important benefit of Eqs. 3.13 and 3.14 stems from the fact that 87% of the data used to develop the equations came from splice tests in which all of the bars were spliced at one location. As a result, the equations are already calibrated based on splice strength, removing the need for a separate development length modification factor to calculate the length of most splices. The development tests with $(c + K_{tr})/d_b \leq 4$ used to develop the equations produced an average test/prediction ratio of 1.07, indicating that development and splice strengths are approximately equal. This has also been seen in previous research (Orangun, Jirsa, Breen 1975, 1977). Therefore, Eqs. 3.13 and 3.14 can be applied directly to the calculation of both splice and development lengths.

CHAPTER 4: SPLICE TESTS OF ULTRA-HIGH RELATIVE RIB AREA BARS

4.1 General

This chapter describes the testing and analysis of splice specimens containing No. 8 (25 mm) threaded bars that are commercially available for use as high-strength prestressing bars (Fig. 2.5). Beam-end specimens used to evaluate the bond strength of these bars were described in Chapter 2. The threaded deformation pattern produces a very high relative rib area (R_r = 0.284). These bars do not have a longitudinal rib. This allows the transverse ribs to interlock when spliced bars are tied together. To investigate the effects of rib interlock on splice strength, specimens were tested in which the ribs were allowed to interlock and in which interlock was prevented.

4.2 Experimental Program

A total of 6 splice specimens, cast in groups 3, 4 and 7, were tested. Each group contained 1 to 3 specimens. The main test parameters were rib interlock and the degree of confinement provided by transverse reinforcement. Four of the six specimens contained transverse reinforcement in the splice region. Interlocking of the ribs was prevented in one specimen with and one specimen without transverse reinforcement.

4.2.1 Test Specimens

The specimens used in this study were 16 ft (4.9 m) long beams, similar to the specimens used to evaluate the splice strength of No. 11 (36 mm) bars described in section 3.2.1, with nominal depths of 15.5 to 16 in. (394 to 406 mm) and a nominal width of 12 in. (305 mm). The specimens were tested as simply supported beams

with cantilevered ends (Fig. 3.2). Each specimen contained two bottom-cast splices located at the center of the beam. Splice lengths were 24 or 36 in. (610 or 914 mm) with 2 in. (51 mm) nominal side cover. Bottom cover was 1.25 or 2 in. (32 or 51 mm). Continuous No. 5 (16 mm) bars were used as top reinforcement. No. 3 (9.5 mm) closed stirrups were equally spaced within the splice region in specimens used to evaluate the effects of transverse reinforcement. Additional No. 3 (9.5 mm) stirrups were placed in the cantilevered ends to provide shear strength. Actual member dimensions are given in Table 4.1.

4.2.2 Materials

Reinforcing Steel: The test bars used in this study, designated T-8, were manufactured by Williams Form Engineering Corporation for use as high-strength prestressing bars conforming to ASTM A 722 with a yield strength reported by the manufacturer of 139 ksi (958 MPa). The high strength and threaded deformation pattern of these bars allows a very small center-to-center rib spacing, 0.250 in. (6.35 mm), with an average rib height of 0.065 in. (1.65 mm). This provides a relative rib area of 0.284, determined using the procedure described in Appendix A, which is considerably higher than values of 0.056-0.086 exhibited by commercially produced conventional reinforcing bars. Conventional ASTM Grade 60 bars were used for transverse and top reinforcement.

Concrete: Air-entrained concrete was supplied by a local ready mix plant and contained Type I portland cement, Kansas River sand and 3/4 in. (19 mm) maximum nominal size crushed limestone coarse aggregate. A water-cement ratio of 0.36 and a water reducing admixture were used to produce concrete strengths of 4090 to 5110

psi (28 to 35 MPa) at test ages of 5 or 7 days. Mix proportions and concrete properties are given in Table 4.2.

4.2.3 Specimen Fabrication

The specimens were fabricated using the same procedures as the splice specimens described in Chapter 3 (see section 3.2.3). For the specimens in Groups 3 and 4, the spliced bars were tied together with the ribs interlocked as shown in Fig. 4.1a. Interlock was prevented for the specimens in Group 7 by tying three 1 in. × 1 in. × 1/32 in. thick steel shims between the spliced bars (Fig. 4.1b). One shim was located at the center of the splice, and the other two were located at each end.

4.2.4 Test Procedure

The specimens were tested according to the procedure described in section 3.2.4.

4.3 Results and Observations

Load-deflection curves for the 6 specimens are shown in Fig. 4.2, where the deflection is the sum of the average deflection at the load points and deflection at the middle of the beam. Loads, moments, and bar stresses at failure are given in Table 4.1.

Two beams (specimens 3.1 and 3.2) failed due to a compression failure of the concrete, without producing splice failures. Specimen 3.1 showed very little cracking in the splice region. Because the specimen was obviously not close to splice failure, the concrete cover was not removed. Specimen 3.2 developed several longitudinal cracks within the splice region and may have been close to splice failure when the

concrete crushed. When the cover was removed after the test, the concrete surrounding the bar was completely intact and showed no signs of damage.

The two beams without transverse reinforcement in the splice region (specimens 3.3 and 7.3) failed much more violently than the beams with relative rib areas ranging from 0.109 to 0.127 without transverse reinforcement (described in Chapter 3). The concrete cover in the splice region was completely thrown off of the bars when splice failure occurred.

The two beams with transverse reinforcement that produced splice failures (specimens 4.3 and 7.4) failed less violently than the beams without transverse reinforcement, but failure was more sudden than for the beams with transverse reinforcement described in Chapter 3. The load-deflection curve for specimen 4.3 (Fig. 4.2) shows that the load dropped slightly after the peak load. This drop in load was accompanied by a loud "popping" sound. The load then began to increase again, but complete splice failure occurred before the load exceeded the previous maximum.

Concrete damage at the steel-concrete interface was very extensive for all specimens that produced splice failures. Shearing of the concrete around the perimeter of the bar, similar to that described in Chapter 3 for the high relative rib area bars with transverse reinforcement, was observed in specimens both with and without transverse reinforcement. However, in the current case, this damage occurred along nearly the entire splice length of the threaded bar specimens, instead of only near the discontinuous end.

4.4 Evaluation of Test Results

The splice strengths obtained for the 6 specimens with threaded bars are compared to the strengths of No. 8 bars described in Chapter 3 and to the strengths

predicted using Eqs. 3.1 and 3.10 for splices without and with transverse reinforcement, respectively. Test/prediction ratios are given in Table 4.3.

4.4.1 Splices Without Transverse Reinforcement

Specimens 3.3 and 7.3 were tested without transverse reinforcement in the splice region. These specimens were identical, except for the concrete strength [f'_c = 5110 and 4160 psi (35 and 29 MPa) for specimens 3.3 and 7.3, respectively] and rib interlock (interlock allowed in specimen 3.3 and prevented in specimen 7.3).

The test/prediction ratios, based on Eq. 3.1, were 1.11 and 1.09 for specimens 3.3 and 7.3, respectively. The small difference in ratios between the two specimens indicates that interlocking of the ribs had almost no effect on bond strength when confining reinforcement was not present. Test/prediction ratios for the 133 specimens used to develop Eq. 3.1 averaged 1.00 and ranged from 0.72 to 1.29 (Darwin et al. 1995a, 1996a). The 9 tests of No. 8 (25 mm) bars (R_r = 0.069 to 0.140) without transverse reinforcement reported by Idun and Darwin (1995) produced test/prediction ratios ranging from 0.94 to 1.13 with an average of 1.03. The two tests described in this chapter seem to suggest that a relative rib area of 0.284 may increase bond strength by about 10%, compared to bars with R_r below 0.14, even without transverse reinforcement. However, more tests are needed to determine if this apparent increase is real or the result of experimental scatter.

4.4.2 Splices With Transverse Reinforcement

The additional bond strength provided by transverse reinforcement, T_s, normalized with respect to $f'^{1/4}_c$ for the four threaded bar specimens is plotted versus the effective transverse reinforcement, NA_{tr}/n, in Fig. 4.3. For comparison, the values

for the No. 8 (25 mm) bars tested in concrete containing limestone coarse aggregate described in Chapter 3 are also plotted. Fig. 4.3 illustrates that the transverse reinforcement was significantly more effective in the threaded bar specimens.

At the time the specimens in Group 3 were designed, only five tests of high relative rib area bars with transverse reinforcement had been completed by Idun and Darwin (1995). The additional bond strength due to transverse reinforcement for the threaded bars was much higher than anticipated, based on the limited data available. As a result, the first two specimens with transverse reinforcement (specimens 3.1 and 3.2) failed due to crushing of the concrete, without producing splice failures. In specimen 3.1, compression failure and a large amount of transverse reinforcement combined to produce a low test/prediction ratio of 0.83, based on Eq. 3.10. However, even though the full strength of the splice was not reached, specimen 3.2 produced a test/prediction ratio of 1.27.

The remaining two specimens with transverse reinforcement produced splice failures and were identical, except that in specimen 4.3 the ribs were allowed to interlock while in specimen 7.4 interlock was prevented. The splice strengths of these specimens show that, unlike the specimens without transverse reinforcement, interlocking of the ribs has a significant impact on bond strength. Bar stresses at splice failure were 107 and 80 ksi (738 and 552 MPa) for specimens 4.3 and 7.4, respectively. Allowing the ribs to interlock resulted in a 34 % increase in total splice strength. The influence of rib interlock is even more apparent when comparing the additional bond strength due to transverse reinforcement for the two specimens. The values of $T_s/f'_c{}^{1/4}$ were 5990 and 3295 in.^{2} (3.86 and 2.13 m^2) for specimens 4.3 and 7.4, respectively, which shows that allowing the ribs to interlock, in this case, resulted in an 82% increase in the effectiveness of the transverse reinforcement.

Specimens 4.3 and 7.4 produced test/prediction ratios of 1.39 and 1.04, respectively. The No. 8 (25 mm) bars tested in concrete containing limestone coarse aggregate discussed in Chapter 3 produced test/prediction ratios ranging from 0.77 to 1.14, with an average of 0.92. Compared to these tests, the threaded bar specimen without rib interlock produced a test/prediction ratio 13% higher than the average, but within the range. The specimen with rib interlock produced a test/prediction ratio 51% higher than the average.

Overall, the test results indicate that Eq. 3.10 accurately predicts the splice strength of bars with relative rib areas as high as 0.284, if the ribs do not interlock. However, for splices with transverse reinforcement, Eq. 3.10 severely underpredicts splice strength when rib interlock is allowed.

CHAPTER 5: MOMENT-ROTATION TESTS

5.1 General

Darwin and Graham (1993a, 1993b) used beam-end specimens to evaluate the bond strength of machined bars with relative rib areas ranging from 0.05 to 0.20. Among their conclusions was that the initial stiffness of the load-slip curve increases as relative rib area increases. A discussion in response to the paper by Darwin and Graham (1993b) expressed concern that "the length of flexural reinforcement which attains yield at a plastic hinge will be reduced by stiffer bond characteristics, resulting in reduced plastic hinge rotation capacity" (Cairns 1994).

This chapter describes the testing and analysis of beam specimens used to investigate the effects of increased relative rib area on the load-deflection and moment-rotation response of beams with continuous reinforcement.

5.2 Experimental Program

A total of 4 beam specimens, cast in groups 16 and 17, were tested. Each group contained two specimens. These beams were cast with the splice specimens in groups 16 and 17 (described in Chapter 3). The main test parameters were relative rib area and reinforcement ratio. The specimens consisted of two matched pairs of beams. The specimens in group 16 contained two No. 8 (25 mm) bars, resulting in a reinforcement ratio, ρ, of 43% of the balanced reinforcement ratio, ρ_b (based on actual material properties). The specimens in group 17 contained three No. 8 (25 mm) bars, resulting in $\rho = 0.68\rho_b$. One beam in each group contained conventional bars, while the other beam contained high relative rib area bars.

5.2.1 Test Specimens

The beams used in this study were 16 ft (4.9 m) long, with nominal widths and depths of 12 and 16 in. (305 and 406 mm), respectively. The specimens were tested as simply supported beams with one concentrated load at the center as shown in Fig. 5.1. Each specimen contained 2 or 3 continuous bottom-cast test bars (Fig. 5.2) with nominal bottom and side covers of 2 in. (51 mm). No. 3 (9.5 mm) closed stirrups spaced 6 in. (152 mm) on center were included along the entire length of the beams to provide shear strength. No. 4 (13 mm) bars were used as top reinforcement to hold the stirrups in place. Actual member dimensions are given in Table 5.1.

5.2.2 Materials

Reinforcing Steel: All bars met the requirements of ASTM A 615, except that the experimental bars did not contain bar markings. Two deformation patterns were tested and are shown in Fig. 5.3. The bars were selected because of their similar yield strengths and the range of relative rib area. The conventional bars, designated 8N0, have a relative rib area of 0.069 and a yield strength of 78.0 ksi (538 MPa). The experimental bars, designated 8N3, have a relative rib area of 0.119 and a yield strength of 80.6 ksi (556 MPa). Both bars were produced from the same heat of steel. Relative rib areas were measured according to the procedure described in Appendix A. The yield strengths reported were determined from tests of three samples of each bar designation. Test bar properties are given in Table 5.2. Conventional ASTM Grade 60 No. 3 and No. 4 (9.5 and 13 mm) bars were used for stirrups and top reinforcement, respectively.

Concrete: Air-entrained concrete was supplied by a local ready-mix plant and contained Type I portland cement, Kansas River sand, and 3/4 in. (19 mm)

maximum nominal size crushed limestone coarse aggregate. A water-cement ratio of 0.44 was used to produce concrete compressive strengths of 5170 and 4760 psi (36 and 33 MPa) at test ages of 23 and 20 days for the specimens in groups 16 and 17, respectively. Mix proportions and concrete properties are given in Table 5.3.

5.2.3 Specimen Fabrication

Formwork: The formwork described in section 3.2.3 for splice specimens was also used for the specimens described in this chapter.

Reinforcing Steel Cages: The reinforcing steel cages for the specimens described in this chapter were similar to those described in section 3.2.3 for splice specimens, except that the bottom No. 8 (25 mm) test bars were continuous and No. 3 (9.5 mm) stirrups spaced 6 in. (152 mm) on center were provided along the entire length of the specimen. No. 4 (13 mm) bars were used as top reinforcement. In specimens containing conventional reinforcement, the test bars were positioned so that the bar markings were centered on the centerline of the beam to minimize their effect on the response of the specimen. The high relative rib area reinforcement did not have bar markings. The test bars were cleaned with acetone to remove debris once before placing the bars in the forms and again just prior to casting.

As shown in Fig. 5.4, six transverse 1/2 in. (12.7 mm) diameter all-thread rods were cast in the specimen to provide attachment points for the LVDTs used to measure rotation at the center of the beam. These rods were located 3.5 in. (89 mm) from the top and bottom of the specimen. Two rods were located at the center of the beam and two were located 17 in. (432 mm) on each side of the center of the beam. A length of 17 in. (432 mm) on each side of the center was chosen based on estimates of the plastic hinge length (Park and Paulay 1975).

Placement and Curing Procedure: The specimens were cast from the same batches of concrete as the splice specimens in groups 16 and 17. Concrete was placed in two lifts, each approximately one-half the depth of the specimen. In the first lift, concrete was placed first in the two ends (approximately one-third the specimen length) followed by the center of the specimen. In the second lift, the placement order was reversed so that the center of all beams was placed first, followed by the ends. Each lift was vibrated with a 1 1/2 in. (38 mm) square internal vibrator on alternate sides of the beam at 1 ft (0.3 mm) intervals.

The specimens were cured in the same manner as the splice specimens described in Chapter 3 (see section 3.2.3).

Three additional 6 × 12 in. (152 × 305 mm) cylinders were cast in each group so the moment-rotation specimens could be tested on a different day than the splice specimens.

5.2.4 Test Procedure

The specimens were tested as simply supported beams with a concentrated load applied at the center (Fig. 5.1). The beams were supported 6 in. (305 mm) from the ends by pin and roller supports mounted on concrete pedestals. Steel plates, attached to the specimen with a thin layer of high strength gypsum cement (Hydrostone), separated the beam from the supports. A downward load was applied at the center of the beam using two 60-ton hollow-core hydraulic jacks powered by an Amsler hydraulic testing machine. Two 1 1/2 in.(38 mm) diameter steel rods were used to transfer the force from the jacks to a steel spreader beam mounted across the specimen. The rods were attached to the spreader beam with semi-cylindrical rollers

to keep the applied load vertical. The beams were painted with diluted white latex paint to make cracks more visible. Load was applied at about 3 kips (13 kN) per minute up to approximately 90% of the yield load. During this period, load was held constant at 5 kip (22 kN) increments as cracks were marked. Above 90% of the yield load, the beams were loaded continuously to failure, after which any additional cracks that had formed were marked.

A spring-loaded LVDT bearing against the bottom of the beam was used to measure the centerline deflection. Load on the beam was measured using the load rods, which were instrumented as load cells using four strain gages in a full bridge configuration. Flexural rotation of the beam on each side of the load point was measured using two LVDTs, as shown in Fig. 5.4. These LVDTs were attached to the 1/2 in. (12.7 mm) diameter all-thread rods cast in the specimen. Two LVDTs were mounted on the north face of the beam and measured rotation on the east side of the load point. The other two LVDTs were mounted on the south face of the beam and measured rotation on the west side of the load point. Cracks were marked on both sides of the beam, opposite the faces on which the rotations were measured (i.e. cracks were marked on the north face of the beam west of the load point and on the south face of the beam east of the load point).

Load cell and LVDT readings were acquired using a Hewlett-Packard data acquisition system controlled by a computer and stored on the computer's hard disk. Up to 90% of the yield load, readings were taken at approximately 10 second intervals. After 90% of the yield load, readings were taken at approximately 1 second intervals.

5.3 Results, Observations and Evaluation

Load-deflection curves for the specimens in groups 16 and 17 are shown in Figs. 5.5a and b, respectively. Moment-rotation curves for the specimens in groups 16 and 17 are shown in Figs. 5.6a and b, respectively.

Rotation of the beam on each side of the load point was calculated from

$$\theta = \tan^{-1}\left(\frac{\Delta_t + \Delta_b}{a}\right) \tag{5.1}$$

where θ = rotation, rad.

Δ_t = deflection of the top LVDT, in., positive in compression (Fig. 5.4)

Δ_b = deflection of the bottom LVDT, in., positive in tension (Fig. 5.4)

a = average vertical distance between the top and bottom LVDTs, in. (Table 5.1 and Fig. 5.4)

The rotations plotted in Figs. 5.6a and b are the averages for both sides of the load point. Individual moment-rotation curves for each side of the load point are shown in Appendix B.

As expected, the specimens with three No. 8 (25 mm) bars produced higher loads and stiffnesses up to the yield load than did the specimens with two No. 8 (25 mm) bars. After reaching the yield load, the stiffnesses of the load-deflection and moment-rotation curves were greatly reduced as a plastic hinge developed near the load point. Loading was continued until a significant drop in load was produced by crushing of the concrete near the load point. Specimens with three No. 8 (25 mm) bars failed in compression soon after yielding, while specimens with two No. 8 (25 mm) bars produced significant additional displacement and rotation after yielding.

The load-deflection and moment-rotation curves (Figs. 5.5 and 5.6, respectively) for matched pairs of specimens are nearly identical. These figures indicate that an increase in relative rib area does not have a measurable effect on the displacement or rotational capacity of beams in which plastic hinges form.

Crack patterns for the specimens are shown in Figs. 5.7-5.10. Flexural cracks initially formed near the load point. As the load increased, these cracks grew while more cracks developed farther away from the load point. After completion of the tests, cracking was more extensive near the load point. Figs. 5.7-5.10 show that the crack patterns for matched pairs of beams are very similar and that the spacing and distribution of flexural cracks is not affected by the relative rib area of the test bar.

As shown in Figs. 5.7-5.10, compression failure occurred only on the west half of all specimens, except for a small amount of crushing on the east half of specimen 16.5 (Fig. 5.8a). This was probably due to the unsymmetric support conditions (one pin and one roller support) that may have caused a slight change in the length of the span on the end of the beam supported by the roller as the specimen was loaded.

Overall, the test results do not support the concerns expressed about the effects of increased relative rib area on the rotational capacity provided by plastic hinges in beams containing high relative rib area bars.

CHAPTER 6: SPLICE LENGTH COMPARISONS AND ESTIMATED MATERIAL SAVINGS

6.1 General

In this chapter, the development and splice length criteria described in Chapter 3, for both conventional and high relative rib area bars, are compared to the more detailed of the expressions in ACI 318-95 described in Chapter 1 (Eq. 1.3). The effects of using new (high relative rib area) bars on splice and development lengths for coated and uncoated bars with and without transverse reinforcement using the criteria developed in this study are also discussed. To obtain estimates of reductions in splice lengths and material savings, splice lengths for bars in actual structures are calculated using the criteria in ACI 318-95 and the criteria described in Chapter 3. Comparisons are also made between the more precise of the equations in Chapter 3, Eq. 3.13, that includes the increase in bond strength when $c_M > c_m$ and the larger effective cover when c_{si} controls, and the simpler equation, Eq. 3.14, that is obtained from Eq. 3.13 by setting $c_M = c_m$ and c_s equal to the smaller of the side cover or one-half the clear spacing between bars.

6.2 Comparison of ACI 318-95 Criteria to the Criteria in Chapter 3

This section discusses several important differences between the ACI criteria and the criteria described in Chapter 3 and their impact on splice and development lengths. In some cases, the ACI criteria result in an underestimate of the development length necessary to produce a desired bar stress, resulting in decreased safety. In other cases, the ACI criteria result in an overestimate of the necessary development length, resulting in decreased economy. The criteria described in Chapter 3 provide a more uniform factor of safety than the ACI criteria, without being overconservative,

because they are based on accurate expressions and include a reliability-based strength reduction factor.

To simplify the comparisons presented in sections 6.2.1 to 6.2.4 between the ACI criteria and the criteria described in Chapter 3, Eq. 3.14 is used because the definition of c in Eq. 3.14 is the same as in the ACI criteria. Using Eq. 3.14 also eliminates the need to specify the value c_M and whether c_{si} controls, allowing more general comparisons between the two criteria. However, it should be noted that development/splice lengths calculated using Eq. 3.14 will always be greater than or equal to those calculated using Eq. 3.13.

6.2.1 Relationship Between Bond Force and Development Length

The ACI expression, Eq. 1.3, assumes that the relationship between bond force and development length is linear and proportional. Therefore, to increase the force, or stress, in a bar by a given percentage requires that same percentage increase in development length. In the criteria described in Chapter 3, the relationship between bond force and development length is also linear, but not proportional. Therefore, to increase the stress in a bar by a given percentage requires more than that percentage increase in development length.

The effect of the relationship between bar stress and development length is shown in Fig. 6.1 for No. 8 (25 mm) bars without transverse reinforcement with $c/d_b = 2$ and $f'_c = 5000$ psi (34.5 MPa). This figure shows that, on the average, the ACI derived development length will be inadequate for design stresses greater than 62 ksi (427 MPa). Fig. 6.1 also shows that the ACI equation requires shorter development lengths, and is therefore unconservative compared to Eq. 3.14, when the stress in the bar is greater than 45 ksi (310 MPa).

6.2.2 Effect of Concrete Strength

The ACI equation uses $f'_c{}^{1/2}$ to represent the effect of concrete strength on bond strength but limits $f'_c{}^{1/2}$ to a maximum of 100 psi (0.69 MPa). Therefore, no additional decrease in development length is obtained when the concrete strength is above 10,000 psi (69 MPa). Darwin et al. (1995a, 1996a) showed that using $f'_c{}^{1/2}$ to represent the effect of concrete strength underestimates bond strength for low strength concrete and overestimates bond strength for high strength concrete. The equations developed in Chapter 3 use $f'_c{}^{1/4}$ to represent the effect of concrete strength, which provides a more accurate representation than $f'_c{}^{1/2}$ for concrete strengths ranging from 2,500 to 16,000 psi (17.2 to 110.3 MPa), the range of strengths used to develop the equations.

6.2.3 Effect of Transverse Reinforcement

Although the symbol used for the term representing the effect of transverse reinforcement, K_{tr}, is the same in both the ACI equation and the equations described in Chapter 3, the expressions for K_{tr} are different. In the ACI equation, $K_{tr} = A_{tr}f_{yt}/(1500\ sn)$. In the equations of Chapter 3, $K_{tr} = 35.3\ (9.6\ R_r + 0.28)(0.72\ d_b + 0.28)A_{tr}/sn = 35.3\ t_r t_d A_{tr}/sn$.

The two expressions for K_{tr} differ in two important ways. The first is that the ACI expression for K_{tr} includes the yield strength of the transverse reinforcement, f_{yt}. As discussed in Chapter 3, Darwin et al. (1995a, 1996a) found that the yield strength of the transverse reinforcement does not effect the increase in splice strength due to transverse reinforcement. Therefore, f_{yt} is not included in the expressions for K_{tr} in the equations of Chapter 3. The second important difference is that the expression for K_{tr} in the equations of Chapter 3 contains two terms, t_r and t_d, that account for the

increase in the effectiveness of transverse reinforcement as relative rib area and bar size increase, respectively. The ACI equations do not account for the effects of relative rib area and bar size on the effectiveness of transverse reinforcement.

Compared to the expression for K_{tr} in the equations of Chapter 3, the ACI expression underpredicts the effect of transverse reinforcement for No. 10 (29 mm) and larger conventional bars (average $R_r = 0.0727$) and No. 6 (19 mm) and larger new bars (average $R_r = 0.1275$) when $f_{yt} = 60$ ksi (414 MPa). For $f_{yt} = 40$ ksi (276 MPa), the ACI expression underpredicts the effectiveness of the transverse reinforcement for No. 6 (19 mm) and larger conventional bars and all sizes of new bars.

Another important difference between the ACI equation and the equations of Chapter 3 is the upper limit on the amount of useable confinement, represented by the term $(c + K_{tr})/d_b$. In the ACI equation, $(c + K_{tr})/d_b$ is limited to a maximum value of 2.5. As discussed in Chapter 3, Darwin et al. (1995a, 1996a) found that ratios of test to predicted strengths for the tests used to develop the expressions presented in Chapter 3 average above 1.0 unless $(c + K_{tr})/d_b$ exceeds a value of 4.

6.2.4 Splice Lengths

Under the provisions of ACI 318-95, splice lengths are calculated based on the class of the splice. Splices where the area of reinforcement provided is at least twice that required by analysis and one-half or less of the total reinforcement is spliced at one location are defined as Class A splices, with a splice length equal to the development length, l_d. All other splices are defined as Class B splices, with a splice length equal to 1.3 l_d.

As discussed in Chapter 3, the equations of Chapter 3 can be used to calculate both splice and development lengths, without the need for a separate factor for splices.

Bars Not Confined By Transverse Reinforcement: Ratios of the development/splice lengths obtained using Eq. 3.14 to the Class A splice (or development) lengths and the Class B splice lengths obtained using the ACI criteria are given in Table 6.1 for bars without transverse reinforcement and $c/d_b \leq 2.5$. This table shows that, for No. 6 (19 mm) and smaller bars, splice lengths obtained using Eq. 3.14 range from 11% to 56% longer than Class A splice lengths obtained using the ACI criteria, and from 15% shorter to 20% longer than Class B splice lengths obtained using the ACI criteria. For No. 7 (22 mm) and larger bars, splice lengths obtained using Eq. 3.14 range from 5% to 25% longer than Class A splice lengths obtained using the ACI criteria, and from 19% to 4% shorter than Class B splice lengths obtained using the ACI criteria. Only Grade 60 (414 MPa) No. 7 (22 mm) and larger bars are considered because Grade 40 (276 MPa) bars are only available in No. 6 (19 mm) and smaller sizes.

For No. 6 (19 mm) and smaller bars, the significant increase in splice lengths obtained using Eq. 3.14, compared to the Class A splice lengths obtained using the ACI criteria, are a result of the 0.8 factor in the ACI equation for these bars and the assumption that bar stress is proportional to development length in the ACI equation. As shown in Fig. 6.2, in which bar stress is plotted as a function of l_d/d_b for No. 6 and smaller bars with $c/d_b = 2.5$ and $f'_c = 5000$ psi (34.5 MPa), these two factors combine to produce increasingly unconservative predictions of bar stress, compared to the stress predicted by Eq. 3.14, when l_d/d_b exceeds 11.2. This observation is supported by the test data for bars without transverse reinforcement used to develop the equations in Chapter 3. Test/predicted bar stress ratios for the tests are plotted versus l_d/d_b in Figs. 6.3 and 6.4 for the ACI development length equation and Eq. 3.14, respectively. Individual test data are presented in Table C.1. Fig. 6.3 shows that the

best-fit lines for test/predicted bar stress based on the ACI equation decrease sharply, especially for No. 6 (19 mm) and smaller bars, as l_d/d_b increases. Fig. 6.4 shows that the best-fit lines for test/predicted bar stress based on Eq. 3.14 decrease only slightly as l_d/d_b increases and are nearly the same for No. 6 (19 mm) and smaller and No. 7 (22 mm) and larger bars. Figs. 6.3 and 6.4 also illustrate the reduction in scatter of test/prediction ratios for Eq. 3.14 compared to the ACI equation.

Under the criteria in Chapter 3, the upper limit on the amount of useable confinement, represented by the term c/d_b for bars without transverse reinforcement, is increased from 2.5, in the ACI criteria, to 4.0 allowing splice lengths for bars with large covers to be reduced. Ratios of development/splice lengths obtained using Eq. 3.14 to Class A and Class B splice lengths obtained using the ACI criteria are given in Table 6.2 for $c/d_b = 4$. For No. 6 (19 mm) and smaller bars, splice lengths obtained using Eq. 3.14 range from 18% shorter to 29% longer than Class A splice lengths obtained using the ACI criteria, and from 37% to 1% shorter than Class B splice lengths obtained using the ACI criteria. For No. 7 (22 mm) and larger bars, splice lengths obtained using Eq. 3.14 range from 34% to 11% shorter than Class A splice lengths obtained using the ACI criteria, and from 50% to 32% shorter than Class B splice lengths obtained using the ACI criteria.

Bars Confined By Transverse Reinforcement: To compare splice lengths for the ACI criteria with the criteria described in Chapter 3, specific configurations must be used because of the large number of variables involved.

Tables 6.3 and 6.4 compare development (or Class A splice) lengths and Class B splice lengths for the ACI criteria and Eq. 3.14 for members with 2 in. (51 mm) cover and No. 3 or No. 4 (9.5 or 13 mm) stirrups, respectively, spaced 6 in. (152 mm) on center. Shown in these tables are development and splice lengths for No. 6 (19

mm) Grade 40 (276 MPa) bars in 3000 and 6000 psi (21 and 41 MPa) concrete and No. 6, No. 8, and No. 11 (19, 25, and 36 mm) Grade 60 (414 MPa) bars in concrete with strengths ranging from 3000 to 15000 psi (21 to 104 MPa) at 3000 psi (21 MPa) intervals. Considering both Tables 6.3 and 6.4 (see summary in Table 6.4), development/splice lengths calculated using Eq. 3.14 for conventional bars range from 28% shorter to 22% longer and average 8% shorter than development (or Class A splice) lengths calculated using the ACI criteria, and range from 45% to 1% shorter and average 24% shorter than Class B splice lengths calculated using the ACI criteria. Development/splice lengths calculated using Eq. 3.14 for high relative rib area bars range from 34% shorter to 8% longer and average 9% shorter than development (or Class A splice) lengths calculated using the ACI criteria, and range from 50% to 1% shorter and average 28% shorter than Class B splice lengths calculated using the ACI criteria. Development/splice lengths for high relative rib area bars range from 16% to 0% shorter and average 5% shorter than conventional bars using Eq. 3.14. The cases shown in the tables where no savings are produced from the use of high relative rib area bars are a result of the application of one of two limits: $l_d/d_b \geq 16$ or $(c + K_{tr})/d_b \leq 4$.

Larger reductions in splice and development lengths for high relative rib area bars compared to conventional bars can be obtained for small covers or bar spacings and large amounts of transverse reinforcement. This will be discussed in section 6.3.

Larger reductions in splice and development lengths can also be obtained when Eq. 3.13 is used, because this equation takes advantage of (1) the increase in bond strength when $c_M > c_m$ and (2) the larger effective cover when c_{si} controls. It should be noted that Eq. 3.14 is obtained from Eq. 3.13 by setting c_M equal to c_m and c_s equal to the smaller of the side cover or one-half the clear spacing between bars and

is therefore calibrated to minimum splice or development strength. The effect of $c_M > c_m$ was not considered in the development of the ACI equations. Therefore, it is calibrated to the average value of c_M / c_m for the tests used to develop the equation.

6.3 Effect of Relative Rib Area

This section describes the effects of relative rib area on development and splice lengths. The ACI equation does not account for the increase in bond strength as relative rib area increases for bars confined by transverse reinforcement. Therefore, splice length comparisons are limited to comparisons between conventional and high relative rib area reinforcement using the criteria described in Chapter 3.

6.3.1 Uncoated Reinforcement

For bars without transverse reinforcement, the criteria described in Chapter 3 predict the same development lengths for both conventional and high relative rib area bars. However, when the bars are confined by transverse reinforcement, significant reductions in development length can be obtained with the use of the new bars. This reduction can be seen by taking the ratio of l_d for new bars to l_d for conventional bars. Using Eq. 3.14, this ratio reduces to

$$\frac{l_d\,(\text{new})}{l_d\,(\text{conv.})} = \frac{c + K_{tr}\,(\text{conv.})}{c + K_{tr}\,(\text{new})} \tag{6.1}$$

where $K_{tr}(\text{conv.}) = 34.5\, t_d A_{tr}/sn = 34.5\,(0.72\, d_b + 0.28)\, A_{tr}/sn$

$K_{tr}(\text{new}) = 53\, t_d A_{tr}/sn = 53\,(0.72\, d_b + 0.28)\, A_{tr}/sn$

This ratio is valid only when $l_d/d_b \geq 16$ and $(c + K_{tr})/d_b \leq 4$.

The maximum reduction in development length will occur when $c/d_b = 1$ (the minimum allowed under ACI 318-95) and $[c + K_{tr}(new)]/d_b = 4$. In this case, $K_{tr}(new)/d_b = 3$ and $K_{tr}(conv.)/d_b = (34.5/53)\ 3 = 0.65 \times 3 = 1.95$. Using Eq. 6.1, $l_d(new)/l_d(conv.) = 0.74$, for a 26% reduction in development length. For $c/d_b = 1$ and $K_{tr}(new)/d_b = 2$ and 1, the reductions become 23% and 17%, respectively. Tables 6.5 and 6.6 summarize values of $l_d(new)/l_d(conv.)$ for $c/d_b = 1$, 1.5, 2, 2.5, and 3 and $K_{tr}(new)/d_b = 1$, 2, and 3. Table 6.5 summarizes the ratios for Grade 60 (414 MPa) reinforcement in concrete with strengths ranging from 3,000 to 15,000 psi (21 to 104 MPa) at 3000 psi (21 MPa) intervals and shows that the savings decrease as cover and bar spacing increase or when $[c + K_{tr}(new)]/d_b > 4$. Savings also decrease for concrete strengths above 6000 psi (41 MPa) because the limit of $l_d/d_b \geq 16$ begins to control the development length of the new bars. Table 6.6 summarizes the ratios for Grade 40 (276 MPa) reinforcement in concrete with strengths of 3000 and 6000 psi (21 and 41 MPa) and shows that generally smaller savings are obtainable with Grade 40 (276 MPa) reinforcement because the limit of $l_d/d_b \geq 16$ has a larger effect.

6.3.2 Epoxy-Coated Reinforcement

Bars Not Confined by Transverse Reinforcement: As discussed in Chapter 3, the ratio of coated to uncoated bar bond strength (β) for high relative rib area bars ($\beta = 0.88$) is higher than that of conventional bars ($\beta = 0.74$ from Hester et al. 1991, 1993). The fact that the relationship between bond strength and development length is linear but not proportional results in a ratio of coated to uncoated bar development length that varies with f'_c and f_y. Using Eq. 3.14, the ratio of coated to uncoated bar development length becomes

$$\frac{l_d\,(\text{coated})}{l_d\,(\text{uncoated})} = \frac{\dfrac{f_y}{\beta f_c'^{1/4}} - 1900}{\dfrac{f_y}{f_c'^{1/4}} - 1900} \tag{6.2}$$

This ratio is valid only when $l_d/d_b \geq 16$ and $(c + K_{tr})/d_b \leq 4$.

Ratios of coated to uncoated bar development length for new and conventional reinforcement are summarized in Table 6.7 for Grade 40 (276 MPa) reinforcement in concrete with strengths of 3000 and 6000 psi (21 and 41 MPa) and for Grade 60 (414 MPa) reinforcement in concrete with strengths ranging from 3,000 to 15,000 psi (21 to 104 MPa). For new bars with $c/d_b = 1$, the ratio of l_d(coated)/l_d(uncoated) is fairly constant at about 1.2, ranging from 1.18 for Grade 60 (414 MPa) reinforcement in 3000 psi (21 MPa) concrete to 1.23 for Grade 40 (276 MPa) reinforcement in 6000 psi (41 MPa) concrete. For conventional bars with $c/d_b = 1$, the ratio of l_d(coated)/l_d(uncoated) ranges from 1.46 to 1.60 which is similar to the current development length modification factor of 1.5 in ACI 318-95 for coated bars with small cover or bar spacing. The values for conventional and new bars with $c/d_b = 4$ show that the ratios will decrease for high strength concrete as the limit of $l_d/d_b \geq 16$ controls development length. In general, when the limits of the equation do not control, the ratios decrease as f_y increases and f'_c decreases.

Table 6.8 compares the ratio of l_d(new) to l_d(conv.) for Grade 40 and Grade 60 (276 and 414 MPa) coated bars. This table shows that l_d(new)/l_d(conv.) for coated bars with $c/d_b = 1$ ranges from 0.77 to 0.81, resulting in about a 20% decrease in development length due to the use of high relative rib area bars. This saving is important because it applies to all coated bars, even those without transverse reinforcement. The ratios for $c/d_b = 4$ again show that savings decrease for higher

concrete strengths when the development length for the new bars is controlled by the limit of $l_d/d_b \geq 16$.

Bars Confined by Transverse Reinforcement: Larger reductions in development length for coated high relative rib area reinforcement can be obtained when the bars are confined by transverse reinforcement.

Table 6.9 summarizes ratios of l_d(new)/l_d(conv.) for Grade 60 (414 MPa) coated bars with transverse reinforcement for c/d_b = 1, 1.5, 2, 2.5, and 3 and K_{tr}(new)/d_b = 1, 2, and 3 in concrete with strengths ranging from 3,000 to 15,000 psi (21 to 104 MPa) at 3000 psi (21 MPa) intervals. As shown in Table 6.9, the ratios of l_d(new)/l_d(conv.) range from 0.58 to 0.85, resulting in a 42% to 15% reduction in development length for coated high relative rib area bars confined by transverse reinforcement. As seen for uncoated bars, the savings are highest for small covers or bar spacings and large amounts of transverse reinforcement.

Ratios of l_d(new)/l_d(conv.) for Grade 40 coated bars with transverse reinforcement are given in Table 6.10 for c/d_b = 1, 1.5, 2, 2.5, and 3 and K_{tr}(new)/d_b = 1, 2, and 3 in concrete with strengths of 3000 and 6000 psi (21 and 41 MPa). Development lengths for the new coated bars range from 40% to 0% shorter than conventional bars. The savings for Grade 40 (276 MPa) bars are smaller because of the limit of $l_d/d_b \geq 16$ controlling many of the development lengths.

6.4 Actual Structures

To determine the effect of the design equations described in Chapter 3 on splice lengths and material quantities, two structures were examined. The first structure is a composite bridge containing both coated and uncoated reinforcement.

The second structure is the lateral load resisting frame system of a twelve story office building containing only uncoated reinforcement.

The splices in these structures were redesigned according to the ACI 318-95 design criteria, using the detailed expression in Code section 12.2.3, and the two equations (Eqs. 3.13 and 3.14) developed in this study for both conventional and new (high relative rib area) bars so comparisons could be made for typical amounts of cover and transverse reinforcement encountered in design.

6.4.1 Bridge

The bridge structure examined was a 247 ft (75.3 m) long and 38 ft (11.6 m) wide three span steel and concrete composite bridge containing a total of 93,341 lb (42,339 kg) of Grade 60 (414 MPa) reinforcing steel as originally designed. The two piers contained 17,410 lb (7,897 kg) of uncoated reinforcing steel. The remaining 75,931 lb (34,442 kg) of reinforcing steel was epoxy-coated reinforcement located in the abutments and deck.

The data used to calculate splice lengths for the bridge are given in Table 6.11. The original splice lengths, taken from the bridge plans, and the splice lengths calculated using the ACI 318-95 equation and Eqs. 3.13 and 3.14, for both conventional and new bars, are given in Table 6.12. In cases where two bars with different diameters are spliced together, the smaller bar diameter was used to calculate the splice length.

Splice length ratios comparing the different design criteria are given in Table 6.13. Average ratios are calculated by weighting each splice configuration equally. Splice lengths for both conventional and new bars are, on average, significantly

shorter using Eqs. 3.13 and 3.14 than those using ACI 318-95 and those from the original design.

Considering all of the reinforcement in the bridge, splice lengths for conventional bars using Eq. 3.13 range from 52% to 102% and average 74% of the splice lengths using the criteria of ACI 318-95. These percentages range from 52% to 134% and average 79% when Eq. 3.14 is used. For new bars using Eq. 3.13, splice lengths range from 41% to 90% and average 65% of the splice lengths using ACI 318-95. These percentages range from 42% to 109% and average 69% when Eq. 3.14 is used. Splice length ratios for new to conventional bars range from 0.78 to 1.0 and average 0.89 and 0.88 using Eqs. 3.13 and 3.14, respectively.

It is important to note that the only splice length ratios comparing the criteria in Chapter 3 to the ACI criteria that are greater than 1 result from the one Class A splice configuration (labeled splice No. 25) in the bridge. Although both the original and the ACI 318-95 splice lengths for this configuration are safe according to the criteria in Chapter 3, assuming they are never stressed to more than one-half the design yield strength of 60 ksi (414 MPa), they are not sufficient to develop the full design yield strength of the bars should an unanticipated overload situation occur. With the exception of this one Class A splice, the splice lengths in the bridge using the criteria of Chapter 3 are all shorter than the splice lengths using the ACI criteria, and produce maximum ratios of 0.90 for conventional and new bars using Eq. 3.13 and for new bars using Eq. 3.14 and 0.97 for conventional bars using Eq. 3.14.

The effect of ignoring the increase in splice strength as c_M/c_m increases can be seen by looking at the ratio of splice lengths calculated from Eq. 3.13 to those calculated from Eq. 3.14 (which conservatively assumes that $c_M/c_m = 1$). As shown

in Table 6.13, these ratios range from about 0.75 to 1.0 and average 0.95, resulting in an overestimate of splice length by as much as 33%.

All of the splices of uncoated reinforcement in the bridge were either not confined by transverse reinforcement or were so heavily confined that the values of $(c + K_{tr})/d_b$ (using the definitions for c and K_{tr} in Chapter 3) were above the limiting value of 4. These two conditions produce identical splice lengths for conventional and new bars under the criteria of Chapter 3. Although no reduction in splice length occurred from the use of the new bars, the equations of Chapter 3 produce significantly shorter splice lengths that average 67% and 69% of the ACI splice lengths using Eqs. 3.13 and 3.14, respectively.

Splice lengths for the coated bars in the bridge using Eqs. 3.13 and 3.14 for conventional bars average 78% and 84% of the ACI splice lengths, respectively. The less detrimental effect of epoxy coating on the bond strength of high relative rib area bars results in even shorter splice lengths that average 65% and 69% of the ACI splice lengths using Eqs. 3.13 and 3.14, respectively, and about 82% of the splice lengths for conventional bars using either equation.

Changes in the weight of the reinforcing steel in the bridge resulting from the changes in splice lengths are shown in Table 6.14. Negative values represent a decrease in the amount of steel (a reduction in splice length), and positive values represent an increase in the amount of steel.

For the uncoated bars in the bridge, using ACI 318-95 criteria produces a 0.92% reduction in the amount of steel compared to the original design. As mentioned previously, splice lengths for conventional and new uncoated bars in the bridge are equal using the criteria of Chapter 3 which produce 1.91% and 1.82% reductions in steel weight using Eqs. 3.13 and 3.14, respectively. The savings are

slightly greater using Eq. 3.13 because this equation accounts for the increase in splice strength as c_M/c_m increases, while in Eq. 3.14 c_M/c_m is conservatively assumed to be equal to 1. Using Eqs. 3.13 and 3.14 reduces the amount of steel by about 1% compared to using the ACI 318-95 equation.

For the coated bars in the bridge, using ACI 318-95 criteria produces a 0.39% increase in the amount of steel compared to the original design. The weight of the coated bars in the bridge for the criteria in Chapter 3 is greatly affected by the one Class A splice configuration (labeled splice no. 25) in the structure. As discussed previously, this is the only configuration for which the criteria in Chapter 3 produce a longer splice length than the ACI criteria. However, as shown in Table 6.11, this configuration is repeated 218 times throughout the structure. As shown in Table 6.14, the increase in steel weight from this one splice configuration cancels out much of the savings produced by the remaining configurations. For conventional bars, using Eqs. 3.13 and 3.14 produce 0.53% and 0.02% reductions in steel weight, respectively. For new bars, the two equations produce 1.04% and 0.65% reductions in steel weight, respectively. Compared to the amount of steel using the ACI 318-95 criteria, steel weight is reduced by 0.91% and 0.41% for conventional bars and by 1.43% and 1.03% for new bars using Eqs. 3.13 and 3.14, respectively. Comparing the steel weights for conventional and new bars using the criteria of Chapter 3 shows that the use of new bars results in 0.52% and 0.64% reductions for the two equations.

Overall, using the ACI 318-95 criteria results in a 0.14% increase in the total amount of steel in the bridge compared to the original design. For conventional bars, total steel weight is reduced 0.78% and 0.36%, while for new bars, steel weight is reduced 1.21% and 0.87% using Eqs. 3.13 and 3.14, respectively. Compared to the amount of steel using ACI 318-95, total steel weight is reduced by 0.93% and 0.50%

for conventional bars and 1.35% and 1.01% for new bars using the two equations in Chapter 3. Comparing the steel weights for conventional and new bars using the criteria of Chapter 3 shows that the use of new bars results in 0.42% and 0.51% reductions for the two equations.

The analysis of the bridge structure demonstrates that significant reductions in splice length are obtained using the design criteria in Chapter 3. The reductions in splice length result in less congested reinforcement, allowing easier concrete placement and reducing the risk of segregation, along with a reduction in the amount of reinforcing steel in the structure. The reductions in splice length, congestion, and amount of reinforcing steel are greatest when the design criteria in Chapter 3 are used in conjunction with high relative rib area reinforcing bars, especially when the bars are epoxy-coated.

6.4.2 Building

The second structure investigated is a 12 story office building in which a cast-in-place reinforced concrete frame system is used to resist lateral loads. The remainder of the building is constructed with precast concrete elements, except for the floor slabs and some of the interior beams. Only the splices in the beams and columns of the cast-in-place frame were examined in this study. All splice lengths were recalculated based on the ACI design criteria and the criteria in Chapter 3.

The frame contains a total of 3,193,283 lb (1,448,448 kg) of Grade 60 (414 MPa) uncoated reinforcing steel, as originally designed. Approximately 40% of the steel is located in the beams and 60% is located in the columns. Concrete strength is either 5000 or 6000 psi (34.5 or 41.4 MPa).

Beams: Individual splice data, splice lengths, changes in steel weight, and splice length ratios for the splices in the beams are given in Appendix D (see Table D.1) for each of the design criteria considered. Maximum, minimum, and average splice length ratios for the splices in the beams are summarized in Table 6.15.

Splice lengths calculated using both the ACI 318-95 design criteria and the criteria in Chapter 3 are, on average, significantly shorter than those of the original design. Average splice lengths range from 62% of the original lengths using the ACI criteria to 43% of the original lengths using Eq. 3.13 for high relative rib area bars.

Table 6.15 also shows that splice lengths calculated using the criteria of Chapter 3 average about 80% and 70% of the splice lengths calculated using the ACI equation for conventional and new bars, respectively. For conventional bars, Eq. 3.13 produces splice lengths ranging from 60% to 91% and averaging 78% of ACI splice lengths, while Eq. 3.14 produces splice lengths ranging from 68% to 91% and averaging 83% of the ACI splice lengths. For high relative rib area bars, Eq. 3.13 produces splice lengths ranging from 54% to 86% and averaging 70% of the ACI splice lengths, while Eq. 3.14 produces splice lengths ranging from 56% to 86% and averaging 73% of the ACI splice lengths. Under the criteria described in Chapter 3, splice lengths for high relative rib area bars range from 83% to 95% and average 89% of those for conventional bars. Splice lengths using the more precise Eq. 3.13 average 95% of the splice lengths using the simplified Eq. 3.14.

The reductions in the splice lengths for the beams are reflected in the beam steel weights for each design criteria shown in Table 6.16. Using the ACI 318-95 criteria, the total beam steel weight is reduced 4.4% to 1,207,800 lb (547,848 kg) compared to the original weight of 1,250,137 lb (567,053 kg). Using Eqs. 3.13 and 3.14 for conventional bars, the weight is reduced to 1,187,657 and 1,194,219 lb

(538,712 and 541,689 kg), respectively, resulting in a 1.7% and 1.1% reduction in weight compared to the ACI design. For new bars, the weight is reduced to 1,180,158 and 1,185,233 lb (535,311 and 537,613 kg), resulting in a 2.3% and 1.9% reduction in weight compared to the ACI design. Comparing the weights for conventional to new bars under the criteria of Chapter 3 shows that the use of high relative rib area bars results in a 0.6% and 0.8% reduction in weight using Eqs. 3.13 and 3.14, respectively.

Columns: Individual splice data, splice lengths, changes in steel weight, and splice length ratios for the splices in the columns are given in Appendix D (see Table D.2) for each of the design criteria considered. Maximum, minimum, and average splice length ratios for the splices in the columns are summarized in Table 6.15.

All splices in the columns are splices of No. 11 (36 mm) bars that are heavily confined by transverse reinforcement. Using the ACI criteria, the large amounts of transverse reinforcement result in values of $(c + K_{tr})/d_b \geq 2.5$ (the maximum allowed in the ACI equation) for all splices. Therefore, all splice lengths are equal to 46.7 and 42.6 in. (1186 and 1082 mm) for splices in 5000 and 6000 psi (34.5 and 41.4 MPa) concrete, respectively. All splice lengths calculated using both equations in Chapter 3 are shorter than the splice lengths necessary for compression splices. Therefore, all splice lengths for both conventional and new bars are equal to the 30 d_b compression splice length given in ACI 318-95 section 12.16.1 multiplied by the 0.83 factor of section 12.17.2.4, resulting in a splice length of 35.1 in. (892 mm). As shown in Table 6.15, these splice lengths average 56% and 45% of the original splice lengths for the ACI equation and the equations in Chapter 3, respectively. Even though the splice lengths calculated under the criteria of Chapter 3 are controlled by the compression splice lengths, they still average 80% of the ACI splice lengths. However, this also results in no savings for using high relative rib area bars.

Changes in column steel weight due to the decrease in the column splice lengths are given in Table 6.16. Using the ACI criteria, total column steel weight is reduced by 3.9% to 1,867,942 lb (847,284 kg), compared to the original weight of 1,943,146 lb (881,396 kg). Using the criteria in Chapter 3, the column steel weight is further reduced to 1,849,032 lb (838,707 kg), which represents a 1.0% reduction compared to the weight obtained using the ACI criteria.

Total: Considering all splices and steel in the beams and columns, the ACI criteria produce splice lengths that are, on average, 61% of the original splice lengths, resulting in a reduction in total steel weight of 3.7% compared to the original design. For conventional bars, Eqs. 3.13 and 3.14 produce splice lengths that are, on average, 47% and 50% of the original and 79% and 82% of the ACI splice lengths, respectively. These reductions translate into 4.9% and 4.7% reductions in total steel weight compared to the original weight and 1.3% and 1.1% reductions compared to the ACI design for the two equations. Because compression splice lengths control for the column splices, the overall reduction in steel weight produced by the use of high relative rib area bars compared to conventional bars is only 0.3% for both Eq. 3.13 and 3.14, while average splice length for the beams and columns is reduced by about 9%.

6.5 Advantages of Proposed Design Criteria and High Relative Rib Area Bars

The design criteria described in Chapter 3 require only a slight amount of additional computational effort to calculate development lengths compared to the ACI criteria, but eliminate the need for a separate modification factor for Class B splices. The criteria in Chapter 3 are also based on a more accurate expression than the criteria in ACI 318-95 that, combined with a reliability-based strength reduction factor,

produce a more uniform factor of safety without compromising the economy of a structure.

Perhaps the principal advantage of the new bars is the reduction in steel congestion obtained through the use of shorter splices. When this congestion is caused by close bar spacing and large amounts of transverse reinforcement, the benefits of using high relative rib area bars are the greatest. This means that the new bars will have their largest effect on reducing congestion in the most highly congested areas. As shown by the comparisons for the structures discussed in section 6.4, the effects of using high relative rib area bars depend heavily on the specific splice configurations. Splice lengths for high relative rib area bars are identical to those for conventional bars when transverse reinforcement is not present, but can be significantly shorter when transverse reinforcement is present. On the other hand, splice lengths for epoxy-coated bars are significantly reduced when high relative rib area bars are used in preference to conventional bars. This advantage is a maximum when the bars are confined by transverse reinforcement.

CHAPTER 7: FINITE ELEMENT STUDIES

7.1 General

Brown, Darwin, and McCabe (1993) studied bond using finite element models of a beam-end specimen similar to those described in Chapter 2. The portion of the beam-end specimen that was modeled is shown in Fig. 7.1. In their analysis, cracking of the concrete was modeled only on the vertical plane of symmetry and the reinforcing steel was modeled as a square bar with ribs only on the vertical face. In the current study, the modeling procedure used by Brown et al. (1993) is extended to include multiple crack planes that radiate from the bar, while the bar is modeled using a round, rather than square, cross-section. Only beam-end specimens without transverse reinforcement confining the bar are considered.

The study is conducted in two phases. In the first phase, small models in which only one rib is modeled on the bar are used to investigate the effects of the number of sides on the cross-section of the bar and the number of planes on which cracking of the concrete is modeled. Based on the results of the first phase, a bar shape and number of crack planes are selected for further study using larger models with multiple ribs.

The results of this study are used to gain insight into the fundamental behavior of bond that could aid in the development of a rational, rather than empirical, model for predicting bond strength. The study also provides information that will be useful for modeling splices in beams using the finite element method.

7.2 Finite Element Model

The finite element models in this study represent the portion of a beam-end specimen with a 1 in. (25 mm) diameter bar shown in Fig. 7.1. Based on symmetry,

only one-half of the width of the specimen is modeled. All of the key elements in the bond of reinforcing steel to concrete are explicitly modeled, including cracking of the concrete, bearing of the ribs of the bar on the surrounding concrete, and friction and cohesion between the steel and concrete.

The models are generated using PATRAN 3, release 1.4 (1995). To optimize the solution procedure, nodes are renumbered to minimize the bandwidth using both the Cuthill-McGee and Gibbs-Spool methods. The node numbering for the method producing the minimum bandwidth is retained. The models are analyzed using the POLO-FINITE, release 8.3-12, general purpose finite element software system (Lopez, Dodds, Rehak, and Schmidt 1994).

7.2.1 Fracture Mechanics Model

As discussed in Chapter 2, failure of beam-end specimens generally involves the formation of a dominant crack that runs along the length of the bar, through the top cover, along with other planar cracks radiating from the bar. These cracks arise from tensile stresses in the concrete, produced by bearing of the ribs on the concrete, resulting in Mode I cracking (Fig. 7.2a).

In this study, Mode I cracking is represented using the fictitious crack model developed by Hillerborg et al. (1976) and discussed in Chapter 1. In the fictitious crack model, cracks are assumed to initiate when the stress in the concrete reaches the tensile strength, f'_t. As the crack width increases, the ability of the concrete to transfer stress across the crack, due to interlock of the aggregate and crack bridging around pieces of aggregate, decreases and reaches zero at a crack width w_1. As shown in Fig. 1.2, the stress-crack opening displacement relationship used in this study decreases linearly from f'_t at zero crack width to zero at a crack width of w_1.

The values of f'_t and w_1 used in this study are 0.4 ksi and 0.0029 in. (2.76 MPa and 0.074 mm), respectively. Using a linear relationship for the descending branch of the stress-crack opening displacement relationship, the fracture energy, G_c, can be calculated from Eq. 1.6 as $G_c = 0.5\ f'_t\ w_1 = 0.58$ lb/in. (100 N/m).

In the finite element models presented in this chapter, cracking of the concrete is modeled on the vertical plane of symmetry and on planes radiating from the center of the bar at various angles. Rod elements, oriented perpendicular to the crack planes, are used to transfer stress from one side of the crack to the other. Each crack rod element has two nodes that are initially coincident. Each node has one degree of freedom parallel to the element.

Crack rods along the vertical plane of symmetry represent one-half of the total crack along this plane and are shown in Fig. 7.3. One node is connected to the concrete substructure, while the other node is constrained against movement perpendicular to the crack plane.

Crack rods that do not lie on the vertical plane of symmetry represent the total crack that forms along these planes and are shown in Fig. 7.4. The two nodes for these elements are connected to the concrete substructures on either side of the crack plane.

The stress-crack opening displacement relationship for the concrete is represented by the stress-strain curve for the crack rods shown in Fig. 7.5. Before the stress in the crack rods reaches the tensile strength of the concrete, the stiffness is very high, with a modulus of elasticity, E, of 400,000 ksi (2,758,000 MPa). After reaching the tensile strength of the concrete, stresses in the crack rods are determined based on the linear descending branch of the stress-strain curve and reach zero stress at a strain of 0.0029, which corresponds to a crack width, w_1, of 0.0029 in. (0.074

mm). At strains above 0.0029, the stress is zero. Because the crack rods along the plane of symmetry represent one-half of the total crack, these rods are given a length of 0.5 in. (12.7 mm), while rods on the other planes are given a length of 1 in. (25.4 mm). The area of each crack rod is equal to the tributary area of the concrete elements attached to the same nodes. As shown in Fig. 7.6, the tributary areas are determined by connecting the midpoints of the sides of the concrete elements surrounding the node for each crack rod.

On crack planes not on the plane of symmetry, two additional rod elements are added at each crack rod location to constrain the concrete substructures from sliding relative to one another in the plane of the crack. As shown in Fig. 7.7, both of these constraint rods are oriented with their longitudinal axis in the plane of the crack, one parallel and one perpendicular to the center line of the bar, to prevent Mode II and Mode III cracking (Figs. 7.2b and 7.2c), respectively. Both constraint rods are connected to the same nodes and have the same area and length as the crack rods at the same location. The constraint rods remain linear throughout the analysis, with E = 400,000 ksi (2,758,000 MPa).

7.2.2 Concrete-Steel Interface Representation

The interface between the concrete and steel is modeled using 3-dimensional link elements. As shown in Fig. 7.8, these elements consist of three springs that connect the two nodes of the element. The first spring is oriented normal to the interface surface. The other two springs are mutually perpendicular and lie in the plane of the interface surface. The two nodes are connected to the concrete and steel bar substructures. A third node is used to orient the interface element so that it lies in the plane of the surface of the rib.

Brown et al. (1993) investigated the response of models with interface elements on the entire surface of the ribs and with interface elements only on the compression face of the ribs. They found that interface elements not on the compression face of the ribs no longer contribute to the bond strength after small bar displacements. However, the solution of the model is slowed considerably as these elements change material states. Placing interface elements only on the compression face of the ribs not only decreases the solution time, but gives a good match with the response of models with interface elements on the entire surface of the ribs and has a minimal effect on bond strength. Based on these results, interface elements are placed only on the compression face of the ribs in the current study.

When the node on a rib face lies along a crack plane, two interface elements are used to connect the bar to the concrete substructures on either side of the crack plane. Similarly, when the node on a rib face lies at the intersection of two elements that form rib faces that do not lie in the same plane, two interface elements are used (one oriented normal to the face on each side of the node). In all other cases, only one interface element is used for each node on a rib face.

The contact area assigned to each interface element is chosen so that the sum of the contact areas is equal to that of a rib face with a height of 0.06 in. (1.52 mm) on a 1 in. (25.4 mm) diameter round bar. Tributary areas for the interface elements, based on the shape of the bar in the model, are multiplied by the ratio of the area of the round bar rib face to the total area of the rib face of the shape in the model to arrive at the modified contact area. Tributary areas are calculated similar to those of the crack rod elements discussed in the previous section. The contact area remains constant during the analysis and does not change as the concrete slides relative to the rib face.

The behavior of the interface elements is governed by a Mohr-Coulomb failure surface as shown in Fig. 7.9. This failure surface is defined by the cohesion, c, and the coefficient of friction, μ, between the concrete and the steel and is given by

$$|\sigma_s| = c - \mu\sigma_n \tag{7.1}$$

where $\sigma_s = (\sigma_{sy}^2 + \sigma_{sz}^2)^{1/2}$= the shear stress, σ_{sy} and σ_{sz} are the mutually perpendicular shear stresses in the element, and σ_n is the normal stress in the element. In the analyses, the coefficient of friction, μ, is equal to 0.59 based on the results of tests to determine the coefficient of friction between concrete and uncoated reinforcing steel reported by Idun and Darwin (1995).

The value of c depends on which of the three possible states the element is in. These three states are shown in Fig. 7.9 and include contact/stick, contact/slip, and separation.

In the contact/stick state, defined as (Lopez et al. 1994)

$$|\sigma_s| \leq c - \mu\sigma_n \tag{7.2}$$

c is set to a value of 0.25 ksi (1.72 MPa). This value is the same as that used by Brown et al. (1993). In this state, the shear stress in the element has not exceeded the allowable stress determined by the failure surface, and there is no relative movement between the concrete and the steel. The stiffness matrix for the contact/stick state is given by

$$K_{stick} = \begin{bmatrix} k_n & 0 & 0 \\ 0 & k_{sy} & 0 \\ 0 & 0 & k_{sz} \end{bmatrix} \tag{7.3}$$

where k_n is the normal stiffness and k_{sy} and k_{sz} are the shear stiffnesses. The modulus of elasticity is set to 40,000 ksi (276,000 MPa) to limit the relative displacement between the concrete and steel before the interface elements reach the failure surface. Each of the springs has a length of 1 in. (25.4 mm).

The contact/slip state is reached when the shear stress exceeds the allowable stress determined by Eq. 7.2. Once the contact/slip state has been reached, the value of c is set to zero, representing a loss of cohesion between the concrete and steel. In this state, relative movement in the plane of the interface occurs between the two nodes of the element. The stiffness matrix for the contact/slip state is given by

$$K_{slip} = \begin{bmatrix} k_n & 0 & 0 \\ 0 & \mu k_{sy} & 0 \\ 0 & 0 & \mu k_{sz} \end{bmatrix} \tag{7.4}$$

The separation state occurs when tension stresses arise in the element and the two nodes separate. The stiffness matrix for this state is given by

$$K_{sep} = \begin{bmatrix} \alpha k_n & 0 & 0 \\ 0 & \alpha k_{sy} & 0 \\ 0 & 0 & \alpha k_{sz} \end{bmatrix} \tag{7.5}$$

The parameter α is used to maintain numerical stability of the model by producing a non-singular stiffness in the interface element in the separation state. The value of α is 0.001 in this study. This state occurs only near the end of the analysis, during iterations (see section 7.2.5) that do not converge to a solution.

7.2.3 Concrete Substructure

The concrete substructure is modeled using 8-node isoparametric brick elements. Each node has translational degrees of freedom in the local x, y, and z directions. The elements remain linear elastic throughout the analysis with a modulus of elasticity of 4000 ksi (27.6 MPa) and a Poisson's ratio of 0.2. Crushing of the concrete in front of the ribs is not modeled.

7.2.4 Reinforcing Steel Substructure

The reinforcing steel substructure is also modeled using 8-node isoparametric brick elements that remain linear elastic throughout the analysis. Because various shapes for the cross-section of the bar are investigated in this study, the area, and therefore, the longitudinal stiffness of the reinforcing steel substructure changes between models. To minimize the effects of the change in stiffness on the results of the study, the modulus of elasticity, E, for the steel elements is modified so that the stiffness of the bar for each model corresponds to that of a 1 in. (25.4 mm) diameter round bar with E = 29,000 ksi (200,000 MPa). This is accomplished by multiplying 29,000 ksi (200,000 MPa) by the ratio of the cross-sectional area of a 1 in. (25.4 mm) diameter round bar to the cross-sectional area of the bar in the model to arrive at an effective modulus of elasticity for the steel elements. A Poisson's ratio of 0.30 is used for the steel elements in all of the models.

7.2.5 Solution Procedure

Load is applied to the model by imposing small increments of displacement (load steps) to the nodes at the end of the reinforcing bar substructure. Initially, small increments of displacement, 0.0001 in. (0.00254 mm), are used because of the highly

nonlinear response of the interface elements as they progress from the contact/stick to the contact/slip state. After most of the interface elements have reached the contact/slip state, larger increments of displacement, 0.0005 in. (0.0127 mm), are used. Near the peak load, the model again becomes highly nonlinear because of crack rod elements reaching the descending branch of the stress-strain curve. In this region, it is necessary to reduce the displacement increments to allow the solution to converge for each load step.

Because the models contain elements with nonlinear material properties, an iterative Newton-Raphson solution procedure is used to arrive at a solution for each load step. The iterative solution procedure begins by assuming that the element properties are the same as those for the solution to the previous load step. For the crack rod elements, the secant stiffness, the slope of a line from the origin to the point on the stress-strain curve corresponding to the strain in the element, is used. As discussed previously, the stiffness of the interface elements depends on the state the element is in. Stresses and strains in each element for the current load step are then calculated based on these properties.

The next step is to compute the residual loads, which represent the difference between the nodal loads applied to the structure and the nodal loads calculated based on the current material properties and strains. Residual loads for the crack rod elements are based on the difference between the stress calculated from the secant stiffness assumed at the beginning of the iteration and the stress corresponding to the strain in the element from the stress-strain curve for the element. Residual loads for the interface elements arise when the elements change from one state to another. As mentioned previously, the value for the cohesion and the shear stiffnesses for the

element change when the state of the element changes. The residual loads are based on the difference in shear between the original and the new failure surfaces.

Convergence for the current load step is achieved if the ratio of the Euclidean norm (square root of the sum of the squares) of the residual load vector to the Euclidean norm of the applied load vector is less than a value known as the convergence parameter. In the current study, a convergence parameter of 0.5% is used. If the ratio is above 0.5%, the element properties are updated and another iteration is performed for the current load step.

7.3 Single-Rib Models

In the first phase of the study, small models, with only one rib represented on the bar, are used to investigate the behavior of models with different cross-sectional bar shapes and various numbers of potential crack planes radiating from the bar. The results of this phase serve as the basis for selecting a bar shape and number of potential crack planes for use in larger models with multiple ribs discussed in section 7.4.

7.3.1 Finite Element Models

The finite element models in this portion of the study were selected to allow the effects of bar shape and number of potential crack planes to be investigated using small models that could be quickly constructed and analyzed. The models are based on the finite element models of beam-end specimens analyzed by Brown et al. (1993), but the overall size is reduced.

As shown in Fig. 7.10, the models are 2.5 in. (63.5 mm) wide and 6 in. (152 mm) long. The overall height is 4.5 in. (114 mm) with 2.5 in. (63.5 mm) of concrete below the bar and 1 in. (25.4 mm) cover above the bar.

In all models, the rib height is 0.06 in. (1.52 mm) with a rib face angle of 45°. The rib is located 0.82 in. (20.8 mm) from the front face of the model to represent a 0.5 in. (12.7 mm) lead length, as was used for the beam-end specimens described in Chapter 2, plus one-half of the center-to-center rib spacing of 0.64 in. (16.3 mm). Typical bar and concrete substructures are shown in Fig. 7.11.

Bar Shapes: Models with four different cross-sectional bar shapes are analyzed. The different shapes, shown in Fig. 7.12, were chosen to determine the number of sides necessary to accurately model a 1 in. (25.4 mm) diameter round bar. The shapes are labeled, such as 4H, with the number denoting the number of sides on the perimeter and the letter denoting whether the top side is horizontal (H) or not horizontal (N).

The 4H bar is square with ribs on all sides and the top side horizontal. Bars with eight sides around the perimeter are investigated using two different bar orientations. For the first orientation (8H), the top side of the bar is horizontal. For the second orientation (8N), the top side is at an angle of 22.5° relative to a horizontal line. The final shape (16N) is a 16-sided bar with the top side at an angle of 11.25° relative to a horizontal line.

Crack Planes: The two configurations for potential crack planes investigated are shown in Fig. 7.13. For the first configuration (labeled 45), crack planes are included on the vertical plane of symmetry and on planes at 45°, 90°, and 135° relative to the vertical plane, passing through the center of the bar. In the second configuration (labeled 22.5), additional crack planes are added to those in the first

configuration on planes at 22.5°, 67.5°, 112.5°, and 157.5° relative to the vertical plane. All crack planes extend the entire length of the model.

All four bar shapes are modeled with both crack configurations, for a total of eight models. The model labels indicate the bar shape followed by the crack configuration. The number of nodes and elements for each model is summarized in Table 7.1.

Boundary Conditions: The boundary conditions, shown in Fig. 7.10, were chosen so that a compressive strut does not intersect the bar when the end of the bar is displaced. Nodes on the bottom surface of the model are constrained against moving vertically (z direction). Nodes at the back of the bottom surface are constrained against moving longitudinally (y direction). Nodes for the reinforcing steel substructure that lie on the plane of symmetry are constrained against moving laterally (x direction).

7.3.2 Results and Observations

As displacement is applied to the nodes at the end of the bar, the interface elements progress from the contact/stick to the contact/slip state. This generally occurs within the first 5 load steps [total displacement = 0.0005 in. (0.0127 mm)]. As displacement of the end of the bar is increased, cracking begins to occur (see section 7.2.1). Initially, all of the crack planes open slightly near the compression face of the rib. Near the peak load, some crack planes begin to dominate, while other crack planes close. Opening of the crack planes reduces the clamping force on the bar, producing a reduction in the total force in the bar. After the peak load is reached, the force in the bar decreases rapidly with little increase in displacement of the end of the

bar. The analysis is terminated after the force in the bar begins to drop and a load step fails to converge to a solution because of extensive cracking.

Load-Displacement Response: Load-displacement curves for models with the 45 and 22.5 crack configurations are shown in Figs. 7.14 and 7.15, respectively. The total load, or bar force, for each model is obtained by summing the reactions at the nodes on the end of the bar at which the displacement is applied and multiplying by two because only one-half of the specimen is modeled. The bar displacement plotted is the total displacement of nodes on the end of the bar. As shown in Figs. 7.14 and 7.15, the initial stiffness of the load-displacement curves is nearly identical for all models. Peak loads and displacements at peak load are given in Table 7.2.

The load-displacement curves for the models with the 4H, 8N, and 16N bar shapes and both crack plane configurations are compared in Fig. 7.16. This figure shows that the load-displacement response and the peak loads for these models differ somewhat based on bar shape, but are not sensitive to the differences in the two crack plane configurations. For the fourth bar shape, 8H, however, the load-displacement response of the two models do differ slightly from one another, as shown in Fig. 7.17. In this case, the 8H-45 model produces slightly higher bar forces than the 8H-22.5 model prior to the peak load. The peak loads, however, are nearly identical.

As shown in Table 7.2, the highest peak loads are produced by the models with the 4H and 8H bar shapes. The average peak loads for both crack configurations are 13,360 and 12,870 lb (59.4 and 57.2 kN) for the 4H and 8H bar shapes, respectively, while the average peak loads for the 8N and 16N bar shapes are 11,790 and 12,050 lb (52.4 and 53.6 kN), respectively.

Cracking Response: Load-crack width curves for models with the 45 and 22.5 crack configurations are shown in Figs. 7.18 and 7.19, respectively. The crack

width plotted is twice the lateral (x direction) displacement of the node on the concrete substructure at the intersection of the plane of symmetry, the front face of the model, and the top surface of the model. Crack widths at peak load are given in Table 7.2.

As shown in Figs. 7.18 and 7.19, the initial response is very similar for all models. However, above a bar force of about 5,000 lb (22.2 kN), the curves begin to differ, with the largest bar force at a given crack width produced by models with the 4H bar shape followed by the 8H, 16N and 8N bar shapes. These figures also show that the crack widths for the models with the 4H bar shape increase up to a bar force of about 13,000 lb (57.8 kN) and then decrease until the peak load is reached.

The load-crack width curves for the models with the 4H, 8N, and 16N bar shapes and both crack plane configurations are compared in Fig. 7.20. This figure shows that, as with the load-displacement response, the load-crack width response for models with the same bar shape are nearly identical, regardless of which crack plane configuration is used.

As shown in Fig. 7.21, the load-crack width response of the two models containing the 8H bar shape is affected by the crack plane configuration. The 8H-45 model produces higher bar forces at a given crack width than the 8H-22.5 model prior to the peak load. However, both models produce nearly identical crack widths at failure, resulting in nearly the same clamping force applied by the concrete to the bar as shown by the peak loads of 12,892 and 12,855 lb (57.3 and 57.2 kN) for the 8H-45 and 8H-22.5 models, respectively.

In all models, except 4H-45, 4H-22.5, and 8H-22.5, the dominant splitting plane is the vertical plane of symmetry, similar to that shown in Fig. 7.22 for the 16N-

45 model at peak load. Some splitting also occurs along other planes but does not lead to failure of the specimen.

For the 4H-45 and 4H-22.5 models, the dominant splitting plane is the 45° crack plane, as shown in Fig. 7.23 for the 4H-22.5 model at peak load. Initially, splitting along the 45° plane begins near the bar and forces the top segment of the concrete substructure to twist, resulting in an increase in crack width along the vertical plane. At a bar force of about 13,000 lb (57.8 kN), splitting along the 45° plane reaches the top surface of the model. As this plane continues to open, the crack rods along it transfer less of a twisting force to the top segment of the concrete substructure, and the crack width along the vertical plane begins to decrease.

For the 8H-22.5 model, dominant splitting planes form through the top cover of the bar and on the 67.5° and 157.5° crack planes, as shown in Fig. 7.24. As splitting on the 157.5° crack plane increases, the boundary conditions on the bottom plane of the model restrain crack growth on this plane. This causes the solution to become unstable, converging for only one load step past the peak load. The difference in crack pattern from the 8H-45 model explains the differences observed in the bar force-displacement curves (Fig. 7.17) and bar force-crack width curves (Fig. 7.21).

Table 7.2 shows that crack widths at peak load are nearly identical for models with the 8H, 8N, and 16N bar shapes, ranging from 0.00515 in. (0.131 mm) for the 8H-45 model to 0.00528 in. (0.134 mm) for the 16N-22.5 model. Crack widths at peak load for the 4H-45 and 4H-22.5 models, however, are only about one-half of these values because the dominant splitting plane is the 45° crack plane.

7.3.3 Evaluation

The results and observations presented in section 7.3.2 form the basis for selecting a bar shape and crack plane configuration for further study using models with multiple ribs.

Due to their unusual cracking response, the 4H-45, 4H-22.5, and 8H-22.5 models are rejected as possible candidates for further study. The response of the 8N-45, 8N-22.5, 16N-45, and 16N-22.5 models are very similar to one another, while the peak load for 8H-45 model is unusually high compared to the other four models. The 8H-45 model is rejected for this reason.

The choice between the remaining four models (8N-45, 8N-22.5, 16N-45, and 16N-22.5) is based on the number of nodes and elements required and how accurately the model represents a round bar. As shown in Table 7.1, the models with crack planes at 22.5° intervals (8N-22.5 and 16N-22.5) require a substantial increase in the number of nodes and elements compared to the models with crack planes at 45° intervals (8N-45 and 16N-45), with very little effect on model response. This increase would be much bigger for the larger, multiple rib models and is not justified when considering the very small effect the additional crack planes have on the response of the models. While there is a small increase in the number of nodes and elements for the 16N-45 model, compared to the 8N-45, due to the number of nodes and elements used to model the bar, this increase is justified due to the more accurate representation of a round bar provided by the 16N bar shape. Therefore, the bar shape and crack plane configuration used in the 16N-45 model are chosen for further investigation in the multiple-rib models.

7.4 Multiple-Rib Models

Based on the results presented in section 7.3, a model with a 16-sided bar shape and potential crack planes at 45° intervals is chosen for further study using larger, multiple-rib models. A total of eight models with 1, 3, 6 or 12 ribs and 1 or 2 in. (25.4 or 50.8 mm) cover are analyzed. The overall dimensions of the models are larger than those of the single-rib models and match those used by Brown et al. (1993). The portion of a beam-end specimen represented is shown in Fig. 7.1.

7.4.1 Finite Element Models

As shown in Fig. 7.25, the finite element models are 4.5 in. (114 mm) wide and 12 in. (305 mm) long. The overall height is 7 or 8 in. (178 or 203 mm) with 5 in. (127 mm) of concrete below the bar and 1 or 2 in. (25.4 or 50.8 mm) cover above the bar. Based on symmetry, only one-half of the width of the specimen is modeled.

The reinforcing bar substructure for all models and the concrete substructure for the model with 2 in. (50.8 mm) cover are shown in Figs. 7.26a and 7.26b, respectively. The number of nodes and elements in the models are given in Table 7.3.

The reinforcing bar substructure has a 16-sided cross-section (16N in Fig. 7.12). The rib dimensions are the same as those used for the single-rib models, with a rib height of 0.06 in. (1.52 mm), a center-to-center spacing of 0.64 in. (16.3 mm), and a face angle of 45°, matching those used by Brown et al. (1993). As in the single-rib models, the first rib is located 0.82 in. (20.8 mm) from the front face of the model to represent a 0.5 in. (12.7 mm) lead length plus one-half of the center-to-center spacing, and interface elements are included only on the compression face of the ribs.

To simplify the modeling, a single model, containing a reinforcing bar substructure with 12 ribs, is used for each value of cover. 1, 3, and 6 rib models are

created by removing the interface elements on the 11, 9, and 6 ribs farthest from the front face, respectively. Besides reducing the number of models created, this procedure has the added advantage of maintaining the same finite element mesh for all models with the same cover.

The boundary conditions are similar to those used for the single-rib models and are shown in Fig. 7.25. Nodes on the bottom surface of the model are constrained against moving vertically (z direction). Nodes at the center line of the bottom surface (oriented in the x direction) are constrained against moving longitudinally (y direction). Nodes for the reinforcing steel substructure that lie on the plane of symmetry are constrained against moving laterally (x direction). These boundary conditions were shown by Brown et al. (1993) to produce stress conditions near the bar that are similar to those in a beam-end specimen.

7.4.2 Results and Observations

The eight models described in the previous section are used to determine the effects of cover and embedded length, or number of ribs, on the response of the model. The overall response is similar to that of the 16N-45 model, described in section 7.3, on which the multiple-rib models are based. The specific response of each of the models is discussed in this section.

For models with interface elements on more than one rib, the interface elements on the rib nearest the loaded end of the bar progress from the contact/stick state to the contact/slip state first. As displacement of the end of the bar is increased, interface elements farther from the loaded end of the bar progress to the contact/slip state.

Load-Displacement Response: Load-displacement curves for the eight models are shown in Fig. 7.27. Peak loads and the displacement at the end of the bar at peak load are given in Table 7.4.

Fig. 7.27 shows that the initial stiffness of the load-displacement curves increases as the number of ribs on the bar increases. Models with 1 in. (25.4 mm) cover produce a smaller bar force at a given displacement than models with the same number of ribs and 2 in. (50.8 mm) cover.

As displacement of the end of the bar increases, an initial drop in load corresponding to the vertical crack plane beginning to open occurs. After the initial drop in load, bar force begins to increase again, but the stiffness of the load-displacement curve is much lower. In the models with 2 in. (50.8 mm) cover and 3, 6, and 12 ribs, the peak load occurs after the initial drop in load. For all other models, the peak load occurs just prior to the initial drop in load. After the initial drop in load, the solution for the 12 rib model with 1 in. cover converges for only extremely small increments of displacement and produces a very short descending branch of the load-displacement curve.

The initial drop in load corresponds to the beginning of splitting on the vertical crack plane and a reduction in the clamping forces on the bar produced by the concrete along this plane. However, as the vertical crack plane continues to open, the clamping forces produced by other crack planes increase, resulting in an increase in the force in the bar. This will be discussed further in the section describing the cracking response of the models.

Load-Slip Response: Load versus loaded and unloaded end slip curves for the models are shown in Figs. 7.28 and 7.29, respectively. Values of loaded and unloaded end slip at peak load are given in Table 7.4. The nodal displacements used

to calculate loaded and unloaded end slip were chosen to replicate, as closely as possible, the methods used for actual beam-end specimens. Loaded end slip is the difference between the longitudinal (y direction) displacements of the loaded end of the bar and the concrete node on the 90° crack plane at the outside of the model. Unloaded end slip is the difference between the longitudinal displacements of the node on the perimeter of the unloaded end of the bar at the location of the 90° crack plane and the two nodes on the 90° crack plane at the perimeter of the bar. All of the nodes used to calculate unloaded end slip are initially coincident.

The loaded end slip curves for each model are very similar to the load-displacement curves for the same model. At a certain load, the value of loaded end slip is less than the bar displacement due to the deformation of the concrete substructure. As expected, the unloaded end slip curves are stiffer than the loaded end slip curves, especially for models with 3, 6, and 12 ribs.

As shown in Table 7.4, all models with 2 in. (50.8 mm) cover produce higher values of loaded and unloaded end slip at peak load than the model with the same number of ribs and 1 in. (25.4 mm) cover. For the 3, 6, and 12 rib models, the difference in slip values at peak load between models with 1 and 2 in. (25.4 and 50.8 mm) cover is larger than for the 1 rib models. This occurs because the peak loads for the models with 3, 6, and 12 ribs and 2 in. (25.4 mm) cover occur after the initial drop in load, producing a much larger value of bar displacement at peak load than for the other models.

Cracking Response: Load-crack width curves for the models are shown in Fig. 7.30. The crack width plotted is twice the lateral (x direction) displacement of the node on the concrete substructure at the intersection of the plane of symmetry, the

front face of the model, and the top surface of the model. Crack widths at peak load are given in Table 7.4.

As shown in Fig. 7.30, models with 1 in. (25.4 mm) cover produce larger crack widths at a given load than the models with the same number of ribs and 2 in. (50.8 mm) cover. After the initial drop in load, crack widths increase more rapidly than before the initial drop in load as additional displacement is applied to the end of the bar. For all models, the crack width corresponding to the initial peak load is smaller in the 2 in. (50.8 mm) cover model than in the 1 in. (25.4 mm) cover model with the same number of ribs.

As shown in Table 7.4, the models in which the peak load occurs before the initial drop in load [all models with 1 in. (25.4 mm) cover and the 1 rib model with 2 in. (50.8 mm) cover] produce crack widths at peak load ranging from 0.0064 to 0.0078 in. (0.163 to 0.198 mm). The models in which the peak load occurs after the initial drop in load [the 3, 6, and 12 rib models with 2 in. (50.8) cover] produce much larger crack widths at peak load that range from 0.0147 to 0.0159 in. (0.373 to 0.404 mm).

The dominant splitting plane for all models develops along the vertical plane of symmetry. As the vertical crack plane begins to dominate near the initial peak load, other crack planes also begin to open.

For the 3, 6, and 12 rib models with 2 in. (50.8 mm) cover, the deformed shape at the initial peak load, shown in Fig. 7.31a for the model with 6 ribs, shows that splitting has occurred along the vertical plane of symmetry, while the 90° crack plane is just beginning to open. The deformed shape at the peak load, shown in Fig. 7.31b, shows that significant additional splitting has occurred along the vertical plane and that the 90° crack plane has continued to open.

For all models with 1 in. (25.4 mm) cover and the 1 rib model with 2 in. (50.8 mm) cover, the deformed shape at the peak load, shown in Fig. 7.32a for the 6 rib model with 1 in. (25.4 mm) cover, is very similar to the deformed shape for the initial peak load of the 6 rib model with 2 in. (50.8 mm) cover (Fig. 7.31a). However, as shown in Fig. 7.32b for a bar displacement of 0.012 in. (0.305 mm), as the displacement at the end of the bar is increased for these models, the 45° crack plane begins to open, while the 90° crack plane closes. This may explain why these models did not produce a higher peak load after the initial drop in load occurs, because less force is required to split the 45° crack plane, compared to the 90° crack plane.

7.4.3 Evaluation

The results for the multiple-rib models discussed in section 7.4.2 provides insight into some of the observations from the analysis of the splice and development data on which the design equations in Chapter 3 are based.

As mentioned in Chapters 3 and 6, the design criteria in Chapter 3 are based on the assumption that the relationship between bond strength and development length is linear, but not proportional. The peak load for each of the models, given in Table 7.4, is plotted as a function of the product of the development length, l_d, and the cover to the center of the bar, $c_m + 0.5d_b$, in Fig. 7.33. This figure shows that the relationship between bond strength and $l_d(c_m + 0.5d_b)$ is nearly linear. An extrapolation of the relationship in Fig. 7.33 shows that a substantial bond force should exist for $l_d(c_m + 0.5d_b) = 0$. Clearly, no bond force could be produced if $l_d(c_m + 0.5d_b) = 0$, but these results show that the initial portion of the embedment length mobilizes a significant portion of the clamping force of the concrete. Increasing the embedment length, or number of ribs, mobilizes additional clamping force. However,

the increase is not in proportion to the increase in embedment length, which supports the assumption used in the design criteria in Chapter 3.

Although the relationship shown in Fig. 7.33 is nearly linear, bond strengths for larger values of $l_d(c_m + 0.5d_b)$ are slightly lower than expected based on the bond strengths for smaller values. In actual structures, crushing of the concrete in front of the ribs, which is not represented in the current study, would allow additional slip at the ribs where crushing occurs. This would result in an increase bond strength for larger embedment lengths, by producing a more uniform distribution of the clamping forces along bar, and a more linear relationship between bond strength and $l_d(c_m + 0.5d_b)$ than that shown in Fig. 7.33.

The design expression given in Eq. 3.13 includes a term that accounts for the observation that bond strength increases as the ratio of c_M to c_m increases. An analysis of the stresses in the interface elements for the finite element models provides some insight as to why this may occur.

Figs. 7.34a to 7.34c show the average normal stresses in the interface elements for each rib in the 3 rib model with 2 in. (50.8 mm) cover as a function of their position around the circumference of the bar. The average stresses plotted are the average for all interface elements at each angle. The angles are defined in the same way as the crack planes shown in Fig. 7.13.

The average normal stresses corresponding to a bar displacement of 0.0055 in. (0.140 mm) and a bar force of 18,339 lb (81.6 kN), a point on the ascending branch of the load-displacement curve prior to the initial drop in load, are shown in Fig. 7.34a. This figure shows that, for each rib, the normal stresses are nearly uniform around the perimeter of the bar. The stresses are slightly higher on rib 3 than on ribs 1 and 2, due

to splitting occurring near the front of the model and reducing the local clamping force applied by the concrete to the bar.

The average normal stresses corresponding to a bar displacement of 0.0105 in. (0.267 mm) and a bar force of 30,888 lb (137.4 kN), the initial peak load for the model, are shown in Fig. 7.34b. This figure shows that normal stresses increase from rib 1 to rib 2 to rib 3, due to splitting near the front of the model, but are still fairly uniform around the perimeter of the bar.

The average normal stresses corresponding to a bar displacement of 0.0144 in. (0.366 mm) and a bar force of 32,711 lb (145.5 kN), the peak load for the model, are shown in Fig. 7.34c. At the peak load, normal stresses in the interface elements are highest on the top and bottom of the bar. This occurs because splitting has occurred on the vertical plane, allowing the concrete substructure to move laterally and reducing the stresses in the interface elements near 90°. However, there are still significant stresses in the interface elements on the top and bottom of the bar because the 90° crack plane is just beginning to open. It would be expected that if the cover along the 90° crack plane were decreased, more splitting would occur on this plane and the stresses at the top and bottom of the bar would be reduced. This would result in a decrease in the total force in the bar as c_M/c_m decreases, which supports the use of the term related to c_M/c_m in Eq. 3.13.

CHAPTER 8: SUMMARY AND CONCLUSIONS

8.1 Summary

The effects of deformation properties on the bond of steel reinforcing bars to concrete are studied using beam-end and splice tests. Development and splice length design equations that account for the effects of bar size, relative rib area, and epoxy coating on bond strength are presented. These design equations are applied to splices in actual structures to investigate both the economic and practical construction benefits resulting from the use of high relative rib area bars. Beams with continuous reinforcement are used to study the effects of relative rib area on the behavior of beams in which plastic hinges develop. The fundamental behavior of bond is studied using finite element analysis.

Beam-end tests are used to investigate the effects of bar size, relative rib area, and the ratio of rib width (measured parallel to the longitudinal axis of the bar) to center-to-center rib spacing. Specimens both with and without transverse stirrups confining the test bar were used. Seventy-two specimens containing 5/8 and 1 in. (16 and 25 mm) diameter bars with relative rib areas, R_r, of 0.05, 0.10, and 0.20 were tested to investigate the effects of bar size and relative rib area on bond strength. Fifty-five specimens containing 1 in. (25 mm) bars with relative rib areas of 0.10 and 0.20 were tested to investigate the effects of the ratio of rib width to center-to-center rib spacing, W_r. For each value of R_r, the rib width was varied, while maintaining a constant center-to-center rib spacing, to produce values of W_r ranging from 0.182 to 0.727. Twelve specimens containing 1 in. (25 mm) diameter threaded bars with a relative rib area of 0.28 were tested to investigate the bond performance of bars with an ultra-high relative rib area.

Splice tests are used to investigate the effects of bar size, relative rib area, epoxy coating, and the amount of transverse reinforcement confining the bars on splice strength. Thirty tests of beams containing No. 5 and No. 11 (16 and 36 mm) bars are combined with sixty-three tests of beams containing No. 8 (25 mm) bars reported by Idun and Darwin (1995) and Hester, Salamizavaregh, Darwin and McCabe (1991, 1993). The combined results include tests using bars with R_r ranging from 0.065 to 0.140. Accurate splice strength equations that account for the effects of bar size, relative rib area, and epoxy coating on bond strength are presented. These equations are combined with a reliability-based strength reduction factor developed by Darwin, Idun, Zuo and Tholen (1995b) to arrive at design equations for splice and development lengths. The new design equations are applied to splices in a bridge and the lateral load resisting frame system of a building to investigate the economic and practical construction benefits resulting from the use of high R_r bars.

Six splice specimens containing 1 in. (25 mm) diameter threaded bars with a relative rib area of 0.28 were tested to investigate the splice strength of bars with an ultra-high relative rib area. The main test parameters include (1) the degree of confinement provided by transverse reinforcement and (2) interlocking of the ribs.

Four beam specimens containing continuous reinforcing bars were used to investigate the effects of R_r on the rotational capacity of beams in which plastic hinges develop. Two specimens containing conventional No. 8 (25 mm) bars (R_r = 0.069) and two specimens containing high relative rib area No. 8 (25 mm) bars (R_r = 0.119) were tested.

Finite element models representing a portion of a beam-end specimen are used to gain insight into the fundamental behavior of bond that could aid in the development of a rational, rather than empirical, model for predicting bond strength.

All of the key elements of bond are represented. Various cross-sectional shapes for the reinforcing bar and multiple crack planes that radiate from the bar are investigated to determine the configuration that best represents a round bar.

8.2 Observations and Conclusions

The following observations and conclusions are based on the results and analyses presented in this report.

8.2.1 Beam-End Tests

1. Under all conditions of confinement, bond strength increases with an increase in bar diameter.
2. Bond strength increases when transverse reinforcement is added, compared to the bond strength of bars without transverse reinforcement. The amount of the increase in bond strength due to transverse reinforcement increases with an increase in bar diameter and relative rib area, independent of the specific combination of rib height and spacing.
3. The width of the longitudinal splitting crack that accompanies bar slip is not affected by rib height prior to specimen failure. Therefore, rib heights for commercially produced bars do not need to be limited due to concerns about increased crack width in reinforced concrete members.
4. The width of the longitudinal splitting crack that accompanies bar slip increases with an increase in relative rib area, due to the greater wedging action provided by bars with higher relative rib areas.
5. Bond strength decreases when the ratio of rib width to center-to-center rib spacing is greater than 0.66 and 0.45 for specimens without and with

transverse reinforcement, respectively. Therefore, rib widths for commercially produced bars should be limited to no greater than 45% of the center-to-center rib spacing.

8.2.2 Splice Tests

1. The splice strength of uncoated bars not confined by transverse reinforcement does not appear to be affected by deformation pattern for bars with relative rib areas ranging from 0.065 to 0.140.
2. The splice strength of bars confined by transverse reinforcement increases with an increase in the relative rib area of the spliced bars.
3. The splice strength of bars confined by transverse reinforcement increases with an increase in the diameter of the spliced bars.
4. The increase in splice strength provided by transverse reinforcement is influenced by the properties of the coarse aggregate used in the concrete. For a given concrete compressive strength, higher strength coarse aggregates provide higher bond strengths.
5. Epoxy coating appears to have a less detrimental effect on the splice strength of high relative rib area bars than on the splice strength of conventional bars.

8.2.3 Splice Tests of Ultra-High Relative Rib Area Bars

1. The splice strength of ultra-high relative rib area bars not confined by transverse reinforcement may be up to 10% higher than that of conventional bars. However, more tests are needed to determine if this apparent increase is real or the result of experimental scatter.

2. The splice strength of ultra-high relative rib area bars confined by transverse reinforcement increases significantly if the ribs are allowed to interlock.

8.2.4 Moment-Rotation Tests

1. For beams with continuous reinforcement, the relative rib area of the reinforcing bar does not appear to effect the distribution of flexural cracks for beams in which plastic hinges develop.
2. For beams with continuous reinforcement, the relative rib area of the reinforcing bar does not appear to effect the displacement or rotational capacity of beams in which plastic hinges develop.

8.2.5 Splice Length Comparisons and Estimated Material Savings

1. The use of reinforcing bars with an average relative rib area of 0.1275 (minimum $R_r = 0.12$) can provide up to a 26% decrease in splice length for uncoated bars and up to a 42% decrease in splice length for epoxy-coated bars compared to conventional reinforcement. The savings obtainable with the high relative rib area bars are highest for low covers and bar spacings and high amounts of confining transverse reinforcement. The reduction in splice length decreases with increases in cover and bar spacing and decreases in transverse reinforcement. The relative savings with high R_r bars also decreases for high levels of confinement that result in bar pullout rather than concrete splitting governing bond strength.
2. Even when transverse reinforcement confining the splice is not present, the use of high relative rib area epoxy-coated bars can provide up to a

23% decrease in splice length compared to conventional epoxy-coated bars.

3. The shorter development and splice lengths necessary for high R_r bars reduce steel congestion, resulting in practical construction, as well as economic, benefits compared to conventional bars.
4. For uncoated No. 6 (19 mm) and smaller bars without transverse reinforcement, splice lengths obtained using Eq. 3.14 (the more conservative of the two design equation presented in Chapter 3) can range from 18% shorter to 56% longer than Class A splice (or development) lengths obtained using the ACI 318-95 criteria and from 37% shorter to 20% longer than Class B splice lengths obtained using the ACI 318-95 criteria. For uncoated No. 7 (22 mm) and larger bars without transverse reinforcement, splice lengths obtained using Eq. 3.14 can range from 34% shorter to 25% longer than Class A splice (or development) lengths obtained using the ACI 318-95 criteria and from 50% to 4% shorter than Class B splice lengths obtained using the ACI 318-95 criteria. A comparison with test data shows that the shorter splice lengths obtained using ACI 318-95 correspond to increasingly unconservative estimates of bond strength as l_d/d_b increases, especially for small bars.
5. For typical splice configurations, the design criteria presented in Chapter 3 produce significant reductions in splice length. Compared to designs using the ACI 318-95 criteria, splice lengths obtained using Eqs. 3.13 and 3.14:
   a. average 26% and 21% shorter and produce 0.93% and 0.50% reductions in total steel weight, respectively, for conventional bars in the bridge structure investigated.

b. average 35% and 31% shorter and produce 1.35% and 1.01% reductions in total steel weight, respectively, for high R_r bars in the bridge structure investigated.

c. average 21% and 18% shorter and produce 1.27% and 1.06% reductions in total steel weight, respectively, for conventional bars in the building structure investigated.

d. average 28% and 25% shorter and produce 1.51% and 1.35% reductions in total steel weight, respectively, for high R_r bars in the building structure investigated.

8.2.6 Finite Element Studies

1. Of the configurations investigated, a bar with a 16-sided cross section and potential cracking planes at 45° intervals provides the best representation of a round bar.
2. An increase in bond force and slip at the peak load results from an increase in cover.
3. The relationship between bond strength and the product of embedded length and cover to the center of the bar is nearly linear.
4. An increase in bond strength results from an increase in embedded length. However, the increase in bond strength is not in proportion to the increase in embedded length.

8.3 Recommendations for Future Study

Research at the University of Kansas investigating the effects of deformation pattern on the bond performance of reinforcing bars is continuing. The current study

has addressed several key aspects related to bond performance, but further research is needed in the following areas.

1. The bond performance of high relative rib area bars in high strength concrete.
2. The bond performance of epoxy-coated bars in high strength concrete.
3. The bond performance of high relative rib area bars when used as top-cast bars.
4. The effects of unsymmetrical bar placement on bond strength.
5. The effects of shear along the development or splice length on bond strength.
6. The effects of splicing bars in multiple layers on splice strength.
7. The bond performance of high relative rib area bars when subjected to cyclic loading.
8. The effects of splice length and relative rib area on crack widths in beam specimens.
9. Finite element analyses in which crushing of the concrete and transverse reinforcement are represented.
10. Finite element analyses in which splices of reinforcing bars are modeled.

REFERENCES

AASHTO Highway Sub-Committee on Bridges and Structures. (1992). *Standard Specifications for Highway Bridges*, 15th Edition, American Association of State Highway and Transportation Officials, Washington, D.C., 686 pp.

Abrams, D. A. (1913). "Tests of Bond Between Concrete and Steel," *Bulletin* No. 71, Engineering Experiment Station, University of Illinois, Urbana, IL, Dec., 238 pp.

ACI Committee 318. (1963). *Building Code Requirements for Reinforced Concrete (ACI 318-63)*, American Concrete Institute, Detroit, MI, 144 pp.

ACI Committee 318. (1989). *Building Code Requirements for Reinforced Concrete (ACI 318-89) and Commentary - ACI 318R-89*, American Concrete Institute, Detroit, MI, 353 pp.

ACI Committee 318. (1989) (Revised 1992). *Building Code Requirements for Reinforced Concrete (ACI 318-89) (Revised 1992) and Commentary - ACI 318R-89 (Revised 1992)*, American Concrete Institute, Detroit, MI, 347 pp.

ACI Committee 318. (1994). "Proposed Revisions to Building Code Requirements for Reinforced Concrete (ACI 318-89) (Revised 1992) and Commentary - ACI 318R-89 (Revised)," *Concrete International*, Vol. 16, No. 12, Dec., pp. 76-128.

ACI Committee 318. (1995). *Building Code Requirements for Structural Concrete (ACI 318-95) and Commentary (ACI 318R-95)*, American Concrete Institute, Farmington Hills, MI, 369 pp.

ASTM A 615/A 615M-95b. (1996). "Standard Specification for Deformed and Plain Billet-Steel Bars for Concrete Reinforcement," *1996 Annual Book of ASTM Standards*, Vol. 1.04, American Society for Testing and Materials, Philadelphia, PA, pp. 302-307.

ASTM A 616/A 616M-95b. (1996). "Standard Specification for Rail-Steel Deformed and Plain Bars for Concrete Reinforcement," *1996 Annual Book of ASTM Standards*, Vol. 1.04, American Society for Testing and Materials, Philadelphia, PA, pp. 308-312.

ASTM A 617/A 617M-95b. (1996). "Standard Specification for Axle-Steel Deformed and Plain Bars for Concrete Reinforcement," *1996 Annual Book of ASTM Standards*, Vol. 1.04, American Society for Testing and Materials, Philadelphia, PA, pp. 313-317.

ASTM A 706/A 706M-95b. (1996). "Standard Specification for Low-Alloy Steel Deformed Bars for Concrete Reinforcement," *1996 Annual Book of ASTM Standards*, Vol. 1.04, American Society for Testing and Materials, Philadelphia, PA, pp. 344-348.

ASTM A 722-90. (1996). "Standard Specification for Uncoated High-Strength Steel Bar for Prestressing Concrete," *1996 Annual Book of ASTM Standards*, Vol. 1.04, American Society for Testing and Materials, Philadelphia, PA, pp. 359-362.

ASTM A 775/A 775M-95. (1996). "Standard Specification for Epoxy-Coated Reinforcing Steel Bars," *1996 Annual Book of ASTM Standards*, Vol. 1.04, American Society for Testing and Materials, Philadelphia, PA, pp. 408-414.

Azizinamini, A.; Stark, M.; Roller, John H.; and Ghosh, S. K. (1993). "Bond Performance of Reinforcing Bars Embedded in High-Strength Concrete," *ACI Structural Journal*, Vol. 95, No. 5, Sept.-Oct., pp. 554-561.

Azizinamini, A.; Chisala, M.; and Ghosh, S. K. (1995). "Tension Development Length of Reinforcing Bars Embedded in High-Strength Concrete," *Engineering Structures*, in press.

Barsom, John, and Rolfe, Stanley. (1987). *Fracture and Fatigue Control in Structures*, 2nd edition, Prentice-Hall, pp. 30-38.

Brettmann, Barrie B.; Darwin, David; and Donahey, Rex C. (1984). "Effects of Superplasticizers on Concrete-Steel Bond Strength," *SL Report* 84-1, University of Kansas Center for Research, Lawrence, Kansas, April, 32 pp.

Brettmann, Barrie B.; Darwin, David; and Donahey, Rex C. (1986). "Bond of Reinforcement to Superplasticized Concrete," ACI Journal, *Proceedings* Vol. 83, No. 1, Jan.-Feb., pp. 98-107.

Brown, Christian J.; Darwin, David; and McCabe, Steven L. (1993). "Finite Element Fracture Analysis of Steel-Concrete Bond," *SM Report* No. 36, University of Kansas Center for Research, Lawrence, Kansas, Nov., 100 pp.

Cairns, J. (1994). "Disc. 90-S65," *ACI Structural Journal*, Vol. 91, No. 5, Sept.-Oct., pp. 626-629.

Chamberlin, S. J. (1956). "Spacing of Reinforcement in Beams," ACI Journal, *Proceedings* Vol. 53, No. 1, July, pp. 113-134.

Chamberlin, S. J. (1958). "Spacing of Spliced Bars in Beams," ACI Journal, *Proceedings* Vol. 54, No. 8, Feb., pp. 689-698.

Chinn, James; Ferguson, Phil M.; and Thompson, J. Neils. (1955). "Lapped Splices in Reinforced Concrete Beams," ACI Journal, *Proceedings* Vol. 52, No. 2, Oct., pp. 201-214.

Choi, Oan Chul; Hadje-Ghaffari, Hossain; Darwin, David; and McCabe, Steven L. (1990a). "Bond of Epoxy-Coated Reinforcement to Concrete: Bar Parameters," *SL Report* 90-1, University of Kansas Center for Research, Lawrence, Kansas, Jan., 43 pp.

Choi, Oan Chul; Darwin, David; and McCabe, Steven L. (1990b). "Bond Strength of Epoxy-Coated Reinforcement to Concrete," *SM Report* No. 25, University of Kansas Center for Research, Lawrence, Kansas, July, 217 pp.

Choi, Oan Chul; Hadje-Ghaffari, Hossain; Darwin, David; and McCabe, Steven L. (1991). "Bond of Epoxy-Coated Reinforcement: Bar Parameters," *ACI Materials Journal*, Vol. 88, No. 2, Mar.-Apr., pp. 207-217.

Clark, A. P. (1946). "Comparative Bond Efficiency of Deformed Concrete Reinforcing Bars," ACI Journal, *Proceedings* Vol. 43, No. 4, Dec., pp. 381-400.

Clark, A. P. (1949). "Bond of Concrete Reinforcing Bars," ACI Journal, *Proceedings* Vol. 46, No. 3, Nov., pp. 161-184.

Darwin, David; McCabe, Steven L.; Idun, Emmanuel K.; and Schoenekase, Steven P. (1992a). "Development Length Criteria: Bars Without Transverse Reinforcement," *SL Report* 92-1, University of Kansas Center for Research, Lawrence, Kansas, Apr., 62 pp.

Darwin, David; McCabe, Steven L.; Idun, Emmanuel K.; and Schoenekase, Steven P. (1992b). "Development Length Criteria: Bars Not Confined by Transverse Reinforcement," *ACI Structural Journal*, Vol. 89, No. 6, Nov.-Dec., pp. 709-720.

Darwin, David, and Graham, Ebenezer K. (1993a). "Effect of Deformation Height and Spacing on Bond Strength of Reinforcing Bars," *SL Report* 93-1, University of Kansas Center for Research, Lawrence, Kansas, Jan., 68 pp.

Darwin, David, and Graham, Ebenezer K. (1993b). "Effect of Deformation Height and Spacing on Bond Strength of Reinforcing Bars," *ACI Structural Journal*, Vol. 90, No. 6, Nov.-Dec., pp. 646-657.

Darwin, David; Zuo, Jun; Tholen, Michael L.; and Idun, Emmanuel K. (1995a). "Development Length Criteria for Conventional and High Relative Rib Area Reinforcing Bars," *SL Report* 95-4, University of Kansas Center for Research, Lawrence, Kansas, May, 70 pp.

Darwin, David; Idun, Emmanuel K.; Zuo, Jun; and Tholen, Michael L. (1995b). "Reliability-Based Strength Reduction Factor for Bond," *SL Report* 95-5, University of Kansas Center for Research, Lawrence, Kansas, May, 47 pp.

Darwin, David; Zuo, Jun; Tholen, Michael L.; and Idun, Emmanuel K. (1996a). "Development Length Criteria for Conventional and High Relative Rib Area Reinforcing Bars," *ACI Structural Journal*, Vol. 93, No. 3, May-June, pp. 347-359.

DeVries, Richard A.; Moehle, Jack P.; and Hester, Weston. (1991). "Lap Splice Strength of Plain and Epoxy-Coated Reinforcement," *Report* No. UCB/SEMM-91/02, University of California, Berkeley, California, Jan., 86 pp.

Donahey, Rex C., and Darwin, David. (1983). "Effects of Construction Procedures on Bond in Bridge Decks," *SM Report* No. 7, University of Kansas Center for Research, Lawrence, Kansas, 129 pp.

Donahey, Rex C., and Darwin, David. (1985). "Bond of Top-Cast Bars in Bridge Decks," ACI Journal, *Proceedings* Vol. 82, No. 1, Jan.-Feb., pp. 57-66.

Esfahani, M. R., and Rangan, B. V. (1996). "Studies on Bond Between Concrete and Reinforcing Bars," School of Civil Engineering, Curtin University of Technology, Perth, Western Australia, 315 pp.

Ferguson, Phil M., and Thompson, J. Neils. (1962). "Development Length of High Strength Reinforcing Bars in Bond," ACI Journal, *Proceedings* Vol. 59, No. 7, July, pp. 887-922.

Ferguson, Phil M., and Breen, John E. (1965). "Lapped Splices for High Strength Reinforcing Bars," ACI Journal, *Proceedings* Vol. 62, No. 9, Sept., pp. 1063-1078.

Gerstle, Walter H., and Xie, Ming. (1992). "FEM Modeling of Fictitious Crack Propagation in Concrete," *Journal of Engineering Mechanics*, ASCE, Vol. 118, No. 2, Feb., pp. 416-434.

Hadje-Ghaffari, Hossain; Darwin, David; and McCabe, Steven L. (1991). "Effects of Epoxy-Coating on the Bond of Reinforcing Steel to Concrete," *SM Report* No. 28, University of Kansas Center for Research, Lawrence, Kansas, July, 288 pp.

Hamad, Bilal S., and Jirsa, James O. (1990). "Influence of Epoxy Coating on Stress Transfer from Steel to Concrete," *Proceedings*, First Materials Engineering Congress, ASCE, New York, Vol. 2, pp. 125-134.

Hamad, Bilal S., and Jirsa, James O. (1993). "Strength of Epoxy-Coated Reinforcing Bar Splices Confined with Transverse Reinforcement," *ACI Structural Journal*, Vol. 90, No. 1, Jan.-Feb., pp. 77-88.

Hester, Cynthia J,; Salamizavaregh, Shahin; Darwin, David; and McCabe, Steven L. (1991). "Bond of Epoxy-Coated Reinforcement to Concrete: Splices," *SL Report* 91-1, University of Kansas Center for Research, Lawrence, Kansas, May, 66 pp.

Hester, Cynthia J,; Salamizavaregh, Shahin; Darwin, David; and McCabe, Steven L. (1993). "Bond of Epoxy-Coated Reinforcement: Splices," *ACI Structural Journal*, Vol. 90, No. 1, Jan.-Feb., pp. 89-102.

Hillerborg, A.; Modeer, M.; and Petersson, P. E. (1976). "Analysis of Crack Formation and Crack Growth in Concrete by Means of Fracture Mechanics and Finite Elements," *Cement and Concrete Research*, Vol. 6, No. 6, Nov., pp. 773-782.

Idun, Emmanuel K., and Darwin, David. (1995). "Improving the Development Characteristics of Steel Reinforcing Bars," *SM Report* No. 41, University of Kansas Center for Research, Lawrence, Kansas, Aug., 267 pp.

Ingraffea, A. R.; Gerstle, W. H.; Gergely, P.; and Saouma, V. (1984). "Fracture Mechanics of Bond in Reinforced Concrete," *Journal of Structural Engineering*, ASCE, Vol. 110, No. 4, April, pp. 871-890.

Keuser, M., and Mehlhorn, G. (1987). "Finite Element Models for Bond Problems," *Journal of Structural Engineering*, ASCE, Vol. 113, No. 10, Oct., pp. 2160-2173.

Lopez, L. A.; Dodds, R. H. Jr.; Rehak, D. R.; and Schmidt, R. J. (1994). *Polo-Finite: A Structural Mechanics System for Linear and Nonlinear Analysis*. A technical report by the University of Illinois at Urbana-Champaign.

Losberg, Anders, and Olsson, Per-Ake. (1979). "Bond Failure of Deformed Reinforcing Bars Based on the Longitudinal Splitting Effect of the Bars," ACI Journal, *Proceedings* Vol. 76, No. 1, Jan., pp. 5-18.

Lutz, L. A., and Gergely, P. (1967). "Mechanics of Bond and Slip of Deformed Bars in Concrete," ACI Journal, *Proceedings* Vol. 64, No. 11, Nov., pp. 711-721.

Maeda, M.; Otani, S.; and Aoyama, H. (1991). "Bond Splitting Strength in Reinforced Concrete Members," *Transactions of the Japan Concrete Inst.*, Vol. 13, pp. 581-588.

Mathey, Robert G., and Clifton, James R. (1976). "Bond of Coated Reinforcing Bars in Concrete," *Journal of the Structural Division*, ASCE, Vol. 102, No. ST1, Jan., pp. 215-229.

Mathey, Robert G., and Watstein, David. (1961). "Investigation of Bond in Beam and Pull-Out Specimens with High-Yield-Strength Deformed Bars," ACI Journal, *Proceedings* Vol. 57, No. 9, Mar., pp. 1071-1090.

Ngo, D., and Scordelis, Alexander C. (1967). "Finite Element Analysis of Reinforced Concrete Beams," ACI Journal, *Proceedings* Vol. 64, No. 3, Mar., pp. 152-163.

Orangun, C. O.; Jirsa, J. O.; and Breen, J. E. (1975). "The Strength of Anchored Bars: A Reevaluation of Test Data on Development Length and Splices," *Research Report* No. 154-3F, Center for Highway Research, The University of Texas at Austin, Jan., 78 pp.

Orangun, C. O.; Jirsa, J. O.; and Breen, J. E. (1977). "A Reevaluation of Test Data on Development Length and Splices," ACI Journal, *Proceedings* Vol. 74, No. 3, Mar., pp. 114-122.

Park, R., and Paulay, T. (1975). *Reinforced Concrete Structures*, John Wiley and Sons, New York, 769 pp.

PATRAN 3 Modeling Software. The MacNeal-Schwendler Corporation, 815 Colorado Boulevard, Los Angeles, CA 90041.

Rashid, Y. R. (1968). "Ultimate Strength Analysis of Prestressed Concrete Pressure Vessels," *Nuclear Engineering and Design*, Vol. 7, No. 4, Apr., pp. 334-344.

Rehm, G. (1957). "The Fundamental Law of Bond," *Proceedings*, Symposium on Bond and Crack Formation in Reinforced Concrete, Stockholm, RILEM, Paris, (published by Tekniska Hogskolans Rotaprinttrychkeri, Stockholm, 1958).

Rehm, G. (1961). "Uber die Grundlagen des Verbundes Zwischen Stahl und Beton." *Deutscher Ausschuss für Stahlbeton.* No. 1381, pp. 59, (C & CA Library Translation No. 134, 1968. "The Basic Principle of the Bond between Steel and Concrete.").

Rezansoff, T.; Akanni, A.; and Sparling, B. (1993). "Tensile Lap Splices under Static Loading: A Review of The Proposed ACI 318 Code Provisions," *ACI Structural Journal*, Vol. 90, No. 4, July-Aug., pp. 374-384.

Rots, J. G. (1989). "Bond of Reinforcement," *RILEM-Fracture Mechanics of Concrete Structures--From Theory to Applications*, Stockholm, pp. 245-250.

Sakurada, T.; Morohashi, N.; and Tanaka, R. (1993). "Effect of Transverse Reinforcement on Bond Splitting Strength of Lap Splices," *Transactions of the Japan Concrete Inst.*, Vol. 15, pp. 573-580.

Skorobogatov, S. M., and Edwards, A. D. (1979). "The Influence of the Geometry of Deformed Steel Bars on Their Bond Strength in Concrete," *The Institute of Civil Engineers*, Proceedings Vol. 67, Part 2, June, pp. 327-339.

Soretz, S., and Holzenbein, H. (1979). "Influence of Rib Dimensions of Reinforcing Bars on Bond and Bendability," ACI Journal, *Proceedings* Vol. 76, No. 1, Jan., pp. 111-127.

Tan, Changzheng; Darwin, David; Tholen, Michael L.; and Zuo, Jun. (1996). "Splice Strength of Epoxy-Coated High Relative Rib Area Bars," *SL Report* 96-2, University of Kansas Center for Research, Lawrence, Kansas, May, 69 pp.

Thompson, M. A.; Jirsa, J. O.; Breen, J. E.; and Meinheit, D. F. (1975). "The Behavior of Multiple Lap Splices in Wide Sections," *Research Report* No. 154-1, Center for Highway Research, The University of Texas at Austin, Feb., 75 pp.

Treece, Robert A., and Jirsa, James O. (1987). "Bond Strength of Epoxy-Coated Reinforcing Bars," *PMFSEL Report* No. 87-1, Phil M. Ferguson Structural Engineering Laboratory, The University of Texas at Austin, Jan., 85 pp.

Treece, Robert A., and Jirsa, James O. (1989). "Bond Strength of Epoxy-Coated Reinforcing Bars," *ACI Materials Journal*, Vol. 86, No. 2, Mar.-Apr., pp. 167-174.

Yao, Budan, and Murray, D. W. (1995). "Study of Concrete Cracking and Bond Using a Distributed Discrete Crack Finite Element Model," *ACI Materials Journal*, Vol. 92, No. 1, Jan.-Feb., pp. 93-104.

Zekany, A. J.; Neumann, S.; and Jirsa, J. O. (1981). "The Influence of Shear on Lapped Splices in Reinforced Concrete," *Research Report* No. 242-2, Center for Transportation Research, Bureau of Engineering Research, University of Texas at Austin, July, 88 pp.

Table 2.1
Test bar data

Nominal Bar Diam. (in.)	Pattern Designation*	Deformation Height (in.)	Deformation Spacing (in.)	Rib Width** (in.)	Relative Rib Area	W_r***
1	M11-8	0.050	0.263	0.050	0.200	0.190
1	M12-8	0.050	0.525	0.100	0.100	0.190
1	M13-8	0.050	1.050	0.200	0.050	0.190
1	M21-8	0.075	0.403	0.075	0.200	0.186
1	M22-8	0.075	0.806	0.150	0.100	0.186
1	M23-8	0.075	1.613	0.300	0.050	0.186
1	M31-8	0.100	0.550	0.100	0.200	0.182
1	M32-8	0.100	1.100	0.200	0.100	0.182
1	M33-8	0.100	2.200	0.400	0.050	0.182
5/8	M11-5	0.031	0.163	0.031	0.200	0.190
5/8	M12-5	0.031	0.325	0.063	0.100	0.194
5/8	M13-5	0.031	0.651	0.125	0.050	0.192
5/8	M21-5	0.047	0.253	0.047	0.200	0.186
5/8	M22-5	0.047	0.505	0.094	0.100	0.186
5/8	M23-5	0.047	1.011	0.188	0.050	0.186
5/8	M31-5	0.063	0.347	0.063	0.200	0.182
5/8	M32-5	0.063	0.693	0.125	0.100	0.180
5/8	M33-5	0.063	1.387	0.250	0.050	0.180
1	M11A-8	0.050	0.263	0.153	0.200	0.582
1	M12D-8	0.050	0.525	0.222	0.100	0.423
1	M12E-8	0.050	0.525	0.325	0.100	0.619
1	M31D-8	0.100	0.550	0.185	0.200	0.336
1	M31E-8	0.100	0.550	0.310	0.200	0.564
1	M32B-8	0.100	1.100	0.500	0.100	0.455
1	M32C-8	0.100	1.100	0.800	0.100	0.727
1	T-8	0.065	0.250		0.284	

* Pattern Designation: 1. Machined bars (MHXA-D) 2. Threaded bars (T-D)
H = deformation height: 1 = low, 2 = medium, 3 = high
X = rib spacing: 1 = small, 2 = medium, 3 = large
A = rib width designation (blank, A, B, C, D or E)
D = nominal bar diameter in 1/8 in.

** Rib width parallel to the longitudinal axis of the bar measured at the top of the ribs

*** W_r = rib width ratio = ratio of rib width to center-to-center spacing of deformations

1 in. = 25.4 mm

Table 2.2
Concrete mix proportions (lb/yd^3) and properties

Group	w/c Ratio	Cement	Water	Fine Agg.*	Coarse Agg.**	wr*** (oz)	Slump (in.)	Conc. Temp. (F)	Air Cont. (%)	Test Age (days)	Cylinder Strength (psi)
2	0.41	550	225	1564	1588	0	4.00	75	2.3	17	4900
4	0.36	582	208	1575	1608	3	1.25	88	3.3	7	5440
5	0.36	582	208	1575	1608	3	2.25	62	4.0	18	5440
6	0.36	582	208	1575	1608	3	2.00	69	4.8	8	4910
7	0.36	582	208	1575	1608	3	1.75	54	3.0	7	5360
8	0.36	582	208	1575	1608	3	2.75	57	2.8	7	4760
9	0.36	582	208	1575	1608	3	1.75	59	2.5	5	4890
10a	0.36	582	208	1575	1608	3	2.00	72	3.2	7	5130
10b										8	5380

* Kansas River Sand - Lawrence Sand Co., Lawrence, KS
Bulk Specific Gravity (SSD) = 2.62; Absorption = 0.5%; Fineness Modulus = 2.89

** Crushed Limestone - Fogel's Quarry, Ottawa, KS
Bulk Specific Gravity (SSD) = 2.58; Absorption = 2.7%; Max. Size = 3/4 in.;
Unit Weight = 90.5 lb/ft^3

*** Water Reducer per 100 lb Cement

1 in. = 25.4 mm; 1 lb = 4.45 N; 1 lb/ft^3 = 21.97 g/m^3; 1 lb/yd^3 = 0.5933 kg/m^3;
1 oz = 29.57 cm^3; 1 psi = 6.89 kPa

Table 2.3
Beam-end specimen properties and test results

Spec. Label*	Rib Ht. (in.)	Relative Rib Area	W_r**	Bonded Length (in.)	Cover (in.)	Concrete Strength (psi)	Stirrups	Just Before Failure: Bond Str. (kips)	Just Before Failure: Mod. Bond Str.+ (kips)	Just Before Failure: Crack Width (mils)	At Failure: Bond Str. (kips)	At Failure: Mod. Bond Str.+ (kips)	At Failure: Crack Width (mils)	Crack Wid. After Failure++ (in.)
Bar Size Study Specimens														
6M11-5N	0.03	0.20	0.190	7.5	2.000	4910		16.73	16.80	9.00	16.73	16.81	9.93	0.059
10M11-5N	0.03	0.20	0.190	7.5	2.125	5130		17.88	17.77	6.72	17.89	17.77	7.77	0.065
AVG.								17.30	17.28	7.86	17.31	17.29	8.85	0.062
6M12-5N	0.03	0.10	0.194	7.5	2.125	4910		16.88	16.96	4.31	16.91	16.98	4.59	0.078
10M12-5N	0.03	0.10	0.194	7.5	2.125	5130		16.88	16.77	3.62	16.90	16.79	4.50	0.086
AVG.								16.88	16.86	3.97	16.91	16.89	4.54	0.082
6M13-5N	0.03	0.05	0.192	7.5	2.063	4910		16.97	17.04	2.36	17.00	17.08	2.78	0.060
10M13-5N	0.03	0.05	0.192	7.5	2.125	5130		18.30	18.18	3.80	18.31	18.20	4.19	0.056
AVG.								17.63	17.61	3.08	17.66	17.64	3.49	0.058
6M21-5N	0.05	0.20	0.186	7.5	2.063	4910		16.08	16.15	6.74	16.10	16.18	7.72	0.093
10M21-5N	0.05	0.20	0.186	7.5	2.125	5130		18.58	18.46	6.04	18.60	18.48	7.09	0.084
AVG.								17.33	17.30	6.39	17.35	17.33	7.40	0.089
6M22-5N	0.05	0.10	0.186	7.5	2.063	4910		18.90	18.99	3.93	18.93	19.01	4.38	0.094
10M22-5N	0.05	0.10	0.186	7.5	2.000	5130		17.37	17.26	4.86	17.39	17.28	5.89	0.094
AVG.								18.14	18.12	4.40	18.16	18.14	5.13	0.094
6M23-5N	0.05	0.05	0.186	7.5	2.000	4910		17.63	17.71	1.87	17.65	17.73	2.37	0.056
10M23-5N	0.05	0.05	0.186	7.5	2.125	5130		18.38	18.26	2.68	18.39	18.28	5.77	0.075
AVG.								18.00	17.99	2.28	18.02	18.00	4.07	0.065
6M31-5N	0.06	0.20	0.182	7.5	2.000	4910		18.26	18.34	14.94	18.27	18.35	16.50	0.104
10M31-5N	0.06	0.20	0.182	7.5	2.063	5130		17.82	17.70	9.63	17.82	17.70	10.67	0.086
AVG.								18.04	18.02	12.28	18.04	18.03	13.59	0.095

Table 2.3
Beam-end specimen properties and test results (continued)

Spec. Label*	Rib Ht. (in.)	Relative Rib Area	W_r**	Bonded Length (in.)	Cover (in.)	Concrete Strength (psi)	Stirrups	Just Before Failure: Bond Str. (kips)	Just Before Failure: Mod. Bond Str.+ (kips)	Just Before Failure: Crack Width (mils)	At Failure: Bond Str. (kips)	At Failure: Mod. Bond Str.+ (kips)	At Failure: Crack Width (mils)	Crack Wid. After Failure++ (in.)
6M32-5N	0.06	0.10	0.180	7.5	2.063	4910		16.06	16.14	4.42	16.08	16.15	5.18	0.167
10M32-5N	0.06	0.10	0.180	7.5	2.125	5130		18.81	18.68	7.88	18.81	18.69	8.38	0.109
AVG.								17.43	17.41	6.15	17.45	17.42	6.78	0.138
6M33-5N	0.06	0.05	0.180	7.5	2.125	4910		15.34	15.41	1.86	15.35	15.41	2.07	0.131
10M33-5N	0.06	0.05	0.180	7.5	2.000	5130		17.21	17.10	3.63	17.21	17.10	4.19	0.069
AVG.								16.27	16.25	2.74	16.28	16.26	3.13	0.100
7M11-5S	0.03	0.20	0.190	7.5	2.125	5360	3 - No. 3	25.45	25.01	14.38	25.46	25.02	15.09	0.150
9M11-5S	0.03	0.20	0.190	7.5	2.063	4890	3 - No. 3	25.64	25.79	15.77	25.64	25.79	16.28	0.140
AVG.								25.55	25.40	15.07	25.55	25.40	15.69	0.145
7M12-5S	0.03	0.10	0.194	7.5	2.000	5360	3 - No. 3	25.66	25.22	10.27	25.67	25.23	10.79	0.106
9M12-5S	0.03	0.10	0.194	7.5	2.063	4890	3 - No. 3	25.16	25.30	12.04	25.18	25.32	12.76	0.152
AVG.								25.41	25.26	11.15	25.43	25.28	11.78	0.129
7M13-5S	0.03	0.05	0.192	7.5	2.063	5360	3 - No. 3	22.67	22.28	10.52	22.69	22.29	10.97	0.118
9M13-5S	0.03	0.05	0.192	7.5	2.000	4890	3 - No. 3	21.55	21.67	9.41	21.56	21.68	9.82	0.087
AVG.								22.11	21.98	9.97	22.12	21.99	10.40	0.103
7M21-5S	0.05	0.20	0.186	7.5	2.063	5360	3 - No. 3	26.44	25.99	29.89	26.45	26.00	30.62	0.284
9M21-5S	0.05	0.20	0.186	7.5	2.000	4890	3 - No. 3	25.64	25.79	48.97	25.65	25.79	49.94	0.116
AVG.								26.04	25.89	39.43	26.05	25.89	40.28	0.200
7M22-5S	0.05	0.10	0.186	7.5	2.063	5360	3 - No. 3	24.78	24.35	14.07	24.78	24.35	14.51	0.176
9M22-5S	0.05	0.10	0.186	7.5	1.875	4890	3 - No. 3	25.06	25.19	11.85	25.07	25.21	12.59	0.199
AVG.								24.92	24.77	12.96	24.92	24.78	13.55	0.188
7M23-5S	0.05	0.05	0.186	7.5	2.000	5360	3 - No. 3	23.04	22.64	8.63	23.06	22.66	9.10	0.129
9M23-5S	0.05	0.05	0.186	7.5	2.125	4890	3 - No. 3	21.78	21.90	7.41	21.78	21.90	7.95	0.172
AVG.								22.41	22.27	8.02	22.42	22.28	8.52	0.150

Table 2.3
Beam-end specimen properties and test results (continued)

Spec. Label*	Rib Ht. (in.)	Relative Rib Area	W_r**	Bonded Length (in.)	Cover (in.)	Concrete Strength (psi)	Stirrups	Just Before Failure: Bond Str. (kips)	Just Before Failure: Mod. Bond Str.+ (kips)	Just Before Failure: Crack Width (mils)	At Failure: Bond Str. (kips)	At Failure: Mod. Bond Str.+ (kips)	At Failure: Crack Width (mils)	Crack Wid. After Failure++ (in.)
7M31-5S	0.06	0.20	0.182	7.5	2.063	5360	3 - No. 3	26.20	25.75	9.36	26.22	25.76	9.83	0.152
9M31-5S	0.06	0.20	0.182	7.5	2.000	4890	3 - No. 3	26.09	26.24	20.43	26.11	26.26	21.46	0.130
AVG.								26.15	26.00	14.90	26.16	26.01	15.64	0.141
7M32-5S	0.06	0.10	0.180	7.5	2.000	5360	3 - No. 3	24.04	23.62	11.83	24.05	23.63	12.44	0.212
9M32-5S	0.06	0.10	0.180	7.5	2.125	4890	3 - No. 3	25.43	25.57	13.83	25.44	25.59	14.41	0.164
AVG.								24.73	24.60	12.83	24.74	24.61	13.43	0.188
7M33-5S	0.06	0.05	0.180	7.5	2.125	5360	3 - No. 3	23.40	22.99	14.03	23.42	23.01	14.49	0.191
9M33-5S	0.06	0.05	0.180	7.5	2.063	4890	3 - No. 3	21.59	21.71	11.61	21.59	21.71	12.02	0.095
AVG.								22.49	22.35	12.82	22.50	22.36	13.25	0.143
6M11-8N	0.050	0.20	0.190	7.5	2.250	4910		17.57	17.65	5.58	17.58	17.66	6.74	0.123
10M11-8N	0.050	0.20	0.190	7.5	2.063	5130		21.80	21.66	7.49	21.80	21.66	9.42	0.126
AVG.								19.68	19.65	6.54	19.69	19.66	8.08	0.125
6M12-8N	0.050	0.10	0.190	7.5	2.000	4910		20.46	20.56	5.20	20.49	20.58	6.47	0.158
10M12-8N	0.050	0.10	0.190	7.5	2.125	5130		18.44	18.32	8.75	18.46	18.34	9.71	0.071
AVG.								19.45	19.44	6.98	19.47	19.46	8.09	0.114
6M13-8N	0.050	0.05	0.190	7.5	2.125	4910		19.68	19.77	3.11	19.71	19.80	3.52	0.082
10M13-8N	0.050	0.05	0.190	7.5	2.125	5130		20.35	20.22	4.26	20.36	20.23	4.69	0.100
AVG.								20.01	19.99	3.69	20.04	20.02	4.11	0.091
6M21-8N	0.075	0.20	0.186	7.5	2.188	4910		18.81	18.90	3.86	18.82	18.90	4.53	0.129
10M21-8N	0.075	0.20	0.186	7.5	2.063	5130		20.18	20.05	5.34	20.22	20.09	6.48	0.117
AVG.								19.49	19.47	4.60	19.52	19.50	5.51	0.123
6M22-8N	0.075	0.10	0.186	7.5	2.000	4910		19.07	19.16	4.77	19.07	19.16	5.88	0.182
10M22-8N	0.075	0.10	0.186	7.5	2.063	5130		18.22	18.10	4.94	18.25	18.13	5.42	0.140
AVG.								18.65	18.63	4.86	18.66	18.64	5.65	0.161

Table 2.3
Beam-end specimen properties and test results (continued)

Spec. Label*	Rib Ht. (in.)	Relative Rib Area	W_r**	Bonded Length (in.)	Cover (in.)	Concrete Strength (psi)	Stirrups	Just Before Failure: Bond Str. (kips)	Just Before Failure: Mod. Bond Str.+ (kips)	Just Before Failure: Crack Width (mils)	At Failure: Bond Str. (kips)	At Failure: Mod. Bond Str.+ (kips)	At Failure: Crack Width (mils)	Crack Wid. After Failure++ (in.)
6M23-8N	0.075	0.05	0.186	7.5	1.938	4910		19.66	19.75	1.24	19.67	19.76	1.32	0.095
10M23-8N	0.075	0.05	0.186	7.5	2.063	5130		16.95	16.84	3.08	16.99	16.88	3.25	0.084
AVG.								18.30	18.29	2.16	18.33	18.32	2.29	0.089
6M31-8N	0.100	0.20	0.182	7.5	1.875	4910		18.02	18.10	4.81	18.03	18.11	5.78	0.158
10M31-8N	0.100	0.20	0.182	7.5	2.188	5130		22.53	22.38	7.40	22.54	22.39	8.88	0.189
AVG.								20.27	20.24	6.10	20.28	20.25	7.33	0.173
6M32-8N	0.100	0.10	0.182	7.5	2.000	4910		20.27	20.37	3.86	20.29	20.38	4.70	0.209
10M32-8N	0.100	0.10	0.182	7.5	2.063	5130		21.26	21.12	2.89	21.27	21.13	3.34	0.077
AVG.								20.76	20.74	3.37	20.78	20.75	4.02	0.143
6M33-8N	0.100	0.05	0.182	7.5	2.125	4910		19.55	19.64	4.40	19.56	19.65	4.92	0.102
10M33-8N	0.100	0.05	0.182	7.5	2.125	5130		18.46	18.34	3.61	18.49	18.37	4.40	0.077
AVG.								19.00	18.99	4.01	19.02	19.01	4.66	0.090
7M11-8S	0.050	0.20	0.190	7.5	2.063	5360	3 - No. 3	28.47	27.98	2.51	28.51	28.02	2.80	0.220
9M11-8S	0.050	0.20	0.190	7.5	2.063	4890	3 - No. 3	29.09	29.25	8.48	29.10	29.26	9.19	0.248
AVG.								28.78	28.61	5.49	28.80	28.64	5.99	0.234
7M12-8S	0.050	0.10	0.190	7.5	2.125	5360	3 - No. 3	29.33	28.82	4.93	29.34	28.83	5.21	0.307
9M12-8S	0.050	0.10	0.190	7.5	2.063	4890	3 - No. 3	27.39	27.54	8.99	27.40	27.56	9.74	0.178
AVG.								28.36	28.18	6.96	28.37	28.19	7.47	0.242
7M13-8S	0.050	0.05	0.190	7.5	2.188	5360	3 - No. 3	26.16	25.71	6.88	26.17	25.72	7.26	0.110
9M13-8S	0.050	0.05	0.190	7.5	2.063	4890	3 - No. 3	26.20	26.35	15.68	26.26	26.40	16.19	0.154
AVG.								26.18	26.03	11.28	26.22	26.06	11.73	0.132
7M21-8S	0.075	0.20	0.186	7.5	2.188	5360	3 - No. 3	29.20	28.69	8.60	29.20	28.69	9.23	0.196
9M21-8S	0.075	0.20	0.186	7.5	2.125	4890	3 - No. 3	28.15	28.31	10.36	28.16	28.31	11.02	0.127
AVG.								28.67	28.50	9.48	28.68	28.50	10.12	0.162

Table 2.3
Beam-end specimen properties and test results (continued)

Spec. Label*	Rib Ht. (in.)	Relative Rib Area	W_r**	Bonded Length (in.)	Cover (in.)	Concrete Strength (psi)	Stirrups	Just Before Failure			At Failure			Crack Wid. After Failure++ (in.)
								Bond Str. (kips)	Mod. Bond Str.+ (kips)	Crack Width (mils)	Bond Str. (kips)	Mod. Bond Str.+ (kips)	Crack Width (mils)	
7M22-8S	0.075	0.10	0.186	7.5	2.063	5360	3 - No. 3	27.76	27.28	12.43	27.77	27.29	12.94	0.253
9M22-8S	0.075	0.10	0.186	7.5	1.938	4890	3 - No. 3	30.39	30.56	10.04	30.41	30.58	10.99	0.174
AVG.								29.08	28.92	11.24	29.09	28.93	11.97	0.214
7M23-8S	0.075	0.05	0.186	7.5	2.063	5360	3 - No. 3	26.06	25.61	10.21	26.08	25.63	11.21	0.115
9M23-8S	0.075	0.05	0.186	7.5	2.000	4890	3 - No. 3	25.96	26.11	7.59	25.97	26.12	8.10	0.124
AVG.								26.01	25.86	8.90	26.03	25.87	9.66	0.120
7M31-8S	0.100	0.20	0.182	7.5	2.063	5360	3 - No. 3	28.27	27.78	10.77	28.27	27.78	11.84	0.269
9M31-8S	0.100	0.20	0.182	7.5	1.938	4890	3 - No. 3	31.54	31.71	12.07	31.56	31.74	12.71	0.137
AVG.								29.90	29.75	11.42	29.91	29.76	12.28	0.203
7M32-8S	0.100	0.10	0.182	7.5	1.938	5360	3 - No. 3	29.13	28.63	8.94	29.15	28.65	9.44	0.118
9M32-8S	0.100	0.10	0.182	7.5	2.125	4890	3 - No. 3	27.35	27.50	11.91	27.36	27.52	13.07	0.113
AVG.								28.24	28.07	10.42	28.26	28.08	11.25	0.115
7M33-8S	0.100	0.05	0.182	7.5	2.188	5360	3 - No. 3	27.17	26.70	6.44	27.18	26.71	6.78	0.165
9M33-8S	0.100	0.05	0.182	7.5	2.000	4890	3 - No. 3	27.25	27.40	4.56	27.26	27.41	5.01	0.110
AVG.								27.21	27.05	5.50	27.22	27.06	5.90	0.138
Rib Width Study Specimens														
2M11-8N	0.050	0.20	0.190	12.0	2.188	4900		29.77	29.92	2.27	29.89	30.04	9.05	N. M.
4M11-8N	0.050	0.20	0.190	12.0	1.938	5440		27.30	26.73	11.90	27.30	26.73	13.99	0.099
AVG.								28.54	28.33	7.09	28.60	28.39	11.52	0.099
2M11A-8N	0.050	0.20	0.582	12.0	2.250	4900		29.00	29.15	2.88	29.21	29.36	7.26	N. M.
4M11A-8N	0.050	0.20	0.582	12.0	1.938	5440		28.02	27.44	3.74	28.04	27.45	4.06	0.030
AVG.								28.51	28.29	3.31	28.63	28.41	5.66	0.030

Table 2.3
Beam-end specimen properties and test results (continued)

Spec. Label*	Rib Ht. (in.)	Relative Rib Area	W_r**	Bonded Length (in.)	Cover (in.)	Concrete Strength (psi)	Stirrups	Just Before Failure: Bond Str. (kips)	Just Before Failure: Mod. Bond Str.+ (kips)	Just Before Failure: Crack Width (mils)	At Failure: Bond Str. (kips)	At Failure: Mod. Bond Str.+ (kips)	At Failure: Crack Width (mils)	Crack Wid. After Failure++ (in.)
2M12-8N	0.050	0.10	0.190	12.0	2.125	4900		31.49	31.65	4.25	31.61	31.77	169.18	0.169
4M12-8N	0.050	0.10	0.190	12.0	2.125	5440		26.53	25.98	8.00	26.53	25.98	9.27	0.131
AVG.								29.01	28.81	6.13	29.07	28.87	89.23	0.150
2M12D-8N	0.050	0.10	0.423	12.0	2.125	4900		29.29	29.44	2.88	29.31	29.46	3.55	0.074
4M12D-8N	0.050	0.10	0.423	12.0	2.000	5440		29.94	29.32	6.18	29.96	29.33	6.82	0.096
AVG.								29.62	29.38	4.53	29.64	29.40	5.19	0.085
2M12E-8N	0.050	0.10	0.619	12.0	2.125	4900		29.44	29.59	3.69	29.56	29.71	58.05	0.056
4M12E-8N	0.050	0.10	0.619	12.0	2.125	5440		28.05	27.46	4.81	28.06	27.47	5.55	0.029
AVG.								28.75	28.53	4.25	28.81	28.59	31.80	0.042
2M31-8N	0.100	0.20	0.182	12.0	2.125	4900		29.18	29.33	3.13	29.29	29.44	7.60	0.161
4M31-8N	0.100	0.20	0.182	12.0	1.938	5440		25.61	25.08	4.40	25.62	25.09	5.29	0.155
AVG.								27.40	27.20	3.77	27.46	27.26	6.45	0.158
2M31D-8N	0.100	0.20	0.336	12.0	2.125	4900		27.41	27.55	5.14	27.51	27.65	9.96	0.137
4M31D-8N	0.100	0.20	0.336	12.0	1.875	5440		26.53	25.98	12.60	26.56	26.01	13.27	0.122
AVG.								26.97	26.76	8.87	27.04	26.83	11.62	0.130
2M31E-8N	0.100	0.20	0.564	12.0	2.125	4900		30.05	30.20	3.30	30.16	30.31	7.36	N. M.
4M31E-8N	0.100	0.20	0.564	12.0	2.063	5440		25.86	25.32	6.07	25.86	25.32	7.29	0.028
AVG.								27.96	27.76	4.69	28.01	27.82	7.33	0.028
2M32-8N	0.100	0.10	0.182	12.0	2.125	4900		32.99	33.16	7.14	33.12	33.29	292.13	0.289
4M32-8N	0.100	0.10	0.182	12.0	2.188	5440		28.07	27.48	7.04	28.07	27.48	8.41	0.212
AVG.								30.53	30.32	7.09	30.60	30.39	150.27	0.251
2M32B-8N	0.100	0.10	0.455	12.0	2.063	4900		30.69	30.85	4.83	30.78	30.94	201.96	0.201
4M32B-8N	0.100	0.10	0.455	12.0	2.250	5440		29.03	28.42	6.82	29.03	28.42	7.54	0.127
AVG.								29.86	29.63	5.83	29.91	29.68	104.75	0.164

Table 2.3
Beam-end specimen properties and test results (continued)

Spec. Label*	Rib Ht. (in.)	Relative Rib Area	W_r**	Bonded Length (in.)	Cover (in.)	Concrete Strength (psi)	Stirrups	Just Before Failure: Bond Str. (kips)	Just Before Failure: Mod. Bond Str.+ (kips)	Just Before Failure: Crack Width (mils)	At Failure: Bond Str. (kips)	At Failure: Mod. Bond Str.+ (kips)	At Failure: Crack Width (mils)	Crack Wid. After Failure++ (in.)
2M32C-8N	0.100	0.10	0.727	12.0	2.125	4900		30.89	31.05	2.50	31.15	31.31	58.50	0.057
4M32C-8N	0.100	0.10	0.727	12.0	2.250	5440		23.90	23.40	0.39	23.92	23.42	0.54	0.042
AVG.								27.40	27.22	1.45	27.54	27.36	29.52	0.050
5M11-8S	0.050	0.20	0.190	12.0	2.125	5440	4 - No. 3	45.67	44.72	41.49	45.69	44.74	42.35	0.142
8M11-8S	0.050	0.20	0.190	12.0	2.063	4760	4 - No. 3	47.57	48.16	17.95	47.58	48.17	18.74	0.178
10M11-8S	0.050	0.20	0.190	12.0	2.125	5380	4 - No. 3	48.25	47.37	22.04	48.25	47.37	22.63	0.108
AVG.								47.16	46.75	27.16	47.17	46.76	27.91	0.143
5M11A-8S	0.050	0.20	0.582	12.0	2.188	5440	4 - No. 3	41.93	41.06	12.10	41.93	41.06	12.60	0.032
8M11A-8S	0.050	0.20	0.582	12.0	2.125	4760	4 - No. 3	44.05	44.59	16.42	44.07	44.62	16.87	0.036
10M11A-8S	0.050	0.20	0.582	12.0	2.125	5380	4 - No. 3	41.77	41.01	6.82	41.80	41.04	7.01	0.014
AVG.								42.58	42.22	11.78	42.60	42.24	12.16	0.028
5M12-8S	0.050	0.10	0.190	12.0	2.125	5440	4 - No. 3	46.64	45.67	28.47	46.67	45.70	29.38	0.265
8M12-8S	0.050	0.10	0.190	12.0	2.063	4760	4 - No. 3	45.41	45.97	16.40	45.43	46.00	16.64	0.375
10M12-8S	0.050	0.10	0.190	12.0	2.000	5380	4 - No. 3	47.74	46.87	16.96	47.76	46.89	17.42	0.292
AVG.								46.60	46.17	20.61	46.62	46.19	21.15	0.311
5M12D-8S	0.050	0.10	0.423	12.0	2.063	5440	4 - No. 3	43.75	42.84	21.96	43.75	42.84	22.72	0.112
8M12D-8S	0.050	0.10	0.423	12.0	2.188	4760	4 - No. 3	45.61	46.17	17.65	45.61	46.18	18.18	0.114
10M12D-8S	0.050	0.10	0.423	12.0	2.188	5380	4 - No. 3	45.83	45.00	20.51	45.84	45.01	21.49	0.104
AVG.								45.06	44.67	20.04	45.07	44.67	20.79	0.110
5M12E-8S	0.050	0.10	0.619	12.0	2.125	5440	4 - No. 3	39.47	38.65	13.53	39.47	38.65	13.91	0.027
8M12E-8S	0.050	0.10	0.619	12.0	2.250	4760	4 - No. 3	43.16	43.69	12.65	43.17	43.70	13.23	0.041
10M12E-8S	0.050	0.10	0.619	12.0	2.188	5380	4 - No. 3	41.79	41.03	8.70	41.81	41.05	9.05	0.026
AVG.								41.47	41.12	11.62	41.48	41.13	12.06	0.031

Table 2.3
Beam-end specimen properties and test results (continued)

Spec. Label*	Rib Ht. (in.)	Relative Rib Area	W_r**	Bonded Length (in.)	Cover (in.)	Concrete Strength (psi)	Stirrups	Just Before Failure			At Failure			Crack Wid. After Failure++ (in.)
								Bond Str. (kips)	Mod. Bond Str.+ (kips)	Crack Width (mils)	Bond Str. (kips)	Mod. Bond Str.+ (kips)	Crack Width (mils)	
5M31-8S	0.100	0.20	0.182	12.0	2.063	5440	4 - No. 3	47.85	46.85	32.33	47.87	46.87	33.03	0.369
8M31-8S	0.100	0.20	0.182	12.0	2.063	4760	4 - No. 3	49.04	49.64	27.70	49.05	49.66	28.59	0.337
10M31-8S	0.100	0.20	0.182	12.0	2.188	5380	4 - No. 3	50.99	50.06	30.84	50.99	50.07	31.85	0.319
AVG.								49.29	48.85	30.29	49.30	48.86	31.16	0.342
5M31D-8S	0.100	0.20	0.336	12.0	2.000	5440	4 - No. 3	47.94	46.94	27.07	47.96	46.96	28.08	0.137
8M31D-8S	0.100	0.20	0.336	12.0	2.000	4760	4 - No. 3	48.96	49.56	27.35	48.97	49.57	28.35	0.205
10M31D-8S	0.100	0.20	0.336	12.0	2.125	5380	4 - No. 3	49.13	48.24	13.75	49.15	48.26	14.67	0.245
AVG.								48.67	48.25	22.72	48.69	48.26	23.70	0.196
5M31E-8S	0.100	0.20	0.564	12.0	2.125	5440	4 - No. 3	42.89	42.00	10.24	42.90	42.00	11.06	0.057
8M31E-8S	0.100	0.20	0.564	12.0	2.063	4760	4 - No. 3	45.75	46.32	16.91	45.77	46.33	17.44	0.071
10M31E-8S	0.100	0.20	0.564	12.0	2.125	5380	4 - No. 3	47.98	47.11	21.82	48.00	47.13	22.47	0.054
AVG.								45.54	45.14	16.32	45.56	45.16	16.99	0.061
5M32-8S	0.100	0.10	0.182	12.0	2.188	5440	4 - No. 3	43.59	42.68	24.09	43.60	42.69	25.22	0.379
8M32-8S	0.100	0.10	0.182	12.0	2.063	4760	4 - No. 3	48.33	48.93	19.18	48.34	48.94	19.78	0.280
10M32-8S	0.100	0.10	0.182	12.0	2.188	5380	4 - No. 3	49.68	48.78	26.98	49.70	48.80	27.74	0.388
AVG.								47.20	46.80	23.42	47.21	46.81	24.24	0.349
5M32B-8S	0.100	0.10	0.455	12.0	2.000	5440	4 - No. 3	43.97	43.05	17.57	43.99	43.07	18.37	0.169
8M32B-8S	0.100	0.10	0.455	12.0	2.250	4760	4 - No. 3	46.52	47.09	15.06	46.53	47.10	15.86	0.216
10M32B-8S	0.100	0.10	0.455	12.0	2.000	5380	4 - No. 3	47.25	46.39	15.69	47.27	46.41	16.26	0.161
AVG.								45.91	45.51	16.11	45.93	45.53	16.83	0.182
5M32C-8S	0.100	0.10	0.727	12.0	2.000	5440	4 - No. 3	36.15	35.40	10.97	36.16	35.41	11.44	0.041
8M32C-8S	0.100	0.10	0.727	12.0	2.125	4760	4 - No. 3	41.90	42.41	11.08	41.91	42.43	11.74	0.032
10M32C-8S	0.100	0.10	0.727	12.0	2.063	5380	4 - No. 3	40.19	39.46	2.76	40.19	39.46	3.23	0.022
AVG.								39.41	39.09	8.27	39.42	39.10	8.80	0.031

Table 2.3
Beam-end specimen properties and test results (continued)

Spec. Label*	Rib Ht. (in.)	Relative Rib Area	W_r**	Bonded Length (in.)	Cover (in.)	Concrete Strength (psi)	Stirrups	Just Before Failure			At Failure			Crack Wid. After Failure++ (in.)
								Bond Str. (kips)	Mod. Bond Str.+ (kips)	Crack Width (mils)	Bond Str. (kips)	Mod. Bond Str.+ (kips)	Crack Width (mils)	
Threaded Bar Study Specimens														
4T-12S-2A	0.07	0.284	N. M.	12.0	2.063	5440	4 - No. 3	52.53	51.43	35.52	52.55	51.45	36.83	0.485
4T-12S-2B	0.07	0.284	N. M.	12.0	2.000	5440	4 - No. 3	51.10	50.03	18.65	51.11	50.04	19.80	0.107
4T-12S-2C	0.07	0.284	N. M.	12.0	2.188	5440	4 - No. 3	52.99	51.88	29.36	52.99	51.88	30.45	0.273
AVG.								52.21	51.12	27.84	52.22	51.13	29.03	0.289
4T-12N-2A	0.07	0.284	N. M.	12.0	1.875	5440		29.69	29.07	N. M.	29.70	29.08	N. M.	N. M.
4T-12N-2B	0.07	0.284	N. M.	12.0	1.938	5440		29.25	28.64	7.74	29.26	28.65	8.25	0.101
4T-12N-2C	0.07	0.284	N. M.	12.0	2.000	5440		28.58	27.98	6.01	28.60	28.00	6.67	0.094
AVG.								29.17	28.56	6.88	29.19	28.58	7.46	0.097
4T-12N-3A	0.07	0.284	N. M.	12.0	2.875	5440		31.88	31.21	7.41	31.88	31.21	8.56	0.117
4T-12N-3B	0.07	0.284	N. M.	12.0	2.875	5440		32.64	31.96	13.77	32.65	31.97	14.86	0.120
4T-12N-3C	0.07	0.284	N. M.	12.0	2.813	5440		35.56	34.82	9.91	35.61	34.87	11.14	0.126
AVG.								33.36	32.66	10.36	33.38	32.68	11.52	0.121
4T-8.5N-3A	0.07	0.284	N. M.	8.5	2.938	5440		45.31	44.36	N. M.	45.32	44.37	N. M.	N. M.
4T-8.5N-3B	0.07	0.284	N. M.	8.5	2.813	5440		44.62	43.69	N. M.	44.66	43.73	N. M.	N. M.
4T-8.5N-3C	0.07	0.284	N. M.	8.5	2.750	5440		46.15	45.19	N. M.	46.18	45.22	N. M.	N. M.
AVG.								45.36	44.41		45.39	44.44		

Table 2.3
Beam-end specimen properties and test results (continued)

Spec. Label*	Rib Ht. (in.)	Relative Rib Area	W_r**	Bonded Length (in.)	Cover (in.)	Concrete Strength (psi)	Stirrups	Just Before Failure: Bond Str. (kips)	Just Before Failure: Mod. Bond Str.+ (kips)	Just Before Failure: Crack Width (mils)	At Failure: Bond Str. (kips)	At Failure: Mod. Bond Str.+ (kips)	At Failure: Crack Width (mils)	Crack Wid. After Failure++ (in.)

* Specimen Label: 1. Machined bars (GMHXA-DC) 2. Threaded bars (GT-BC-NR)

G = group number (2, 4 - 10)
M = machined bar
T = threaded bar
H = deformation height: 1 = low, 2 = medium, 3 = high
X = rib spacing: 1 = small, 2 = medium, 3 = large
A = rib width designation (blank, A, B, C, D or E)
D = nominal bar diameter in 1/8 in.
B = bonded length in in. (8.5 or 12)
C = confinement: N = no transverse stirrups, S = transverse stirrups
N = nominal cover in in. (2 or 3)
R = replication mark: A, B or C

** W_r = rib width ratio = ratio of rib width to center-to-center spacing of deformations

\+ Modified bond strength = bond strength $(5000/f'_c)^{1/4}$

++ N. M. = not measured

1 in. = 25.4 mm; 1 psi = 6.89 kPa; 1 kip = 4.45 kN; 1 mil = 0.001 in. = 25.4 mm

Table 2.4
Ratios of test to base bond strength

Specimen Label*	Rib Height (in.)	Rib Spacing (in.)	Rib Width (in.)	W_r**	Relative Rib Area	Stirrups	Bond Strength (kips)	Test/Base Bond Str.
2M11-8N	0.050	0.263	0.050	0.190	0.20		29.89	1.000
4M11-8N	0.050	0.263	0.050	0.190	0.20		27.30	1.000
AVG.							28.60	1.000
2M11A-8N	0.050	0.263	0.153	0.582	0.20		29.21	0.977
4M11A-8N	0.050	0.263	0.153	0.582	0.20		28.04	1.027
AVG.							28.63	1.002
2M12-8N	0.050	0.525	0.100	0.190	0.10		31.61	1.000
4M12-8N	0.050	0.525	0.100	0.190	0.10		26.53	1.000
AVG.							29.07	1.000
2M12D-8N	0.050	0.525	0.222	0.423	0.10		29.31	0.927
4M12D-8N	0.050	0.525	0.222	0.423	0.10		29.96	1.129
AVG.							29.64	1.028
2M12E-8N	0.050	0.525	0.325	0.619	0.10		29.56	0.935
4M12E-8N	0.050	0.525	0.325	0.619	0.10		28.06	1.058
AVG.							28.81	0.996
2M31-8N	0.100	0.550	0.100	0.182	0.20		29.29	1.000
4M31-8N	0.100	0.550	0.100	0.182	0.20		25.62	1.000
AVG.							27.46	1.000
2M31D-8N	0.100	0.550	0.185	0.336	0.20		27.51	0.939
4M31D-8N	0.100	0.550	0.185	0.336	0.20		26.56	1.037
AVG.							27.04	0.988
2M31E-8N	0.100	0.550	0.310	0.564	0.20		30.16	1.030
4M31E-8N	0.100	0.550	0.310	0.564	0.20		25.86	1.009
AVG.							28.01	1.020
2M32-8N	0.100	1.100	0.200	0.182	0.10		33.12	1.000
4M32-8N	0.100	1.100	0.200	0.182	0.10		28.07	1.000
AVG.							30.60	1.000
2M32B-8N	0.100	1.100	0.500	0.455	0.10		30.78	0.929
4M32B-8N	0.100	1.100	0.500	0.455	0.10		29.03	1.034
AVG.							29.91	0.982
2M32C-8N	0.100	1.100	0.800	0.727	0.10		31.15	0.941
4M32C-8N	0.100	1.100	0.800	0.727	0.10		23.92	0.852
AVG.							27.54	0.896
5M11-8S	0.050	0.263	0.050	0.190	0.20	4 - No. 3	45.69	1.000
8M11-8S	0.050	0.263	0.050	0.190	0.20	4 - No. 3	47.58	1.000
10M11-8S	0.050	0.263	0.050	0.190	0.20	4 - No. 3	48.25	1.000
AVG.							47.17	1.000
5M11A-8S	0.050	0.263	0.153	0.582	0.20	4 - No. 3	41.93	0.918
8M11A-8S	0.050	0.263	0.153	0.582	0.20	4 - No. 3	44.07	0.926
10M11A-8S	0.050	0.263	0.153	0.582	0.20	4 - No. 3	41.80	0.866
AVG.							42.60	0.903
5M12-8S	0.050	0.525	0.100	0.190	0.10	4 - No. 3	46.67	1.000
8M12-8S	0.050	0.525	0.100	0.190	0.10	4 - No. 3	45.43	1.000
10M12-8S	0.050	0.525	0.100	0.190	0.10	4 - No. 3	47.76	1.000
AVG.							46.62	1.000

Table 2.4
Ratios of test to base bond strength (continued)

Specimen Label*	Rib Height (in.)	Rib Spacing (in.)	Rib Width (in.)	W_r**	Relative Rib Area	Stirrups	Bond Strength (kips)	Test/Base Bond Str.
5M12D-8S	0.050	0.525	0.222	0.423	0.10	4 - No. 3	43.75	0.937
8M12D-8S	0.050	0.525	0.222	0.423	0.10	4 - No. 3	45.61	1.004
10M12D-8S	0.050	0.525	0.222	0.423	0.10	4 - No. 3	45.84	0.960
AVG.							45.07	0.967
5M12E-8S	0.050	0.525	0.325	0.619	0.10	4 - No. 3	39.47	0.846
8M12E-8S	0.050	0.525	0.325	0.619	0.10	4 - No. 3	43.17	0.950
10M12E-8S	0.050	0.525	0.325	0.619	0.10	4 - No. 3	41.81	0.876
AVG.							41.48	0.890
5M31-8S	0.100	0.550	0.100	0.182	0.20	4 - No. 3	47.87	1.000
8M31-8S	0.100	0.550	0.100	0.182	0.20	4 - No. 3	49.05	1.000
10M31-8S	0.100	0.550	0.100	0.182	0.20	4 - No. 3	50.99	1.000
AVG.							49.30	1.000
5M31D-8S	0.100	0.550	0.185	0.336	0.20	4 - No. 3	47.96	1.002
8M31D-8S	0.100	0.550	0.185	0.336	0.20	4 - No. 3	48.97	0.998
10M31D-8S	0.100	0.550	0.185	0.336	0.20	4 - No. 3	49.15	0.964
AVG.							48.69	0.988
5M31E-8S	0.100	0.550	0.310	0.564	0.20	4 - No. 3	42.90	0.896
8M31E-8S	0.100	0.550	0.310	0.564	0.20	4 - No. 3	45.77	0.933
10M31E-8S	0.100	0.550	0.310	0.564	0.20	4 - No. 3	48.00	0.941
AVG.							45.56	0.924
5M32-8S	0.100	1.100	0.200	0.182	0.10	4 - No. 3	43.60	1.000
8M32-8S	0.100	1.100	0.200	0.182	0.10	4 - No. 3	48.34	1.000
10M32-8S	0.100	1.100	0.200	0.182	0.10	4 - No. 3	49.70	1.000
AVG.							47.21	1.000
5M32B-8S	0.100	1.100	0.500	0.455	0.10	4 - No. 3	43.99	1.009
8M32B-8S	0.100	1.100	0.500	0.455	0.10	4 - No. 3	46.53	0.963
10M32B-8S	0.100	1.100	0.500	0.455	0.10	4 - No. 3	47.27	0.951
AVG.							45.93	0.974
5M32C-8S	0.100	1.100	0.800	0.727	0.10	4 - No. 3	36.16	0.829
8M32C-8S	0.100	1.100	0.800	0.727	0.10	4 - No. 3	41.91	0.867
10M32C-8S	0.100	1.100	0.800	0.727	0.10	4 - No. 3	40.19	0.809
AVG.							39.42	0.835

* Specimen Label: Machined bars (GMHXA-DC)
G = group number (2, 4, 5, 8, or 10)
M = machined bar
H = deformation height: 1 = low, 2 = medium, 3 = high
X = rib spacing: 1 = small, 2 = medium, 3 = large
A = rib width designation (blank, A, B, C, D or E)
D = nominal bar diameter in 1/8 in.
C = confinement: N = no transverse stirrups, S = transverse stirrups

** W_r = rib width ratio = ratio of rib width to center-to-center spacing of deformations

1 in. = 25.4 mm; 1 kip = 4.45 kN

Table 2.5
Beam-end specimen properties and test results from Darwin and Graham (1993a, 1993b)

Spec. Label*	Rib Ht. (in.)	Relative Rib Area	W_r**	Bonded Length (in.)	Cover (in.)	Concrete Strength (psi)	Stirrups	Bond Str. (kips)	Mod. Bond Str.+ (kips)
5M11-12-.5A	0.050	0.20	0.190	12.0	2.125	4560		29.08	29.76
5M11-12-.5B	0.050	0.20	0.190	12.0	2.125	4610		29.88	30.49
5M11-12-.5C	0.050	0.20	0.190	12.0	2.063	4610		28.78	29.37
AVG.								29.25	29.87
5M12-12-.5A	0.050	0.10	0.190	12.0	2.063	4610		31.40	32.04
5M12-12-.5B	0.050	0.10	0.190	12.0	2.125	4610		34.13	34.83
5M12-12-.5C	0.050	0.10	0.190	12.0	2.125	4560		29.90	30.60
AVG.								31.81	32.49
5M13-12-.5A	0.050	0.05	0.190	12.0	2.125	4610		29.72	30.33
5M13-12-.5B	0.050	0.05	0.190	12.0	2.188	4610		28.05	28.63
5M13-12-.5C	0.050	0.05	0.190	12.0	2.188	4560		31.24	31.97
AVG.								29.67	30.31
5M21-12-.5A	0.075	0.20	0.186	12.0	2.375	4610		30.60	31.23
5M21-12-.5B	0.075	0.20	0.186	12.0	2.125	4560		25.42	26.01
5M21-12-.5C	0.075	0.20	0.186	12.0	2.125	4610		31.34	31.98
AVG.								29.12	29.74
5M22-12-.5A	0.075	0.10	0.186	12.0	2.000	4610		31.46	32.11
5M22-12-.5B	0.075	0.10	0.186	12.0	2.125	4560		29.62	30.31
5M22-12-.5C	0.075	0.10	0.186	12.0	2.250	4610		26.00	26.53
AVG.								29.03	29.65
5M23-12-.5A	0.075	0.05	0.186	12.0	2.000	4610		31.24	31.88
5M23-12-.5B	0.075	0.05	0.186	12.0	2.063	4560		30.77	31.49
5M23-12-.5C	0.075	0.05	0.186	12.0	2.063	4610		28.08	28.66
AVG.								30.03	30.67
5M31-12-.5A	0.100	0.20	0.182	12.0	2.063	4560		31.13	31.86
5M31-12-.5B	0.100	0.20	0.182	12.0	2.063	4610		29.99	30.61
5M31-12-.5C	0.100	0.20	0.182	12.0	2.188	4560		29.03	29.71
AVG.								30.05	30.72
5M32-12-.5A	0.100	0.10	0.182	12.0	1.938	4560		29.95	30.65
5M32-12-.5B	0.100	0.10	0.182	12.0	1.938	4610		30.26	30.88
5M32-12-.5C	0.100	0.10	0.182	12.0	2.063	4610		30.11	30.73
AVG.								30.11	30.75
5M33-12-.5A	0.100	0.05	0.182	12.0	2.125	4610		32.11	32.77
5M33-12-.5B	0.100	0.05	0.182	12.0	2.188	4610		27.97	28.54
5M33-12-.5C	0.100	0.05	0.182	12.0	2.125	4610		25.75	26.28
AVG.								28.61	29.20
6M11-12-.5A	0.050	0.20	0.190	12.0	2.125	4600	4 - No. 3	41.82	42.70
6M11-12-.5B	0.050	0.20	0.190	12.0	2.125	4720	4 - No. 3	46.06	46.73
6M11-12-.5C	0.050	0.20	0.190	12.0	2.063	4530	4 - No. 3	41.85	42.90
AVG.								43.24	44.11

Table 2.5
Beam-end specimen properties and test results
from Darwin and Graham (1993a, 1993b) (continued)

Spec. Label*	Rib Ht. (in.)	Relative Rib Area	W_r**	Bonded Length (in.)	Cover (in.)	Concrete Strength (psi)	Stirrups	Bond Str. (kips)	Mod. Bond Str.+ (kips)
6M12-12-.5A	0.050	0.10	0.190	12.0	2.125	4600	4 - No. 3	39.84	40.68
6M12-12-.5B	0.050	0.10	0.190	12.0	1.938	4720	4 - No. 3	41.56	42.16
6M12-12-.5C	0.050	0.10	0.190	12.0	1.938	4530	4 - No. 3	38.35	39.31
AVG.								39.92	40.72
6M13-12-.5A	0.050	0.05	0.190	12.0	2.063	4600	4 - No. 3	33.38	34.08
6M13-12-.5B	0.050	0.05	0.190	12.0	2.313	4720	4 - No. 3	37.11	37.65
6M13-12-.5C	0.050	0.05	0.190	12.0	2.188	4530	4 - No. 3	38.89	39.86
AVG.								36.46	37.20
6M21-12-.5A	0.075	0.20	0.186	12.0	2.250	4720	4 - No. 3	42.56	43.18
6M21-12-.5B	0.075	0.20	0.186	12.0	2.188	4530	4 - No. 3	45.18	46.31
6M21-12-.5C	0.075	0.20	0.186	12.0	2.000	4600	4 - No. 3	45.14	46.09
AVG.								44.29	45.19
6M22-12-.5A	0.075	0.10	0.186	12.0	2.125	4720	4 - No. 3	41.73	42.34
6M22-12-.5B	0.075	0.10	0.186	12.0	2.188	4530	4 - No. 3	40.92	41.94
6M22-12-.5C	0.075	0.10	0.186	12.0	2.000	4600	4 - No. 3	37.92	38.72
AVG.								40.19	41.00
6M23-12-.5A	0.075	0.05	0.186	12.0	2.063	4720	4 - No. 3	36.56	37.09
6M23-12-.5B	0.075	0.05	0.186	12.0	2.063	4530	4 - No. 3	36.84	37.76
6M23-12-.5C	0.075	0.05	0.186	12.0	2.063	4600	4 - No. 3	36.23	36.99
AVG.								36.54	37.28
6M31-12-.5A	0.100	0.20	0.182	12.0	2.000	4530	4 - No. 3	40.84	41.86
6M31-12-.5B	0.100	0.20	0.182	12.0	1.938	4600	4 - No. 3	44.18	45.11
6M31-12-.5C	0.100	0.20	0.182	12.0	2.063	4720	4 - No. 3	45.83	46.50
AVG.								43.62	44.49
6M32-12-.5A	0.100	0.10	0.182	12.0	2.000	4530	4 - No. 3	34.98	35.85
6M32-12-.5B	0.100	0.10	0.182	12.0	2.125	4600	4 - No. 3	39.71	40.55
6M32-12-.5C	0.100	0.10	0.182	12.0	2.125	4720	4 - No. 3	44.74	45.39
AVG.								39.81	40.60
6M33-12-.5A	0.100	0.05	0.182	12.0	1.938	4530	4 - No. 3	34.59	35.45
6M33-12-.5B	0.100	0.05	0.182	12.0	2.000	4600	4 - No. 3	31.55	32.21
6M33-12-.5C	0.100	0.05	0.182	12.0	2.063	4720	4 - No. 3	27.44	27.84
AVG.								31.19	31.84
9M11-8.5-4A	0.050	0.20	0.190	8.5	3.000	5990		55.51	53.06
9M11-8.5-4B	0.050	0.20	0.190	8.5	3.250	5040		45.50	45.41
AVG.								50.51	49.23
9M12-8.5-4A	0.050	0.10	0.190	8.5	3.125	5990		54.68	52.27
9M12-8.5-4B	0.050	0.10	0.190	8.5	3.250	5040		42.70	42.62
AVG.								48.69	47.44
9M13-8.5-4A	0.050	0.05	0.190	8.5	3.000	5990		49.27	47.09
9M13-8.5-4B	0.050	0.05	0.190	8.5	3.000	5040		42.50	42.42
AVG.								45.89	44.75

Table 2.5
Beam-end specimen properties and test results from Darwin and Graham (1993a, 1993b) (continued)

Spec. Label*	Rib Ht. (in.)	Relative Rib Area	W_r**	Bonded Length (in.)	Cover (in.)	Concrete Strength (psi)	Stirrups	Bond Str. (kips)	Mod. Bond Str.+ (kips)
9M21-8.5-4	0.075	0.20	0.186	8.5	3.000	5990		55.04	52.61
9M22-8.5-4	0.075	0.10	0.186	8.5	3.000	5990		53.25	50.90
9M23-8.5-4	0.075	0.05	0.186	8.5	3.063	5990		48.28	46.15
9M31-8.5-4A	0.100	0.20	0.182	8.5	3.000	5990		50.58	48.35
9M31-8.5-4B	0.100	0.20	0.182	8.5	3.063	5040		47.40	47.31
9M31-8.5-4C	0.100	0.20	0.182	8.5	3.000	5040		49.00	48.90
AVG.								48.99	48.18
9M32-8.5-4A	0.100	0.10	0.182	8.5	3.125	5990		51.84	49.55
9M32-8.5-4B	0.100	0.10	0.182	8.5	3.125	5040		45.60	45.51
AVG.								48.72	47.53
9M33-8.5-4A	0.100	0.05	0.182	8.5	3.063	5990		44.29	42.33
9M33-8.5-4B	0.100	0.05	0.182	8.5	3.063	5040		42.30	42.22
AVG.								43.30	42.28

* Specimen Label: Machined bars (GMHX-B-LR)
G = group number (5, 6 or 9)
M = machined bar
H = deformation height: 1 = low, 2 = medium, 3 = high
X = rib spacing: 1 = small, 2 = medium, 3 = large
B = bonded length, in.
L = lead length, in.
R = replication mark (A, B or C)

** W_r = rib width ratio = ratio of rib width to center-to-center spacing of deformations

\+ Modified bond strength = bond strength $(5000/f'_c)^{1/4}$

1 in. = 25.4 mm; 1 psi = 6.89 kPa; 1 kip = 4.45 kN

Table 3.1
Splice specimen properties and test results

Specimen No. +	Bar ++ Designation	n	l_s (in.)	d_b (in.)	c_{so} (in.)	c_{si} (in.)	c_b (in.)	b (in.)	h (in.)	l (ft)	l_c (ft)	d (in.)	f'_c (psi)	N	d_s (in.)	f_{y1} (ksi)	P (kips)	M_u (k-in.)	f_s* (ksi)
12.1	5N0	4	10.0	0.625	1.875	0.521	1.335	12.07	15.56	13.00	4.00	13.90	4120	2	0.500	84.7	14.34	708	45.42
12.2	5C2	4	10.0	0.625	1.953	0.516	1.297	12.12	15.57	13.00	4.00	13.94	4120	2	0.500	84.7	14.40	711	45.48
12.3	5N0	3	10.0	0.625	2.032	1.039	1.291	12.14	15.50	13.00	4.00	13.88	4120	1	0.375	64.6	11.54	573	48.52
12.4	5C2	3	10.0	0.625	2.063	1.032	1.264	12.12	15.56	13.00	4.00	13.96	4120	1	0.375	64.6	12.48	618	52.02
13.1	5C2	3	12.0	0.625	1.532	1.289	1.303	12.18	15.51	13.00	4.00	13.88	4110	1	0.375	64.6	13.33	659	55.82
13.2	5N0	3	12.0	0.625	1.563	1.266	1.315	12.11	15.50	13.00	4.00	13.86	4110	1	0.375	64.6	13.38	661	56.10
13.3	5C2**	3	16.0	0.625	2.047	1.000	1.325	12.15	15.52	13.00	4.00	13.86	4110				12.84	636	53.91
13.4	5C2	3	16.0	0.625	2.094	1.016	1.354	12.19	15.60	13.00	4.00	13.92	4110				14.38	710	59.96
14.3	5C2	3	17.0	0.625	2.032	1.031	1.295	12.14	15.51	13.00	4.00	13.89	4200				15.06	743	62.84
14.4	5C2**	3	17.0	0.625	2.063	1.000	1.320	12.14	15.59	13.00	4.00	13.94	4200				13.76	680	57.34
14.5	5N0	2	12.0	0.625	1.594	3.156	1.210	12.13	15.45	13.00	4.00	13.91	4200	2	0.375	64.6	9.64	482	60.15
14.6	5C2	2	12.0	0.625	1.532	3.188	1.277	12.05	15.49	13.00	4.00	13.89	4200	2	0.375	64.6	10.17	507	63.45
15.1	11F3	2	27.0	1.410	1.516	1.500	1.902	12.11	16.11	16.00	6.00	13.46	5250	9	0.500	84.7	44.97	2449	67.33
15.2	11N0	2	27.0	1.410	1.610	1.469	1.924	12.11	16.12	16.00	6.00	13.46	5250	9	0.500	84.7	41.96	2287	62.89
15.3	11N0	2	40.0	1.410	1.516	1.531	1.820	12.04	16.19	16.00	6.00	13.63	5250	10	0.375	64.6	41.92	2287	62.07
15.4	11F3	2	40.0	1.410	1.563	1.469	1.884	12.08	16.13	16.00	6.00	13.50	5250	10	0.375	64.6	51.57	2808	76.93
15.5	11F3	2	40.0	1.410	3.063	2.984	1.908	18.05	16.12	16.00	6.00	13.47	5250				36.65	2013	54.12
15.6	11F3**	2	40.0	1.410	2.922	3.063	1.932	18.07	16.10	16.00	6.00	13.42	5250				32.45	1787	48.19
16.1	11F3**	2	40.0	1.410	3.063	2.906	1.833	18.04	15.93	16.00	6.00	13.35	5180				32.68	1799	48.83
16.2	11F3	2	40.0	1.410	3.016	2.969	1.895	18.07	16.28	16.00	6.00	13.64	5180				35.92	1974	52.38
16.3	11F3	2	40.0	1.410	3.047	2.969	1.791	18.03	16.16	16.00	6.00	13.62	5180	4	0.375	64.6	42.18	2312	61.42
16.4	11B0	2	40.0	1.410	3.063	3.000	1.846	18.06	16.00	16.00	6.00	13.45	5180	4	0.375	64.6	41.45	2272	61.19
17.3	11F3	2	38.0	1.410	3.047	2.984	1.888	18.03	16.12	16.00	6.00	13.48	4710	8	0.375	64.6	46.74	2558	68.85
17.4	11B0	2	38.0	1.410	3.094	3.000	1.866	18.07	16.09	16.00	6.00	13.49	4710	8	0.375	64.6	44.77	2451	65.98
17.5	11B0	2	30.0	1.410	3.079	3.000	1.907	18.09	16.09	16.00	6.00	13.45	4710	7	0.500	84.7	39.69	2175	58.72
17.6	11F3	2	30.0	1.410	3.063	2.969	1.911	18.07	16.20	16.00	6.00	13.54	4710	7	0.500	84.7	47.03	2572	68.92
18.1	11F3	2	40.0	1.410	1.484	4.500	1.845	18.05	16.11	16.00	6.00	13.52	4700	10	0.375	64.6	55.06	3007	80.72
18.2	11F3**	2	40.0	1.410	2.984	3.000	1.922	18.07	16.14	16.00	6.00	13.48	4700	6	0.375	68.9	38.88	2134	57.48
18.3	11F3	2	40.0	1.410	3.031	3.000	1.911	18.05	16.08	16.00	6.00	13.43	4700	6	0.375	64.6	46.85	2564	69.33
18.4	11B0	2	40.0	1.410	3.016	3.031	1.871	18.08	16.23	16.00	6.00	13.62	4700	6	0.375	64.6	45.49	2491	66.33

Note: Refer to last page of table for footnotes.

Table 3.1
Splice specimen properties and test results (continued)

Specimen No. +	Bar ++ Designation	n	l_s (in.)	d_b (in.)	c_{so} (in.)	c_{si} (in.)	c_b (in.)	b (in.)	h (in.)	l (ft)	l_c (ft)	d (in.)	f'_c (psi)	N	d_s (in.)	f_{yt} (ksi)	P (kips)	M_u (k-in.)	f_s* (ksi)

\+ Specimen No.
G.P, G = group number (12-18), P = casting order in the group (1-6)

++ Bar Designation
#AA, # = bar size (No. 5 or No. 11), AA = bar manufacturer and deformation pattern

B0	Conventional Birmingham Steel bar	F3	New Florida Steel bars
C2	New Chaparral Steel bars	N0	Conventional North Star Steel bar

* Bar stress is computed based on working stress if f_s does not exceed bar yield stress, otherwise computed based on ultimate strength
M_u and f_s include effects of beam self weight and loading system

** Spliced bars were coated

1 in. = 25.4 mm; 1 ft = 305 mm; 1 psi = 6.89 kPa; 1 ksi = 6.89 MPa; 1 kip = 4.45 kN; 1 k-in. = 0.113 kN-m

Table 3.2
Properties of reinforcing bars

Bar + Designation	Yield Str. (ksi)	Nominal Diameter (in.)	Weight (lb/ft)	% Light or Heavy	Rib Spacing (in.)	Rib Height ASTM (in.)	Rib Height Avg. * (in.)	Relative Rib Area	Coating Thick.** (mils)
5N0	66.4	0.625	1.015	2.6% L	0.350	0.036	0.035	0.082	-
5C2	61.8	0.625	1.013	2.9% L	0.275	0.042	0.041	0.109	9.9
11N0	65.5	1.410	5.157	2.9% L	0.911	0.079	0.075	0.072	-
11B0	66.7	1.410	5.102	4.0% L	0.825	0.070	0.066	0.070	-
11F3	77.8	1.410	5.145	3.2% L	0.615	0.090	0.088	0.127	6.3

\+ Bar Designation
#AA, # = bar size (No. 5 or No. 11), AA = bar manufacturer and deformation pattern

- B0 Conventional Birmingham Steel bar
- C2 New Chaparral Steel bars
- F3 New Florida Steel bars
- N0 Conventional North Star Steel bar

\- No coated bars tested

* Average rib height between longitudinal ribs

** Average coating thicknesses for epoxy-coated bars belonging to bar designation

1 ksi = 6.89 MPa; 1 in. = 25.4 mm; 1 lb/ft = 1.49 kg/m; 1 mil = 0.001 in. = 25.4 μm

Table 3.3
Concrete mix proportions (lb/yd^3) and properties

Group	w/c Ratio	Cement	Water	Fine Agg.*	Coarse Agg.**	wr (oz)	Slump (in.)	Concrete Temp (F)	Air Content (%)	Test Age (days)	Cylinder Strength (psi)
12	0.36	582	208	1575	1608	3	2.50	88	5.50	6	4120
13	0.36	582	208	1575	1608	3	2.50	91	5.20	6	4110
14	0.44	508	224	1554	1650	0	2.50	90	2.90	10	4200
15	0.44	508	224	1554	1650	0	2.50	83	2.30	19	5250
16	0.44	508	224	1554	1650	0	3.25	59	3.10	22	5180
17	0.44	508	224	1554	1650	0	2.50	59	4.00	21	4710
18	0.44	508	224	1554	1650	0	2.50	65	3.70	30	4700

* Kansas River Sand - Lawrence Sand Co., Lawrence, KS
Bulk Specific Gravity (SSD) = 2.62; Absorption = 0.5 %; Fineness Modulus = 2.89

** Crushed Limestone - Fogel's Quarry, Ottawa, KS
Bulk Specific Gravity (SSD) = 2.58; Absorption = 2.7 %; Max. Size = 3/4 in.;
Unit Weight = 90.5 lb/cu. ft

wr Water Reducer per 100 lb Cement

1 lb/yd^3 = 0.5933 kg/m^3; 1 oz = 29.57 cm^3; 1 psi = 6.89 kPa

Table 3.4
Splice specimen properties and test results from Idun and Darwin (1995)

Specimen No. +	Bar ++ Designation	Relative Rib Area	n	l_s (in.)	d_b (in.)	c_{so} (in.)	c_{si} (in.)	c_b (in.)	b (in.)	h (in.)	l (ft)	l_c (ft)	d (in.)	f'_c (psi)	N	d_s (in.)	f_{yt} (ksi)	M_u (k-in.)	f_s+++ (ksi)
1.1	8C1	0.101	2	16.0	1.000	2.969	2.938	2.938	16.08	17.22	13.00	4.00	13.76	5020				1021	51.63
1.2	8C1	0.101	2*	16.0	1.000	2.032	2.281	1.938	24.06	16.25	13.00	4.00	13.79	5020				1746	44.60
1.3	8C1	0.101	3	16.0	1.000	2.032	1.438	1.938	16.07	16.21	13.00	4.00	13.75	5020				1310	45.01
1.4	8C1**	0.101	3	16.0	1.000	2.032	1.375	1.938	16.11	16.20	13.00	4.00	13.74	5020				1079	37.09
1.5	8C1	0.101	3	16.0	1.000	2.063	1.375	1.938	16.07	16.19	13.00	4.00	13.74	5020	5	0.500	70.8	1518	52.22
1.6	8C1	0.101	3	16.0	1.000	2.063	1.438	1.938	16.05	16.19	13.00	4.00	13.74	5020	3	0.500	70.8	1511	51.98
2.1	8S0	0.071	2	24.0	1.000	2.250	1.706	1.328	12.12	15.56	16.00	6.00	13.70	5250	7	0.375	69.9	1214	62.43
2.2***	8F1	0.140	2	24.0	1.000	2.125	1.801	1.406	12.12	15.52	16.00	6.00	13.58	5250	7	0.375	69.9	1526	77.60
2.3	8F1	0.140	2	24.0	1.000	2.125	1.780	1.969	12.11	16.06	16.00	6.00	13.56	5250	4	0.375	69.9	1413	73.45
2.4	8F1	0.140	2	24.0	1.000	2.000	1.914	1.313	12.13	15.64	16.00	6.00	13.79	5250				1059	54.08
2.5	8F1	0.140	2	24.0	1.000	2.063	1.856	1.813	12.13	16.01	16.00	6.00	13.67	5250				1138	58.67
2.6	8F1**	0.140	2	24.0	1.000	2.000	1.917	1.938	12.12	16.19	16.00	6.00	13.71	5250				961	49.37
3.4	8C0	0.085	2	24.0	1.000	2.110	1.857	2.000	12.14	16.26	16.00	6.00	13.73	5110	4	0.375	69.9	1087	55.77
3.5	8C0	0.085	3	28.0	1.000	1.001	0.965	1.906	12.17	16.17	16.00	6.00	13.74	3810	8	0.375	69.9	1479	52.02
4.1	8S0	0.071	2	24.0	1.000	2.063	1.926	1.250	12.16	15.49	16.00	6.00	13.72	4090	6	0.500	70.8	1211	62.51
4.2	8F1	0.140	2	24.0	1.000	2.094	1.848	1.313	12.17	15.59	16.00	6.00	13.74	4090	8	0.375	69.9	1403	72.33
4.4	8C1	0.101	2	24.0	1.000	2.032	1.978	1.219	12.15	15.47	16.00	6.00	13.73	4090	4	0.375	69.9	1141	58.85
4.5	8C1	0.101	2	24.0	1.000	2.063	1.936	1.844	12.12	16.15	16.00	6.00	13.79	4090				994	51.06
4.6	8C1**	0.101	2	24.0	1.000	2.094	1.926	2.000	12.16	16.23	16.00	6.00	13.72	4090				808	41.72
5.1	8SH0	0.065	3	24.0	1.000	2.016	1.914	1.250	18.22	15.57	16.00	6.00	13.79	4190	7	0.375	69.9	1888	64.61
5.2	8F1	0.140	3	24.0	1.000	2.078	1.867	1.359	18.12	15.62	16.00	6.00	13.73	4190	7	0.375	69.9	1902	65.42
5.3	8F1	0.140	2	24.0	1.000	2.063	1.849	1.281	12.11	15.50	16.00	6.00	13.68	4190	7	0.375	69.9	1311	67.86
5.4	8SH0	0.065	2	24.0	1.000	1.985	1.980	1.250	12.12	15.46	16.00	6.00	13.68	4190	7	0.375	69.9	1137	58.88
5.5	8C0	0.085	2	24.0	1.000	2.063	1.904	1.406	12.12	15.60	16.00	6.00	13.67	4190	4	0.375	69.9	896	46.42
5.6	8F1	0.140	2	22.0	1.000	2.094	1.807	1.313	12.11	15.69	16.00	6.00	13.84	4190	5	0.500	70.8	1297	66.36
6.1	8SH0	0.065	3	24.0	1.000	2.063	0.422	1.906	12.18	16.12	16.00	6.00	13.69	4220	8	0.500	66.4	1797	63.24
6.2	8F1	0.140	3	24.0	1.000	2.000	0.438	2.000	12.11	16.15	16.00	6.00	13.62	4220	8	0.500	66.4	2115	74.92
6.3	8F1	0.140	2	16.0	1.000	2.000	1.906	1.344	12.13	15.51	16.00	6.00	13.63	4220	2	0.375	64.6	887	46.09
6.4	8C0	0.085	2	16.0	1.000	2.094	1.844	1.344	12.11	15.45	16.00	6.00	13.58	4220	2	0.375	64.6	703	36.68
6.5	8F1	0.140	2	24.0	1.000	2.000	1.906	1.969	12.10	16.13	16.00	6.00	13.63	4220				1031	53.59
6.6	8F1**	0.140	2	24.0	1.000	2.032	1.875	1.969	12.15	16.13	16.00	6.00	13.63	4220				955	49.63
7.1	8F1	0.140	2	16.0	1.000	2.079	1.797	1.875	12.00	16.18	16.00	6.00	13.77	4160	2	0.375	64.6	908	46.72
7.2	8C1	0.101	2	18.0	1.000	1.469	2.531	1.313	12.06	15.54	16.00	6.00	13.72	4160	5	0.500	84.7	1081	55.82
7.5	8F1	0.140	3	24.0	1.000	2.032	0.399	2.000	11.97	16.17	16.00	6.00	13.64	4160	8	0.500	84.7	2068	73.17

Table 3.4
Splice specimen properties and test results from Idun and Darwin (1995) (continued)

Specimen No. +	Bar ++ Designation	Relative Rib Area	n	l_s (in.)	d_b (in.)	c_{so} (in.)	c_{si} (in.)	c_b (in.)	b (in.)	h (in.)	l (ft)	l_c (ft)	d (in.)	f'_c (psi)	N	d_s (in.)	f_{yt} (ksi)	M_u (k-in.)	f_s+++ (ksi)
7.6	8C1	0.101	2	16.0	1.000	2.032	1.969	1.938	12.01	16.22	16.00	6.00	13.77	4160	2	0.375	64.6	862	44.34
8.1	8N0	0.069	3	24.0	1.000	2.032	0.453	1.953	12.13	16.23	16.00	6.00	13.76	3830	8	0.500	84.7	1983	69.67
8.2	8N3	0.119	3	24.0	1.000	2.047	0.430	1.969	12.16	16.20	16.00	6.00	13.69	3830	8	0.500	84.7	2247	79.32
8.3	8N0	0.069	2	24.0	1.000	2.000	1.953	2.000	12.11	16.05	16.00	6.00	13.53	3830				1171	61.47
8.4	8N3	0.119	2	16.0	1.000	2.063	1.891	1.906	12.10	16.35	16.00	6.00	13.91	3830	2	0.375	64.6	959	48.90
9.1	8N3	0.119	2	24.0	1.000	2.032	1.875	1.954	12.14	16.19	16.00	6.00	13.70	4230	2	0.375	64.6	1226	63.40
9.2	8F1	0.140	2	18.0	1.000	2.063	1.844	1.290	12.10	15.67	16.00	6.00	13.84	4230	6	0.375	64.6	1351	69.06
9.3	8N0	0.069	2	24.0	1.000	2.094	1.907	1.818	12.19	16.12	16.00	6.00	13.78	4230	2	0.375	64.6	1076	55.25
9.4	8F1	0.140	2	24.0	1.000	2.016	1.891	1.915	12.11	16.17	16.00	6.00	13.72	4230	2	0.375	64.6	1259	65.00
10.1	8N3**	0.119	2	26.0	1.000	2.016	1.907	1.896	12.15	16.16	16.00	6.00	13.72	4250				1120	57.79
10.2	8N3	0.119	2	26.0	1.000	2.063	1.875	1.933	12.13	16.25	16.00	6.00	13.78	4250				1191	61.17
10.3	8N0	0.069	2	26.0	1.000	2.094	1.844	1.798	12.11	16.09	16.00	6.00	13.77	4250	2	0.375	64.6	1144	58.85
10.4	8N0	0.069	2	20.0	1.000	2.079	1.875	1.916	12.07	16.19	16.00	6.00	13.75	4250	5	0.500	84.7	1204	61.98
11.1	8F1	0.140	3	18.0	1.000	2.000	0.453	1.928	12.20	16.14	16.00	6.00	13.68	4380	6	0.500	84.7	1902	66.94
11.2	8N0	0.069	2	18.0	1.000	2.094	1.844	1.881	12.19	16.13	16.00	6.00	13.72	4380	4	0.500	84.7	1202	61.94
11.3	8N3	0.119	2	18.0	1.000	2.063	1.844	1.943	12.13	16.08	16.00	6.00	13.60	4380	4	0.500	84.7	1200	62.44
11.4	8F1	0.140	2	24.0	1.000	2.094	1.844	1.928	12.15	16.23	16.00	6.00	13.77	4380	2	0.375	64.6	1217	62.49
14.1	8C1	0.101	3	36.0	1.000	2.032	0.484	1.877	12.12	16.26	16.00	6.00	13.86	4200	3	0.375	64.6	1725	59.96
14.2***	8C1	0.101	3	21.0	1.000	2.016	0.469	1.897	12.19	16.13	16.00	6.00	13.72	4200	7	0.500	84.7	1788	62.83

\+ Specimen No.
G.P, G = group number (1-11 or 14), P = casting order in the group (1-6), Note: Groups 8-11 cast in concrete containing basalt coarse aggregate.

++ Bar Designation
#AA, # = bar size (No. 8), AA = bar manufacturer and deformation pattern

C0	Conventional Chaparral Steel bar	N0	Conventional North Star Steel bar	S0	Conventional Structural Metals, Inc. bar
C1	New Chaparral Steel bars	N3	New North Star Steel bar	SH0	Conventional Sheffield Steel bar
F1	New Florida Steel bars				

+++ Bar stress is computed based on working stress if f_s does not exceed bar yield stress, otherwise computed based on ultimate strength
M_u and f_s include effects of beam self weight and loading system

* Contained 2 splices and 2 continuous bars

** Spliced bars were coated

*** Specimens with $f_s > f_y$

1 in. = 25.4 mm; 1 ft = 305 mm; 1 psi = 6.89 kPa; 1 ksi = 6.89 MPa; 1 kip = 4.45 kN; 1 k-in. = 0.113 kN-m

Table 3.5
Splice specimen properties and test results from Hester et al. (1991, 1993)

Specimen No. +	Bar ++ Designation	Relative Rib Area	n	l_s (in.)	d_b (in.)	c_{so} (in.)	c_{si} (in.)	c_b (in.)	b (in.)	h (in.)	l (ft)	l_c (ft)	d (in.)	f'_c (psi)	N	d_s (in.)	f_{y1} (ksi)	M_u (k-in.)	f_s +++ (ksi)
1.2	8N0	0.078	3	16.00	1.000	2.000	1.500	2.000	16.00	16.00	13.00	4.00	13.50	5990	2	0.375	77.3	1604	56.00
2.2	8C0	0.071	3	16.00	1.000	2.000	1.500	1.830	16.00	16.28	13.00	4.00	13.95	6200	2	0.375	54.1	1305	43.99
3.2	8S0	0.070	3	16.00	1.000	2.000	1.500	2.080	16.06	16.24	13.00	4.00	13.66	6020	2	0.375	68.9	1348	46.47
4.2	8S0	0.070	3	16.00	1.000	2.000	1.500	2.040	16.09	16.36	13.00	4.00	13.82	6450	2	0.375	68.9	1384	47.06
4.3	8S0	0.070	3	16.00	1.000	2.000	1.500	2.100	16.09	16.28	13.00	4.00	13.68	6450	3	0.375	68.9	1456	50.04
5.2	8C0	0.071	3	16.00	1.000	2.000	1.500	2.060	16.10	16.42	13.00	4.00	13.86	5490	2	0.375	54.1	1367	46.51
5.3	8C0	0.071	3	16.00	1.000	2.000	1.500	2.060	16.09	16.12	13.00	4.00	13.56	5490	3	0.375	54.1	1244	43.31
6.2	8C0	0.071	3	22.75	1.000	2.000	1.500	2.170	16.06	16.20	13.00	4.00	13.53	5850	3	0.375	54.1	1620	56.45
6.3	8C0	0.071	3	22.75	1.000	2.000	1.500	2.160	16.03	16.17	13.00	4.00	13.51	5850	4	0.375	54.1	1595	55.67
7.2	8C0	0.071	2	16.00	1.000	2.000	4.000	2.030	16.00	16.30	13.00	4.00	13.77	5240	3	0.375	54.1	1019	51.49

\+ Specimen No.
G.P, G = group number (1-7), P = casting order in the group (1-3)

++ Bar Designation
#AA, # = bar size (No. 8), AA = bar manufacturer and deformation pattern

- C0 Conventional Chaparral Steel bar
- N0 Conventional North Star Steel bar
- S0 Conventional Structural Metals, Inc. bar

+++ Bar stress is computed based on working stress if f_s does not exceed bar yield stress, otherwise computed based on ultimate strength.
M_u and f_s include effect of beam self weight and loading system.

1 in. = 25.4 mm; 1 ft = 305 mm; 1 psi = 6.89 kPa; 1 ksi = 6.89 MPa; 1 kip = 4.45 kN; 1 k-in. = 0.113 kN-m

Table 3.6
Comparison of splice strengths for epoxy-coated (C) and uncoated (U) high R_r bars

Bar Size	Bar Designation	R_r*	Specimen No.	Surface Condition	Bar Stress (ksi)	C ** / U
No. 5	5C2	0.109	13.4	U	59.96	
			13.3	C	53.91	0.899
			14.3	U	62.84	
			14.4	C	57.34	0.912
No. 8	8C1	0.101	1.3	U	45.01	
			1.4	C	37.09	0.824
			4.5	U	51.06	
			4.6	C	41.72	0.817
	8N3	0.119	10.1	U	61.17	
			10.2	C	57.79	0.945
	8F1	0.140	2.5	U	58.67	
			2.6	C	49.37	0.841
			6.5	U	53.59	
			6.6	C	49.63	0.926
No. 11	11F3	0.127	15.5	U	54.12	
			15.6	C	48.19	0.890
			16.2	U	52.38	
			16.1	C	48.83	0.932
			18.3 ***	U	69.33	
			18.2 ***	C	57.48	0.829
Average						0.882

* R_r = relative rib area

** C/U = ratio of splice strengths of coated to uncoated bars

*** Splices confined by stirrups

1 ksi = 6.89 MPa

Table 3.7

Analysis of effects of relative rib area, R_r, and bar diameter, d_b, on increase in splice strength, represented by $T_s/f'^{1/4}_c$, provided by transverse reinforcement, represented by NA_{tr}/n (T_s in lb, f'_c in psi, and A_{tr} in in.^{2})

Bars	No. of Tests	Weighted Mean R_r	m^+	b^{++}	Mean^{+++} Slope, M	$M^{++++}_{R_r=0.075}$	t_r*	M/t_r**
Conv. No. 5 (L)***	4	0.082	1347	100	1397	1348	1.036	1310
5C2 (L)	4	0.109	1524	122	1585		1.176	1196
Conv. No. 8 (L)***	19	0.073	1727	-228	1612	1606	1.004	1643
8C1 (L)	7	0.101	1901	100	1951		1.214	1563
8F1 (L)	10	0.140	2594	84	2636		1.641	1625
Conv. No. 8 (B)	5	0.069	2415	-382	2224	2295	0.969	
8N3 (B)	4	0.119	3078	-36	3060		1.333	
8F1 (B)	4	0.140	3879	5	3881		1.691	
Conv. No. 11 (L)	6	0.071	1876	333	2043	2138	0.956	2134
11F3 (L)	7	0.127	2909	732	3275		1.532	2188

$^+$ Slope of the best-fit line

$^{++}$ Intercept of best-fit line at $NA_{tr}/n = 0$

$^{+++}$ $M = (2m + b)/2$

$^{++++}$ Based on best-fit line for each bar size and concrete type

* $t_r = M/M_{R_r=0.075}$

** $t_r = 9.6\,R_r + 0.28$ (used to calculate t_d)

*** L = limestone coarse aggregate
B = basalt coarse aggregate

1 lb = 4.45 N; 1 psi = 6.89 kPa; 1 in. = 25.4 mm

Table 4.1
Threaded bar splice specimen properties and test results

Specimen No. +	Bar ++ Designation	n	l_s (in.)	d_b (in.)	c_{so} (in.)	c_{si} (in.)	c_b (in.)	b (in.)	h (in.)	l (ft)	l_c (ft)	d (in.)	f'_c (psi)	N	d_s (in.)	f_{yt} (ksi)	P (kips)	M_u (k-in.)	f_s* (ksi)
3.1**	T-8	2	36.0	1.000	2.047	1.683	1.281	12.09	15.62	16.00	6.00	13.76	5110	12	0.375	69.9	45.32	2469	132.87
3.2**	T-8	2	24.0	1.000	2.032	1.714	1.938	12.13	16.17	16.00	6.00	13.65	5110	6	0.375	69.9	45.18	2460	133.70
3.3	T-8	2	36.0	1.000	1.969	1.775	1.906	12.10	16.09	16.00	6.00	13.61	5110				29.93	1639	84.92
4.3	T-8	2	24.0	1.000	2.032	1.730	1.281	12.15	15.51	16.00	6.00	13.65	4090	4	0.375	69.9	37.91	2067	107.35
7.3***	T-8	2	36.0	1.000	1.953	1.703	1.844	12.11	16.16	16.00	6.00	13.74	4160				26.71	1508	77.74
7.4***	T-8	2	24.0	1.000	2.063	1.625	1.313	12.06	15.65	16.00	6.00	13.76	4160	4	0.375	64.6	27.72	1562	80.40

\+ Specimen No.
G.P, G = group number (3, 4 or 7), P = casting order in the group (1-4)

++ Bar Designation
A-#, A = bar manufacturer and deformation pattern, # = bar size (No. 8)

T Williams Form Engineering Corporation high-strength prestressing bar (R_r = 0.284)

* Bar stress is computed based on working stress if concrete did not crush, otherwise computed based on ultimate strength
M_u and f_s include effects of beam self weight and loading system

** Concrete crushed on compression face prior to splice failure

*** Spliced bars were separated to prevent interlocking of the ribs

1 in. = 25.4 mm; 1 ft = 305 mm; 1 psi = 6.89 kPa; 1 ksi = 6.89 MPa; 1 kip = 4.45 kN; 1 k-in. = 0.113 kN-m

Table 4.2
Concrete mix proportions (lb/yd^3) and properties

Group	w/c Ratio	Cement	Water	Fine Agg.*	Coarse Agg.**	wr (oz)	Slump (in.)	Concrete Temp. (F)	Air Content (%)	Test Age (days)	Cylinder Strength (psi)
3	0.36	582	208	1575	1608	3	2.75	93	3.70	7	5110
4	0.36	582	208	1575	1608	3	1.75	95	4.50	5	4090
7	0.36	582	208	1575	1608	3	5.25	67	3.50	7	4160

* Kansas River Sand - Lawrence Sand Co., Lawrence, KS
Bulk Specific Gravity (SSD) = 2.62; Absorption = 0.5 %; Fineness Modulus = 2.89

** Crushed Limestone - Fogel's Quarry, Ottawa, KS
Bulk Specific Gravity (SSD) = 2.58; Absorption = 2.7 %; Max. Size = 3/4 in.;
Unit Weight = 90.5 lb/cu. ft

wr Water Reducer per 100 lb Cement

1 lb/yd^3 = 0.5933 kg/m^3; 1 oz = 29.57 cm^3; 1 psi = 6.89 kPa

Table 4.3
Test/prediction ratios for threaded bar splice tests

Specimen No.	l_s (in.)	d_b (in.)	c_M (in.)	c_m (in.)	$\frac{NA_{tr}}{n}$ (in.^{2})	f'_c (psi)	f_s (ksi)	$T_b/f'^{1/4}_c$ Test (in.^{2})	$T_c/f'^{1/4}_c$ Eq. 3.1$^+$ (in.^{2})	$T_s/f'^{1/4}_c$ Test (in.^{2})	$T_s/f'^{1/4}_c$ Eq. 3.7a^{++} (in.^{2})	$T_b/f'^{1/4}_c$ Eq. 3.10^{+++} (in.^{2})	Test / Prediction
Beams without transverse reinforcement													
3.3	36.0	1.000	1.969	1.906	-	5110	84.92	7935	7163	-	-	7163	1.108
7.3*	36.0	1.000	1.953	1.844	-	4160	77.74	7647	7040	-	-	7040	1.086
Beams with transverse reinforcement													
3.1**	36.0	1.000	1.933	1.281	1.32	5110	132.87	12415	6013	6402	8900	14913	0.833
3.2**	24.0	1.000	1.964	1.938	0.66	5110	133.70	12493	5376	7116	4483	9859	1.267
4.3	24.0	1.000	1.980	1.281	0.44	4090	107.35	10605	4614	5990	3011	7625	1.391
7.4*	24.0	1.000	1.875	1.313	0.44	4160	80.40	7909	4613	3295	3011	7624	1.037

* Spliced bars were separated to prevent interlocking of the ribs

** Concrete crushed on compression face prior to splice failure

$^+$ Eq. 3.1 $= \dfrac{T_c}{f'^{1/4}_c} = [63\, l_d\, (c_m + 0.5\, d_b) + 2130\, A_b]\left(0.1\dfrac{c_M}{c_m} + 0.9\right)$

$^{++}$ Eq. 3.7a $= \dfrac{T_s}{f'^{1/4}_c} = 2226\,(9.6\, R_r + 0.28)\,(0.72\, d_b + 0.28)\dfrac{NA_{tr}}{n} + 66$

$^{+++}$ Eq. 3.10 $= \dfrac{T_c + T_s}{f'^{1/4}_c}$

1 in. = 25.4 mm; 1 psi = 6.89 kPa; 1 ksi = 6.89 MPa

Table 5.1
Moment-rotation test specimen properties

Spec. No.+	Bar ++ Desig.	Number of Bars	c_{so} (in.)	c_{si} (in.)	c_b (in.)	d (in.)	b (in.)	h (in.)	l (ft)	l_c (ft)	a (in.)
16.5	8N0	2	2.125	2.813	1.926	13.67	12.00	16.10	16.00	15.00	9.04
16.6	8N3	2	2.078	2.875	1.971	13.61	12.06	16.09	16.00	15.00	9.01
17.1	8N0	3	2.094	1.156	1.919	13.67	12.04	16.08	16.00	15.00	9.01
17.2	8N3	3	2.031	1.094	1.915	13.72	12.06	16.13	16.00	15.00	9.05

Table 5.2
Properties of reinforcing bars

Bar ++ Designation	Yield Str. (ksi)	Nominal Diameter (in.)	Weight (lb/ft)	% Light or Heavy	Rib Spacing (in.)	Rib Height ASTM (in.)	Rib Height Avg. * (in.)	Relative Rib Area
8N0	78.0	1.000	2.594	2.8%L	0.650	0.057	0.054	0.069
8N3	80.3	1.000	2.730	2.2%H	0.487	0.072	0.068	0.119

Table 5.3
Concrete mix proportions (lb/yd^3) and properties

Group	w/c Ratio	Cement	Water	Fine Agg.**	Coarse Agg.**	Slump (in.)	Concrete Temp (F)	Air Content (%)	Test Age (days)	Cylinder Strength (psi)
16	0.44	508	224	1554	1650	3.25	59	3.10	23	5170
17	0.44	508	224	1554	1650	2.50	59	4.00	20	4760

\+ Specimen No.
G.P, G = group number (16 or 17), P = casting order in the group (1, 2, 5, or 6)

++ Bar Designation
#AA, # = bar size (No. 8), AA = bar manufacturer and deformation pattern

N0 Conventional North Star Steel bar N3 New North Star Steel bar

* Average rib height between longitudinal ribs

** See Table 3.3 for aggregate properties

1 in. = 25.4 mm; 1 ft = 305 mm; 1 psi = 6.89 kPa; 1 ksi = 6.89 MPa;
1 lb/ft = 1.49 kg/m; 1 lb/yd^3 = 0.5933 kg/m^3

Table 6.1
Splice length ratios, l_s(Eq. 3.14)/l_s(ACI), comparing Eq. 3.14 and ACI Class A and Class B splices for uncoated bars not confined by transverse reinforcement with $c/d_b \leq 2.5$

f'_c (psi)	No. 6 and smaller bars				No. 7 and larger bars	
	f_y = 40 ksi		f_y = 60 ksi		f_y = 60 ksi	
	Class A*	Class B	Class A*	Class B	Class A*	Class B
3000	1.11	0.85	1.31	1.01	1.05	0.81
6000	1.19	0.91	1.47	1.13	1.18	0.90
9000			1.56	1.20	1.25	0.96
12000			1.48	1.14	1.18	0.91
15000			1.36	1.05	1.09	0.84

* Class A splice length is equal to development length
1 psi = 6.89 kPa; 1 ksi = 6.89 MPa

Table 6.2
Splice length ratios, l_s(Eq. 3.14)/l_s(ACI), comparing Eq. 3.14 and ACI Class A and Class B splices for uncoated bars not confined by transverse reinforcement with $c/d_b = 4$

f'_c (psi)	No. 6 and smaller bars				No. 7 and larger bars	
	f_y = 40 ksi		f_y = 60 ksi		f_y = 60 ksi	
	Class A*	Class B	Class A*	Class B	Class A*	Class B
3000	0.91	0.70	0.82	0.63	0.66	0.50
6000	1.29	0.99	0.92	0.71	0.73	0.57
9000			1.05	0.81	0.84	0.65
12000			1.11	0.85	0.89	0.68
15000			1.11	0.85	0.89	0.68

* Class A splice length is equal to development length
1 psi = 6.89 kPa; 1 ksi = 6.89 MPa

Table 6.3
Comparison of development and splice lengths for bars with 2 in. cover confined by No. 3 stirrups spaced 6 in. on center

				ACI 318-95		Eq. 3.14[+]		New** / Conv.*	Eq. 3.14[+] / ACI l_d	Eq. 3.14[+] / ACI l_d	Eq. 3.14[+] / ACI l_s	Eq. 3.14[+] / ACI l_s
d_b (in.)	f_y (ksi)	f'_c (psi)	c/d_b	l_d (in.)	l_s (in.)	l_d (Conv.*) (in.)	l_d (New**) (in.)	Eq. 3.14[+]	Conv.*	New**	Conv.*	New**
0.75	40	3000	3.167	13.15	17.09	12.00	12.00	1.000	0.913	0.913	0.702	0.702
0.75	40	6000	3.167	12.00	12.08	12.00	12.00	1.000	1.000	1.000	0.993	0.993
0.75	60	3000	3.167	19.72	25.63	16.76	16.16	0.965	0.850	0.820	0.654	0.631
0.75	60	6000	3.167	13.94	18.13	13.28	12.81	0.965	0.952	0.918	0.732	0.706
0.75	60	9000	3.167	12.00	14.80	12.00	12.00	1.000	1.000	1.000	0.811	0.811
0.75	60	12000	3.167	12.00	14.04	12.00	12.00	1.000	1.000	1.000	0.855	0.855
0.75	60	15000	3.167	12.00	14.04	12.00	12.00	1.000	1.000	1.000	0.855	0.855
1.00	60	3000	2.500	32.86	42.72	27.52	24.83	0.902	0.837	0.756	0.644	0.581
1.00	60	6000	2.500	23.24	30.21	21.80	19.67	0.902	0.938	0.847	0.722	0.651
1.00	60	9000	2.500	18.97	24.67	18.89	17.04	0.902	0.996	0.898	0.766	0.691
1.00	60	12000	2.500	18.00	23.40	16.99	16.00	0.942	0.944	0.889	0.726	0.684
1.00	60	15000	2.500	18.00	23.40	16.00	16.00	1.000	0.889	0.889	0.684	0.684
1.41	60	3000	1.918	47.51	61.76	48.63	43.24	0.889	1.024	0.910	0.788	0.700
1.41	60	6000	1.918	33.59	43.67	38.53	34.26	0.889	1.147	1.020	0.882	0.784
1.41	60	9000	1.918	27.43	35.66	33.38	29.68	0.889	1.217	1.082	0.936	0.832
1.41	60	12000	1.918	26.02	33.83	30.03	26.70	0.889	1.154	1.026	0.888	0.789
1.41	60	15000	1.918	26.02	33.83	27.59	24.53	0.889	1.060	0.943	0.816	0.725
							Max.	1.000	1.217	1.082	0.993	0.993
							Min.	0.889	0.837	0.756	0.644	0.581
							Avg.	0.943	0.995	0.936	0.791	0.746

* Conventional bars, $R_r = 0.0727$

** High relative rib area bars, $R_r = 0.1275$

[+] Eq. 3.14 $= \dfrac{l_d}{d_b} = \dfrac{\dfrac{f_y}{f_c'^{1/4}} - 1900}{72\left(\dfrac{c + K_{tr}}{d_b}\right)}$

1 in. = 25.4 mm; 1 psi = 6.89 kPa; 1 ksi = 6.89 MPa

Table 6.4
Comparison of development and splice lengths for bars with 2 in. cover confined by No. 4 stirrups spaced 6 in. on center

				ACI 318-95		Eq. 3.14[+]		New** / Conv.*	Eq. 3.14[+] / ACI l_d	Eq. 3.14[+] / ACI l_d	Eq. 3.14[+] / ACI l_s	Eq. 3.14[+] / ACI l_s
d_b (in.)	f_y (ksi)	f'_c (psi)	c/d_b	l_d (in.)	l_s (in.)	l_d (Conv.*) (in.)	l_d (New**) (in.)	Eq. 3.14[+]	Conv.*	New**	Conv.*	New**
0.75	40	3000	3.167	13.15	17.09	12.00	12.00	1.000	0.913	0.913	0.702	0.702
0.75	40	6000	3.167	12.00	12.08	12.00	12.00	1.000	1.000	1.000	0.993	0.993
0.75	60	3000	3.167	19.72	25.63	16.16	16.16	1.000	0.820	0.820	0.631	0.631
0.75	60	6000	3.167	13.94	18.13	12.81	12.81	1.000	0.918	0.918	0.706	0.706
0.75	60	9000	3.167	12.00	14.80	12.00	12.00	1.000	1.000	1.000	0.811	0.811
0.75	60	12000	3.167	12.00	14.04	12.00	12.00	1.000	1.000	1.000	0.855	0.855
0.75	60	15000	3.167	12.00	14.04	12.00	12.00	1.000	1.000	1.000	0.855	0.855
1.00	60	3000	2.500	32.86	42.72	23.62	21.55	0.913	0.719	0.656	0.553	0.504
1.00	60	6000	2.500	23.24	30.21	18.71	17.07	0.913	0.805	0.735	0.619	0.565
1.00	60	9000	2.500	18.97	24.67	16.21	16.00	0.987	0.854	0.843	0.657	0.649
1.00	60	12000	2.500	18.00	23.40	16.00	16.00	1.000	0.889	0.889	0.684	0.684
1.00	60	15000	2.500	18.00	23.40	16.00	16.00	1.000	0.889	0.889	0.684	0.684
1.41	60	3000	1.918	46.34	60.24	40.86	34.33	0.840	0.882	0.741	0.678	0.570
1.41	60	6000	1.918	32.77	42.60	32.37	27.19	0.840	0.988	0.830	0.760	0.638
1.41	60	9000	1.918	26.75	34.78	28.04	23.56	0.840	1.048	0.881	0.806	0.677
1.41	60	12000	1.918	25.38	32.99	25.23	22.56	0.894	0.994	0.889	0.765	0.684
1.41	60	15000	1.918	25.38	32.99	23.18	22.56	0.973	0.913	0.889	0.703	0.684
							Max.	1.000	1.048	1.000	0.993	0.993
							Min.	0.840	0.719	0.656	0.553	0.504
							Avg.	0.953	0.920	0.876	0.733	0.700

Table 6.4
Comparison of development and splice lengths for bars with 2 in. cover confined by No. 4 stirrups spaced 6 in. on center (continued)

d_b (in.)	f_y (ksi)	f'_c (psi)	c/d_b	ACI 318-95 l_d (in.)	ACI 318-95 l_s (in.)	Eq. 3.14+ l_d (Conv.*) (in.)	Eq. 3.14+ l_d (New**) (in.)	New** Conv.* Eq. 3.14+	Eq. 3.14+ ACI l_d Conv.*	Eq. 3.14+ ACI l_d New**	Eq. 3.14+ ACI l_s Conv.*	Eq. 3.14+ ACI l_s New**
For all data in Tables 6.3 and 6.4							Max.	1.000	1.217	1.082	0.993	0.993
							Min.	0.840	0.719	0.656	0.553	0.504
							Avg.	0.948	0.957	0.906	0.762	0.723

* Conventional bars, $R_r = 0.0727$

** High relative rib area bars, $R_r = 0.1275$

\+ Eq. 3.14 $= \dfrac{l_d}{d_b} = \dfrac{\dfrac{f_y}{f_c'^{1/4}} - 1900}{72\left(\dfrac{c + K_{tr}}{d_b}\right)}$

1 in. = 25.4 mm; 1 psi = 6.89 kPa; 1 ksi = 6.89 MPa

Table 6.5

Ratios of development length, l_d(new)/l_d(conv.), comparing new (high R_r) and conventional Grade 60 reinforcing bars confined by transverse reinforcement (based on Eq. 3.14)

c/d_b	f'_c = 3000 psi K_{tr}(new)/d_b*			f'_c = 6000 psi K_{tr}(new)/d_b*			f'_c = 9000 psi K_{tr}(new)/d_b*			f'_c = 12000 psi K_{tr}(new)/d_b*			f'_c = 15000 psi K_{tr}(new)/d_b*		
	1	2	3	1	2	3	1	2	3	1	2	3	1	2	3
1	0.83	0.77	0.74	0.83	0.77	0.74	0.83	0.77	0.80	0.83	0.77	0.89	0.83	0.77	0.97
1.5	0.86	0.80	0.86	0.86	0.80	0.86	0.86	0.80	0.93	0.86	0.84	1.00	0.86	0.92	1.00
2	0.88	0.83	0.99	0.88	0.83	0.99	0.88	0.89	1.00	0.88	0.99	1.00	0.88	1.00	1.00
2.5	0.90	0.95	1.00	0.90	0.95	1.00	0.90	1.00	1.00	0.95	1.00	1.00	1.00	1.00	1.00
3	0.91	1.00	1.00	0.91	1.00	1.00	0.99	1.00	1.00	1.00	1.00	1.00	1.00	1.00	1.00

* K_{tr}(conv.) = 0.65 K_{tr}(new), $(c + K_{tr})/d_b \leq 4$

1 psi = 6.89 kPa

Table 6.6

Ratios of development length, l_d(new)/l_d(conv.), comparing new (high R_r) and conventional Grade 40 reinforcing bars confined by transverse reinforcement (based on Eq. 3.14)

c/d_b	f'_c = 3000 psi K_{tr}(new)/d_b*			f'_c = 6000 psi K_{tr}(new)/d_b*		
	1	2	3	1	2	3
1	0.83	0.77	0.97	0.83	1.00	1.00
1.5	0.86	0.92	1.00	0.94	1.00	1.00
2	0.88	1.00	1.00	1.00	1.00	1.00
2.5	1.00	1.00	1.00	1.00	1.00	1.00
3	1.00	1.00	1.00	1.00	1.00	1.00

* K_{tr}(conv.) = 0.65 K_{tr}(new), $(c + K_{tr})/d_b \leq 4$

1 psi = 6.89 kPa

Table 6.7
Ratios of development length, l_d(coated)/l_d(uncoated), for new (high R_r) and conventional reinforcing bars not confined by transverse reinforcement (based on Eq. 3.14)

f'_c (psi)	Conventional bars*				New bars**			
	f_y = 40 ksi		f_y = 60 ksi		f_y = 40 ksi		f_y = 60 ksi	
	c/d_b=1	c/d_b=4	c/d_b=1	c/d_b=4	c/d_b=1	c/d_b=4	c/d_b=1	c/d_b=4
3000	1.54	1.17	1.46	1.46	1.21	1.00	1.18	1.18
6000	1.60	1.00	1.49	1.49	1.23	1.00	1.19	1.19
9000			1.51	1.39			1.20	1.11
12000			1.53	1.27			1.20	1.00
15000			1.54	1.18			1.21	1.00

* Average R_r = 0.0727, β = 0.74

** Average R_r = 0.1275, β = 0.88

1 psi = 6.89 kPa; 1 ksi = 6.89 MPa

Table 6.8
Ratios of development length, l_d(new)/l_d(conv.), comparing new (high R_r) and conventional coated reinforcing bars not confined by transverse reinforcement (based on Eq. 3.14)

f'_c (psi)	f_y = 40 ksi		f_y = 60 ksi	
	c/d_b=1	c/d_b=4	c/d_b=1	c/d_b=4
3000	0.78	0.85	0.81	0.81
6000	0.77	1.00	0.80	0.80
9000			0.79	0.79
12000			0.79	0.79
15000			0.79	0.85

1 psi = 6.89 kPa; 1 ksi = 6.89 MPa

Table 6.9

Ratios of development length, l_d(new)/l_d(conv.), comparing new (high R_r) and conventional Grade 60 coated reinforcing bars confined by transverse reinforcement (based on Eq. 3.14)

c/d_b	f'_c = 3000 psi K_{tr}(new)/d_b*			f'_c = 6000 psi K_{tr}(new)/d_b*			f'_c = 9000 psi K_{tr}(new)/d_b*			f'_c = 12000 psi K_{tr}(new)/d_b*			f'_c = 15000 psi K_{tr}(new)/d_b*		
	1	2	3	1	2	3	1	2	3	1	2	3	1	2	3
1	0.67	0.62	0.60	0.66	0.61	0.59	0.65	0.61	0.59	0.65	0.61	0.58	0.65	0.60	0.63
1.5	0.69	0.65	0.70	0.69	0.64	0.69	0.68	0.64	0.68	0.68	0.63	0.68	0.68	0.63	0.73
2	0.71	0.67	0.80	0.71	0.66	0.79	0.70	0.65	0.78	0.70	0.65	0.78	0.69	0.70	0.84
2.5	0.73	0.77	0.81	0.72	0.76	0.80	0.71	0.75	0.79	0.71	0.75	0.79	0.71	0.81	0.85
3	0.74	0.81	0.81	0.73	0.80	0.80	0.72	0.79	0.79	0.72	0.79	0.79	0.77	0.85	0.85

* K_{tr}(conv.) = 0.65 K_{tr}(new), $(c + K_{tr})/d_b \leq 4$

1 psi = 6.89 kPa

Table 6.10

Ratios of development length, l_d(new)/l_d(conv.), comparing new (high R_r) and conventional Grade 40 coated reinforcing bars confined by transverse reinforcement (based on Eq. 3.14)

c/d_b	f'_c = 3000 psi K_{tr}(new)/d_b*			f'_c = 6000 psi K_{tr}(new)/d_b*		
	1	2	3	1	2	3
1	0.65	0.60	0.63	0.63	0.62	0.80
1.5	0.68	0.63	0.74	0.66	0.76	0.94
2	0.69	0.70	0.84	0.72	0.90	1.00
2.5	0.71	0.81	0.85	0.86	1.00	1.00
3	0.78	0.85	0.85	0.99	1.00	1.00

* K_{tr}(conv.) = 0.65 K_{tr}(new), $(c + K_{tr})/d_b \leq 4$

1 psi = 6.89 kPa

Table 6.11
Splice data for bridge structure

Splice No.	Number of Bars	Coated	Top Bar	d_b* bar a (in.)	d_b* bar b (in.)	Cover c_b (in.)	Cover c_{so} (in.)	Cover c_{si} (in.)	Transverse Reinf. A_{tr}/n ($in.^2$)	Transverse Reinf. s (in.)
1	112	N	N	0.625	0.625	2.00	NA	2.38	0.000	
2	4	N	N	0.625	0.625	2.00	2.00	NA	0.000	
3	6	N	Y	0.500	0.500	2.63	11.50	9.00	0.310	12.00
4	10	N	Y	0.500	0.500	2.63	2.63	4.25	0.310	12.00
5	10	N	Y	0.500	0.500	2.63	2.63	4.25	0.310	12.00
6	26	N	Y	0.625	0.625	2.00	3.00	5.38	0.000	
7	26	N	Y	0.625	0.625	2.00	3.00	5.38	0.000	
8	112	N	N	0.625	0.625	2.00	NA	2.38	0.000	
9	4	N	N	0.625	0.625	2.00	2.00	NA	0.000	
10	6	N	Y	0.500	0.500	2.63	11.50	9.00	0.310	12.00
11	10	N	Y	0.500	0.500	2.63	2.63	4.25	0.310	12.00
12	10	N	Y	0.500	0.500	2.63	2.63	4.25	0.310	12.00
13	8	Y	N	1.000	1.000	3.75	2.75	10.00	0.440	17.00
14	8	Y	Y	1.000	1.000	4.13	2.75	8.50	0.440	17.00
15	20	Y	N	0.750	0.750	3.13	2.25	7.88	0.000	
16	4	Y	N	0.750	0.750	3.13	2.25	7.88	0.000	
17	96	Y	N	0.750	0.750	2.00	NA	7.75	0.000	
18	96	Y	N	0.750	0.750	2.00	NA	7.75	0.000	
19	4	Y	N	0.750	0.750	2.00	2.40	8.25	0.000	
20	4	Y	N	0.750	0.750	2.00	2.40	8.25	0.000	

Table 6.11
Splice data for bridge structure (continued)

Splice No.	Number of Bars	Coated	Top Bar	d_b* bar a (in.)	d_b* bar b (in.)	Cover c_b (in.)	Cover c_{so} (in.)	Cover c_{si} (in.)	Transverse Reinf. A_{tr}/n ($in.^2$)	Transverse Reinf. s (in.)
21	48	Y	N	0.500	0.625	3.13	NA	11.00	0.200	11.00
22	48	Y	N	0.500	0.625	3.13	NA	11.00	0.200	11.00
23	8	Y	N	0.625	0.750	2.38	1.88	3.00	0.073	13.75
24	8	Y	N	0.625	0.750	2.38	1.88	3.00	0.073	13.75
25**	218	Y	N	0.625	0.625	1.00	NA	10.38	0.000	
26	4	Y	N	0.500	0.750	2.38	1.88	3.00	0.073	13.75
27	4	Y	N	0.500	0.750	2.38	1.88	3.00	0.073	13.75
28	24	Y	Y	0.500	0.500	2.75	NA	10.00	0.440	32.75
29	288	Y	N	0.500	0.500	1.63	NA	6.00	0.200	11.00
30	16	Y	N	0.500	0.500	2.00	2.00	3.00	0.200	12.00
31	4	Y	Y	0.500	0.500	2.50	2.50	NA	0.000	
32	384	Y	N	0.500	0.500	1.50	3.00	1.44	0.000	
33	48	Y	N	0.500	0.500	3.13	NA	11.00	0.200	11.00
34	256	Y	N	0.375	0.375	1.50	NA	1.13	0.000	
35	24	Y	N	0.75	0.75	1.63	3.25	5.69	0.000	

* Bar size a spliced to bar size b

** Class A splice, all other splices are Class B

Note: $f_y = f_{yt} = 60{,}000$ psi and $f'_c = 4{,}000$ psi

1 in. = 25.4 mm; 1 psi = 6.89 kPa

Table 6.12
Splice lengths for bridge structure

Splice No.	Orig. l_s (in.)	ACI '95 l_s (in.)	l_s (Eq. 3.13+) Conv.* (in.)	l_s (Eq. 3.13+) New** (in.)	l_s (Eq. 3.14++) Conv.* (in.)	l_s (Eq. 3.14++) New** (in.)
1	26.00	18.50	12.71	12.71	13.24	13.24
2	26.00	18.50	13.24	13.24	13.24	13.24
3	18.00	19.24	12.00	12.00	12.74	12.74
4	24.00	19.24	12.74	12.74	12.74	12.74
5	24.00	19.24	12.74	12.74	12.74	12.74
6	24.00	24.05	16.12	16.12	17.22	17.22
7	24.00	24.05	16.12	16.12	17.22	17.22
8	26.00	18.50	12.71	12.71	13.24	13.24
9	26.00	18.50	13.24	13.24	13.24	13.24
10	18.00	19.24	12.00	12.00	12.74	12.74
11	24.00	19.24	12.74	12.74	12.74	12.74
12	24.00	19.24	12.74	12.74	12.74	12.74
13	51.00	55.50	28.56	22.93	28.80	23.17
14	51.00	62.90	37.02	29.69	37.44	30.12
15	22.00	26.64	23.55	18.91	24.69	19.86
16	22.00	26.64	23.55	18.91	24.69	19.86
17	36.00	33.30	20.58	16.31	27.29	21.95
18	36.00	33.30	20.58	16.31	27.29	21.95
19	36.00	33.30	26.63	21.40	27.29	21.95
20	36.00	33.30	26.63	21.40	27.29	21.95
21	15.00	17.76	13.58	12.00	14.40	12.00
22	15.00	17.76	13.58	12.00	14.40	12.00
23	31.00	22.20	18.80	14.66	19.39	15.13
24	31.00	22.20	18.80	14.66	19.39	15.13
25	18.00	25.41	25.86	20.50	34.29	27.59
26	31.00	17.76	14.31	12.00	14.40	12.00
27	31.00	17.76	14.31	12.00	14.40	12.00
28	21.00	23.09	17.65	13.99	18.72	15.06
29	15.00	17.76	13.58	12.00	14.40	12.00
30	19.00	17.76	14.40	12.00	14.40	12.00
31	21.00	23.09	18.72	15.06	18.72	15.06
32	16.00	22.20	16.21	13.03	17.07	13.73
33	15.00	17.76	13.58	12.00	14.40	12.00
34	15.00	13.32	12.00	12.00	12.34	12.00
35	29.00	33.30	28.78	23.02	32.40	26.07

$$+ \quad \text{Eq. 3.13} = \frac{l_d}{d_b} = \frac{\frac{f_y}{f_c'^{1/4}} - 1900\left(0.1\frac{c_M}{c_m} + 0.9\right)}{72\left(\frac{c + K_{tr}}{d_b}\right)} \qquad ++ \quad \text{Eq. 3.14} = \frac{l_d}{d_b} = \frac{\frac{f_y}{f_c'^{1/4}} - 1900}{72\left(\frac{c + K_{tr}}{d_b}\right)}$$

Note: Definition of c in Eq. 3.13 is different than c in Eq. 3.14 (see Chapter 3)

* Conventional reinforcement (avg. $R_r = 0.0727$)

** New reinforcement (avg. $R_r = 0.1275$)

1 in. = 25.4 mm

Table 6.13
Splice length ratios for bridge structure

Spl. No.	ACI '95 Orig.	Eq. 3.13^{+} Orig. Conv.*	Eq. 3.13^{+} Orig. New**	Eq. 3.14^{++} Orig. Conv.*	Eq. 3.14^{++} Orig. New**	Eq. 3.13^{+} ACI '95 Conv.*	Eq. 3.13^{+} ACI '95 New**	Eq. 3.14^{++} ACI '95 Conv.*	Eq. 3.14^{++} ACI '95 New**	Eq. 3.13^{+} Eq. 3.14^{++} Conv.*	Eq. 3.13^{+} Eq. 3.14^{++} New**	New** Conv.* Eq. 3.13^{+}	New** Conv.* Eq. 3.14^{++}
1	0.712	0.489	0.489	0.509	0.509	0.687	0.687	0.716	0.716	0.959	0.959	1.000	1.000
2	0.712	0.509	0.509	0.509	0.509	0.716	0.716	0.716	0.716	1.000	1.000	1.000	1.000
3	1.069	0.667	0.667	0.708	0.708	0.624	0.624	0.662	0.662	0.942	0.942	1.000	1.000
4	0.802	0.531	0.531	0.531	0.531	0.662	0.662	0.662	0.662	1.000	1.000	1.000	1.000
5	0.802	0.531	0.531	0.531	0.531	0.662	0.662	0.662	0.662	1.000	1.000	1.000	1.000
6	1.002	0.672	0.672	0.717	0.717	0.670	0.670	0.716	0.716	0.936	0.936	1.000	1.000
7	1.002	0.672	0.672	0.717	0.717	0.670	0.670	0.716	0.716	0.936	0.936	1.000	1.000
8	0.712	0.489	0.489	0.509	0.509	0.687	0.687	0.716	0.716	0.959	0.959	1.000	1.000
9	0.712	0.509	0.509	0.509	0.509	0.716	0.716	0.716	0.716	1.000	1.000	1.000	1.000
10	1.069	0.667	0.667	0.708	0.708	0.624	0.624	0.662	0.662	0.942	0.942	1.000	1.000
11	0.802	0.531	0.531	0.531	0.531	0.662	0.662	0.662	0.662	1.000	1.000	1.000	1.000
12	0.802	0.531	0.531	0.531	0.531	0.662	0.662	0.662	0.662	1.000	1.000	1.000	1.000
13	1.088	0.560	0.450	0.565	0.454	0.515	0.413	0.519	0.418	0.992	0.990	0.803	0.804
14	1.233	0.726	0.582	0.734	0.591	0.589	0.472	0.595	0.479	0.989	0.986	0.802	0.804
15	1.211	1.071	0.859	1.122	0.903	0.884	0.710	0.927	0.746	0.954	0.952	0.803	0.804
16	1.211	1.071	0.859	1.122	0.903	0.884	0.710	0.927	0.746	0.954	0.952	0.803	0.804
17	0.925	0.572	0.453	0.758	0.610	0.618	0.490	0.819	0.659	0.754	0.743	0.793	0.804
18	0.925	0.572	0.453	0.758	0.610	0.618	0.490	0.819	0.659	0.754	0.743	0.793	0.804
19	0.925	0.740	0.594	0.758	0.610	0.800	0.643	0.819	0.659	0.976	0.975	0.804	0.804
20	0.925	0.740	0.594	0.758	0.610	0.800	0.643	0.819	0.659	0.976	0.975	0.804	0.804

Table 6.14
Change in steel weight for bridge structure

Splice No.	ACI '95	Change in weight of steel (lb) Eq. 3.13[+]		Eq. 3.14[++]	
		Conv.*	New**	Conv.*	New**
1	-73.02	-129.41	-129.41	-124.19	-124.19
2	-2.61	-4.44	-4.44	-4.44	-4.44
3	0.41	-2.00	-2.00	-1.76	-1.76
4	-2.65	-6.27	-6.27	-6.27	-6.27
5	-2.65	-6.27	-6.27	-6.27	-6.27
6	0.11	-17.81	-17.81	-15.33	-15.33
7	0.11	-17.81	-17.81	-15.33	-15.33
8	-73.02	-129.41	-129.41	-124.19	-124.19
9	-2.61	-4.44	-4.44	-4.44	-4.44
10	0.41	-2.00	-2.00	-1.76	-1.76
11	-2.65	-6.27	-6.27	-6.27	-6.27
12	-2.65	-6.27	-6.27	-6.27	-6.27
13	8.01	-39.94	-49.96	-39.51	-49.53
14	21.18	-24.89	-37.92	-24.13	-37.16
15	11.61	3.89	-7.74	6.73	-5.35
16	2.32	0.78	-1.55	1.35	-1.07
17	-32.46	-185.29	-236.58	-104.69	-168.80
18	-32.46	-185.29	-236.58	-104.69	-168.80
19	-1.35	-4.69	-7.31	-4.36	-7.03
20	-1.35	-4.69	-7.31	-4.36	-7.03
21	11.51	-5.94	-12.52	-2.50	-12.52
22	11.51	-5.94	-12.52	-2.50	-12.52
23	-8.81	-12.22	-16.36	-11.63	-15.89
24	-8.81	-12.22	-16.36	-11.63	-15.89
25	140.43	148.95	47.32	308.66	181.62
26	-6.63	-8.35	-9.51	-8.31	-9.51
27	-6.63	-8.35	-9.51	-8.31	-9.51
28	2.79	-4.48	-9.37	-3.04	-7.93
29	44.24	-22.81	-48.10	-9.59	-48.10
30	-1.11	-4.10	-6.23	-4.10	-6.23
31	0.46	-0.51	-1.32	-0.51	-1.32
32	132.51	4.48	-63.47	22.85	-48.50
33	7.37	-3.80	-8.02	-1.60	-8.02
34	-13.48	-24.06	-24.06	-21.30	-24.06
35	12.91	-0.65	-17.95	10.23	-8.81

Table 6.14
Change in steel weight for bridge structure (continued)

Splice No.	ACI '95	Change in weight of steel (lb) Eq. 3.13+ Conv.*	Eq. 3.13+ New**	Eq. 3.14++ Conv.*	Eq. 3.14++ New**
All reinforcement					
Weight (lb)	93474	92608	92216	93008	92533
Change from original (lb)	132.97	-732.50	-1125.32	-333.43	-808.47
Change from original (%)	0.14	-0.78	-1.21	-0.36	-0.87
Uncoated reinforcement					
Weight (lb)	17249	17078	17078	17094	17094
Change from original (lb)	-160.80	-332.38	-332.38	-316.50	-316.50
Change from original (%)	-0.92	-1.91	-1.91	-1.82	-1.82
Coated reinforcement					
Weight (lb)	76225	75531	75138	75914	75439
Change from original (lb)	293.77	-400.12	-792.94	-16.94	-491.98
Change from original (%)	0.39	-0.53	-1.04	-0.02	-0.65

$$+ \quad \text{Eq. 3.13} = \frac{l_d}{d_b} = \frac{\frac{f_y}{f_c'^{1/4}} - 1900\left(0.1\frac{c_M}{c_m} + 0.9\right)}{72\left(\frac{c + K_{tr}}{d_b}\right)}$$

$$++ \quad \text{Eq. 3.14} = \frac{l_d}{d_b} = \frac{\frac{f_y}{f_c'^{1/4}} - 1900}{72\left(\frac{c + K_{tr}}{d_b}\right)}$$

Note: Definition of c in Eq. 3.13 is different than c in Eq. 3.14 (see Chapter 3)

* Conventional reinforcement (avg. $R_r = 0.0727$)

** New reinforcement (avg. $R_r = 0.1275$)

1 lb = 0.454 kg

Table 6.15
Summary of splice length ratios for lateral load resisting frame system

	ACI '95 Orig.	Eq. 3.13[+] Orig. Conv.*	Eq. 3.13[+] Orig. New**	Eq. 3.14[++] Orig. Conv.*	Eq. 3.14[++] Orig. New**	Eq. 3.13[+] ACI '95 Conv.*	Eq. 3.13[+] ACI '95 New**	Eq. 3.14[++] ACI '95 Conv.*	Eq. 3.14[++] ACI '95 New**	Eq. 3.13[+] Eq. 3.14[++] Conv.*	Eq. 3.13[+] Eq. 3.14[++] New**	New** Conv.* Eq. 3.13[+]	New** Conv.* Eq. 3.14[++]
Beams													
Max.	1.090	0.781	0.740	0.934	0.853	0.906	0.864	0.906	0.864	1.000	1.000	0.957	0.954
Min.	0.444	0.336	0.285	0.341	0.291	0.600	0.536	0.677	0.564	0.809	0.825	0.833	0.831
Avg.	0.622	0.480	0.427	0.516	0.455	0.782	0.697	0.826	0.731	0.949	0.954	0.890	0.885
Columns													
Max.	0.598	0.450	0.450	0.450	0.450	0.824	0.824	0.824	0.824	1.000	1.000	1.000	1.000
Min.	0.546	0.450	0.450	0.450	0.450	0.752	0.752	0.752	0.752	1.000	1.000	1.000	1.000
Avg.	0.564	0.450	0.450	0.450	0.450	0.800	0.800	0.800	0.800	1.000	1.000	1.000	1.000
All Members													
Max.	1.090	0.781	0.740	0.934	0.853	0.906	0.864	0.906	0.864	1.000	1.000	1.000	1.000
Min.	0.444	0.336	0.285	0.341	0.291	0.600	0.536	0.677	0.564	0.809	0.825	0.833	0.831
Avg.	0.610	0.473	0.432	0.502	0.454	0.786	0.719	0.820	0.746	0.960	0.964	0.914	0.910

$$^{+}\ \text{Eq. 3.13} = \frac{l_d}{d_b} = \frac{\dfrac{f_y}{f_c'^{1/4}} - 1900\left(0.1\dfrac{c_M}{c_m} + 0.9\right)}{72\left(\dfrac{c + K_{tr}}{d_b}\right)}$$

$$^{++}\ \text{Eq. 3.14} = \frac{l_d}{d_b} = \frac{\dfrac{f_y}{f_c'^{1/4}} - 1900}{72\left(\dfrac{c + K_{tr}}{d_b}\right)}$$

Note: Definition of c in Eq. 3.13 is different than c in Eq. 3.14 (see Chapter 3)

* Conventional reinforcement (avg. $R_r = 0.0727$)

** New reinforcement (avg. $R_r = 0.1275$)

Table 6.16
Summary of steel weights and savings in lateral load resisting building frames

Design Criteria	Beam Steel	Column Steel	All Steel
Original design			
Weight (lb)	1250137	1943146	3193283
ACI 318-95			
Weight (lb)	1207800	1867942	3075742
Change from original (lb)	-42337	-75204	-117541
Change from original (%)	-3.39	-3.87	-3.68
Eq. 3.13^{+} (Conv.*)			
Weight (lb)	1187657	1849032	3036689
Change from original (lb)	-62480	-94114	-156594
Change from original (%)	-5.00	-4.84	-4.90
Eq. 3.13^{+} (New**)			
Weight (lb)	1180158	1849032	3029190
Change from original (lb)	-69979	-94114	-164093
Change from original (%)	-5.60	-4.84	-5.14
Eq. 3.14^{++} (Conv.*)			
Weight (lb)	1194219	1849032	3043251
Change from original (lb)	-55918	-94114	-150032
Change from original (%)	-4.47	-4.84	-4.70
Eq. 3.14^{++} (New**)			
Weight (lb)	1185233	1849032	3034265
Change from original (lb)	-64904	-94114	-159018
Change from original (%)	-5.19	-4.84	-4.98

$^{+}$ Eq. 3.13 $= \dfrac{l_d}{d_b} = \dfrac{\dfrac{f_y}{f_c'^{1/4}} - 1900\left(0.1\dfrac{c_M}{c_m} + 0.9\right)}{72\left(\dfrac{c + K_{tr}}{d_b}\right)}$

$^{++}$ Eq. 3.14 $= \dfrac{l_d}{d_b} = \dfrac{\dfrac{f_y}{f_c'^{1/4}} - 1900}{72\left(\dfrac{c + K_{tr}}{d_b}\right)}$

Note: Definition of c in Eq. 3.13 is different than c in Eq. 3.14 (see Chapter 3)

* Conventional reinforcement (avg. $R_r = 0.0727$)

** New reinforcement (avg. $R_r = 0.1275$)

1 lb = 0.454 kg

Table 7.1
Single-rib finite element models

Model Designation[+]	Substructure					
	Concrete	Reinf. Steel	Crack Rods*	Constraint Rods**	Interface***	Total
4H-45						
No. of Nodes	1116	234	178	-	-	1528
No. of Elements	562	110	437	518	24	1651
4H-22.5						
No. of Nodes	1488	234	178	-	-	1900
No. of Elements	562	110	809	1262	32	2775
8H-45						
No. of Nodes	1116	234	178	-	-	1528
No. of Elements	562	110	437	518	32	1659
8H-22.5						
No. of Nodes	1488	234	178	-	-	1900
No. of Elements	562	110	809	1262	32	2775
8N-45						
No. of Nodes	1116	234	178	-	-	1528
No. of Elements	562	110	437	518	24	1651
8N-22.5						
No. of Nodes	1488	234	178	-	-	1900
No. of Elements	562	110	809	1262	32	2775
16N-45						
No. of Nodes	1116	360	178	-	-	1654
No. of Elements	562	212	437	518	32	1761
16N-22.5						
No. of Nodes	1488	360	178	-	-	2026
No. of Elements	562	212	809	1262	32	2877

[+] Model Designation, #O-A

# = number of sides on cross-section of bar (4, 8, or 16)
O = orientation of top side of bar (H = horizontal, N = not horizontal)
A = angle between crack planes in concrete substructure, degrees (22.5 or 45)

* No. of nodes shown are only those nodes not included in the concrete substructure

** All nodes are included in the concrete substructure

*** All nodes are included in the concrete or reinforcing steel substructures

Table 7.2
Bond force (peak load) and corresponding values of bar displacement and crack width for single-rib finite element models

Model Designation[+]	Bond Force (lb)	Bar Displacement (in.)	Crack Width (in.)
4H-45	13377	0.00974	0.00257
4H-22.5	13350	0.00972	0.00258
8H-45	12892	0.00900	0.00515
8H-22.5	12855	0.00895	0.00520
8N-45	11801	0.00850	0.00520
8N-22.5	11781	0.00850	0.00525
16N-45	12065	0.00860	0.00519
16N-22.5	12041	0.00860	0.00528

[+] Model Designation, #O-A

# = number of sides on cross-section of bar (4, 8, or 16)
O = orientation of top side of bar (H = horizontal, N = not horizontal)
A = angle between crack planes in concrete substructure, degrees (22.5 or 45)

1 lb = 4.45 N; 1 in. = 25.4 mm

Table 7.3
Multiple-rib finite element models

Embedded Length[+] (No. of Ribs)	Substructure	1 in. Cover No. of Nodes	1 in. Cover No. of Elements	2 in. Cover No. of Nodes	2 in. Cover No. of Elements
0.82 in. (1 Rib)	Concrete	4296	2358	4560	2530
	Reinf. Steel	1090	636	1090	636
	Crack Rods*	650	1647	738	1823
	Constraint Rods**	-	1994	-	2170
	Interface***	-	32	-	32
	Total	6036	6667	6388	7191
2.10 in. (3 Rib)	Concrete	4296	2358	4560	2530
	Reinf. Steel	1090	636	1090	636
	Crack Rods*	650	1647	738	1823
	Constraint Rods**	-	1994	-	2170
	Interface***	-	96	-	96
	Total	6036	6731	6388	7255
4.02 in. (6 Rib)	Concrete	4296	2358	4560	2530
	Reinf. Steel	1090	636	1090	636
	Crack Rods*	650	1647	738	1823
	Constraint Rods**	-	1994	-	2170
	Interface***	-	192	-	192
	Total	6036	6827	6388	7351
7.86 in. (12 Rib)	Concrete	4296	2358	4560	2530
	Reinf. Steel	1090	636	1090	636
	Crack Rods*	650	1647	738	1823
	Constraint Rods**	-	1994	-	2170
	Interface***	-	384	-	384
	Total	6036	7019	6388	7543

[+] Includes 1/2 in. lead length

* No. of nodes shown are only those nodes not included in the concrete substructure

** All nodes are included in the concrete substructure

*** All nodes are included in the concrete or reinforcing steel substructures

1 in. = 25.4 mm

Table 7.4
Bond force (peak load) and corresponding values of bar displacement, crack width, and slips for multiple-rib finite element models

No. of Ribs	Cover (in.)	Bond Force (lb)	Bar Displacement (in.)	Crack Width (in.)	Loaded End Slip (in.)	Unloaded End Slip (in.)
1	1	23905	0.01360	0.00734	0.01270	0.01104
3	1	27016	0.00960	0.00782	0.00843	0.00586
6	1	31545	0.00880	0.00675	0.00714	0.00316
12	1	39601	0.00993	0.00673	0.00769	0.00093
1	2	27885	0.01481	0.00640	0.01357	0.01175
3	2	32711	0.01440	0.01465	0.01377	0.00958
6	2	38567	0.01374	0.01594	0.01269	0.00630
12	2	45564	0.01423	0.01535	0.01266	0.00232

1 lb = 4.45 N; 1 in. = 25.4 mm

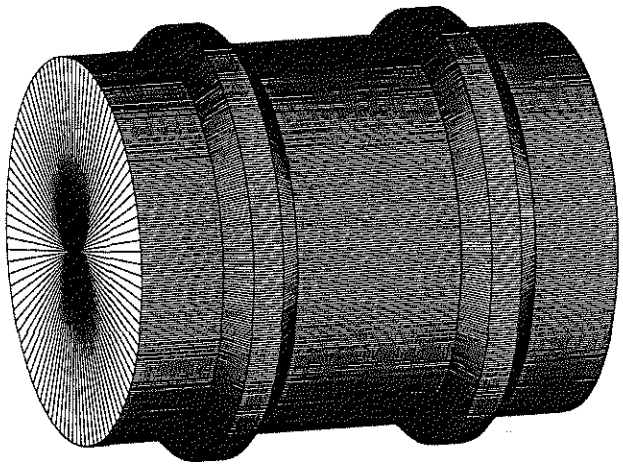

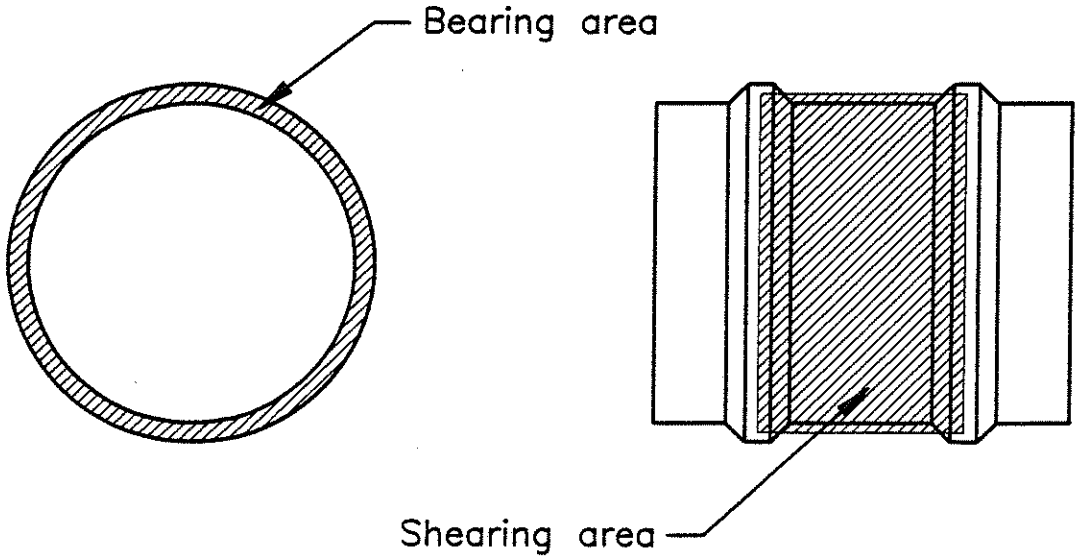

$$R_r = \frac{\text{Bearing area}}{\text{Shearing area}}$$

Fig. 1.1 Schematic illustrating relative rib area, R_r

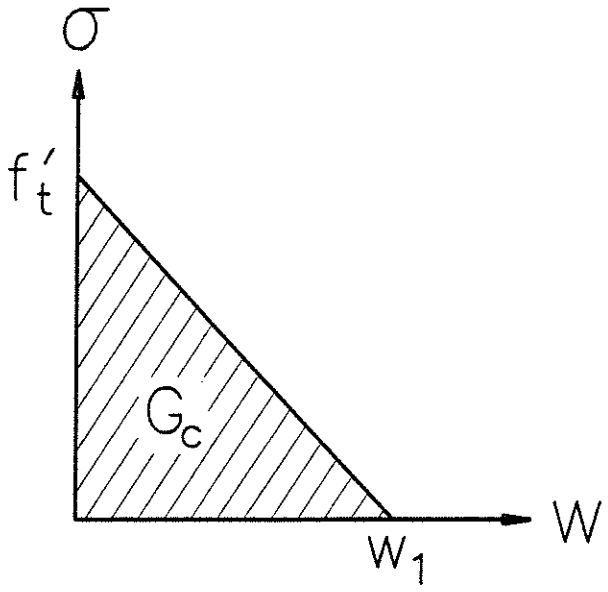

Fig. 1.2 Representation of fracture energy, G_c, using a linear approximation for the stress-crack opening displacement relationship

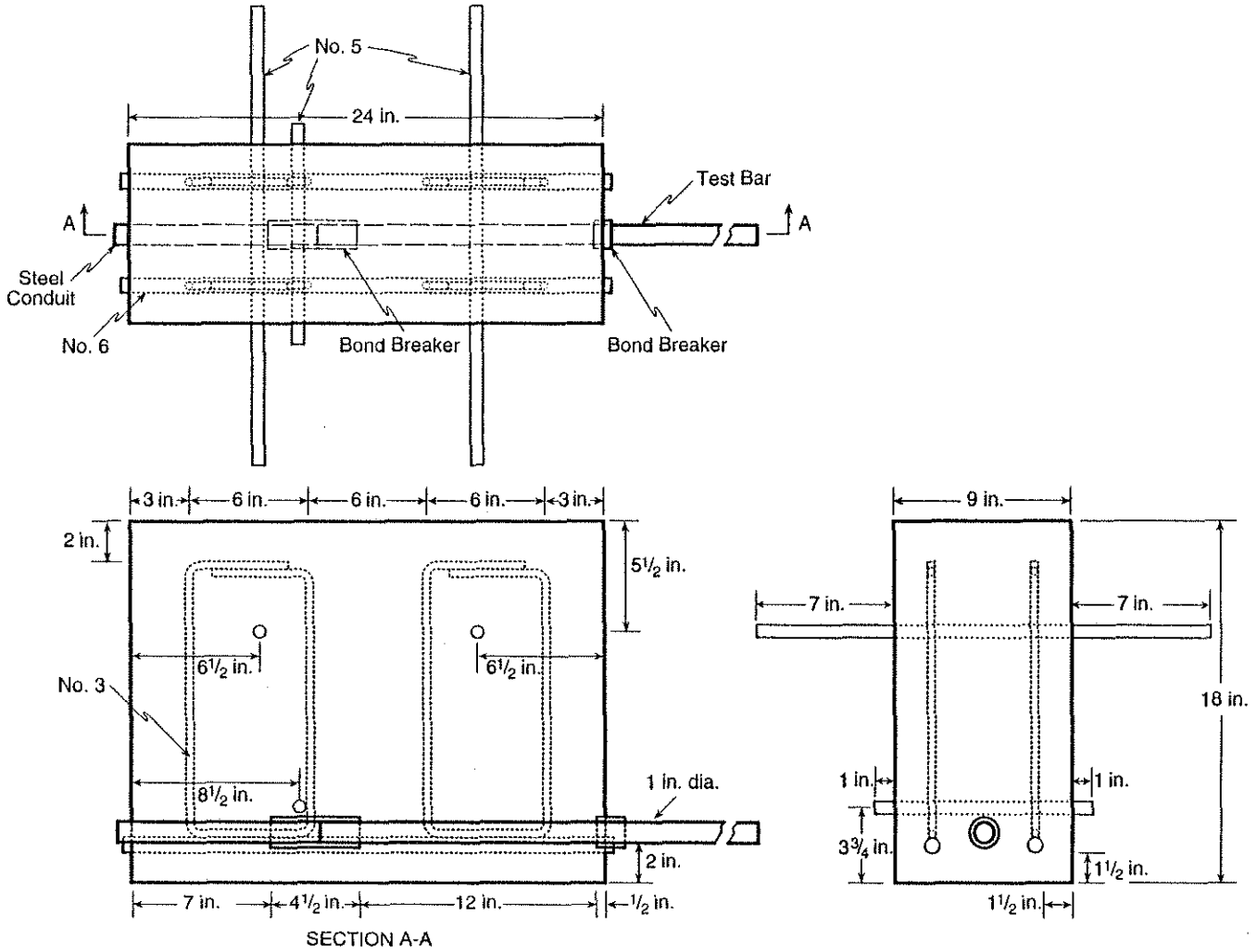

Fig. 2.1a Beam-end test specimen for evaluating the bond strength of reinforcing bars not confined by transverse reinforcement (1 in. = 25.4 mm)

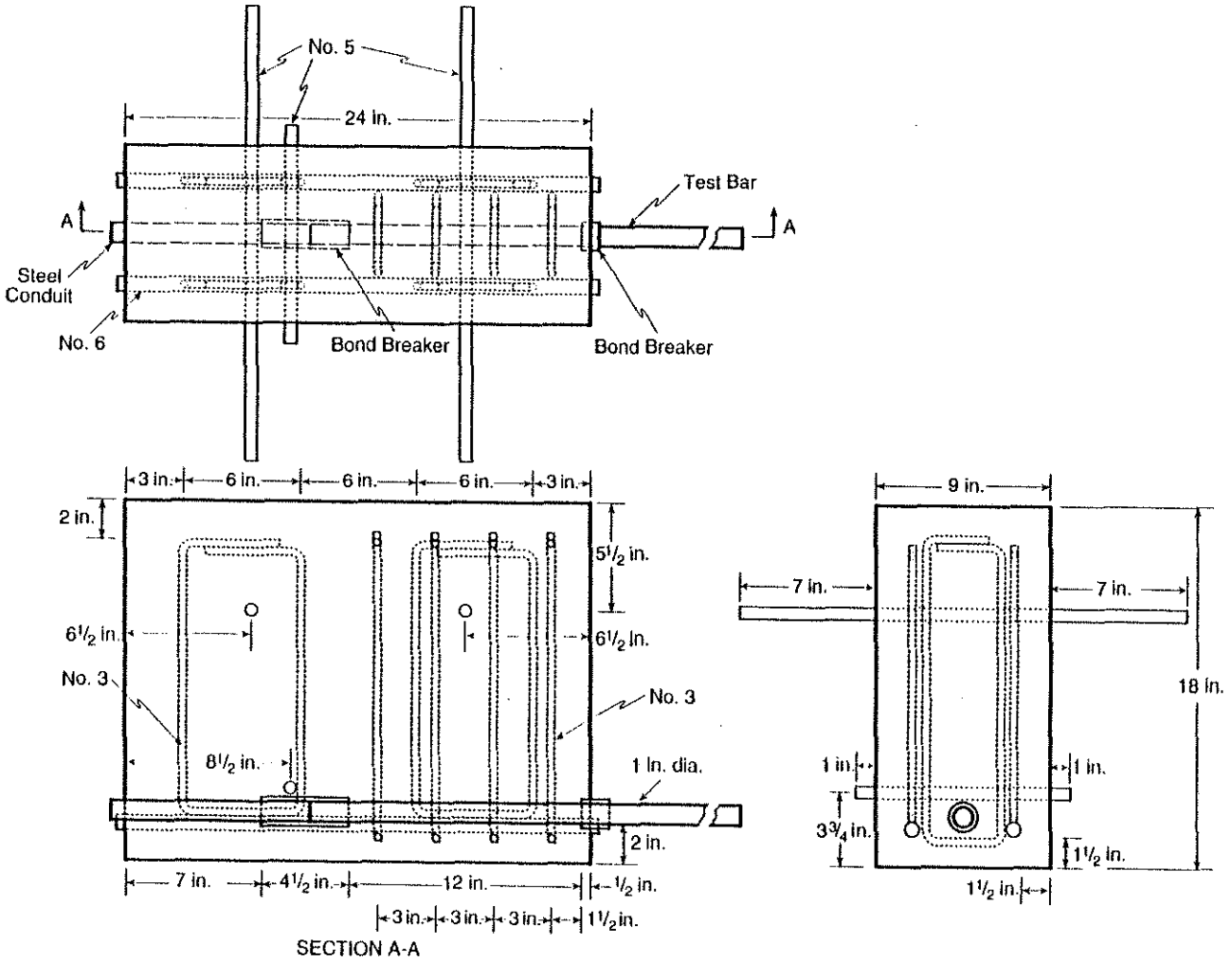

Fig. 2.1b Beam-end test specimen for evaluating the bond strength of reinforcing bars confined by transverse reinforcement (1 in. = 25.4 mm)

Pattern Designation	Relative Rib Area	
M11–8	0.20	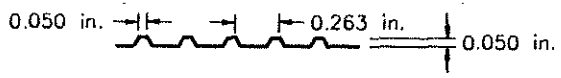
M12–8	0.10	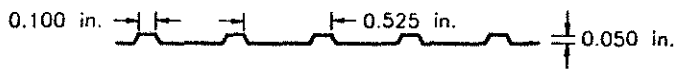
M13–8	0.05	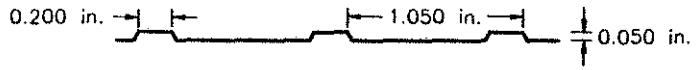
M21–8	0.20	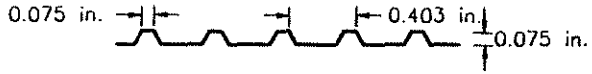
M22–8	0.10	
M23–8	0.05	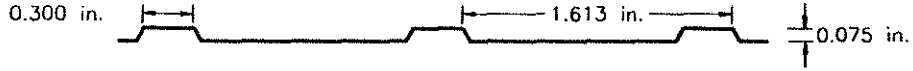
M31–8	0.20	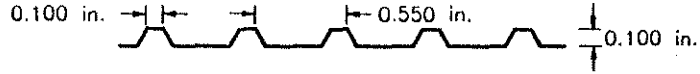
M32–8	0.10	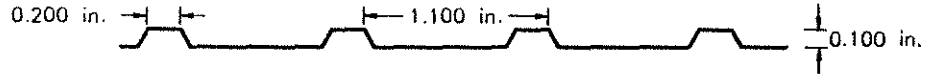
M33–8	0.05	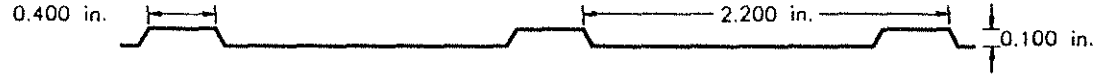

Fig. 2.2 Machined bar deformation patterns for 1 in. (25 mm) diameter bars. Face angle = 60° for all bars (1 in. = 25.4 mm)

Pattern Designation	Relative Rib Area	
M11–5	0.20	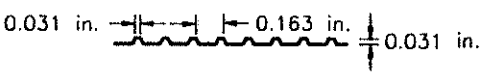
M12–5	0.10	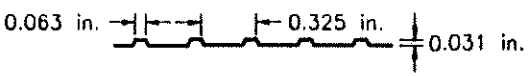
M13–5	0.05	
M21–5	0.20	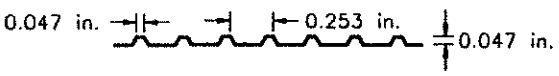
M22–5	0.10	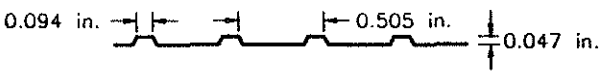
M23–5	0.05	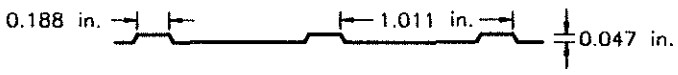
M31–5	0.20	
M32–5	0.10	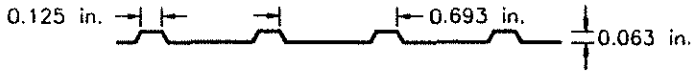
M33–5	0.05	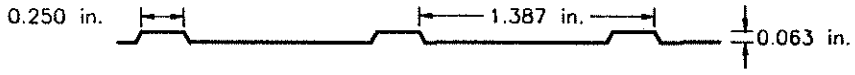

Fig. 2.3 Machined bar deformation patterns for 5/8 in. (16 mm) diameter bars. Face angle = 60° for all bars (1 in. = 25.4 mm)

Pattern Designation	Relative Rib Area	
M11A–8	0.20	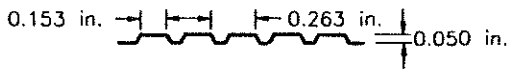
M12D–8	0.10	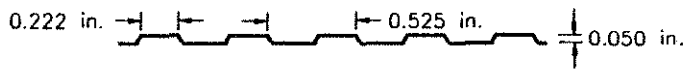
M12E–8	0.10	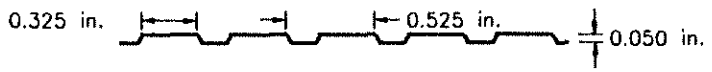
M31D–8	0.20	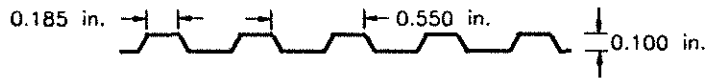
M31E–8	0.20	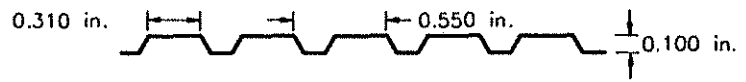
M32B–8	0.10	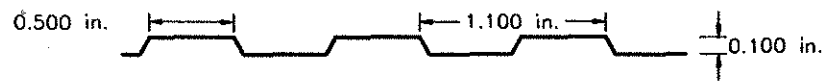
M32C–8	0.10	

Fig. 2.4 Machined bar deformation patterns for 1 in. (25 mm) diameter bars with increased rib width. Face angle = 60° for all bars (1 in. = 25.4 mm)

T-8

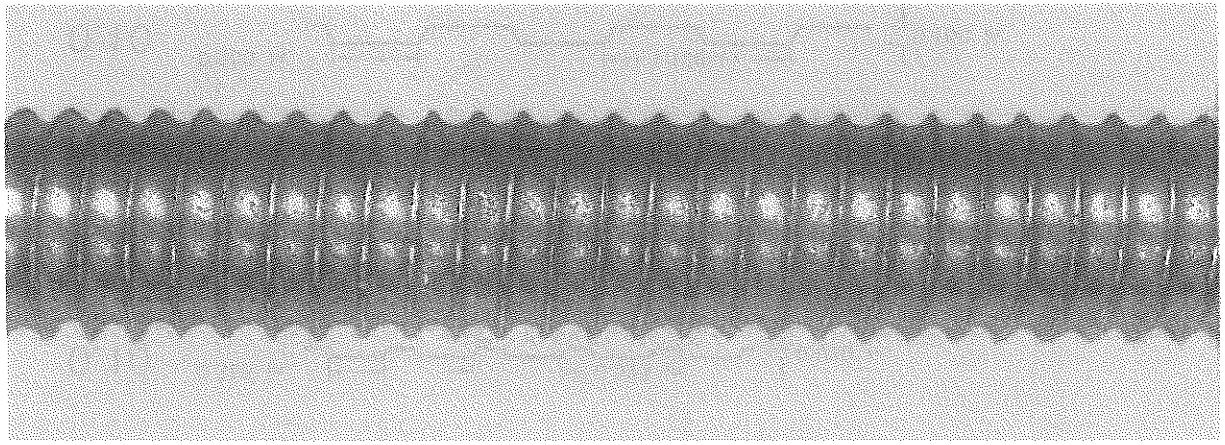

Fig. 2.5 Threaded bar deformation pattern

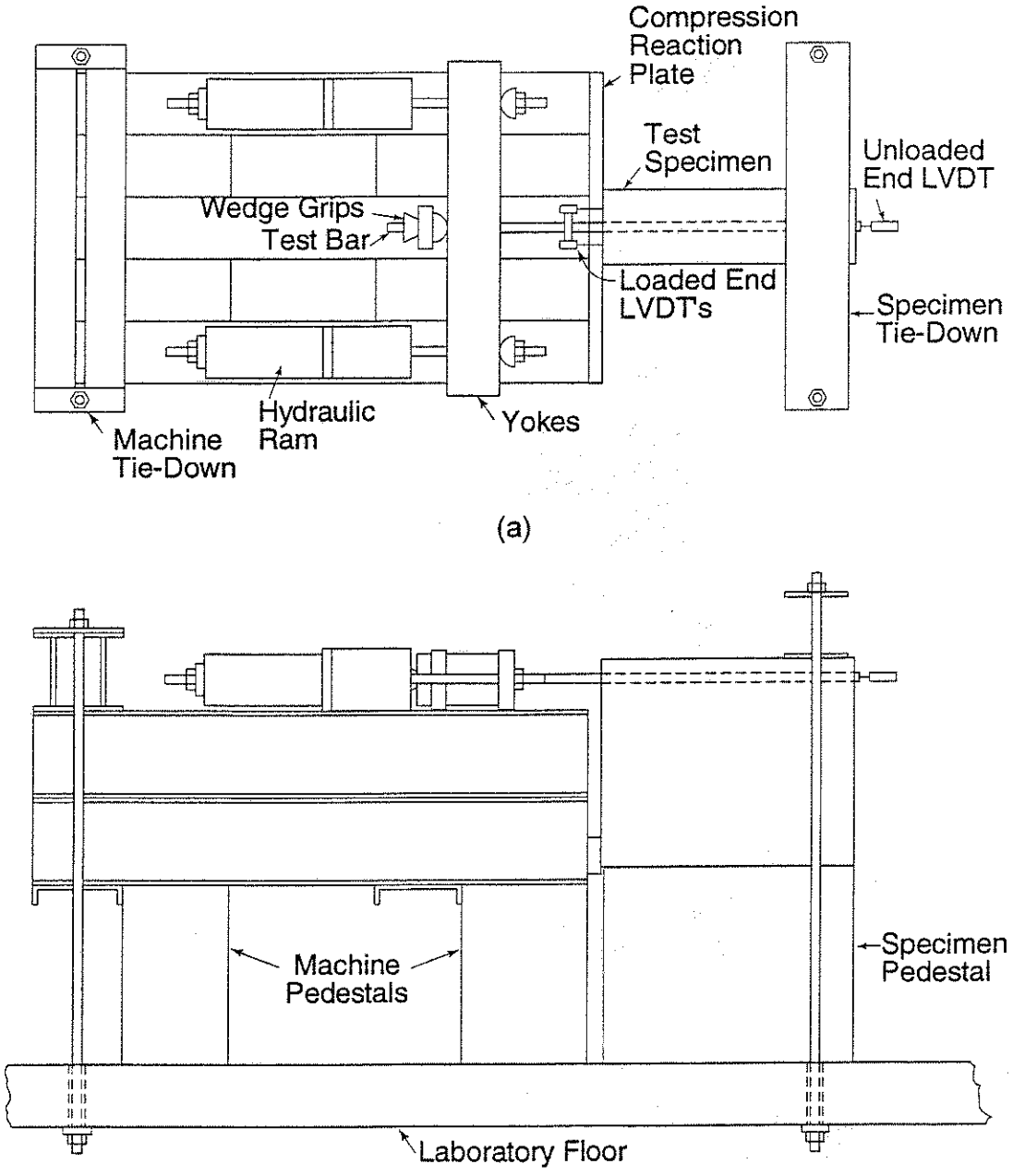

Fig. 2.6 Schematic of beam-end test apparatus, (a) plan view, (b) side view

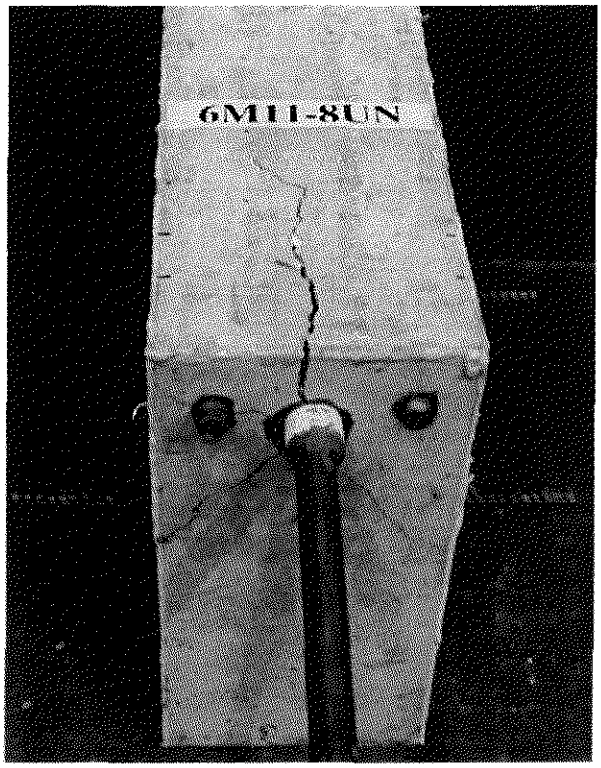

Fig. 2.7a Beam-end test specimen without transverse stirrups after failure. Cracks on the front face of specimen below the bar form an inverted V

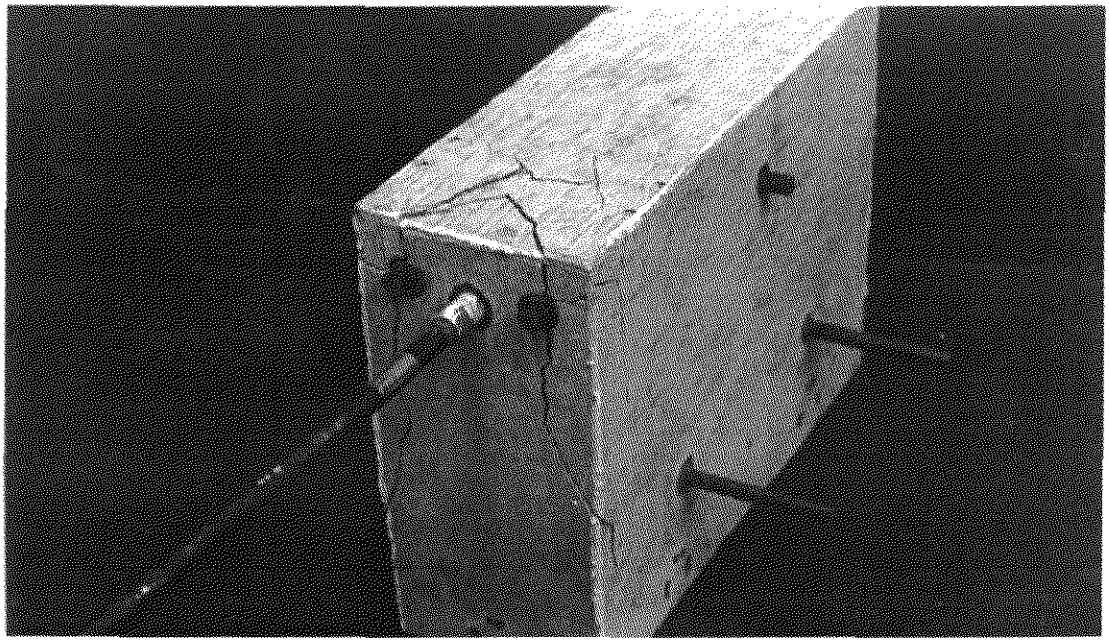

Fig. 2.7b Beam-end test specimen with transverse stirrups after failure

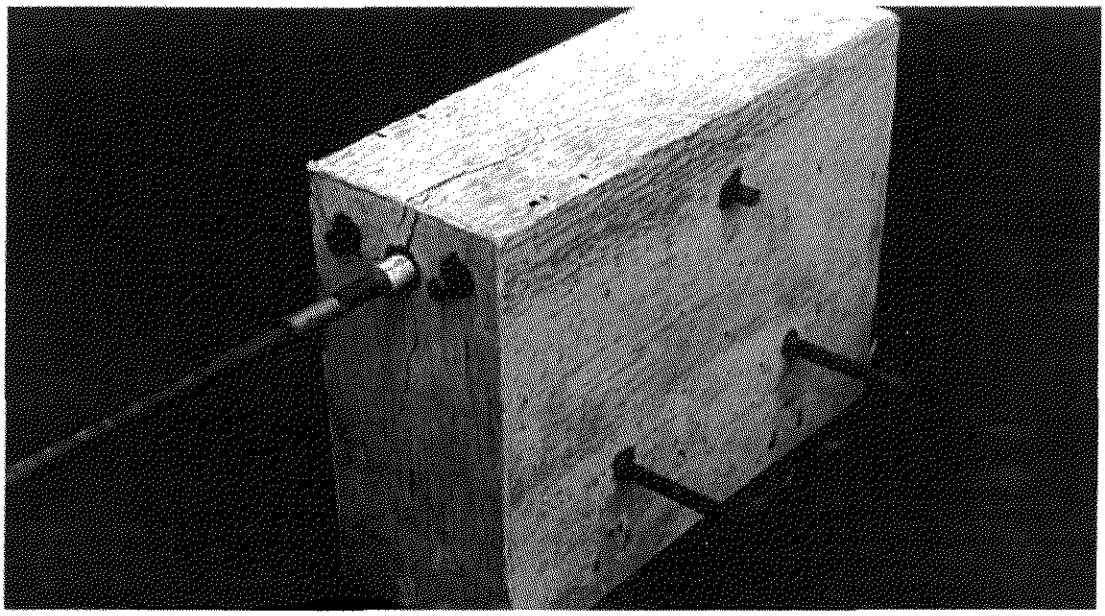

Fig. 2.7c Beam-end test specimen without transverse stirrups after failure. Cracks on the front face of specimen below the bar form an inverted Y with vertical crack passing through the location of the test bar

Fig. 2.7d Beam-end test specimen without transverse stirrups after failure. Cracks on the front face of specimen form horizontally through the side cover

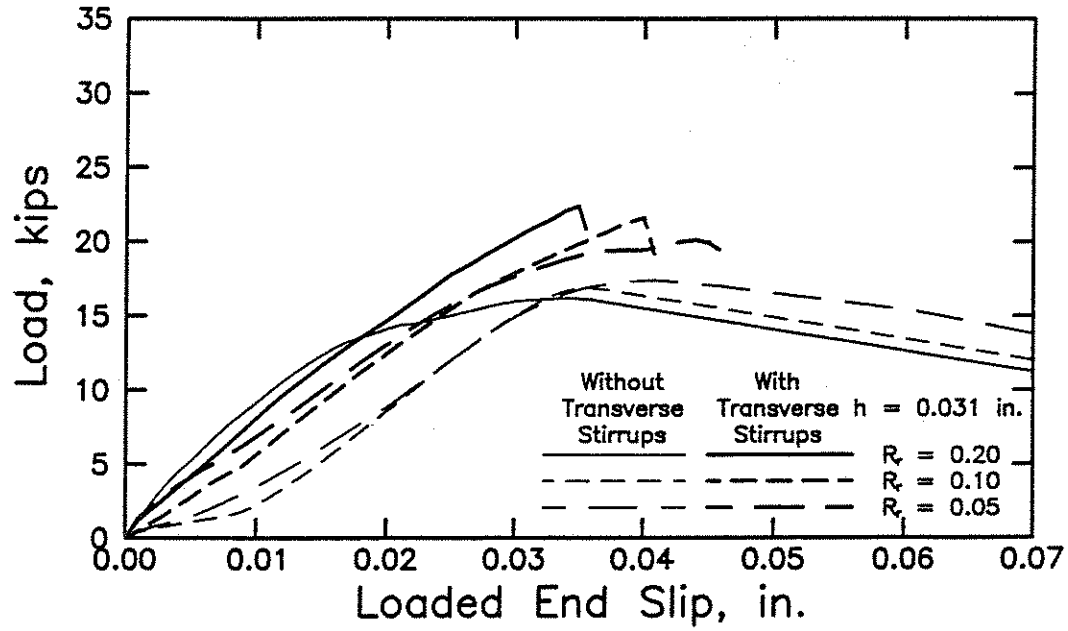

(a)

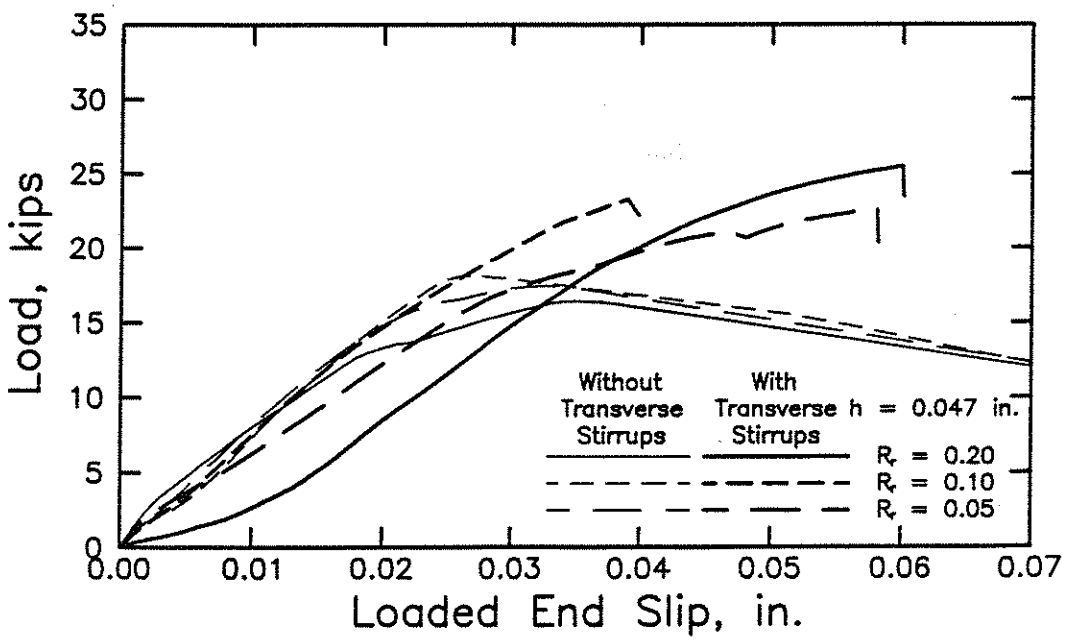

(b)

Figs. 2.8a&b Average load-loaded end slip curves for specimens with 7 1/2 in. (191 mm) bonded length, 1/2 in. (13 mm) lead length, and 2 in. (51 mm) cover, (a) 5/8 in. (16 mm) bars with deformation patterns M11-5, M12-5, and M13-5, (b) 5/8 in. (16 mm) bars with deformation patterns M21-5, M22-5, and M23-5 (1 in. = 25.4 mm, 1 kip = 4.45 kN)

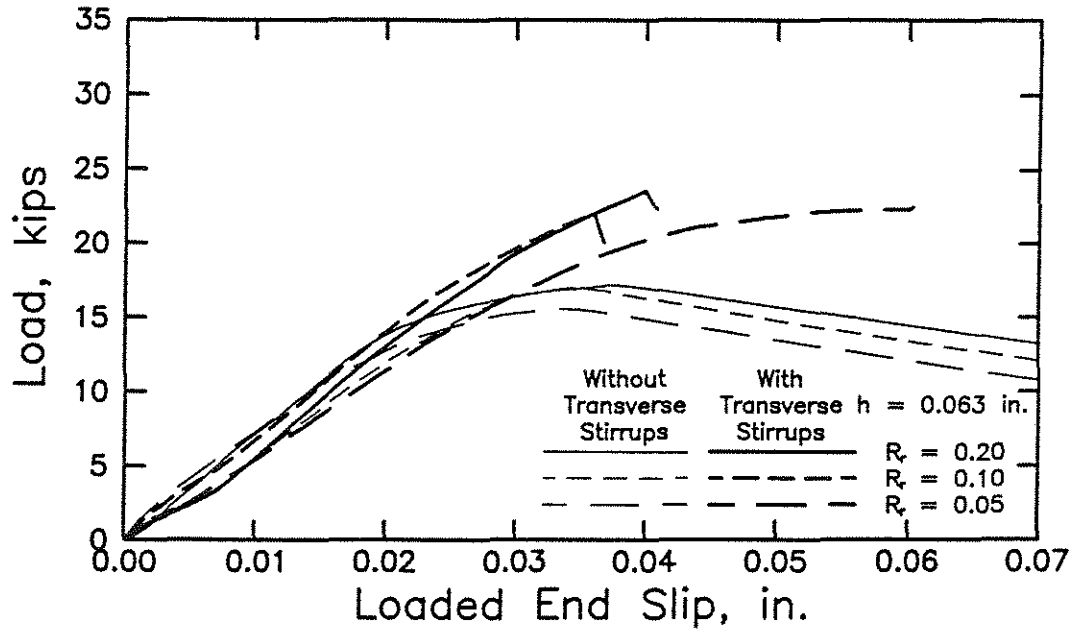

(c)

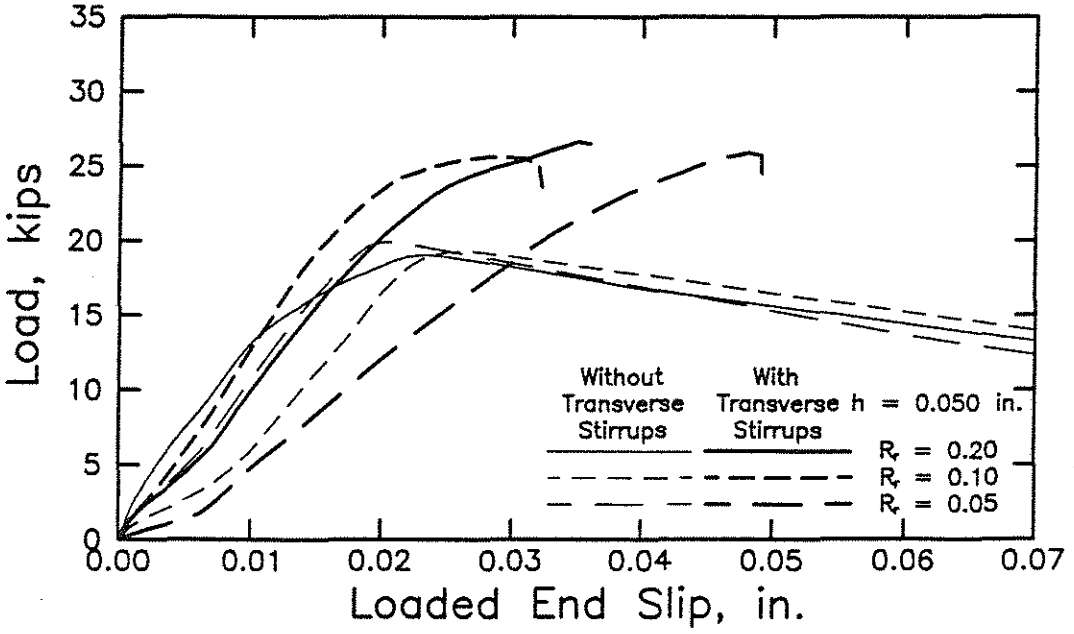

(d)

Figs. 2.8c&d Average load-loaded end slip curves for specimens with 7 1/2 in. (191 mm) bonded length, 1/2 in. (13 mm) lead length, and 2 in. (51 mm) cover, (c) 5/8 in. (16 mm) bars with deformation patterns M31-5, M32-5, and M33-5, (d) 1 in. (25 mm) bars with deformation patterns M11-8, M12-8, and M13-8 (1 in. = 25.4 mm, 1 kip = 4.45 kN)

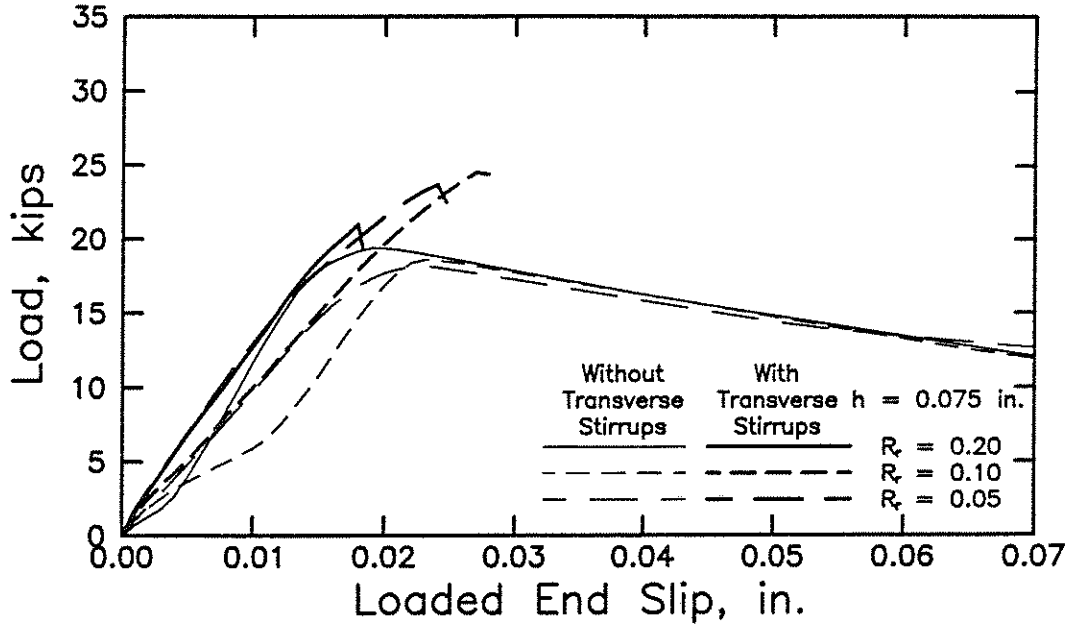

(e)

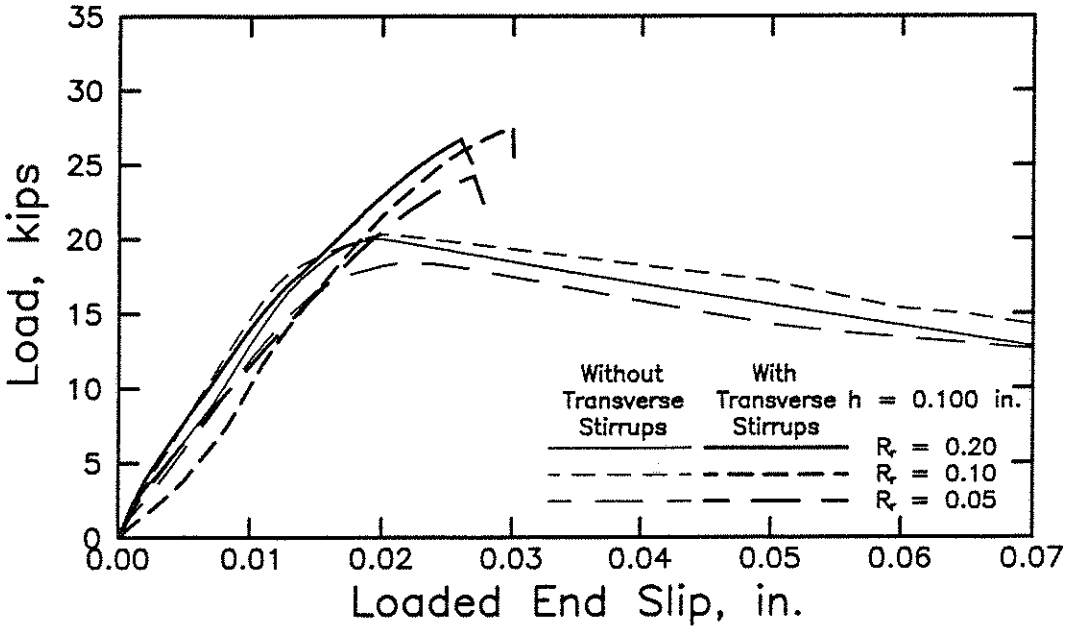

(f)

Figs. 2.8e&f Average load-loaded end slip curves for specimens with 7 1/2 in. (191 mm) bonded length, 1/2 in. (13 mm) lead length, and 2 in. (51 mm) cover, (e) 1 in. (25 mm) bars with deformation patterns M21-8, M22-8, and M23-8, (f) 1 in. (25 mm) bars with deformation patterns M31-8, M32-8, and M33-8 (1 in. = 25.4 mm, 1 kip = 4.45 kN)

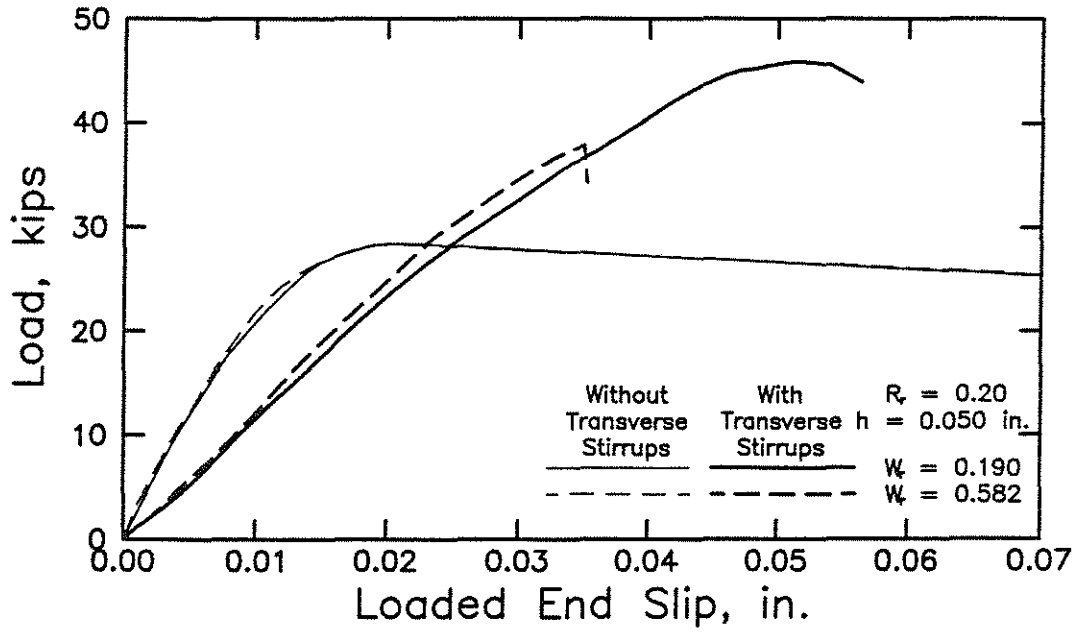

(g)

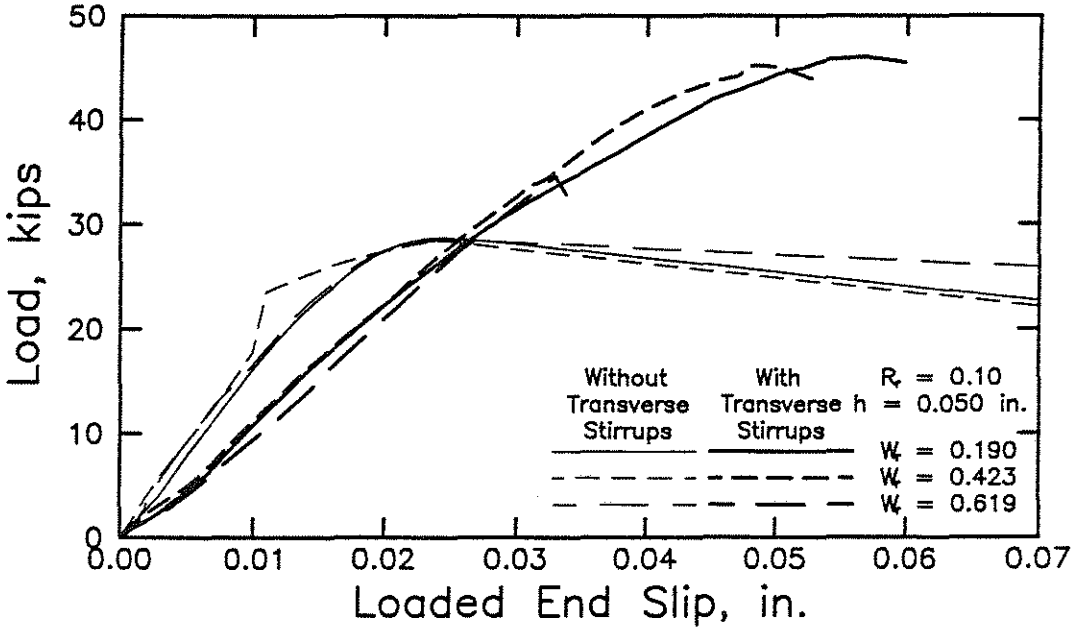

(h)

Figs. 2.8g&h Average load-loaded end slip curves for specimens with 12 in. (305 mm) bonded length, 1/2 in. (13 mm) lead length, and 2 in. (51 mm) cover, (g) 1 in. (25 mm) bars with deformation patterns M11-8 and M11A-8, (h) 1 in. (25 mm) bars with deformation patterns M12-8, M12D-8, and M12E-8 (1 in. = 25.4 mm, 1 kip = 4.45 kN)

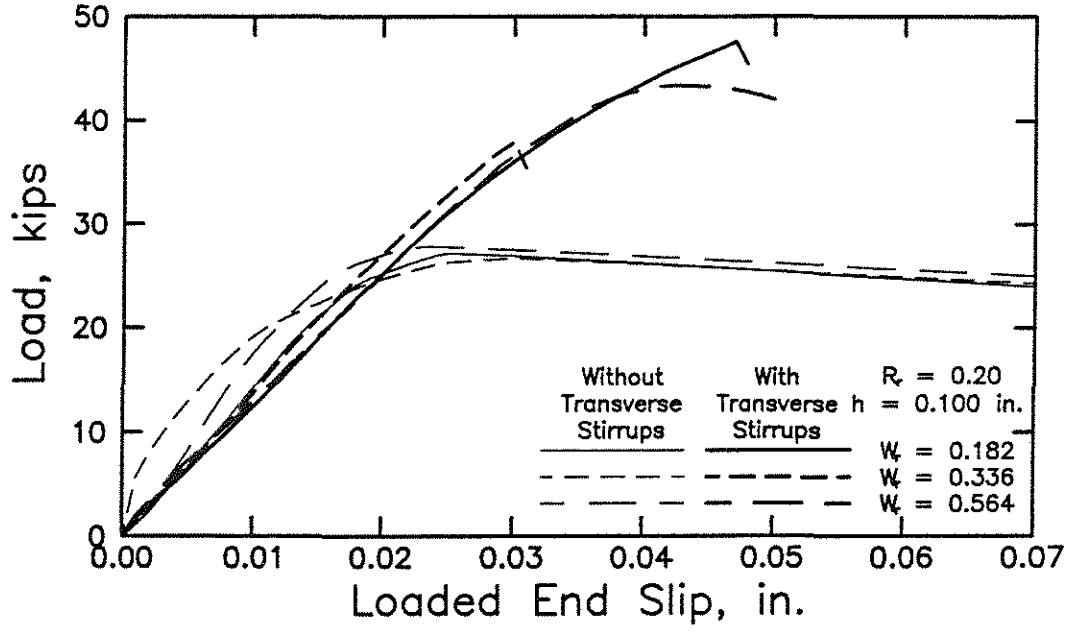

(i)

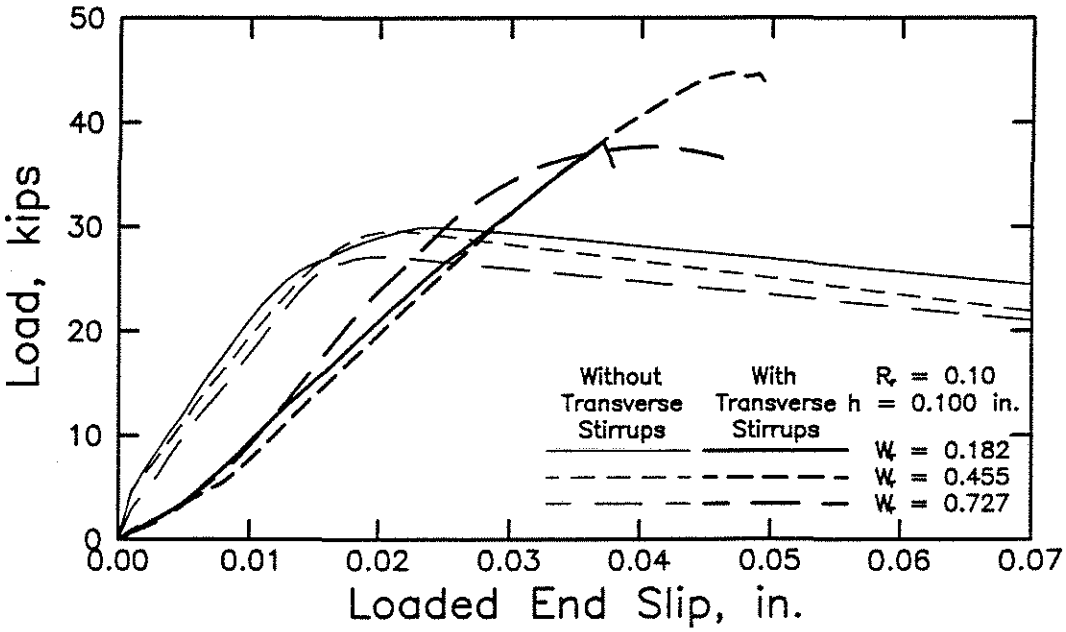

(j)

Figs. 2.8i&j Average load-loaded end slip curves for specimens with 12 in. (305 mm) bonded length, 1/2 in. (13 mm) lead length, and 2 in. (51 mm) cover, (i) 1 in. (25 mm) bars with deformation patterns M31-8, M31D-8, and M31E-8, (j) 1 in. (25 mm) bars with deformation patterns M32-8, M32B-8, and M32C-8 (1 in. = 25.4 mm, 1 kip = 4.45 kN)

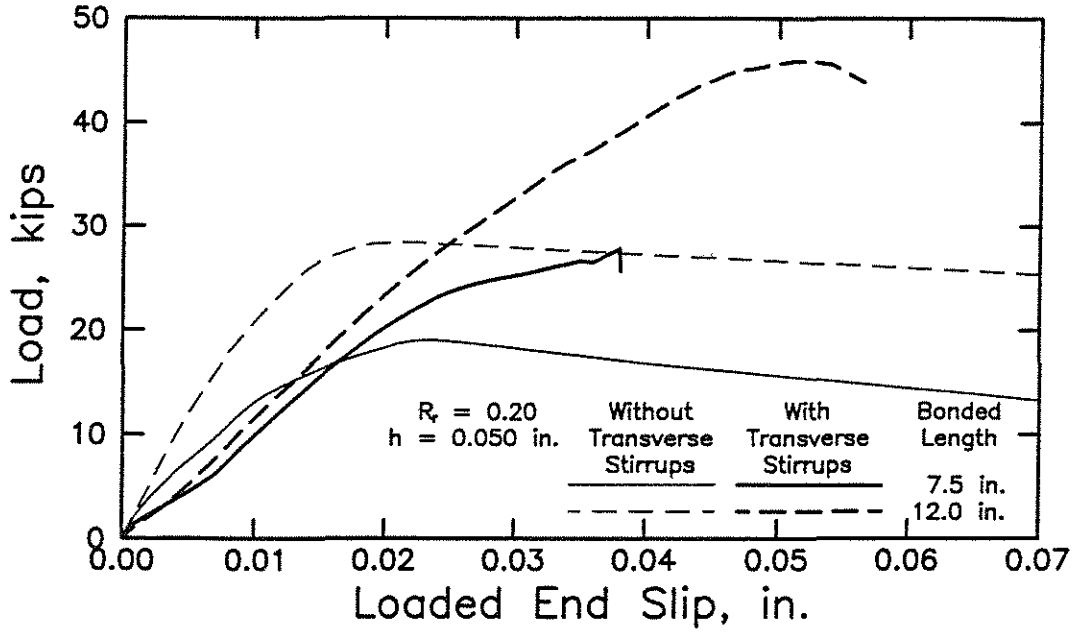

(k)

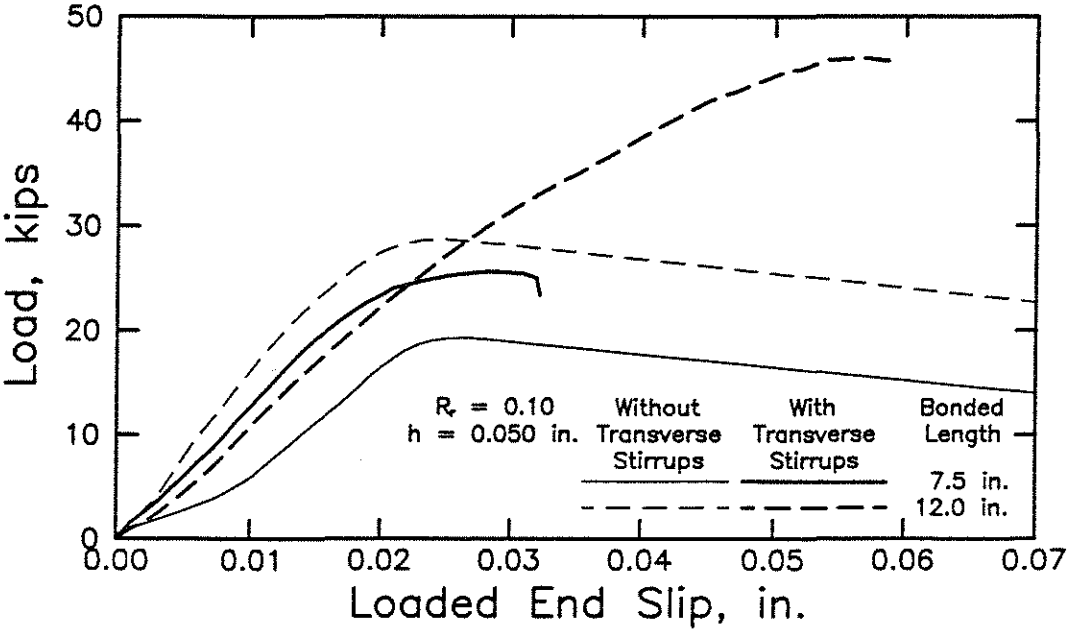

(l)

Figs. 2.8k&l Comparison of average load-loaded end slip curves for specimens with 1/2 in. (13 mm) lead length and 2 in. (51 mm) cover, (k) 1 in. (25 mm) bars with deformation pattern M11-8, (l) 1 in. (25 mm) bars with deformation pattern M12-8 (1 in. = 25.4 mm, 1 kip = 4.45 kN)

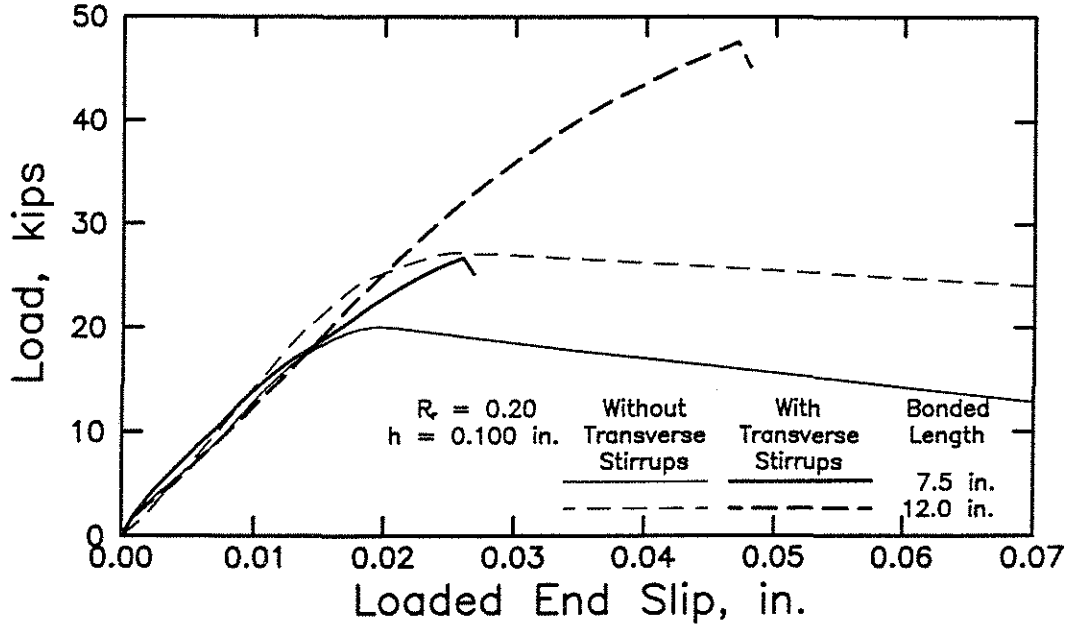

(m)

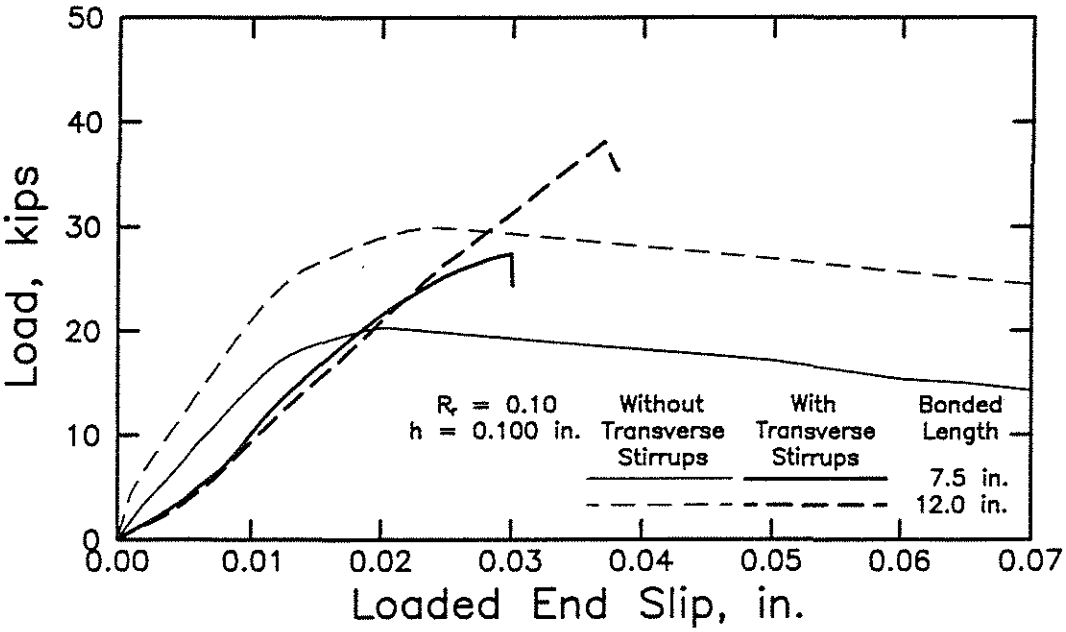

(n)

Figs. 2.8m&n Comparison of average load-loaded end slip curves for specimens with 1/2 in. (13 mm) lead length and 2 in. (51 mm) cover, (m) 1 in. (25 mm) bars with deformation pattern M31-8, (n) 1 in. (25 mm) bars with deformation pattern M32-8 (1 in. = 25.4 mm, 1 kip = 4.45 kN)

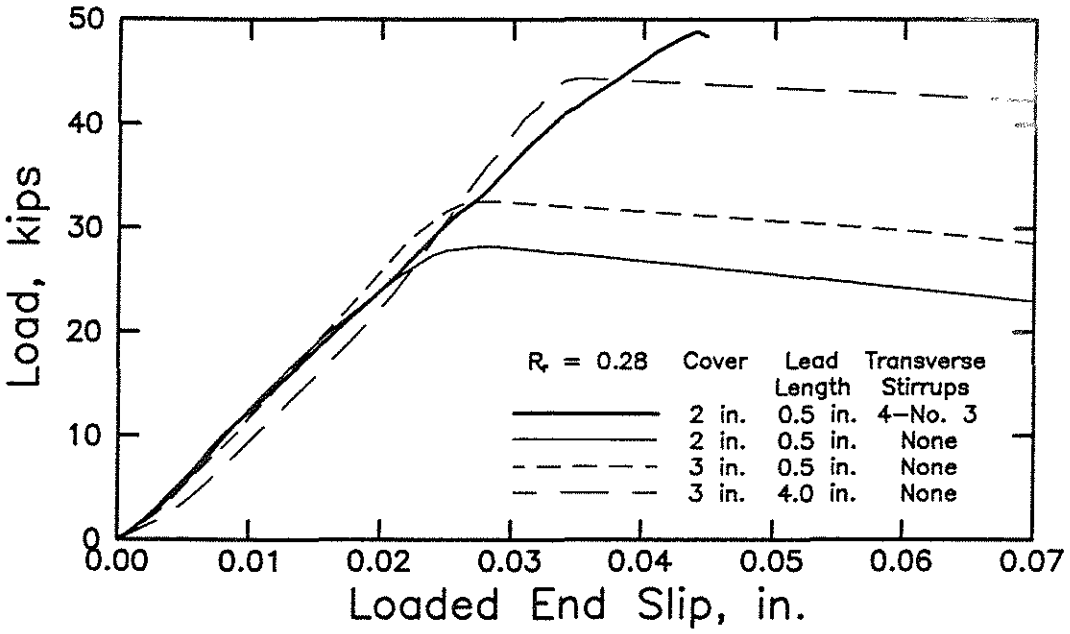

Fig. 2.8o Average load-loaded end slip curves for specimens with 12.5 in. (318 mm) embedment length containing threaded bars with deformation pattern T-8 (1 in. = 25.4 mm, 1 kip = 4.45 kN)

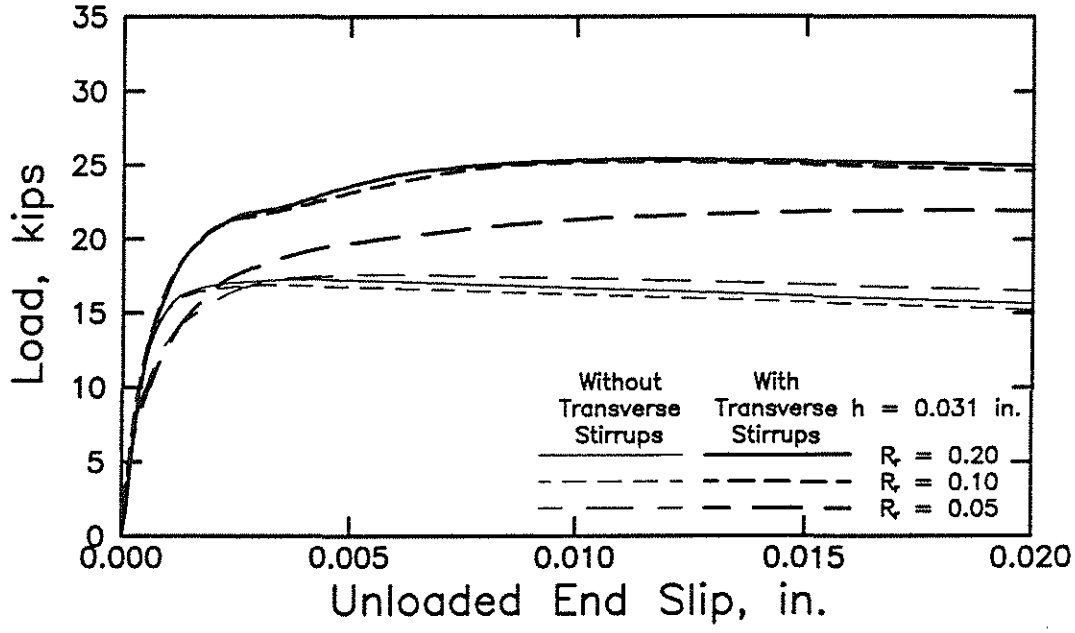

(a)

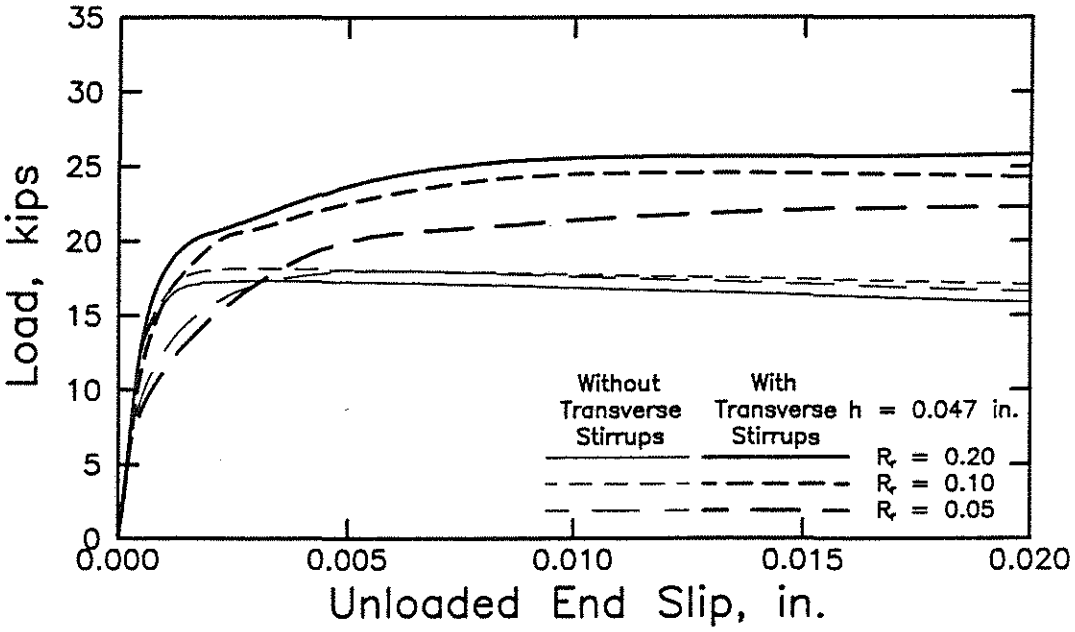

(b)

Figs. 2.9a&b Average load-unloaded end slip curves for specimens with 7 1/2 in. (191 mm) bonded length, 1/2 in. (13 mm) lead length, and 2 in. (51 mm) cover, (a) 5/8 in. (16 mm) bars with deformation patterns M11-5, M12-5, and M13-5, (b) 5/8 in. (16 mm) bars with deformation patterns M21-5, M22-5, and M23-5 (1 in. = 25.4 mm, 1 kip = 4.45 kN)

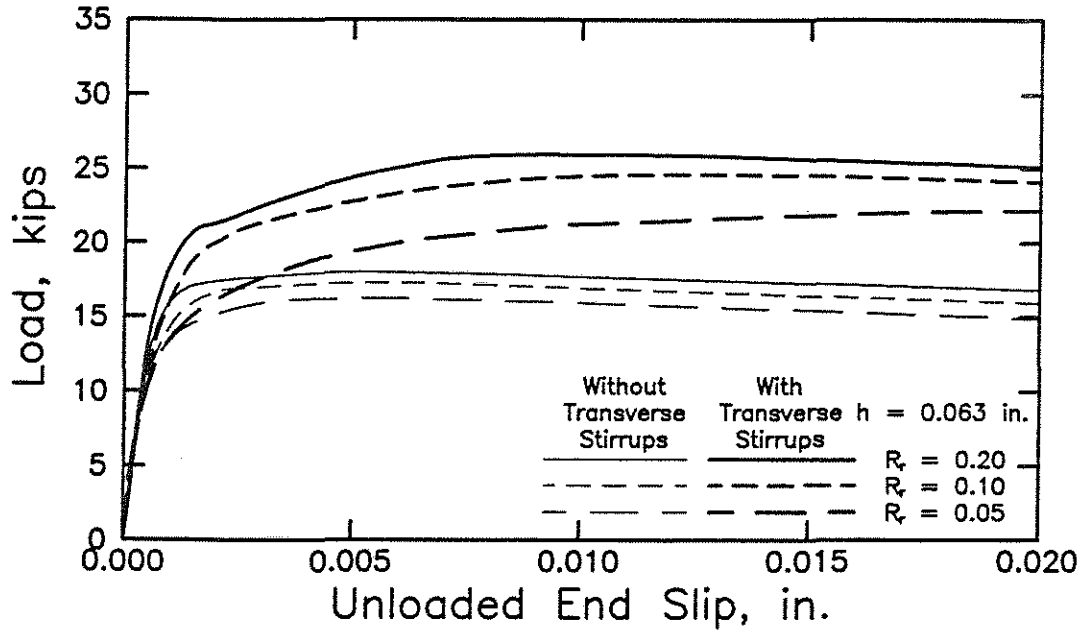

(c)

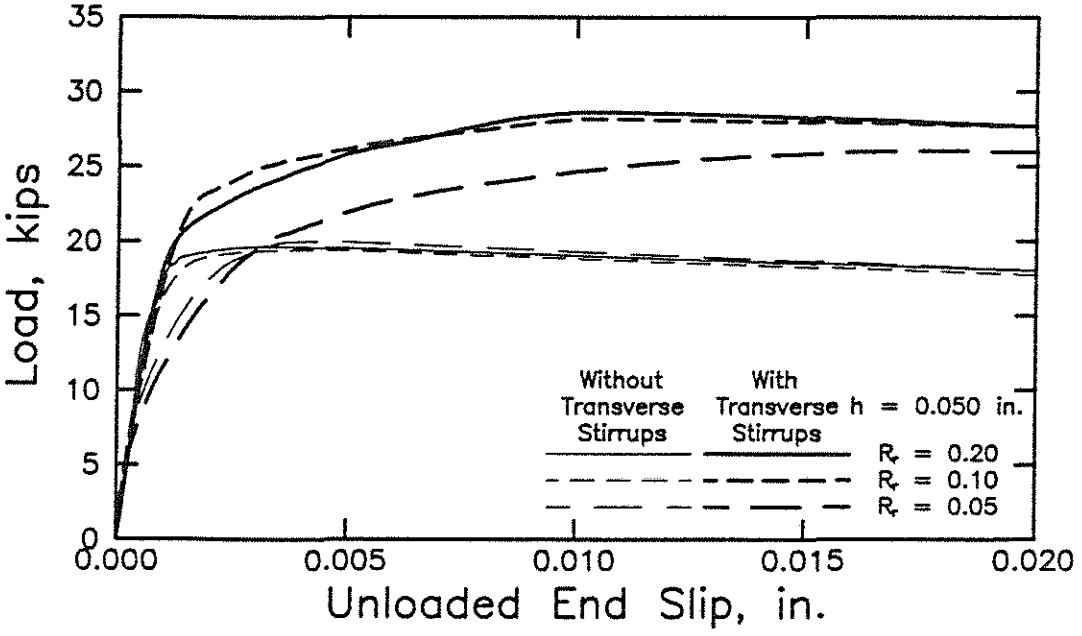

(d)

Figs. 2.9c&d Average load-unloaded end slip curves for specimens with 7 1/2 in. (191 mm) bonded length, 1/2 in. (13 mm) lead length, and 2 in. (51 mm) cover, (c) 5/8 in. (16 mm) bars with deformation patterns M31-5, M32-5, and M33-5, (d) 1 in. (25 mm) bars with deformation patterns M11-8, M12-8, and M13-8 (1 in. = 25.4 mm, 1 kip = 4.45 kN)

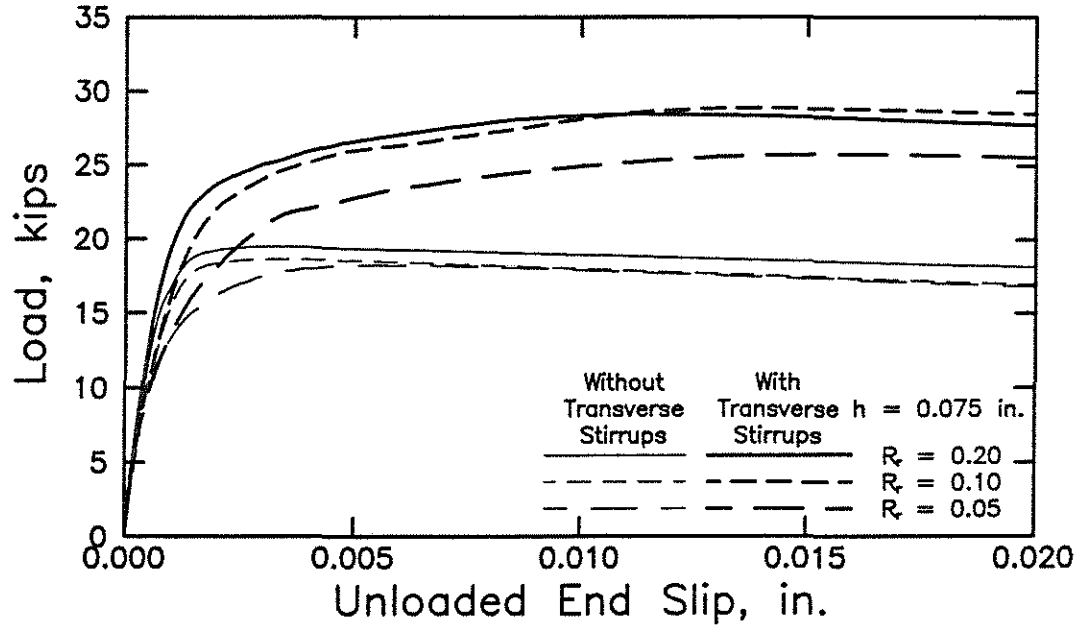

(e)

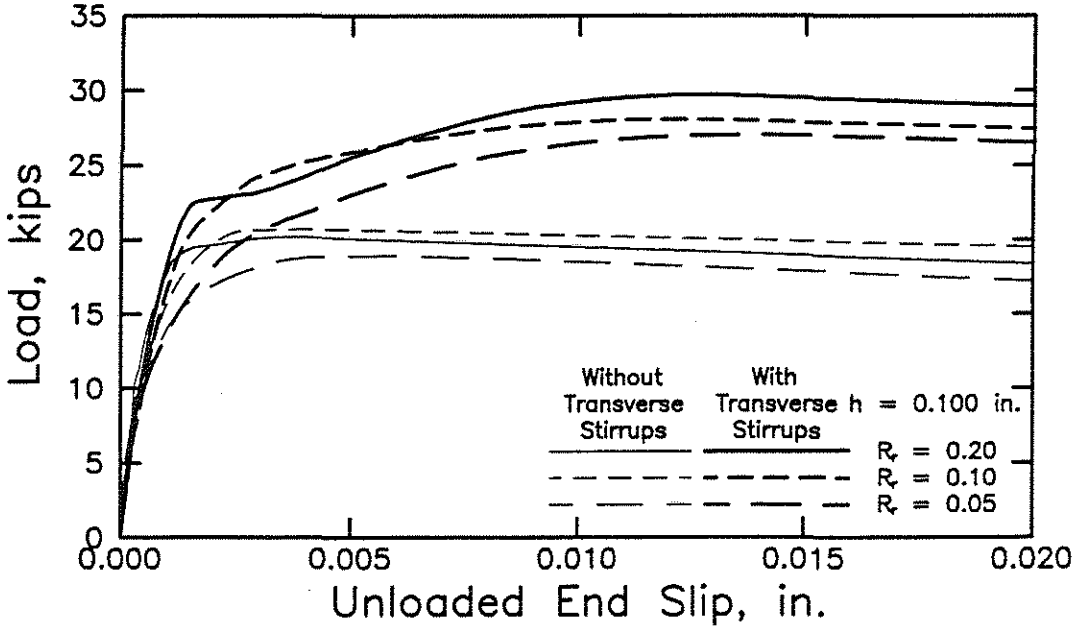

(f)

Figs. 2.9e&f Average load-unloaded end slip curves for specimens with 7 1/2 in. (191 mm) bonded length, 1/2 in. (13 mm) lead length, and 2 in. (51 mm) cover, (e) 1 in. (25 mm) bars with deformation patterns M21-8, M22-8, and M23-8, (f) 1 in. (25 mm) bars with deformation patterns M31-8, M32-8, and M33-8 (1 in. = 25.4 mm, 1 kip = 4.45 kN)

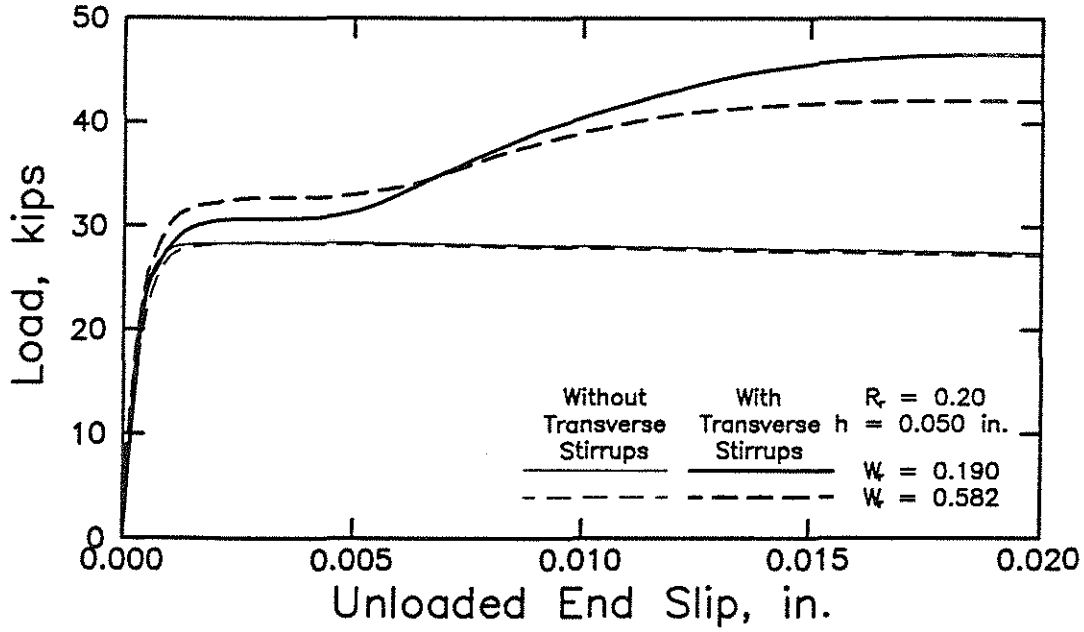

(g)

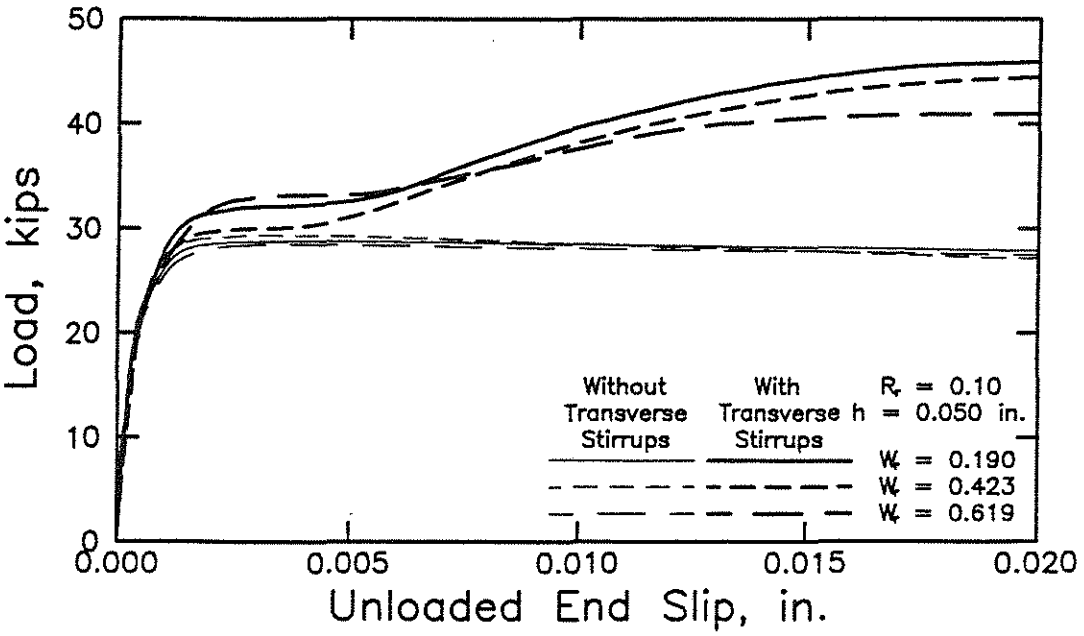

(h)

Figs. 2.9g&h Average load-unloaded end slip curves for specimens with 12 in. (305 mm) bonded length, 1/2 in. (13 mm) lead length, and 2 in. (51 mm) cover, (g) 1 in. (25 mm) bars with deformation patterns M11-8 and M11A-8, (h) 1 in. (25 mm) bars with deformation patterns M12-8, M12D-8, and M12E-8 (1 in. = 25.4 mm, 1 kip = 4.45 kN)

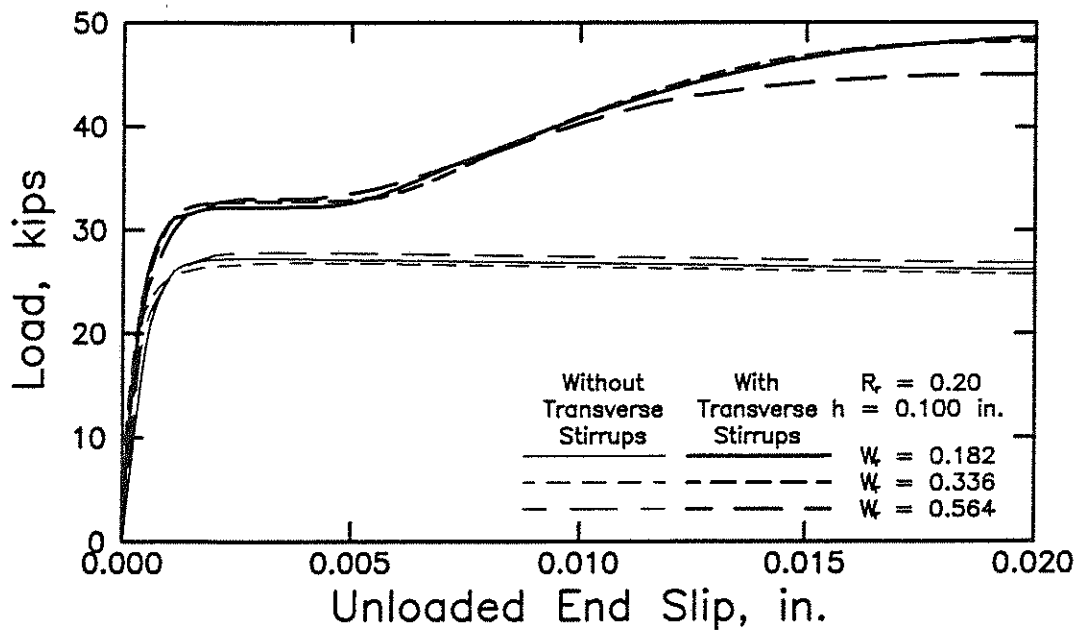

(i)

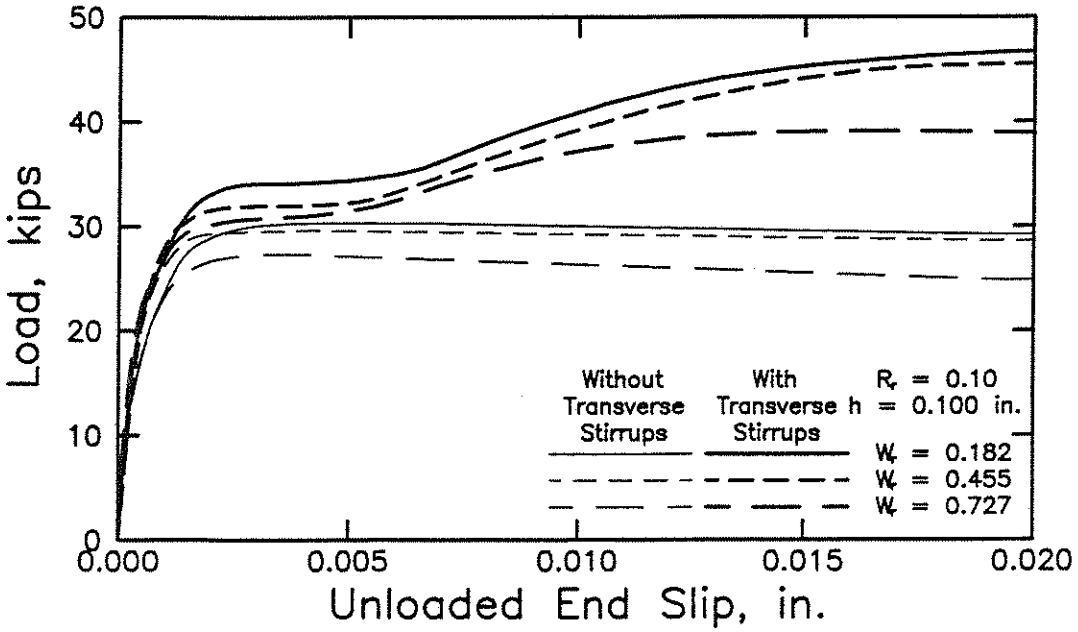

(j)

Figs. 2.9i&j Average load-unloaded end slip curves for specimens with 12 in. (305 mm) bonded length, 1/2 in. (13 mm) lead length, and 2 in. (51 mm) cover, (i) 1 in. (25 mm) bars with deformation patterns M31-8, M31D-8, and M31E-8, (j) 1 in. (25 mm) bars with deformation patterns M32-8, M32B-8, and M32C-8 (1 in. = 25.4 mm, 1 kip = 4.45 kN)

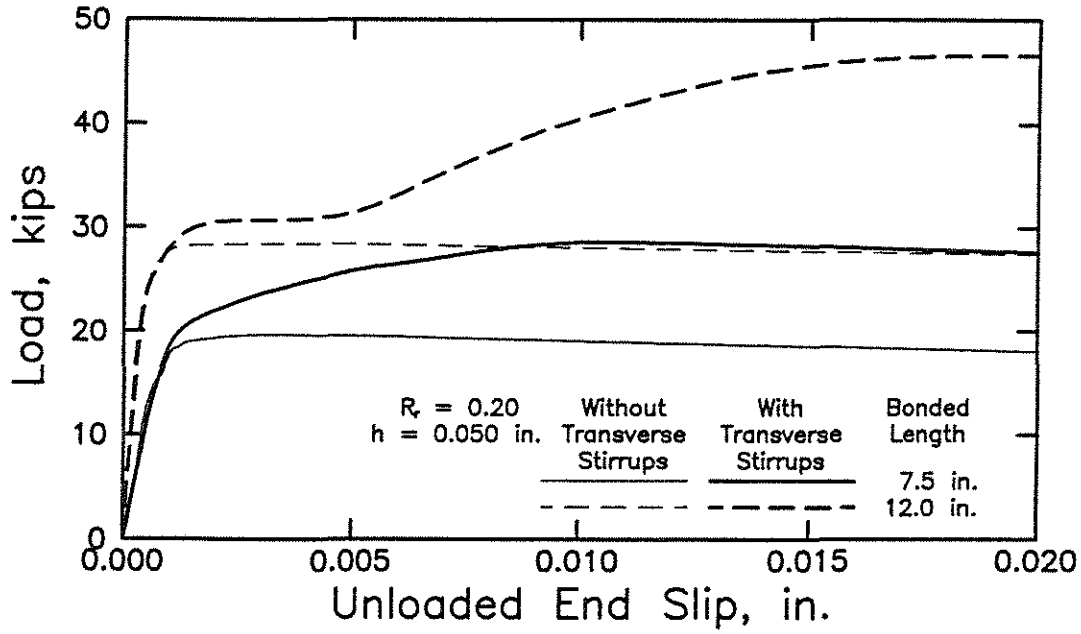

(k)

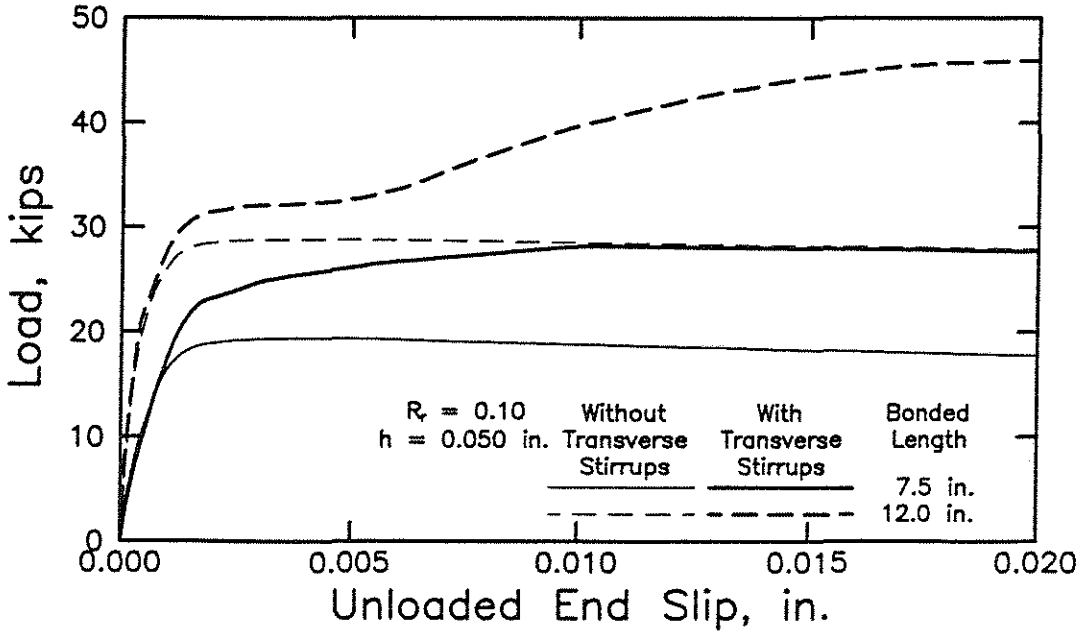

(l)

Figs. 2.9k&l Comparison of average load-unloaded end slip curves for specimens with 1/2 in. (13 mm) lead length and 2 in. (51 mm) cover, (k) 1 in. (25 mm) bars with deformation pattern M11-8, (l) 1 in. (25 mm) bars with deformation pattern M12-8 (1 in. = 25.4 mm, 1 kip = 4.45 kN)

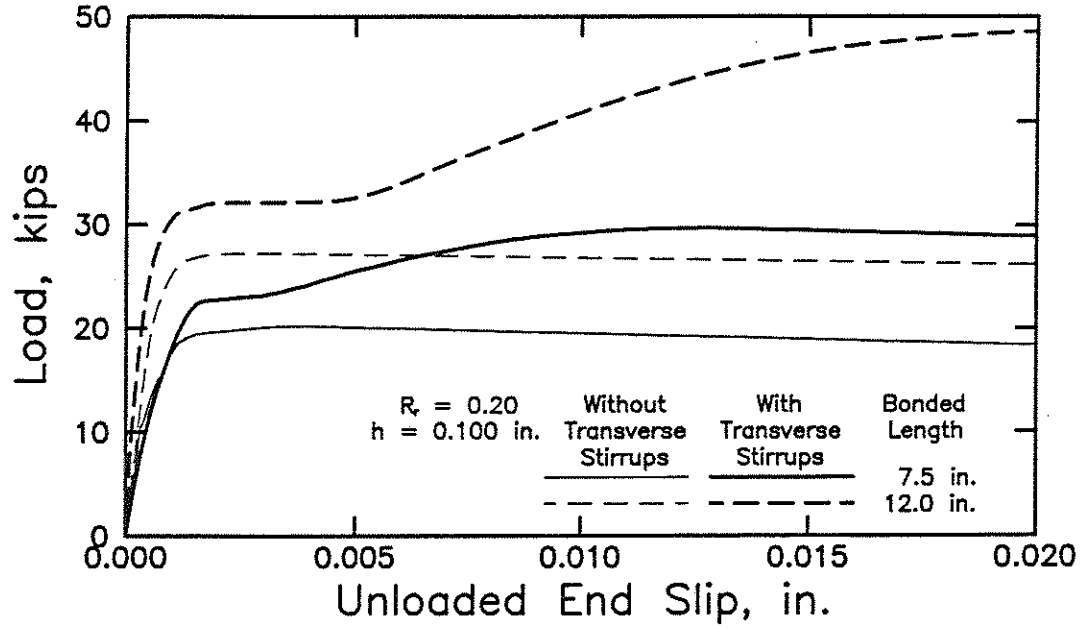

(m)

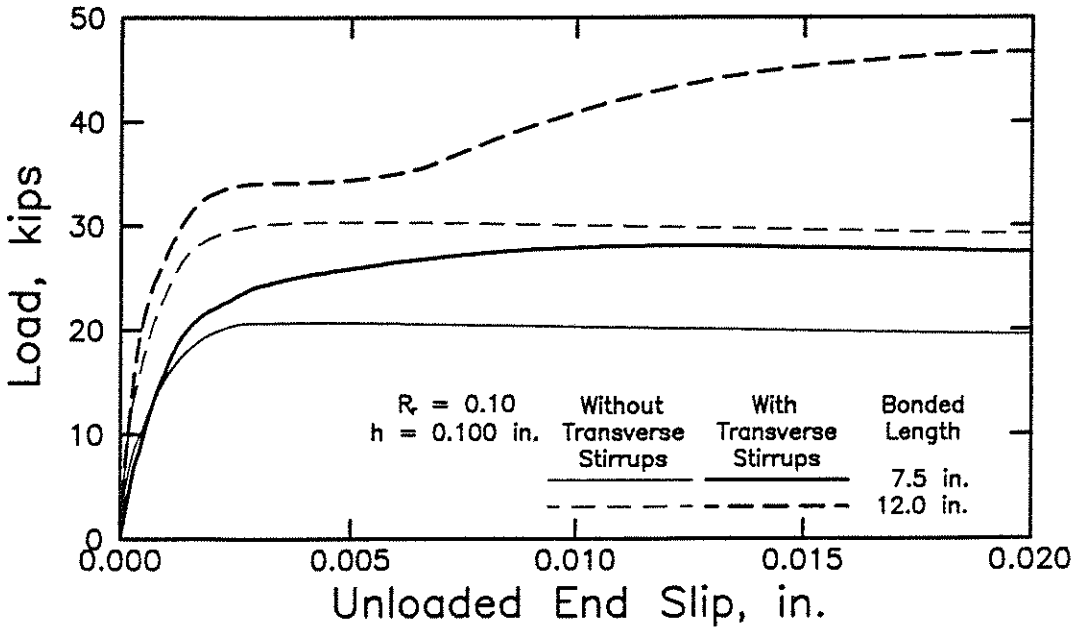

(n)

Figs. 2.9m&n Comparison of average load-unloaded end slip curves for specimens with 1/2 in. (13 mm) lead length and 2 in. (51 mm) cover, (m) 1 in. (25 mm) bars with deformation pattern M31-8, (n) 1 in. (25 mm) bars with deformation pattern M32-8 (1 in. = 25.4 mm, 1 kip = 4.45 kN)

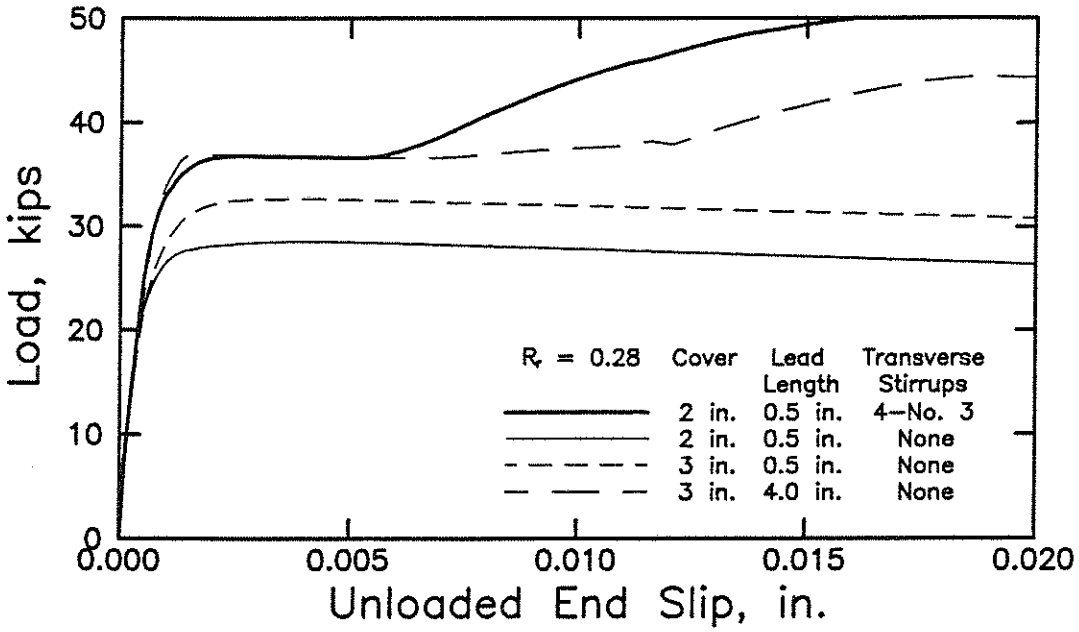

Fig. 2.9o Average load-unloaded end slip curves for specimens with 12.5 in. (318 mm) embedment length containing threaded bars with deformation pattern T-8 (1 in. = 25.4 mm, 1 kip = 4.45 kN)

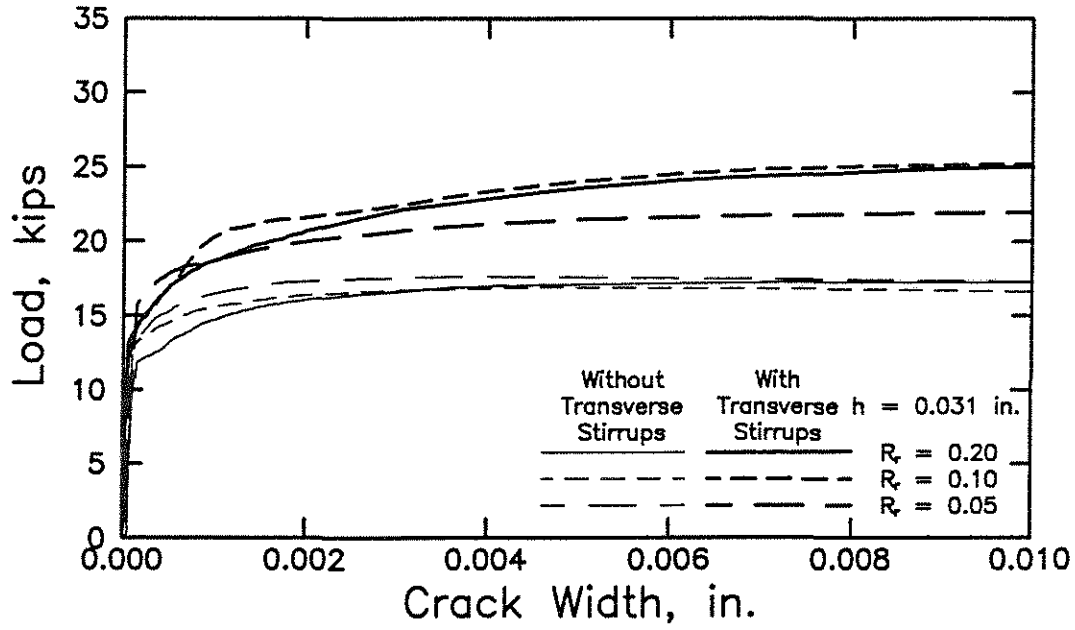

(a)

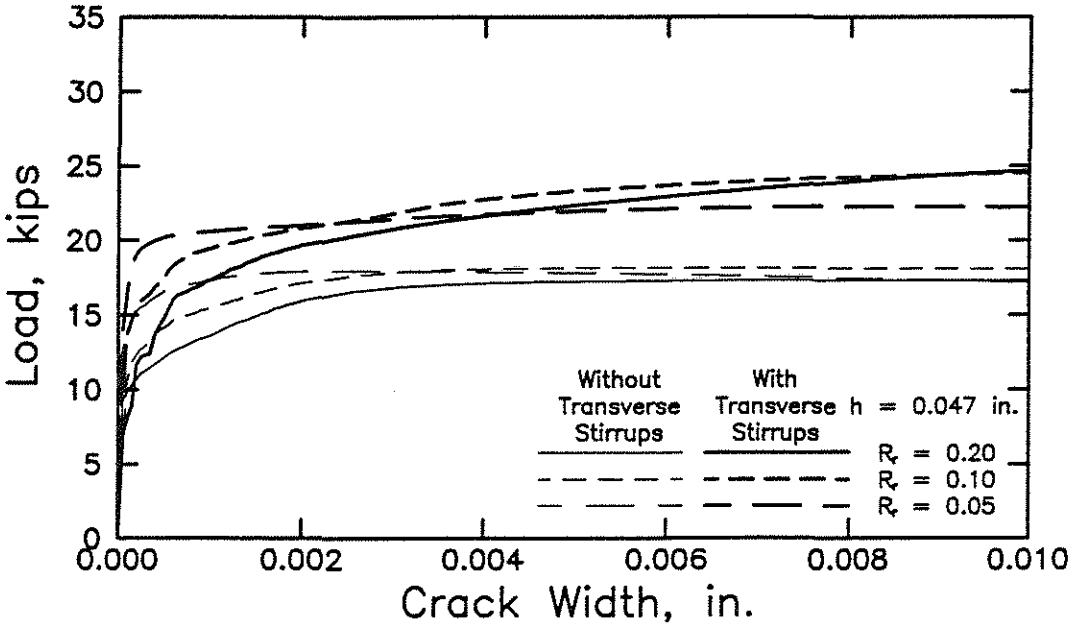

(b)

Figs. 2.10a&b Average load-crack width curves for specimens with 7 1/2 in. (191 mm) bonded length, 1/2 in. (13 mm) lead length, and 2 in. (51 mm) cover, (a) 5/8 in. (16 mm) bars with deformation patterns M11-5, M12-5, and M13-5, (b) 5/8 in. (16 mm) bars with deformation patterns M21-5, M22-5, and M23-5 (1 in. = 25.4 mm, 1 kip = 4.45 kN)

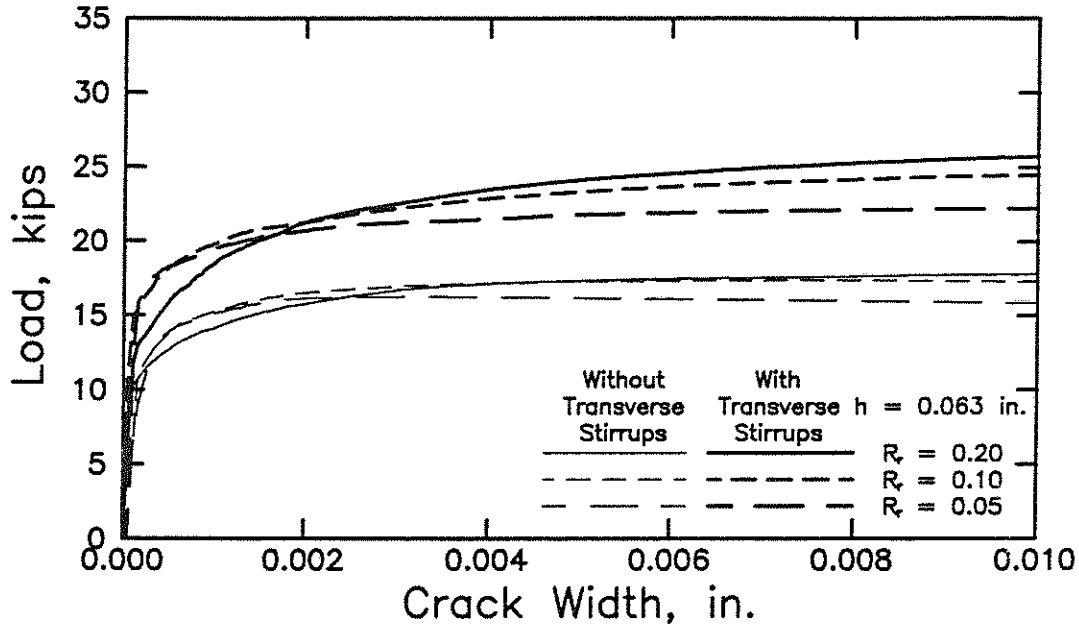

(c)

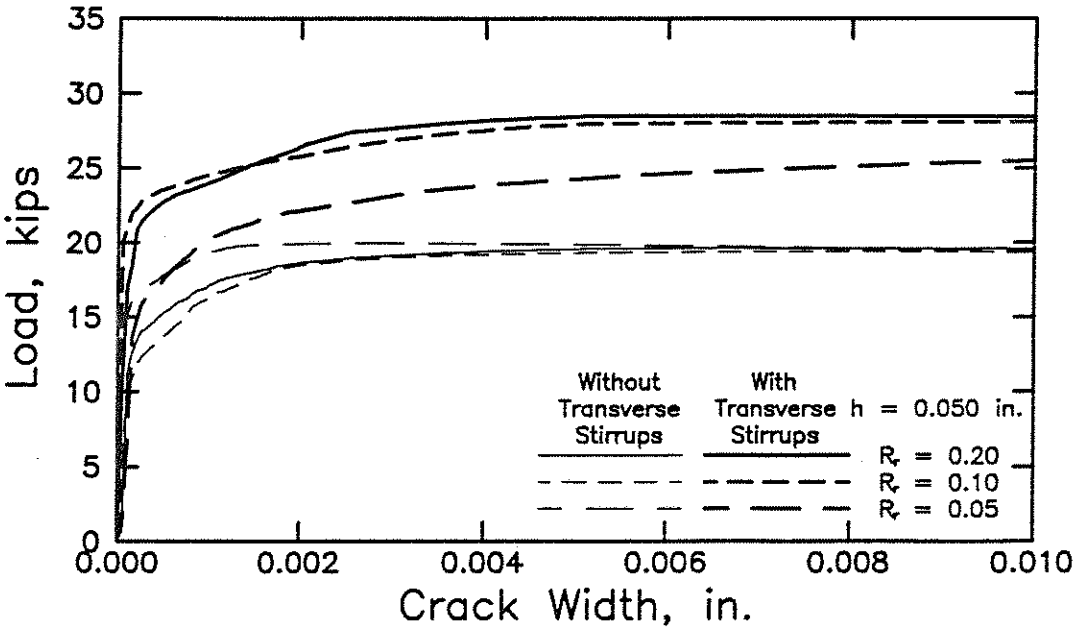

(d)

Figs. 2.10c&d Average load-crack width curves for specimens with 7 1/2 in. (191 mm) bonded length, 1/2 in. (13 mm) lead length, and 2 in. (51 mm) cover, (c) 5/8 in. (16 mm) bars with deformation patterns M31-5, M32-5, and M33-5, (d) 1 in. (25 mm) bars with deformation patterns M11-8, M12-8, and M13-8 (1 in. = 25.4 mm, 1 kip = 4.45 kN)

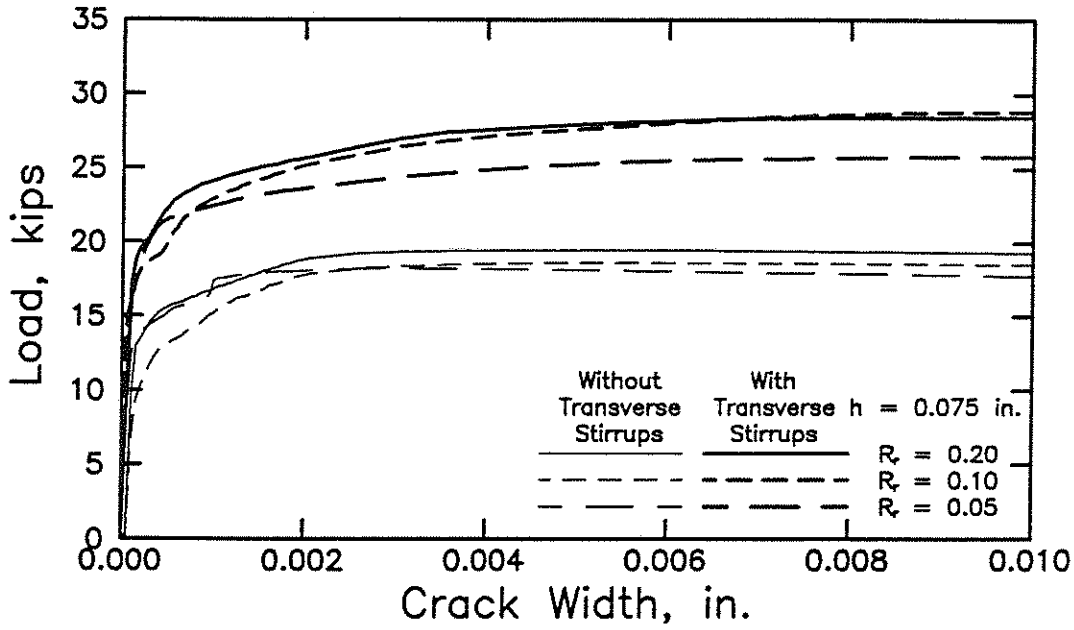

(e)

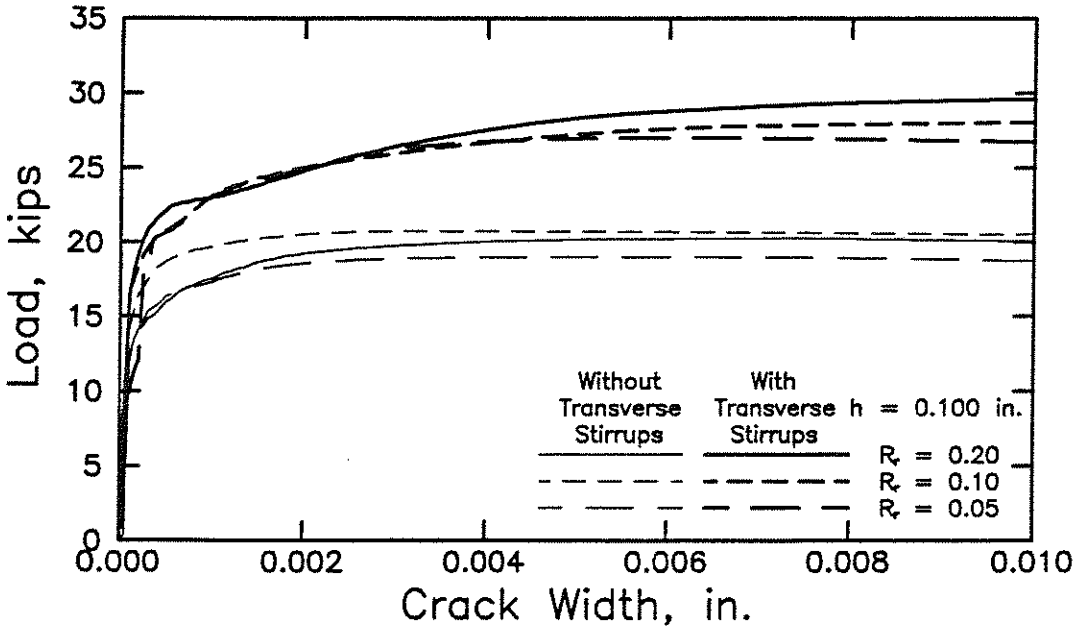

(f)

Figs. 2.10e&f Average load-crack width curves for specimens with 7 1/2 in. (191 mm) bonded length, 1/2 in. (13 mm) lead length, and 2 in. (51 mm) cover, (e) 1 in. (25 mm) bars with deformation patterns M21-8, M22-8, and M23-8, (f) 1 in. (25 mm) bars with deformation patterns M31-8, M32-8, and M33-8 (1 in. = 25.4 mm, 1 kip = 4.45 kN)

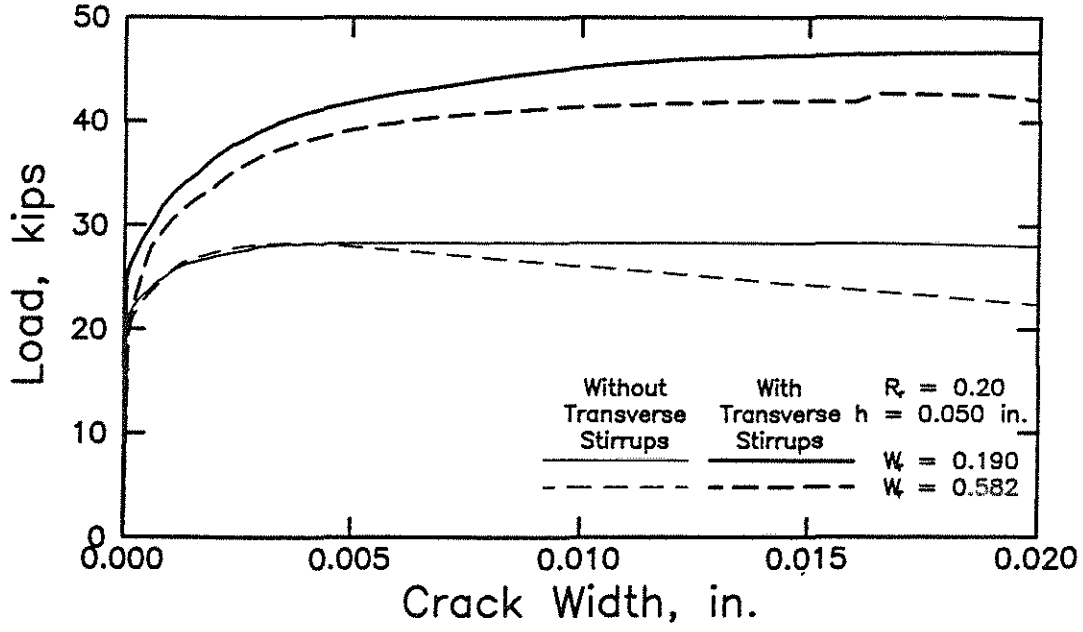

(g)

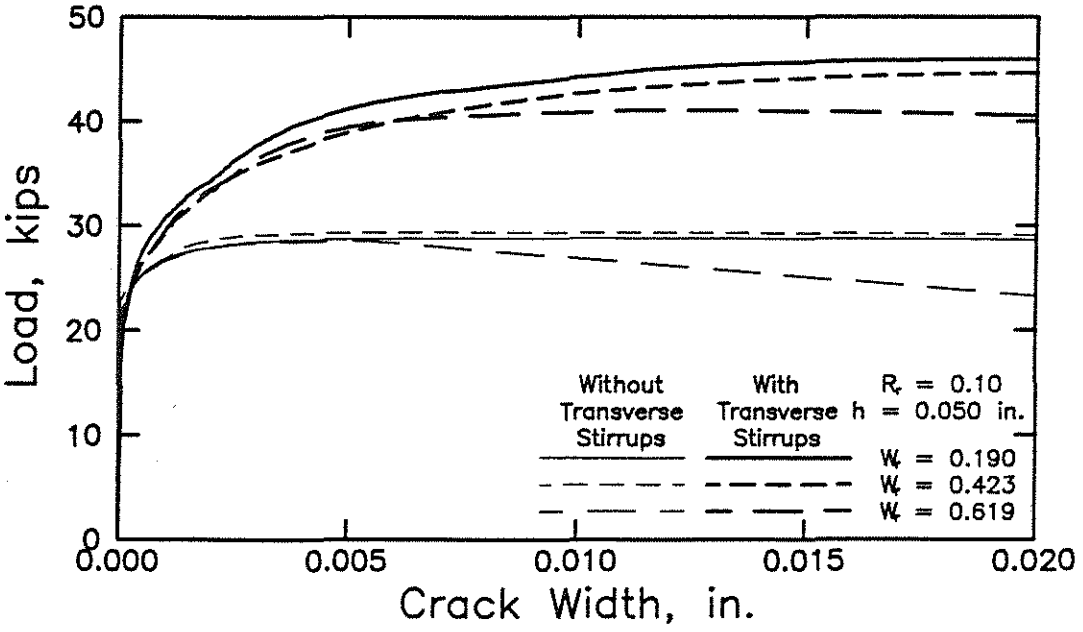

(h)

Figs. 2.10g&h Average load-crack width curves for specimens with 12 in. (305 mm) bonded length, 1/2 in. (13 mm) lead length, and 2 in. (51 mm) cover, (g) 1 in. (25 mm) bars with deformation patterns M11-8 and M11A-8, (h) 1 in. (25 mm) bars with deformation patterns M12-8, M12D-8, and M12E-8 (1 in. = 25.4 mm, 1 kip = 4.45 kN)

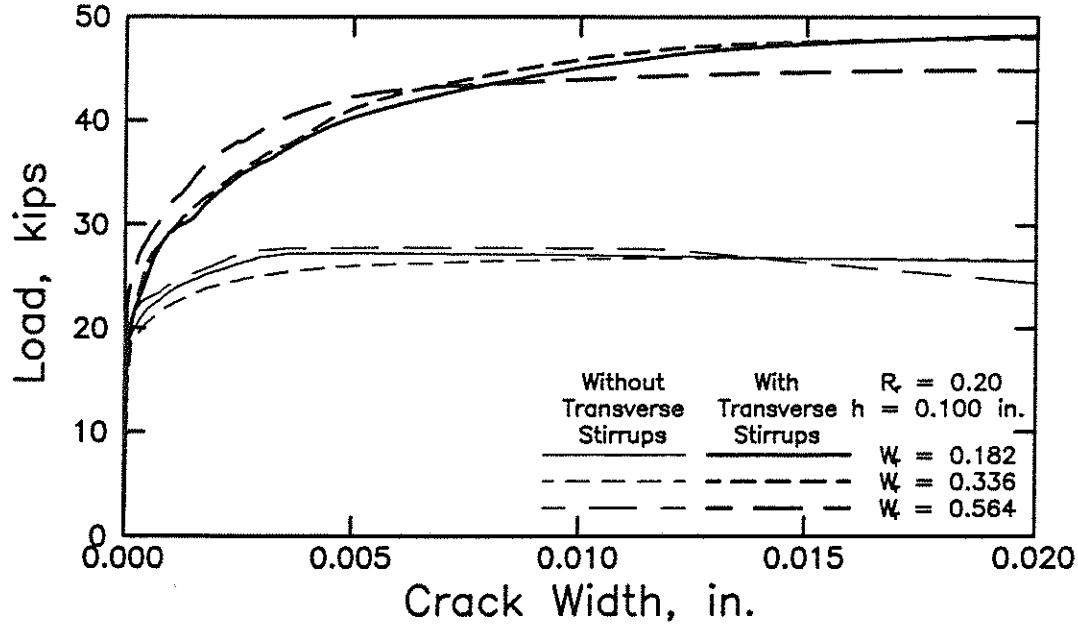

(i)

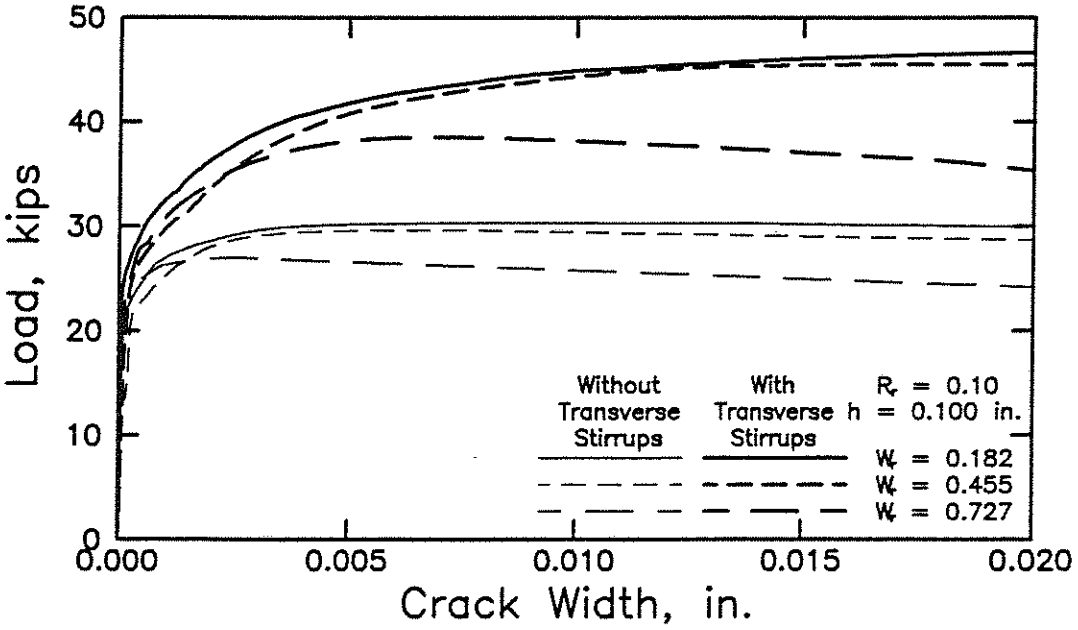

(j)

Figs. 2.10i&j Average load-crack width curves for specimens with 12 in. (305 mm) bonded length, 1/2 in. (13 mm) lead length, and 2 in. (51 mm) cover, (i) 1 in. (25 mm) bars with deformation patterns M31-8, M31D-8, and M31E-8, (j) 1 in. (25 mm) bars with deformation patterns M32-8, M32B-8, and M32C-8 (1 in. = 25.4 mm, 1 kip = 4.45 kN)

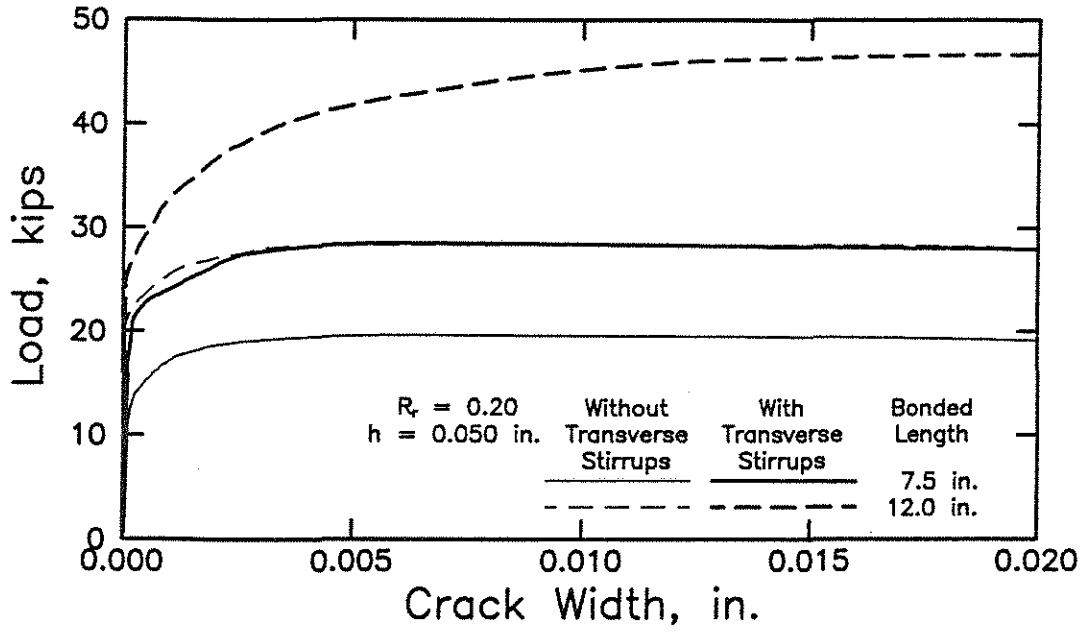

(k)

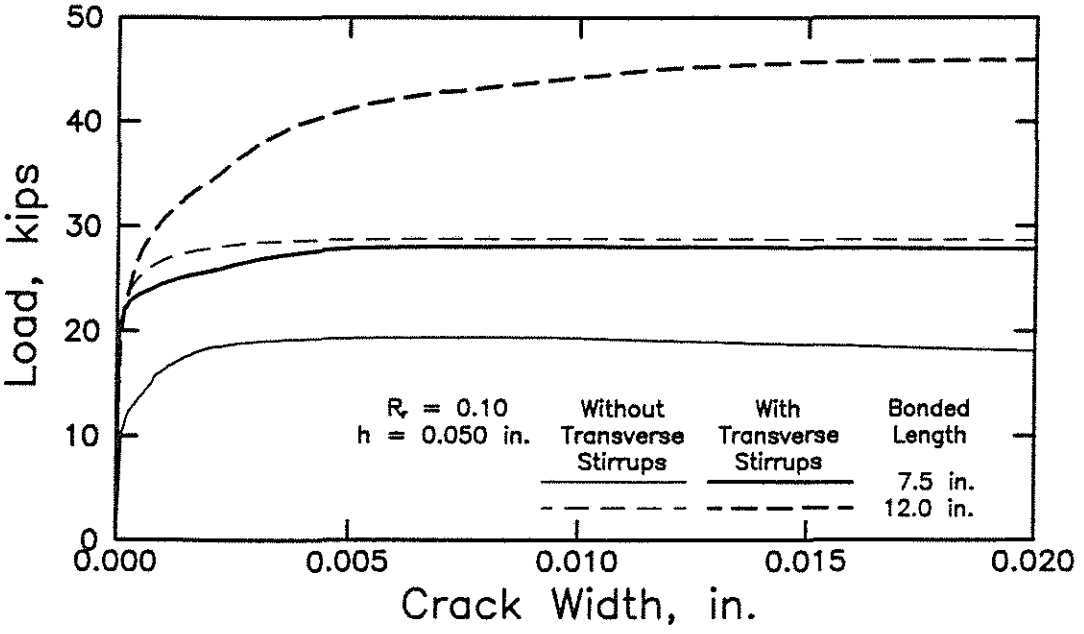

(l)

Figs. 2.10k&l Comparison of average load-crack width curves for specimens with 1/2 in. (13 mm) lead length and 2 in. (51 mm) cover, (k) 1 in. (25 mm) bars with deformation pattern M11-8, (l) 1 in. (25 mm) bars with deformation pattern M12-8 (1 in. = 25.4 mm, 1 kip = 4.45 kN)

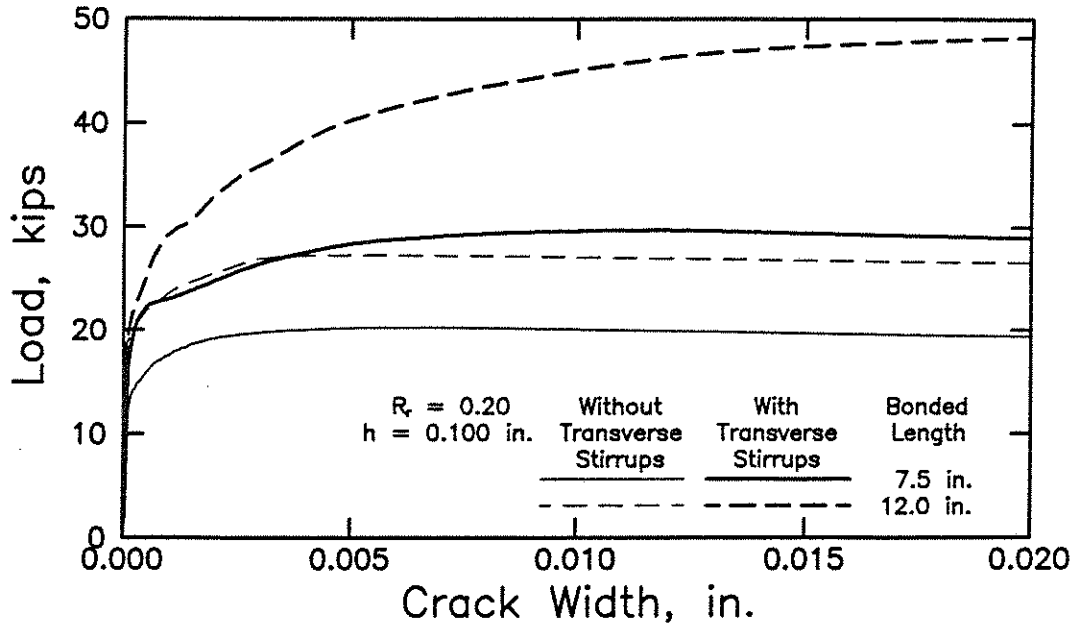

(m)

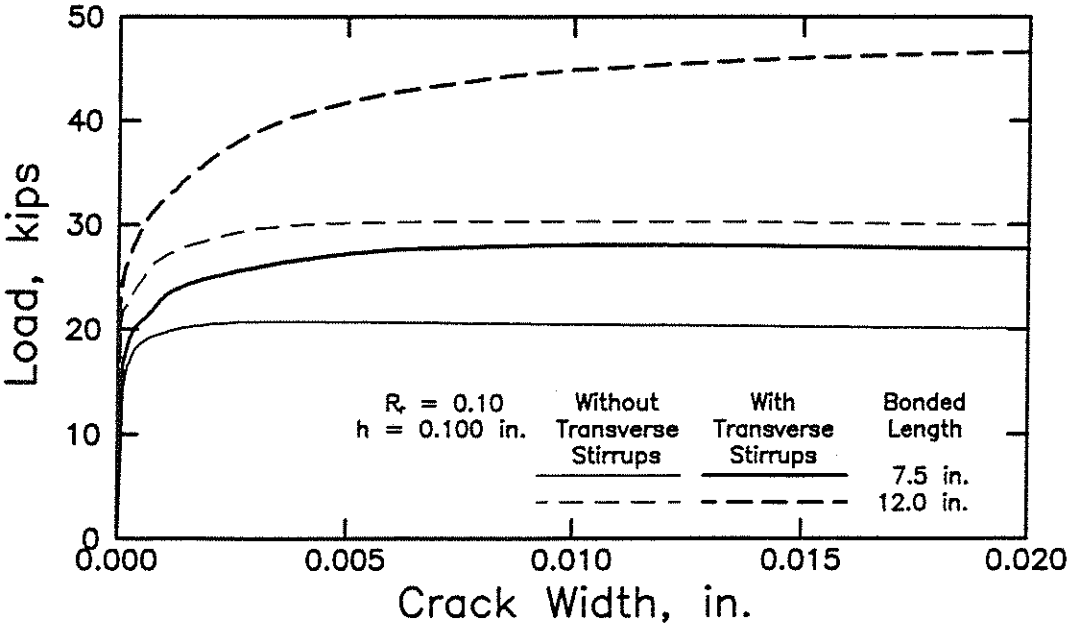

(n)

Figs. 2.10m&n Comparison of average load-crack width curves for specimens with 1/2 in. (13 mm) lead length and 2 in. (51 mm) cover, (m) 1 in. (25 mm) bars with deformation pattern M31-8, (n) 1 in. (25 mm) bars with deformation pattern M32-8 (1 in. = 25.4 mm, 1 kip = 4.45 kN)

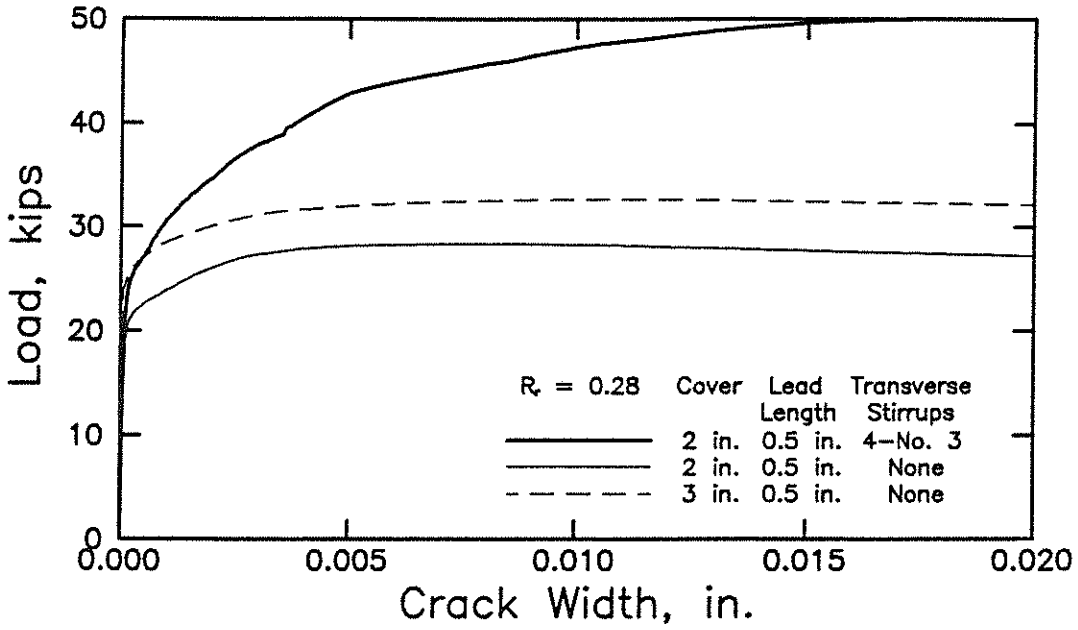

Fig. 2.10o Average load-crack width curves for specimens with 12.5 in. (318 mm) embedment length containing threaded bars with deformation pattern T-8 (1 in. = 25.4 mm, 1 kip = 4.45 kN)

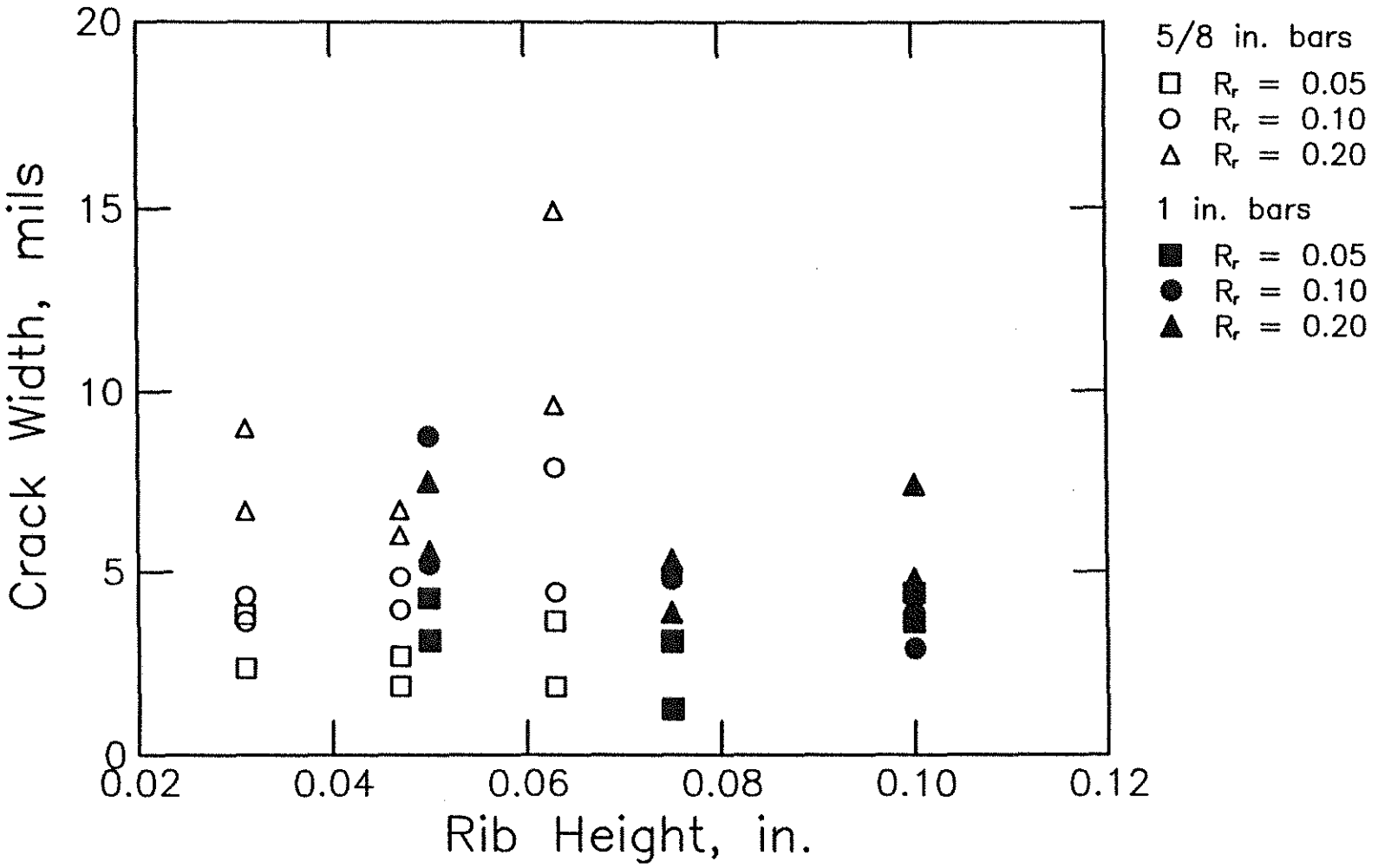

Fig. 2.11a Crack width before failure versus rib height for specimens with 7.5 in. (191 mm) bonded length without transverse stirrups (1 in. = 25.4 mm)

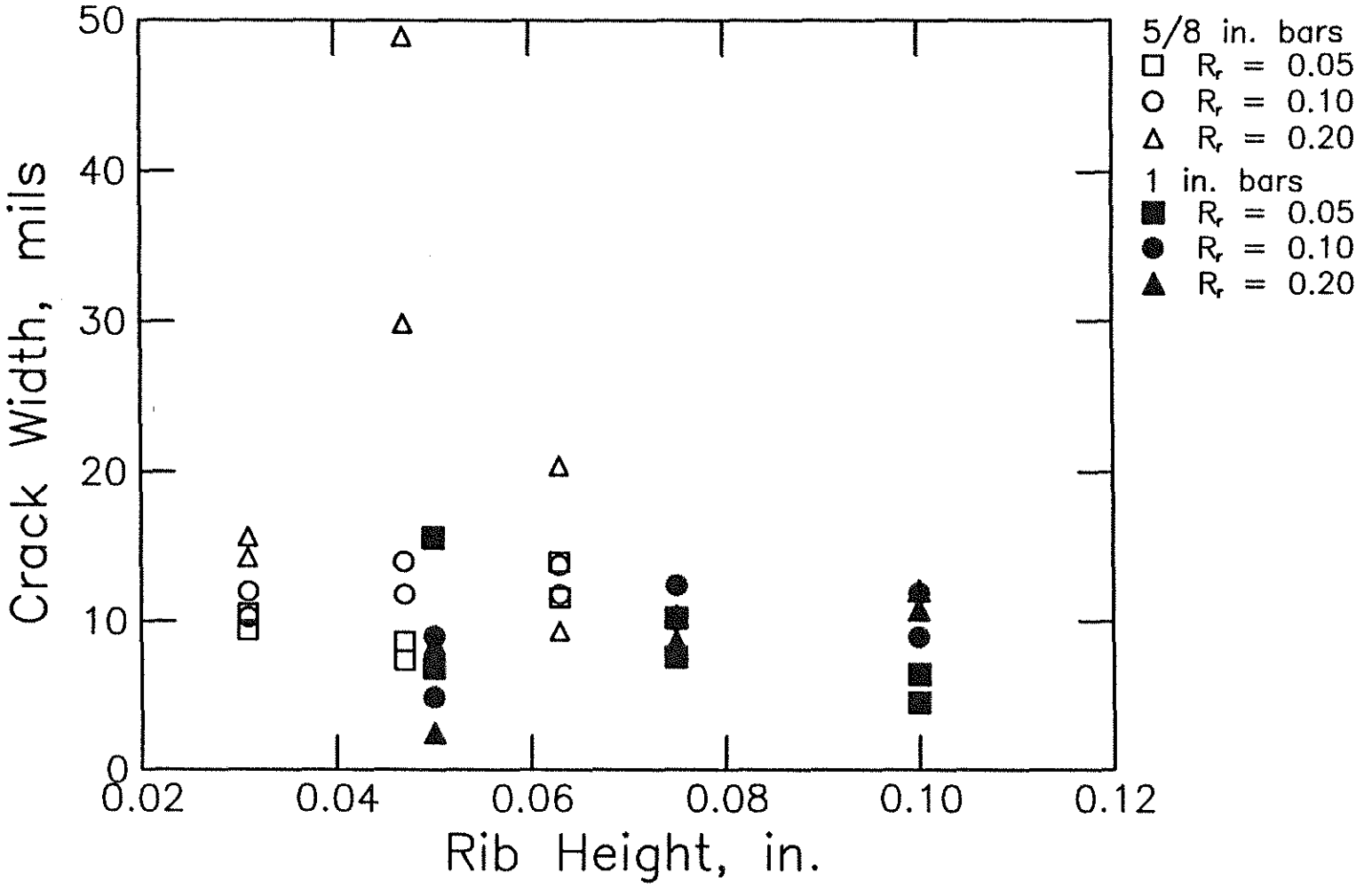

Fig. 2.11b Crack width before failure versus rib height for specimens with 7.5 in. (191 mm) bonded length with transverse stirrups (1 in. = 25.4 mm)

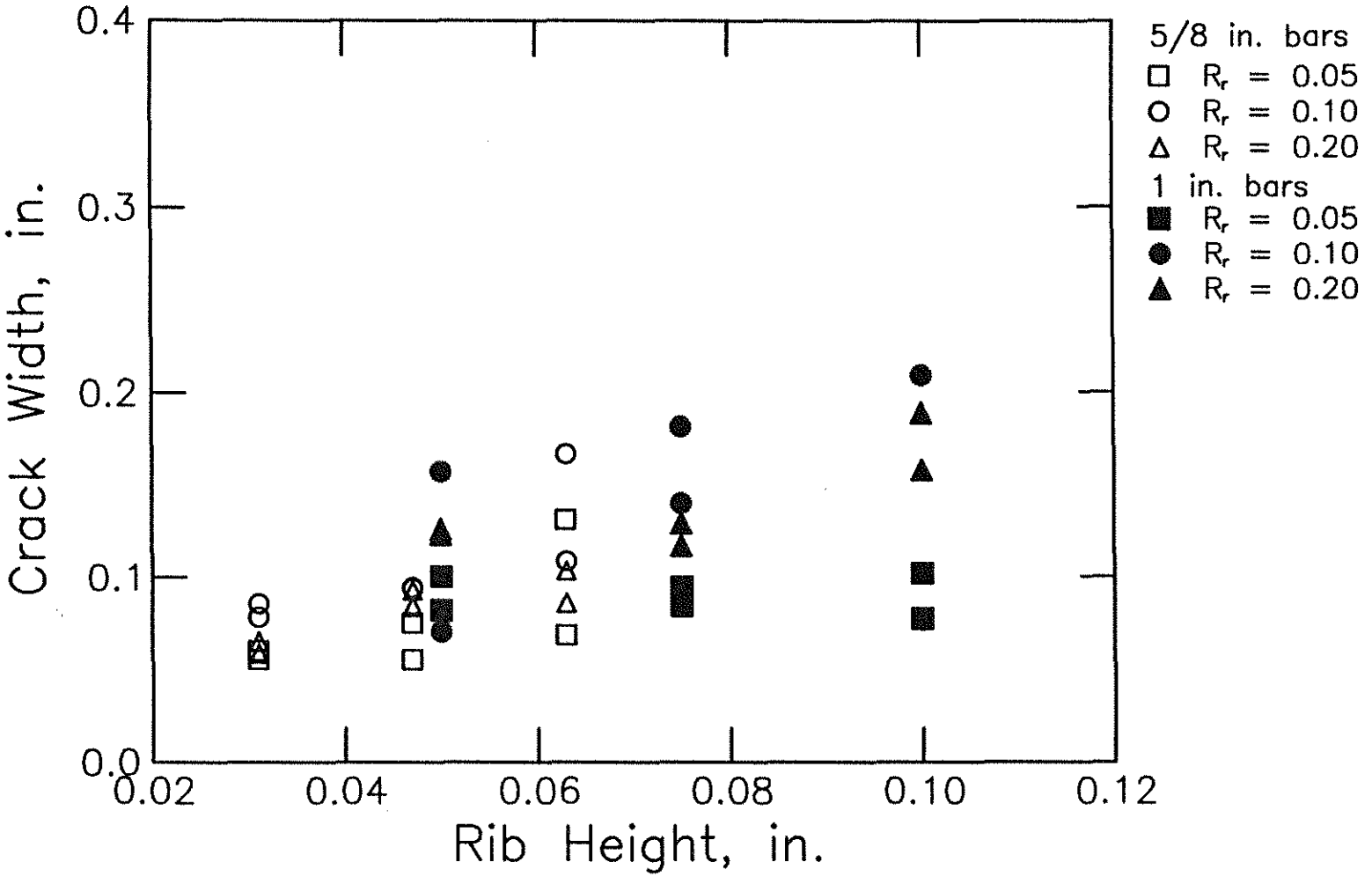

Fig. 2.12a Crack width after failure versus rib height for specimens with 7.5 in. (191 mm) bonded length without transverse stirrups (1 in. = 25.4 mm)

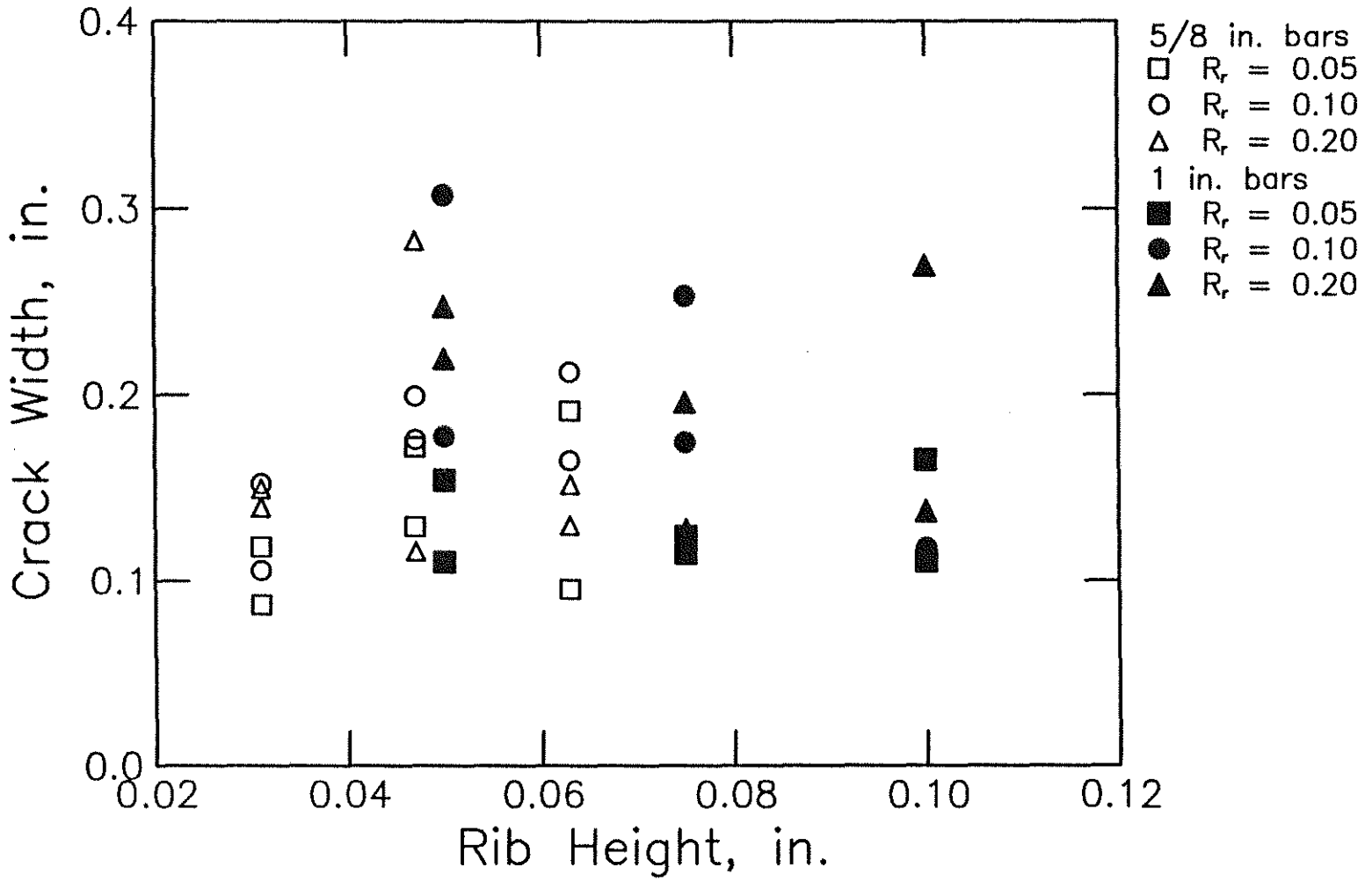

Fig. 2.12b Crack width after failure versus rib height for specimens with 7.5 in. (191 mm) bonded length with transverse stirrups (1 in. = 25.4 mm)

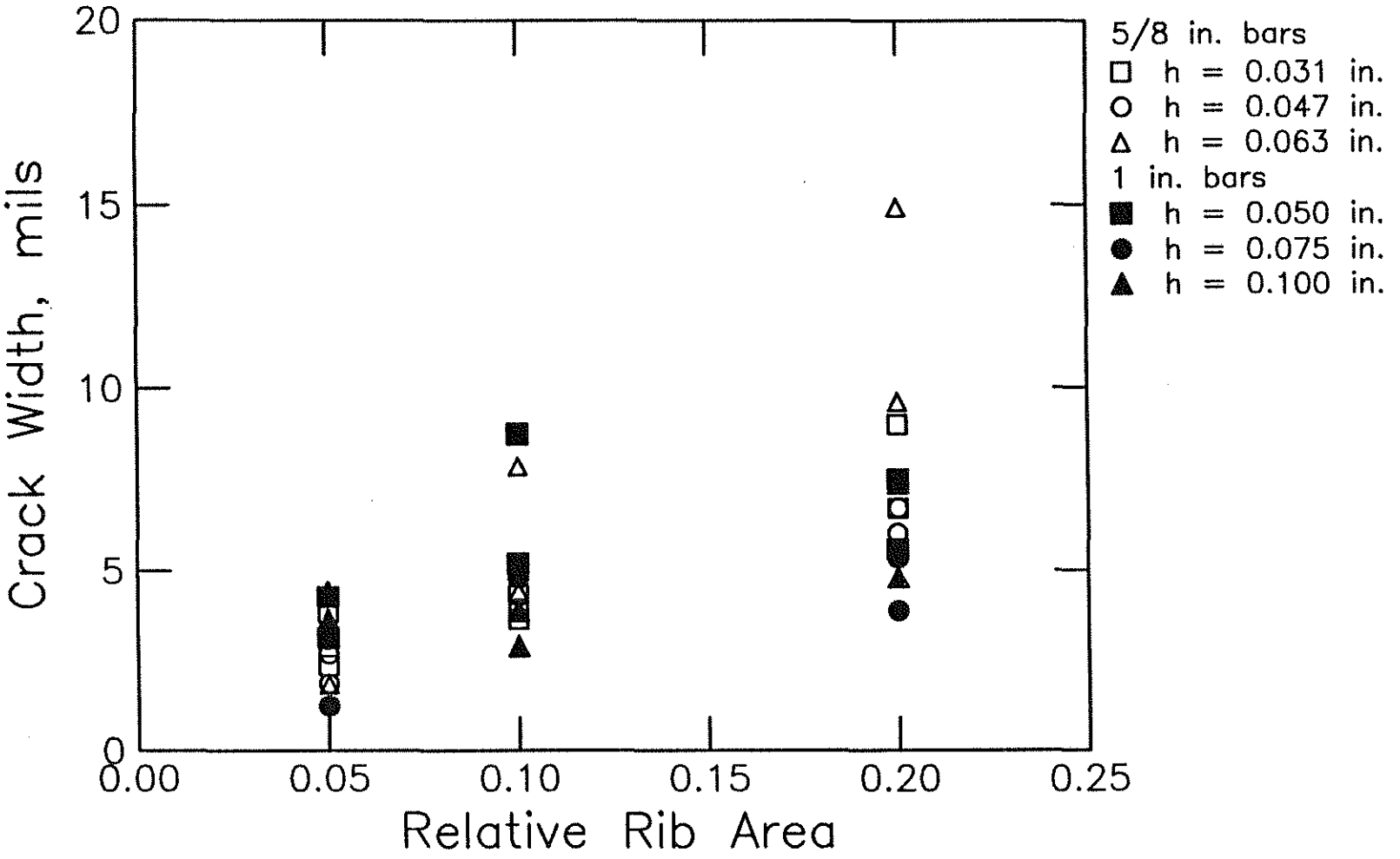

Fig. 2.13a Crack width before failure versus relative rib area for specimens with 7.5 in. (191 mm) bonded length without transverse stirrups (1 in. = 25.4 mm)

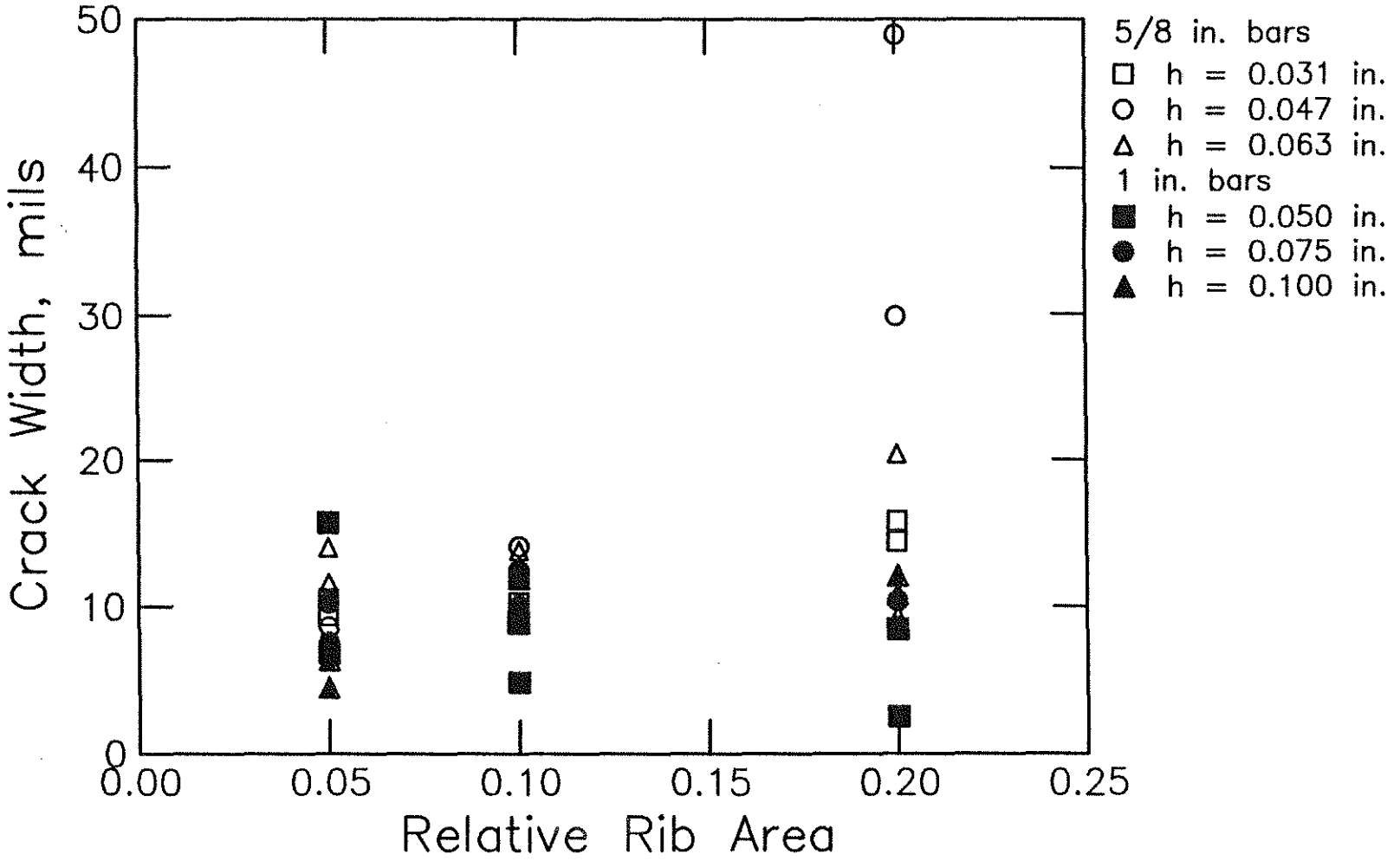

Fig. 2.13b Crack width before failure versus relative rib area for specimens with 7.5 in. (191 mm) bonded length with transverse stirrups (1 in. = 25.4 mm)

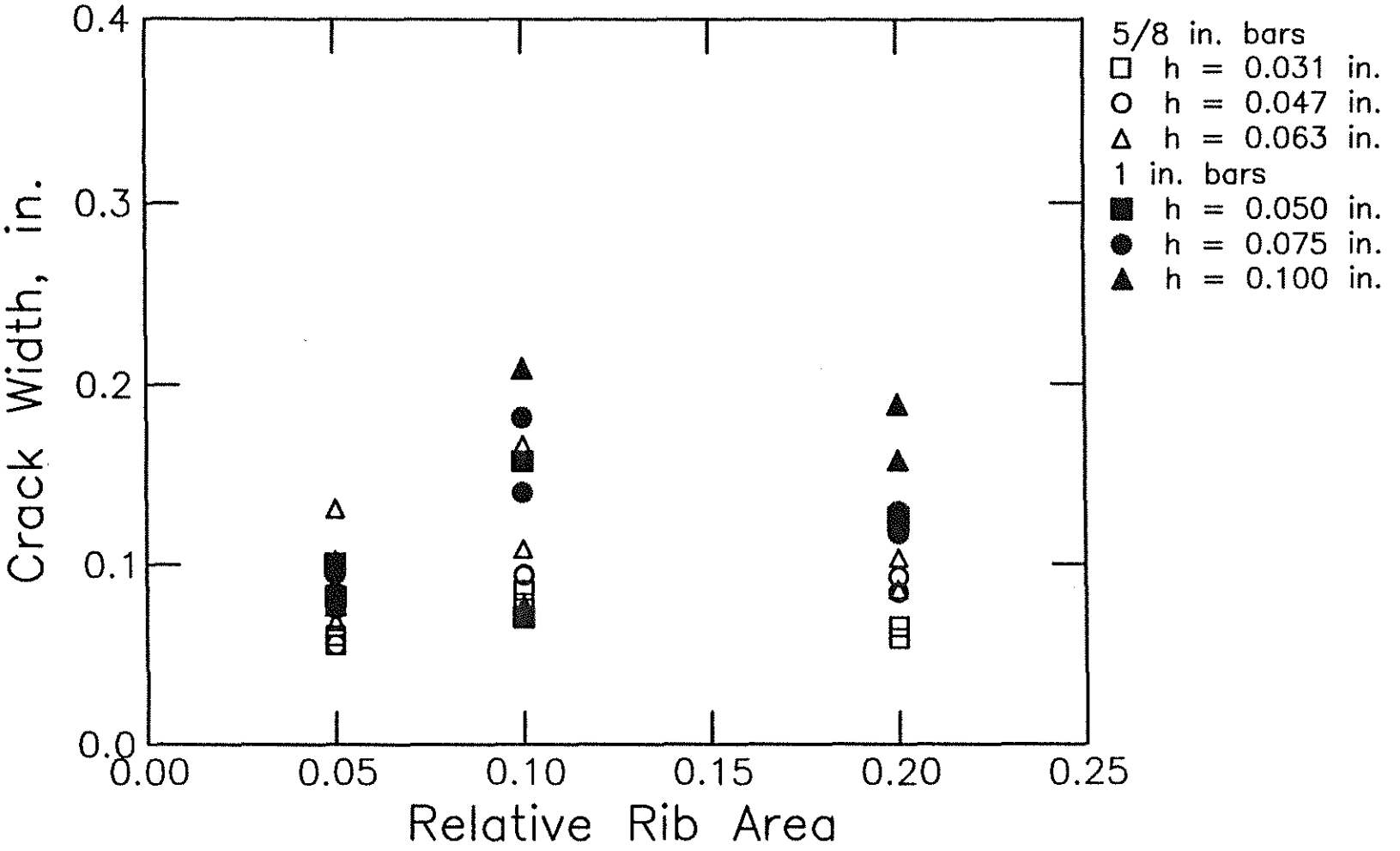

Fig. 2.14a Crack width after failure versus relative rib area for specimens with 7.5 in. (191 mm) bonded length without transverse stirrups (1 in. = 25.4 mm)

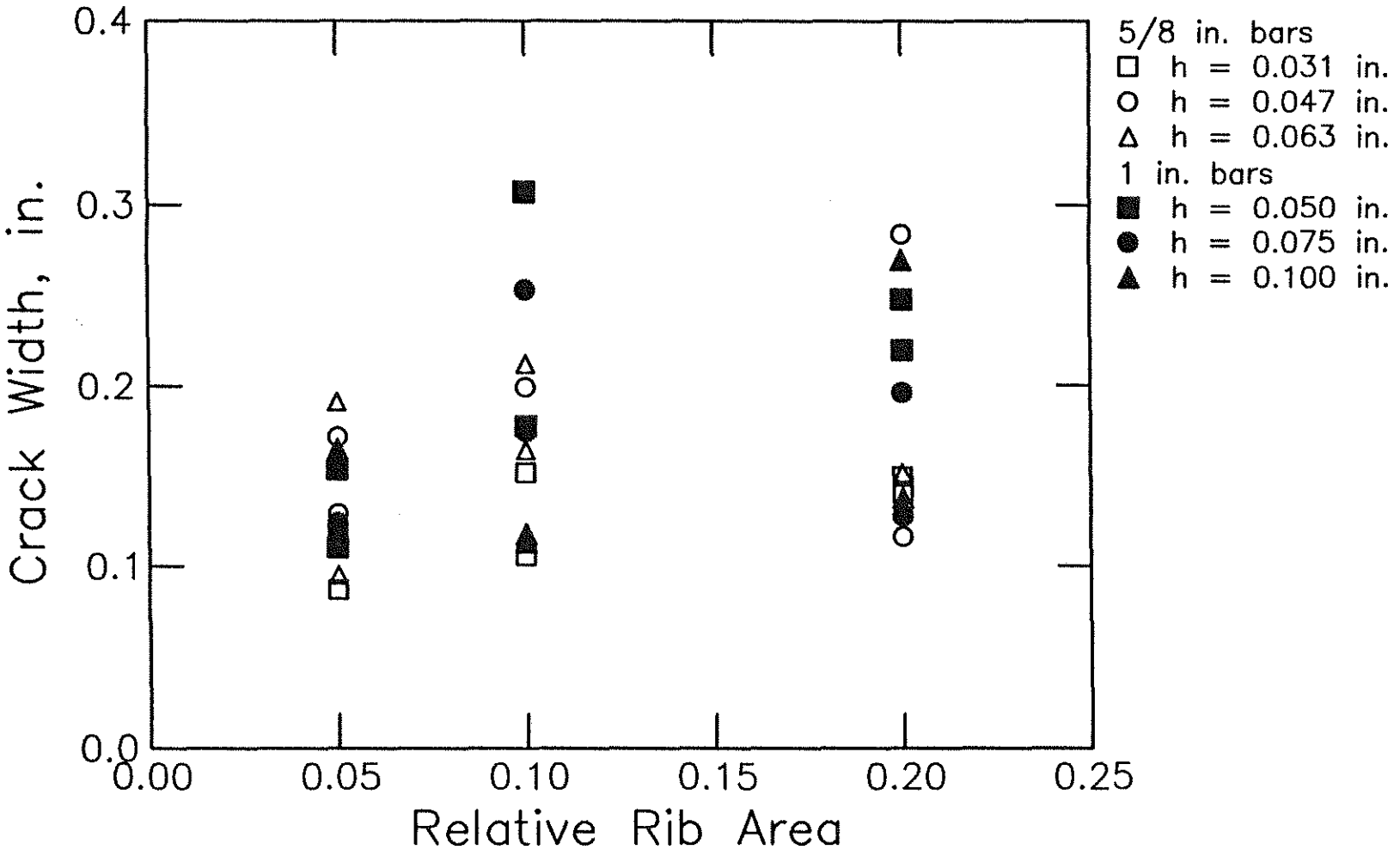

Fig. 2.14b Crack width after failure versus relative rib area for specimens with 7.5 in. (191 mm) bonded length with transverse stirrups (1 in. = 25.4 mm)

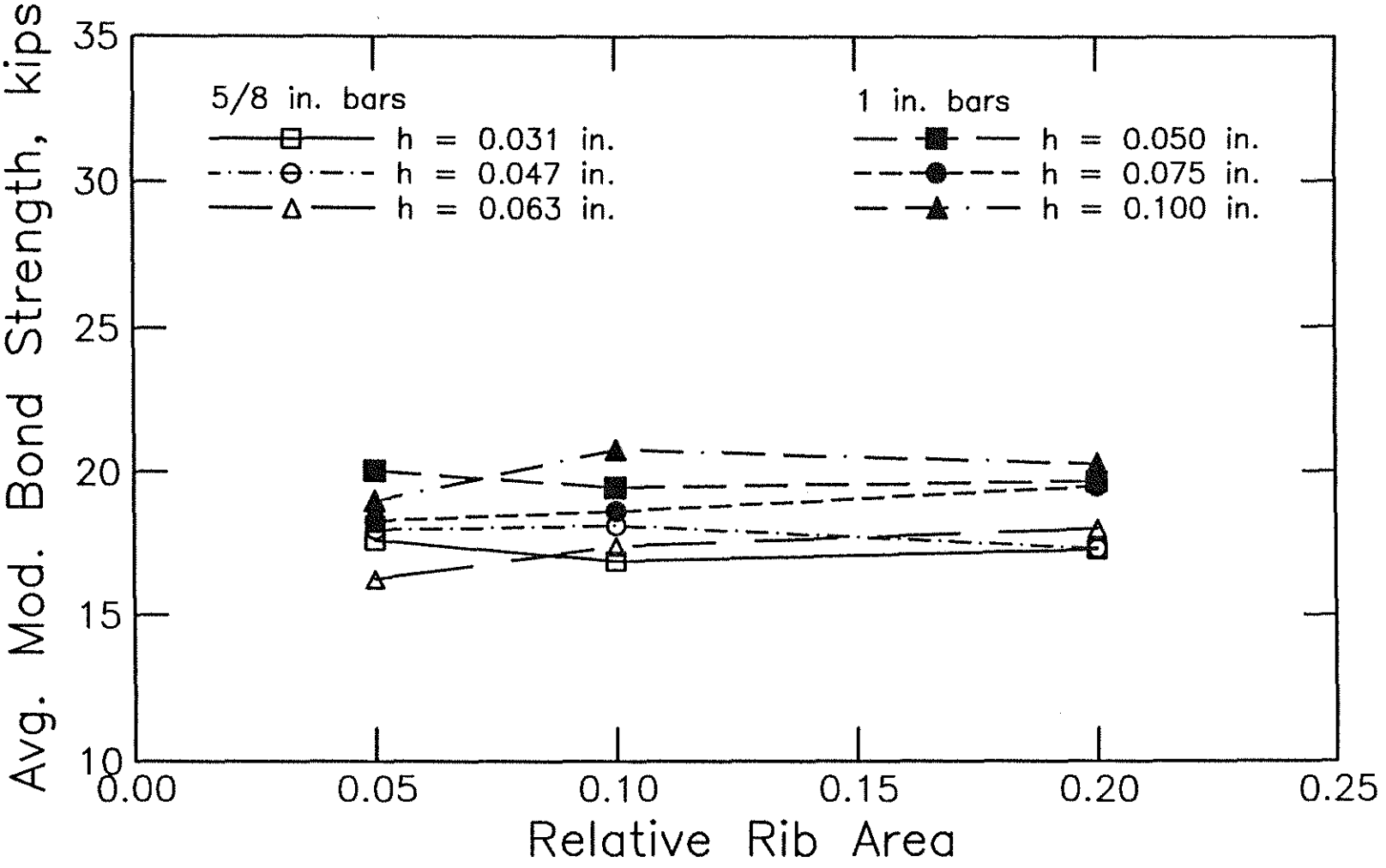

Fig. 2.15a Average modified bond strength versus relative rib area for specimens with 7.5 in. (191 mm) bonded length without transverse stirrups (1 kip = 4.45 kN)

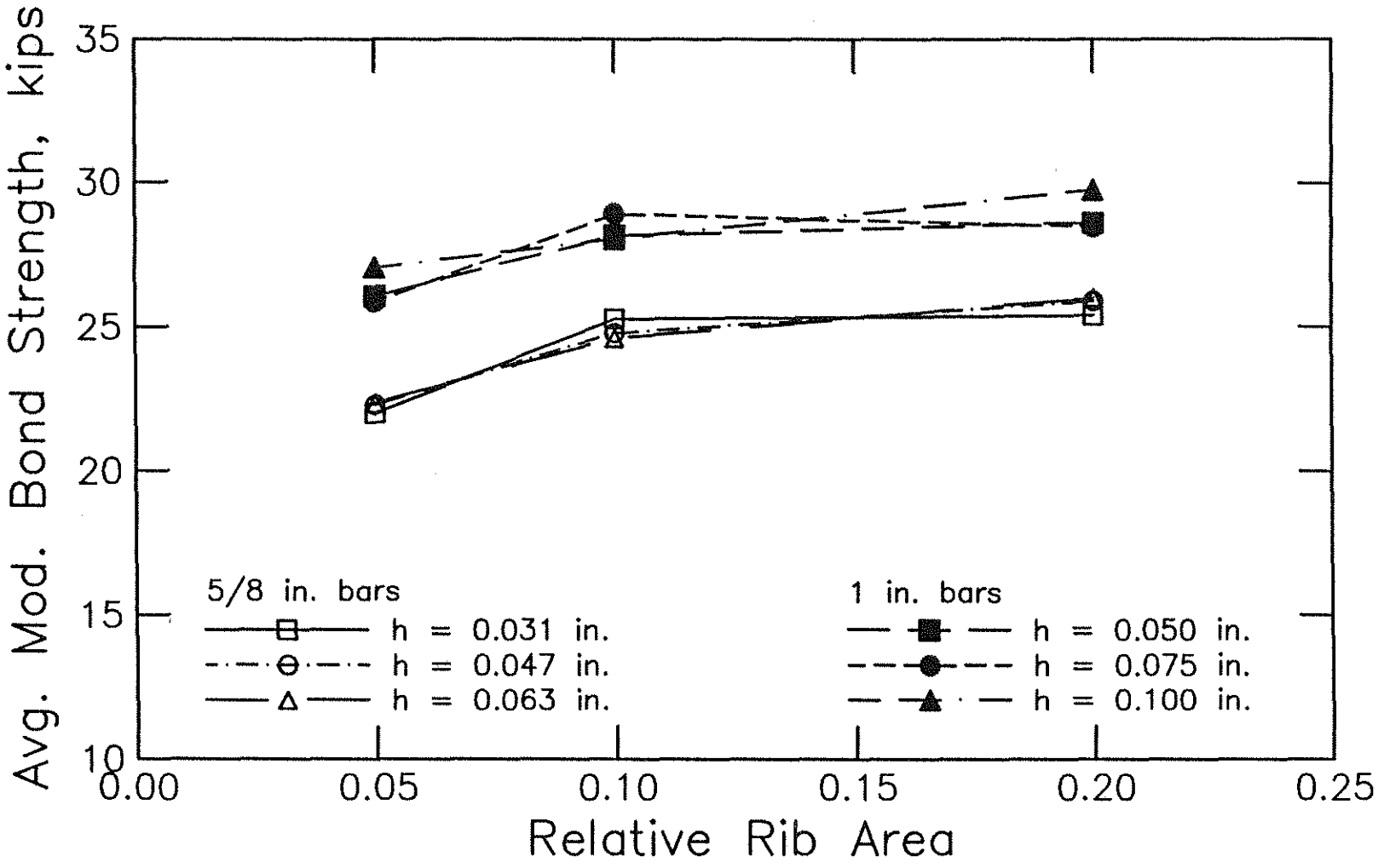

Fig. 2.15b Average modified bond strength versus relative rib area for specimens with 7.5 in. (191 mm) bonded length with transverse stirrups (1 kip = 4.45 kN)

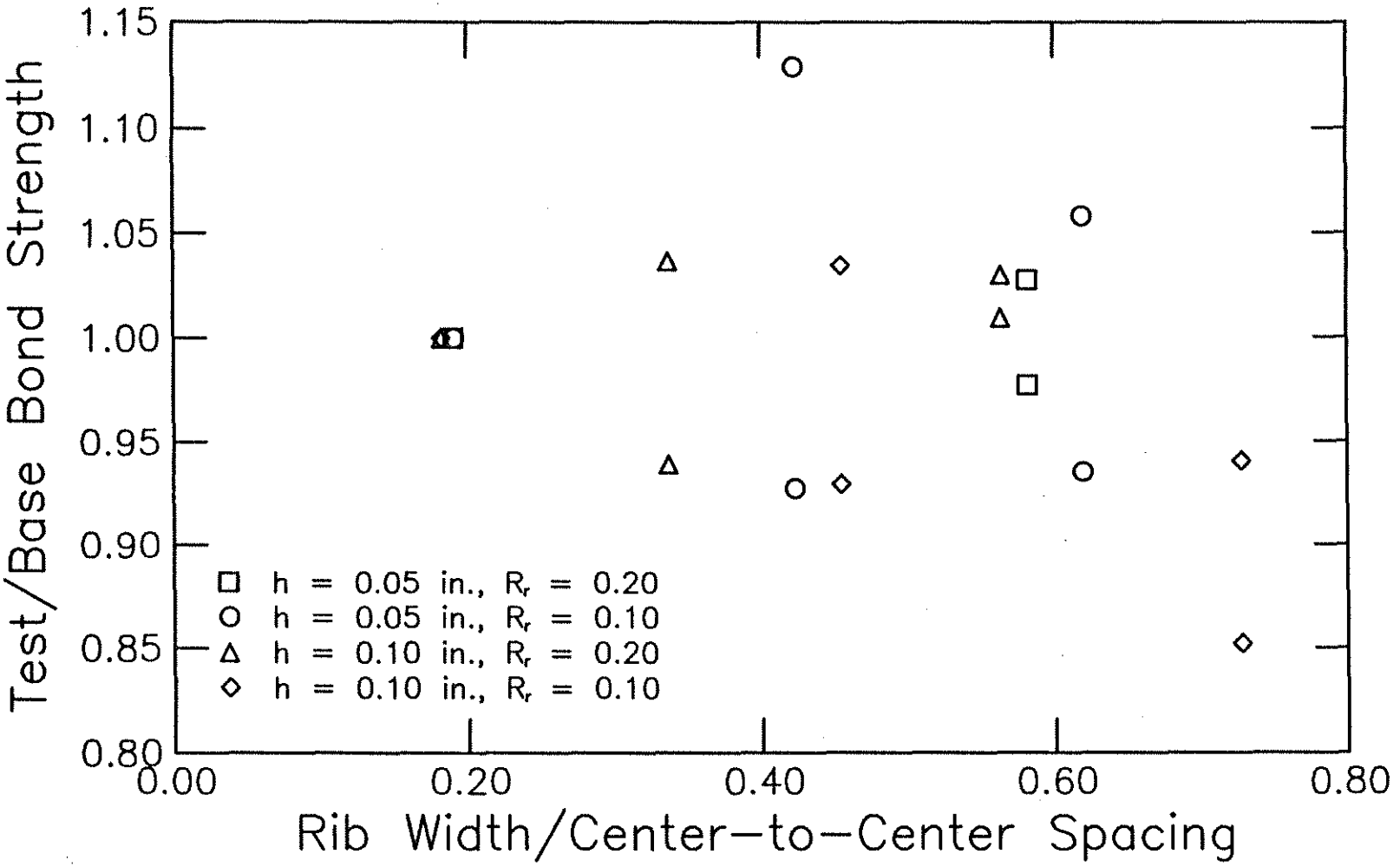

Fig. 2.16a Ratio of test to base bond strength versus ratio of rib width to center-to-center rib spacing for specimens with 12 in. (305 mm) bonded length without transverse stirrups

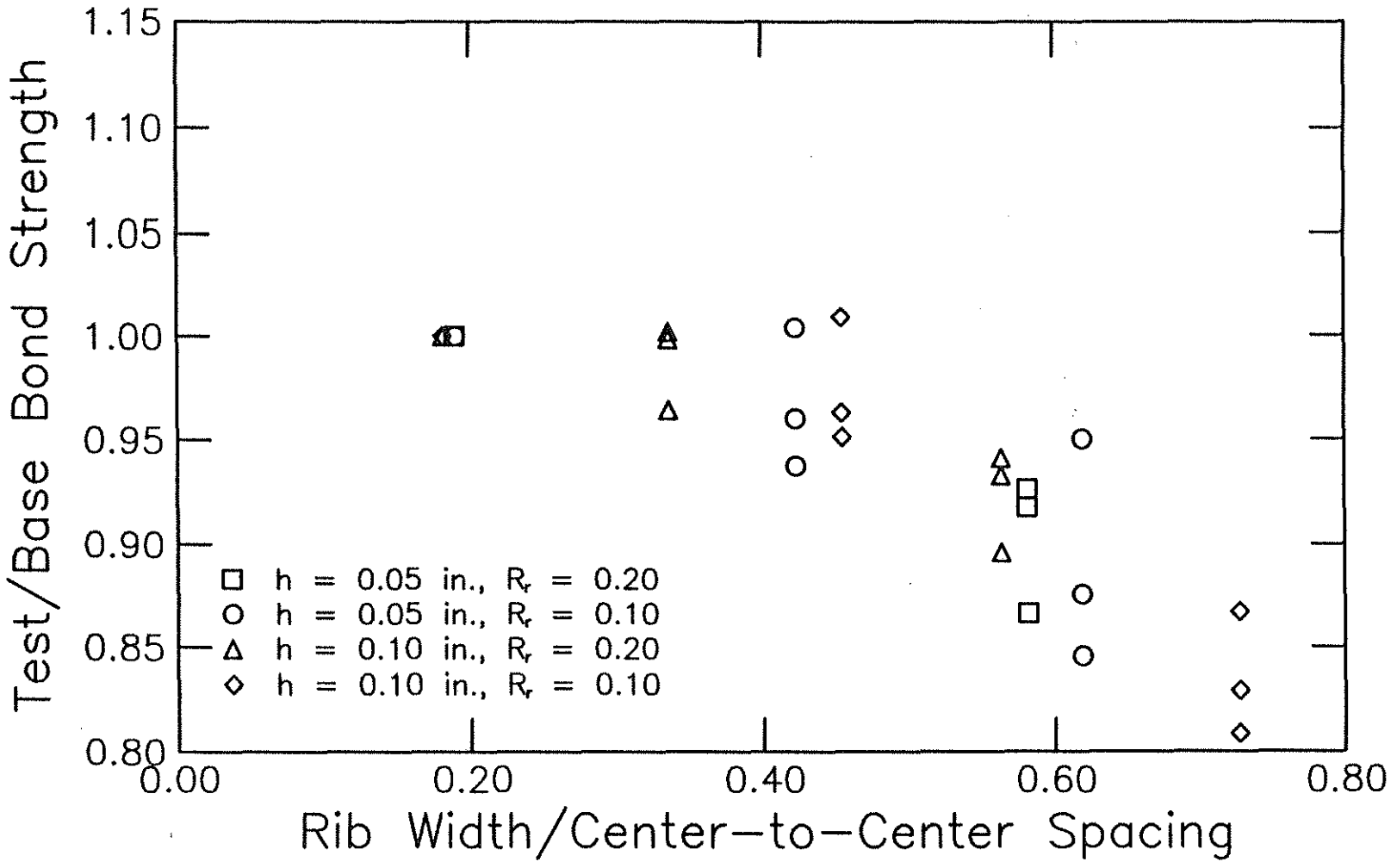

Fig. 2.16b Ratio of test to base bond strength versus ratio of rib width to center-to-center rib spacing for specimens with 12 in. (305 mm) bonded length with transverse stirrups

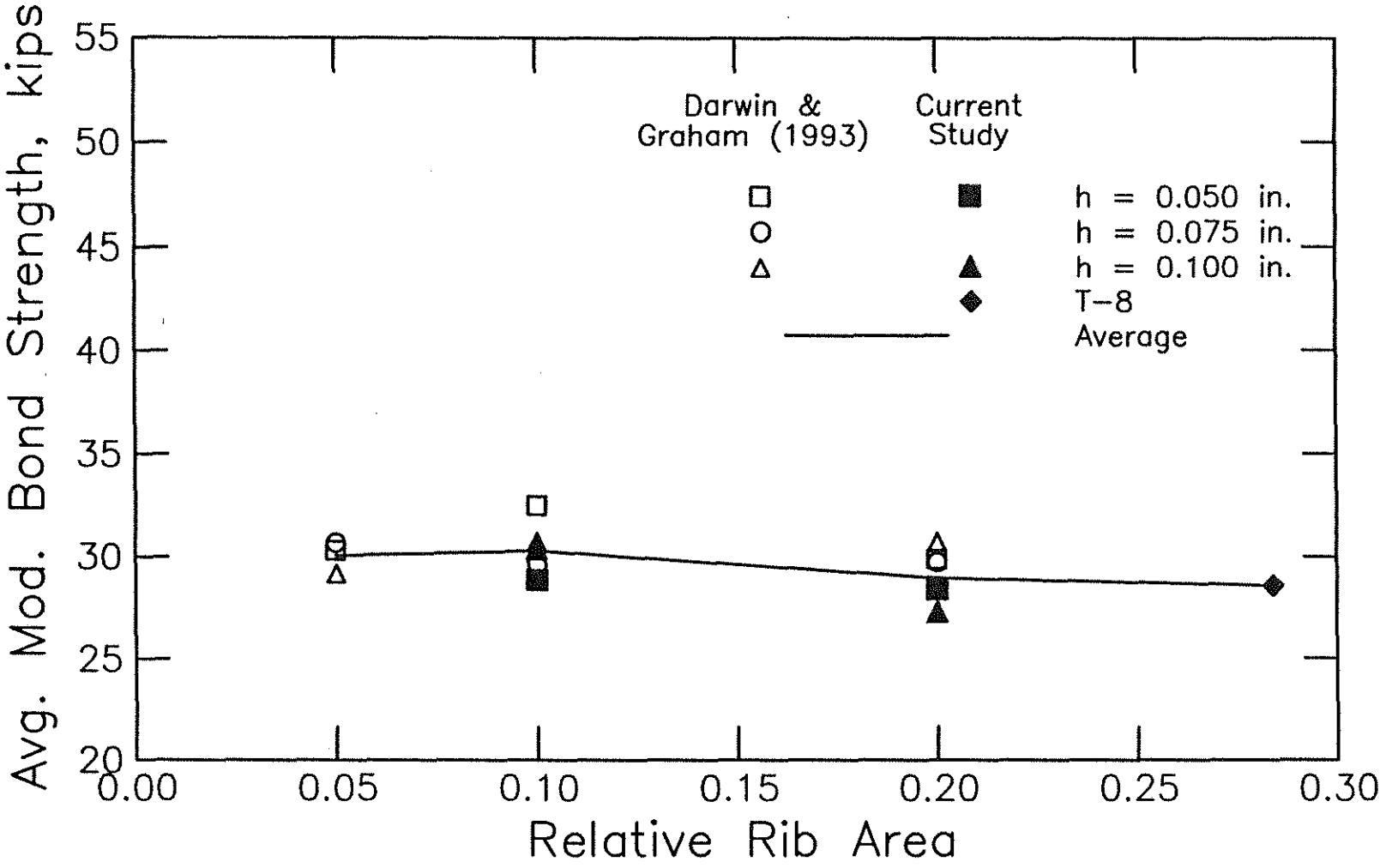

Fig 2.17 Average modified bond strength versus relative rib area for specimens without transverse stirrups [cover = 2 in. (51 mm), lead length = 1/2 in. (13 mm), bonded length = 12 in. (305 mm)] (1 kip = 4.45 kN)

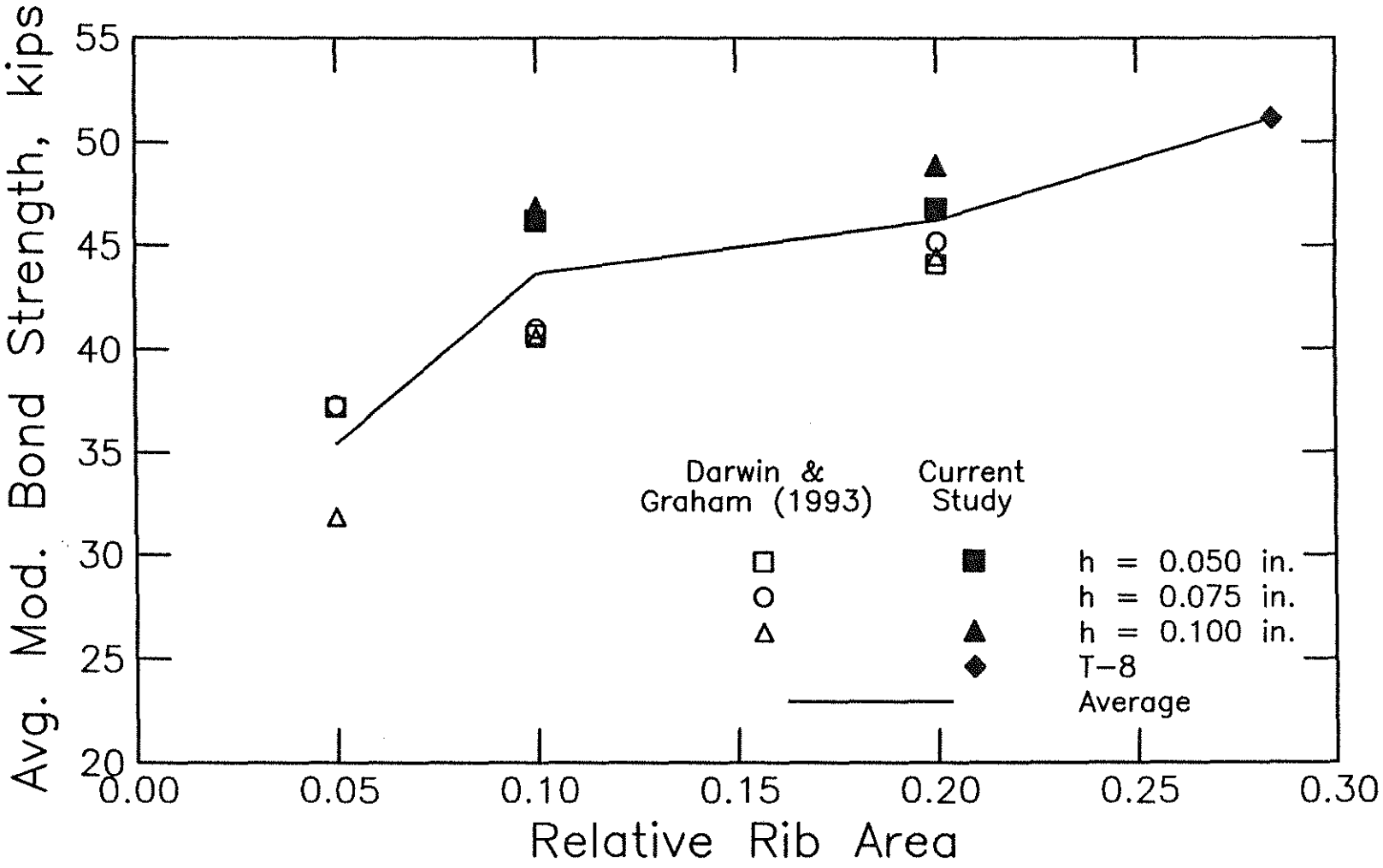

Fig 2.18 Average modified bond strength versus relative rib area for specimens with transverse stirrups [cover = 2 in. (51 mm), lead length = 1/2 in. (13 mm), bonded length = 12 in. (305 mm)] (1 kip = 4.45 kN)

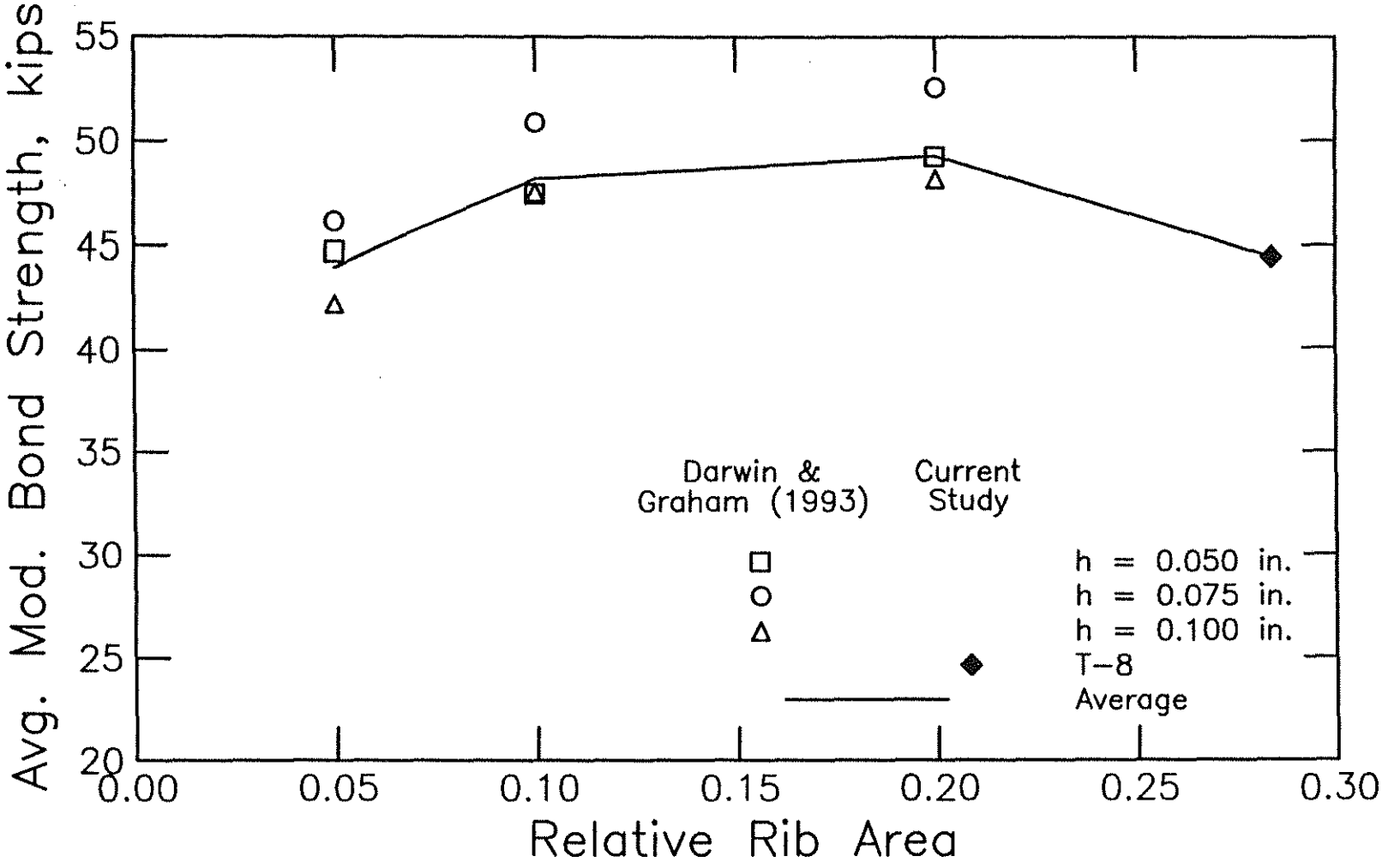

Fig 2.19 Average modified bond strength versus relative rib area for specimens without transverse stirrups [cover = 3 in. (76 mm), lead length = 4 in. (102 mm), bonded length = 8 1/2 in. (216 mm)] (1 kip = 4.45 kN)

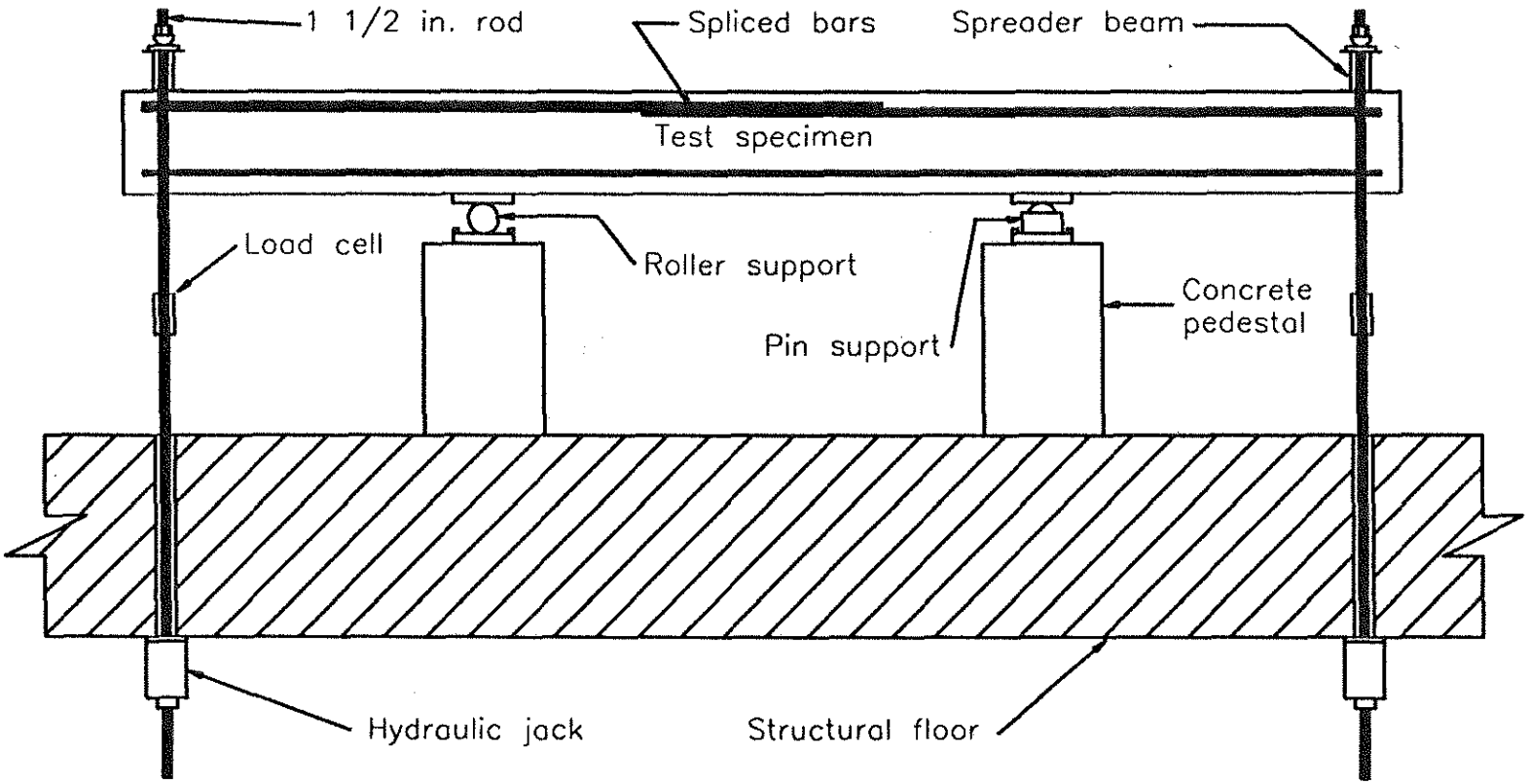

Fig. 3.1 Schematic of test apparatus

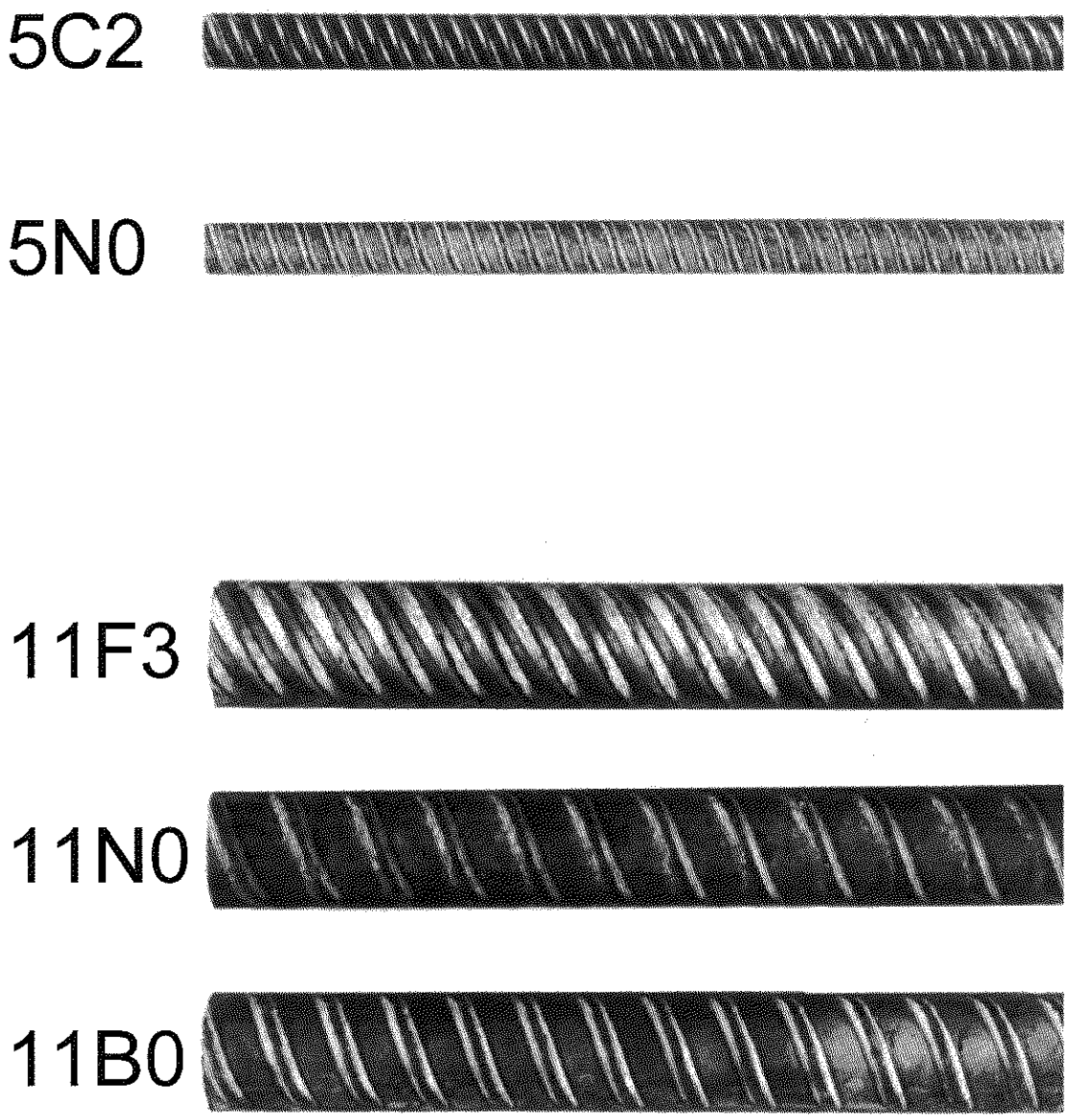

Fig. 3.2 Reinforcing bar deformation patterns, No. 5 and No. 11 (16 and 36 mm) bars

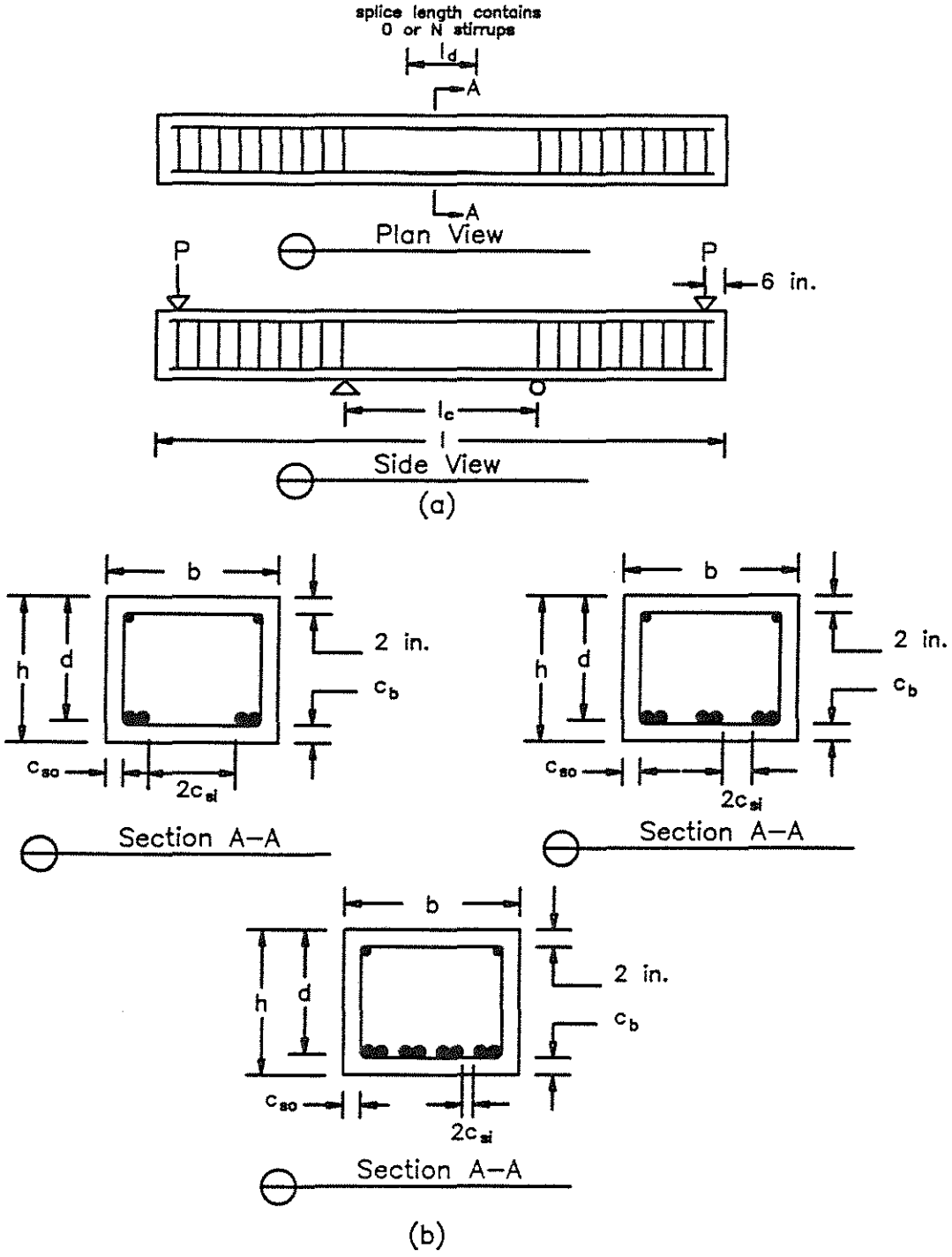

Fig. 3.3 Splice test specimens, (a) as tested, (b) configurations as cast (1 in. = 25.4 mm)

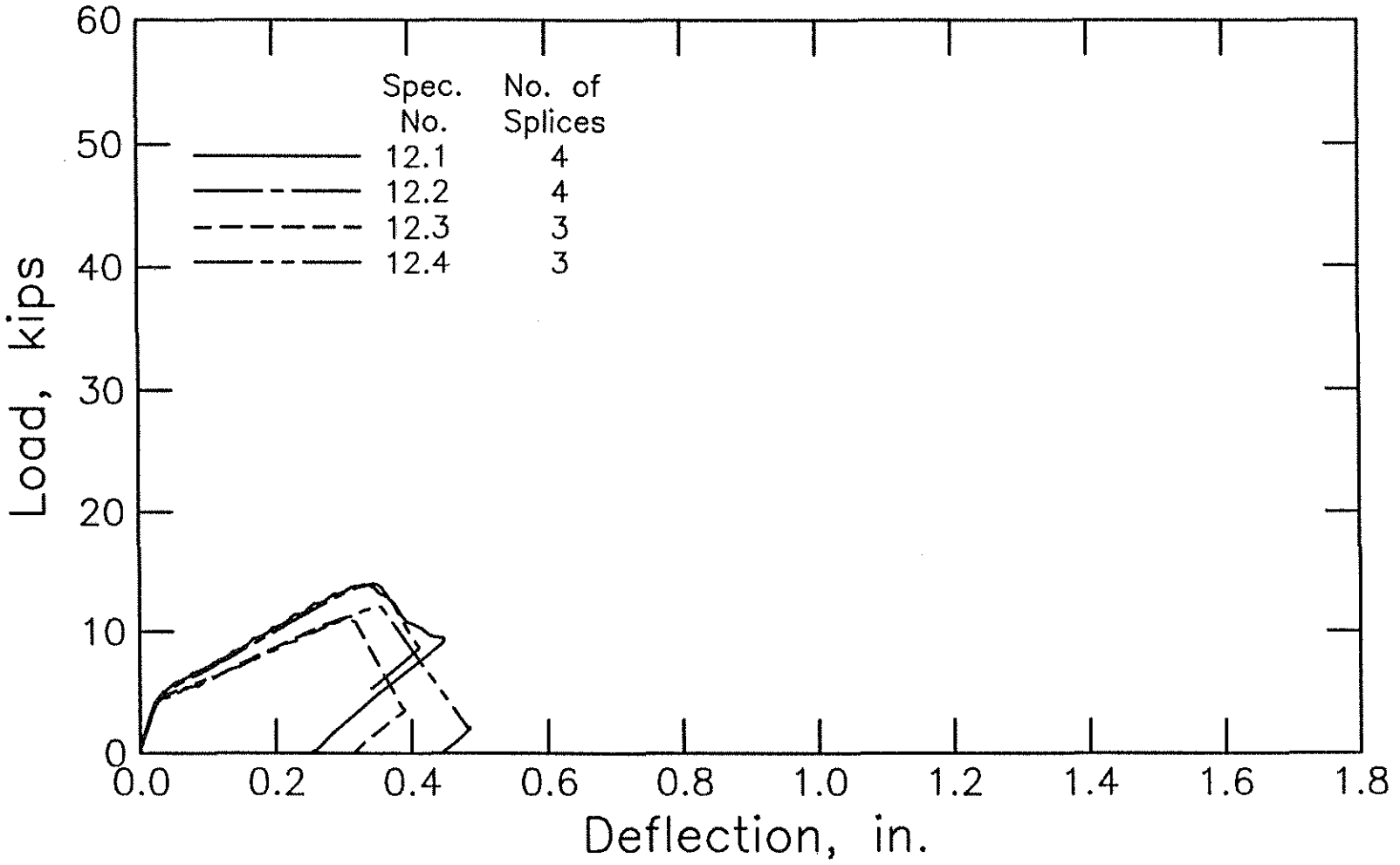

Fig. 3.4a Load-deflection curves for splice specimens in Group 12 (1 kip = 4.45 kN, 1 in. = 25.4 mm)

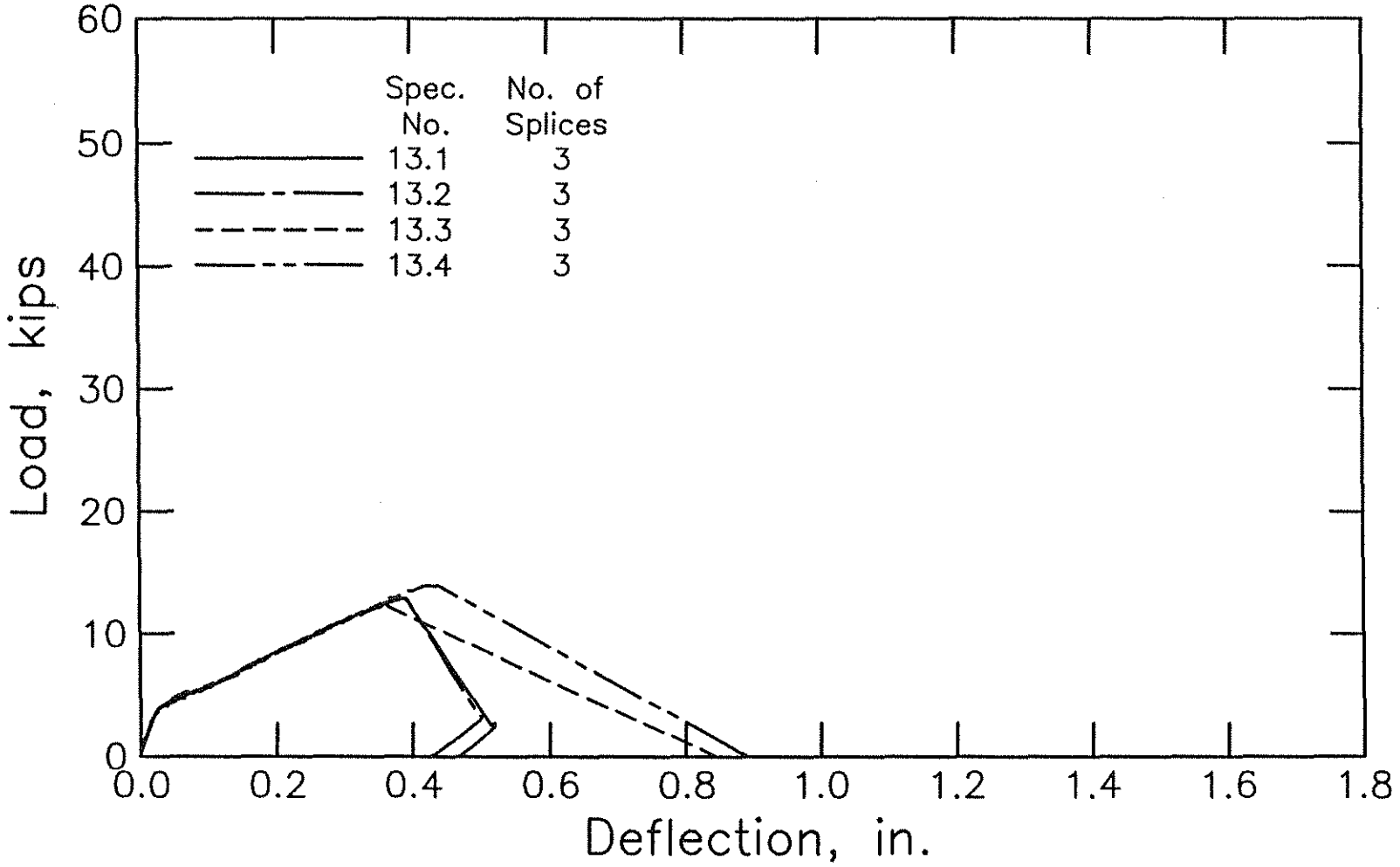

Fig. 3.4b Load-deflection curves for splice specimens in Group 13 (1 kip = 4.45 kN, 1 in. = 25.4 mm)

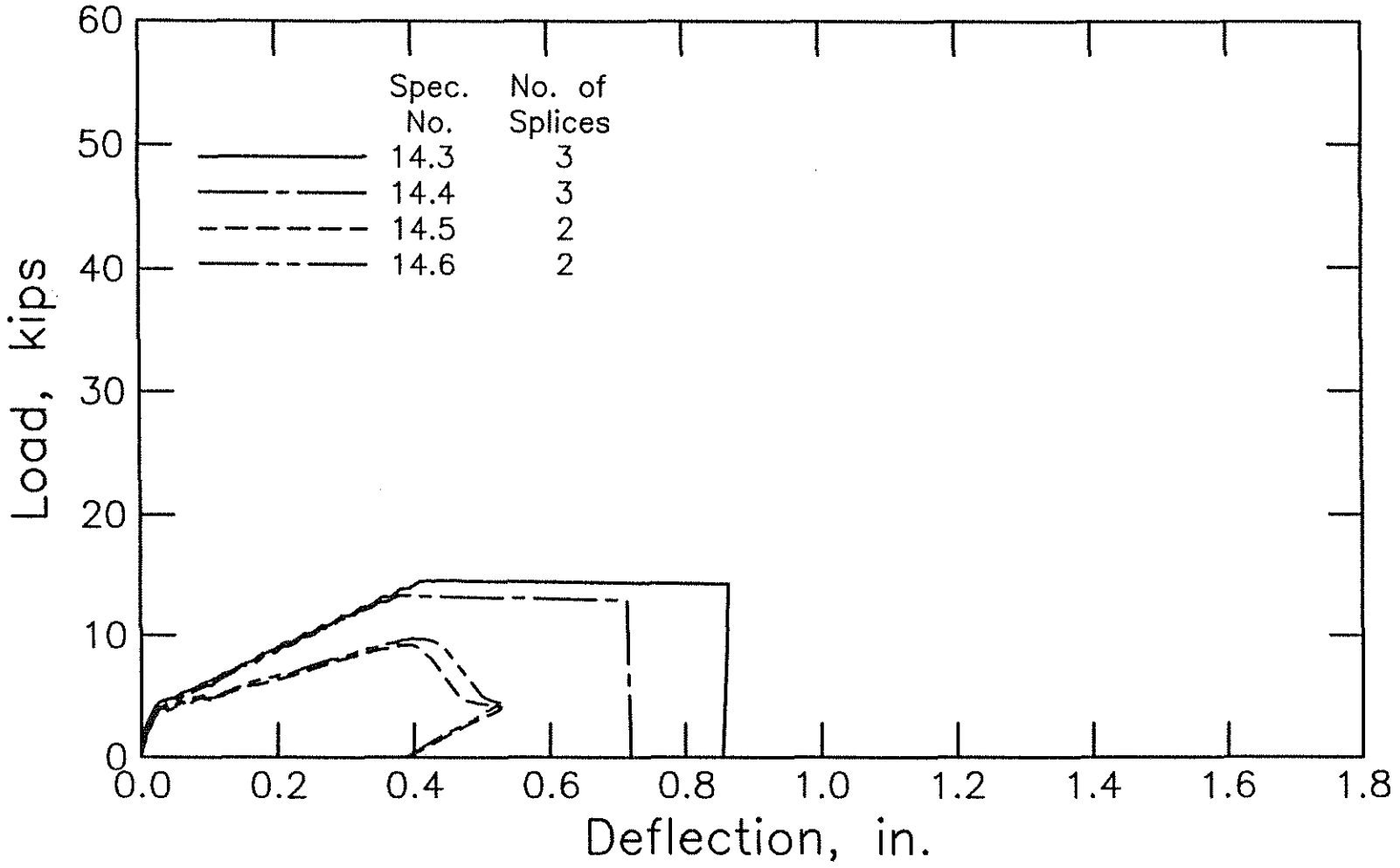

Fig. 3.4c Load-deflection curves for splice specimens in Group 14 (1 kip = 4.45 kN, 1 in. = 25.4 mm)

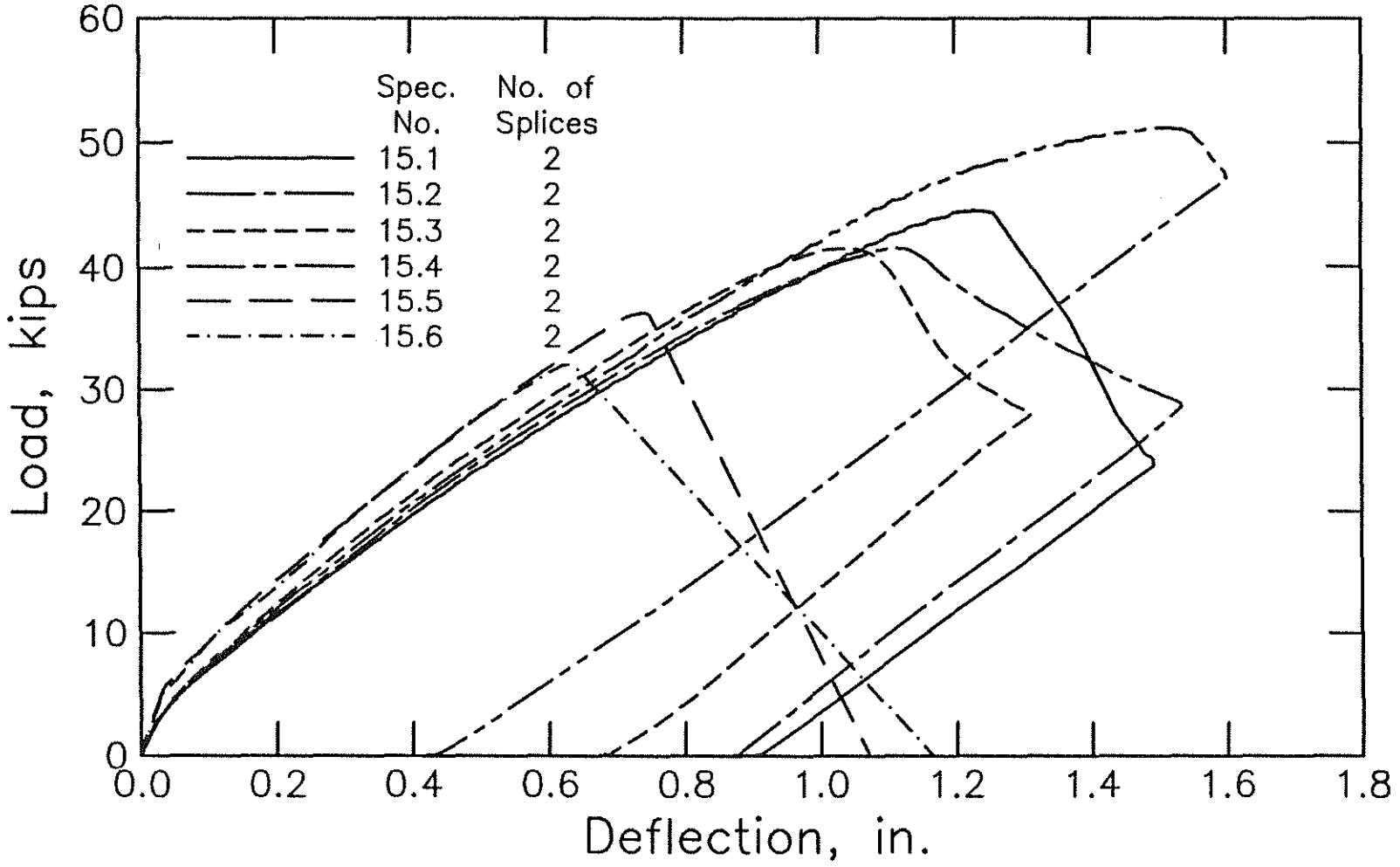

Fig. 3.4d Load-deflection curves for splice specimens in Group 15 (1 kip = 4.45 kN, 1 in. = 25.4 mm)

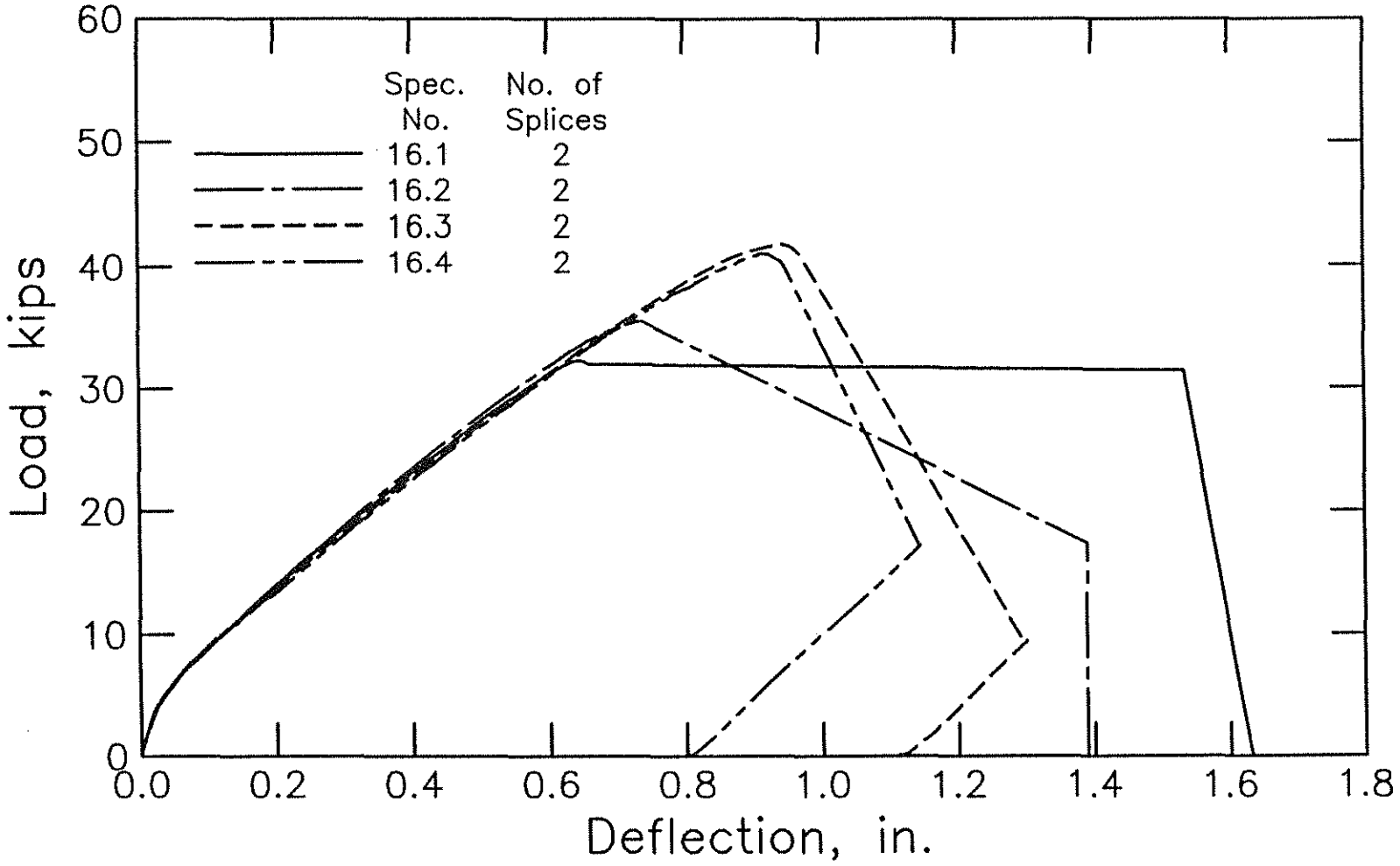

Fig. 3.4e Load-deflection curves for splice specimens in Group 16 (1 kip = 4.45 kN, 1 in. = 25.4 mm)

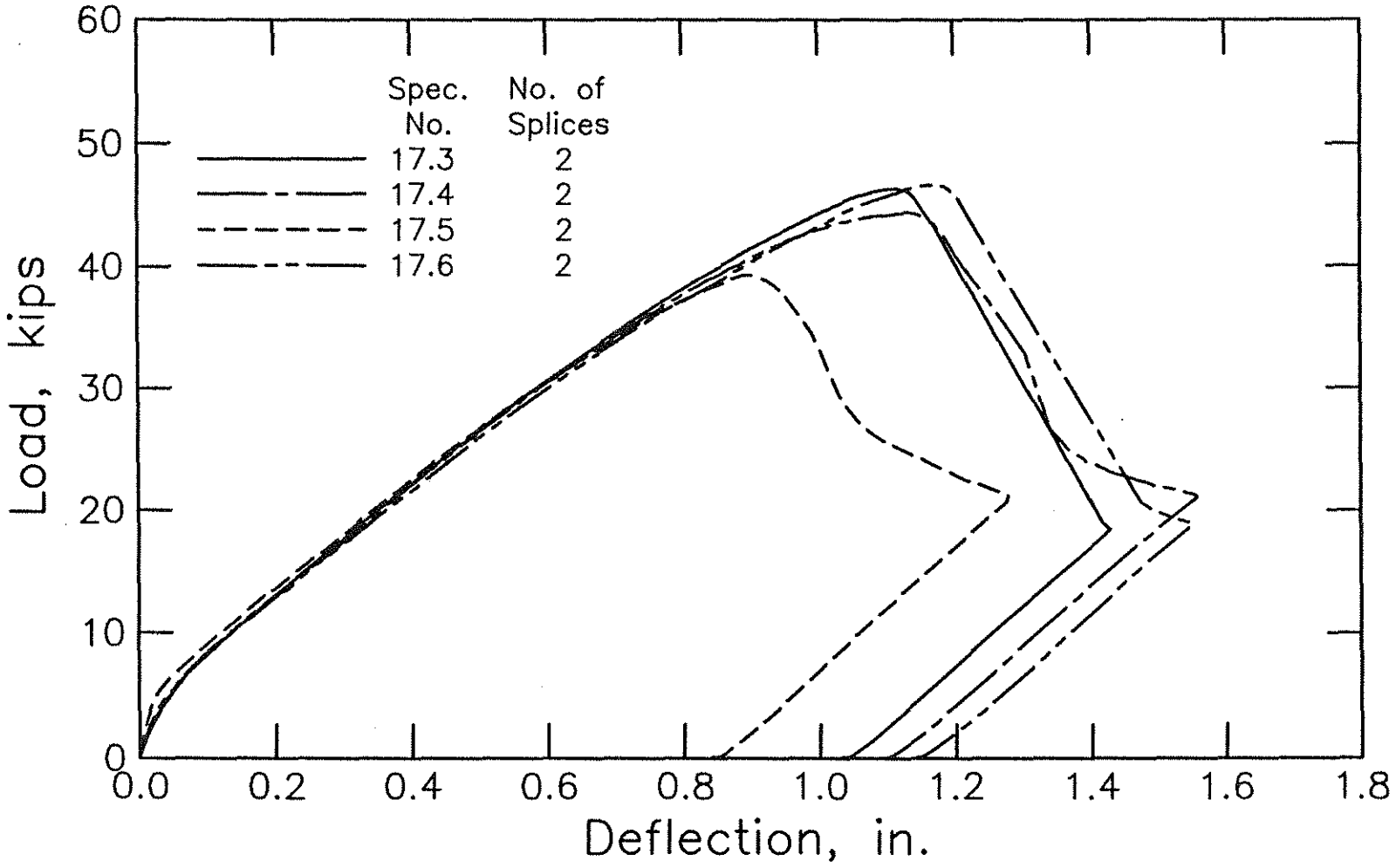

Fig. 3.4f Load-deflection curves for splice specimens in Group 17 (1 kip = 4.45 kN, 1 in. = 25.4 mm)

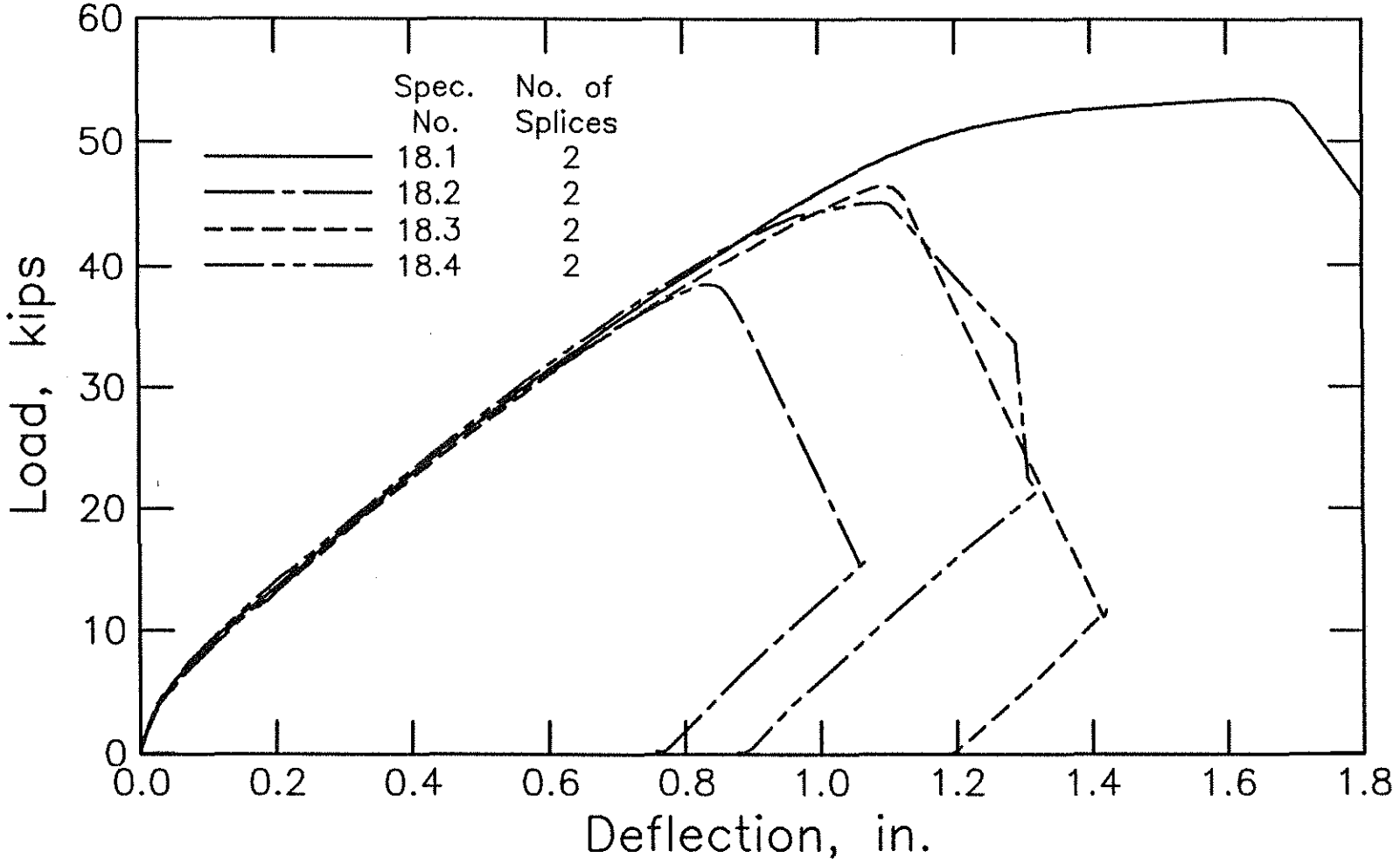

Fig. 3.4g Load-deflection curves for splice specimens in Group 18 (1 kip = 4.45 kN, 1 in. = 25.4 mm)

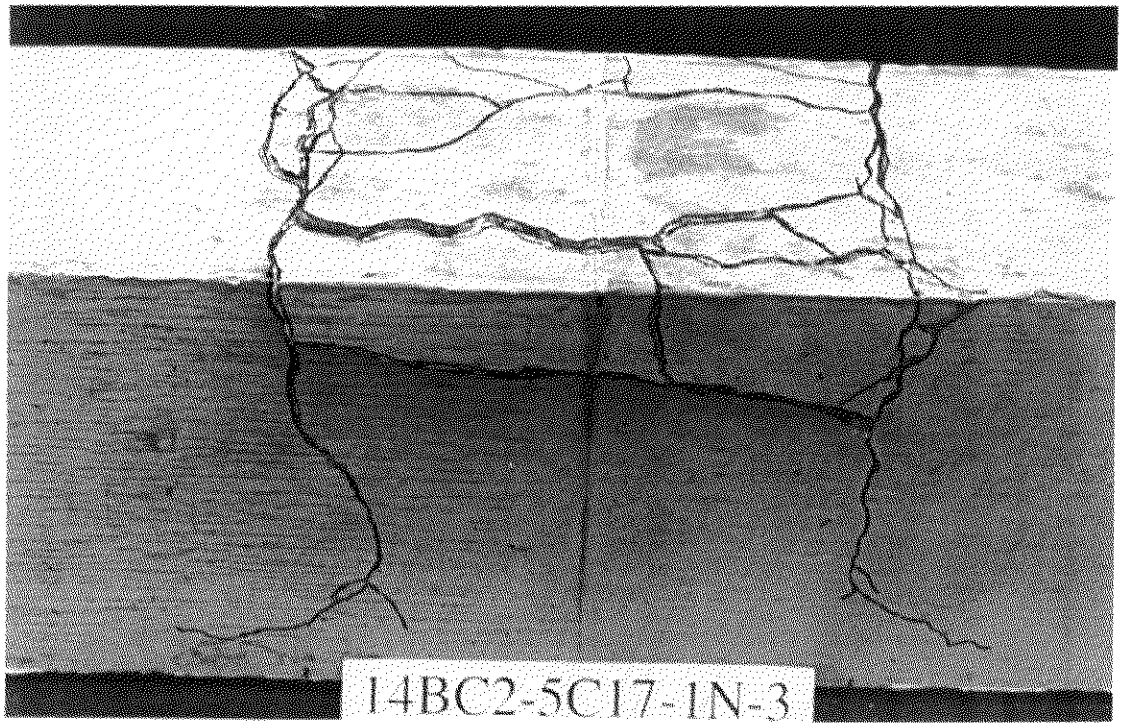

(a)

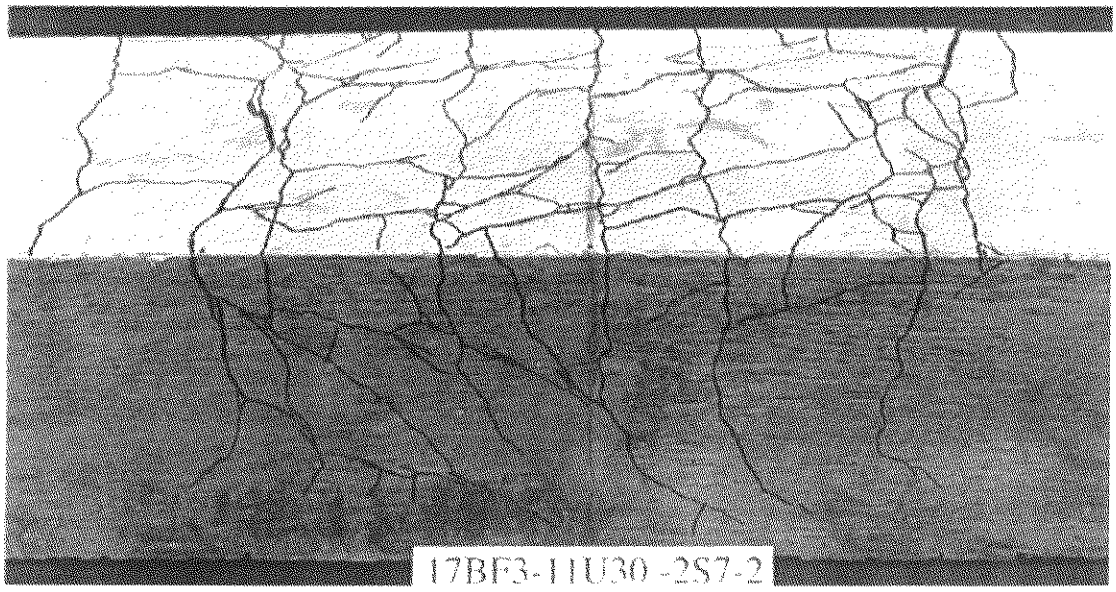

(b)

Fig. 3.5 Cracked splice specimens after failure, (a) without confining reinforcement, (b) with confining reinforcement

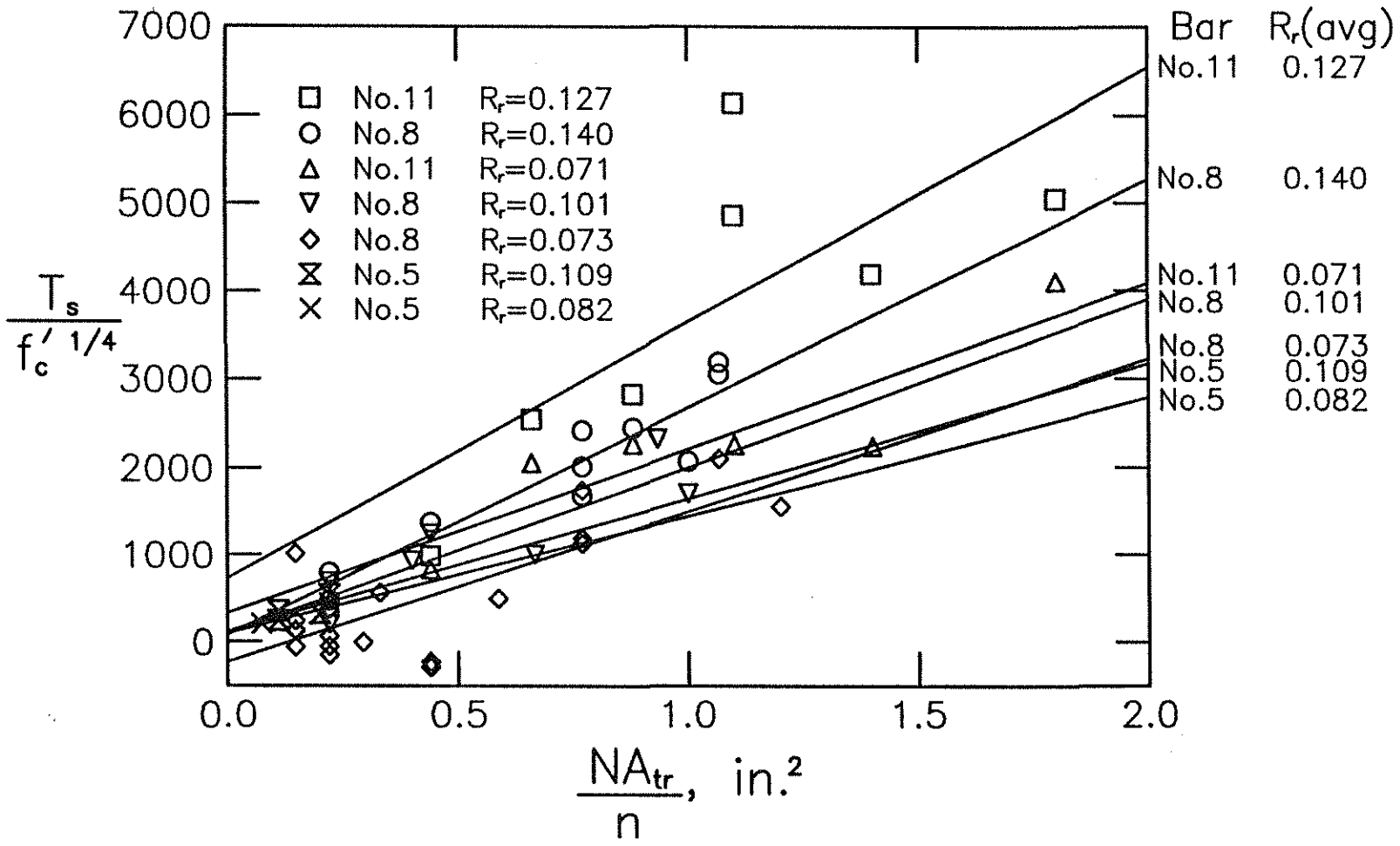

Fig. 3.6 Increase in bond force, T_s, normalized with respect to $f'_c{}^{1/4}$ versus effective transverse reinforcement, NA_{tr}/n, for splices in concrete containing limestone coarse aggregate (T_s in lb, f'_c in psi, A_{tr} in in.^{2}) (1 lb = 4.45 N, 1 psi = 6.89 kPa, 1 in. = 25.4 mm)

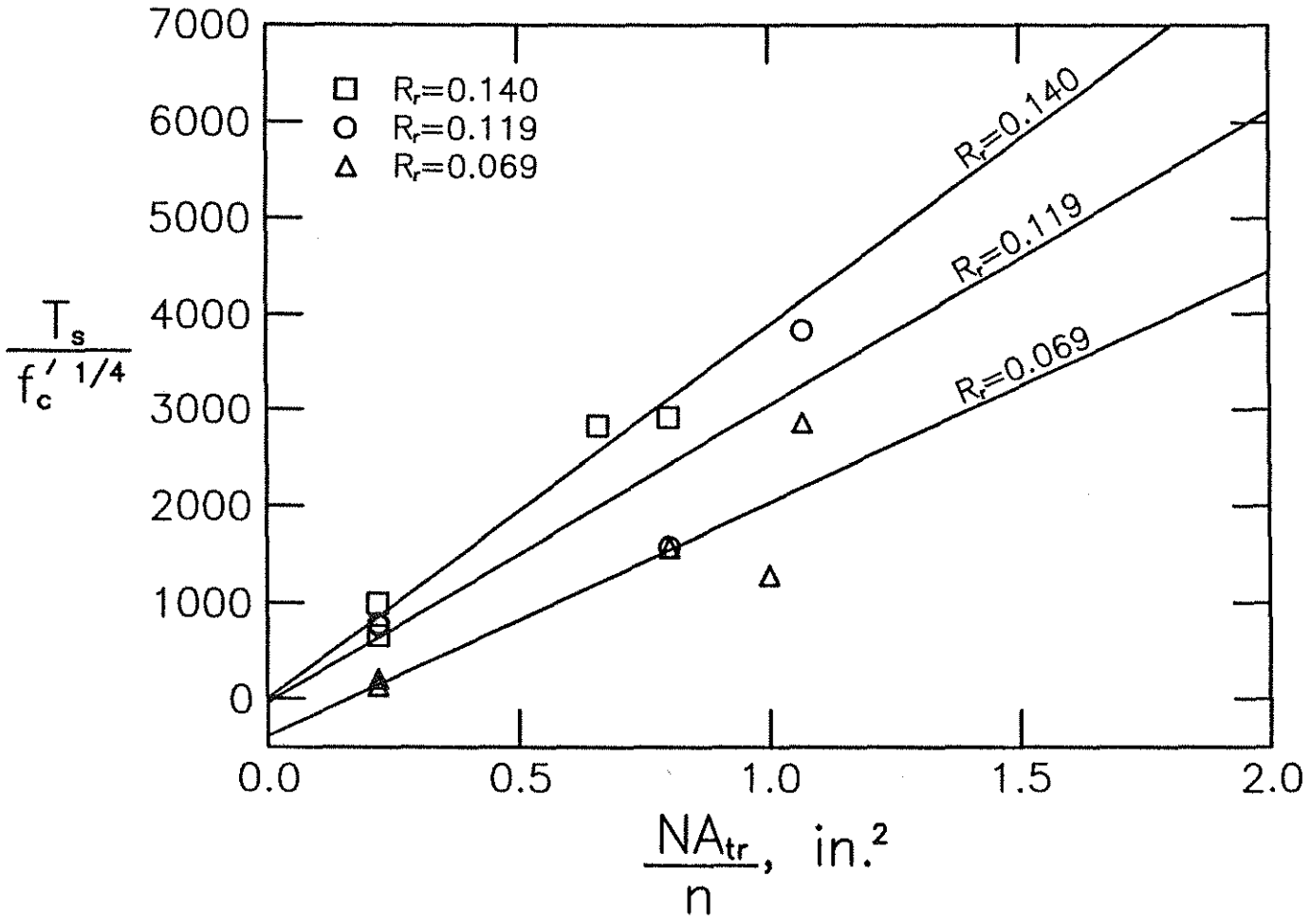

Fig. 3.7 Increase in bond force, T_s, normalized with respect to $f'_c{}^{1/4}$ versus effective transverse reinforcement, NA_{tr}/n, for splices in concrete containing basalt coarse aggregate (T_s in lb, f'_c in psi, A_{tr} in in.^{2}) (1 lb = 4.45 N, 1 psi = 6.89 kPa, 1 in. = 25.4 mm)

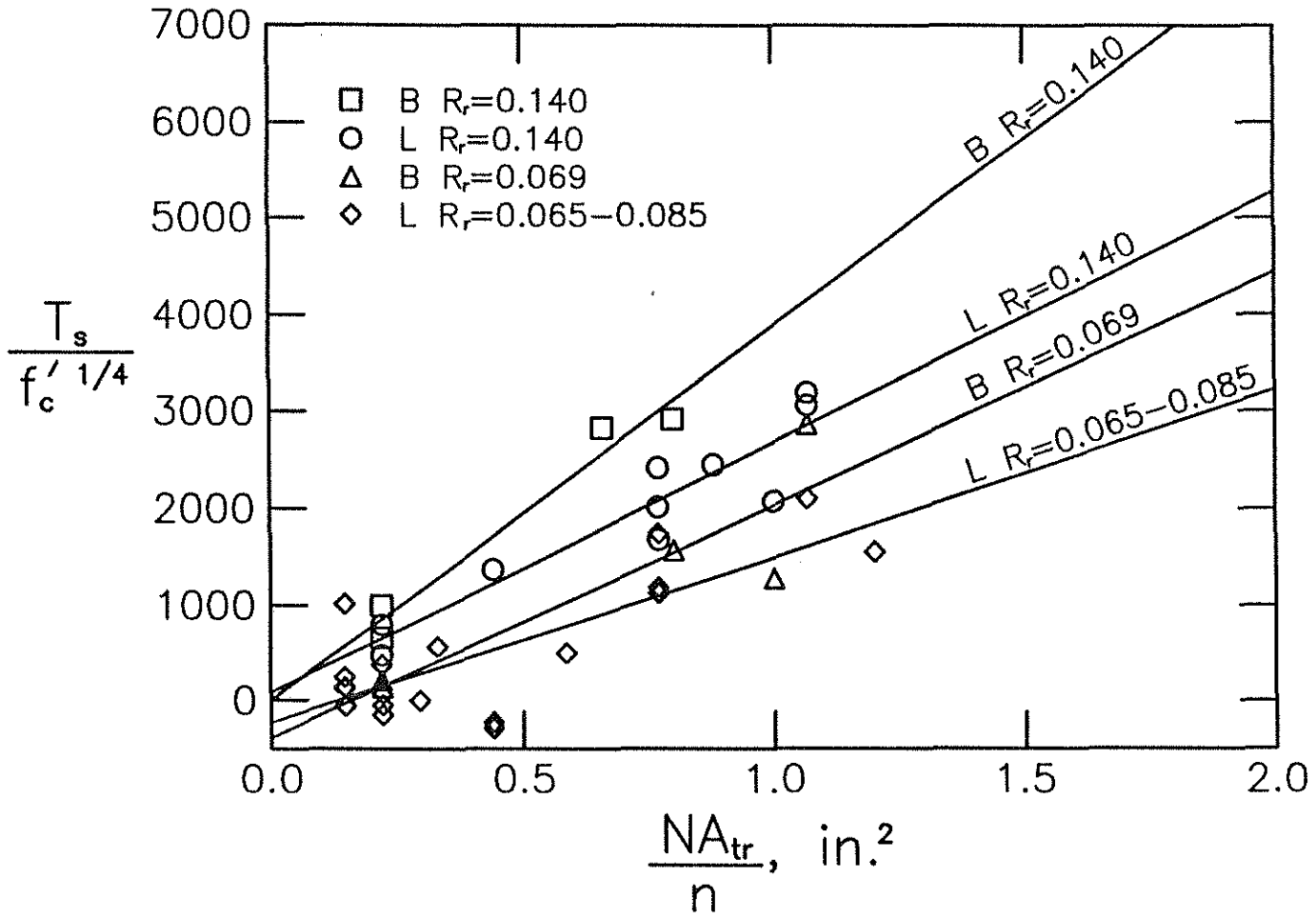

Fig. 3.8 Comparison of increases in bond force, T_s, normalized with respect to $f'^{1/4}_c$ for No. 8 (25 mm) bars as affected by coarse aggregate, B = basalt, L = limestone, (T_s in lb, f'_c in psi, A_{tr} in in.^{2}) (1 lb = 4.45 N, 1 psi = 6.89 kPa, 1 in. = 25.4 mm)

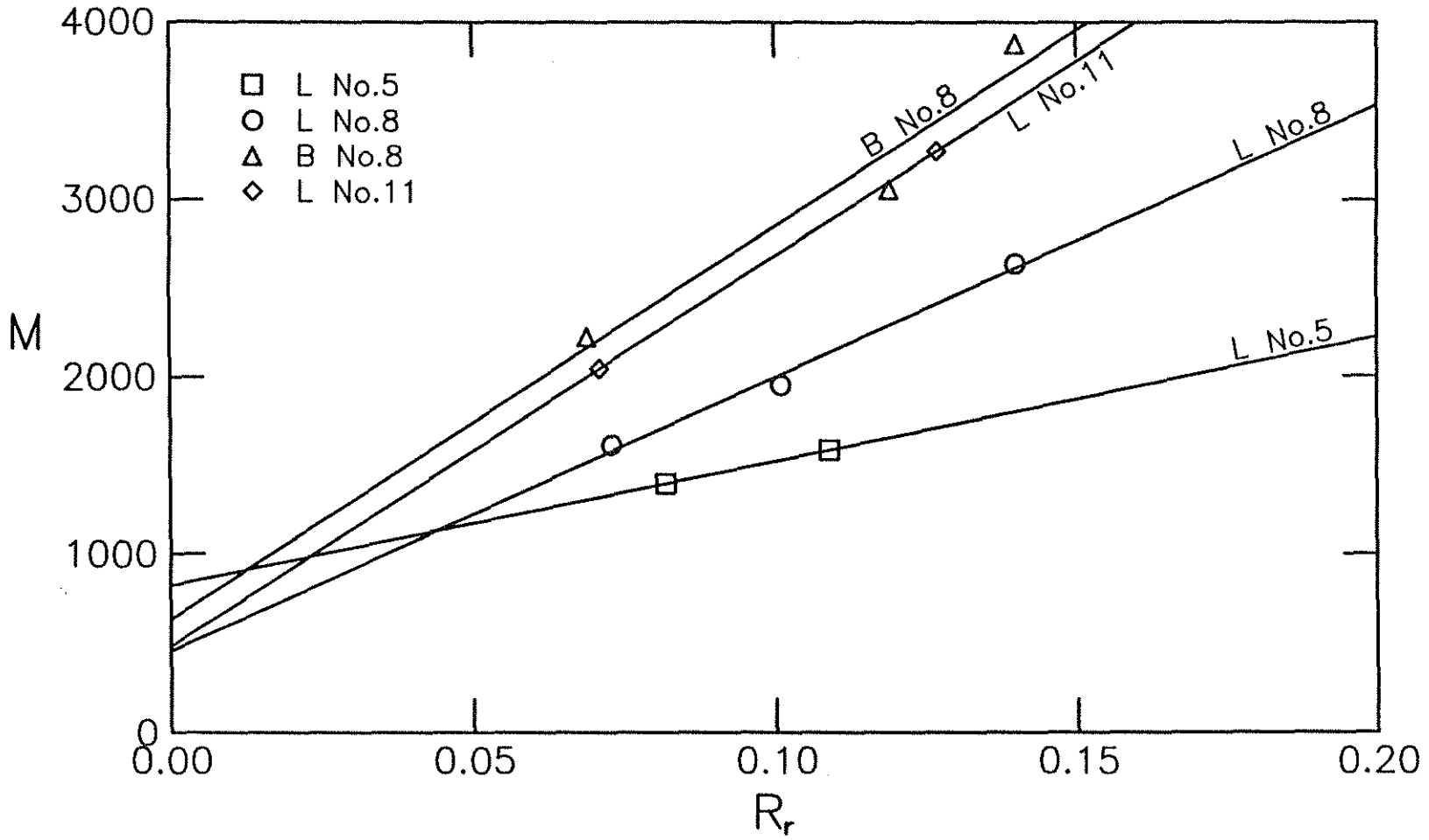

Fig. 3.9 Mean slope from Eq. 3.2, M, versus relative rib area, R_r, for No. 5, No. 8, and No. 11 (16, 25, and 36 mm) bars cast in concrete containing limestone coarse aggregate (L) and No. 8 (25 mm) bars cast in concrete containing basalt coarse aggregate (B)

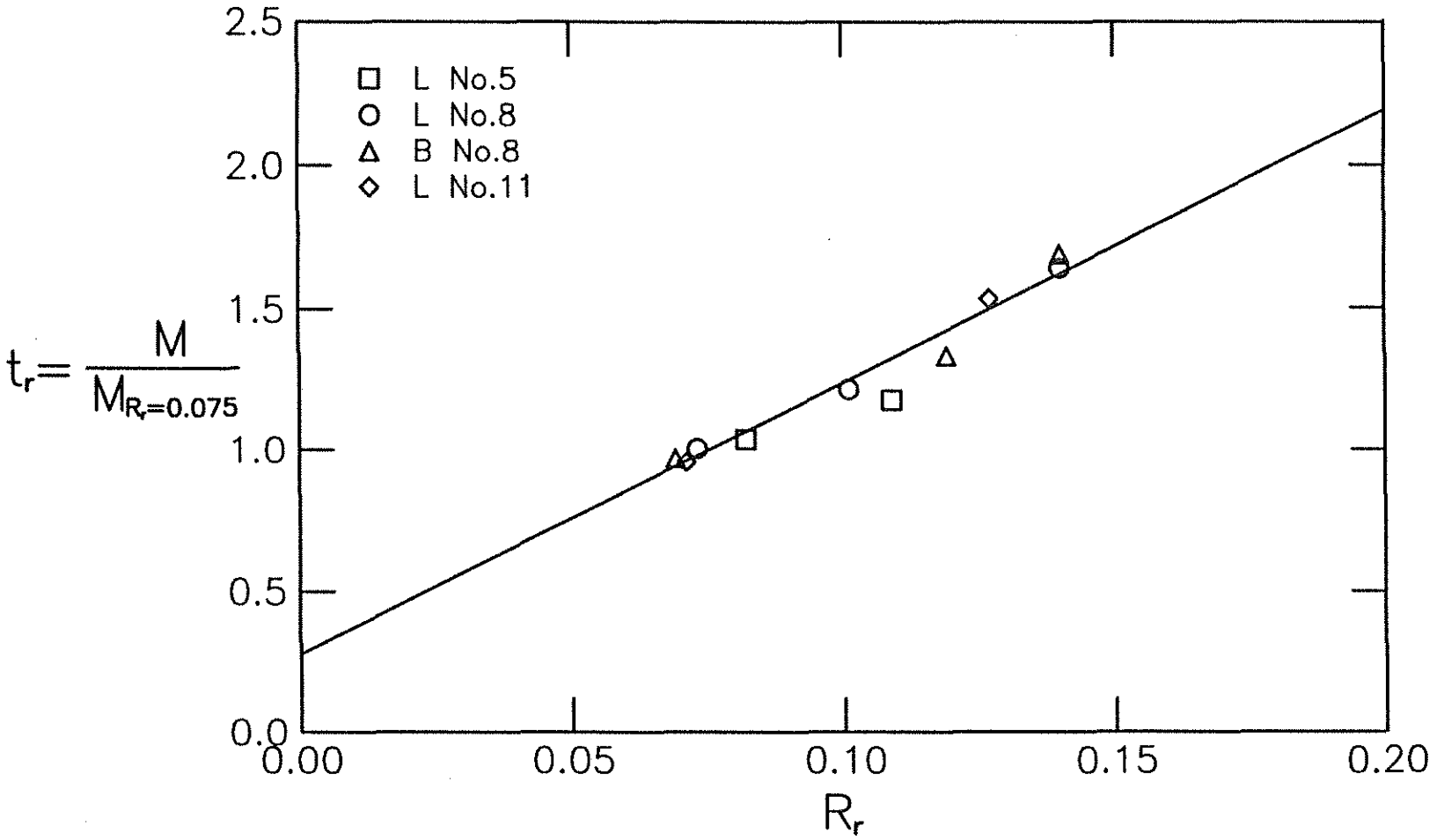

Fig. 3.10 Factor representing effect of relative rib area on increase in bond strength due to confining reinforcement, $M/M_{R_r=0.075}$, versus relative rib area, R_r

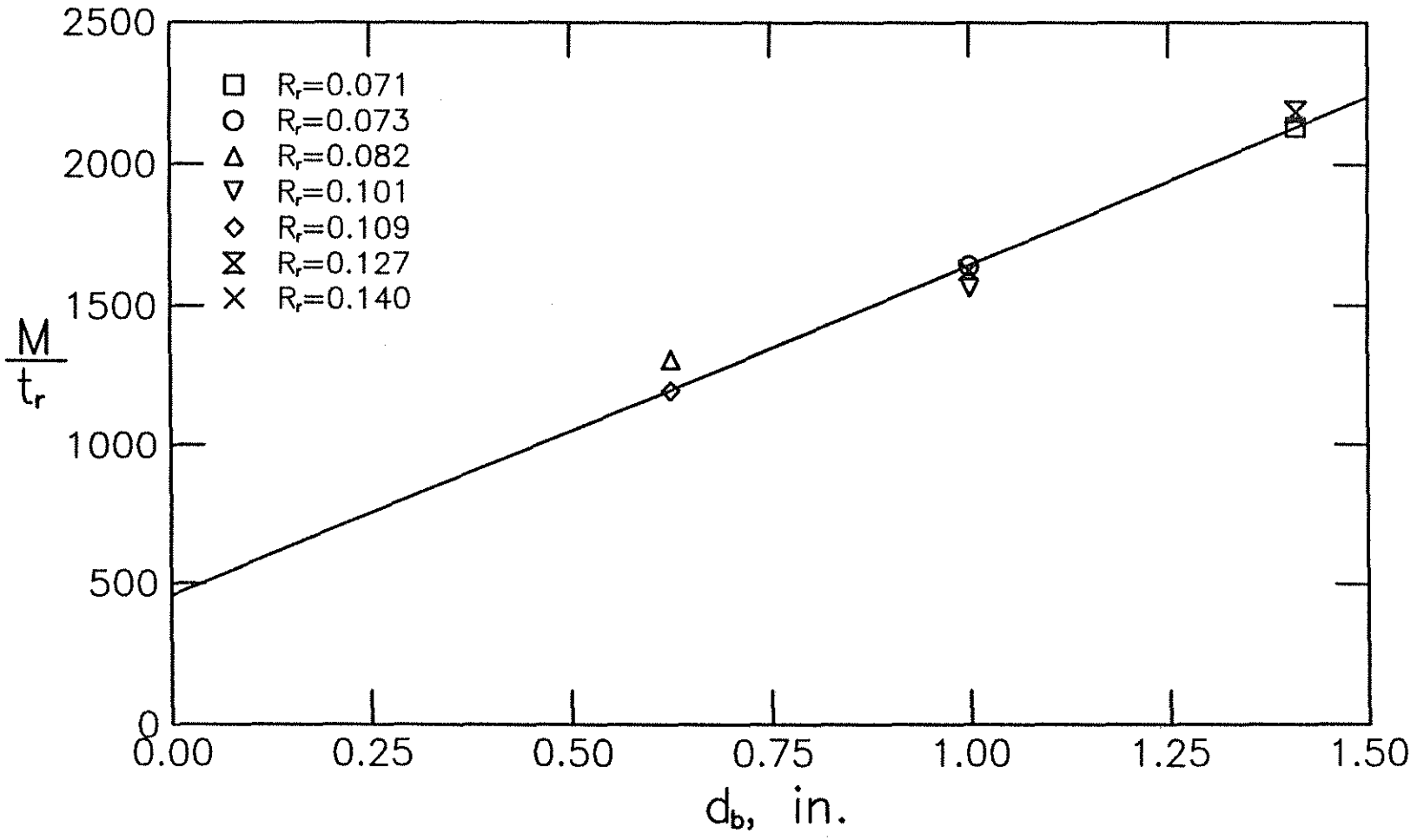

Fig. 3.11 Mean slope from Eq. 3.2, M, normalized with respect to $t_r = 9.6\ R_r + 0.28$ versus nominal bar diameter, d_b (1 in. = 25.4 mm)

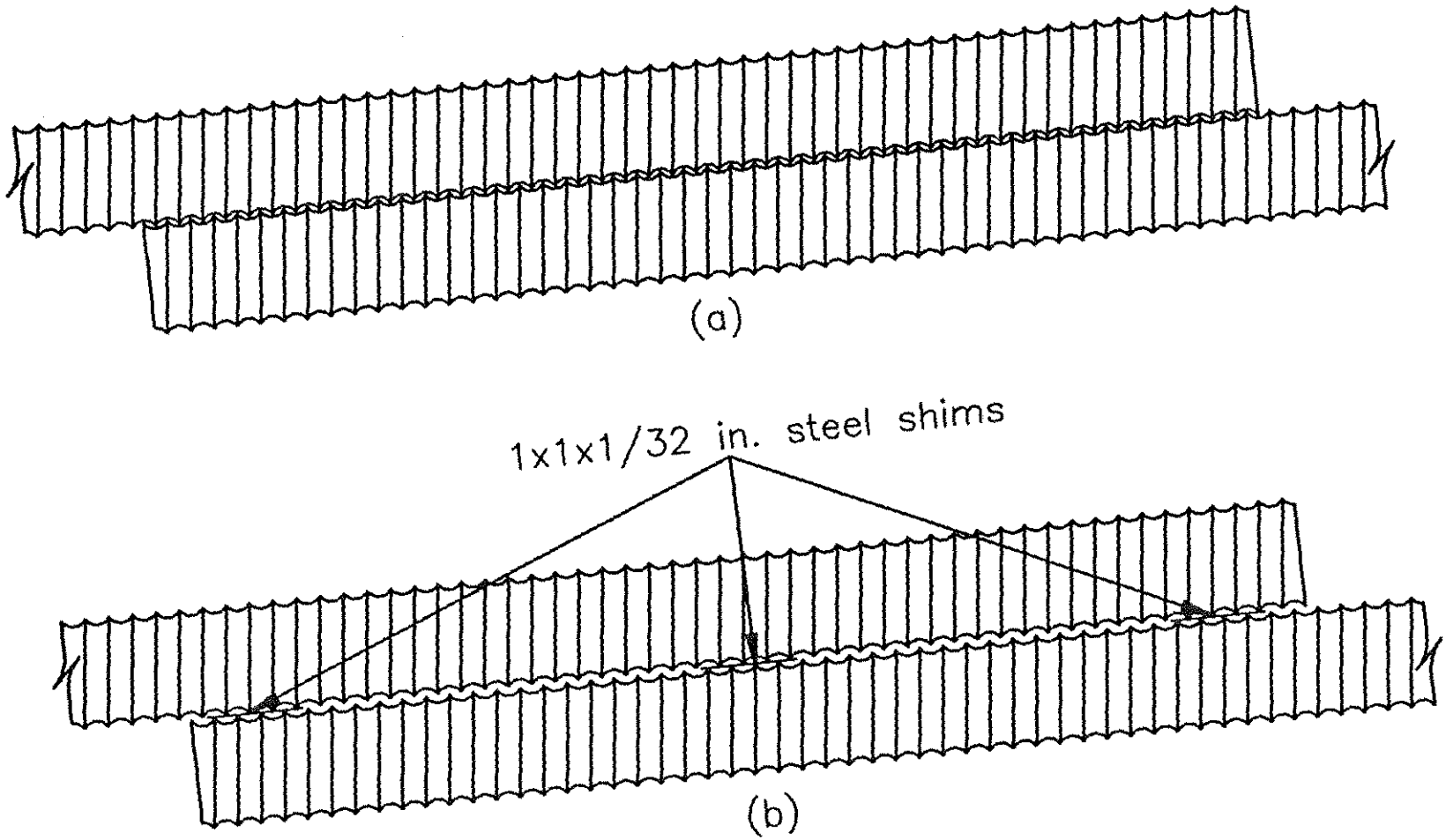

Fig. 4.1 Schematic of threaded bar splice configurations, (a) ribs interlocked, (b) rib interlock prevented (1 in. = 25.4 mm)

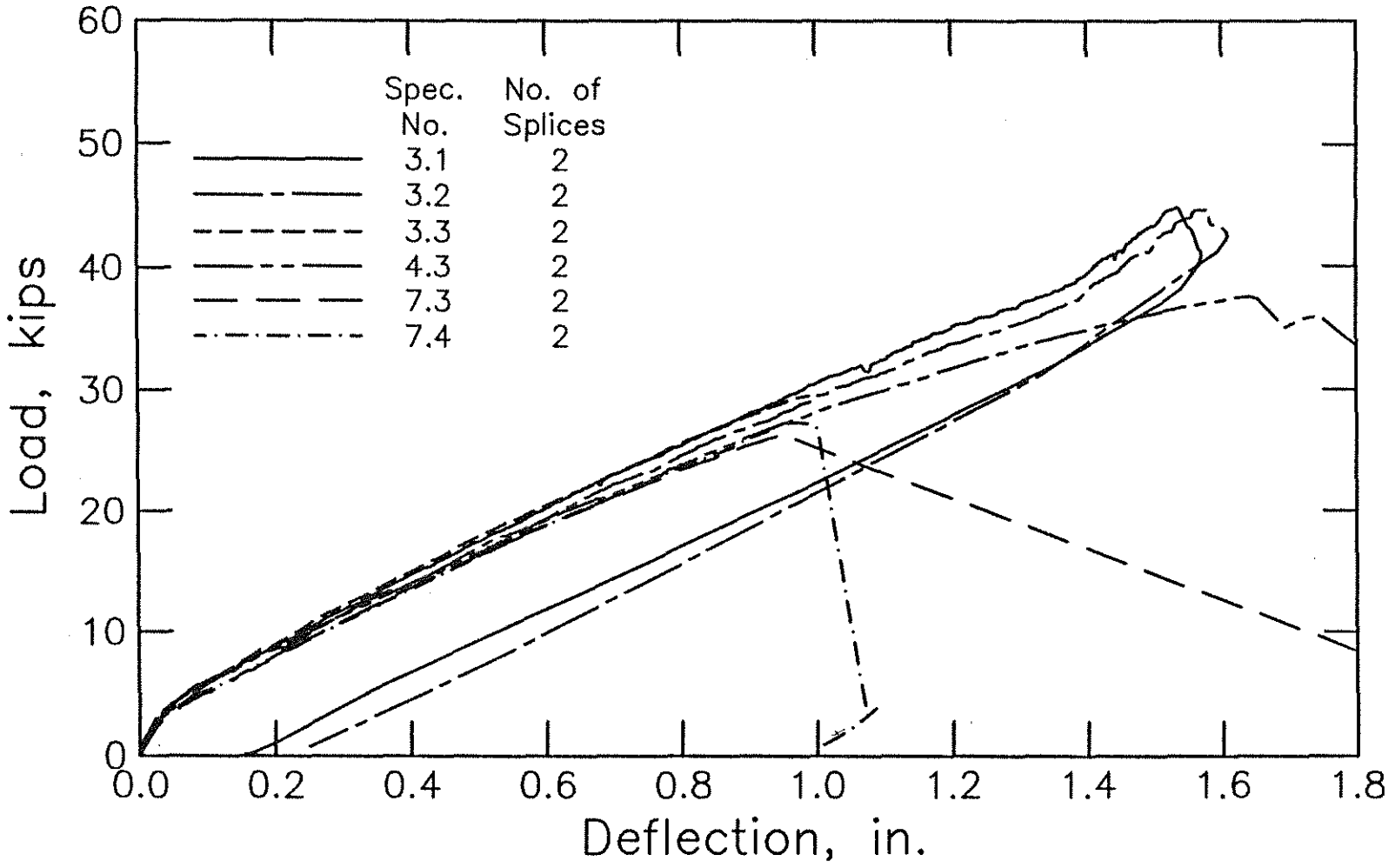

Fig. 4.2 Load-deflection curves for threaded bar splice specimens in Groups 3, 4, and 7 (Note: data not available for specimen 3.3 after peak load) (1 kip = 4.45 kN, 1 in. = 25.4 mm)

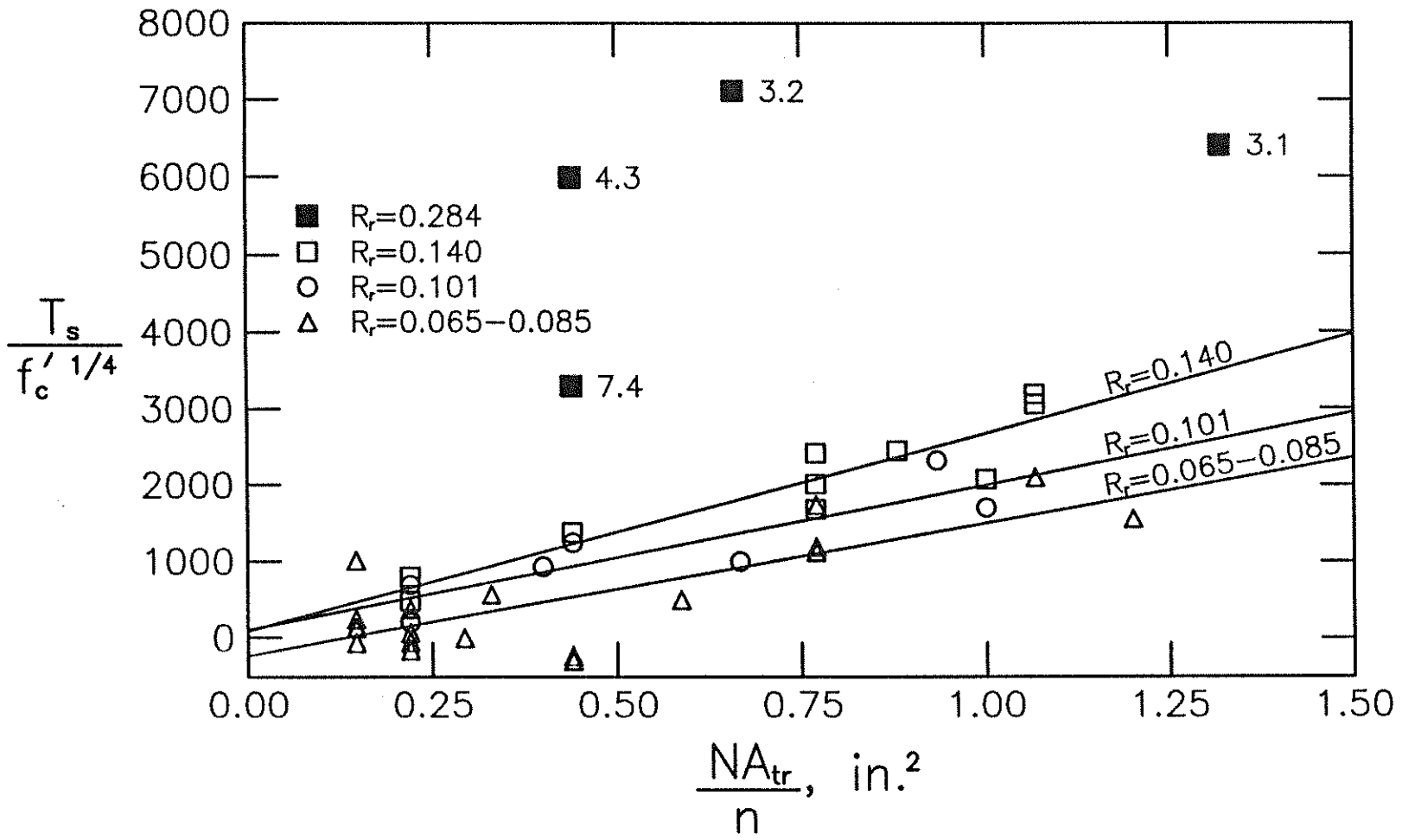

Fig. 4.3 Increase in bond force, T_s, normalized with respect to $f'_c{}^{1/4}$ versus effective transverse reinforcement, NA_{tr}/n, for No. 8 (25 mm) bar splices in concrete containing limestone coarse aggregate (T_s in lb, f'_c in psi, A_{tr} in in.^{2}) (1 lb = 4.45 N, 1 psi = 6.89 kPa, 1 in. = 25.4 mm)

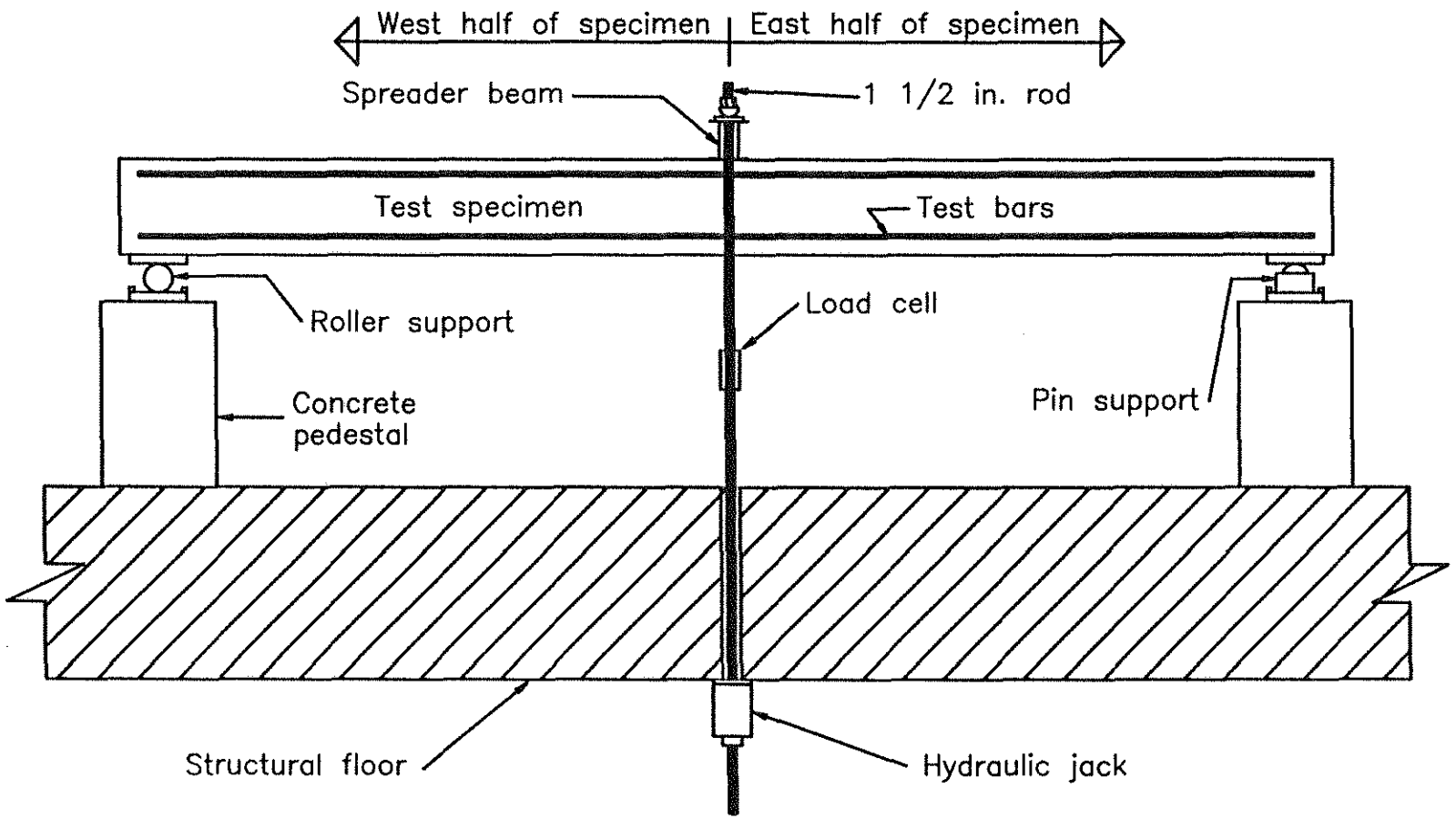

Fig. 5.1 Schematic of test apparatus

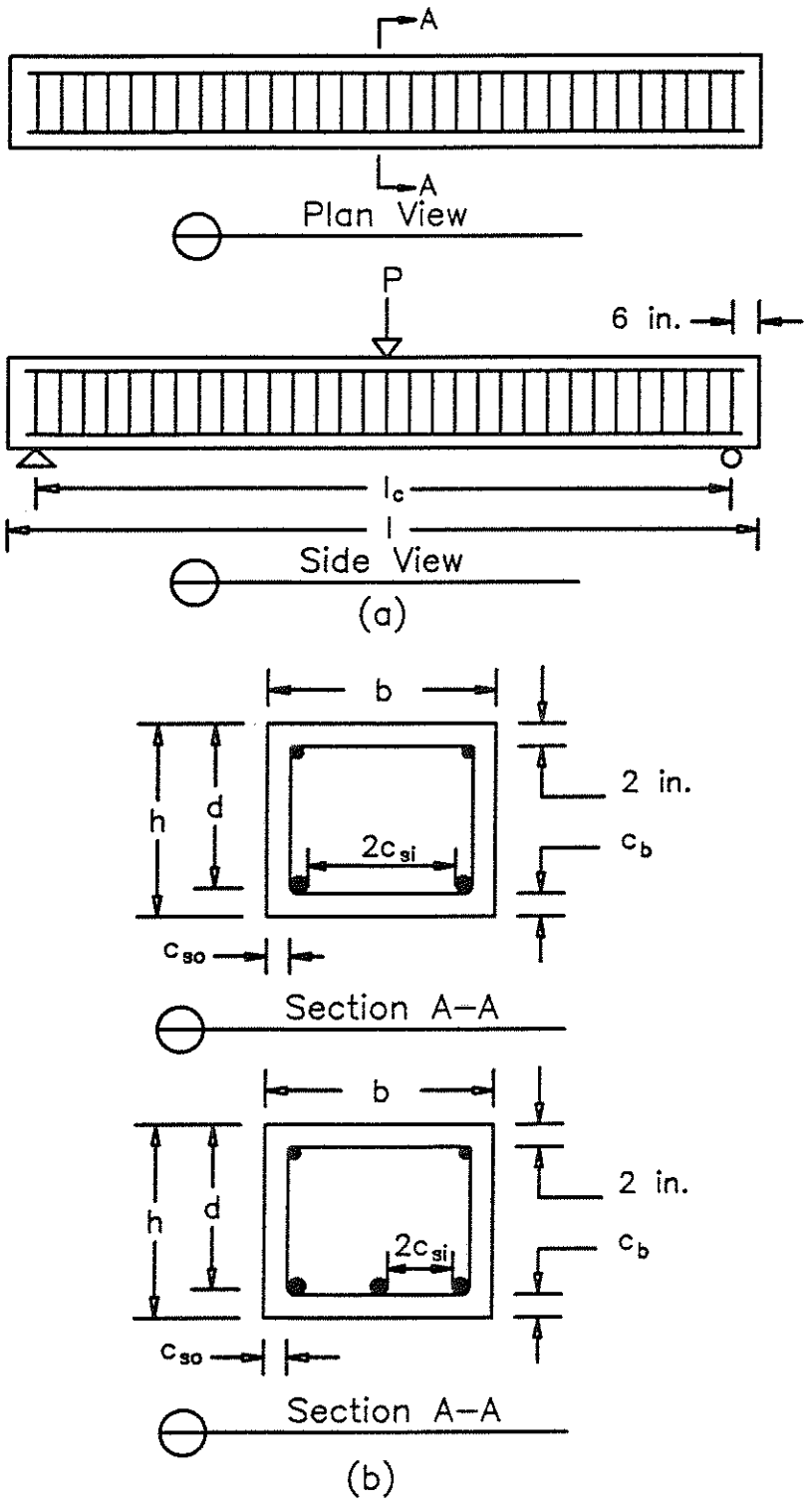

Fig. 5.2 Moment-rotation test specimens, (a) as tested, (b) configurations as cast (1 in. = 25.4 mm)

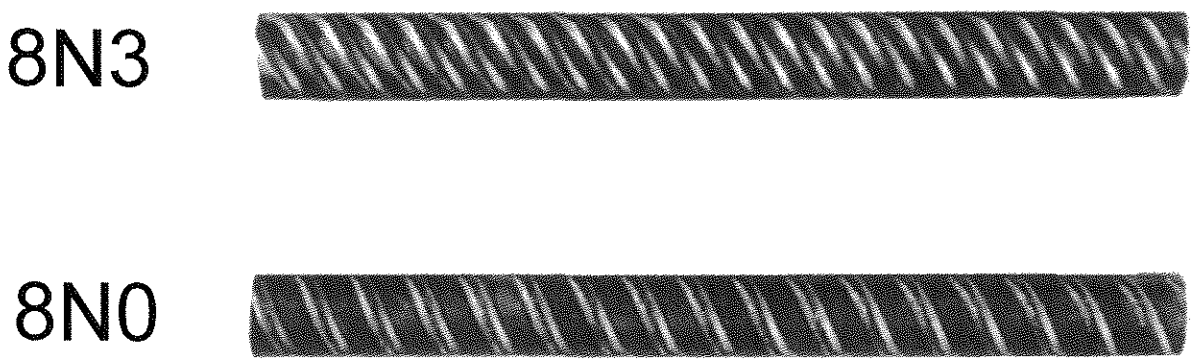

Fig. 5.3 Reinforcing bar deformation patterns, No. 8 (25 mm) bars

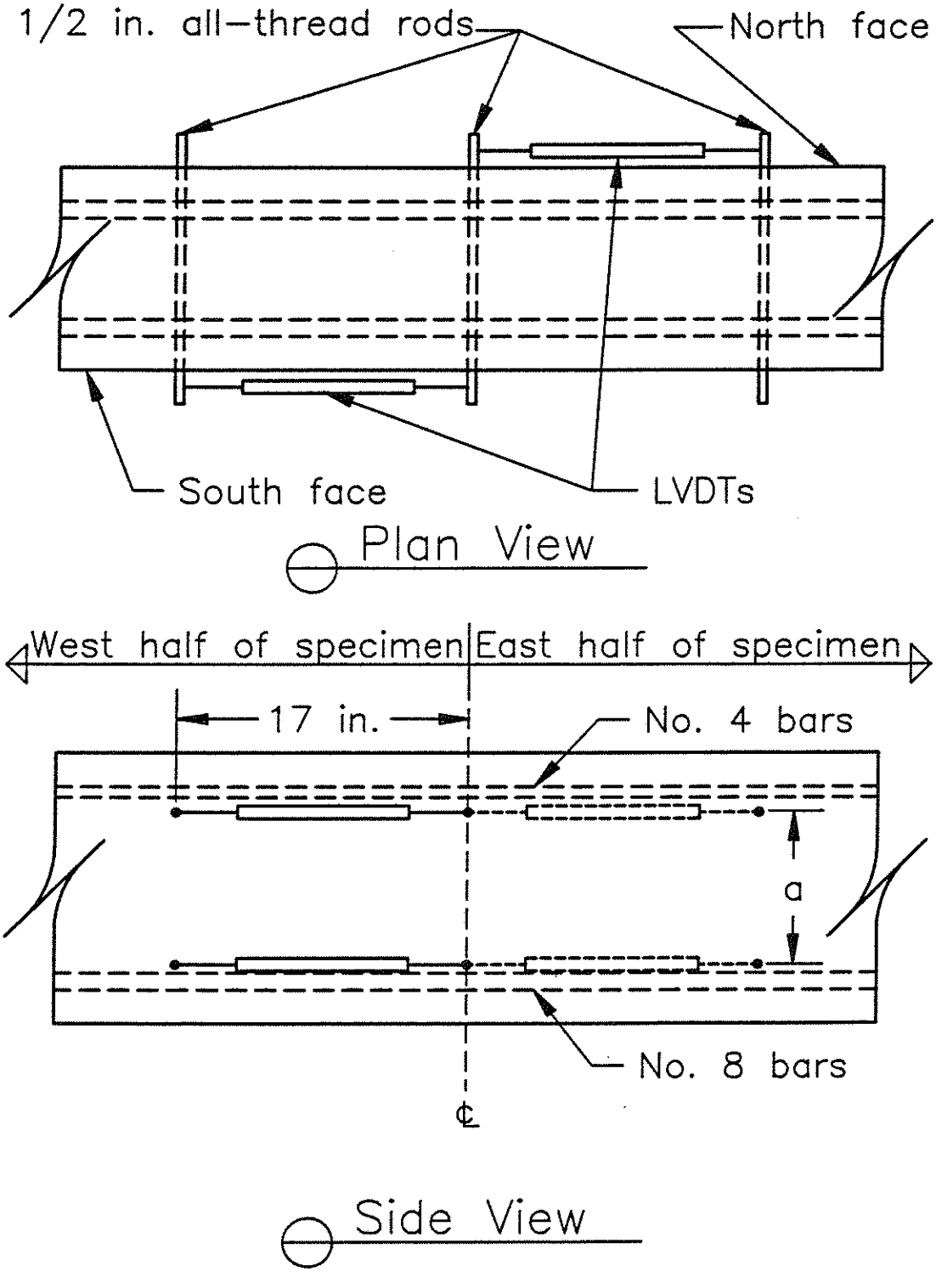

Fig. 5.4 Schematic of rotation measurement setup (1 in. = 25.4 mm)

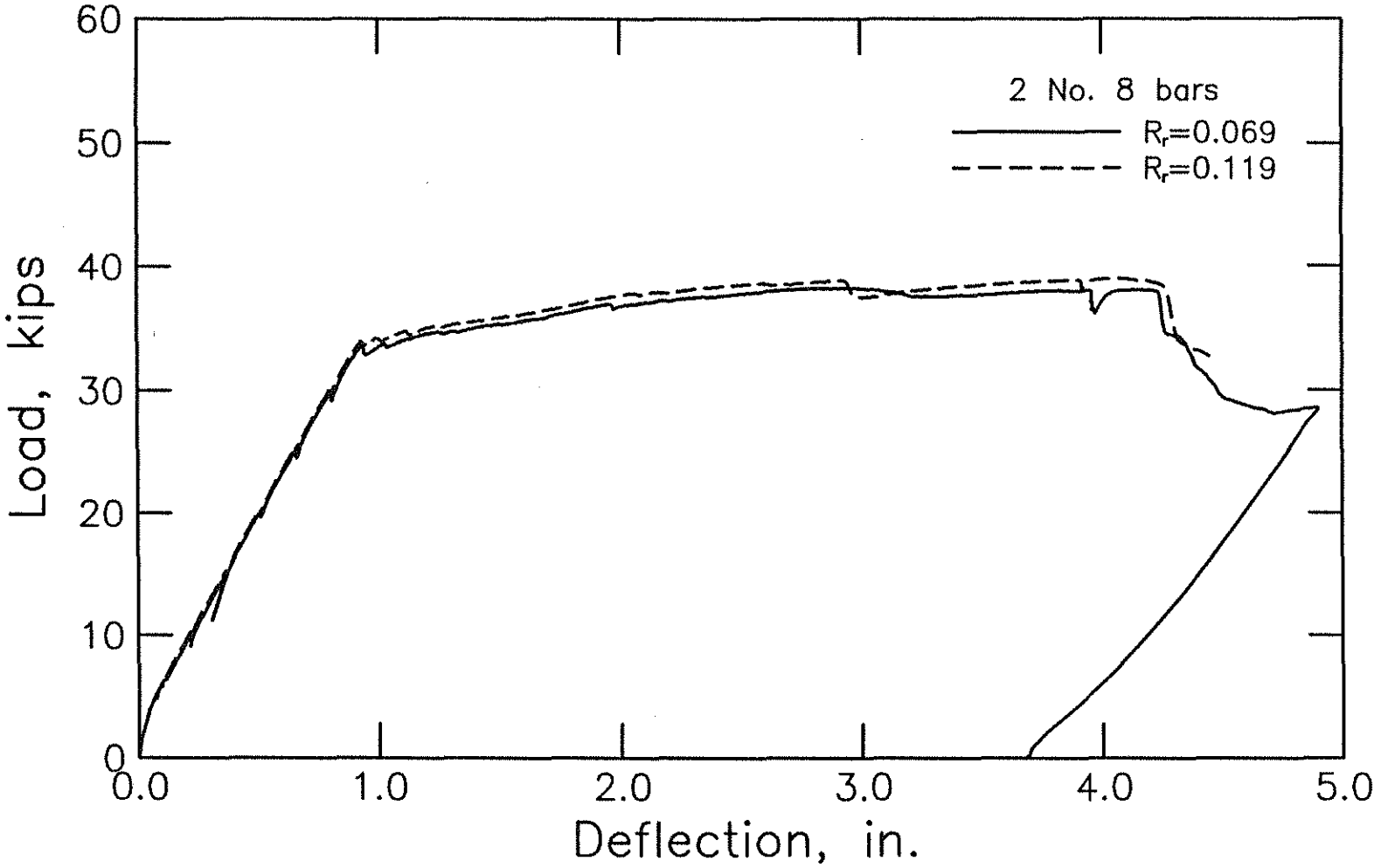

Fig. 5.5a Load-deflection curves for moment-rotation test specimens in Group 16, $\rho = 0.43\rho_{bal}$ (1 kip = 4.45 kN, 1 in. = 25.4 mm)

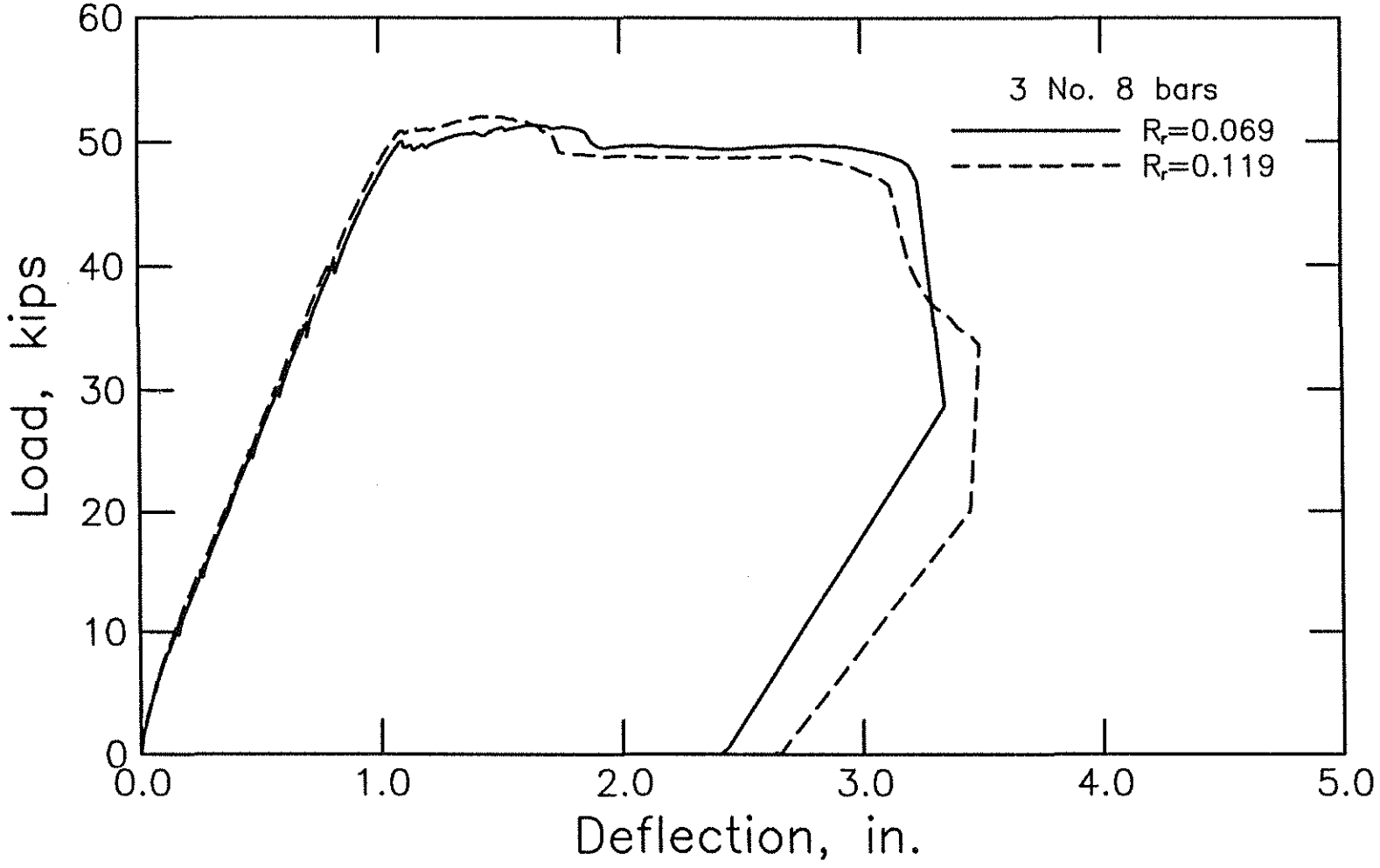

Fig. 5.5b Load-deflection curves for moment-rotation test specimens in Group 17, $\rho = 0.68\rho_{bal}$ (1 kip = 4.45 kN, 1 in. = 25.4 mm)

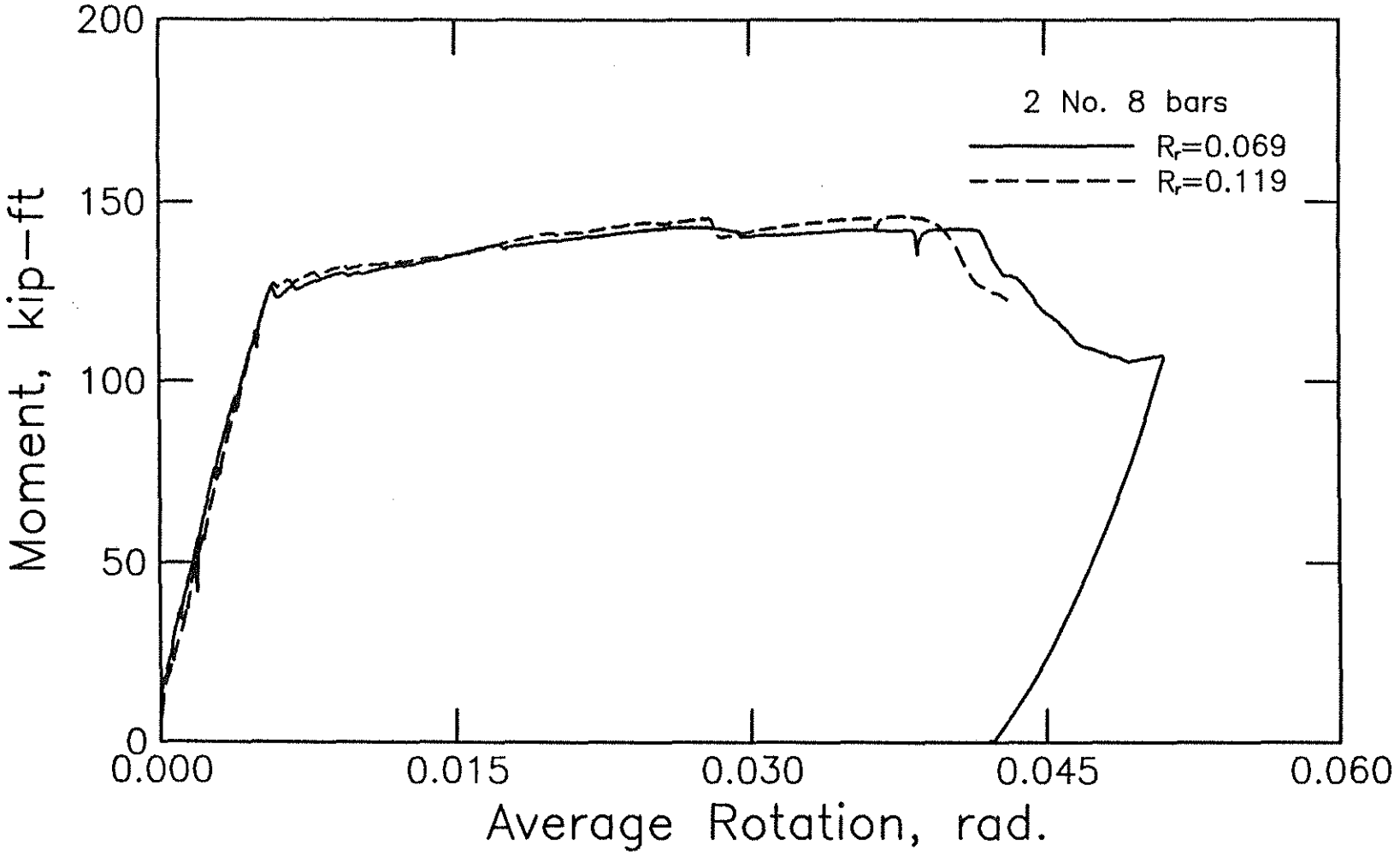

Fig. 5.6a Moment-rotation curves for moment-rotation test specimens in Group 16, $\rho = 0.43\rho_{bal}$ (1 kip-ft = 1.356 kN-m)

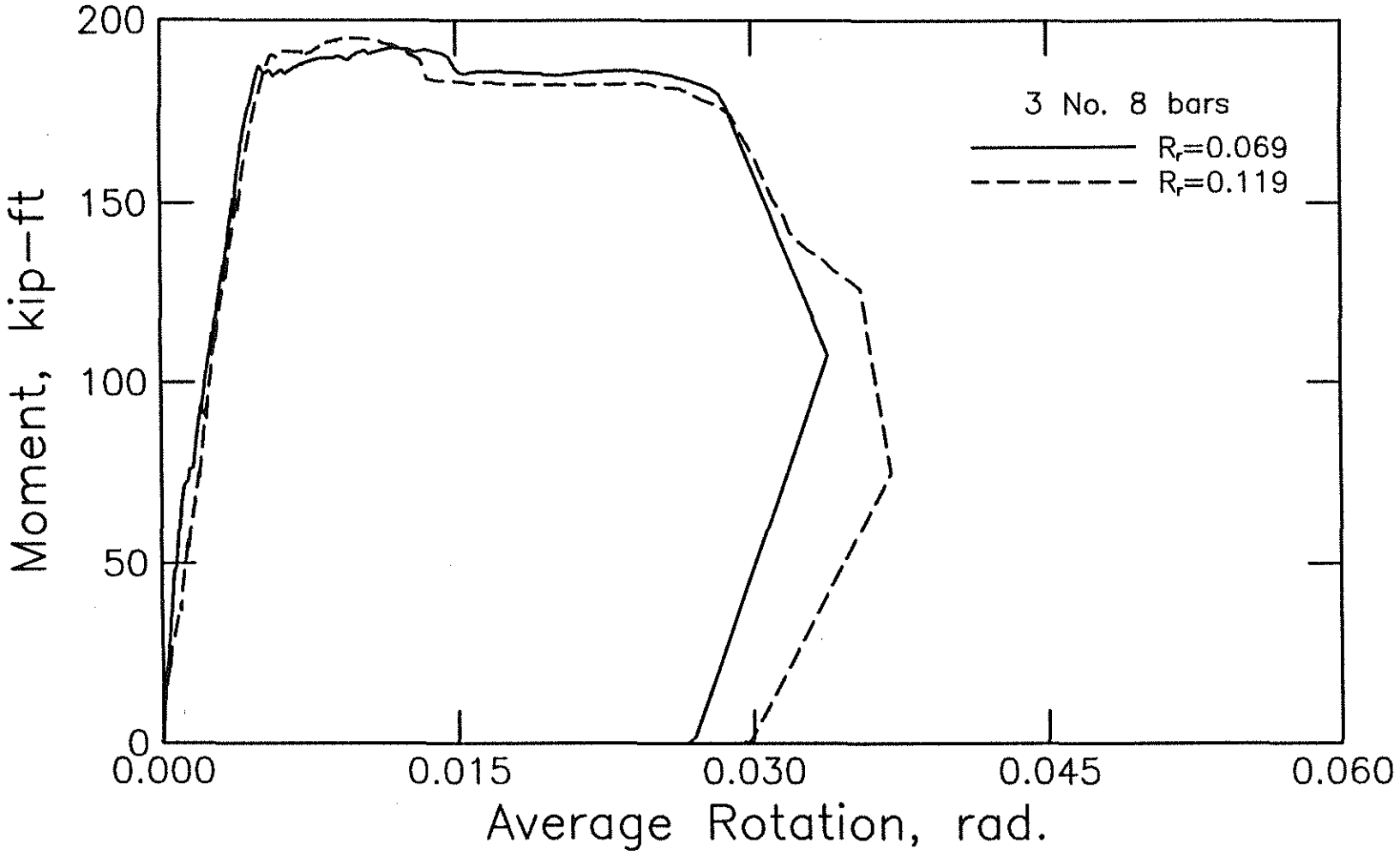

Fig. 5.6b Moment-rotation curves for moment-rotation test specimens in Group 17, $\rho = 0.68\rho_{bal}$ (1 kip-ft = 1.356 kN-m)

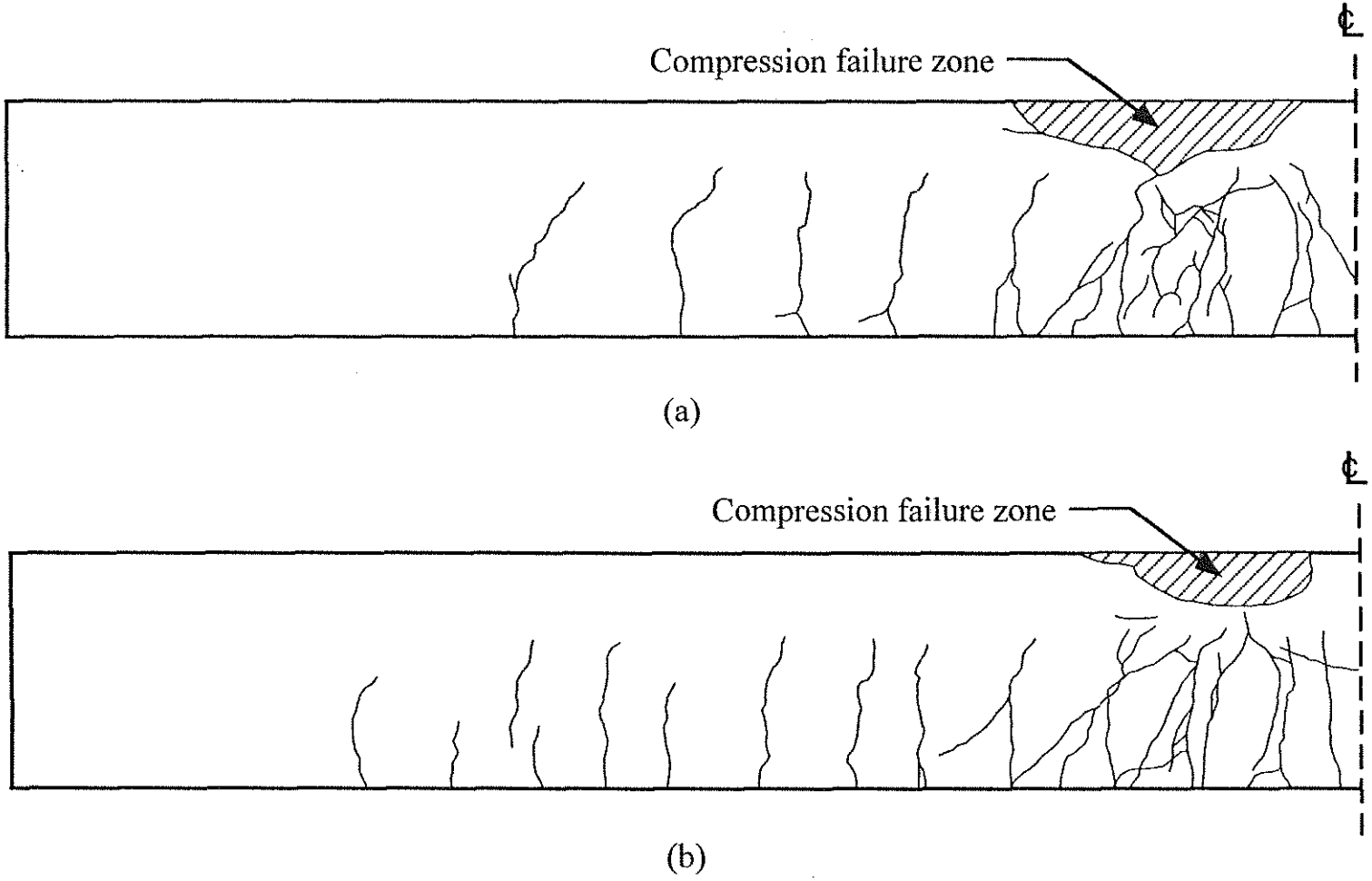

Fig. 5.7 Crack patterns for west half of beams with two No. 8 (25 mm) bars, $\rho = 0.43\rho_{bal}$: (a) $R_r = 0.069$, (b) $R_r = 0.119$

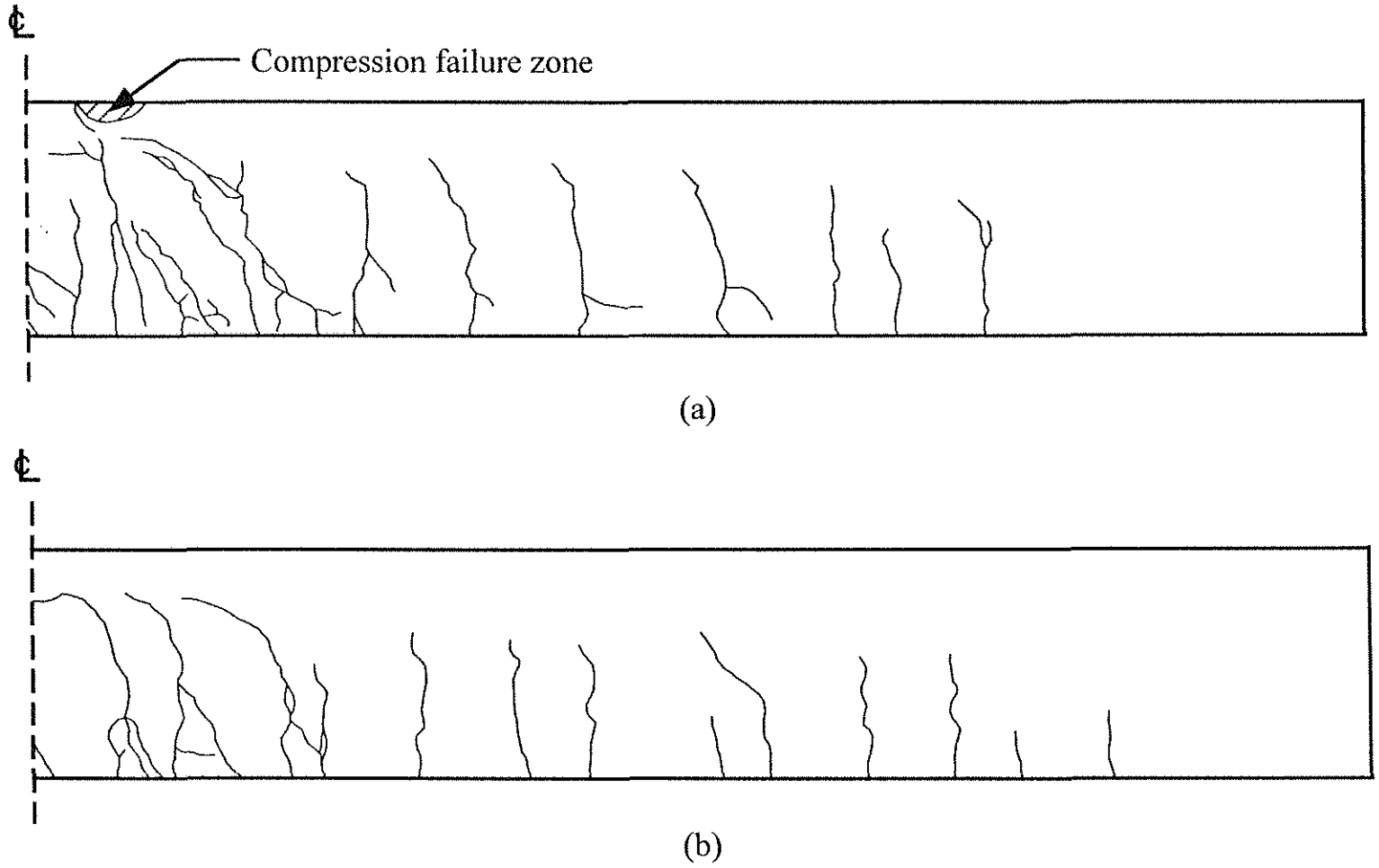

Fig. 5.8 Crack patterns for east half of beams with two No. 8 (25 mm) bars, $\rho = 0.43\rho_{bal}$: (a) $R_r = 0.069$, (b) $R_r = 0.119$

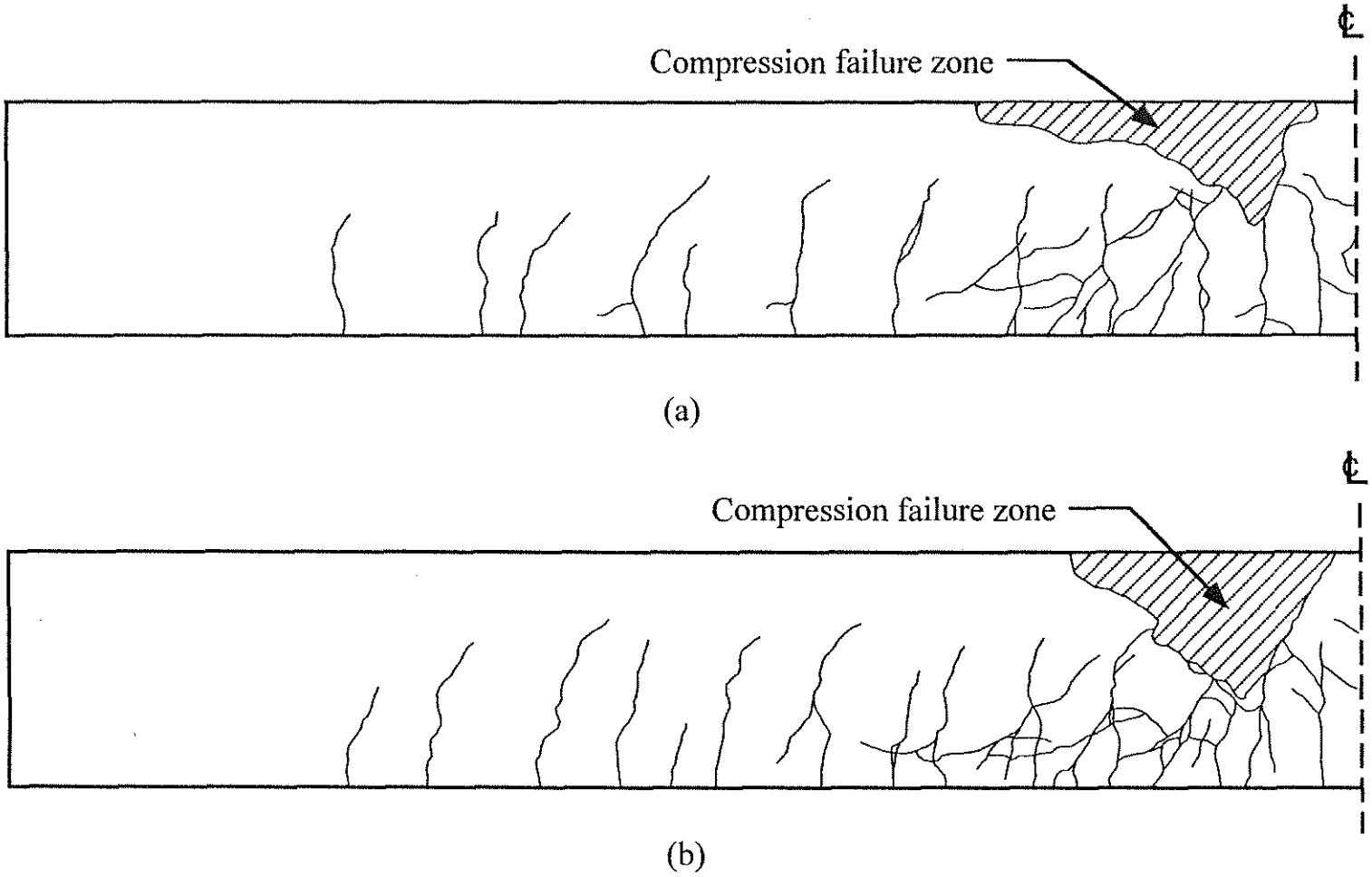

Fig. 5.9 Crack patterns for west half of beams with three No. 8 (25 mm) bars, $\rho = 0.68\rho_{bal}$: (a) $R_r = 0.069$, (b) $R_r = 0.119$

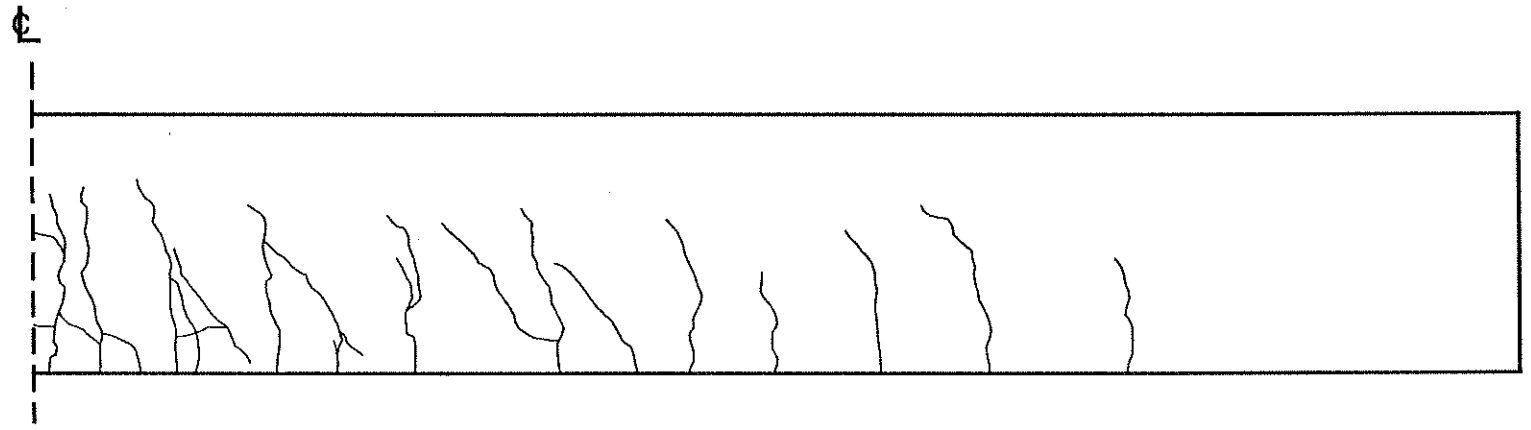

(a)

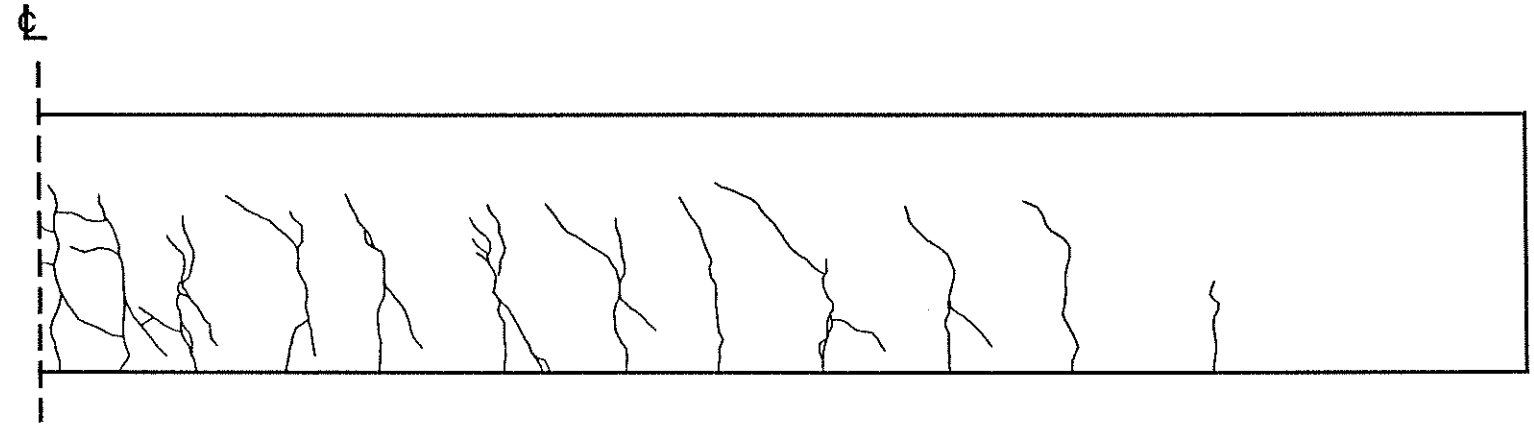

(b)

Fig. 5.10 Crack patterns for east half of beams with three No. 8 (25 mm) bars, $\rho = 0.68\rho_{bal}$: (a) $R_r = 0.069$, (b) $R_r = 0.119$

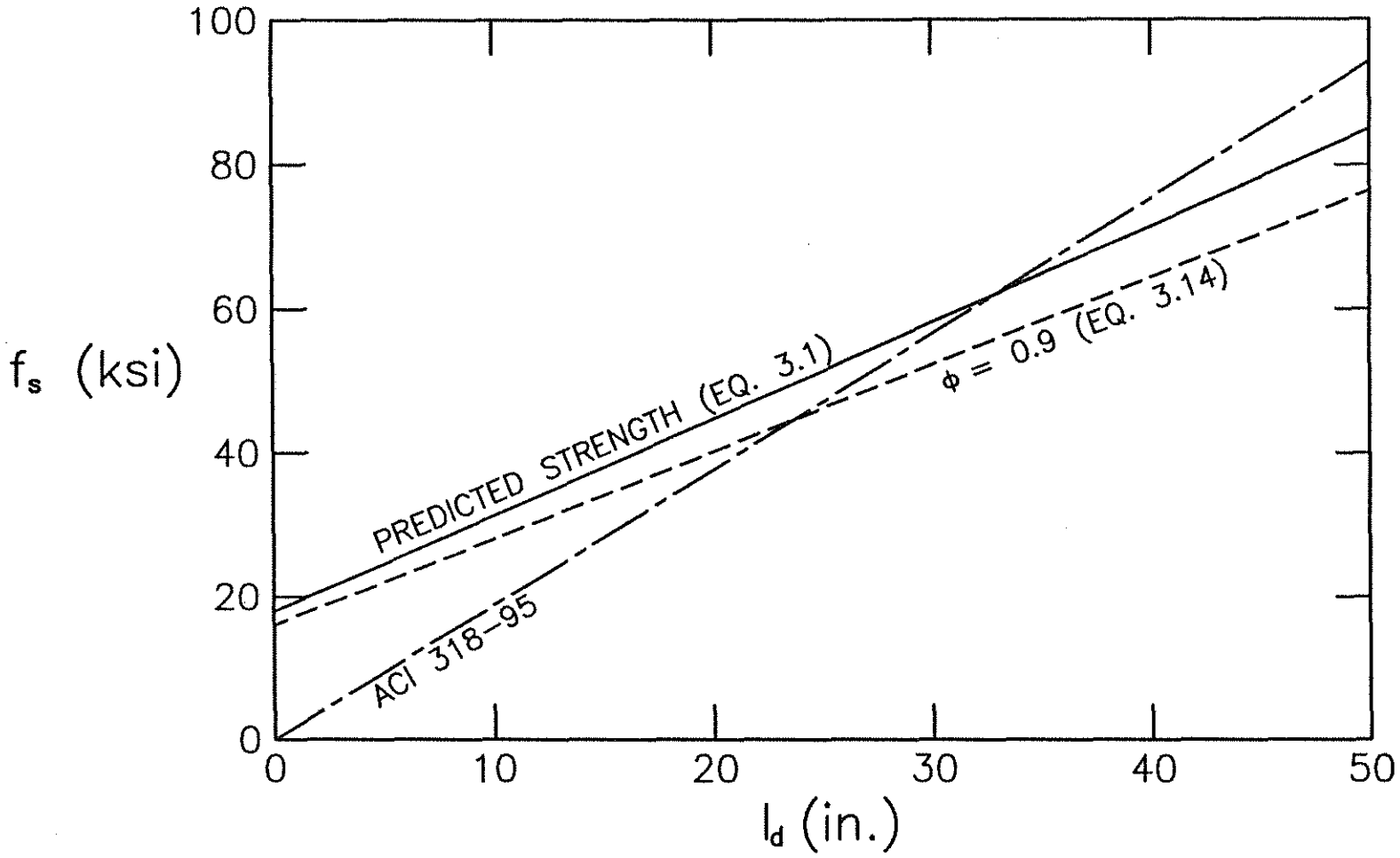

Fig. 6.1 Predicted bar stress, f_s, versus development length, l_d, comparing the criteria in Chapter 3 to the ACI criteria for No. 8 (25 mm) bars not confined by transverse reinforcement with $c/d_b = 2$ and $f'_c = 5000$ psi (34.5 MPa) (1 ksi = 6.89 Mpa)

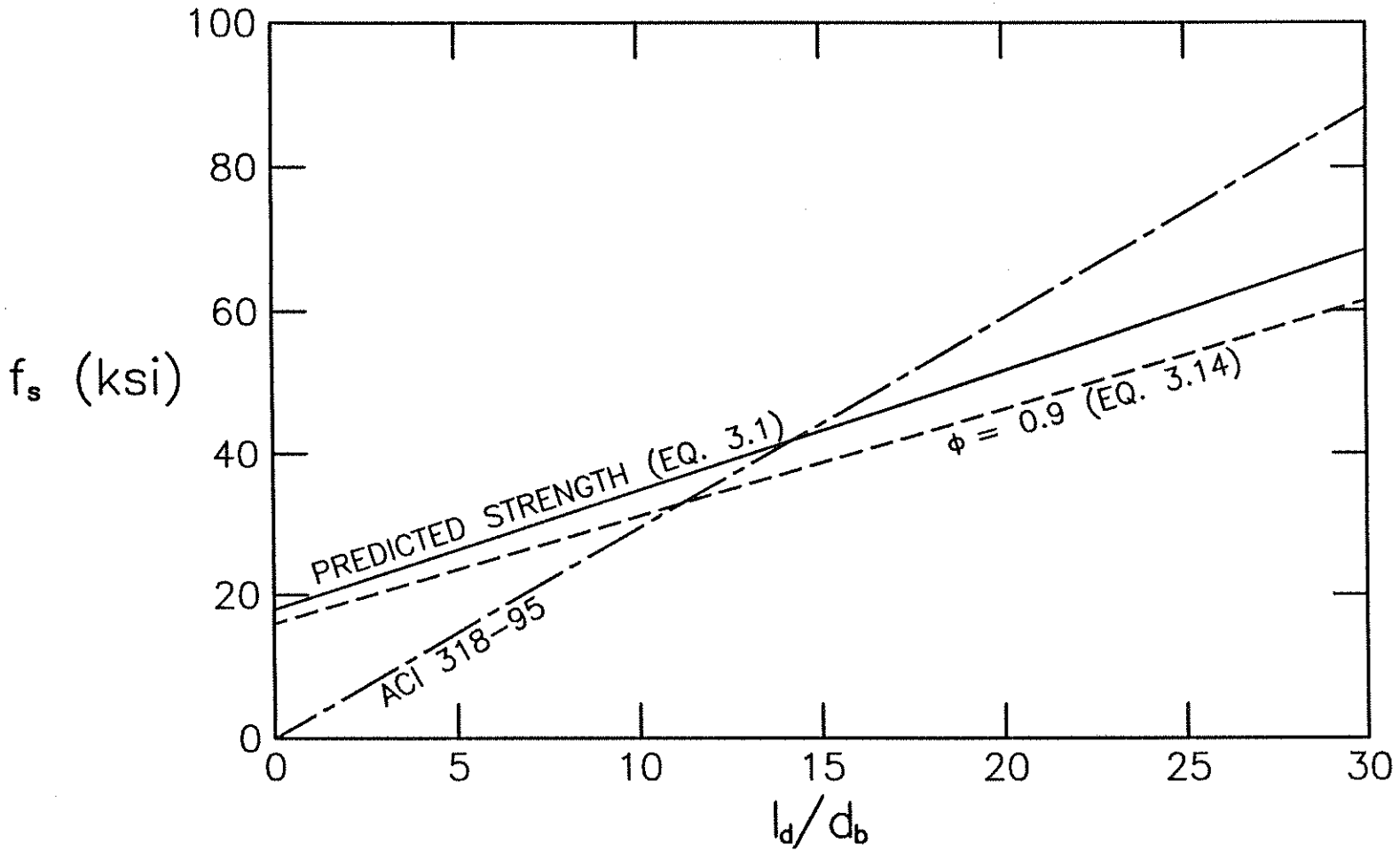

Fig. 6.2 Predicted bar stress, f_s, versus l_d/d_b comparing the criteria in Chapter 3 to the ACI criteria for No. 6 (19 mm) and smaller bars not confined by transverse reinforcement with $c/d_b = 2.5$ and $f'_c = 5000$ psi (34.5 MPa) (1 ksi = 6.89 Mpa)

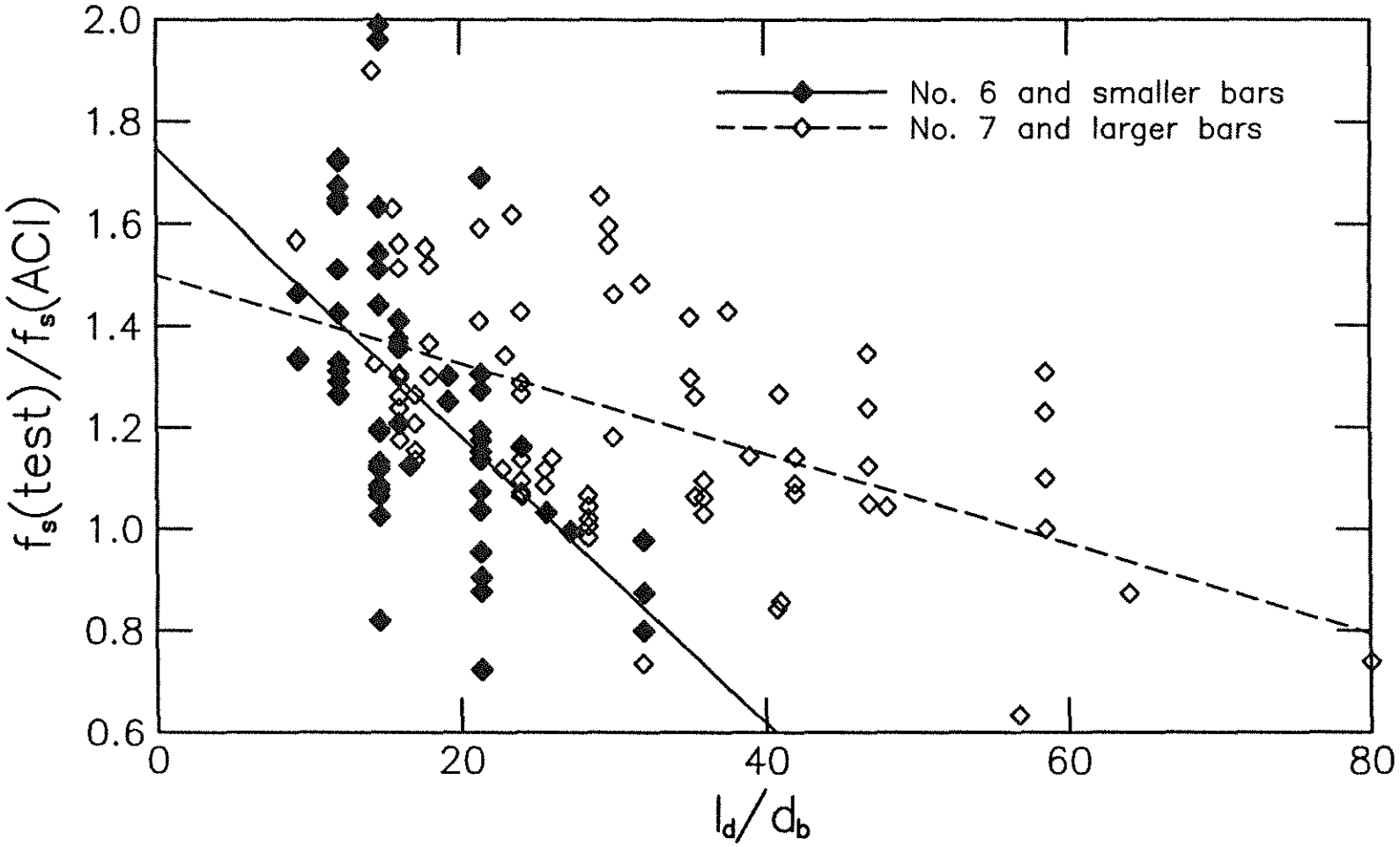

Fig. 6.3 Ratio of bar stress at failure to bar stress predicted by ACI 318-95 versus l_d/d_b for 119 tests without transverse reinforcement

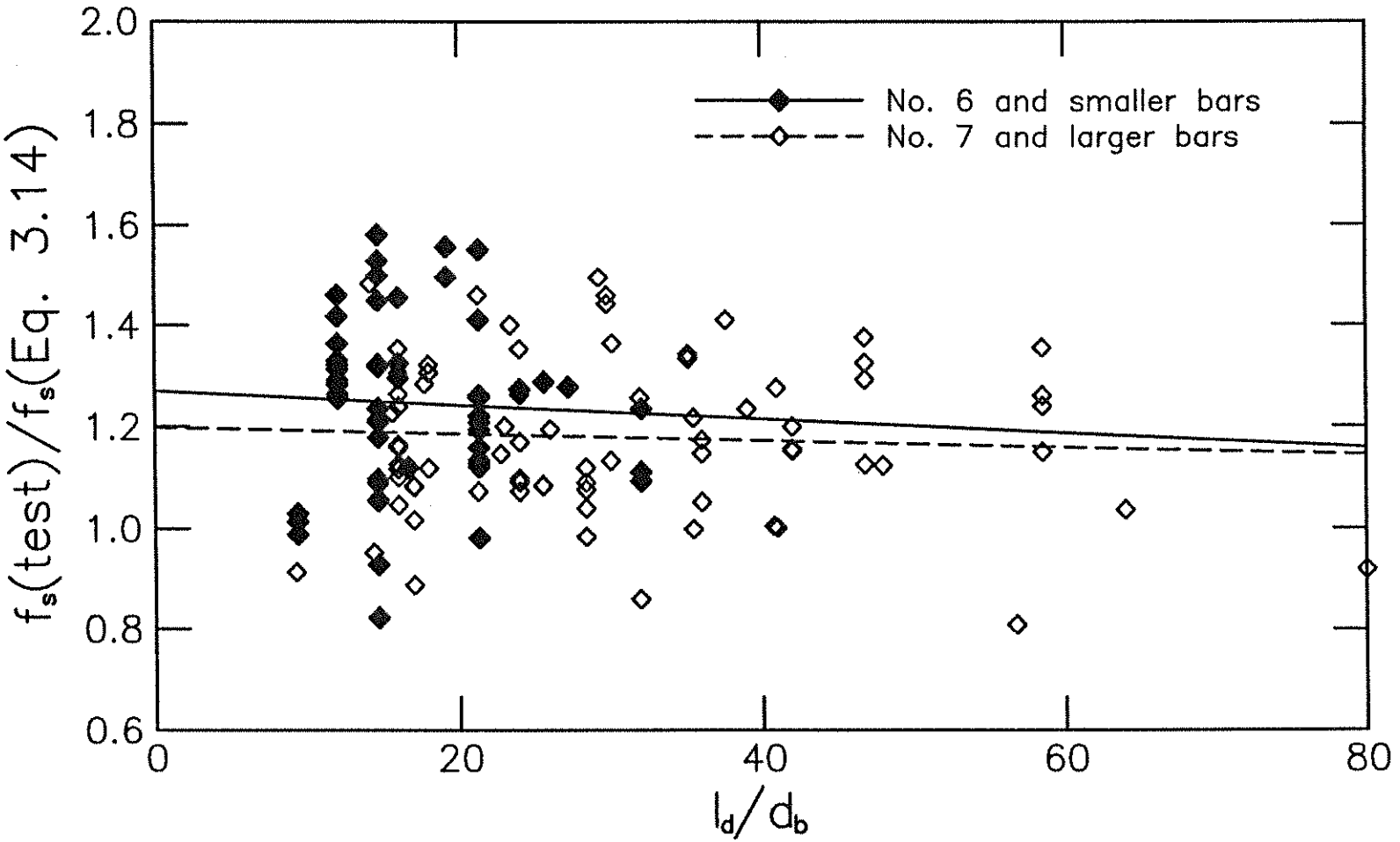

Fig. 6.4 Ratio of bar stress at failure to bar stress predicted by Eq. 3.14 versus l_d/d_b for 119 tests without transverse reinforcement

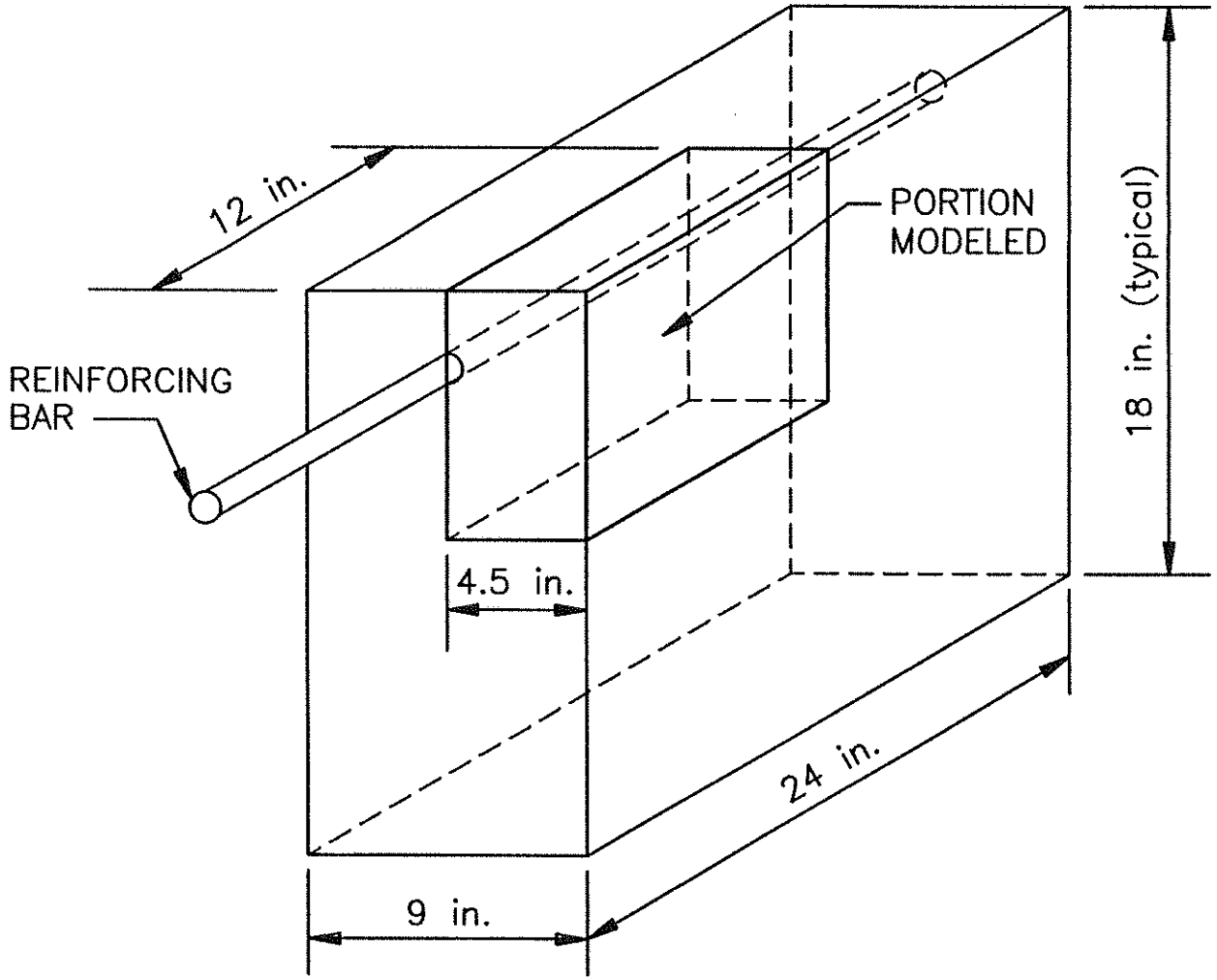

Fig. 7.1 Portion of experimental beam-end specimen represented by finite element models (1 in. = 25.4 mm)

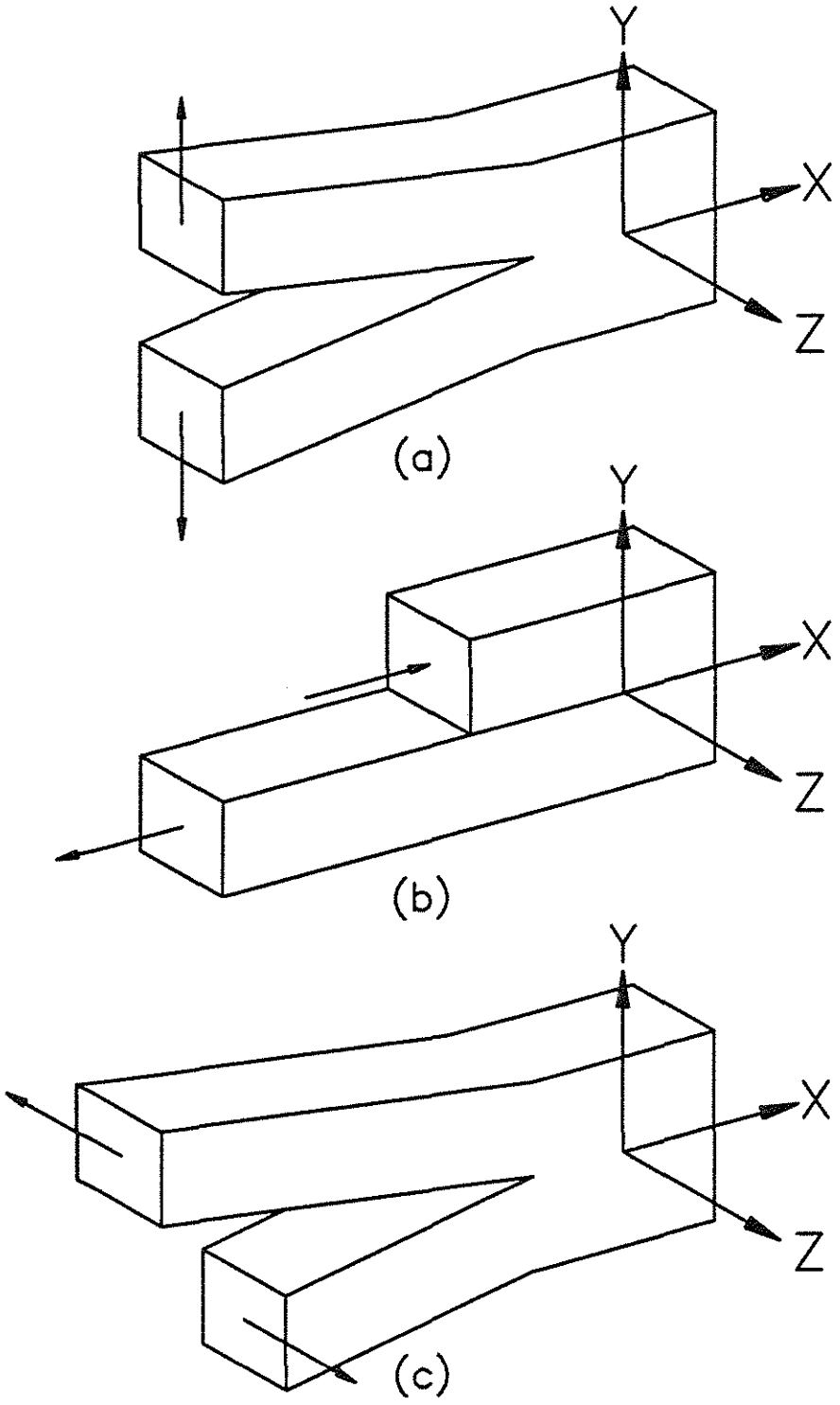

Fig. 7.2 Cracking modes, (a) Mode I, (b) Mode II, (c) Mode III (after Barsom and Rolfe 1987)

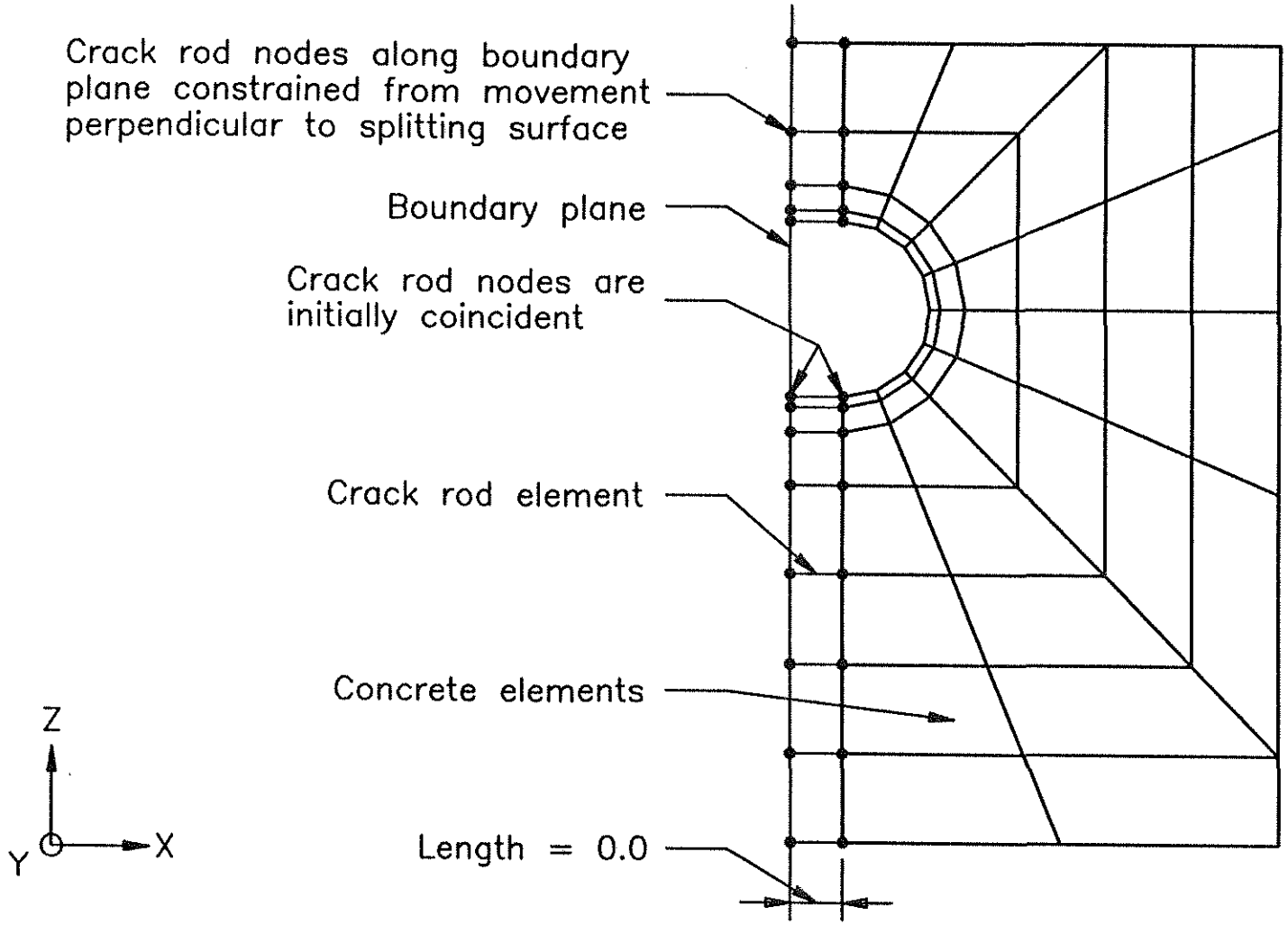

Fig. 7.3 Connection of crack rods on vertical plane to concrete elements (end view)

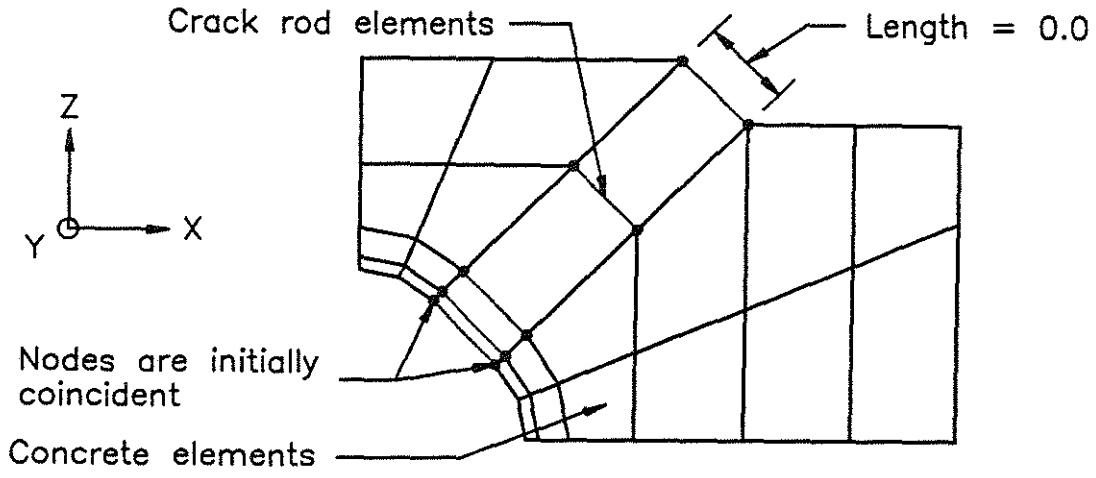

Fig. 7.4 Connection of crack rods on nonvertical planes to concrete elements (end view)

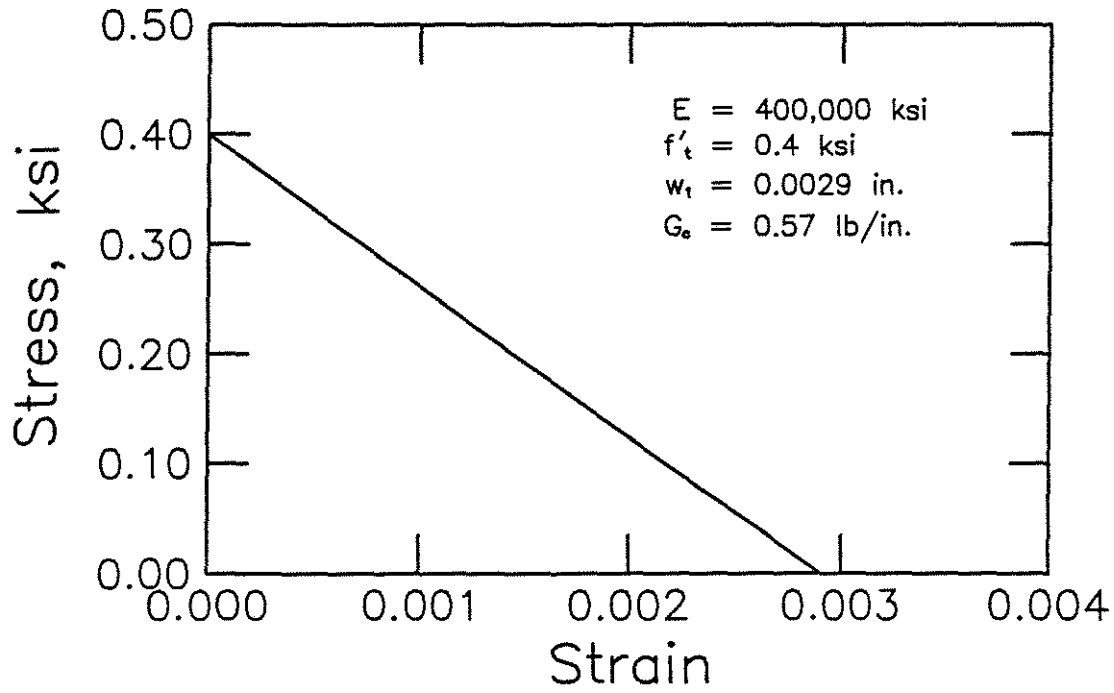

Fig. 7.5 Stress-strain curve for crack rod elements (1 in. = 25.4 mm, 1 ksi = 6.89 MPa, 1 lb/in. = 175 N/m)

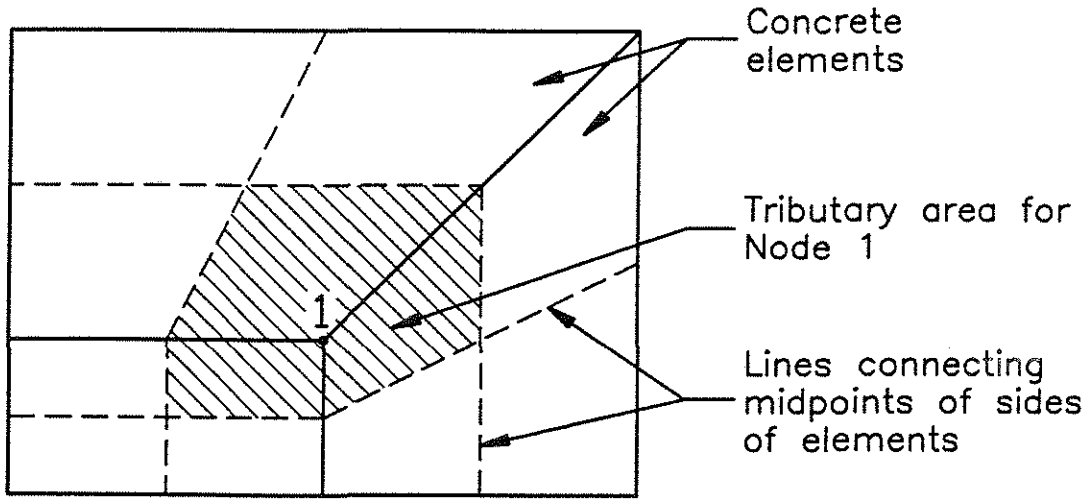

Fig. 7.6 Tributary area for crack rod elements

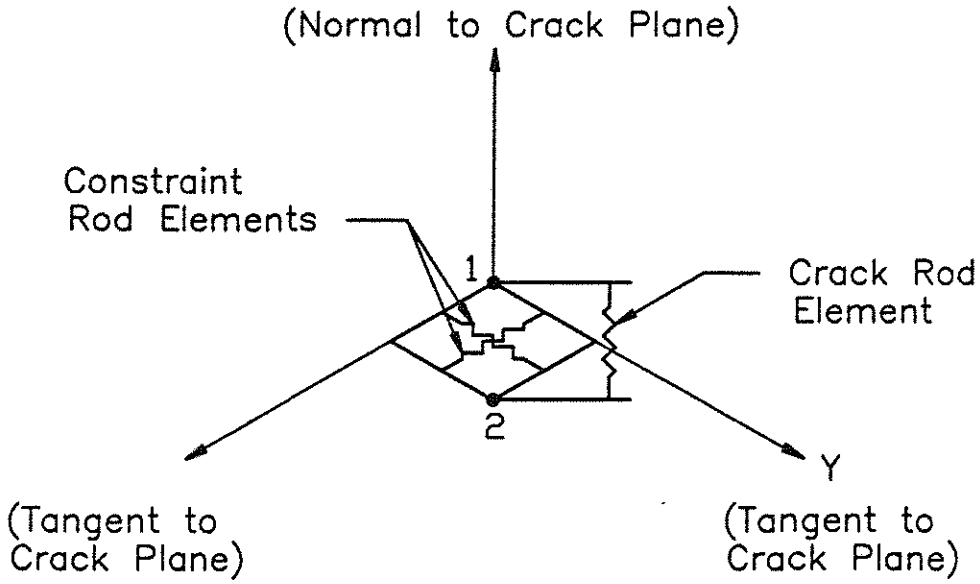

Fig. 7.7 Crack and constraint rod elements on nonvertical crack planes

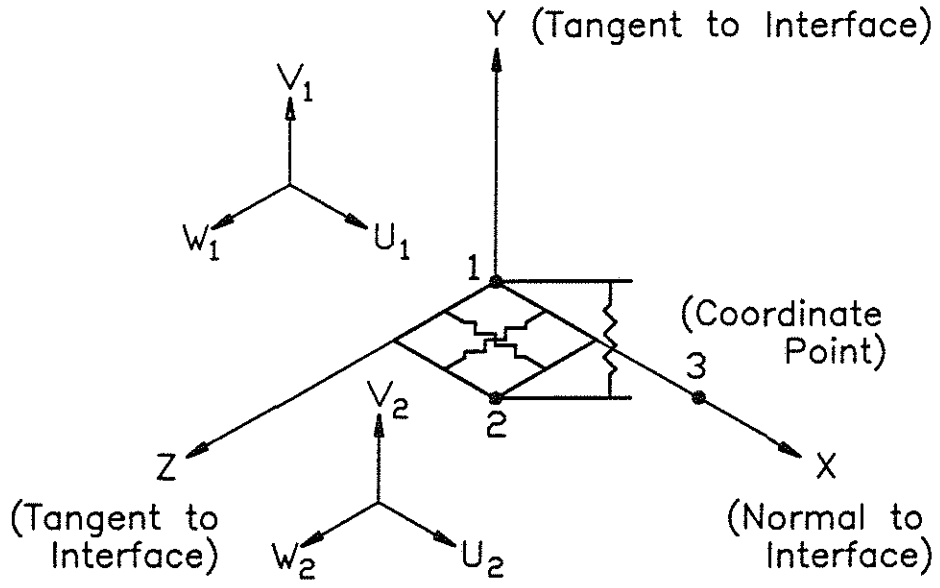

Fig. 7.8 Three-dimensional interface link element (after Lopez et al. 1994)

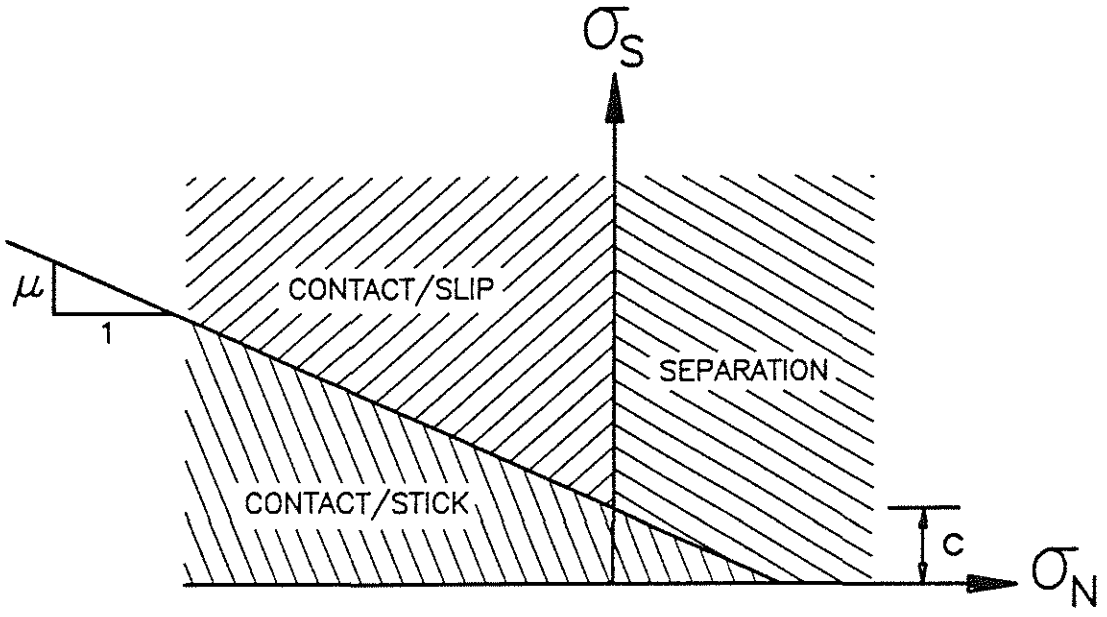

Fig. 7.9 Interface element material states on Mohr-Coulomb surface

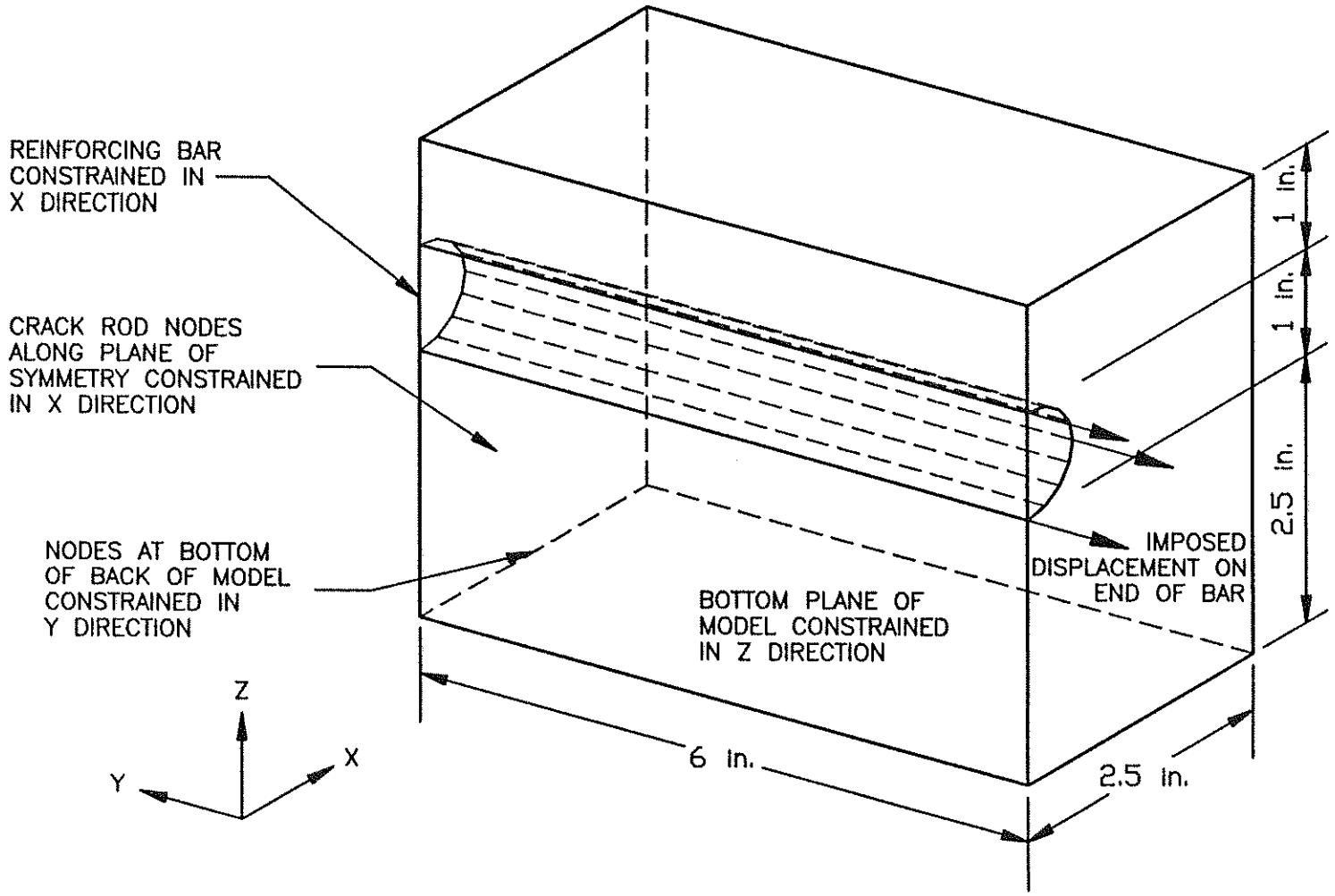

Fig. 7.10 Dimensions and boundary conditions for single-rib finite element models (1 in. = 25.4 mm)

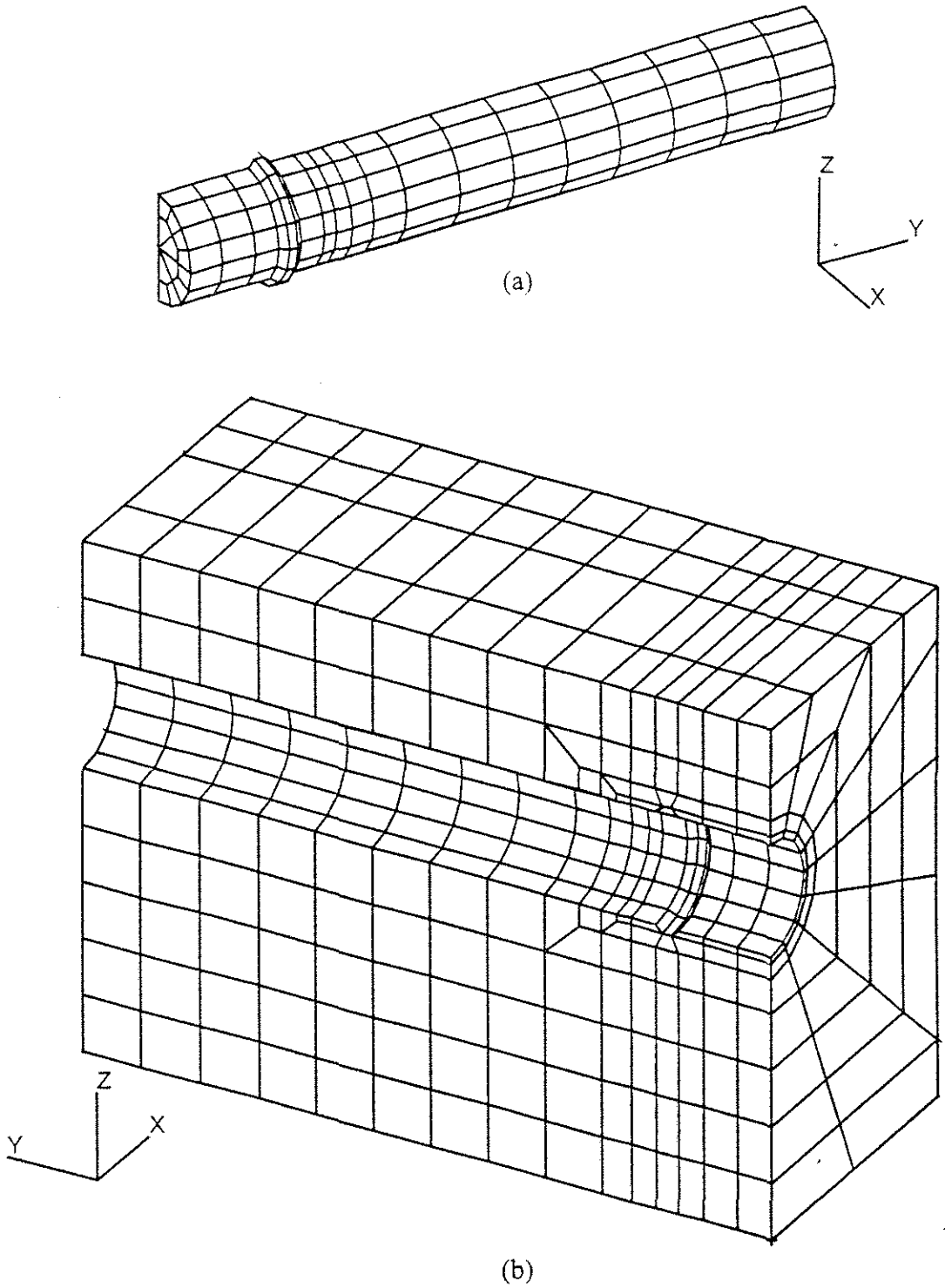

Fig. 7.11 Finite element mesh for single-rib model, (a) reinforcing steel substructure, (b) concrete substructure

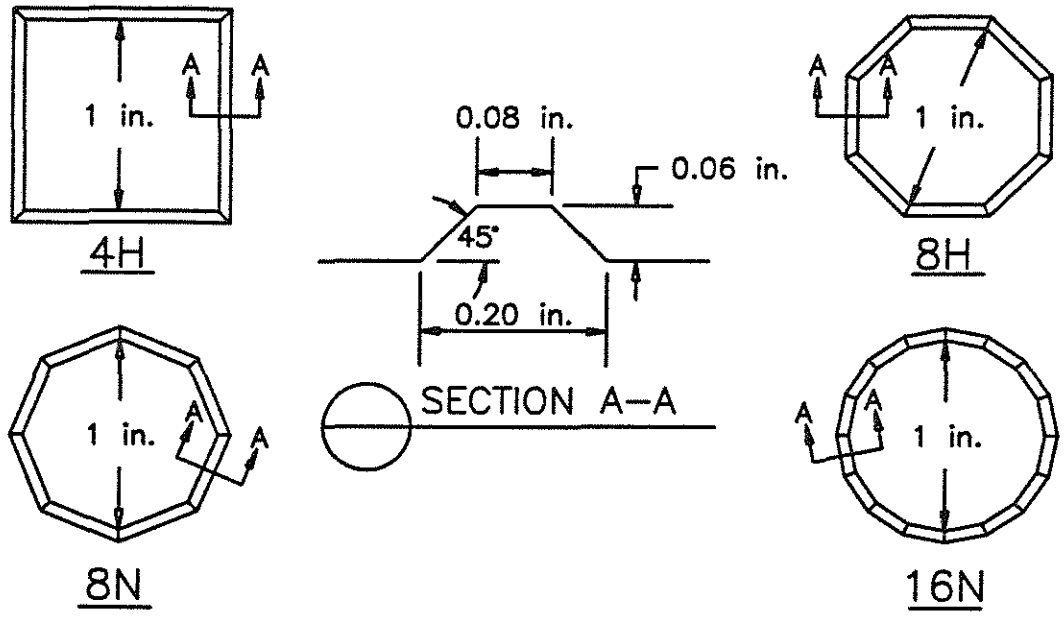

Fig. 7.12 Bar shapes investigated using single-rib finite element models (1 in. = 25.4 mm)

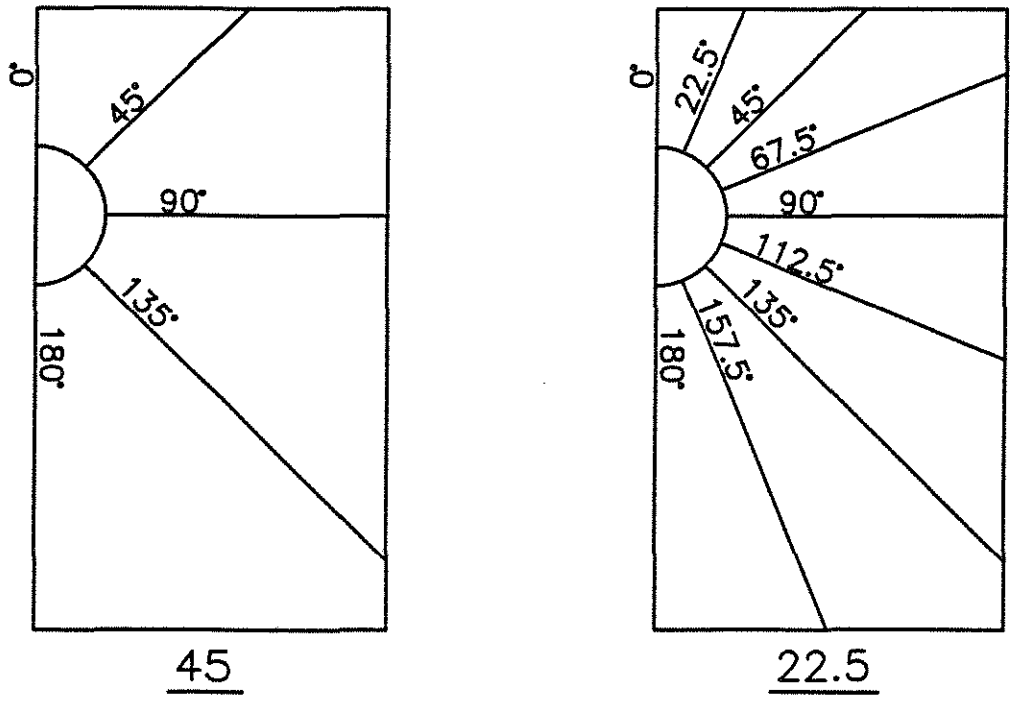

Fig. 7.13 Crack plane configurations investigated using single-rib finite element models

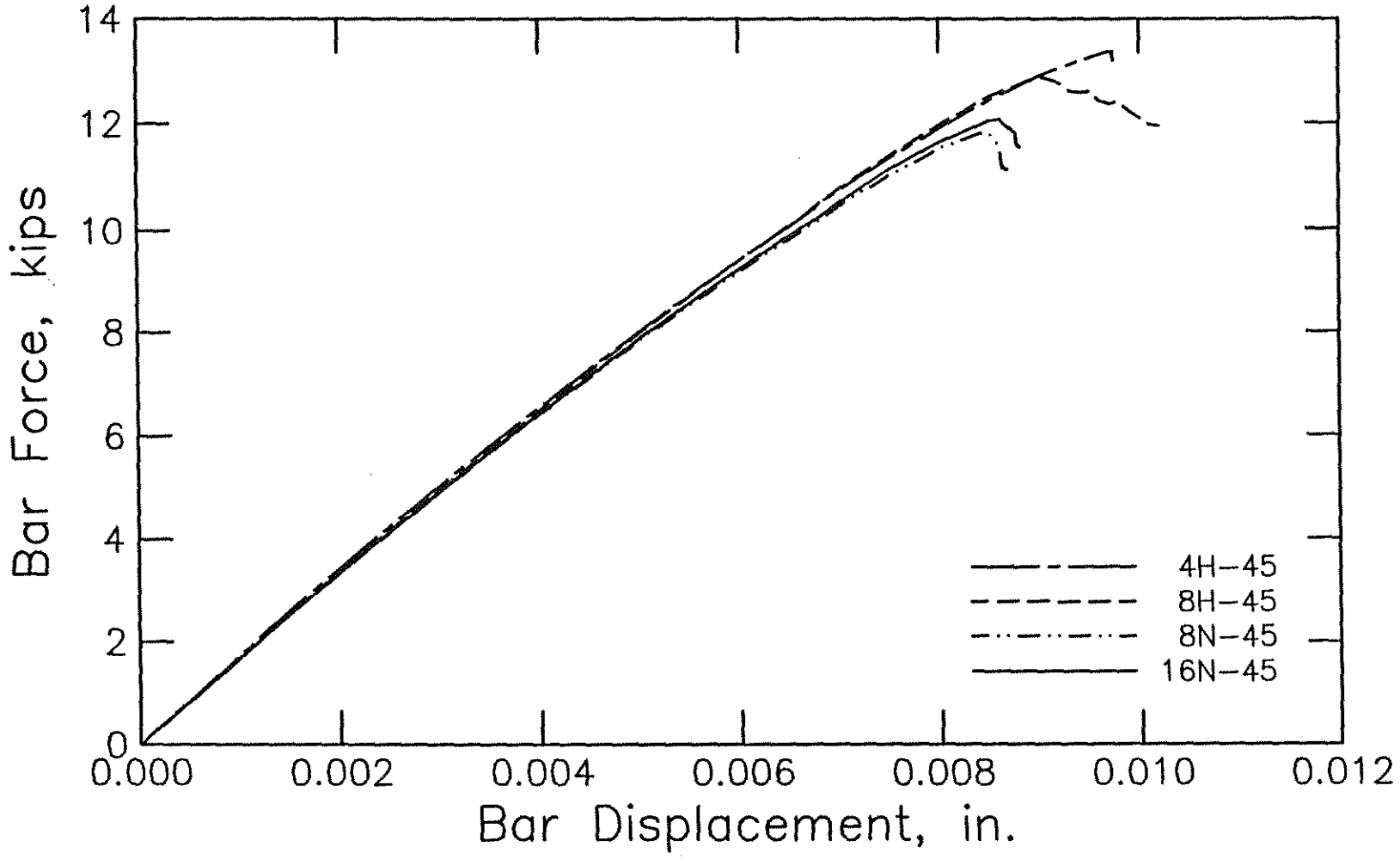

Fig. 7.14 Bar force-displacement curves for single-rib models with crack planes at 45° intervals (1 in. = 25.4 mm, 1 kip = 4.45 kN)

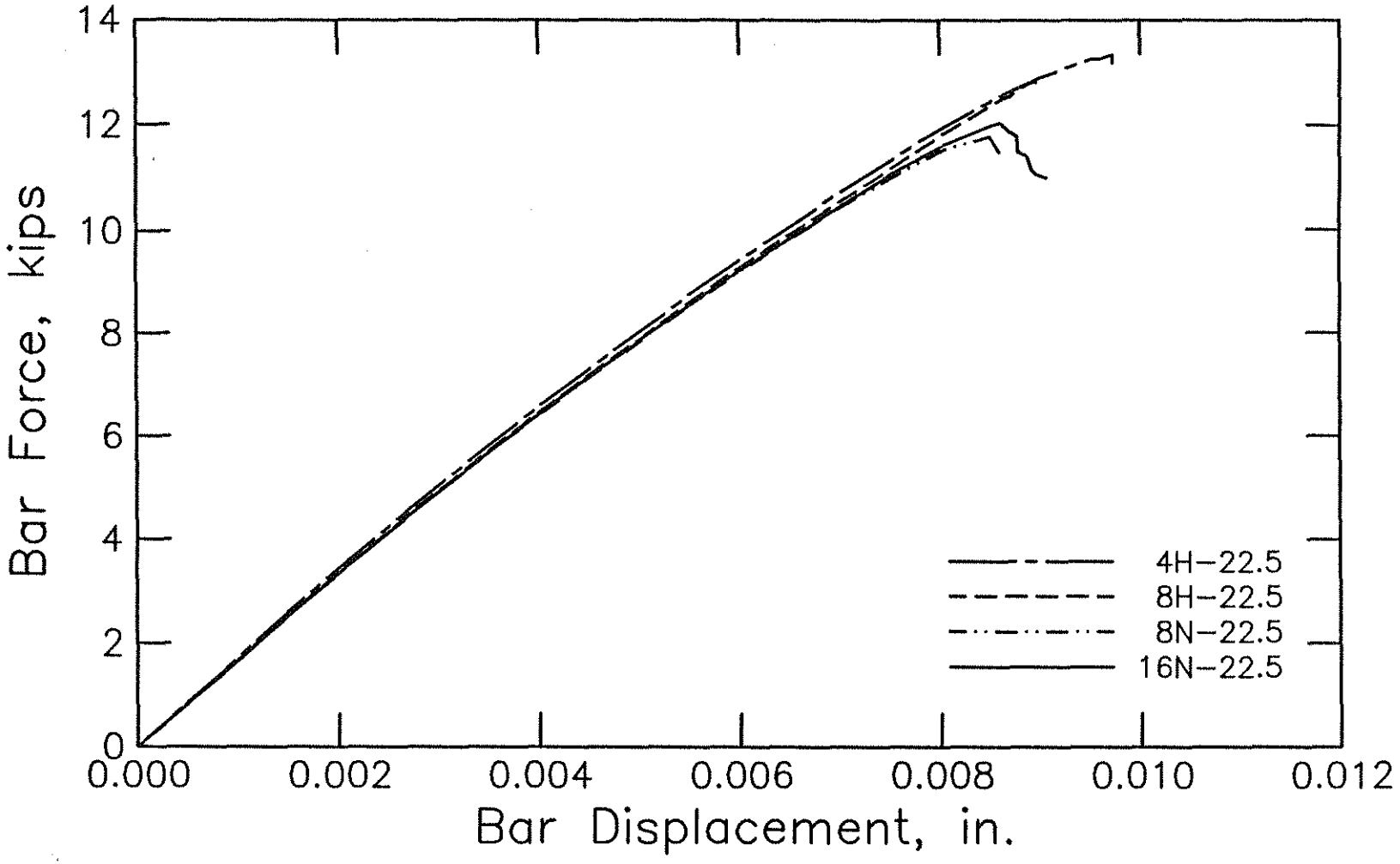

Fig. 7.15 Bar force-displacement curves for single-rib models with crack planes at 22.5° intervals (1 in. = 25.4 mm, 1 kip = 4.45 kN)

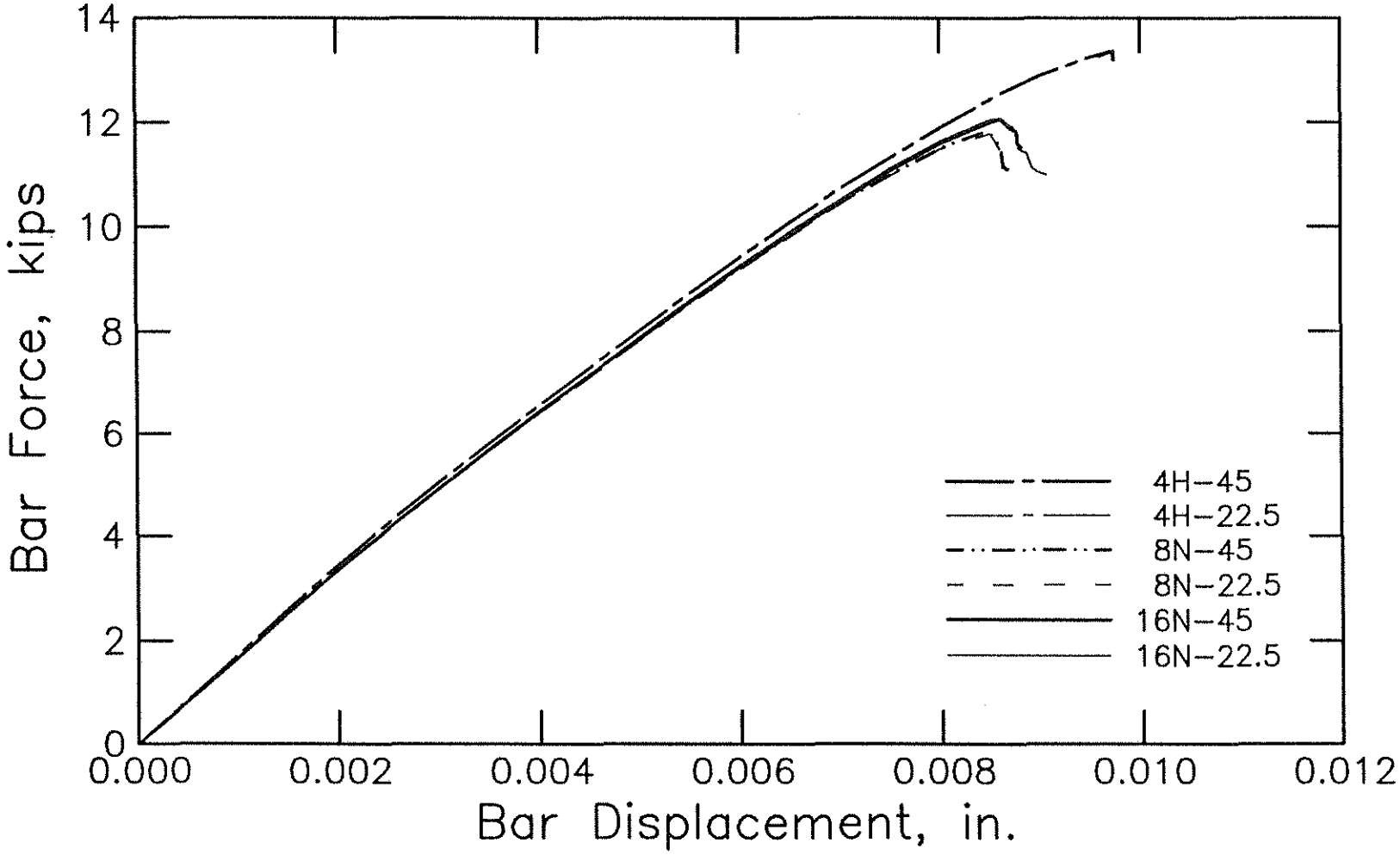

Fig. 7.16 Bar force-displacement curves for single-rib models with the 4H, 8N and 16N bar shapes (1 in. = 25.4 mm, 1 kip = 4.45 kN)

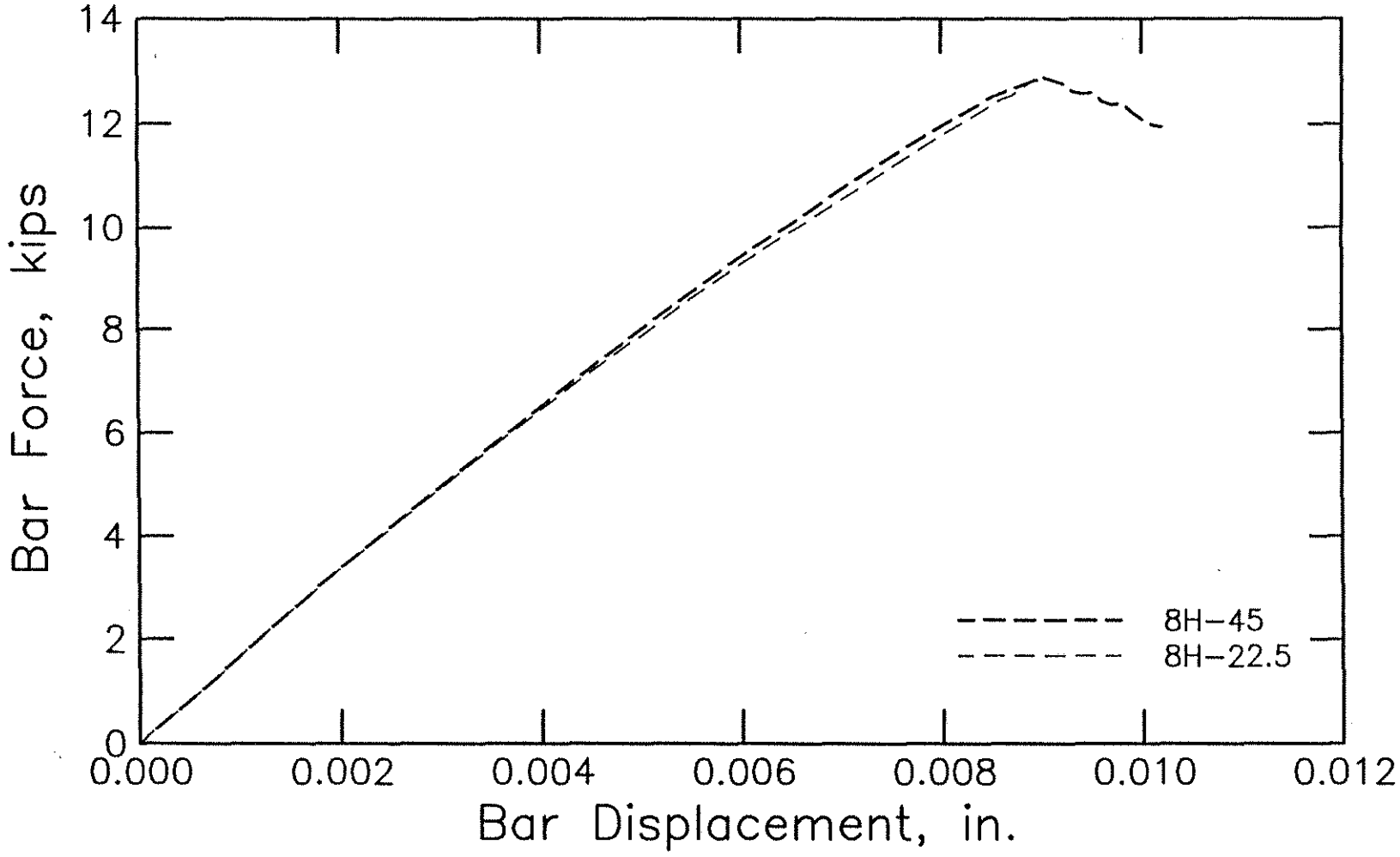

Fig. 7.17 Bar force-displacement curves for single-rib models with the 8H bar shape (1 in. = 25.4 mm, 1 kip = 4.45 kN)

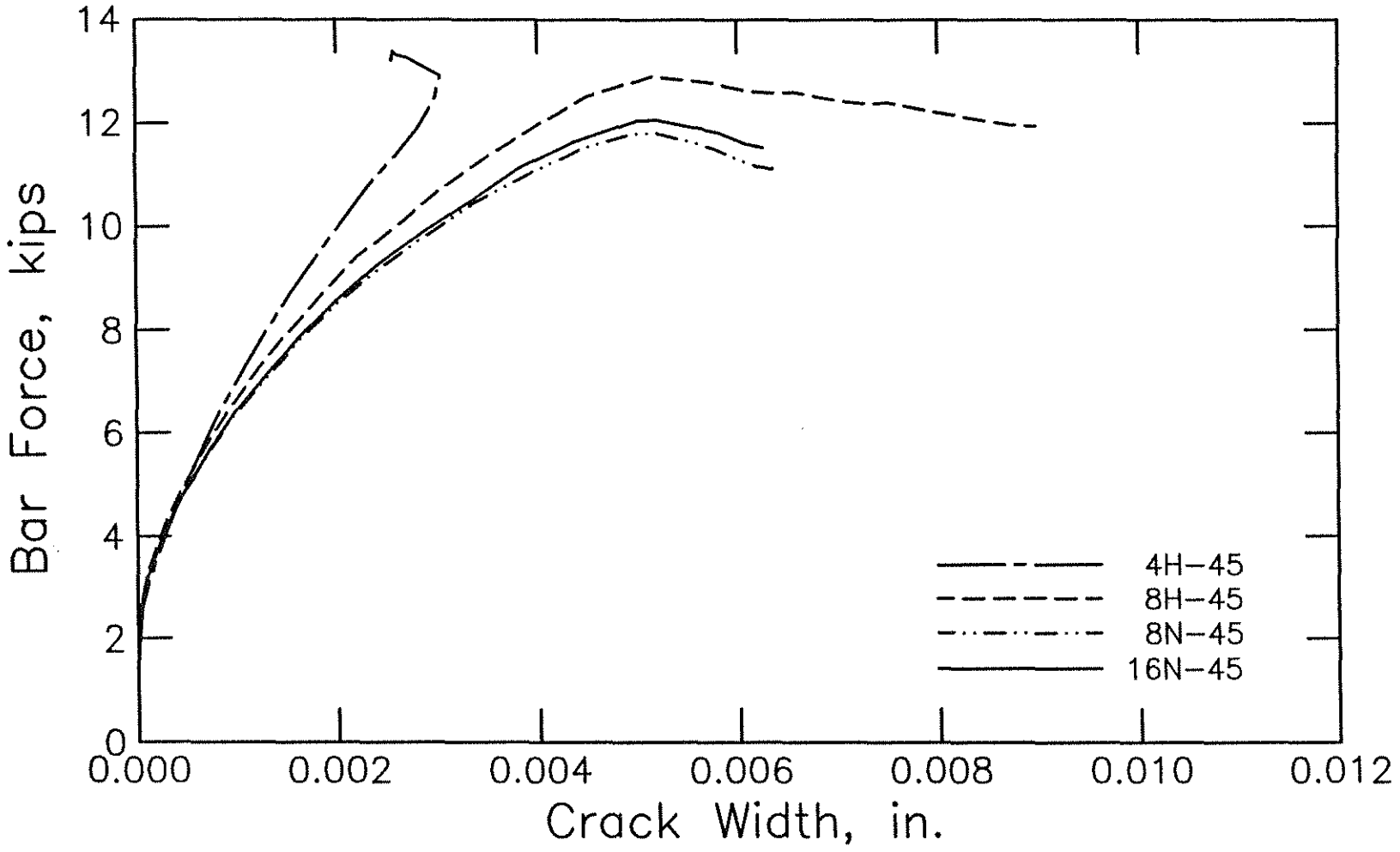

Fig. 7.18 Bar force-crack width curves for single-rib models with crack planes at 45° intervals (1 in. = 25.4 mm, 1 kip = 4.45 kN)

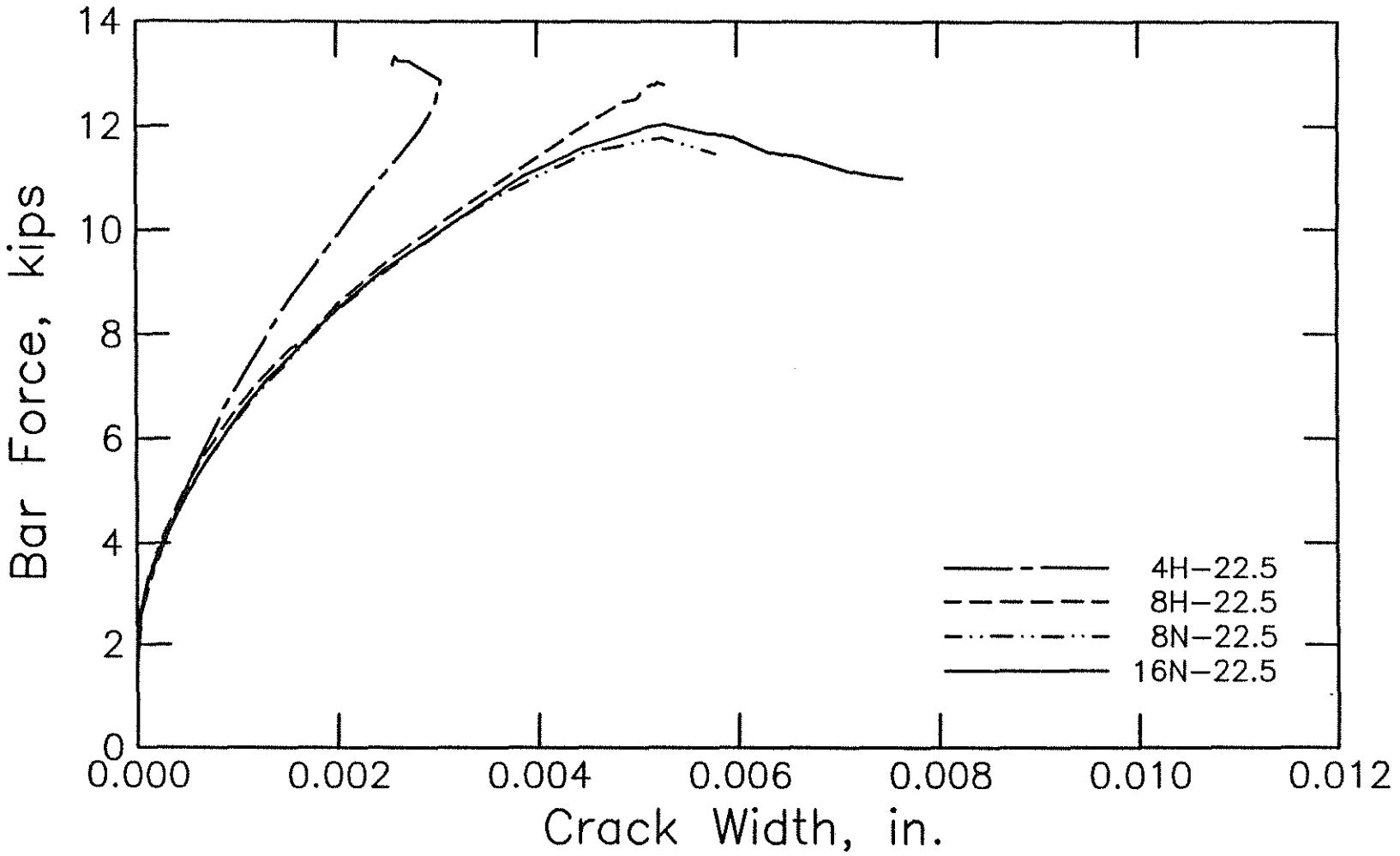

Fig. 7.19 Bar force-crack width curves for single-rib models with crack planes at 22.5° intervals (1 in. = 25.4 mm, 1 kip = 4.45 kN)

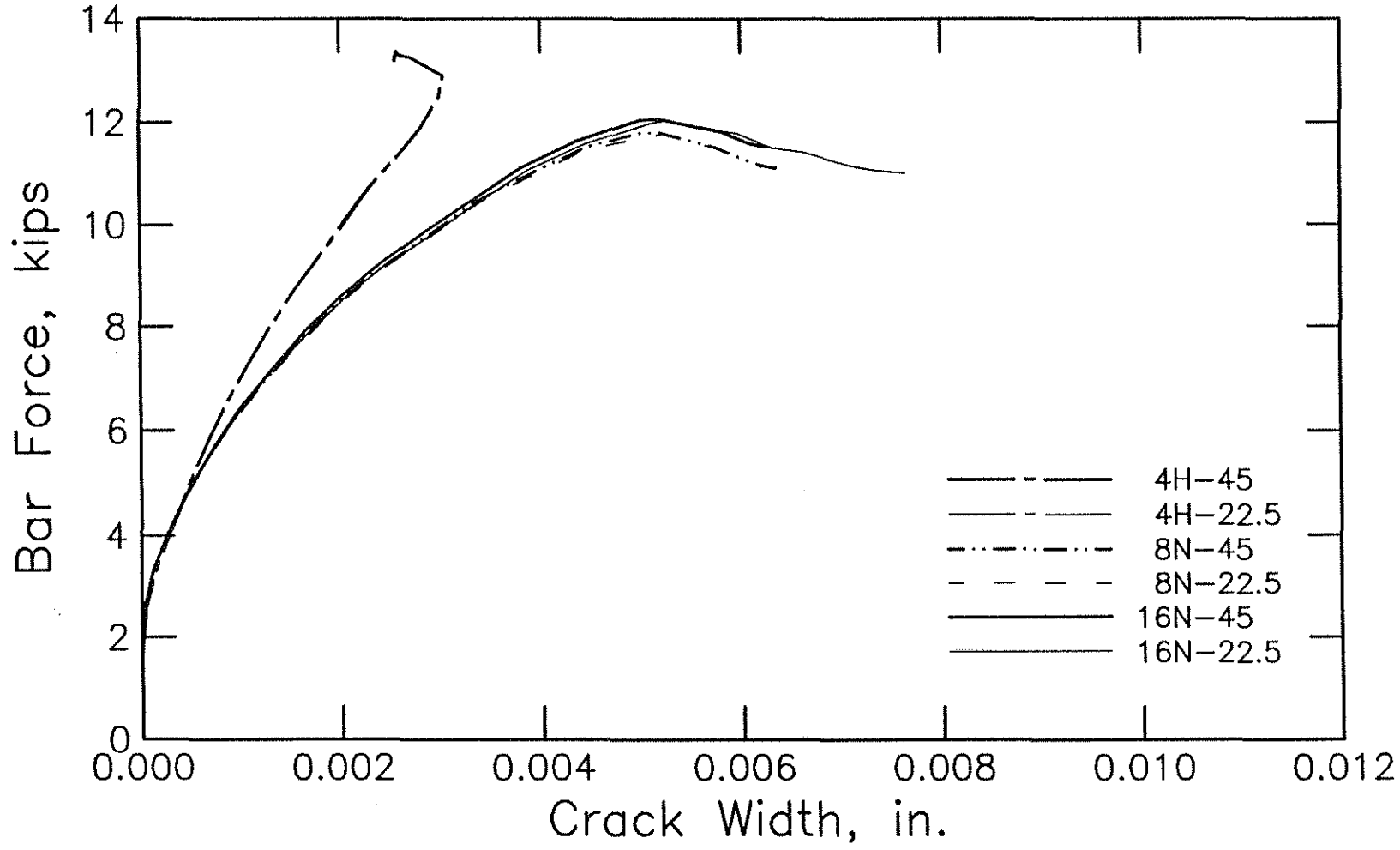

Fig. 7.20 Bar force-crack width curves for single-rib models with the 4H, 8N and 16N bar shapes (1 in. = 25.4 mm, 1 kip = 4.45 kN)

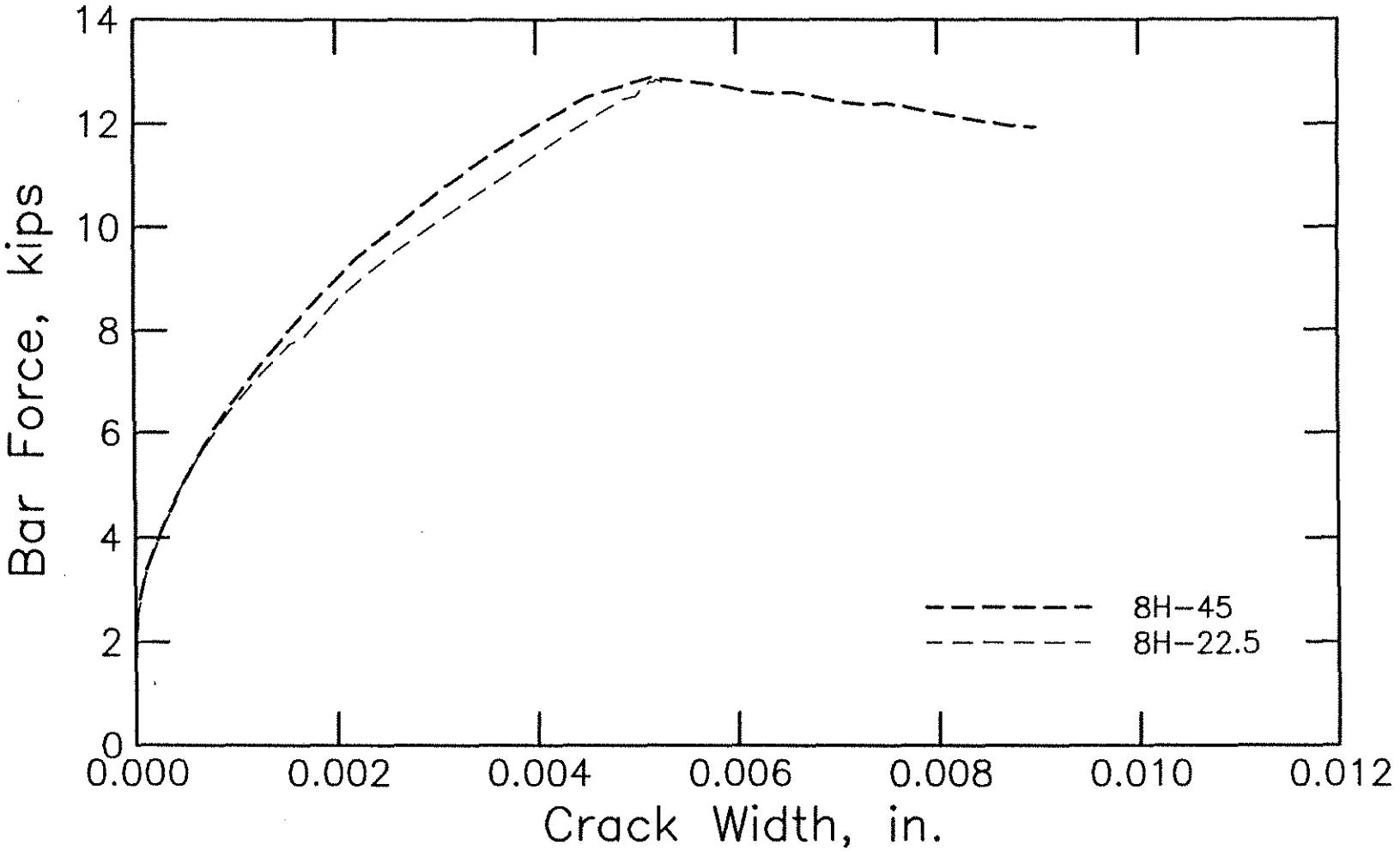

Fig. 7.21 Bar force-crack width curves for single-rib models with the 8H bar shape (1 in. = 25.4 mm, 1 kip = 4.45 kN)

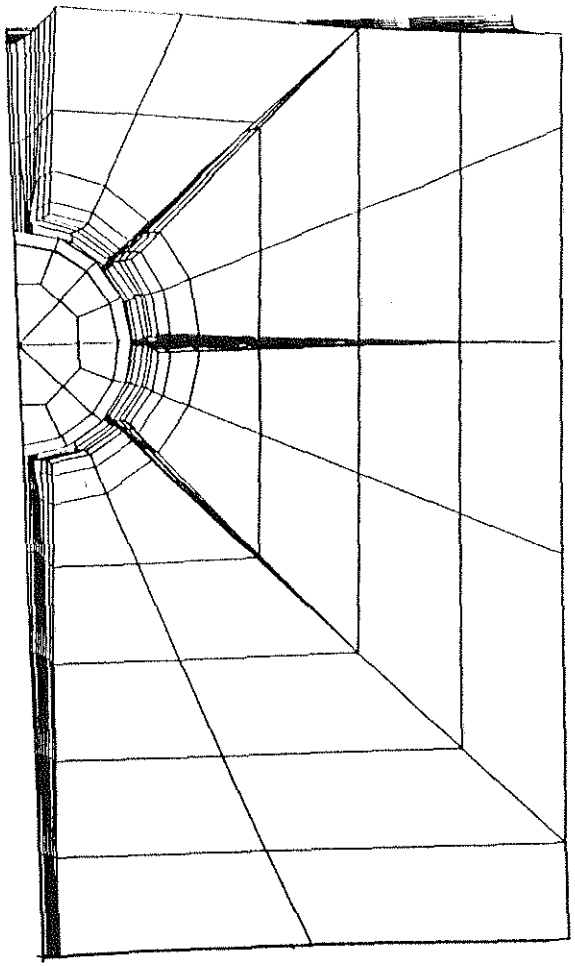

Fig. 7.22 Deformed shape for 16N-45 model at peak load

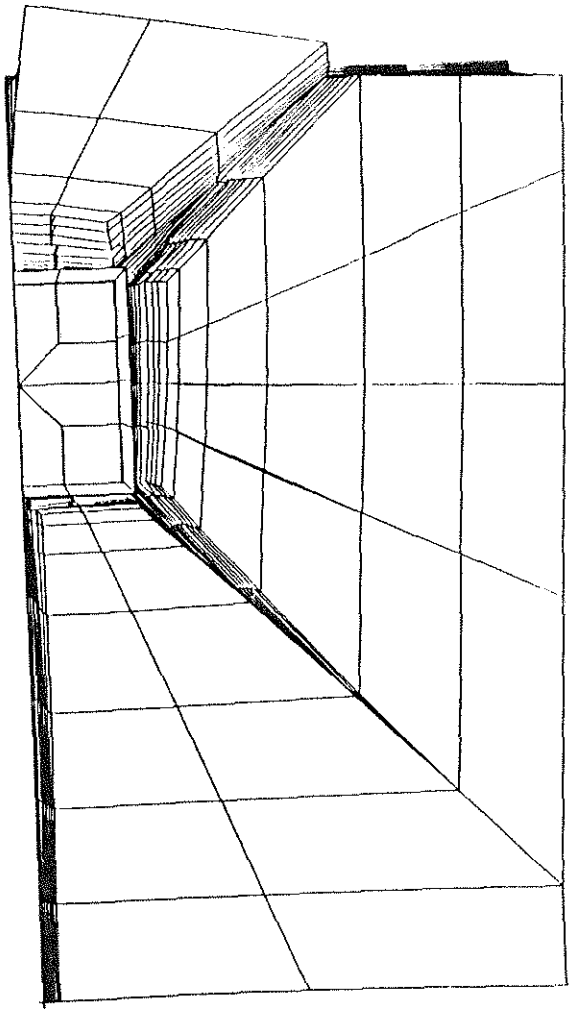

Fig. 7.23 Deformed shape for 4H-22.5 model at peak load

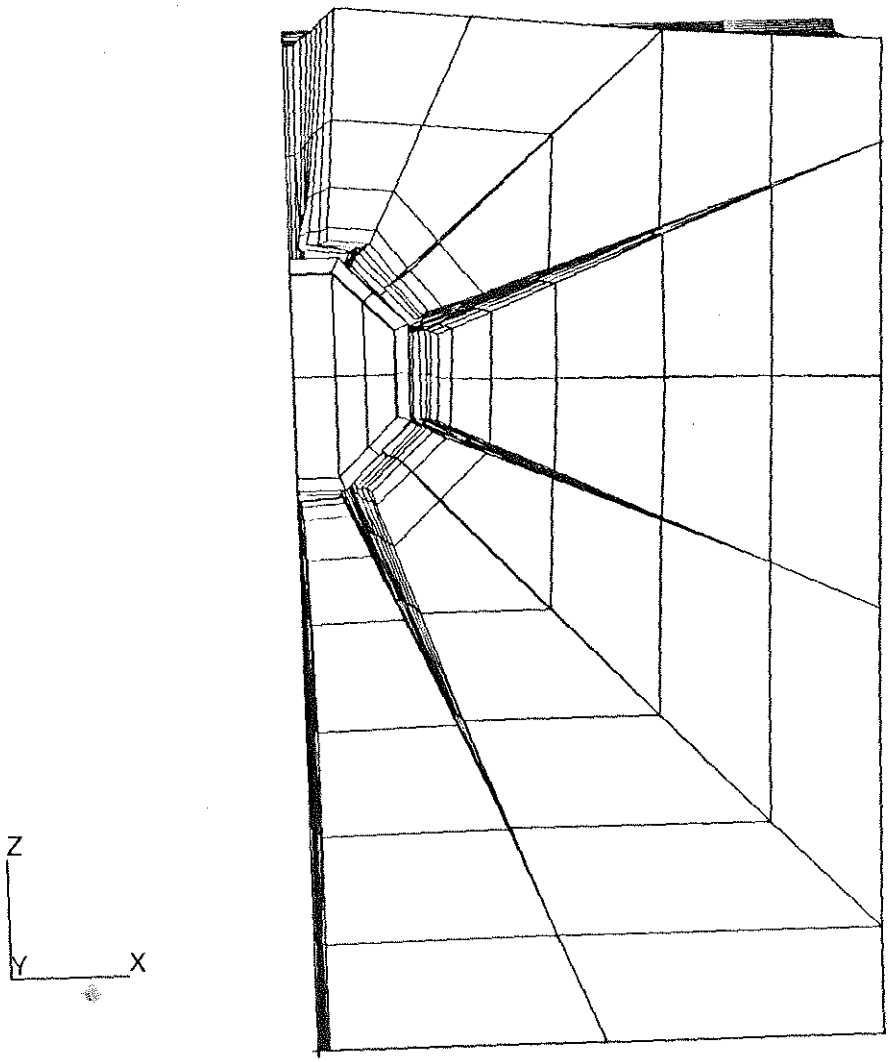

Fig. 7.24 Deformed shape for 8H-22.5 model at peak load

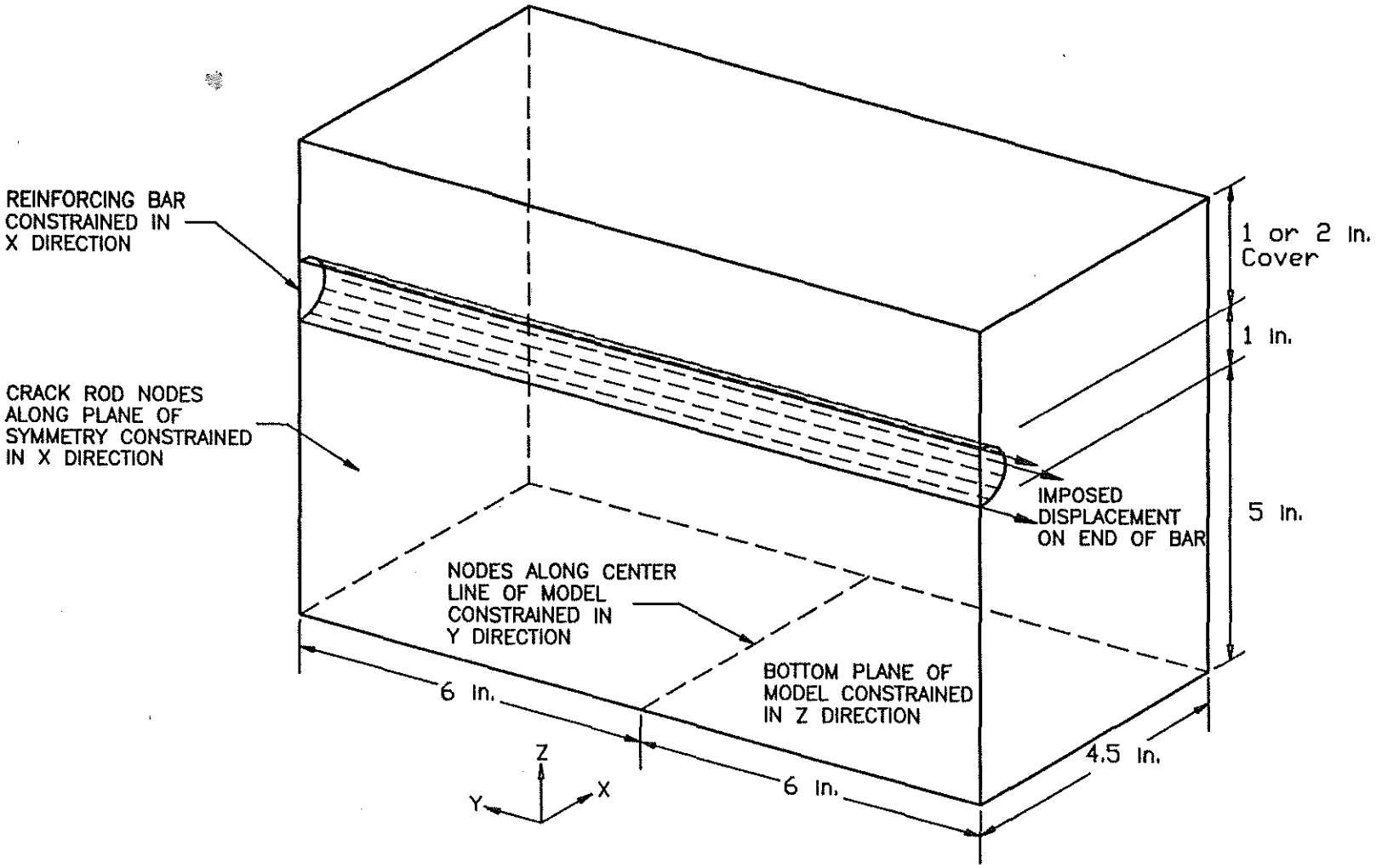

Fig. 7.25 Dimensions and boundary conditions for multiple-rib finite element models (1 in. = 25.4 mm)

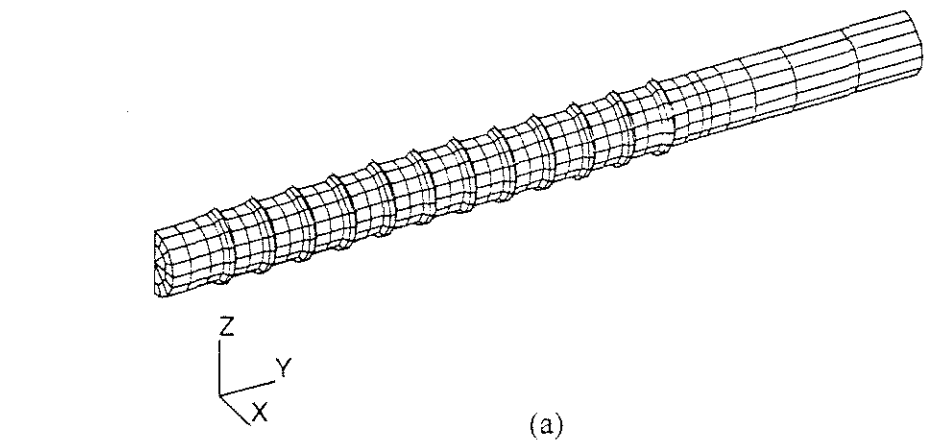

(a)

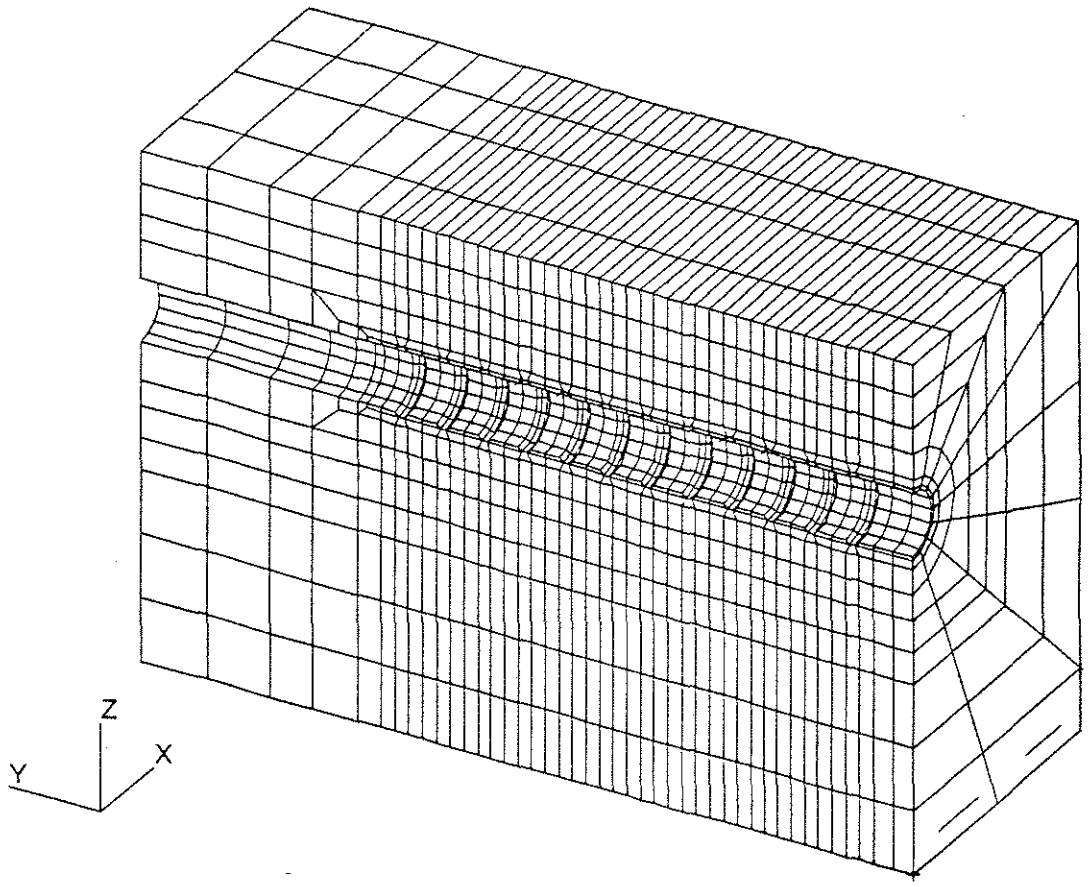

(b)

Fig. 7.26 Finite element mesh for multiple-rib model with 2 in. (50.8 mm) cover, (a) reinforcing steel substructure, (b) concrete substructure

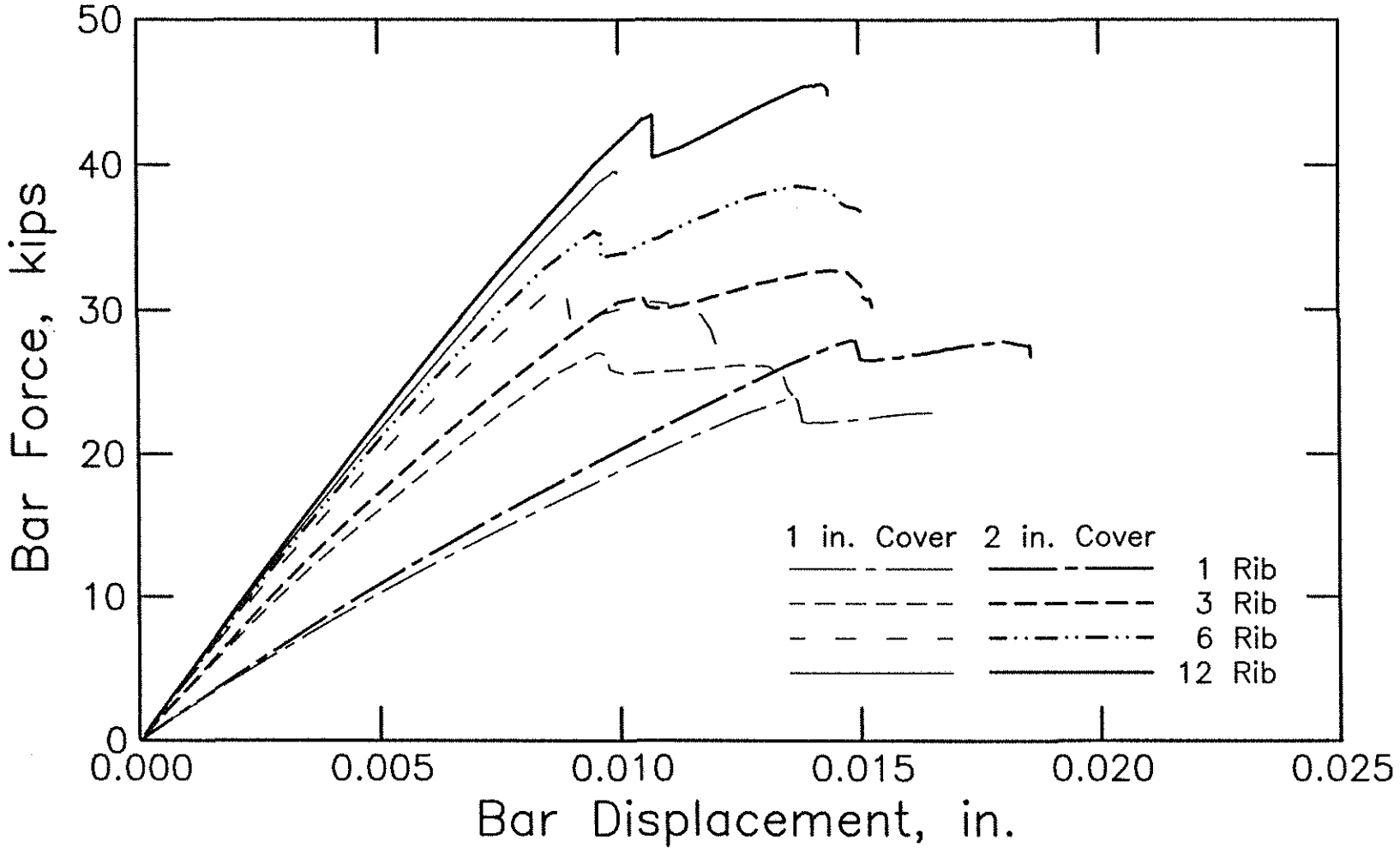

Fig. 7.27 Bar force-displacement curves for multiple-rib models (1 in. = 25.4 mm, 1 kip = 4.45 kN)

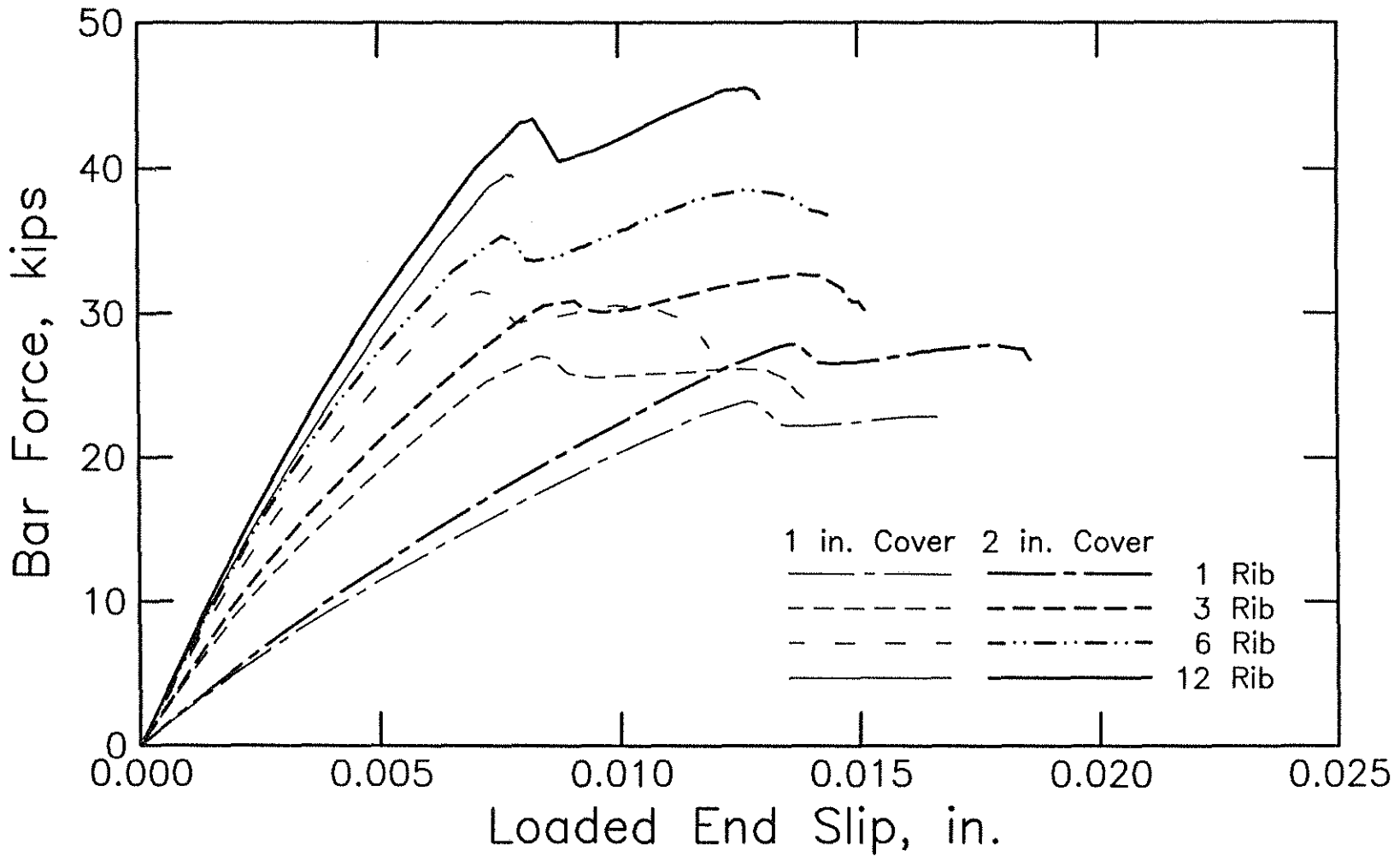

Fig. 7.28 Bar force-loaded end slip curves for multiple-rib models (1 in. = 25.4 mm, 1 kip = 4.45 kN)

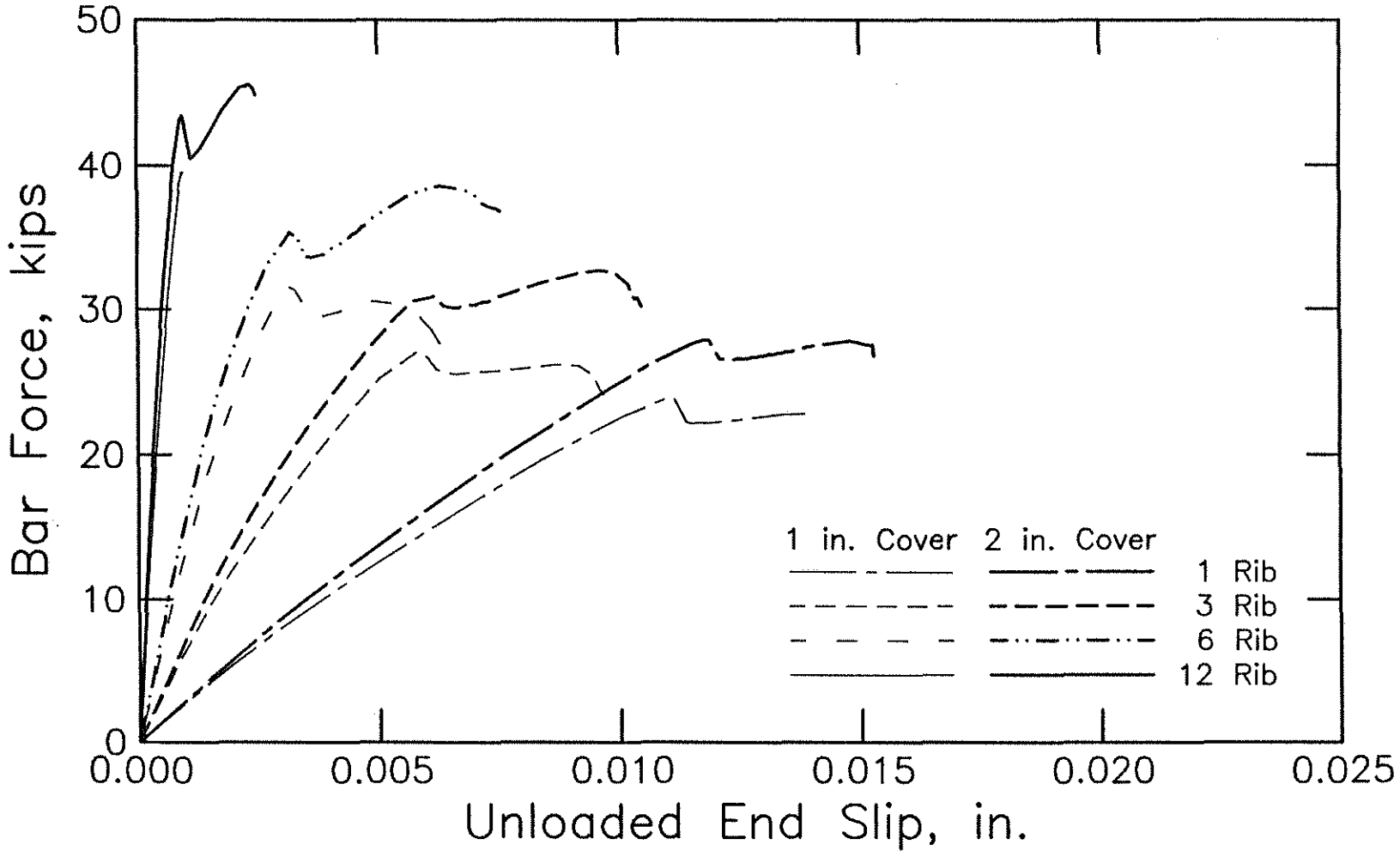

Fig. 7.29 Bar force-unloaded end slip curves for multiple-rib models (1 in. = 25.4 mm, 1 kip = 4.45 kN)

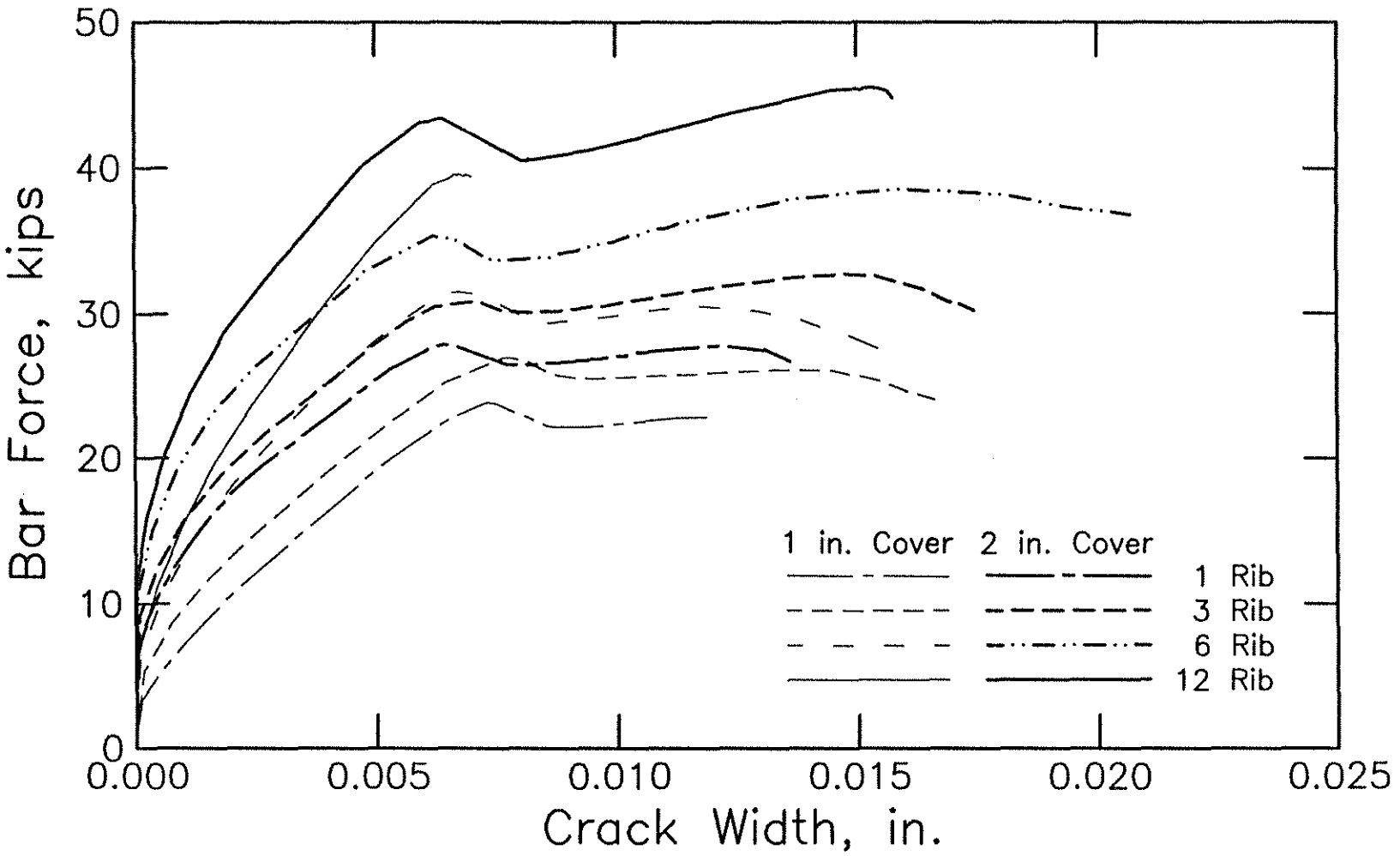

Fig. 7.30 Bar force-crack width curves for multiple-rib models (1 in. = 25.4 mm, 1 kip = 4.45 kN)

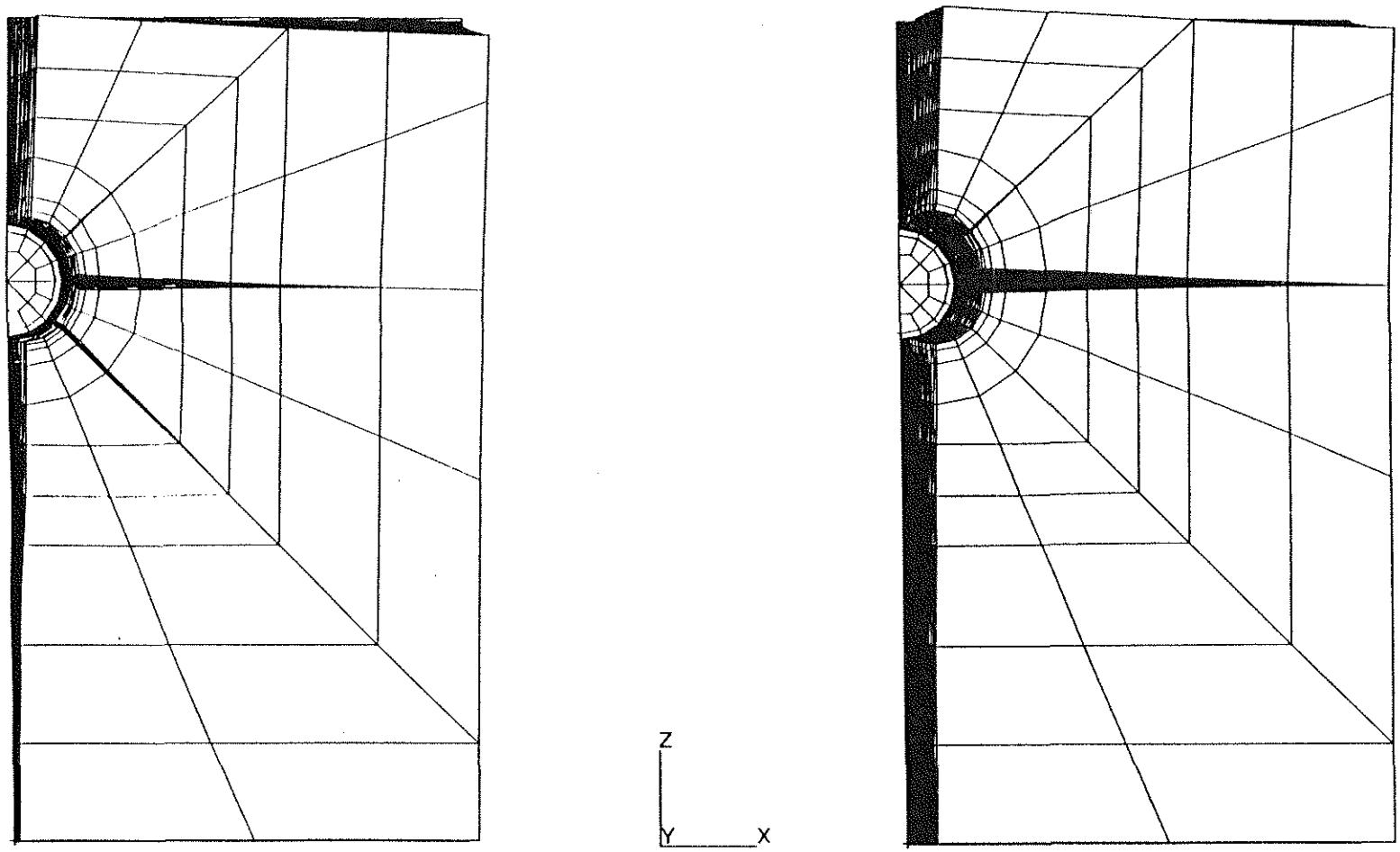

(a) (b)

Fig. 7.31 Deformed shape for multiple-rib model with 6 ribs and 2 in. (50.8 mm) cover, (a) at initial peak load, (b) at peak load

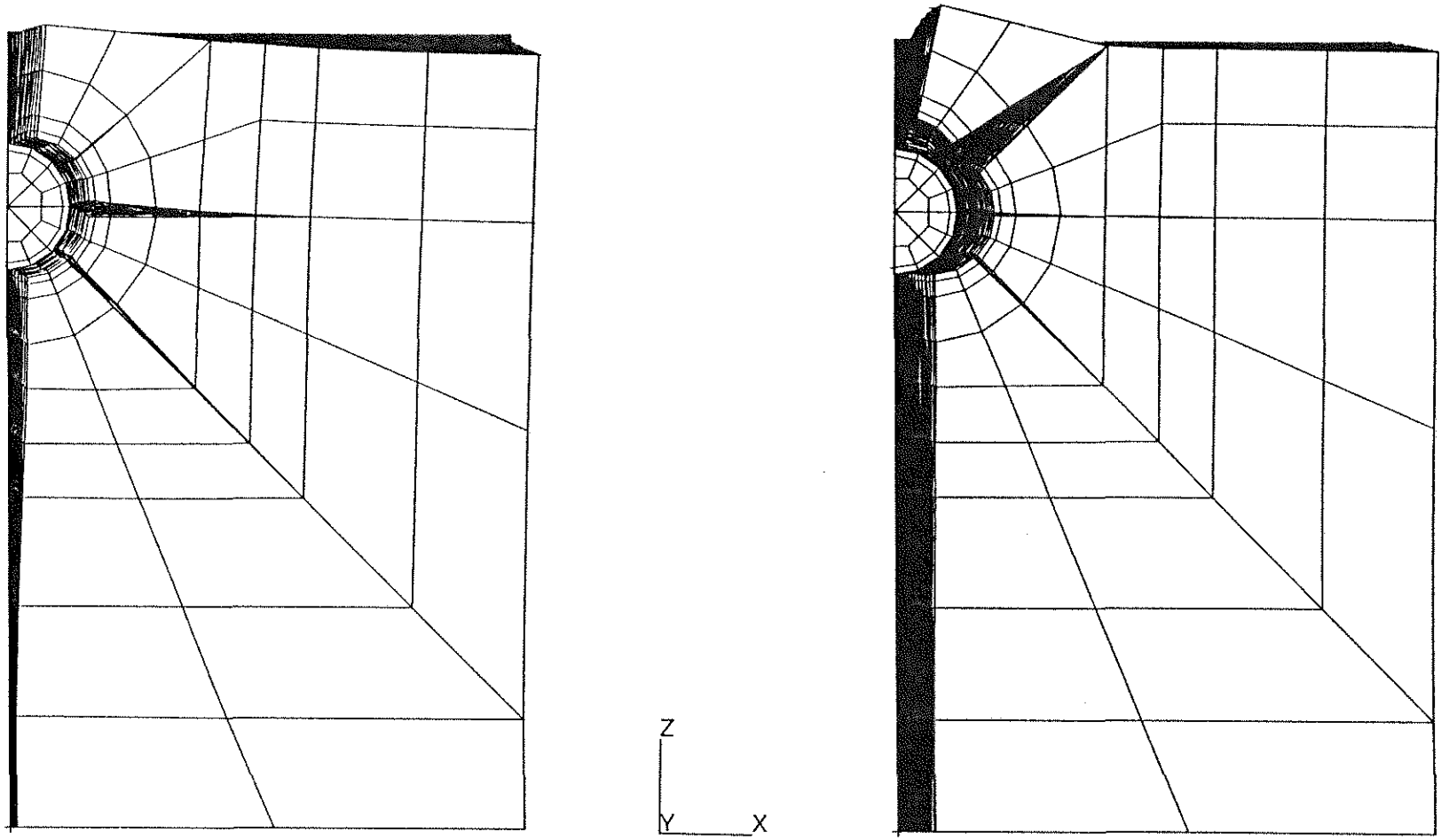

(a) (b)

Fig. 7.32 Deformed shape for multiple-rib model with 6 ribs and 1 in. (25.4 mm) cover, (a) at peak load, (b) bar displacement = 0.012 in. (0.305 mm)

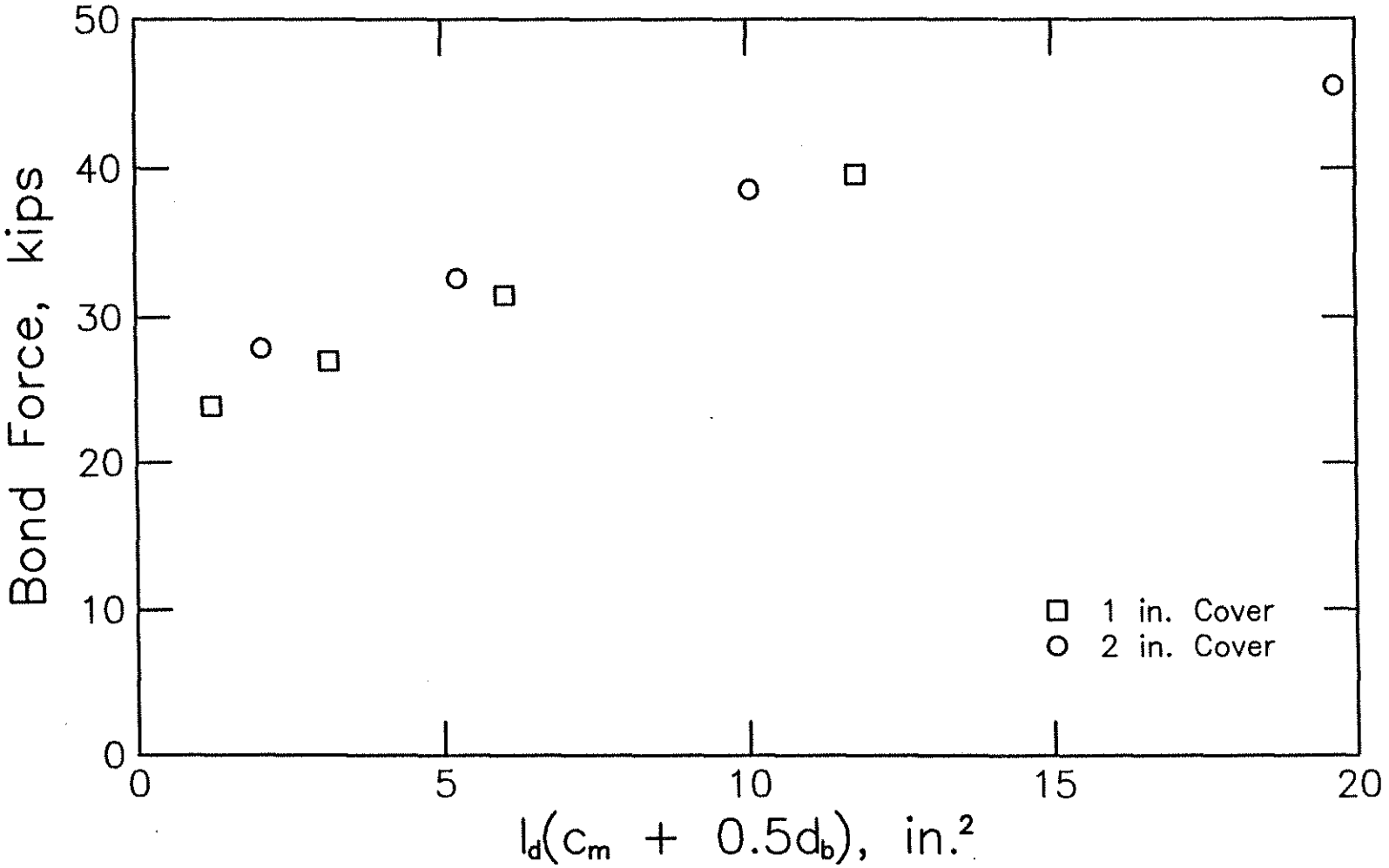

Fig. 7.33 Bar force versus $l_d(c_m + 0.5d_b)$ for multiple rib models (1 in.^{2} = 645 mm^2, 1 kip = 4.45 kN)

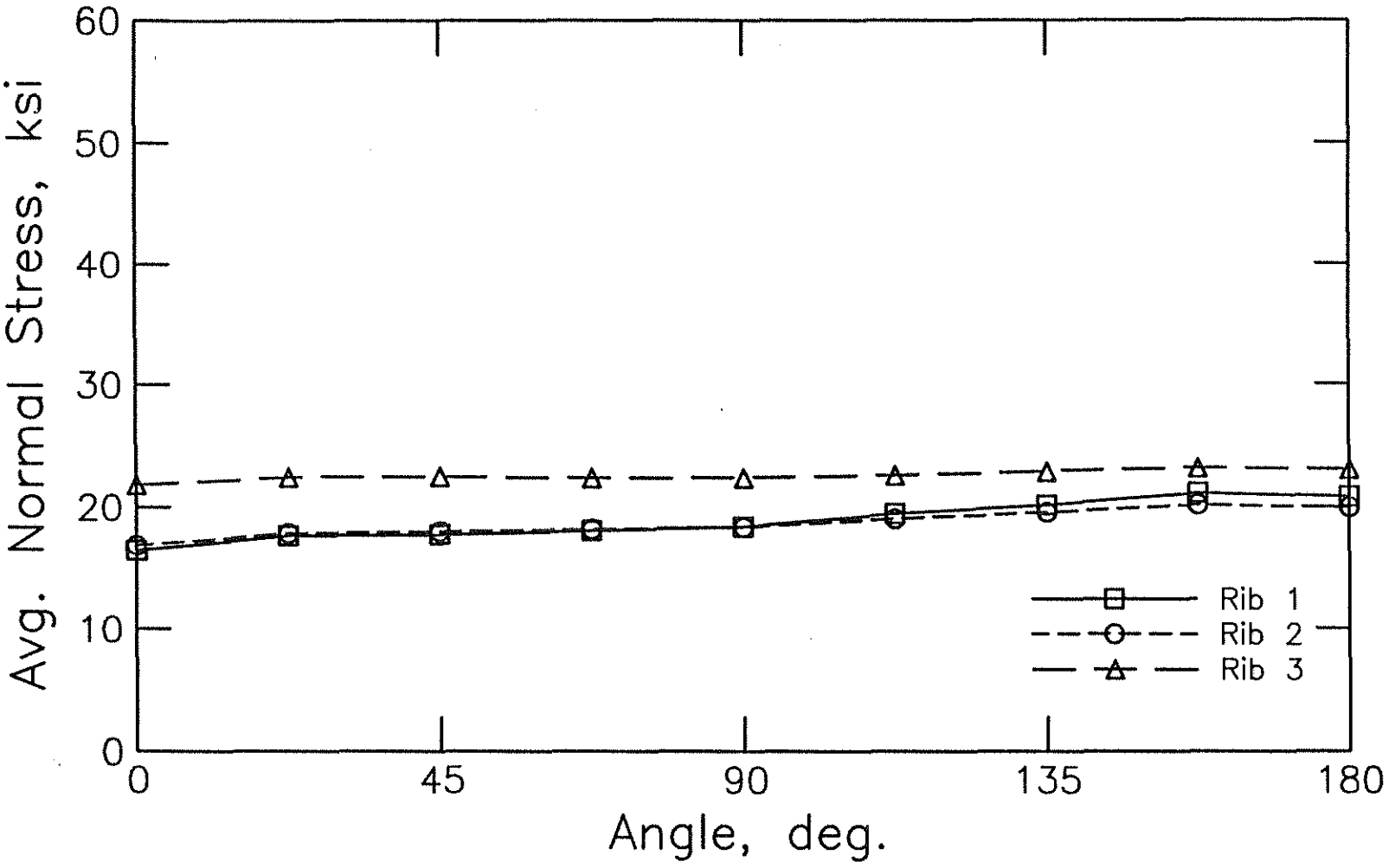

Fig. 7.34a Average normal stress in interface elements around perimeter of bar for 3 rib model with 2 in. (50.8 mm) cover: bar displacement = 0.0055 in. (0.140 mm), bar force = 18,339 lb (81.6 kN) (1 ksi = 6.89 MPa)

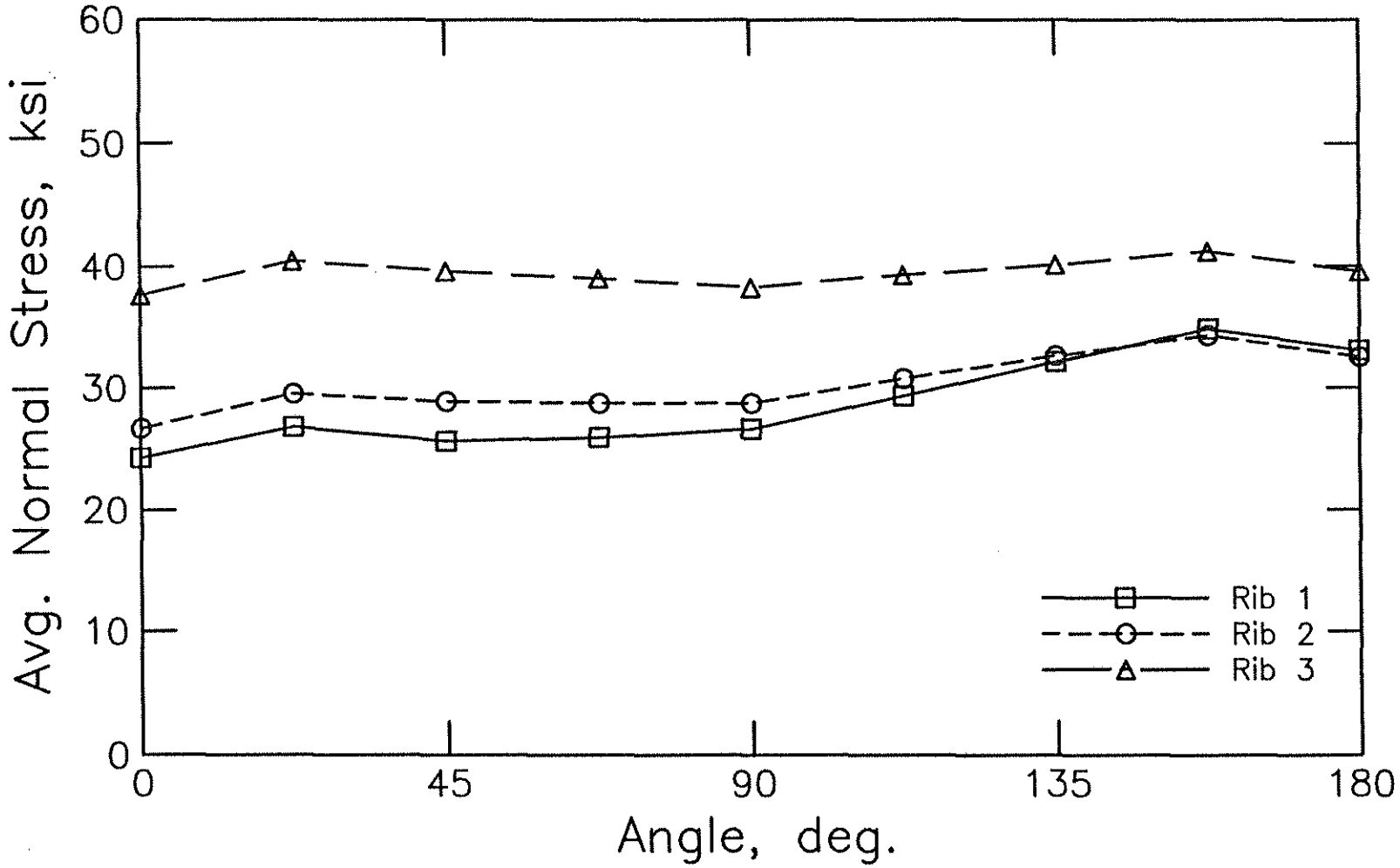

Fig. 7.34b Average normal stress in interface elements around perimeter of bar for 3 rib model with 2 in. (50.8 mm) cover: bar displacement = 0.0105 in. (0.267 mm), bar force = 30,888 lb (137.4 kN) (1 ksi = 6.89 MPa)

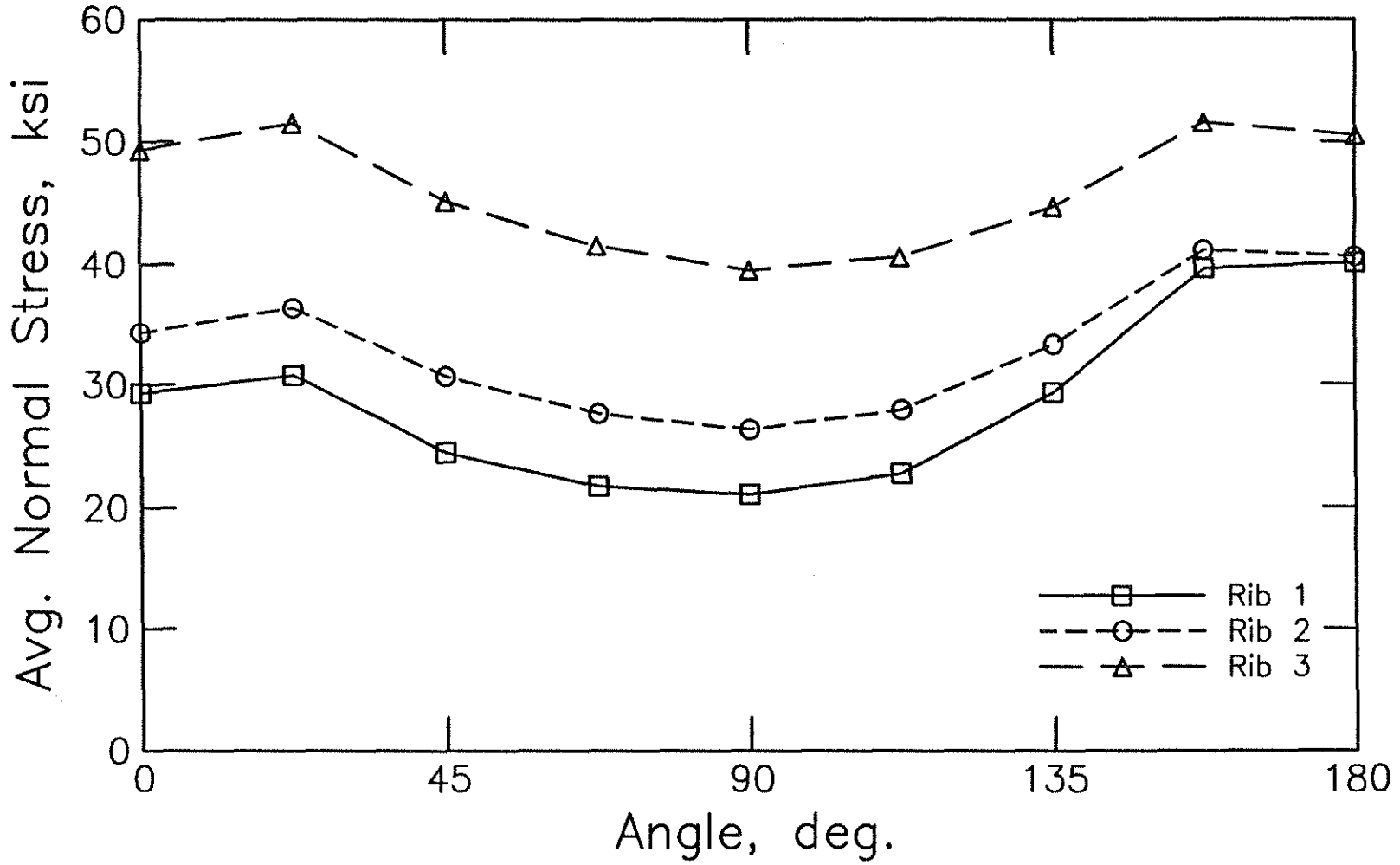

Fig. 7.34c Average normal stress in interface elements around perimeter of bar for 3 rib model with 2 in. (50.8 mm) cover: bar displacement = 0.0144 in. (0.366 mm), bar force = 32,711 lb (145.5 kN) (1 ksi = 6.89 MPa)

APPENDIX A: METHOD FOR MEASURING THE RELATIVE RIB AREA OF REINFORCING BARS

A.1 General

Measurements of the gap width, rib spacing and rib height are used to calculate the relative rib area of reinforcing bars, which is defined as the ratio of the projected rib area normal to the bar axis to the product of the nominal bar perimeter and the average center-to-center rib spacing. The rib heights are measured at ten points around the perimeter of the bar (Fig. A.1), which include points at 45, 90 and 135 degrees relative to a line between the center of the longitudinal ribs and at the base of each longitudinal rib. These measurements are used in equations that describe the radii to the outside of the ribs and to the barrel of the bar which are used, in turn, to calculate the bearing area of the ribs.

A.2 Bar Preparation

A sample of the bar, approximately three feet long, is selected and cleaned to remove dust and debris. The bar is cut so that the bases of the longitudinal ribs are exposed at one end of the bar. Lines are drawn on the end of the bar to mark the 10 positions around the perimeter of the bar where measurements are to be taken (Fig. A.1). First, a line is drawn which connects the center of the two longitudinal ribs (the base line); the midpoint of this line is treated as the centroid of the bar. Lines are then drawn at 45, 90 and 135 degrees relative to the base line, passing through the centroid. The bases of the longitudinal ribs provide the final four positions for obtaining measurements (Fig. A.1). These lines are used to align the bar so that rib height measurements can be taken at these points around the perimeter.

A.3 Measuring Setup

A steel angle and a dial gauge with a pointed tip are used to measure the rib heights (Fig. A.2). The angle is firmly attached to a table and is used to hold the bar at the desired orientation as the measurements are being taken. The dial gauge is mounted on a stand with a magnetic base and positioned so that the tip is directly above the centroid of the bar when the bar is placed in the corner of the angle.

A.4 Measurement Method

The bar is positioned against the side of the angle so that the tip of the dial gauge is aligned with one of the ten positions around the perimeter of the bar. Once the bar is positioned correctly, locking pliers are attached to the bar and used to maintain the desired orientation; the pliers are positioned on the bar so that the outside of one jaw rests against the bottom of the angle. This procedure helps maintain the correct bar orientation as measurements are taken at successive ribs.

The distance from the steel angle to the top of a rib or the barrel of the bar is measured at ten locations, evenly distributed along the length of the bar. Rib heights are equal to the difference between measurements taken at the top of the rib and the barrel of the bar (midway between the measured rib and an adjacent rib). Readings are taken until all ten ribs are measured at the current angle. The bar is then rotated to the next measuring position. The process is repeated for all ten positions around the perimeter of the bar. The rib and barrel measurements for each orientation are averaged to obtain a representative rib profile for the bar. If the stroke of the dial gauge is not sufficient to measure the entire distance from the steel angle to the tops of the ribs, the vertical distance between the angle and the tip of the dial gauge at zero reading is measured. This distance is then added to all dial gauge readings.

The center-to-center rib spacing and gap width for the longitudinal ribs are measured using calipers. The rib spacing is determined by measuring the distance between the faces of two widely separated ribs and dividing by the number of ribs in this distance. The gap widths are measured at the points where the longitudinal ribs meet the barrel of the bar. Five evenly spaced measurements are taken for each rib and averaged.

If the bar has an extra longitudinal rib (or ribs), such as for designating the steel grade, the height and width are also measured. The height is determined by taking the difference between a measurement at the top of the rib and the average of measurements on both sides of the rib where it meets the barrel of the bar. The width is measured similar to the gap width. Measurements on extra longitudinal ribs are taken midway between transverse ribs at ten locations along the bar.

A.5 Calculations

The measurements described in the previous section are used to calculate the relative rib area of the bar, R_r, which is defined as

$$R_r = \frac{\text{projected rib area normal to bar axis}}{\text{nominal bar perimeter} \times \text{center - to - center rib spacing}} \qquad \text{(A.1)}$$

where the nominal bar perimeter is the product of π and the nominal bar diameter.

The first step in determining the projected rib area is to determine the radii of the bar to both the barrel and the top of the ribs. This is done by first determining the diameter of the bar to the outside of the ribs, at each of the positions measured around the perimeter of the bar. Next, by assuming that the barrel of the bar is symmetric about the centroid, the radius of the barrel at each orientation can be determined by

subtracting the average rib heights along each diameter from the appropriate diameter and dividing by two. The outside radius to the top of the ribs for each of the ten orientations is determined by adding the rib height to the appropriate barrel radius. Note that this does not result in a symmetric rib radius about the centroid, but gives the rib radius at ten points around the perimeter of the bar.

The next step is to determine the angles, α, between the base line and lines from the centroid of the bar to the points where the longitudinal ribs meet the barrel of the bar (Fig. A.3). This angle is determined on each side of the base line for each longitudinal rib from

$$\alpha = \arcsin\left(\frac{0.5 \times \text{average gap width}}{\text{radius of the barrel next to the longitudinal rib}}\right) \qquad \text{(A.2)}$$

The projected rib area is calculated by dividing the bar into four quadrants, with each quadrant encompassing an area 90 degrees on either side of the center of a longitudinal rib. The projected rib area for each quadrant is calculated by fitting an equation to the radii of the rib and barrel of the form

$$r = A + B\theta + C\theta^2 + D\theta^3 \qquad \text{(A.3)}$$

where r is the radius of either the rib or barrel of the bar, θ is the angle defined as 0 on a line perpendicular to the base line passing through the centroid (Fig. A.3) and A, B, C and D are constants. The constants are determined from the following constraints:

1) at $\theta = 0$, r = the radius of the rib or barrel at $\theta = 0$ (position 3 or 8 in Fig. A.1)

2) at $\theta = 0$, $dr/d\theta = 0$

3) at $\theta = \pi/4$, r = the radius of the rib or barrel at $\theta = \pi/4$ (position 2, 4, 7 or 9 in Fig. A.1)

4) at $\theta = \pi/2 - \alpha$, r = the radius of the rib or barrel where the longitudinal rib meets the barrel of the bar (position 1, 5, 6 or 10 in Fig. A.1)

The projected rib area, A_p for each quadrant of the bar is then calculated from

$$A_p = \int_0^{\pi/2-\alpha} \frac{r_{rib}^2}{2} d\theta - \int_0^{\pi/2-\alpha} \frac{r_{bar}^2}{2} d\theta \qquad (A.4)$$

where r_{rib} and r_{bar} are the radii of the rib and barrel (r in Eq. A.3) as a function of θ. The values of A_p are summed for the four quadrants to obtain the total bearing area of the rib which is then used in Eq. A.1 to calculate R_r.

If the bar contains an extra longitudinal rib (or ribs), the area of this rib is subtracted from the total projected bearing area. It is assumed that this rib has a parabolic cross-sectional shape with an area equal to 2/3 of the product of the width and the height.

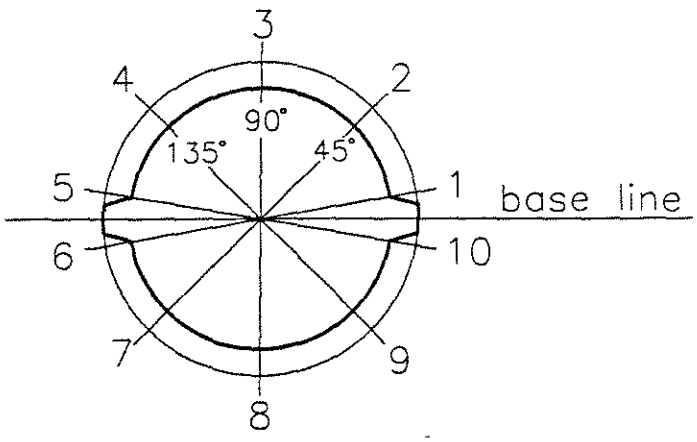

Fig. A.1 Ten positions around the perimeter of the bar where measurements are taken

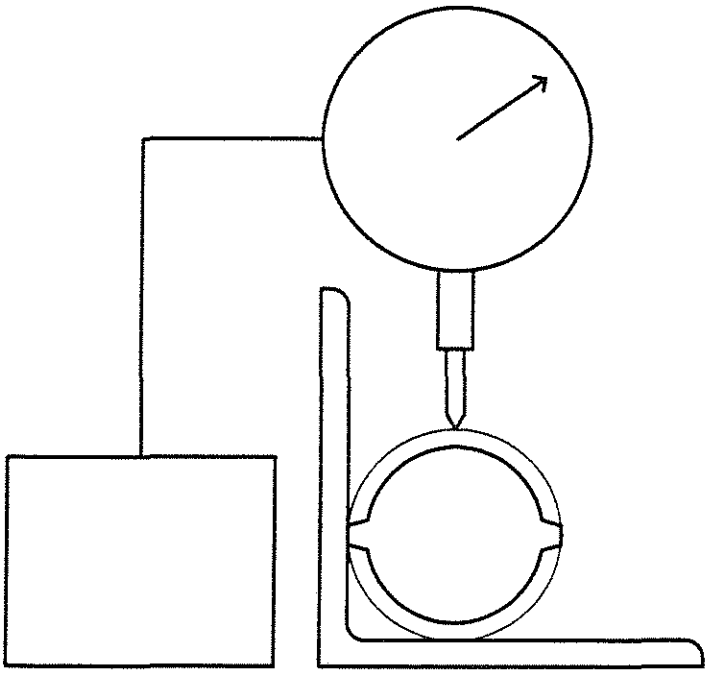

Fig. A.2 Schematic of measuring setup

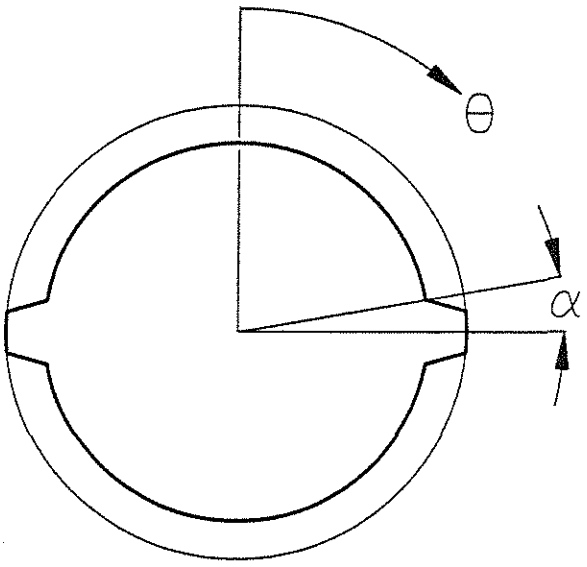

Fig. A.3 Definitions of α and θ for first quadrant

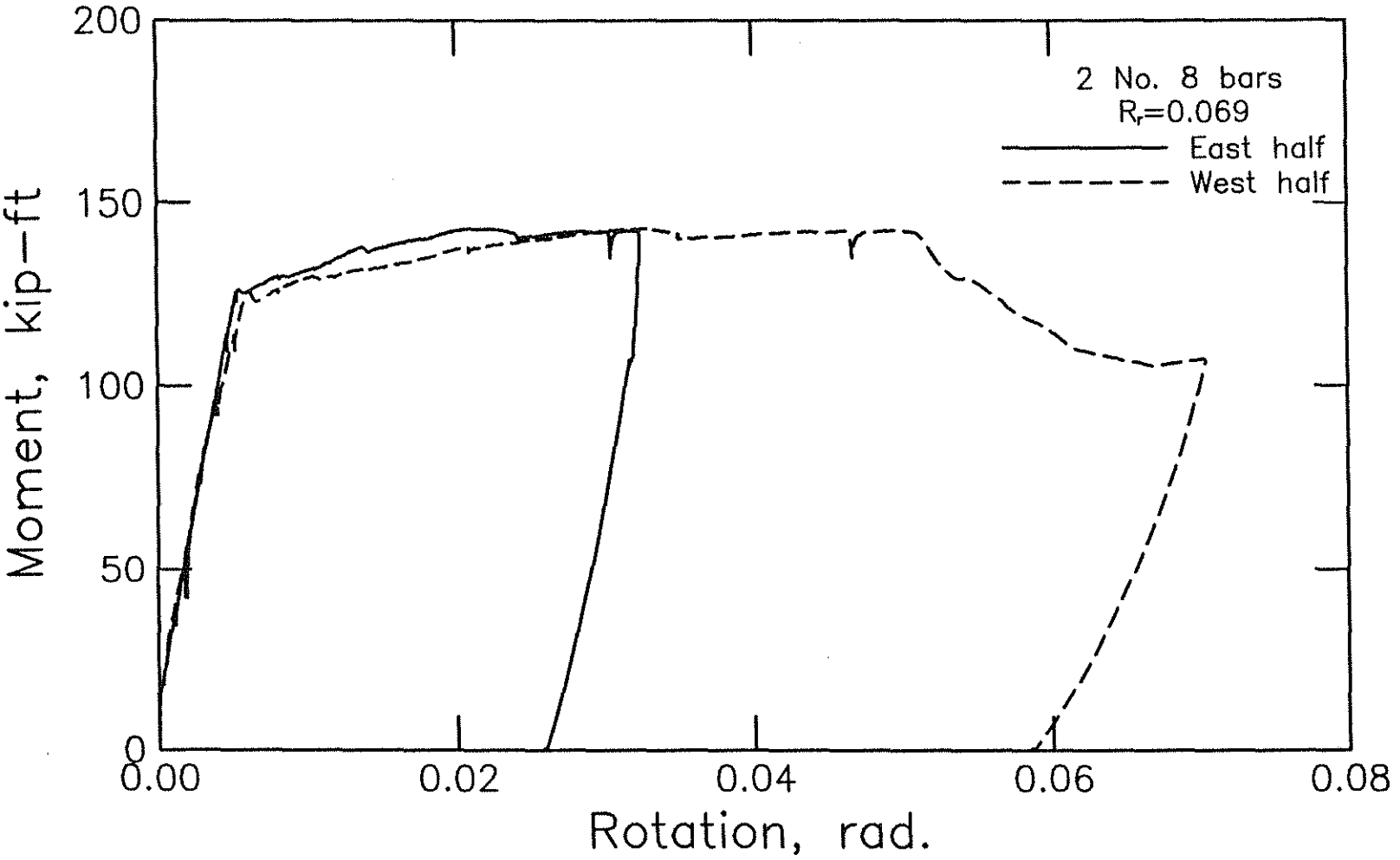

Fig. B.1 Moment-rotation curves for moment-rotation test specimen 16.5, $\rho = 0.43\rho_{bal}$ (1 kip-ft = 1.356 kN-m)

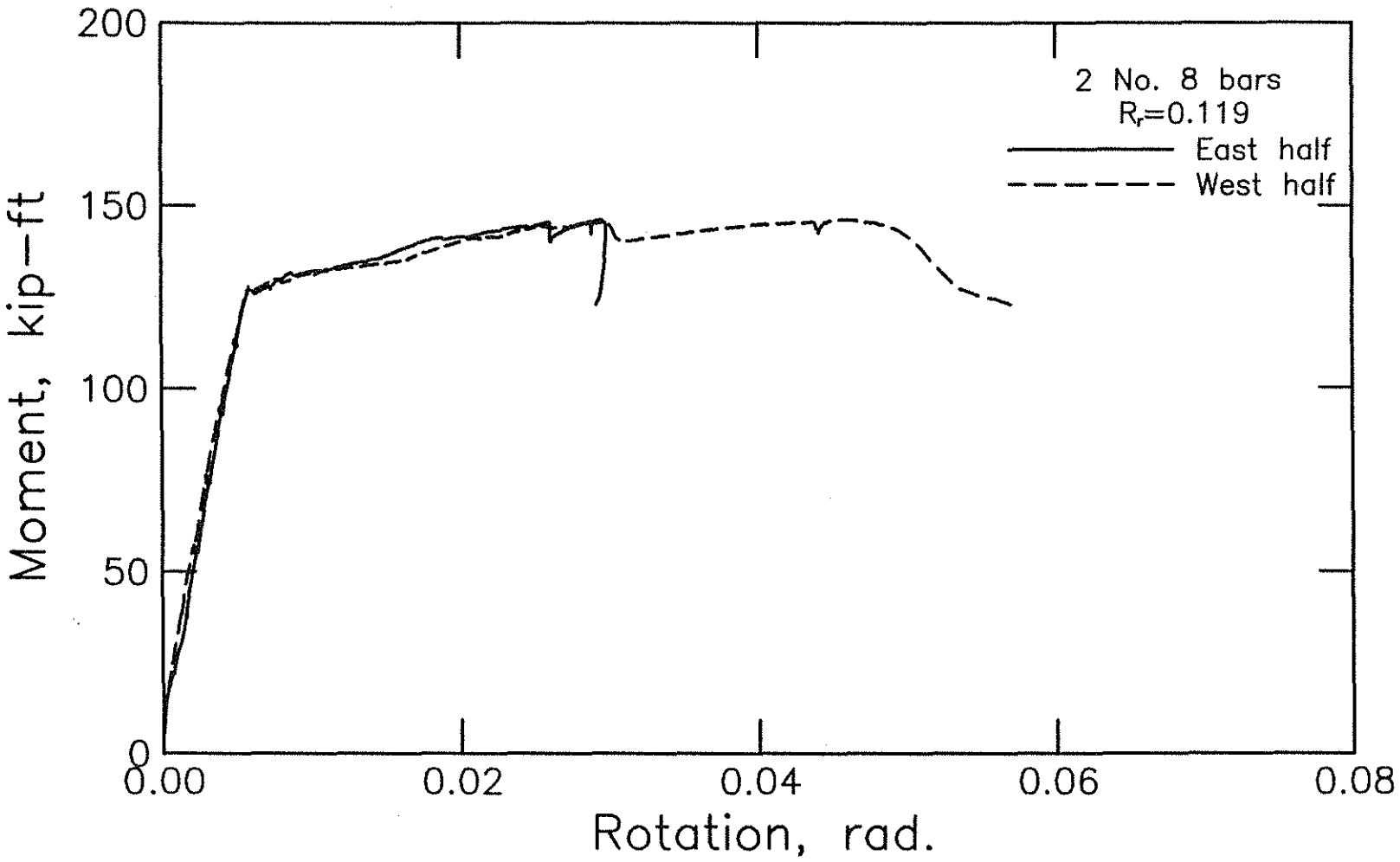

Fig. B.2 Moment-rotation curves for moment-rotation test specimen 16.6, $\rho = 0.43\rho_{bal}$ (1 kip-ft = 1.356 kN-m)

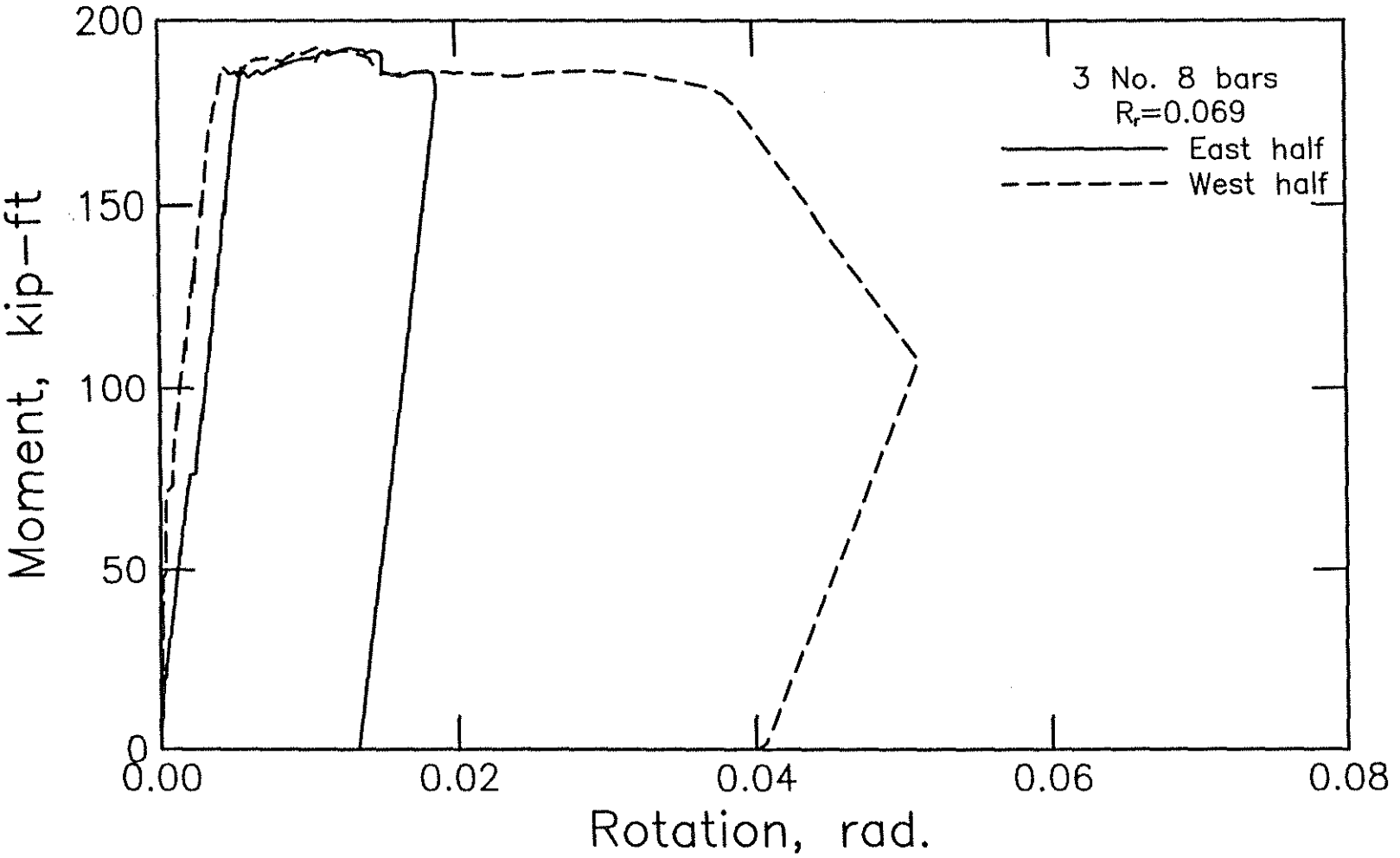

Fig. B.3 Moment-rotation curves for moment-rotation test specimen 17.1, $\rho = 0.68\rho_{bal}$ (1 kip-ft = 1.356 kN-m)

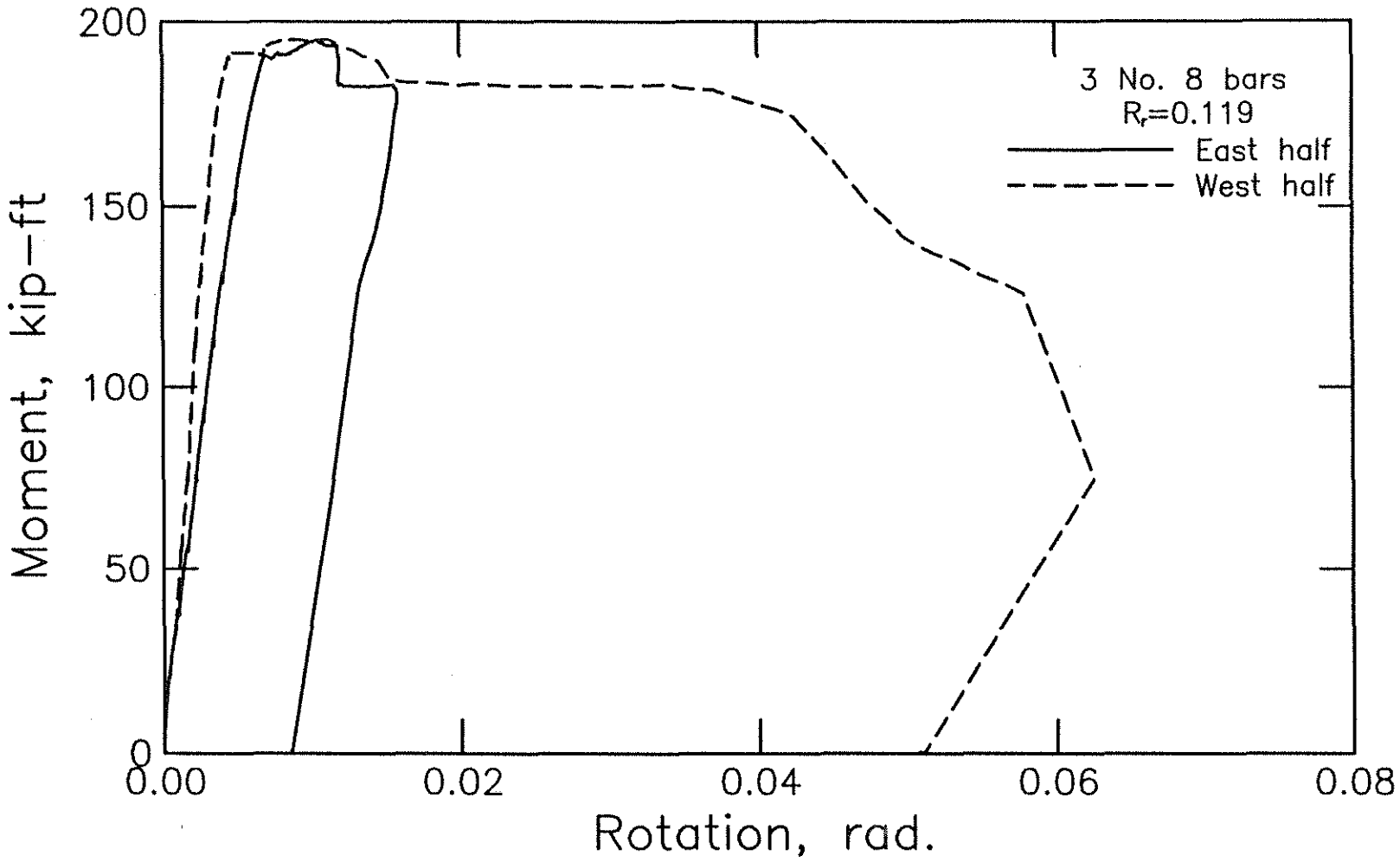

Fig. B.4 Moment-rotation curves for moment-rotation test specimen 17.2, $\rho = 0.68\rho_{bal}$ (1 kip-ft = 1.356 kN-m)

Table C.1

Data and test/prediction ratios for developed and spliced bars without confining reinforcement (cited in section 6.2.4)

Test No.	n	l_s	d_b	A_b	c_{so}	c_{si}	c_b	b	h	d	f'_c	f_y	f_s (test)	f_s (ACI '95)	f_s (Eq. 3.14)	$\frac{f_s(\text{test})}{f_s(\text{ACI '95})}$	$\frac{f_s(\text{test})}{f_s(\text{Eq. 3.14})}$
		(in.)	(in.)	($in.^2$)	(in.)	(in.)	(in.)	(in.)	(in.)	(in.)	(psi)	(ksi)	(ksi)	(ksi)	(ksi)		
Chinn et al. (1955)																	
D31	1	5.50	0.375	0.110	1.470		0.830	3.69	-	-	4700	79.00	60.35	41.90	39.46	1.441	1.530
D36	1	5.50	0.375	0.110	1.470		0.560	3.69	-	-	4410	79.00	48.95	32.36	32.64	1.513	1.500
D10	1	7.00	0.750	0.440	1.060		1.480	3.62	-	-	4370	57.00	26.27	19.68	25.90	1.335	1.014
D20	1	7.00	0.750	0.440	1.125		1.420	3.75	-	-	4230	57.00	26.95	20.23	26.16	1.332	1.030
D22	1	7.00	0.750	0.440	1.095		0.800	3.69	-	-	4480	57.00	23.89	16.31	24.16	1.465	0.989
D13	1	11.00	0.750	0.440	2.905		1.440	7.31	-	-	4820	57.00	48.93	41.07	37.12	1.191	1.318
D14	1	11.00	0.750	0.440	1.095		0.830	3.69	-	-	4820	57.00	32.63	27.27	29.97	1.197	1.089
D15	1	11.00	0.750	0.440	2.875		0.620	7.25	-	-	4290	57.00	42.24	21.24	26.71	1.989	1.581
D21	1	11.00	0.750	0.440	2.905		1.470	7.31	-	-	4480	57.00	43.35	40.25	36.80	1.077	1.178
D29	1	11.00	0.750	0.440	1.095		1.390	3.69	-	-	7480	57.00	44.60	41.44	36.92	1.076	1.208
D3	2	11.00	0.750	0.440	1.500	0.500	1.500	9.00	-	-	4350	57.00	36.86	18.81	25.44	1.960	1.449
D32	1	11.00	0.750	0.440	2.875		1.470	7.25	-	-	4700	57.00	46.05	41.23	37.24	1.117	1.237
D38	1	11.00	0.750	0.440	1.560		1.520	4.62	-	-	3160	57.00	28.16	34.35	34.25	0.820	0.822
D39	1	11.00	0.750	0.440	1.095		1.560	3.69	-	-	3160	57.00	27.62	26.93	29.76	1.025	0.928
D5	1	11.00	0.750	0.440	2.000		1.500	5.50	-	-	4180	57.00	44.34	39.51	36.50	1.122	1.215
D6	2	11.00	0.750	0.440	1.500	0.625	1.160	7.25	-	-	4340	57.00	33.17	21.47	26.85	1.545	1.235
D7	1	11.00	0.750	0.440	1.060		1.270	3.62	-	-	4450	57.00	33.85	31.20	32.02	1.085	1.057
D8	2	11.00	0.750	0.440	1.500	0.625	1.480	7.25	-	-	4570	57.00	35.95	22.03	27.20	1.632	1.322
D9	1	11.00	0.750	0.440	1.060		1.440	3.62	-	-	4380	57.00	34.98	30.95	31.89	1.130	1.097
D34	1	12.50	0.750	0.440	1.060		1.490	3.62	-	-	3800	57.00	36.86	32.76	32.94	1.125	1.119
D12	1	16.00	0.750	0.440	1.125		1.620	3.75	-	-	4530	57.00	45.70	47.86	40.79	0.955	1.120
D17	1	16.00	0.750	0.440	1.095		0.800	3.69	-	-	3580	57.00	39.74	33.33	33.31	1.192	1.193
D19*	1	16.00	0.750	0.440	2.905		1.700	7.31	-	-	4230	57.00	59.93	57.81	49.59	1.037	1.208
D23	1	16.00	0.750	0.440	1.060		0.780	3.62	-	-	4450	57.00	39.23	36.53	34.84	1.074	1.126
D24	1	16.00	0.750	0.440	2.875		0.810	7.25	-	-	4450	57.00	43.18	37.48	35.34	1.152	1.222
D30	1	16.00	0.750	0.440	1.095		1.560	3.69	-	-	7480	57.00	52.88	60.27	45.67	0.877	1.158
D4	2	16.00	0.750	0.440	1.500	0.500	1.500	9.00	-	-	4470	57.00	46.84	27.73	30.19	1.689	1.552
D40	1	16.00	0.750	0.440	2.940		0.750	7.38	-	-	5280	57.00	50.55	38.75	35.84	1.304	1.411
D25*	1	24.00	0.750	0.440	1.060		1.530	3.62	-	-	5100	57.00	58.25	72.87	53.31	0.799	1.093
D26	1	24.00	0.750	0.440	1.095		0.750	3.69	-	-	5100	57.00	55.87	57.13	45.26	0.978	1.234
D35	1	24.00	0.750	0.440	1.060		1.450	3.62	-	-	3800	57.00	54.99	62.90	49.53	0.874	1.110
D33	1	20.25	1.410	1.560	1.990		1.550	6.80	-	-	4830	57.00	28.20	21.28	29.63	1.325	0.952
Chamberlin (1956)																	
SII15	1	6.00	0.500	0.200	0.500		1.000	6.00	6.00	4.75	4470	-	34.52	20.06	26.13	1.721	1.321
SII16	1	6.00	0.500	0.200	0.750		1.000	6.00	6.00	4.75	4470	-	38.11	26.74	29.66	1.425	1.285
SIII31	1	6.00	0.500	0.200	0.500		1.000	6.00	6.00	4.75	5870	-	39.66	22.98	27.97	1.725	1.418
SIII32	1	6.00	0.500	0.200	0.750		1.000	6.00	6.00	4.75	5870	-	46.37	30.65	31.76	1.513	1.460
SIII33	1	6.00	0.500	0.200	1.000		1.000	6.00	6.00	4.75	5870	-	48.45	38.31	35.54	1.265	1.363
SII11	1	10.67	0.500	0.200	0.500		1.000	6.00	6.00	4.75	3680	-	41.17	32.35	32.74	1.273	1.257
SIII27	1	10.67	0.500	0.200	0.500		1.000	6.00	6.00	4.75	5870	-	46.43	40.86	36.80	1.136	1.262
SIII28	1	10.67	0.500	0.200	0.750		1.000	6.00	6.00	4.75	5870	-	49.32	54.48	43.52	0.905	1.133
SIII29	1	10.67	0.500	0.200	1.000		1.000	6.00	6.00	4.75	5870	-	49.32	68.10	50.24	0.724	0.982
SIV53	2	12.00	0.500	0.200	2.000	0.500	1.000	6.00	6.00	4.75	4540	-	46.95	40.43	36.87	1.161	1.273
SII23	1	16.00	0.750	0.440	0.750		1.000	9.00	9.00	7.63	4470	-	41.89	35.66	34.37	1.175	1.219
Chamberlin (1958)																	
3a	2	6.00	0.500	0.200	0.500	1.500	1.000	6.00	6.00	4.75	4450	50.00	32.78	20.01	26.10	1.638	1.256
3b	2	6.00	0.500	0.200	0.500	1.000	1.000	6.00	6.00	4.75	4450	50.00	33.00	20.01	26.10	1.649	1.264
3c	2	6.00	0.500	0.200	0.500	0.500	1.000	6.00	6.00	4.75	4450	50.00	33.48	20.01	26.10	1.673	1.283
4a	1	6.00	0.500	0.200	2.500		1.000	6.00	6.00	4.75	4370	50.00	42.64	33.05	33.01	1.290	1.292
4b	1	6.00	0.500	0.200	2.250		1.000	6.00	6.00	4.75	4370	50.00	43.89	33.05	33.01	1.328	1.330
4c	1	6.00	0.500	0.200	2.000		1.000	6.00	6.00	4.75	4370	50.00	43.32	33.05	33.01	1.311	1.312
Ferguson and Breen (1965)																	
8R18a	2	18.00	1.000	0.790	3.250	3.265	1.750	17.03	14.97	12.72	3470	99.00	41.32	31.81	36.96	1.299	1.118
8R24a	2	24.00	1.000	0.790	3.250	3.310	1.670	17.12	15.03	12.86	3530	99.00	58.88	41.26	43.55	1.427	1.352
8F30a	2	30.00	1.000	0.790	3.250	3.295	1.530	17.09	14.97	12.94	3030	74.00	52.78	44.70	46.63	1.181	1.132
8F36a*	2	36.00	1.000	0.790	3.250	3.330	1.410	17.16	15.00	13.09	4650	63.50	66.34	62.52	56.57	1.061	1.173
8F36b	2	36.00	1.000	0.790	3.250	3.220	1.400	16.94	15.03	13.13	3770	74.00	61.30	56.00	53.48	1.095	1.146
8F36k	2	36.00	1.000	0.790	1.420	1.425	1.380	9.69	15.09	13.21	3460	74.00	54.65	53.08	51.95	1.030	1.052
8F39a*	2	39.00	1.000	0.790	3.250	3.280	1.530	17.06	15.09	13.06	3650	63.50	72.90	63.77	59.07	1.143	1.234
8F42a*	2	42.00	1.000	0.790	3.250	3.345	1.500	17.19	15.09	13.09	2660	63.50	65.93	57.76	57.08	1.141	1.155
8F42b*	2	42.00	1.000	0.790	3.250	3.330	1.450	17.16	15.03	13.08	3830	63.50	73.54	67.58	61.34	1.088	1.199
8R42a	2	42.00	1.000	0.790	3.250	3.345	1.560	17.19	15.00	12.94	3310	99.00	71.01	66.37	61.66	1.070	1.152
8R48a	2	48.00	1.000	0.790	3.250	3.265	1.480	17.03	15.00	13.02	3040	99.00	72.88	69.87	64.92	1.043	1.123
8R64a	2	64.00	1.000	0.790	3.250	3.295	1.520	17.09	15.00	12.98	3550	99.00	89.71	102.70	86.51	0.873	1.037

Table C.1

Data and test/prediction ratios for developed and spliced bars without confining reinforcement (continued)

Test No.	n	l_s	d_b	A_b	c_{so}	c_{si}	c_b	b	h	d	f'_c	f_y	f_s (test)	f_s (ACI '95)	f_s (Eq. 3.14$^+$)	$\frac{f_s(\text{test})}{f_s(\text{ACI '95})}$	$\frac{f_s(\text{test})}{f_s(\text{Eq. 3.14}^+)}$
		(in.)	(in.)	(in.^{2})	(in.)	(in.)	(in.)	(in.)	(in.)	(in.)	(psi)	(ksi)	(ksi)	(ksi)	(ksi)		
8R80a	2	80.00	1.000	0.790	3.250	3.265	1.500	17.03	15.03	13.03	3740	99.00	96.41	130.47	104.95	0.739	0.919
11R24a	2	33.00	1.410	1.560	4.590	4.635	1.670	24.09	18.09	15.72	3720	93.00	51.81	32.06	37.01	1.616	1.400
11R30a	2	41.25	1.410	1.560	4.590	4.635	1.310	24.09	18.09	16.08	4030	93.00	58.50	35.39	39.12	1.653	1.495
11F36a	2	49.50	1.410	1.560	4.590	4.635	1.500	24.09	18.00	15.79	4570	73.00	64.16	49.48	48.12	1.297	1.333
11F36b	2	49.50	1.410	1.560	4.590	4.605	1.470	24.03	18.00	15.83	3350	65.00	59.20	41.79	44.12	1.417	1.342
11F42a	2	57.75	1.410	1.560	4.590	4.590	1.480	24.00	18.00	15.82	3530	65.00	63.61	50.28	49.87	1.265	1.276
11F48a*	2	66.00	1.410	1.560	4.590	4.620	1.530	24.16	18.03	15.80	3140	73.00	74.56	55.44	54.21	1.345	1.375
11F48b*	2	66.00	1.410	1.560	4.590	4.665	1.580	24.15	18.22	15.93	3330	65.00	72.24	58.37	55.92	1.238	1.292
11R48a	2	66.00	1.410	1.560	4.590	4.670	1.500	24.16	18.03	15.83	5620	93.00	82.22	73.17	62.08	1.124	1.324
11R48b	2	66.00	1.410	1.560	4.590	4.700	2.060	24.22	18.19	15.43	3100	93.00	71.43	68.14	63.49	1.048	1.125
11F60a*	2	82.50	1.410	1.560	4.590	4.575	1.590	23.97	18.09	15.83	2610	73.00	84.80	64.87	62.59	1.307	1.355
11F60b*	2	82.50	1.410	1.560	4.590	4.590	1.500	24.00	18.09	15.92	4090	65.00	78.02	78.02	67.88	1.000	1.149
11R60a	2	82.50	1.410	1.560	4.590	4.590	1.410	24.00	18.12	16.01	2690	93.00	74.61	60.69	59.19	1.229	1.260
11R60b	2	82.50	1.410	1.560	4.590	4.575	1.750	24.00	18.03	15.58	3460	93.00	87.80	79.90	70.83	1.099	1.240
Thompson et al. (1975)																	
6-12-4/2/2-6/6	6	12.00	0.750	0.440	2.000	2.000	2.000	33.00	13.00	10.63	3730	61.70	57.40	40.72	43.36	1.410	1.324
8-18-4/3/2-6/6	6	18.00	1.000	0.790	2.000	2.000	3.000	36.00	13.00	9.50	4710	59.30	56.26	41.18	42.58	1.366	1.321
8-18-4/3/2.5-4/6	6	18.00	1.000	0.790	2.500	2.000	3.000	36.00	13.00	9.50	2920	59.30	49.33	32.42	37.78	1.521	1.306
8-24-4/2/2-6/6	6	24.00	1.000	0.790	2.000	2.000	2.000	36.00	13.00	10.50	3105	59.30	50.64	44.58	46.43	1.136	1.091
11-25-6/2/3-5/5	5	25.00	1.410	1.560	3.000	3.000	2.000	44.06	13.01	10.30	3920	66.30	44.19	28.40	34.41	1.556	1.284
11-30-4/2/2-6/6	6	30.00	1.410	1.560	2.000	2.000	2.000	40.88	13.01	10.30	2865	60.50	37.99	29.13	35.40	1.304	1.073
11-30-4/2/4-6/6	6	30.00	1.410	1.560	4.000	2.000	2.000	44.88	13.01	10.30	3350	63.40	44.39	31.50	36.81	1.409	1.206
11-30-4/2/2.7-4/6	4	30.00	1.410	1.560	2.700	2.000	2.000	44.88	13.01	10.30	4420	63.30	57.59	36.18	39.45	1.592	1.460
11-45-4/1/2-6/6	6	45.00	1.410	1.560	2.000	2.000	1.000	40.88	13.01	11.30	3520	60.50	45.28	30.53	36.04	1.483	1.256
14-60-4/2/2-5/5	5	60.00	1.693	2.250	2.000	2.000	2.000	37.50	16.15	13.30	2865	57.70	45.23	42.53	45.29	1.063	0.999
14-60-4/2/4-5/5	5	60.00	1.693	2.250	4.000	2.000	2.000	41.50	16.00	13.15	3200	57.70	56.64	44.94	46.56	1.260	1.217
Zekany (1981)																	
9-S3-B-N	5	16.00	1.128	1.000	2.000	1.423	2.000	27.25	16.00	13.44	5650	62.80	47.56	25.04	32.07	1.899	1.483
N-N-80B	4	22.00	1.410	1.560	2.000	1.849	2.000	27.25	16.01	13.30	3825	60.10	37.96	23.30	30.94	1.629	1.227
Choi et al. (1990a, 1991)																	
1-5N0120U	2	12.00	0.625	0.310	2.000	2.000	1.000	10.50	16.00	14.69	5360	63.80	61.51	49.20	41.10	1.250	1.497
1-5N0120U*	3	12.00	0.625	0.310	2.000	2.000	1.000	15.75	16.00	14.69	5360	63.80	63.99	49.20	41.10	1.301	1.557
2-6C0120U	2	12.00	0.750	0.440	2.000	2.000	1.000	11.00	16.01	14.63	6010	70.90	51.40	37.90	35.32	1.356	1.455
2-6S0120U	2	12.00	0.750	0.440	2.000	2.000	1.000	11.00	16.01	14.63	6010	63.80	45.75	37.90	35.32	1.207	1.295
3-8N0160U	2	16.00	1.000	0.790	2.000	2.000	1.500	12.00	16.00	14.00	5980	63.80	43.02	32.99	36.97	1.304	1.164
3-8S0160U	2	16.00	1.000	0.790	2.000	2.000	1.500	12.00	14.00	12.00	5980	67.00	42.82	32.99	36.97	1.298	1.158
4-11C0240U	2	24.00	1.410	1.560	2.000	2.000	2.000	13.65	16.01	13.30	5850	63.10	37.82	33.30	37.18	1.136	1.017
4-11S0240U	2	24.00	1.410	1.560	2.000	2.000	2.000	13.65	16.01	13.30	5850	64.60	40.22	33.30	37.18	1.208	1.082
Hester et al. (1991, 1993)																	
1-8N3160U	3	16.00	1.000	0.790	2.000	1.500	2.000	16.00	16.00	13.50	5990	63.80	50.03	33.02	36.98	1.515	1.353
2-8C3160U	3	16.00	1.000	0.790	2.000	1.500	1.840	16.00	16.33	13.99	6200	69.00	46.24	33.60	37.30	1.376	1.240
3-8S3160U	3	16.00	1.000	0.790	2.000	1.500	2.040	16.09	16.23	13.69	6020	71.10	46.81	33.10	37.03	1.414	1.264
4-8S3160U	3	16.00	1.000	0.790	2.000	1.500	2.100	16.08	16.22	13.62	6450	71.10	42.40	34.27	37.67	1.237	1.125
5-8C3160U	3	16.00	1.000	0.790	2.000	1.500	2.050	16.09	16.27	13.72	5490	69.00	39.82	31.61	36.19	1.260	1.101
6-8C3220U	3	22.75	1.000	0.790	2.000	1.500	2.150	16.06	16.19	13.54	5850	69.00	51.85	46.40	45.27	1.117	1.145
7-8C3160U	2	16.00	1.000	0.790	2.000	4.000	2.120	16.03	16.20	13.58	5240	69.00	45.37	38.61	40.67	1.175	1.116
Rezansoff et al. (1993)																	
2a	3	29.53	0.992	0.775	1.827	0.994	2.008	13.58	12.99	10.49	3958	64.52	58.56	37.50	40.60	1.562	1.442
2b	3	29.53	0.992	0.775	1.827	0.994	2.008	13.58	12.99	10.49	3799	64.52	58.63	36.73	40.18	1.596	1.459
5a	3	35.43	1.177	1.085	1.819	1.183	2.008	15.43	20.00	17.40	4031	68.87	56.08	38.35	41.13	1.462	1.364
5b	3	44.29	1.177	1.085	1.819	1.183	2.008	15.43	20.00	17.40	3726	68.87	65.83	46.09	46.70	1.428	1.410
Azizinamini et al. (1993)																	
BB-8-5-23	2	23.00	1.000	0.790	1.000	1.500	1.000	9.00	14.00	12.50	5290	77.85	47.01	33.46	37.39	1.405	1.257
AB83-8-15-41	2	41.00	1.000	0.790	1.000	1.500	1.000	9.00	14.00	12.50	15120	77.85	73.07	82.00	70.17	0.891	1.041
BB-11-5-24	2	24.00	1.410	1.560	1.410	1.770	1.410	12.00	16.00	13.89	5080	70.80	29.73	24.26	31.56	1.225	0.942
BB-11-5-40	2	40.00	1.410	1.560	1.410	1.770	1.410	12.00	16.00	13.89	5080	70.80	43.03	40.44	41.91	1.064	1.027
BB-11-12-24	2	24.00	1.410	1.560	1.410	1.770	1.410	12.00	16.00	13.89	12730	70.80	44.72	34.04	39.71	1.314	1.126
B-11-12-40	2	40.00	1.410	1.560	1.410	1.770	1.410	12.00	16.00	13.89	13000	70.80	58.78	56.74	53.00	1.036	1.109
BB-11-11-45	3	45.00	1.410	1.560	1.410	1.680	1.410	18.00	18.00	15.89	10900	70.80	48.90	63.83	54.63	0.766	0.895
BB-11-15-36	3	36.00	1.410	1.560	1.410	1.680	1.410	18.00	18.00	15.89	14550	70.80	57.34	51.06	51.15	1.123	1.121
BB-11-5-36	3	36.00	1.410	1.560	1.410	1.680	1.410	18.00	18.00	15.89	6170	73.72	46.75	40.11	41.28	1.166	1.133
BB-11-13-40	3	40.00	1.410	1.560	1.410	1.680	1.410	18.00	18.00	15.89	13600	73.72	57.70	56.74	53.60	1.017	1.076
BB-11-15-13	2	13.00	1.410	1.560	1.410	1.770	1.410	12.00	16.00	13.89	14330	73.72	30.06	18.44	31.68	1.630	0.949
AB83-11-15-57.5	2	57.50	1.410	1.560	1.410	1.770	1.410	12.00	16.00	13.89	13870	73.72	71.66	81.56	68.42	0.879	1.047
AB89-11-15-80	2	80.00	1.410	1.560	1.410	1.770	1.410	12.00	16.00	13.89	15120	73.72	71.17	113.48	89.02	0.627	0.799

Table C.1

Data and test/prediction ratios for developed and spliced bars without confining reinforcement (continued)

Test No.	n	l_s	d_b	A_b	c_{so}	c_{si}	c_b	b	h	d	f'_c	f_y	f_s (test)	f_s (ACI '95)	f_s (Eq. 3.14+)	f_s(test) / f_s(ACI '95)	f_s(test) / f_s(Eq. 3.14+)
		(in.)	(in.)	($in.^2$)	(in.)	(in.)	(in.)	(in.)	(in.)	(in.)	(psi)	(ksi)	(ksi)	(ksi)	(ksi)		
Idun and Darwin (1995)																	
1.1	2	16.00	1.000	0.790	2.969	2.938	2.938	16.08	17.22	13.76	5020	67.70	51.63	37.79	49.33	1.366	1.047
1.2	2	16.00	1.000	0.790	2.032	2.281	1.938	24.06	16.25	13.79	5020	67.70	44.60	36.85	39.63	1.210	1.125
1.3	3	16.00	1.000	0.790	2.032	1.438	1.938	16.07	16.21	13.75	5020	67.70	45.01	29.29	34.79	1.537	1.294
2.4	2	24.00	1.000	0.790	2.000	1.914	1.313	12.13	15.64	13.79	5250	75.40	54.08	42.04	42.84	1.286	1.262
2.5	2	24.00	1.000	0.790	2.063	1.856	1.813	12.13	16.01	13.67	5250	75.40	58.67	53.63	50.20	1.094	1.169
4.5	2	24.00	1.000	0.790	2.063	1.936	1.844	12.12	16.15	13.79	4090	67.70	51.06	47.97	47.59	1.064	1.073
6.5	2	24.00	1.000	0.790	2.000	1.906	1.969	12.10	16.13	13.63	4220	75.40	53.59	50.02	48.82	1.071	1.098
8.3	2	24.00	1.000	0.790	2.000	1.953	2.000	12.11	16.05	13.53	3830	78.00	61.47	48.58	48.29	1.265	1.273
10.2	2	26.00	1.000	0.790	2.063	1.875	1.933	12.13	16.25	13.78	4250	80.60	61.17	53.67	51.24	1.140	1.194
Current Study																	
13.4	3	16.00	0.625	0.310	2.094	1.016	1.354	12.19	15.60	13.92	4110	61.80	59.96	58.12	46.57	1.032	1.287
14.3*	3	17.00	0.625	0.310	2.032	1.031	1.295	12.14	15.51	13.89	4200	61.80	62.84	63.17	49.19	0.995	1.277
15.5	2	40.00	1.410	1.560	3.063	2.984	1.908	18.05	16.12	13.47	5250	80.60	54.12	50.79	48.39	1.066	1.118
16.2	2	40.00	1.410	1.560	3.016	2.969	1.895	18.07	16.28	13.64	5180	80.60	52.38	50.20	48.07	1.043	1.090
															Max.	1.989	1.581
															Min.	0.627	0.799
															Avg.	1.251	1.211
															St. Dev.	0.254	0.157
															COV	0.203	0.130

* Specimens with $f_s > f_y$

\- Data is not available

$$+ \quad \text{Eq. 3.14} = \frac{l_d}{d_b} = \frac{\dfrac{f_y}{f_c'^{1/4}} - 1900}{72\left(\dfrac{c + K_{tr}}{d_b}\right)}$$

1 in. = 25.4 mm; 1 psi = 6.89 kPa; 1 ksi = 6.89 MPa

Table D.1a
Splice data for beams in lateral load resisting frame system

Splice	Top	Spliced Bars* A Bars		B Bars		Cover			Transverse Reinf.		f'_c
						c_b	c_{so}	c_{si}	A_{tr}/n	s	
No.	Bar	# bars	d_b (in.)	# bars	d_b (in.)	(in.)	(in.)	(in.)	($in.^2$)	(in.)	(psi)
1	Y	4	1.410	4	1.410	2.125	NA	2.410	0.310	15.0	6000
2	N	2	1.410	2	1.410	2.125	2.125	2.600	0.155	15.0	6000
3	N	2	1.128	2	1.128	2.125	2.125	2.600	0.155	15.0	6000
4	Y	4	1.410	4	1.410	2.125	NA	2.410	0.310	15.0	6000
5	N	2	1.410	2	1.410	2.125	2.125	2.600	0.155	15.0	6000
6	N	2	1.128	2	1.128	2.125	2.125	2.600	0.155	15.0	6000
7	Y	6	1.410	6	1.410	2.125	NA	0.880	0.207	13.0	6000
8	N	4	1.270	6	1.270	2.125	2.125	2.180	0.310	13.0	6000
9	Y	6	1.410	6	1.410	2.125	NA	0.880	0.207	13.0	6000
10	N	4	1.270	6	1.270	2.125	2.125	2.180	0.310	13.0	6000
11	Y	6	1.410	6	1.410	2.125	NA	0.880	0.207	13.0	6000
12	N	4	1.270	6	1.270	2.125	2.125	2.180	0.310	13.0	6000
13	Y	6	1.410	6	1.410	2.125	NA	0.880	0.207	13.0	6000
14	N	4	1.270	6	1.270	2.125	2.125	2.180	0.310	13.0	6000
15	Y	4	1.270	6	1.270	2.125	NA	2.080	0.310	15.0	6000
16	N	4	1.410	4	1.410	2.125	2.125	2.410	0.310	15.0	6000
17	Y	4	1.270	6	1.270	2.125	NA	2.080	0.310	15.0	6000
18	N	4	1.410	4	1.410	2.125	2.125	2.410	0.310	15.0	6000
19	Y	4	1.270	6	1.270	2.125	NA	2.080	0.310	15.0	6000
20	N	4	1.270	4	1.410	2.125	2.125	2.510	0.310	15.0	6000
21	Y	4	1.270	6	1.270	2.125	NA	2.080	0.310	15.0	6000
22	N	4	1.270	4	1.410	2.125	2.125	2.510	0.310	15.0	6000
23	Y	4	1.410	6	1.270	2.125	NA	2.080	0.310	15.0	6000
24	N	4	1.410	4	1.410	2.125	2.125	2.510	0.310	15.0	6000
25	Y	4	1.410	6	1.270	2.125	NA	2.080	0.310	15.0	6000
26	N	4	1.410	4	1.410	2.125	2.125	2.510	0.310	15.0	6000
27	Y	4	1.270	6	1.270	2.125	NA	2.080	0.310	15.0	6000
28	N	4	1.410	4	1.410	2.125	2.125	2.410	0.310	15.0	6000
29	Y	4	1.270	6	1.270	2.125	NA	2.080	0.310	15.0	6000
30	N	4	1.410	4	1.410	2.125	2.125	2.410	0.310	15.0	6000
31	Y	4	1.410	6	1.410	2.125	NA	1.940	0.310	15.0	5000
32	N	4	1.270	6	1.270	2.125	2.125	2.080	0.310	15.0	5000
33	Y	4	1.410	6	1.410	2.125	NA	1.940	0.310	15.0	5000
34	N	4	1.270	6	1.270	2.125	2.125	2.080	0.310	15.0	5000
35	Y	4	1.410	6	1.410	2.125	NA	1.940	0.310	15.0	5000
36	N	4	1.270	6	1.270	2.125	2.125	2.080	0.310	15.0	5000
37	Y	4	1.410	6	1.410	2.125	NA	1.940	0.310	15.0	5000
38	N	4	1.270	6	1.270	2.125	2.125	2.080	0.310	15.0	5000
39	Y	4	1.410	6	1.410	2.125	NA	1.940	0.155	9.0	5000
40	N	4	1.410	4	1.410	2.125	2.125	2.410	0.155	9.0	5000

Table D.1a
Splice data for beams in lateral load resisting frame system (continued)

Splice	Top	Spliced Bars* A Bars		B Bars		Cover			Transverse Reinf.		f'_c
						c_b	c_{so}	c_{si}	A_{tr}/n	s	
No.	Bar	# bars	d_b (in.)	# bars	d_b (in.)	(in.)	(in.)	(in.)	($in.^2$)	(in.)	(psi)
41	Y	4	1.410	6	1.410	2.125	NA	1.940	0.155	9.0	5000
42	N	4	1.410	4	1.410	2.125	2.125	2.410	0.155	9.0	5000
43	Y	4	1.270	4	1.410	2.000	NA	2.550	0.200	13.0	5000
44	N	4	1.270	4	1.410	2.000	2.000	2.550	0.100	13.0	5000
45	Y	4	1.270	4	1.410	2.000	NA	2.550	0.200	13.0	5000
46	N	4	1.270	4	1.410	2.000	2.000	2.550	0.100	13.0	5000
47	Y	4	1.128	4	1.410	2.125	NA	2.600	0.310	15.0	5000
48	N	4	1.270	4	1.270	2.125	2.125	2.650	0.155	15.0	5000
49	Y	4	1.128	4	1.410	2.125	NA	2.600	0.310	15.0	5000
50	N	4	1.270	4	1.270	2.125	2.125	2.650	0.155	15.0	5000
51	Y	4	1.270	4	1.270	2.000	NA	2.690	0.200	15.0	5000
52	N	2	1.128	2	1.128	2.000	2.000	2.730	0.100	15.0	5000
53	N	2	1.270	2	1.270	2.000	2.000	2.730	0.100	15.0	5000
54	Y	4	1.270	4	1.270	2.000	NA	2.690	0.200	15.0	5000
55	N	2	1.128	2	1.128	2.000	2.000	2.730	0.100	15.0	5000
56	N	2	1.270	2	1.270	2.000	2.000	2.730	0.100	15.0	5000
57	Y	2	1.270	2	1.410	2.125	NA	2.460	0.310	9.0	6000
58	Y	2	1.410	2	1.410	2.125	NA	2.460	0.310	9.0	6000
59	N	2	1.128	2	1.128	2.125	2.125	2.900	0.155	9.0	6000
60	N	2	1.270	2	1.270	2.125	2.125	2.900	0.155	9.0	6000
61	Y	4	1.410	4	1.410	2.125	NA	2.410	0.310	9.0	6000
62	N	2	1.128	2	1.128	2.125	2.125	2.900	0.155	9.0	6000
63	N	2	1.270	2	1.270	2.125	2.125	2.900	0.155	9.0	6000
64	Y	4	1.410	4	1.410	2.125	NA	2.410	0.310	9.0	6000
65	N	2	1.128	2	1.128	2.125	2.125	2.900	0.155	9.0	6000
66	N	2	1.270	2	1.270	2.125	2.125	2.900	0.155	9.0	6000
67	Y	4	1.410	4	1.410	2.125	NA	2.410	0.310	9.0	6000
68	N	2	1.128	2	1.128	2.125	2.125	2.900	0.155	9.0	6000
69	N	2	1.270	2	1.270	2.125	2.125	2.900	0.155	9.0	6000
70	Y	4	1.410	4	1.410	2.125	NA	2.410	0.310	9.0	6000
71	N	2	1.128	2	1.128	2.125	2.125	2.900	0.155	9.0	6000
72	N	2	1.270	2	1.270	2.125	2.125	2.900	0.155	9.0	6000
73	Y	2	1.270	2	1.410	2.125	NA	2.460	0.310	9.0	6000
74	Y	2	1.410	2	1.410	2.125	NA	2.460	0.310	9.0	6000
75	N	2	1.128	2	1.128	2.125	2.125	2.900	0.155	9.0	6000
76	N	2	1.270	2	1.270	2.125	2.125	2.900	0.155	9.0	6000
77	Y	6	1.410	6	1.410	2.125	NA	0.880	0.207	10.5	6000
78	N	4	1.410	4	1.410	2.125	2.125	2.410	0.207	10.5	6000
79	Y	6	1.410	6	1.410	2.125	NA	0.880	0.207	12.0	6000
80	N	4	1.410	4	1.410	2.125	2.125	2.410	0.310	12.0	6000

Table D.1a
Splice data for beams in lateral load resisting frame system (continued)

Splice	Top	Spliced Bars*				Cover			Transverse Reinf.		f'_c
		A Bars		B Bars		c_b	c_{so}	c_{si}	A_{tr}/n	s	
No.	Bar	# bars	d_b (in.)	# bars	d_b (in.)	(in.)	(in.)	(in.)	($in.^2$)	(in.)	(psi)
81	Y	6	1.410	6	1.410	2.125	NA	0.880	0.207	12.0	6000
82	N	4	1.410	4	1.410	2.125	2.125	2.410	0.310	12.0	6000
83	Y	6	1.410	6	1.410	2.125	NA	0.880	0.207	12.0	6000
84	N	4	1.410	4	1.410	2.125	2.125	2.410	0.310	12.0	6000
85	Y	6	1.410	6	1.410	2.125	NA	0.880	0.207	12.0	6000
86	N	4	1.410	4	1.410	2.125	2.125	2.410	0.310	12.0	6000
87	Y	6	1.410	6	1.410	2.125	NA	0.880	0.207	10.5	6000
88	N	4	1.410	4	1.410	2.125	2.125	2.410	0.207	10.5	6000
89	Y	6	1.410	6	1.410	2.125	NA	0.880	0.207	11.0	6000
90	N	4	1.410	4	1.410	2.125	2.125	2.410	0.310	11.0	6000
91	Y	6	1.410	6	1.410	2.125	NA	0.880	0.207	11.0	6000
92	N	4	1.410	4	1.410	2.125	2.125	2.410	0.310	11.0	6000
93	Y	4	1.410	6	1.410	2.125	NA	0.880	0.207	11.0	6000
94	N	4	1.410	4	1.410	2.125	2.125	2.410	0.310	11.0	6000
95	Y	4	1.410	6	1.410	2.125	NA	0.880	0.207	11.0	6000
96	N	4	1.410	4	1.410	2.125	2.125	2.410	0.310	11.0	6000
97	Y	6	1.410	6	1.410	2.125	NA	0.880	0.207	11.0	6000
98	N	4	1.410	4	1.410	2.125	2.125	2.410	0.310	11.0	6000
99	Y	6	1.410	6	1.410	2.125	NA	0.880	0.207	11.0	6000
100	N	4	1.410	4	1.410	2.125	2.125	2.410	0.310	11.0	6000
101	Y	6	1.410	6	1.410	2.125	NA	0.880	0.207	13.0	6000
102	N	4	1.410	4	1.410	2.125	2.125	2.410	0.310	13.0	6000
103	Y	6	1.410	6	1.410	2.125	NA	0.880	0.207	13.0	6000
104	N	4	1.410	4	1.410	2.125	2.125	2.410	0.310	13.0	6000
105	Y	6	1.410	6	1.410	2.125	NA	0.880	0.207	13.0	6000
106	N	4	1.410	4	1.410	2.125	2.125	2.410	0.310	13.0	6000
107	Y	6	1.410	6	1.410	2.125	NA	0.880	0.207	13.0	6000
108	N	4	1.410	4	1.410	2.125	2.125	2.410	0.310	13.0	6000
109	Y	6	1.410	6	1.410	2.125	NA	0.880	0.207	13.0	6000
110	N	4	1.410	4	1.410	2.125	2.125	2.410	0.310	13.0	6000
111	Y	6	1.410	6	1.410	2.125	NA	0.880	0.207	13.0	6000
112	N	4	1.410	4	1.410	2.125	2.125	2.410	0.310	13.0	6000
113	Y	6	1.410	6	1.410	2.125	NA	0.880	0.207	13.0	6000
114	N	4	1.410	4	1.410	2.125	2.125	2.410	0.310	13.0	6000
115	Y	6	1.410	6	1.410	2.125	NA	0.880	0.207	13.0	6000
116	N	4	1.410	4	1.410	2.125	2.125	2.410	0.310	13.0	6000
117	Y	6	1.410	6	1.410	2.125	NA	0.880	0.207	13.0	6000
118	N	4	1.410	4	1.410	2.125	2.125	2.410	0.310	13.0	6000
119	Y	6	1.410	6	1.410	2.125	NA	0.880	0.207	13.0	6000
120	N	4	1.410	4	1.410	2.125	2.125	2.410	0.310	13.0	6000

Table D.1a
Splice data for beams in lateral load resisting frame system (continued)

Splice	Top	Spliced Bars*				Cover			Transverse Reinf.		f'_c
		A Bars		B Bars		c_b	c_{so}	c_{si}	A_{tr}/n	s	
No.	Bar	# bars	d_b (in.)	# bars	d_b (in.)	(in.)	(in.)	(in.)	($in.^2$)	(in.)	(psi)
121	Y	6	1.410	6	1.410	2.125	NA	0.880	0.207	13.0	6000
122	N	4	1.410	4	1.410	2.125	2.125	2.410	0.310	13.0	6000
123	Y	6	1.410	6	1.410	2.125	NA	0.880	0.207	13.0	6000
124	N	4	1.410	4	1.410	2.125	2.125	2.410	0.310	13.0	6000
125	Y	4	1.410	6	1.410	2.125	NA	1.940	0.310	15.0	6000
126	N	4	1.410	4	1.410	2.125	2.125	2.410	0.310	15.0	6000
127	Y	6	1.410	6	1.410	2.125	NA	0.880	0.207	14.0	6000
128	N	4	1.410	4	1.410	2.125	2.125	2.410	0.310	14.0	6000
129	Y	6	1.410	6	1.410	2.125	NA	0.880	0.207	14.0	6000
130	N	4	1.410	4	1.410	2.125	2.125	2.410	0.310	14.0	6000
131	Y	6	1.410	6	1.410	2.125	NA	0.880	0.207	14.0	6000
132	N	4	1.410	4	1.410	2.125	2.125	2.410	0.310	14.0	6000
133	Y	6	1.410	6	1.410	2.125	NA	0.880	0.207	14.0	6000
134	N	4	1.410	4	1.410	2.125	2.125	2.410	0.310	14.0	6000
135	Y	4	1.410	6	1.410	2.125	NA	1.940	0.310	15.0	6000
136	N	4	1.410	4	1.410	2.125	2.125	2.410	0.310	15.0	6000
137	Y	4	1.410	6	1.410	2.125	NA	1.940	0.310	15.0	6000
138	N	4	1.410	4	1.410	2.125	2.125	2.410	0.310	15.0	6000
139	Y	6	1.410	6	1.410	2.125	NA	0.880	0.207	14.0	6000
140	N	4	1.410	4	1.410	2.125	2.125	2.410	0.310	14.0	6000
141	Y	6	1.410	6	1.410	2.125	NA	0.880	0.207	14.0	6000
142	N	4	1.410	4	1.410	2.125	2.125	2.410	0.310	14.0	6000
143	Y	6	1.410	6	1.410	2.125	NA	0.880	0.207	14.0	6000
144	N	4	1.410	4	1.410	2.125	2.125	2.410	0.310	14.0	6000
145	Y	6	1.410	6	1.410	2.125	NA	0.880	0.207	14.0	6000
146	N	4	1.410	4	1.410	2.125	2.125	2.410	0.310	14.0	6000
147	Y	4	1.410	6	1.410	2.125	NA	1.940	0.310	15.0	6000
148	N	4	1.410	4	1.410	2.125	2.125	2.410	0.310	15.0	6000
149	Y	4	1.270	6	1.270	2.125	NA	2.080	0.310	15.0	5000
150	N	4	1.410	4	1.410	2.125	2.125	2.410	0.310	15.0	5000
151	Y	6	1.270	6	1.270	2.125	NA	1.050	0.207	15.0	5000
152	N	4	1.270	4	1.270	2.125	2.125	2.600	0.310	15.0	5000
153	Y	6	1.270	6	1.270	2.125	NA	1.050	0.207	15.0	5000
154	N	4	1.410	4	1.410	2.125	2.125	2.410	0.310	15.0	5000
155	Y	6	1.270	6	1.270	2.125	NA	1.050	0.207	15.0	5000
156	N	4	1.410	4	1.410	2.125	2.125	2.410	0.310	15.0	5000
157	Y	6	1.270	6	1.270	2.125	NA	1.050	0.207	15.0	5000
158	N	4	1.270	4	1.270	2.125	2.125	2.600	0.310	15.0	5000
159	Y	4	1.270	6	1.270	2.125	NA	2.080	0.310	15.0	5000
160	N	4	1.410	4	1.410	2.125	2.125	2.410	0.310	15.0	5000

Table D.1a
Splice data for beams in lateral load resisting frame system (continued)

Splice	Top	Spliced Bars* A Bars		B Bars		Cover			Transverse Reinf.		f'_c
No.	Bar	# bars	d_b (in.)	# bars	d_b (in.)	c_b (in.)	c_{so} (in.)	c_{si} (in.)	A_{tr}/n ($in.^2$)	s (in.)	(psi)
161	Y	4	1.410	4	1.410	2.125	NA	2.410	0.310	8.0	5000
162	N	4	1.270	4	1.270	2.125	2.125	2.510	0.155	8.0	5000
163	Y	4	1.410	4	1.410	2.125	NA	2.410	0.310	8.0	5000
164	N	4	1.270	4	1.270	2.125	2.125	2.600	0.155	8.0	5000
165	Y	4	1.410	4	1.410	2.125	NA	2.410	0.310	8.0	5000
166	N	4	1.270	4	1.270	2.125	2.125	2.600	0.155	8.0	5000
167	Y	4	1.410	4	1.410	2.125	NA	2.410	0.310	8.0	5000
168	N	4	1.270	4	1.270	2.125	2.125	2.600	0.155	8.0	5000
169	Y	4	1.410	4	1.410	2.125	NA	2.410	0.310	8.0	5000
170	N	4	1.270	4	1.270	2.125	2.125	2.600	0.155	8.0	5000
171	Y	4	1.410	4	1.410	2.125	NA	2.410	0.310	8.0	5000
172	N	4	1.270	4	1.270	2.125	2.125	2.510	0.155	8.0	5000
173	Y	4	1.270	4	1.410	2.125	NA	2.510	0.310	10.0	5000
174	N	2	1.128	2	1.410	2.125	2.125	2.550	0.155	10.0	5000
175	N	2	1.270	2	1.410	2.125	2.125	2.550	0.155	10.0	5000
176	Y	4	1.270	4	1.270	2.125	NA	2.600	0.310	10.0	5000
177	N	4	1.410	4	1.410	2.125	2.125	2.410	0.155	10.0	5000
178	Y	4	1.270	4	1.270	2.125	NA	2.600	0.310	10.0	5000
179	N	4	1.410	4	1.410	2.125	2.125	2.410	0.155	10.0	5000
180	Y	4	1.270	4	1.270	2.125	NA	2.600	0.310	10.0	5000
181	N	4	1.410	4	1.410	2.125	2.125	2.410	0.155	10.0	5000
182	Y	4	1.270	4	1.270	2.125	NA	2.600	0.310	10.0	5000
183	N	4	1.410	4	1.410	2.125	2.125	2.410	0.155	10.0	5000
184	Y	4	1.270	4	1.410	2.125	NA	2.510	0.310	10.0	5000
185	N	2	1.128	2	1.410	2.125	2.125	2.550	0.155	10.0	5000
186	N	2	1.270	2	1.410	2.125	2.125	2.550	0.155	10.0	5000
187	Y	4	1.410	4	1.410	2.125	NA	2.410	0.310	12.0	5000
188	N	2	1.128	2	1.270	2.125	2.125	2.650	0.155	12.0	5000
189	N	2	1.270	2	1.270	2.125	2.125	2.650	0.155	12.0	5000
190	Y	4	1.410	4	1.410	2.125	NA	2.410	0.310	12.0	5000
191	N	4	1.270	4	1.270	2.125	2.125	2.600	0.155	12.0	5000
192	Y	4	1.410	4	1.410	2.125	NA	2.410	0.310	12.0	5000
193	N	4	1.270	4	1.270	2.125	2.125	2.600	0.155	12.0	5000
194	Y	4	1.410	4	1.410	2.125	NA	2.410	0.310	12.0	5000
195	N	4	1.270	4	1.270	2.125	2.125	2.600	0.155	12.0	5000
196	Y	4	1.410	4	1.410	2.125	NA	2.410	0.310	12.0	5000
197	N	4	1.270	4	1.270	2.125	2.125	2.600	0.155	12.0	5000
198	Y	4	1.410	4	1.410	2.125	NA	2.410	0.310	12.0	5000
199	N	2	1.128	2	1.270	2.125	2.125	2.650	0.155	12.0	5000
200	N	2	1.270	2	1.270	2.125	2.125	2.650	0.155	12.0	5000

Table D.1a
Splice data for beams in lateral load resisting frame system (continued)

Splice	Top	Spliced Bars* A Bars		B Bars		Cover			Transverse Reinf.		f'_c
No.	Bar	# bars	d_b (in.)	# bars	d_b (in.)	c_b (in.)	c_{so} (in.)	c_{si} (in.)	A_{tr}/n ($in.^2$)	s (in.)	(psi)
201	Y	3	1.128	4	1.128	2.000	NA	4.530	0.200	15.0	5000
202	N	2	1.128	2	1.270	2.000	2.000	2.690	0.100	15.0	5000
203	N	2	1.270	2	1.270	2.000	2.000	2.690	0.100	15.0	5000
204	Y	4	1.128	4	1.128	2.125	NA	2.790	0.310	12.0	5000
205	N	4	1.270	4	1.270	2.125	2.125	2.600	0.155	12.0	5000
206	Y	4	1.128	4	1.128	2.125	NA	2.790	0.310	12.0	5000
207	N	4	1.270	4	1.270	2.125	2.125	2.600	0.155	12.0	5000
208	Y	4	1.128	4	1.128	2.125	NA	2.790	0.310	12.0	5000
209	N	4	1.270	4	1.270	2.125	2.125	2.600	0.155	12.0	5000
210	Y	4	1.128	4	1.128	2.125	NA	2.790	0.310	12.0	5000
211	N	4	1.270	4	1.270	2.125	2.125	2.600	0.155	12.0	5000
212	Y	3	1.128	4	1.128	2.000	NA	4.530	0.200	15.0	5000
213	N	2	1.128	2	1.270	2.000	2.000	2.690	0.100	15.0	5000
214	N	2	1.270	2	1.270	2.000	2.000	2.690	0.100	15.0	5000
215	Y	2	1.128	2	1.128	2.000	NA	2.730	0.200	15.0	6000
216	Y	2	1.270	2	1.270	2.000	NA	2.730	0.200	15.0	6000
217	N	2	1.128	2	1.128	2.000	2.000	2.730	0.100	15.0	6000
218	N	2	1.270	2	1.270	2.000	2.000	2.730	0.100	15.0	6000
219	Y	2	1.128	2	1.128	2.000	NA	2.730	0.200	15.0	6000
220	Y	2	1.270	2	1.270	2.000	NA	2.730	0.200	15.0	6000
221	N	2	1.128	2	1.128	2.000	2.000	2.730	0.100	15.0	6000
222	N	2	1.270	2	1.270	2.000	2.000	2.730	0.100	15.0	6000
223	Y	4	1.410	4	1.410	2.125	NA	2.410	0.310	14.0	6000
224	N	4	1.410	4	1.410	2.125	2.125	2.410	0.310	14.0	6000
225	Y	4	1.410	4	1.410	2.125	NA	2.410	0.310	14.0	6000
226	N	4	1.410	4	1.410	2.125	2.125	2.410	0.310	14.0	6000
227	Y	4	1.410	4	1.410	2.125	NA	2.410	0.310	8.0	6000
228	N	4	1.410	4	1.410	2.125	2.125	2.410	0.155	8.0	6000
229	Y	4	1.410	4	1.410	2.125	NA	2.410	0.310	8.0	6000
230	N	4	1.410	4	1.410	2.125	2.125	2.410	0.155	8.0	6000
231	Y	4	1.410	4	1.410	2.125	NA	2.410	0.310	10.0	6000
232	N	4	1.410	4	1.410	2.125	2.125	2.410	0.155	10.0	6000
233	Y	4	1.410	4	1.410	2.125	NA	2.410	0.310	10.0	6000
234	N	4	1.410	4	1.410	2.125	2.125	2.410	0.155	10.0	6000
235	Y	4	1.410	4	1.410	2.125	NA	2.410	0.310	11.0	6000
236	N	4	1.410	4	1.410	2.125	2.125	2.410	0.155	11.0	6000
237	Y	4	1.410	4	1.410	2.125	NA	2.410	0.310	11.0	6000
238	N	4	1.410	4	1.410	2.125	2.125	2.410	0.155	11.0	6000
239	Y	4	1.410	4	1.410	2.125	NA	2.410	0.310	11.0	6000
240	N	4	1.410	4	1.410	2.125	2.125	2.410	0.155	11.0	6000

Table D.1a
Splice data for beams in lateral load resisting frame system (continued)

Splice	Top	Spliced Bars* A Bars		B Bars		Cover			Transverse Reinf.		f'_c
No.	Bar	# bars	d_b (in.)	# bars	d_b (in.)	c_b (in.)	c_{so} (in.)	c_{si} (in.)	A_{tr}/n ($in.^2$)	s (in.)	(psi)
241	Y	4	1.410	4	1.410	2.125	NA	2.410	0.310	11.0	6000
242	N	4	1.410	4	1.410	2.125	2.125	2.410	0.155	11.0	6000
243	Y	4	1.410	4	1.410	2.125	NA	2.410	0.310	10.0	6000
244	N	4	1.410	4	1.410	2.125	2.125	2.410	0.155	10.0	6000
245	Y	4	1.410	4	1.410	2.125	NA	2.410	0.310	10.0	6000
246	N	4	1.410	4	1.410	2.125	2.125	2.410	0.155	10.0	6000
247	Y	4	1.410	4	1.410	2.125	NA	2.410	0.310	10.0	5000
248	N	4	1.410	4	1.410	2.125	2.125	2.410	0.155	10.0	5000
249	Y	4	1.410	4	1.410	2.125	NA	2.410	0.310	10.0	5000
250	N	4	1.410	4	1.410	2.125	2.125	2.410	0.155	10.0	5000
251	Y	4	1.410	4	1.410	2.125	NA	2.410	0.310	11.0	5000
252	N	4	1.410	4	1.410	2.125	2.125	2.410	0.155	11.0	5000
253	Y	4	1.410	4	1.410	2.125	NA	2.410	0.310	11.0	5000
254	N	4	1.410	4	1.410	2.125	2.125	2.410	0.155	11.0	5000
255	Y	4	1.410	4	1.410	2.125	NA	2.410	0.310	14.0	5000
256	N	2	1.128	2	1.128	2.125	2.125	2.690	0.155	14.0	5000
257	N	2	1.270	2	1.270	2.125	2.125	2.690	0.155	14.0	5000
258	Y	4	1.410	4	1.410	2.125	NA	2.410	0.310	14.0	5000
259	N	2	1.128	2	1.128	2.125	2.125	2.690	0.155	14.0	5000
260	N	2	1.270	2	1.270	2.125	2.125	2.690	0.155	14.0	5000
261	Y	4	1.270	4	1.270	2.125	NA	2.600	0.310	15.0	5000
262	N	4	1.270	4	1.270	2.125	2.125	2.600	0.155	15.0	5000
263	Y	4	1.270	4	1.270	2.125	NA	2.600	0.310	15.0	5000
264	N	4	1.270	4	1.270	2.125	2.125	2.600	0.155	15.0	5000
265	Y	4	1.410	4	1.410	2.125	NA	2.410	0.310	12.0	5000
266	N	2	1.128	2	1.128	2.125	2.125	2.690	0.155	12.0	5000
267	N	2	1.270	2	1.270	2.125	2.125	2.690	0.155	12.0	5000
268	Y	4	1.410	4	1.410	2.125	NA	2.410	0.310	12.0	5000
269	N	2	1.128	2	1.128	2.125	2.125	2.690	0.155	12.0	5000
270	N	2	1.270	2	1.270	2.125	2.125	2.690	0.155	12.0	5000
271	Y	2	1.128	2	1.128	2.000	NA	2.690	0.200	15.0	5000
272	Y	2	1.270	2	1.270	2.000	NA	2.690	0.200	15.0	5000
273	N	2	1.128	2	1.128	2.000	2.000	2.690	0.100	15.0	5000
274	N	2	1.270	2	1.270	2.000	2.000	2.690	0.100	15.0	5000
275	Y	2	1.128	2	1.128	2.000	NA	2.690	0.200	15.0	5000
276	Y	2	1.270	2	1.270	2.000	NA	2.690	0.200	15.0	5000
277	N	2	1.128	2	1.128	2.000	2.000	2.690	0.100	15.0	5000
278	N	2	1.270	2	1.270	2.000	2.000	2.690	0.100	15.0	5000
279	Y	4	1.410	4	1.410	2.125	NA	2.410	0.310	12.0	6000
280	N	2	1.128	2	1.128	2.125	2.125	2.730	0.155	12.0	6000

Table D.1a
Splice data for beams in lateral load resisting frame system (continued)

Splice	Top	Spliced Bars* A Bars		B Bars		Cover			Transverse Reinf.		f'_c
No.	Bar	# bars	d_b (in.)	# bars	d_b (in.)	c_b (in.)	c_{so} (in.)	c_{si} (in.)	A_{tr}/n ($in.^2$)	s (in.)	(psi)
281	N	2	1.270	2	1.270	2.125	2.125	2.730	0.155	12.0	6000
282	Y	4	1.410	4	1.410	2.125	NA	2.410	0.310	12.0	6000
283	N	2	1.128	2	1.128	2.125	2.125	2.730	0.155	12.0	6000
284	N	2	1.270	2	1.270	2.125	2.125	2.730	0.155	12.0	6000
285	Y	4	1.410	4	1.410	2.125	NA	2.410	0.310	12.0	6000
286	N	2	1.128	2	1.128	2.125	2.125	2.730	0.155	12.0	6000
287	N	2	1.270	2	1.270	2.125	2.125	2.730	0.155	12.0	6000
288	Y	6	1.410	6	1.410	2.125	NA	1.480	0.207	9.0	6000
289	N	6	1.410	6	1.410	2.125	2.125	1.480	0.207	9.0	6000
290	Y	6	1.410	6	1.410	2.125	NA	1.480	0.207	9.0	6000
291	N	6	1.410	6	1.410	2.125	2.125	1.480	0.207	9.0	6000
292	Y	6	1.410	6	1.410	2.125	NA	1.480	0.207	9.0	6000
293	N	6	1.410	6	1.410	2.125	2.125	1.480	0.207	9.0	6000
294	Y	6	1.410	6	1.410	2.125	NA	0.880	0.207	10.0	6000
295	N	4	1.410	6	1.410	2.125	2.125	1.940	0.310	10.0	6000
296	Y	6	1.410	6	1.410	2.125	NA	0.880	0.207	10.0	6000
297	N	6	1.410	6	1.410	2.125	2.125	0.880	0.207	10.0	6000
298	Y	6	1.410	6	1.410	2.125	NA	0.880	0.207	10.0	6000
299	N	4	1.410	6	1.410	2.125	2.125	1.940	0.310	10.0	6000
300	Y	6	1.410	6	1.410	2.125	NA	0.880	0.207	10.5	6000
301	N	4	1.410	4	1.410	2.125	2.125	2.410	0.310	10.5	6000
302	Y	6	1.410	6	1.410	2.125	NA	0.880	0.207	10.5	6000
303	N	4	1.410	4	1.410	2.125	2.125	2.410	0.310	10.5	6000
304	Y	6	1.410	6	1.410	2.125	NA	0.880	0.207	10.5	6000
305	N	4	1.410	4	1.410	2.125	2.125	2.410	0.310	10.5	6000
306	Y	6	1.410	6	1.410	2.125	NA	0.880	0.207	13.0	6000
307	N	4	1.410	4	1.410	2.125	2.125	2.410	0.310	13.0	6000
308	Y	6	1.410	6	1.410	2.125	NA	0.880	0.207	13.0	6000
309	N	4	1.410	4	1.410	2.125	2.125	2.410	0.310	13.0	6000
310	Y	6	1.410	6	1.410	2.125	NA	0.880	0.207	13.0	6000
311	N	4	1.410	4	1.410	2.125	2.125	2.410	0.310	13.0	6000
312	Y	6	1.410	6	1.410	2.125	NA	0.880	0.207	13.0	6000
313	N	4	1.270	4	1.410	2.125	2.125	2.510	0.310	13.0	6000
314	Y	6	1.410	6	1.410	2.125	NA	0.880	0.207	14.0	6000
315	N	4	1.410	4	1.410	2.125	2.125	2.410	0.310	14.0	6000
316	Y	6	1.410	6	1.410	2.125	NA	0.880	0.207	13.0	6000
317	N	4	1.270	4	1.410	2.125	2.125	2.510	0.310	13.0	6000
318	Y	6	1.410	6	1.410	2.125	NA	0.880	0.207	10.5	6000
319	N	4	1.410	4	1.410	2.125	2.125	2.410	0.310	10.5	6000
320	Y	6	1.410	6	1.410	2.125	NA	0.880	0.207	10.5	6000

Table D.1a
Splice data for beams in lateral load resisting frame system (continued)

Splice	Top	Spliced Bars* A Bars		B Bars		Cover			Transverse Reinf.		f'_c
No.	Bar	# bars	d_b (in.)	# bars	d_b (in.)	c_b (in.)	c_{so} (in.)	c_{si} (in.)	A_{tr}/n ($in.^2$)	s (in.)	(psi)
321	N	4	1.410	4	1.410	2.125	2.125	2.410	0.310	10.5	6000
322	Y	6	1.410	6	1.410	2.125	NA	0.880	0.207	10.5	6000
323	N	4	1.410	4	1.410	2.125	2.125	2.410	0.310	10.5	6000
324	Y	6	1.410	6	1.410	2.125	NA	0.880	0.207	13.0	5000
325	N	4	1.270	4	1.410	2.125	2.125	2.510	0.310	13.0	5000
326	Y	6	1.410	6	1.410	2.125	NA	0.880	0.207	13.0	5000
327	N	4	1.410	4	1.410	2.125	2.125	2.410	0.310	13.0	5000
328	Y	6	1.410	6	1.410	2.125	NA	0.880	0.207	13.0	5000
329	N	4	1.270	4	1.410	2.125	2.125	2.510	0.310	13.0	5000
330	Y	6	1.410	6	1.410	2.125	NA	0.880	0.207	13.0	5000
331	N	4	1.270	4	1.410	2.125	2.125	2.510	0.310	13.0	5000
332	Y	6	1.410	6	1.410	2.125	NA	0.880	0.207	13.0	5000
333	N	4	1.410	4	1.410	2.125	2.125	2.410	0.310	13.0	5000
334	Y	6	1.410	6	1.410	2.125	NA	0.880	0.207	13.0	5000
335	N	4	1.270	4	1.410	2.125	2.125	2.510	0.310	13.0	5000
336	Y	4	1.410	4	1.410	2.125	NA	2.410	0.310	15.0	5000
337	N	4	1.270	4	1.270	2.125	2.125	2.600	0.310	15.0	5000
338	Y	4	1.410	4	1.410	2.125	NA	2.410	0.310	15.0	5000
339	N	4	1.270	4	1.270	2.125	2.125	2.600	0.310	15.0	5000
340	Y	4	1.410	4	1.410	2.125	NA	2.410	0.310	15.0	5000
341	N	4	1.270	4	1.270	2.125	2.125	2.600	0.310	15.0	5000
342	Y	4	1.410	4	1.410	2.125	NA	2.410	0.310	15.0	5000
343	N	2	1.128	2	1.270	2.125	2.125	2.650	0.310	15.0	5000
344	N	2	1.270	2	1.270	2.125	2.125	2.650	0.310	15.0	5000
345	Y	4	1.410	4	1.410	2.125	NA	2.410	0.310	15.0	5000
346	N	4	1.270	4	1.270	2.125	2.125	2.600	0.310	15.0	5000
347	Y	4	1.410	4	1.410	2.125	NA	2.410	0.310	15.0	5000
348	N	2	1.128	2	1.270	2.125	2.125	2.650	0.310	15.0	5000
349	N	2	1.270	2	1.270	2.125	2.125	2.650	0.310	15.0	5000
350	Y	4	1.270	4	1.410	2.125	NA	2.510	0.310	13.0	5000
351	N	4	1.128	4	1.128	2.125	2.125	2.740	0.155	13.0	5000
352	Y	4	1.410	4	1.410	2.125	NA	2.410	0.310	14.0	5000
353	N	4	1.128	4	1.128	2.125	2.125	2.790	0.155	14.0	5000
354	Y	4	1.270	4	1.410	2.125	NA	2.510	0.310	13.0	5000
355	N	4	1.128	4	1.128	2.125	2.125	2.740	0.155	13.0	5000
356	Y	4	1.410	4	1.410	2.125	NA	2.410	0.310	15.0	5000
357	N	2	1.128	2	1.128	2.125	2.125	2.690	0.155	15.0	5000
358	N	2	1.270	2	1.270	2.125	2.125	2.690	0.155	15.0	5000
359	Y	4	1.410	4	1.410	2.125	NA	2.410	0.310	15.0	5000
360	N	2	1.128	2	1.128	2.125	2.125	2.690	0.155	15.0	5000

Table D.1a
Splice data for beams in lateral load resisting frame system (continued)

Splice	Top	Spliced Bars* A Bars		B Bars		Cover			Transverse Reinf.		f'_c
No.	Bar	# bars	d_b (in.)	# bars	d_b (in.)	c_b (in.)	c_{so} (in.)	c_{si} (in.)	A_{tr}/n ($in.^2$)	s (in.)	(psi)
361	N	2	1.270	2	1.270	2.125	2.125	2.690	0.155	15.0	5000
362	Y	4	1.410	4	1.410	2.125	NA	2.410	0.310	15.0	5000
363	N	2	1.128	2	1.128	2.125	2.125	2.690	0.155	15.0	5000
364	N	2	1.270	2	1.270	2.125	2.125	2.690	0.155	15.0	5000
365	Y	4	1.410	4	1.410	2.125	NA	2.410	0.310	12.0	6000
366	N	2	1.128	2	1.128	2.125	2.125	2.690	0.155	12.0	6000
367	N	2	1.270	2	1.270	2.125	2.125	2.690	0.155	12.0	6000
368	Y	4	1.410	4	1.410	2.125	NA	2.410	0.310	12.0	6000
369	N	2	1.128	2	1.128	2.125	2.125	2.690	0.155	12.0	6000
370	N	2	1.270	2	1.270	2.125	2.125	2.690	0.155	12.0	6000
371	Y	4	1.410	4	1.410	2.125	NA	2.410	0.310	12.0	6000
372	N	2	1.128	2	1.128	2.125	2.125	2.690	0.155	12.0	6000
373	N	2	1.270	2	1.270	2.125	2.125	2.690	0.155	12.0	6000
374	Y	4	1.410	4	1.410	2.125	NA	2.410	0.310	12.0	6000
375	N	2	1.128	2	1.128	2.125	2.125	2.690	0.155	12.0	6000
376	N	2	1.270	2	1.270	2.125	2.125	2.690	0.155	12.0	6000
377	Y	6	1.410	6	1.410	2.125	NA	0.880	0.207	12.0	6000
378	N	4	1.270	6	1.270	2.125	2.125	2.080	0.310	12.0	6000
379	Y	6	1.410	6	1.410	2.125	NA	0.880	0.207	12.0	6000
380	N	6	1.270	6	1.270	2.125	2.125	1.050	0.207	12.0	6000
381	Y	6	1.410	6	1.410	2.125	NA	0.880	0.207	12.0	6000
382	N	6	1.270	6	1.270	2.125	2.125	1.050	0.207	12.0	6000
383	Y	6	1.410	6	1.410	2.125	NA	0.880	0.103	8.0	6000
384	N	4	1.270	6	1.270	2.125	2.125	2.080	0.155	8.0	6000
385	Y	6	1.410	6	1.410	2.125	NA	0.880	0.207	10.0	6000
386	N	4	1.270	6	1.270	2.125	2.125	2.080	0.310	10.0	6000
387	Y	6	1.410	6	1.410	2.125	NA	0.880	0.207	10.0	6000
388	N	6	1.270	6	1.270	2.125	2.125	1.050	0.207	10.0	6000
389	Y	6	1.410	6	1.410	2.125	NA	0.880	0.207	10.0	6000
390	N	6	1.270	6	1.270	2.125	2.125	1.050	0.207	10.0	6000
391	Y	6	1.410	6	1.410	2.125	NA	0.880	0.103	8.0	6000
392	N	4	1.270	6	1.270	2.125	2.125	2.080	0.155	8.0	6000
393	Y	6	1.410	6	1.410	2.125	NA	0.880	0.207	13.0	6000
394	N	4	1.410	4	1.410	2.125	2.125	2.410	0.310	13.0	6000
395	Y	6	1.410	6	1.410	2.125	NA	0.880	0.207	13.0	6000
396	N	4	1.410	4	1.410	2.125	2.125	2.410	0.310	13.0	6000
397	Y	6	1.410	6	1.410	2.125	NA	0.880	0.207	13.0	6000
398	N	4	1.410	4	1.410	2.125	2.125	2.410	0.310	13.0	6000
399	Y	6	1.410	6	1.410	2.125	NA	0.880	0.103	8.0	6000
400	N	4	1.410	4	1.410	2.125	2.125	2.410	0.155	8.0	6000

Table D.1a
Splice data for beams in lateral load resisting frame system (continued)

Splice No.	Top Bar	Spliced Bars* A Bars # bars	A Bars d_b (in.)	B Bars # bars	B Bars d_b (in.)	Cover c_b (in.)	Cover c_{so} (in.)	Cover c_{si} (in.)	Transverse Reinf. A_{tr}/n ($in.^2$)	Transverse Reinf. s (in.)	f'_c (psi)
401	Y	6	1.410	6	1.410	2.125	NA	0.880	0.207	13.0	6000
402	N	4	1.410	4	1.410	2.125	2.125	2.410	0.310	13.0	6000
403	Y	6	1.410	6	1.410	2.125	NA	0.880	0.207	13.0	6000
404	N	4	1.410	4	1.410	2.125	2.125	2.410	0.310	13.0	6000
405	Y	6	1.410	6	1.410	2.125	NA	0.880	0.207	13.0	6000
406	N	4	1.410	4	1.410	2.125	2.125	2.410	0.310	13.0	6000
407	Y	6	1.410	6	1.410	2.125	NA	0.880	0.103	8.0	6000
408	N	4	1.410	4	1.410	2.125	2.125	2.410	0.155	8.0	6000
409	Y	6	1.410	6	1.410	2.125	NA	0.880	0.207	13.0	6000
410	N	4	1.410	4	1.410	2.125	2.125	2.410	0.310	13.0	6000
411	Y	6	1.410	6	1.410	2.125	NA	0.880	0.207	13.0	6000
412	N	4	1.410	4	1.410	2.125	2.125	2.410	0.310	13.0	6000
413	Y	6	1.410	6	1.410	2.125	NA	0.880	0.207	13.0	6000
414	N	4	1.410	4	1.410	2.125	2.125	2.410	0.310	13.0	6000
415	Y	6	1.410	6	1.410	2.125	NA	0.880	0.103	8.0	6000
416	N	4	1.410	4	1.410	2.125	2.125	2.410	0.155	8.0	6000
417	Y	6	1.410	6	1.410	2.125	NA	0.880	0.207	10.0	6000
418	N	4	1.270	6	1.270	2.125	2.125	2.080	0.310	10.0	6000
419	Y	6	1.410	6	1.410	2.125	NA	0.880	0.207	10.0	6000
420	N	6	1.270	6	1.270	2.125	2.125	1.050	0.207	10.0	6000
421	Y	6	1.410	6	1.410	2.125	NA	0.880	0.207	10.0	6000
422	N	6	1.270	6	1.270	2.125	2.125	1.050	0.207	10.0	6000
423	Y	6	1.410	6	1.410	2.125	NA	0.880	0.103	8.0	6000
424	N	4	1.270	6	1.270	2.125	2.125	2.080	0.155	8.0	6000
425	Y	6	1.410	6	1.410	2.125	NA	0.880	0.207	11.0	5000
426	N	4	1.410	4	1.410	2.125	2.125	2.410	0.310	11.0	5000
427	Y	6	1.410	6	1.410	2.125	NA	0.880	0.207	12.0	5000
428	N	4	1.410	4	1.410	2.125	2.125	2.410	0.310	12.0	5000
429	Y	6	1.410	6	1.410	2.125	NA	0.880	0.207	12.0	5000
430	N	4	1.410	4	1.410	2.125	2.125	2.410	0.310	12.0	5000
431	Y	6	1.410	6	1.410	2.125	NA	0.880	0.103	8.0	5000
432	N	4	1.410	4	1.410	2.125	2.125	2.410	0.155	8.0	5000
433	Y	6	1.410	6	1.410	2.125	NA	0.880	0.207	12.0	5000
434	N	4	1.410	4	1.410	2.125	2.125	2.410	0.310	12.0	5000
435	Y	6	1.410	6	1.410	2.125	NA	0.880	0.207	12.0	5000
436	N	4	1.410	4	1.410	2.125	2.125	2.410	0.310	12.0	5000
437	Y	6	1.410	6	1.410	2.125	NA	0.880	0.207	12.0	5000
438	N	4	1.410	4	1.410	2.125	2.125	2.410	0.310	12.0	5000
439	Y	6	1.410	6	1.410	2.125	NA	0.880	0.103	9.0	5000
440	N	4	1.410	4	1.410	2.125	2.125	2.410	0.155	9.0	5000

Table D.1a
Splice data for beams in lateral load resisting frame system (continued)

Splice No.	Top Bar	Spliced Bars* A Bars # bars	A Bars d_b (in.)	B Bars # bars	B Bars d_b (in.)	Cover c_b (in.)	Cover c_{so} (in.)	Cover c_{si} (in.)	Transverse Reinf. A_{tr}/n ($in.^2$)	Transverse Reinf. s (in.)	f'_c (psi)
441	Y	4	1.410	6	1.410	2.125	NA	1.940	0.310	15.0	5000
442	N	4	1.270	4	1.270	2.125	2.125	2.600	0.310	15.0	5000
443	Y	4	1.410	4	1.410	2.125	NA	2.410	0.310	15.0	5000
444	N	4	1.270	4	1.270	2.125	2.125	2.600	0.310	15.0	5000
445	Y	4	1.410	4	1.410	2.125	NA	2.410	0.310	15.0	5000
446	N	4	1.270	4	1.270	2.125	2.125	2.600	0.310	15.0	5000
447	Y	4	1.410	6	1.410	2.125	NA	1.940	0.103	11.0	5000
448	N	4	1.270	4	1.270	2.125	2.125	2.600	0.155	11.0	5000
449	Y	4	1.410	6	1.410	2.125	NA	1.940	0.310	15.0	5000
450	N	4	1.270	4	1.270	2.125	2.125	2.600	0.310	15.0	5000
451	Y	4	1.410	4	1.410	2.125	NA	2.410	0.310	15.0	5000
452	N	4	1.270	4	1.270	2.125	2.125	2.600	0.310	15.0	5000
453	Y	4	1.410	4	1.410	2.125	NA	2.410	0.310	15.0	5000
454	N	4	1.270	4	1.270	2.125	2.125	2.600	0.310	15.0	5000
455	Y	4	1.410	6	1.410	2.125	NA	1.940	0.103	11.0	5000
456	N	4	1.270	4	1.270	2.125	2.125	2.600	0.155	11.0	5000
457	Y	4	1.410	4	1.410	2.125	NA	2.410	0.310	9.0	5000
458	N	2	1.128	2	1.270	2.125	2.125	2.650	0.155	9.0	5000
459	N	2	1.270	2	1.270	2.125	2.125	2.650	0.155	9.0	5000
460	Y	4	1.410	4	1.410	2.125	NA	2.410	0.310	9.0	5000
461	N	4	1.270	4	1.270	2.125	2.125	2.600	0.155	9.0	5000
462	Y	4	1.410	4	1.410	2.125	NA	2.410	0.310	9.0	5000
463	N	4	1.270	4	1.270	2.125	2.125	2.600	0.155	9.0	5000
464	Y	4	1.410	4	1.410	2.125	NA	2.410	0.310	15.0	5000
465	N	2	1.128	2	1.270	2.125	2.125	2.650	0.155	15.0	5000
466	N	2	1.270	2	1.270	2.125	2.125	2.650	0.155	15.0	5000
467	Y	4	1.410	4	1.410	2.125	NA	2.410	0.310	12.0	5000
468	N	2	1.128	2	1.128	2.125	2.125	2.690	0.155	12.0	5000
469	N	2	1.270	2	1.270	2.125	2.125	2.690	0.155	12.0	5000
470	Y	4	1.128	4	1.128	2.000	NA	1.830	0.100	15.0	5000
471	N	4	1.128	4	1.128	2.000	2.000	1.830	0.100	15.0	5000
472	Y	4	1.410	4	1.410	2.125	NA	2.410	0.310	15.0	6000
473	N	2	1.128	2	1.128	2.125	2.125	2.690	0.155	15.0	6000
474	N	2	1.270	2	1.270	2.125	2.125	2.690	0.155	15.0	6000
475	Y	4	1.410	4	1.410	2.125	NA	2.410	0.310	15.0	6000
476	N	2	1.128	2	1.128	2.125	2.125	2.690	0.155	15.0	6000
477	N	2	1.270	2	1.270	2.125	2.125	2.690	0.155	15.0	6000
478	Y	4	1.270	4	1.410	2.125	NA	2.510	0.310	15.0	6000
479	N	2	1.128	2	1.128	2.125	2.125	2.690	0.155	15.0	6000
480	N	2	1.270	2	1.270	2.125	2.125	2.690	0.155	15.0	6000

Table D.1a
Splice data for beams in lateral load resisting frame system (continued)

Splice	Top	Spliced Bars* A Bars		B Bars		Cover			Transverse Reinf.		f'_c
						c_b	c_{so}	c_{si}	A_{tr}/n	s	
No.	Bar	# bars	d_b (in.)	# bars	d_b (in.)	(in.)	(in.)	(in.)	($in.^2$)	(in.)	(psi)
481	Y	4	1.270	4	1.410	2.125	NA	2.510	0.310	15.0	6000
482	N	2	1.128	2	1.128	2.125	2.125	2.690	0.155	15.0	6000
483	N	2	1.270	2	1.270	2.125	2.125	2.690	0.155	15.0	6000
484	Y	6	1.410	6	1.410	2.125	NA	0.880	0.207	13.0	6000
485	N	4	1.270	4	1.410	2.125	2.125	2.510	0.310	13.0	6000
486	Y	6	1.410	6	1.410	2.125	NA	0.880	0.207	14.0	6000
487	N	4	1.270	4	1.270	2.125	2.125	2.600	0.310	14.0	6000
488	Y	6	1.410	6	1.410	2.125	NA	0.880	0.207	14.0	6000
489	N	4	1.270	4	1.270	2.125	2.125	2.600	0.310	14.0	6000
490	Y	6	1.410	6	1.410	2.125	NA	0.880	0.207	14.0	6000
491	N	4	1.270	4	1.410	2.125	2.125	2.510	0.310	14.0	6000
492	Y	6	1.410	6	1.410	2.125	NA	0.880	0.207	13.0	6000
493	N	4	1.270	4	1.410	2.125	2.125	2.510	0.310	13.0	6000
494	Y	6	1.410	6	1.410	2.125	NA	0.880	0.207	14.0	6000
495	N	4	1.270	4	1.270	2.125	2.125	2.600	0.310	14.0	6000
496	Y	6	1.410	6	1.410	2.125	NA	0.880	0.207	14.0	6000
497	N	4	1.270	4	1.270	2.125	2.125	2.600	0.310	14.0	6000
498	Y	6	1.410	6	1.410	2.125	NA	0.880	0.207	14.0	6000
499	N	4	1.270	4	1.410	2.125	2.125	2.510	0.310	14.0	6000
500	Y	4	1.410	6	1.410	2.125	NA	1.940	0.310	15.0	6000
501	N	4	1.410	4	1.410	2.125	2.125	2.410	0.310	15.0	6000
502	Y	6	1.410	6	1.410	2.125	NA	0.880	0.207	15.0	6000
503	N	4	1.410	4	1.410	2.125	2.125	2.410	0.310	15.0	6000
504	Y	6	1.410	6	1.410	2.125	NA	0.880	0.207	15.0	6000
505	N	4	1.410	4	1.410	2.125	2.125	2.410	0.310	15.0	6000
506	Y	4	1.410	6	1.410	2.125	NA	1.940	0.155	8.0	6000
507	N	4	1.410	4	1.410	2.125	2.125	2.410	0.155	8.0	6000
508	Y	4	1.410	6	1.410	2.125	NA	1.940	0.310	15.0	6000
509	N	4	1.410	4	1.410	2.125	2.125	2.410	0.310	15.0	6000
510	Y	6	1.410	6	1.410	2.125	NA	0.880	0.207	15.0	6000
511	N	4	1.410	4	1.410	2.125	2.125	2.410	0.310	15.0	6000
512	Y	6	1.410	6	1.410	2.125	NA	0.880	0.207	15.0	6000
513	N	4	1.410	4	1.410	2.125	2.125	2.410	0.310	15.0	6000
514	Y	4	1.410	6	1.410	2.125	NA	1.940	0.155	8.0	6000
515	N	4	1.410	4	1.410	2.125	2.125	2.410	0.155	8.0	6000
516	Y	4	1.410	6	1.410	2.125	NA	1.940	0.310	15.0	6000
517	N	4	1.410	4	1.410	2.125	2.125	2.410	0.310	15.0	6000
518	Y	6	1.410	6	1.410	2.125	NA	0.880	0.207	15.0	6000
519	N	4	1.410	4	1.410	2.125	2.125	2.410	0.310	15.0	6000
520	Y	4	1.410	6	1.410	2.125	NA	1.940	0.310	15.0	6000

Table D.1a
Splice data for beams in lateral load resisting frame system (continued)

Splice	Top	Spliced Bars* A Bars		B Bars		Cover			Transverse Reinf.		f'_c
						c_b	c_{so}	c_{si}	A_{tr}/n	s	
No.	Bar	# bars	d_b (in.)	# bars	d_b (in.)	(in.)	(in.)	(in.)	($in.^2$)	(in.)	(psi)
521	N	4	1.410	4	1.410	2.125	2.125	2.410	0.310	15.0	6000
522	Y	4	1.410	4	1.410	2.125	NA	2.410	0.310	8.0	6000
523	N	4	1.410	4	1.410	2.125	2.125	2.410	0.155	8.0	6000
524	Y	6	1.410	6	1.410	2.125	NA	0.880	0.207	10.0	6000
525	N	4	1.270	6	1.410	2.125	2.125	2.040	0.310	10.0	6000
526	Y	6	1.410	6	1.410	2.125	NA	0.880	0.207	10.0	6000
527	N	6	1.410	6	1.410	2.125	2.125	0.880	0.207	10.0	6000
528	Y	6	1.410	6	1.410	2.125	NA	0.880	0.207	10.0	6000
529	N	6	1.410	6	1.410	2.125	2.125	0.880	0.207	10.0	6000
530	Y	6	1.410	6	1.410	2.125	NA	0.880	0.207	10.0	6000
531	N	4	1.270	6	1.410	2.125	2.125	2.040	0.310	10.0	6000
532	Y	6	1.410	6	1.410	2.125	NA	0.880	0.207	10.0	5000
533	N	4	1.270	6	1.410	2.125	2.125	2.040	0.310	10.0	5000
534	Y	6	1.410	6	1.410	2.125	NA	0.880	0.207	10.0	5000
535	N	6	1.410	6	1.410	2.125	2.125	0.880	0.207	10.0	5000
536	Y	6	1.410	6	1.410	2.125	NA	0.880	0.207	10.0	5000
537	N	6	1.410	6	1.410	2.125	2.125	0.880	0.207	10.0	5000
538	Y	6	1.410	6	1.410	2.125	NA	0.880	0.207	10.0	5000
539	N	4	1.270	6	1.410	2.125	2.125	2.040	0.310	10.0	5000
540	Y	6	1.410	6	1.410	2.125	NA	0.880	0.207	10.0	5000
541	N	4	1.270	6	1.270	2.125	2.125	2.180	0.310	10.0	5000
542	Y	6	1.410	6	1.410	2.125	NA	0.880	0.207	10.0	5000
543	N	6	1.270	6	1.410	2.125	2.125	0.970	0.207	10.0	5000
544	Y	6	1.410	6	1.410	2.125	NA	0.880	0.207	10.0	5000
545	N	6	1.410	6	1.410	2.125	2.125	0.880	0.207	10.0	5000
546	Y	6	1.410	6	1.410	2.125	NA	0.880	0.207	10.0	5000
547	N	4	1.270	6	1.410	2.125	2.125	2.040	0.310	10.0	5000
548	Y	6	1.410	6	1.410	2.125	NA	0.880	0.207	11.0	5000
549	N	4	1.270	4	1.410	2.125	2.125	2.510	0.310	11.0	5000
550	Y	6	1.410	6	1.410	2.125	NA	0.880	0.207	12.0	5000
551	N	4	1.410	4	1.410	2.125	2.125	2.410	0.310	12.0	5000
552	Y	6	1.410	6	1.410	2.125	NA	0.880	0.207	12.0	5000
553	N	4	1.410	4	1.410	2.125	2.125	2.410	0.310	12.0	5000
554	Y	6	1.410	6	1.410	2.125	NA	0.880	0.207	13.0	5000
555	N	4	1.410	4	1.410	2.125	2.125	2.410	0.310	13.0	5000
556	Y	6	1.410	6	1.410	2.125	NA	0.880	0.207	13.0	5000
557	N	4	1.128	4	1.410	2.125	2.125	2.600	0.310	13.0	5000
558	Y	6	1.410	6	1.410	2.125	NA	0.880	0.207	14.0	5000
559	N	4	1.410	4	1.410	2.125	2.125	2.410	0.310	14.0	5000
560	Y	6	1.410	6	1.410	2.125	NA	0.880	0.207	14.0	5000

Table D.1a
Splice data for beams in lateral load resisting frame system (continued)

Splice	Top	Spliced Bars* A Bars		Spliced Bars* B Bars		Cover			Transverse Reinf.		
						c_b	c_{so}	c_{si}	A_{tr}/n	s	f'_c
No.	Bar	# bars	d_b (in.)	# bars	d_b (in.)	(in.)	(in.)	(in.)	($in.^2$)	(in.)	(psi)
561	N	4	1.410	4	1.410	2.125	2.125	2.410	0.310	14.0	5000
562	Y	4	1.410	6	1.410	2.125	NA	1.940	0.310	15.0	5000
563	N	4	1.128	4	1.410	2.125	2.125	2.600	0.310	15.0	5000
564	Y	4	1.270	4	1.410	2.125	NA	2.510	0.310	10.0	5000
565	N	2	1.128	2	1.270	2.125	2.125	2.650	0.155	10.0	5000
566	N	2	1.270	2	1.270	2.125	2.125	2.650	0.155	10.0	5000
567	Y	4	1.410	4	1.410	2.125	NA	2.410	0.310	9.0	5000
568	N	4	1.270	4	1.270	2.125	2.125	2.600	0.155	9.0	5000
569	Y	4	1.410	4	1.410	2.125	NA	2.410	0.310	9.0	5000
570	N	4	1.270	4	1.270	2.125	2.125	2.600	0.155	9.0	5000
571	Y	4	1.270	4	1.410	2.125	NA	2.510	0.310	10.0	5000
572	N	2	1.128	2	1.270	2.125	2.125	2.650	0.155	10.0	5000
573	N	2	1.270	2	1.270	2.125	2.125	2.650	0.155	10.0	5000
574	Y	4	1.128	4	1.410	2.125	NA	2.600	0.310	15.0	5000
575	N	2	1.128	2	1.128	2.125	2.125	2.690	0.155	15.0	5000
576	N	2	1.270	2	1.270	2.125	2.125	2.690	0.155	15.0	5000
577	Y	4	1.410	4	1.410	2.125	NA	2.410	0.310	15.0	5000
578	N	2	1.128	2	1.128	2.125	2.125	2.690	0.155	15.0	5000
579	N	2	1.270	2	1.270	2.125	2.125	2.690	0.155	15.0	5000
580	Y	4	1.128	4	1.410	2.125	NA	2.600	0.310	15.0	5000
581	N	2	1.128	2	1.128	2.125	2.125	2.690	0.155	15.0	5000
582	N	2	1.270	2	1.270	2.125	2.125	2.690	0.155	15.0	5000
583	Y	4	1.128	4	1.128	2.000	NA	2.830	0.200	15.0	6000
584	N	2	1.128	2	1.128	2.000	2.000	2.730	0.100	15.0	6000
585	N	2	1.270	2	1.270	2.000	2.000	2.730	0.100	15.0	6000
586	Y	4	1.128	4	1.128	2.000	NA	2.830	0.200	15.0	6000
587	N	2	1.128	2	1.128	2.000	2.000	2.730	0.100	15.0	6000
588	N	2	1.270	2	1.270	2.000	2.000	2.730	0.100	15.0	6000
589	Y	4	1.128	4	1.128	2.000	NA	2.830	0.200	15.0	6000
590	N	2	1.128	2	1.128	2.000	2.000	2.730	0.100	15.0	6000
591	N	2	1.270	2	1.270	2.000	2.000	2.730	0.100	15.0	6000
592	Y	4	1.410	6	1.410	2.125	NA	1.940	0.310	15.0	6000
593	N	4	1.410	4	1.410	2.125	2.125	2.410	0.310	15.0	6000
594	Y	4	1.410	4	1.410	2.125	NA	2.410	0.310	15.0	6000
595	N	4	1.410	4	1.410	2.125	2.125	2.410	0.310	15.0	6000
596	Y	4	1.410	6	1.410	2.125	NA	1.940	0.310	15.0	6000
597	N	4	1.410	4	1.410	2.125	2.125	2.410	0.310	15.0	6000
598	Y	6	1.410	6	1.410	2.125	NA	0.880	0.103	8.0	6000
599	N	4	1.410	4	1.410	2.125	2.125	2.410	0.155	8.0	6000
600	Y	6	1.410	6	1.410	2.125	NA	0.880	0.103	8.0	6000

Table D.1a
Splice data for beams in lateral load resisting frame system (continued)

Splice	Top	Spliced Bars* A Bars		Spliced Bars* B Bars		Cover			Transverse Reinf.		
						c_b	c_{so}	c_{si}	A_{tr}/n	s	f'_c
No.	Bar	# bars	d_b (in.)	# bars	d_b (in.)	(in.)	(in.)	(in.)	($in.^2$)	(in.)	(psi)
601	N	4	1.410	4	1.410	2.125	2.125	2.410	0.155	8.0	6000
602	Y	6	1.410	6	1.410	2.125	NA	0.880	0.103	8.0	6000
603	N	4	1.410	4	1.410	2.125	2.125	2.410	0.155	8.0	6000
604	Y	4	1.410	6	1.410	2.125	NA	1.940	0.155	8.0	6000
605	N	4	1.128	4	1.270	2.125	2.125	2.730	0.155	8.0	6000
606	Y	4	1.410	4	1.410	2.125	NA	2.410	0.310	9.0	6000
607	N	4	1.270	4	1.270	2.125	2.125	2.600	0.155	9.0	6000
608	Y	4	1.410	6	1.410	2.125	NA	1.940	0.155	8.0	6000
609	N	4	1.128	4	1.270	2.125	2.125	2.730	0.155	8.0	6000
610	Y	4	1.410	6	1.410	2.125	NA	1.940	0.155	8.0	6000
611	N	4	1.128	4	1.270	2.125	2.125	2.730	0.155	8.0	6000
612	Y	4	1.410	4	1.410	2.125	NA	2.410	0.310	9.0	6000
613	N	4	1.270	4	1.270	2.125	2.125	2.600	0.155	9.0	6000
614	Y	4	1.410	6	1.410	2.125	NA	1.940	0.155	8.0	6000
615	N	4	1.128	4	1.270	2.125	2.125	2.730	0.155	8.0	6000
616	Y	4	1.270	4	1.410	2.125	NA	2.510	0.310	14.0	6000
617	N	3	1.128	4	1.128	2.125	2.125	4.390	0.207	14.0	6000
618	Y	4	1.410	4	1.410	2.125	NA	2.410	0.310	14.0	6000
619	N	3	1.128	3	1.128	2.125	2.125	4.750	0.207	14.0	6000
620	Y	4	1.270	4	1.410	2.125	NA	2.510	0.310	14.0	6000
621	N	3	1.128	4	1.128	2.125	2.125	4.390	0.207	14.0	6000
622	Y	4	1.270	4	1.410	2.125	NA	2.510	0.310	12.0	6000
623	N	2	1.128	2	1.128	2.125	2.125	2.690	0.155	12.0	6000
624	N	2	1.270	2	1.270	2.125	2.125	2.690	0.155	12.0	6000
625	Y	4	1.410	4	1.410	2.125	NA	2.410	0.310	12.0	6000
626	N	2	1.128	2	1.128	2.125	2.125	2.690	0.155	12.0	6000
627	N	2	1.270	2	1.270	2.125	2.125	2.690	0.155	12.0	6000
628	Y	4	1.410	4	1.410	2.125	NA	2.410	0.310	12.0	6000
629	N	2	1.128	2	1.128	2.125	2.125	2.690	0.155	12.0	6000
630	N	2	1.270	2	1.270	2.125	2.125	2.690	0.155	12.0	6000
631	Y	4	1.270	4	1.410	2.125	NA	2.510	0.310	12.0	6000
632	N	2	1.128	2	1.128	2.125	2.125	2.690	0.155	12.0	6000
633	N	2	1.270	2	1.270	2.125	2.125	2.690	0.155	12.0	6000
634	Y	6	1.410	6	1.410	2.125	NA	0.880	0.207	13.0	6000
635	N	4	1.270	4	1.410	2.125	2.125	2.510	0.310	13.0	6000
636	Y	6	1.410	6	1.410	2.125	NA	0.880	0.207	13.0	6000
637	N	4	1.270	4	1.270	2.125	2.125	2.600	0.310	13.0	6000
638	Y	6	1.410	6	1.410	2.125	NA	0.880	0.207	13.0	6000
639	N	4	1.270	4	1.270	2.125	2.125	2.600	0.310	13.0	6000
640	Y	6	1.410	6	1.410	2.125	NA	0.880	0.207	13.0	6000

Table D.1a
Splice data for beams in lateral load resisting frame system (continued)

Splice	Top	Spliced Bars* A Bars		B Bars		Cover			Transverse Reinf.		f'_c
						c_b	c_{so}	c_{si}	A_{tr}/n	s	
No.	Bar	# bars	d_b (in.)	# bars	d_b (in.)	(in.)	(in.)	(in.)	($in.^2$)	(in.)	(psi)
641	N	4	1.270	4	1.410	2.125	2.125	2.510	0.310	13.0	6000
642	Y	6	1.410	6	1.410	2.125	NA	0.880	0.207	13.0	6000
643	N	4	1.270	4	1.410	2.125	2.125	2.510	0.310	13.0	6000
644	Y	6	1.410	6	1.410	2.125	NA	0.880	0.207	13.0	6000
645	N	4	1.270	4	1.270	2.125	2.125	2.600	0.310	13.0	6000
646	Y	6	1.410	6	1.410	2.125	NA	0.880	0.207	13.0	6000
647	N	4	1.270	4	1.270	2.125	2.125	2.600	0.310	13.0	6000
648	Y	6	1.410	6	1.410	2.125	NA	0.880	0.207	13.0	6000
649	N	4	1.270	4	1.410	2.125	2.125	2.510	0.310	13.0	6000
650	Y	4	1.410	4	1.410	2.125	NA	2.410	0.310	9.0	6000
651	N	4	1.410	4	1.410	2.125	2.125	2.410	0.155	9.0	6000
652	Y	4	1.410	4	1.410	2.125	NA	2.410	0.310	9.0	6000
653	N	4	1.410	4	1.410	2.125	2.125	2.410	0.155	9.0	6000
654	Y	4	1.410	4	1.410	2.125	NA	2.410	0.310	9.0	6000
655	N	4	1.410	4	1.410	2.125	2.125	2.410	0.155	9.0	6000
656	Y	4	1.410	4	1.410	2.125	NA	2.410	0.310	9.0	6000
657	N	4	1.410	4	1.410	2.125	2.125	2.410	0.155	9.0	6000
658	Y	4	1.410	4	1.410	2.125	NA	2.410	0.310	9.0	6000
659	N	4	1.410	4	1.410	2.125	2.125	2.410	0.155	9.0	6000
660	Y	4	1.410	4	1.410	2.125	NA	2.410	0.310	9.0	6000
661	N	4	1.410	4	1.410	2.125	2.125	2.410	0.155	9.0	6000
662	Y	4	1.410	4	1.410	2.125	NA	2.410	0.310	9.0	6000
663	N	4	1.410	4	1.410	2.125	2.125	2.410	0.155	9.0	6000
664	Y	4	1.410	4	1.410	2.125	NA	2.410	0.310	9.0	6000
665	N	4	1.410	4	1.410	2.125	2.125	2.410	0.155	9.0	6000
666	Y	4	1.410	4	1.410	2.125	NA	2.410	0.310	14.0	6000
667	N	4	1.410	4	1.410	2.125	2.125	2.410	0.155	14.0	6000
668	Y	4	1.410	4	1.410	2.125	NA	2.410	0.310	14.0	6000
669	N	4	1.410	4	1.410	2.125	2.125	2.410	0.155	14.0	6000
670	Y	4	1.410	4	1.410	2.125	NA	2.410	0.310	14.0	6000
671	N	4	1.410	4	1.410	2.125	2.125	2.410	0.155	14.0	6000
672	Y	4	1.410	4	1.410	2.125	NA	2.410	0.310	14.0	6000
673	N	4	1.410	4	1.410	2.125	2.125	2.410	0.155	14.0	6000
674	Y	4	1.270	4	1.410	2.125	NA	1.510	0.155	11.0	5000
675	N	4	1.128	4	1.128	2.125	2.125	1.790	0.155	11.0	5000
676	Y	4	1.410	4	1.410	2.125	NA	1.410	0.155	12.0	5000
677	N	4	1.128	4	1.128	2.125	2.125	1.790	0.155	12.0	5000
678	Y	4	1.410	4	1.410	2.125	NA	1.410	0.155	12.0	5000
679	N	4	1.128	4	1.128	2.125	2.125	1.790	0.155	12.0	5000
680	Y	4	1.410	4	1.410	2.125	NA	1.410	0.155	12.0	5000

Table D.1a
Splice data for beams in lateral load resisting frame system (continued)

Splice	Top	Spliced Bars* A Bars		B Bars		Cover			Transverse Reinf.		f'_c
						c_b	c_{so}	c_{si}	A_{tr}/n	s	
No.	Bar	# bars	d_b (in.)	# bars	d_b (in.)	(in.)	(in.)	(in.)	($in.^2$)	(in.)	(psi)
681	N	4	1.128	4	1.128	2.125	2.125	1.790	0.155	12.0	5000
682	Y	4	1.270	4	1.410	2.125	NA	1.510	0.155	12.0	5000
683	N	4	1.128	4	1.128	2.125	2.125	1.790	0.155	12.0	5000
684	Y	4	1.270	4	1.270	2.125	NA	1.600	0.155	11.0	5000
685	N	4	1.128	4	1.128	2.125	2.125	1.790	0.155	11.0	5000
686	Y	4	1.270	4	1.270	2.125	NA	1.600	0.155	12.0	5000
687	N	4	1.128	4	1.128	2.125	2.125	1.790	0.155	12.0	5000
688	Y	4	1.270	4	1.410	2.125	NA	1.510	0.155	12.0	5000
689	N	4	1.128	4	1.128	2.125	2.125	1.790	0.155	12.0	5000
690	Y	4	1.410	4	1.270	2.125	NA	1.410	0.155	12.0	5000
691	N	4	1.128	4	1.128	2.125	2.125	1.790	0.155	12.0	5000
692	Y	4	1.270	4	1.410	2.125	NA	1.510	0.155	12.0	5000
693	N	4	1.128	4	1.128	2.125	2.125	1.790	0.155	12.0	5000
694	Y	4	1.270	4	1.270	2.125	NA	1.600	0.155	11.0	5000
695	N	4	1.128	4	1.128	2.125	2.125	1.790	0.155	11.0	5000
696	Y	4	1.270	4	1.270	2.125	NA	1.600	0.155	11.0	5000
697	N	4	1.128	4	1.128	2.125	2.125	1.790	0.155	11.0	5000
698	Y	4	1.270	4	1.410	2.125	NA	1.510	0.155	11.0	5000
699	N	4	1.128	4	1.128	2.125	2.125	1.790	0.155	11.0	5000
700	Y	4	1.410	4	1.410	2.125	NA	1.410	0.155	12.0	5000
701	N	4	1.128	4	1.128	2.125	2.125	1.790	0.155	12.0	5000
702	Y	4	1.410	4	1.410	2.125	NA	1.410	0.155	12.0	5000
703	N	4	1.128	4	1.128	2.125	2.125	1.790	0.155	12.0	5000
704	Y	4	1.128	4	1.128	2.000	NA	1.830	0.100	13.0	5000
705	N	4	1.128	4	1.128	2.000	2.000	1.830	0.100	13.0	5000
706	Y	2	1.128	2	1.128	2.125	NA	2.690	0.310	12.0	6000
707	Y	2	1.270	2	1.270	2.125	NA	2.690	0.310	12.0	6000
708	N	2	1.128	2	1.128	2.125	2.125	2.690	0.155	12.0	6000
709	N	2	1.270	2	1.270	2.125	2.125	2.690	0.155	12.0	6000
710	Y	2	1.128	2	1.128	2.125	NA	2.690	0.310	12.0	6000
711	Y	2	1.270	2	1.270	2.125	NA	2.690	0.310	12.0	6000
712	N	2	1.128	2	1.128	2.125	2.125	2.690	0.155	12.0	6000
713	N	2	1.270	2	1.270	2.125	2.125	2.690	0.155	12.0	6000
714	Y	2	1.128	2	1.128	2.125	NA	2.690	0.310	12.0	6000
715	Y	2	1.270	2	1.270	2.125	NA	2.690	0.310	12.0	6000
716	N	2	1.128	2	1.128	2.125	2.125	2.690	0.155	12.0	6000
717	N	2	1.270	2	1.270	2.125	2.125	2.690	0.155	12.0	6000
718	Y	2	1.128	2	1.128	2.125	NA	2.690	0.310	12.0	6000
719	Y	2	1.270	2	1.270	2.125	NA	2.690	0.310	12.0	6000
720	N	2	1.128	2	1.128	2.125	2.125	2.690	0.155	12.0	6000

Table D.1a
Splice data for beams in lateral load resisting frame system (continued)

Splice	Top	Spliced Bars* A Bars		B Bars		Cover			Transverse Reinf.		f'_c
No.	Bar	# bars	d_b (in.)	# bars	d_b (in.)	c_b (in.)	c_{so} (in.)	c_{si} (in.)	A_{tr}/n ($in.^2$)	s (in.)	(psi)
721	N	2	1.270	2	1.270	2.125	2.125	2.690	0.155	12.0	6000
722	Y	6	1.410	6	1.410	2.125	NA	0.880	0.207	13.0	6000
723	N	4	1.270	4	1.410	2.125	2.125	2.510	0.310	13.0	6000
724	Y	6	1.410	6	1.410	2.125	NA	0.880	0.207	13.0	6000
725	N	4	1.270	4	1.270	2.125	2.125	2.600	0.310	13.0	6000
726	Y	6	1.410	6	1.410	2.125	NA	0.880	0.207	13.0	6000
727	N	4	1.270	4	1.270	2.125	2.125	2.600	0.310	13.0	6000
728	Y	6	1.410	6	1.410	2.125	NA	0.880	0.207	13.0	6000
729	N	4	1.270	4	1.410	2.125	2.125	2.510	0.310	13.0	6000
730	Y	6	1.410	6	1.410	2.125	NA	0.880	0.207	13.0	6000
731	N	4	1.270	4	1.410	2.125	2.125	2.510	0.310	13.0	6000
732	Y	6	1.410	6	1.410	2.125	NA	0.880	0.207	13.0	6000
733	N	4	1.270	4	1.270	2.125	2.125	2.600	0.310	13.0	6000
734	Y	6	1.410	6	1.410	2.125	NA	0.880	0.207	13.0	6000
735	N	4	1.270	4	1.270	2.125	2.125	2.600	0.310	13.0	6000
736	Y	6	1.410	6	1.410	2.125	NA	0.880	0.207	13.0	6000
737	N	4	1.270	4	1.410	2.125	2.125	2.510	0.310	13.0	6000
738	Y	4	1.410	4	1.410	2.125	NA	2.410	0.310	9.0	6000
739	N	4	1.410	4	1.410	2.125	2.125	2.410	0.155	9.0	6000
740	Y	4	1.410	4	1.410	2.125	NA	2.410	0.310	9.0	6000
741	N	4	1.410	4	1.410	2.125	2.125	2.410	0.155	9.0	6000
742	Y	4	1.410	4	1.410	2.125	NA	2.410	0.310	9.0	6000
743	N	4	1.410	4	1.410	2.125	2.125	2.410	0.155	9.0	6000
744	Y	4	1.410	4	1.410	2.125	NA	2.410	0.310	9.0	6000
745	N	4	1.410	4	1.410	2.125	2.125	2.410	0.155	9.0	6000
746	Y	4	1.410	4	1.410	2.125	NA	2.410	0.310	9.0	6000
747	N	4	1.410	4	1.410	2.125	2.125	2.410	0.155	9.0	6000
748	Y	4	1.410	4	1.410	2.125	NA	2.410	0.310	9.0	6000
749	N	4	1.410	4	1.410	2.125	2.125	2.410	0.155	9.0	6000
750	Y	4	1.410	4	1.410	2.125	NA	2.410	0.310	9.0	6000
751	N	4	1.410	4	1.410	2.125	2.125	2.410	0.155	9.0	6000
752	Y	4	1.410	4	1.410	2.125	NA	2.410	0.310	9.0	6000
753	N	4	1.410	4	1.410	2.125	2.125	2.410	0.155	9.0	6000
754	Y	4	1.410	4	1.410	2.125	NA	2.410	0.310	14.0	6000
755	N	4	1.410	4	1.410	2.125	2.125	2.410	0.155	14.0	6000
756	Y	4	1.410	4	1.410	2.125	NA	2.410	0.310	14.0	6000
757	N	4	1.410	4	1.410	2.125	2.125	2.410	0.155	14.0	6000
758	Y	4	1.410	4	1.410	2.125	NA	2.410	0.310	14.0	6000
759	N	4	1.410	4	1.410	2.125	2.125	2.410	0.155	14.0	6000
760	Y	4	1.410	4	1.410	2.125	NA	2.410	0.310	14.0	6000

Table D.1a
Splice data for beams in lateral load resisting frame system (continued)

Splice	Top	Spliced Bars* A Bars		B Bars		Cover			Transverse Reinf.		f'_c
No.	Bar	# bars	d_b (in.)	# bars	d_b (in.)	c_b (in.)	c_{so} (in.)	c_{si} (in.)	A_{tr}/n ($in.^2$)	s (in.)	(psi)
761	N	4	1.410	4	1.410	2.125	2.125	2.410	0.155	14.0	6000
762	Y	3	1.128	3	1.128	2.125	NA	4.750	0.310	12.0	6000
763	N	2	1.128	2	1.128	2.125	2.125	2.690	0.155	12.0	6000
764	N	2	1.270	2	1.270	2.125	2.125	2.690	0.155	12.0	6000
765	Y	3	1.128	3	1.128	2.125	NA	4.750	0.310	12.0	6000
766	Y	3	1.128	3	1.128	2.125	NA	4.750	0.310	12.0	6000
767	Y	4	1.410	6	1.410	2.125	NA	1.940	0.310	13.0	6000
768	N	4	1.270	4	1.270	2.125	2.125	2.600	0.310	13.0	6000
769	Y	4	1.410	4	1.410	2.125	NA	2.410	0.310	15.0	6000
770	N	4	1.270	4	1.270	2.125	2.125	2.600	0.310	15.0	6000
771	Y	4	1.410	6	1.410	2.125	NA	1.940	0.310	13.0	6000
772	N	4	1.270	4	1.270	2.125	2.125	2.600	0.310	13.0	6000
773	Y	4	1.410	4	1.410	2.125	NA	2.410	0.310	8.0	6000
774	N	4	1.270	4	1.410	2.125	2.125	2.510	0.155	8.0	6000
775	Y	4	1.410	4	1.410	2.125	NA	2.410	0.310	8.0	6000
776	N	4	1.270	4	1.270	2.125	2.125	2.600	0.155	8.0	6000
777	Y	4	1.410	4	1.410	2.125	NA	2.410	0.310	8.0	6000
778	N	4	1.270	4	1.410	2.125	2.125	2.510	0.155	8.0	6000
779	Y	4	1.410	4	1.410	2.125	NA	2.410	0.310	11.0	6000
780	N	4	1.270	4	1.410	2.125	2.125	2.510	0.155	11.0	6000
781	Y	4	1.410	4	1.410	2.125	NA	2.410	0.310	11.0	6000
782	N	4	1.270	4	1.270	2.125	2.125	2.600	0.155	11.0	6000
783	Y	4	1.410	4	1.410	2.125	NA	2.410	0.310	11.0	6000
784	N	4	1.270	4	1.410	2.125	2.125	2.510	0.155	11.0	6000
785	Y	4	1.270	4	1.410	2.125	NA	2.510	0.310	13.0	6000
786	N	4	1.128	4	1.270	2.125	2.125	2.740	0.155	13.0	6000
787	Y	4	1.410	4	1.410	2.125	NA	2.410	0.310	14.0	6000
788	N	4	1.270	4	1.270	2.125	2.125	2.600	0.155	14.0	6000
789	Y	4	1.270	4	1.410	2.125	NA	2.510	0.310	13.0	6000
790	N	4	1.128	4	1.270	2.125	2.125	2.740	0.155	13.0	6000
791	Y	3	1.128	4	1.128	2.000	NA	4.530	0.200	15.0	6000
792	N	2	1.128	2	1.128	2.000	2.000	2.730	0.100	15.0	6000
793	N	2	1.270	2	1.270	2.000	2.000	2.730	0.100	15.0	6000
794	Y	4	1.128	4	1.128	2.000	NA	2.830	0.200	15.0	6000
795	N	2	1.128	2	1.128	2.000	2.000	2.730	0.100	15.0	6000
796	N	2	1.270	2	1.270	2.000	2.000	2.730	0.100	15.0	6000
797	Y	3	1.128	4	1.128	2.000	NA	4.530	0.200	15.0	6000
798	N	2	1.128	2	1.128	2.000	2.000	2.730	0.100	15.0	6000
799	N	2	1.270	2	1.270	2.000	2.000	2.730	0.100	15.0	6000
800	Y	4	1.410	6	1.410	2.125	NA	0.940	0.155	10.0	5000

Table D.1a
Splice data for beams in lateral load resisting frame system (continued)

Splice	Top	Spliced Bars* A Bars		Spliced Bars* B Bars		Cover c_b	Cover c_{so}	Cover c_{si}	Transverse Reinf. A_{tr}/n	Transverse Reinf. s	f'_c
No.	Bar	# bars	d_b (in.)	# bars	d_b (in.)	(in.)	(in.)	(in.)	(in.^{2})	(in.)	(psi)
801	N	4	1.128	4	1.128	2.125	2.125	1.790	0.155	10.0	5000
802	Y	4	1.410	6	1.410	2.125	NA	0.940	0.155	10.0	5000
803	Y	2	1.128	3	1.270	2.000	NA	1.260	0.100	16.0	5000
804	Y	2	1.270	3	1.270	2.000	NA	1.260	0.100	16.0	5000
805	N	2	1.128	2	1.128	2.000	2.000	1.730	0.100	16.0	5000
806	N	2	1.270	2	1.270	2.000	2.000	1.730	0.100	16.0	5000
807	Y	2	1.128	3	1.270	2.000	NA	1.260	0.100	16.0	5000
808	Y	2	1.270	3	1.270	2.000	NA	1.260	0.100	16.0	5000
809	N	4	1.128	4	1.410	2.125	2.125	1.600	0.155	8.0	5000
810	Y	4	1.410	4	1.410	2.125	NA	1.410	0.155	10.0	5000
811	N	4	1.128	4	1.410	2.125	2.125	1.600	0.155	8.0	5000
812	Y	2	1.128	2	1.128	2.000	NA	1.730	0.100	10.0	5000
813	Y	2	1.270	2	1.270	2.000	NA	1.730	0.100	10.0	5000
814	N	2	1.128	2	1.128	2.000	2.000	1.730	0.100	10.0	5000
815	N	2	1.270	2	1.270	2.000	2.000	1.730	0.100	10.0	5000
816	N	4	1.128	4	1.128	2.000	2.000	1.780	0.100	9.0	5000
817	Y	4	1.270	4	1.270	2.000	NA	1.640	0.100	10.0	5000
818	N	4	1.128	4	1.128	2.000	2.000	1.780	0.100	9.0	5000

* A bars spliced to B bars
1 in. = 25.4 mm; 1 psi = 6.89 kPa

Table D.1b
Splice lengths and material savings for beams in lateral load resisting frame system (continued)

Spl. No.	Orig. l_s (in.)	ACI '95 l_s (in.)	l_s (Eq. 3.13†) Conv. (in.)	l_s (Eq. 3.13†) New* (in.)	l_s (Eq. 3.14††) Conv. (in.)	l_s (Eq. 3.14††) New* (in.)	Change in weight of steel (lb) ACI '95	Eq. 3.13† Conv.*	Eq. 3.13† New**	Eq. 3.14†† Conv.*	Eq. 3.14†† New**
161	96.00	60.66	40.19	33.48	41.20	34.23	-62.6	-98.8	-110.7	-97.1	-109.4
162	78.00	42.03	32.96	29.42	32.96	29.42	-51.6	-64.6	-69.7	-64.6	-69.7
163	96.00	60.66	40.19	33.48	41.20	34.23	-62.6	-98.8	-110.7	-97.1	-109.4
164	78.00	42.03	32.96	29.42	32.96	29.42	-51.6	-64.6	-69.7	-64.6	-69.7
165	96.00	60.66	40.19	33.48	41.20	34.23	-62.6	-98.8	-110.7	-97.1	-109.4
166	78.00	42.03	32.96	29.42	32.96	29.42	-51.6	-64.6	-69.7	-64.6	-69.7
167	96.00	60.66	40.19	33.48	41.20	34.23	-62.6	-98.8	-110.7	-97.1	-109.4
168	78.00	42.03	32.96	29.42	32.96	29.42	-51.6	-64.6	-69.7	-64.6	-69.7
169	96.00	60.66	40.19	33.48	41.20	34.23	-62.6	-98.8	-110.7	-97.1	-109.4
170	78.00	42.03	32.96	29.42	32.96	29.42	-51.6	-64.6	-69.7	-64.6	-69.7
171	96.00	60.66	40.19	33.48	41.20	34.23	-62.6	-98.8	-110.7	-97.1	-109.4
172	78.00	42.03	32.96	29.42	32.96	29.42	-51.6	-64.6	-69.7	-64.6	-69.7
173	78.00	54.64	36.60	31.39	37.76	32.28	-41.4	-73.3	-82.6	-71.3	-81.0
174	67.00	37.33	28.27	25.80	28.27	25.80	-26.3	-34.3	-36.5	-34.3	-36.5
175	78.00	42.03	34.51	31.35	34.51	31.35	-31.9	-38.5	-41.3	-38.5	-41.3
176	78.00	54.64	36.44	31.26	37.76	32.28	-33.5	-59.6	-67.0	-57.7	-65.6
177	96.00	47.67	41.04	37.12	41.04	37.12	-85.6	-97.3	-104.3	-97.3	-104.3
178	78.00	54.64	36.44	31.26	37.76	32.28	-33.5	-59.6	-67.0	-57.7	-65.6
179	96.00	47.67	41.04	37.12	41.04	37.12	-85.6	-97.3	-104.3	-97.3	-104.3
180	78.00	54.64	36.44	31.26	37.76	32.28	-33.5	-59.6	-67.0	-57.7	-65.6
181	96.00	47.67	41.04	37.12	41.04	37.12	-85.6	-97.3	-104.3	-97.3	-104.3
182	78.00	54.64	36.44	31.26	37.76	32.28	-33.5	-59.6	-67.0	-57.7	-65.6
183	96.00	47.67	41.04	37.12	41.04	37.12	-85.6	-97.3	-104.3	-97.3	-104.3
184	78.00	54.64	36.60	31.39	37.76	32.28	-41.4	-73.3	-82.6	-71.3	-81.0
185	67.00	37.33	28.27	25.80	28.27	25.80	-26.3	-34.3	-36.5	-34.3	-36.5
186	78.00	42.03	34.51	31.35	34.51	31.35	-31.9	-38.5	-41.3	-38.5	-41.3
187	96.00	60.66	45.91	39.83	47.17	40.82	-62.6	-88.7	-99.5	-86.5	-97.7
188	67.00	37.33	29.13	26.92	29.13	26.92	-21.3	-27.2	-28.7	-27.2	-28.7
189	78.00	42.03	35.62	32.78	35.62	32.78	-25.8	-30.4	-32.4	-30.4	-32.4
190	96.00	60.66	45.91	39.83	47.17	40.82	-62.6	-88.7	-99.5	-86.5	-97.7
191	78.00	42.03	35.62	32.78	35.62	32.78	-51.6	-60.8	-64.9	-60.8	-64.9
192	96.00	60.66	45.91	39.83	47.17	40.82	-62.6	-88.7	-99.5	-86.5	-97.7
193	78.00	42.03	35.62	32.78	35.62	32.78	-51.6	-60.8	-64.9	-60.8	-64.9
194	96.00	60.66	45.91	39.83	47.17	40.82	-62.6	-88.7	-99.5	-86.5	-97.7
195	78.00	42.03	35.62	32.78	35.62	32.78	-51.6	-60.8	-64.9	-60.8	-64.9
196	96.00	60.66	45.91	39.83	47.17	40.82	-62.6	-88.7	-99.5	-86.5	-97.7
197	78.00	42.03	35.62	32.78	35.62	32.78	-51.6	-60.8	-64.9	-60.8	-64.9
198	96.00	60.66	45.91	39.83	47.17	40.82	-62.6	-88.7	-99.5	-86.5	-97.7
199	67.00	37.33	29.13	26.92	29.13	26.92	-21.3	-27.2	-28.7	-27.2	-28.7
200	78.00	42.03	35.62	32.78	35.62	32.78	-25.8	-30.4	-32.4	-30.4	-32.4

Table D.1b
Splice lengths and material savings for beams in lateral load resisting frame system (continued)

Spl. No.	Orig. l_s (in.)	ACI '95 l_s (in.)	l_s (Eq. 3.13†) Conv. (in.)	l_s (Eq. 3.13†) New* (in.)	l_s (Eq. 3.14††) Conv. (in.)	l_s (Eq. 3.14††) New* (in.)	Change in weight of steel (lb) ACI '95	Eq. 3.13† Conv.*	Eq. 3.13† New**	Eq. 3.14†† Conv.*	Eq. 3.14†† New**
201	67.00	48.53	33.37	30.93	39.22	36.06	-20.9	-38.1	-40.9	-31.5	-35.1
202	67.00	37.33	32.86	31.36	32.86	31.36	-21.3	-24.5	-25.6	-24.5	-25.6
203	78.00	45.99	40.31	38.36	40.31	38.36	-23.0	-27.0	-28.4	-27.0	-28.4
204	67.00	48.53	31.34	27.53	32.84	28.74	-20.9	-40.4	-44.7	-38.7	-43.4
205	78.00	42.03	35.62	32.78	35.62	32.78	-51.6	-60.8	-64.9	-60.8	-64.9
206	67.00	48.53	31.34	27.53	32.84	28.74	-20.9	-40.4	-44.7	-38.7	-43.4
207	78.00	42.03	35.62	32.78	35.62	32.78	-51.6	-60.8	-64.9	-60.8	-64.9
208	67.00	48.53	31.34	27.53	32.84	28.74	-20.9	-40.4	-44.7	-38.7	-43.4
209	78.00	42.03	35.62	32.78	35.62	32.78	-51.6	-60.8	-64.9	-60.8	-64.9
210	67.00	48.53	31.34	27.53	32.84	28.74	-20.9	-40.4	-44.7	-38.7	-43.4
211	78.00	42.03	35.62	32.78	35.62	32.78	-51.6	-60.8	-64.9	-60.8	-64.9
212	67.00	48.53	33.37	30.93	39.22	36.06	-20.9	-38.1	-40.9	-31.5	-35.1
213	67.00	37.33	32.86	31.36	32.86	31.36	-21.3	-24.5	-25.6	-24.5	-25.6
214	78.00	45.99	40.31	38.36	40.31	38.36	-23.0	-27.0	-28.4	-27.0	-28.4
215	67.00	44.30	34.72	32.02	36.84	33.87	-12.9	-18.3	-19.8	-17.1	-18.8
216	78.00	49.98	42.40	38.94	44.97	41.16	-20.1	-25.5	-28.0	-23.7	-26.4
217	67.00	34.08	30.87	29.46	30.87	29.46	-18.7	-20.5	-21.3	-20.5	-21.3
218	78.00	41.98	37.86	36.03	37.86	36.03	-25.8	-28.8	-30.1	-28.8	-30.1
219	67.00	44.30	34.72	32.02	36.84	33.87	-12.9	-18.3	-19.8	-17.1	-18.8
220	78.00	49.98	42.40	38.94	44.97	41.16	-20.1	-25.5	-28.0	-23.7	-26.4
221	67.00	34.08	30.87	29.46	30.87	29.46	-18.7	-20.5	-21.3	-20.5	-21.3
222	78.00	41.98	37.86	36.03	37.86	36.03	-25.8	-28.8	-30.1	-28.8	-30.1
223	96.00	55.37	44.93	39.54	46.21	40.58	-71.9	-90.5	-100.0	-88.2	-98.2
224	96.00	42.60	35.55	31.21	35.55	31.21	-94.6	-107.1	-114.7	-107.1	-114.7
225	96.00	55.37	44.93	39.54	46.21	40.58	-71.9	-90.5	-100.0	-88.2	-98.2
226	96.00	42.60	35.55	31.21	35.55	31.21	-94.6	-107.1	-114.7	-107.1	-114.7
227	96.00	55.37	37.73	31.43	38.70	32.15	-71.9	-103.2	-114.4	-101.5	-113.1
228	96.00	42.60	36.74	32.64	36.74	32.64	-94.6	-105.0	-112.2	-105.0	-112.2
229	96.00	55.37	37.73	31.43	38.70	32.15	-71.9	-103.2	-114.4	-101.5	-113.1
230	96.00	42.60	36.74	32.64	36.74	32.64	-94.6	-105.0	-112.2	-105.0	-112.2
231	96.00	55.37	40.78	34.76	41.88	35.60	-71.9	-97.8	-108.5	-95.9	-107.0
232	96.00	43.52	38.55	34.87	38.55	34.87	-92.9	-101.8	-108.3	-101.8	-108.3
233	96.00	55.37	40.78	34.76	41.88	35.60	-71.9	-97.8	-108.5	-95.9	-107.0
234	96.00	43.52	38.55	34.87	38.55	34.87	-92.9	-101.8	-108.3	-101.8	-108.3
235	96.00	55.37	42.01	36.15	43.16	37.05	-71.9	-95.6	-106.0	-93.6	-104.4
236	96.00	44.24	39.25	35.76	39.25	35.76	-91.7	-100.5	-106.7	-100.5	-106.7
237	96.00	55.37	42.01	36.15	43.16	37.05	-71.9	-95.6	-106.0	-93.6	-104.4
238	96.00	44.24	39.25	35.76	39.25	35.76	-91.7	-100.5	-106.7	-100.5	-106.7
239	96.00	55.37	42.01	36.15	43.16	37.05	-71.9	-95.6	-106.0	-93.6	-104.4
240	96.00	44.24	39.25	35.76	39.25	35.76	-91.7	-100.5	-106.7	-100.5	-106.7

Table D.1b
Splice lengths and material savings for beams in lateral load resisting frame system (continued)

Spl. No.	Orig. l_s (in.)	ACI '95 l_s (in.)	l_s (Eq. 3.13^{+}) Conv. (in.)	l_s (Eq. 3.13^{+}) New* (in.)	l_s (Eq. 3.14^{++}) Conv. (in.)	l_s (Eq. 3.14^{++}) New* (in.)	Change in weight of steel (lb) ACI '95	Eq. 3.13^{+} Conv.*	Eq. 3.13^{+} New**	Eq. 3.14^{++} Conv.*	Eq. 3.14^{++} New**
241	96.00	55.37	42.01	36.15	43.16	37.05	-71.9	-95.6	-106.0	-93.6	-104.4
242	96.00	44.24	39.25	35.76	39.25	35.76	-91.7	-100.5	-106.7	-100.5	-106.7
243	96.00	55.37	40.78	34.76	41.88	35.60	-71.9	-97.8	-108.5	-95.9	-107.0
244	96.00	43.52	38.55	34.87	38.55	34.87	-92.9	-101.8	-108.3	-101.8	-108.3
245	96.00	55.37	40.78	34.76	41.88	35.60	-71.9	-97.8	-108.5	-95.9	-107.0
246	96.00	43.52	38.55	34.87	38.55	34.87	-92.9	-101.8	-108.3	-101.8	-108.3
247	96.00	60.66	43.44	37.03	44.58	37.90	-62.6	-93.1	-104.4	-91.1	-102.9
248	96.00	47.67	41.04	37.12	41.04	37.12	-85.6	-97.3	-104.3	-97.3	-104.3
249	96.00	60.66	43.44	37.03	44.58	37.90	-62.6	-93.1	-104.4	-91.1	-102.9
250	96.00	47.67	41.04	37.12	41.04	37.12	-85.6	-97.3	-104.3	-97.3	-104.3
251	96.00	60.66	44.76	38.51	45.96	39.44	-62.6	-90.8	-101.8	-88.6	-100.2
252	96.00	48.47	41.78	38.07	41.78	38.07	-84.2	-96.0	-102.6	-96.0	-102.6
253	96.00	60.66	44.76	38.51	45.96	39.44	-62.6	-90.8	-101.8	-88.6	-100.2
254	96.00	48.47	41.78	38.07	41.78	38.07	-84.2	-96.0	-102.6	-96.0	-102.6
255	96.00	60.66	47.86	42.12	49.20	43.20	-62.6	-85.3	-95.4	-82.9	-93.5
256	67.00	37.33	29.79	27.78	29.79	27.78	-16.8	-21.1	-22.2	-21.1	-22.2
257	78.00	42.03	36.46	33.89	36.46	33.89	-25.8	-29.8	-31.6	-29.8	-31.6
258	96.00	60.66	47.86	42.12	49.20	43.20	-62.6	-85.3	-95.4	-82.9	-93.5
259	67.00	37.33	29.79	27.78	29.79	27.78	-16.8	-21.1	-22.2	-21.1	-22.2
260	78.00	42.03	36.46	33.89	36.46	33.89	-25.8	-29.8	-31.6	-29.8	-31.6
261	78.00	54.64	40.63	36.17	42.21	37.48	-33.5	-53.6	-60.0	-51.3	-58.1
262	78.00	42.05	36.81	34.35	36.81	34.35	-51.6	-59.1	-62.6	-59.1	-62.6
263	78.00	54.64	40.63	36.17	42.21	37.48	-33.5	-53.6	-60.0	-51.3	-58.1
264	78.00	42.05	36.81	34.35	36.81	34.35	-51.6	-59.1	-62.6	-59.1	-62.6
265	96.00	60.66	45.91	39.83	47.17	40.82	-62.6	-88.7	-99.5	-86.5	-97.7
266	67.00	37.33	29.13	26.92	29.13	26.92	-16.8	-21.5	-22.7	-21.5	-22.7
267	78.00	42.03	35.62	32.78	35.62	32.78	-25.8	-30.4	-32.4	-30.4	-32.4
268	96.00	60.66	45.91	39.83	47.17	40.82	-62.6	-88.7	-99.5	-86.5	-97.7
269	67.00	37.33	29.13	26.92	29.13	26.92	-16.8	-21.5	-22.7	-21.5	-22.7
270	78.00	42.03	35.62	32.78	35.62	32.78	-25.8	-30.4	-32.4	-30.4	-32.4
271	67.00	48.53	37.10	34.20	39.22	36.06	-10.5	-16.9	-18.6	-15.7	-17.5
272	78.00	54.75	45.30	41.59	47.88	43.82	-16.7	-23.5	-26.1	-21.6	-24.5
273	67.00	37.33	32.86	31.36	32.86	31.36	-16.8	-19.3	-20.2	-19.3	-20.2
274	78.00	45.99	40.31	38.36	40.31	38.36	-23.0	-27.0	-28.4	-27.0	-28.4
275	67.00	48.53	37.10	34.20	39.22	36.06	-10.5	-16.9	-18.6	-15.7	-17.5
276	78.00	54.75	45.30	41.59	47.88	43.82	-16.7	-23.5	-26.1	-21.6	-24.5
277	67.00	37.33	32.86	31.36	32.86	31.36	-16.8	-19.3	-20.2	-19.3	-20.2
278	78.00	45.99	40.31	38.36	40.31	38.36	-23.0	-27.0	-28.4	-27.0	-28.4
279	96.00	55.37	43.10	37.39	44.30	38.34	-71.9	-93.7	-103.8	-91.6	-102.1
280	67.00	34.08	27.36	25.29	27.36	25.29	-18.7	-22.5	-23.6	-22.5	-23.6

Table D.1b
Splice lengths and material savings for beams in lateral load resisting frame system (continued)

Spl. No.	Orig. l_s (in.)	ACI '95 l_s (in.)	l_s (Eq. 3.13^{+}) Conv. (in.)	l_s (Eq. 3.13^{+}) New* (in.)	l_s (Eq. 3.14^{++}) Conv. (in.)	l_s (Eq. 3.14^{++}) New* (in.)	Change in weight of steel (lb) ACI '95	Eq. 3.13^{+} Conv.*	Eq. 3.13^{+} New**	Eq. 3.14^{++} Conv.*	Eq. 3.14^{++} New**
281	78.00	38.37	33.46	30.79	33.46	30.79	-28.4	-31.9	-33.9	-31.9	-33.9
282	96.00	55.37	43.10	37.39	44.30	38.34	-71.9	-93.7	-103.8	-91.6	-102.1
283	67.00	34.08	27.36	25.29	27.36	25.29	-18.7	-22.5	-23.6	-22.5	-23.6
284	78.00	38.37	33.46	30.79	33.46	30.79	-28.4	-31.9	-33.9	-31.9	-33.9
285	96.00	55.37	43.10	37.39	44.30	38.34	-71.9	-93.7	-103.8	-91.6	-102.1
286	67.00	34.08	27.36	25.29	27.36	25.29	-18.7	-22.5	-23.6	-22.5	-23.6
287	78.00	38.37	33.46	30.79	33.46	30.79	-28.4	-31.9	-33.9	-31.9	-33.9
288	96.00	62.86	49.73	42.99	54.94	46.90	-88.0	-122.9	-140.8	-109.1	-130.4
289	96.00	48.36	38.25	33.07	42.26	36.07	-126.6	-153.4	-167.2	-142.8	-159.2
290	96.00	62.86	49.73	42.99	54.94	46.90	-88.0	-122.9	-140.8	-109.1	-130.4
291	96.00	48.36	38.25	33.07	42.26	36.07	-126.6	-153.4	-167.2	-142.8	-159.2
292	96.00	62.86	49.73	42.99	54.94	46.90	-88.0	-122.9	-140.8	-109.1	-130.4
293	96.00	48.36	38.25	33.07	42.26	36.07	-126.6	-153.4	-167.2	-142.8	-159.2
294	96.00	80.89	58.36	49.89	70.32	58.72	-40.1	-100.0	-122.5	-68.2	-99.0
295	96.00	42.60	32.21	27.39	33.69	28.45	-141.9	-169.5	-182.3	-165.5	-179.5
296	96.00	80.89	58.36	49.89	70.32	58.72	-40.1	-100.0	-122.5	-68.2	-99.0
297	96.00	62.22	44.89	38.38	54.10	45.17	-89.7	-135.8	-153.1	-111.3	-135.0
298	96.00	80.89	58.36	49.89	70.32	58.72	-40.1	-100.0	-122.5	-68.2	-99.0
299	96.00	42.60	32.21	27.39	33.69	28.45	-141.9	-169.5	-182.3	-165.5	-179.5
300	96.00	82.24	59.26	50.90	71.58	60.07	-36.6	-97.6	-119.8	-64.9	-95.4
301	96.00	42.60	32.72	27.96	32.72	27.96	-94.6	-112.1	-120.5	-112.1	-120.5
302	96.00	82.24	59.26	50.90	71.58	60.07	-36.6	-97.6	-119.8	-64.9	-95.4
303	96.00	42.60	32.72	27.96	32.72	27.96	-94.6	-112.1	-120.5	-112.1	-120.5
304	96.00	82.24	59.26	50.90	71.58	60.07	-36.6	-97.6	-119.8	-64.9	-95.4
305	96.00	42.60	32.72	27.96	32.72	27.96	-94.6	-112.1	-120.5	-112.1	-120.5
306	96.00	87.85	62.96	55.19	76.86	65.91	-21.7	-87.8	-108.4	-50.8	-79.9
307	96.00	42.60	34.85	30.40	34.85	30.40	-94.6	-108.3	-116.2	-108.3	-116.2
308	96.00	87.85	62.96	55.19	76.86	65.91	-21.7	-87.8	-108.4	-50.8	-79.9
309	96.00	42.60	34.85	30.40	34.85	30.40	-94.6	-108.3	-116.2	-108.3	-116.2
310	96.00	87.85	62.96	55.19	76.86	65.91	-21.7	-87.8	-108.4	-50.8	-79.9
311	96.00	42.60	34.85	30.40	34.85	30.40	-94.6	-108.3	-116.2	-108.3	-116.2
312	96.00	87.85	62.96	55.19	76.86	65.91	-21.7	-87.8	-108.4	-50.8	-79.9
313	78.00	38.37	29.43	25.80	29.43	25.80	-70.2	-86.0	-92.4	-86.0	-92.4
314	96.00	89.68	64.17	56.62	78.60	67.89	-16.8	-84.6	-104.6	-46.2	-74.7
315	96.00	42.60	35.55	31.21	35.55	31.21	-94.6	-107.1	-114.7	-107.1	-114.7
316	96.00	87.85	62.96	55.19	76.86	65.91	-21.7	-87.8	-108.4	-50.8	-79.9
317	78.00	38.37	29.43	25.80	29.43	25.80	-70.2	-86.0	-92.4	-86.0	-92.4
318	96.00	82.24	59.26	50.90	71.58	60.07	-36.6	-97.6	-119.8	-64.9	-95.4
319	96.00	42.60	32.72	27.96	32.72	27.96	-94.6	-112.1	-120.5	-112.1	-120.5
320	96.00	82.24	59.26	50.90	71.58	60.07	-36.6	-97.6	-119.8	-64.9	-95.4

Table D.1b
Splice lengths and material savings for beams in lateral load resisting frame system (continued)

Spl. No.	Orig. l_s (in.)	ACI '95 l_s (in.)	l_s (Eq. 3.13$^+$) Conv. (in.)	l_s (Eq. 3.13$^+$) New* (in.)	l_s (Eq. 3.14^{++}) Conv. (in.)	l_s (Eq. 3.14^{++}) New* (in.)	Change in weight of steel (lb) ACI '95	Eq. 3.13$^+$ Conv.*	Eq. 3.13$^+$ New**	Eq. 3.14^{++} Conv.*	Eq. 3.14^{++} New**
321	96.00	42.60	32.72	27.96	32.72	27.96	-94.6	-112.1	-120.5	-112.1	-120.5
322	96.00	82.24	59.26	50.90	71.58	60.07	-36.6	-97.6	-119.8	-64.9	-95.4
323	96.00	42.60	32.72	27.96	32.72	27.96	-94.6	-112.1	-120.5	-112.1	-120.5
324	96.00	96.23	67.18	58.88	81.83	70.17	0.6	-76.6	-98.6	-37.6	-68.6
325	78.00	42.03	31.34	27.47	31.34	27.47	-63.7	-82.6	-89.5	-82.6	-89.5
326	96.00	96.23	67.18	58.88	81.83	70.17	0.6	-76.6	-98.6	-37.6	-68.6
327	96.00	46.66	37.11	32.36	37.11	32.36	-87.4	-104.3	-112.7	-104.3	-112.7
328	96.00	96.23	67.18	58.88	81.83	70.17	0.6	-76.6	-98.6	-37.6	-68.6
329	78.00	42.03	31.34	27.47	31.34	27.47	-63.7	-82.6	-89.5	-82.6	-89.5
330	96.00	96.23	67.18	58.88	81.83	70.17	0.6	-76.6	-98.6	-37.6	-68.6
331	78.00	42.03	31.34	27.47	31.34	27.47	-63.7	-82.6	-89.5	-82.6	-89.5
332	96.00	96.23	67.18	58.88	81.83	70.17	0.6	-76.6	-98.6	-37.6	-68.6
333	96.00	46.66	37.11	32.36	37.11	32.36	-87.4	-104.3	-112.7	-104.3	-112.7
334	96.00	96.23	67.18	58.88	81.83	70.17	0.6	-76.6	-98.6	-37.6	-68.6
335	78.00	42.03	31.34	27.47	31.34	27.47	-63.7	-82.6	-89.5	-82.6	-89.5
336	96.00	60.66	48.69	43.10	50.07	44.23	-62.6	-83.8	-93.7	-81.3	-91.7
337	78.00	42.03	32.47	28.83	32.47	28.83	-51.6	-65.3	-70.5	-65.3	-70.5
338	96.00	60.66	48.69	43.10	50.07	44.23	-62.6	-83.8	-93.7	-81.3	-91.7
339	78.00	42.03	32.47	28.83	32.47	28.83	-51.6	-65.3	-70.5	-65.3	-70.5
340	96.00	60.66	48.69	43.10	50.07	44.23	-62.6	-83.8	-93.7	-81.3	-91.7
341	78.00	42.03	32.47	28.83	32.47	28.83	-51.6	-65.3	-70.5	-65.3	-70.5
342	96.00	60.66	48.69	43.10	50.07	44.23	-62.6	-83.8	-93.7	-81.3	-91.7
343	67.00	37.33	26.68	23.81	26.68	23.81	-21.3	-28.9	-31.0	-28.9	-31.0
344	78.00	42.03	32.47	28.83	32.47	28.83	-25.8	-32.7	-35.3	-32.7	-35.3
345	96.00	60.66	48.69	43.10	50.07	44.23	-62.6	-83.8	-93.7	-81.3	-91.7
346	78.00	42.03	32.47	28.83	32.47	28.83	-51.6	-65.3	-70.5	-65.3	-70.5
347	96.00	60.66	48.69	43.10	50.07	44.23	-62.6	-83.8	-93.7	-81.3	-91.7
348	67.00	37.33	26.68	23.81	26.68	23.81	-21.3	-28.9	-31.0	-28.9	-31.0
349	78.00	42.03	32.47	28.83	32.47	28.83	-25.8	-32.7	-35.3	-32.7	-35.3
350	78.00	54.64	39.43	34.65	40.74	35.71	-41.4	-68.3	-76.8	-66.0	-74.9
351	67.00	37.33	29.48	27.38	29.48	27.38	-33.6	-42.5	-44.9	-42.5	-44.9
352	96.00	60.66	47.86	42.12	49.20	43.20	-62.6	-85.3	-95.4	-82.9	-93.5
353	67.00	37.33	29.79	27.78	29.79	27.78	-33.6	-42.2	-44.4	-42.2	-44.4
354	78.00	54.64	39.43	34.65	40.74	35.71	-41.4	-68.3	-76.8	-66.0	-74.9
355	67.00	37.33	29.48	27.38	29.48	27.38	-33.6	-42.5	-44.9	-42.5	-44.9
356	96.00	60.66	48.69	43.10	50.07	44.23	-62.6	-83.8	-93.7	-81.3	-91.7
357	67.00	37.33	30.05	28.15	30.05	28.15	-16.8	-20.9	-22.0	-20.9	-22.0
358	78.00	42.05	36.81	34.35	36.81	34.35	-25.8	-29.5	-31.3	-29.5	-31.3
359	96.00	60.66	48.69	43.10	50.07	44.23	-62.6	-83.8	-93.7	-81.3	-91.7
360	67.00	37.33	30.05	28.15	30.05	28.15	-16.8	-20.9	-22.0	-20.9	-22.0

Table D.1b
Splice lengths and material savings for beams in lateral load resisting frame system (continued)

Spl. No.	Orig. l_s (in.)	ACI '95 l_s (in.)	l_s (Eq. 3.13$^+$) Conv. (in.)	l_s (Eq. 3.13$^+$) New* (in.)	l_s (Eq. 3.14^{++}) Conv. (in.)	l_s (Eq. 3.14^{++}) New* (in.)	Change in weight of steel (lb) ACI '95	Eq. 3.13$^+$ Conv.*	Eq. 3.13$^+$ New**	Eq. 3.14^{++} Conv.*	Eq. 3.14^{++} New**
361	78.00	42.05	36.81	34.35	36.81	34.35	-25.8	-29.5	-31.3	-29.5	-31.3
362	96.00	60.66	48.69	43.10	50.07	44.23	-62.6	-83.8	-93.7	-81.3	-91.7
363	67.00	37.33	30.05	28.15	30.05	28.15	-16.8	-20.9	-22.0	-20.9	-22.0
364	78.00	42.05	36.81	34.35	36.81	34.35	-25.8	-29.5	-31.3	-29.5	-31.3
365	96.00	55.37	43.10	37.39	44.30	38.34	-71.9	-93.7	-103.8	-91.6	-102.1
366	67.00	34.08	27.36	25.29	27.36	25.29	-18.7	-22.5	-23.6	-22.5	-23.6
367	78.00	38.37	33.46	30.79	33.46	30.79	-28.4	-31.9	-33.9	-31.9	-33.9
368	96.00	55.37	43.10	37.39	44.30	38.34	-71.9	-93.7	-103.8	-91.6	-102.1
369	67.00	34.08	27.36	25.29	27.36	25.29	-18.7	-22.5	-23.6	-22.5	-23.6
370	78.00	38.37	33.46	30.79	33.46	30.79	-28.4	-31.9	-33.9	-31.9	-33.9
371	96.00	55.37	43.10	37.39	44.30	38.34	-71.9	-93.7	-103.8	-91.6	-102.1
372	67.00	34.08	27.36	25.29	27.36	25.29	-18.7	-22.5	-23.6	-22.5	-23.6
373	78.00	38.37	33.46	30.79	33.46	30.79	-28.4	-31.9	-33.9	-31.9	-33.9
374	96.00	55.37	43.10	37.39	44.30	38.34	-71.9	-93.7	-103.8	-91.6	-102.1
375	67.00	34.08	27.36	25.29	27.36	25.29	-18.7	-22.5	-23.6	-22.5	-23.6
376	78.00	38.37	33.46	30.79	33.46	30.79	-28.4	-31.9	-33.9	-31.9	-33.9
377	96.00	85.80	61.61	53.61	74.93	63.74	-27.1	-91.3	-112.6	-56.0	-85.7
378	78.00	38.37	28.80	25.06	29.15	25.32	-85.3	-105.8	-113.9	-105.1	-113.3
379	96.00	85.80	61.61	53.61	74.93	63.74	-27.1	-91.3	-112.6	-56.0	-85.7
380	78.00	51.29	38.81	34.11	45.98	39.67	-57.5	-84.3	-94.4	-68.9	-82.5
381	96.00	85.80	61.61	53.61	74.93	63.74	-27.1	-91.3	-112.6	-56.0	-85.7
382	78.00	51.29	38.81	34.11	45.98	39.67	-57.5	-84.3	-94.4	-68.9	-82.5
383	96.00	92.95	66.30	59.20	81.71	71.50	-8.1	-78.9	-97.8	-38.0	-65.1
384	78.00	38.37	30.96	27.63	31.35	27.95	-85.3	-101.2	-108.4	-100.4	-107.7
385	96.00	80.89	58.36	49.89	70.32	58.72	-40.1	-100.0	-122.5	-68.2	-99.0
386	78.00	38.37	27.28	23.33	27.59	23.55	-85.3	-109.1	-117.6	-108.5	-117.1
387	96.00	80.89	58.36	49.89	70.32	58.72	-40.1	-100.0	-122.5	-68.2	-99.0
388	78.00	48.47	36.92	31.90	43.40	36.77	-63.5	-88.4	-99.2	-74.4	-88.7
389	96.00	80.89	58.36	49.89	70.32	58.72	-40.1	-100.0	-122.5	-68.2	-99.0
390	78.00	48.47	36.92	31.90	43.40	36.77	-63.5	-88.4	-99.2	-74.4	-88.7
391	96.00	92.95	66.30	59.20	81.71	71.50	-8.1	-78.9	-97.8	-38.0	-65.1
392	78.00	38.37	30.96	27.63	31.35	27.95	-85.3	-101.2	-108.4	-100.4	-107.7
393	96.00	87.85	62.96	55.19	76.86	65.91	-21.7	-87.8	-108.4	-50.8	-79.9
394	96.00	42.60	34.85	30.40	34.85	30.40	-94.6	-108.3	-116.2	-108.3	-116.2
395	96.00	87.85	62.96	55.19	76.86	65.91	-21.7	-87.8	-108.4	-50.8	-79.9
396	96.00	42.60	34.85	30.40	34.85	30.40	-94.6	-108.3	-116.2	-108.3	-116.2
397	96.00	87.85	62.96	55.19	76.86	65.91	-21.7	-87.8	-108.4	-50.8	-79.9
398	96.00	42.60	34.85	30.40	34.85	30.40	-94.6	-108.3	-116.2	-108.3	-116.2
399	96.00	92.95	66.30	59.20	81.71	71.50	-8.1	-78.9	-97.8	-38.0	-65.1
400	96.00	42.60	36.74	32.64	36.74	32.64	-94.6	-105.0	-112.2	-105.0	-112.2

Table D.1b
Splice lengths and material savings for beams in lateral load resisting frame system (continued)

Spl. No.	Orig. l_s (in.)	ACI '95 l_s (in.)	l_s (Eq. 3.13$^+$) Conv. (in.)	l_s (Eq. 3.13$^+$) New* (in.)	l_s (Eq. 3.14^{++}) Conv. (in.)	l_s (Eq. 3.14^{++}) New* (in.)	Change in weight of steel (lb) ACI '95	Eq. 3.13$^+$ Conv.*	Eq. 3.13$^+$ New**	Eq. 3.14^{++} Conv.*	Eq. 3.14^{++} New**
401	96.00	87.85	62.96	55.19	76.86	65.91	-21.7	-87.8	-108.4	-50.8	-79.9
402	96.00	42.60	34.85	30.40	34.85	30.40	-94.6	-108.3	-116.2	-108.3	-116.2
403	96.00	87.85	62.96	55.19	76.86	65.91	-21.7	-87.8	-108.4	-50.8	-79.9
404	96.00	42.60	34.85	30.40	34.85	30.40	-94.6	-108.3	-116.2	-108.3	-116.2
405	96.00	87.85	62.96	55.19	76.86	65.91	-21.7	-87.8	-108.4	-50.8	-79.9
406	96.00	42.60	34.85	30.40	34.85	30.40	-94.6	-108.3	-116.2	-108.3	-116.2
407	96.00	92.95	66.30	59.20	81.71	71.50	-8.1	-78.9	-97.8	-38.0	-65.1
408	96.00	42.60	36.74	32.64	36.74	32.64	-94.6	-105.0	-112.2	-105.0	-112.2
409	96.00	87.85	62.96	55.19	76.86	65.91	-21.7	-87.8	-108.4	-50.8	-79.9
410	96.00	42.60	34.85	30.40	34.85	30.40	-94.6	-108.3	-116.2	-108.3	-116.2
411	96.00	87.85	62.96	55.19	76.86	65.91	-21.7	-87.8	-108.4	-50.8	-79.9
412	96.00	42.60	34.85	30.40	34.85	30.40	-94.6	-108.3	-116.2	-108.3	-116.2
413	96.00	87.85	62.96	55.19	76.86	65.91	-21.7	-87.8	-108.4	-50.8	-79.9
414	96.00	42.60	34.85	30.40	34.85	30.40	-94.6	-108.3	-116.2	-108.3	-116.2
415	96.00	92.95	66.30	59.20	81.71	71.50	-8.1	-78.9	-97.8	-38.0	-65.1
416	96.00	42.60	36.74	32.64	36.74	32.64	-94.6	-105.0	-112.2	-105.0	-112.2
417	96.00	80.89	58.36	49.89	70.32	58.72	-40.1	-100.0	-122.5	-68.2	-99.0
418	78.00	38.37	27.28	23.33	27.59	23.55	-85.3	-109.1	-117.6	-108.5	-117.1
419	96.00	80.89	58.36	49.89	70.32	58.72	-40.1	-100.0	-122.5	-68.2	-99.0
420	78.00	48.47	36.92	31.90	43.40	36.77	-63.5	-88.4	-99.2	-74.4	-88.7
421	96.00	80.89	58.36	49.89	70.32	58.72	-40.1	-100.0	-122.5	-68.2	-99.0
422	78.00	48.47	36.92	31.90	43.40	36.77	-63.5	-88.4	-99.2	-74.4	-88.7
423	96.00	92.95	66.30	59.20	81.71	71.50	-8.1	-78.9	-97.8	-38.0	-65.1
424	78.00	38.37	30.96	27.63	31.35	27.95	-85.3	-101.2	-108.4	-100.4	-107.7
425	96.00	91.47	64.11	55.32	77.47	65.32	-12.0	-84.7	-108.1	-49.2	-81.5
426	96.00	46.66	35.35	30.34	35.35	30.34	-87.4	-107.4	-116.3	-107.4	-116.3
427	96.00	93.99	65.74	57.19	79.77	67.86	-5.3	-80.4	-103.1	-43.1	-74.7
428	96.00	46.66	36.28	31.40	36.28	31.40	-87.4	-105.8	-114.4	-105.8	-114.4
429	96.00	93.99	65.74	57.19	79.77	67.86	-5.3	-80.4	-103.1	-43.1	-74.7
430	96.00	46.66	36.28	31.40	36.28	31.40	-87.4	-105.8	-114.4	-105.8	-114.4
431	96.00	101.82	70.73	63.16	86.99	76.12	15.5	-67.1	-87.2	-23.9	-52.8
432	96.00	46.66	39.11	34.75	39.11	34.75	-87.4	-100.7	-108.5	-100.7	-108.5
433	96.00	93.99	65.74	57.19	79.77	67.86	-5.3	-80.4	-103.1	-43.1	-74.7
434	96.00	46.66	36.28	31.40	36.28	31.40	-87.4	-105.8	-114.4	-105.8	-114.4
435	96.00	93.99	65.74	57.19	79.77	67.86	-5.3	-80.4	-103.1	-43.1	-74.7
436	96.00	46.66	36.28	31.40	36.28	31.40	-87.4	-105.8	-114.4	-105.8	-114.4
437	96.00	93.99	65.74	57.19	79.77	67.86	-5.3	-80.4	-103.1	-43.1	-74.7
438	96.00	46.66	36.28	31.40	36.28	31.40	-87.4	-105.8	-114.4	-105.8	-114.4
439	96.00	104.67	72.54	65.39	89.64	79.27	23.0	-62.3	-81.3	-16.9	-44.4
440	96.00	46.74	40.16	36.03	40.16	36.03	-87.2	-98.9	-106.2	-98.9	-106.2

Table D.1b
Splice lengths and material savings for beams in lateral load resisting frame system (continued)

Spl. No.	Orig. l_s (in.)	ACI '95 l_s (in.)	l_s (Eq. 3.13$^+$) Conv. (in.)	l_s (Eq. 3.13$^+$) New* (in.)	l_s (Eq. 3.14^{++}) Conv. (in.)	l_s (Eq. 3.14^{++}) New* (in.)	Change in weight of steel (lb) ACI '95	Eq. 3.13$^+$ Conv.*	Eq. 3.13$^+$ New**	Eq. 3.14^{++} Conv.*	Eq. 3.14^{++} New**
441	96.00	61.59	49.90	44.09	52.66	46.25	-91.4	-122.5	-137.9	-115.1	-132.2
442	78.00	42.03	32.47	28.83	32.47	28.83	-51.6	-65.3	-70.5	-65.3	-70.5
443	96.00	60.66	48.69	43.10	50.07	44.23	-62.6	-83.8	-93.7	-81.3	-91.7
444	78.00	42.03	32.47	28.83	32.47	28.83	-51.6	-65.3	-70.5	-65.3	-70.5
445	96.00	60.66	48.69	43.10	50.07	44.23	-62.6	-83.8	-93.7	-81.3	-91.7
446	78.00	42.03	32.47	28.83	32.47	28.83	-51.6	-65.3	-70.5	-65.3	-70.5
447	96.00	70.81	57.63	53.92	61.35	57.16	-66.9	-101.9	-111.8	-92.1	-103.2
448	78.00	42.03	35.11	32.11	35.11	32.11	-51.6	-61.5	-65.8	-61.5	-65.8
449	96.00	61.59	49.90	44.09	52.66	46.25	-91.4	-122.5	-137.9	-115.1	-132.2
450	78.00	42.03	32.47	28.83	32.47	28.83	-51.6	-65.3	-70.5	-65.3	-70.5
451	96.00	60.66	48.69	43.10	50.07	44.23	-62.6	-83.8	-93.7	-81.3	-91.7
452	78.00	42.03	32.47	28.83	32.47	28.83	-51.6	-65.3	-70.5	-65.3	-70.5
453	96.00	60.66	48.69	43.10	50.07	44.23	-62.6	-83.8	-93.7	-81.3	-91.7
454	78.00	42.03	32.47	28.83	32.47	28.83	-51.6	-65.3	-70.5	-65.3	-70.5
455	96.00	70.81	57.63	53.92	61.35	57.16	-66.9	-101.9	-111.8	-92.1	-103.2
456	78.00	42.03	35.11	32.11	35.11	32.11	-51.6	-61.5	-65.8	-61.5	-65.8
457	96.00	60.66	41.94	35.36	43.01	36.18	-62.6	-95.7	-107.4	-93.8	-105.9
458	67.00	37.33	27.72	25.10	27.72	25.10	-21.3	-28.2	-30.0	-28.2	-30.0
459	78.00	42.03	33.80	30.46	33.80	30.46	-25.8	-31.7	-34.1	-31.7	-34.1
460	96.00	60.66	41.94	35.36	43.01	36.18	-62.6	-95.7	-107.4	-93.8	-105.9
461	78.00	42.03	33.80	30.46	33.80	30.46	-51.6	-63.4	-68.2	-63.4	-68.2
462	96.00	60.66	41.94	35.36	43.01	36.18	-62.6	-95.7	-107.4	-93.8	-105.9
463	78.00	42.03	33.80	30.46	33.80	30.46	-51.6	-63.4	-68.2	-63.4	-68.2
464	96.00	60.66	48.69	43.10	50.07	44.23	-62.6	-83.8	-93.7	-81.3	-91.7
465	67.00	37.33	30.05	28.15	30.05	28.15	-21.3	-26.5	-27.9	-26.5	-27.9
466	78.00	42.05	36.81	34.35	36.81	34.35	-25.8	-29.5	-31.3	-29.5	-31.3
467	96.00	60.66	45.91	39.83	47.17	40.82	-62.6	-88.7	-99.5	-86.5	-97.7
468	67.00	37.33	29.13	26.92	29.13	26.92	-16.8	-21.5	-22.7	-21.5	-22.7
469	78.00	42.03	35.62	32.78	35.62	32.78	-25.8	-30.4	-32.4	-30.4	-32.4
470	67.00	51.43	42.51	40.57	45.47	43.27	-17.6	-27.8	-30.0	-24.4	-26.9
471	67.00	39.56	32.86	31.36	34.98	33.28	-31.1	-38.7	-40.4	-36.3	-38.2
472	96.00	55.37	45.70	40.46	47.03	41.55	-71.9	-89.1	-98.4	-86.7	-96.4
473	67.00	34.08	28.23	26.44	28.23	26.44	-18.7	-22.0	-23.0	-22.0	-23.0
474	78.00	38.39	34.58	32.26	34.58	32.26	-28.4	-31.1	-32.8	-31.1	-32.8
475	96.00	55.37	45.70	40.46	47.03	41.55	-71.9	-89.1	-98.4	-86.7	-96.4
476	67.00	34.08	28.23	26.44	28.23	26.44	-18.7	-22.0	-23.0	-22.0	-23.0
477	78.00	38.39	34.58	32.26	34.58	32.26	-28.4	-31.1	-32.8	-31.1	-32.8
478	78.00	49.88	38.32	34.10	39.65	35.20	-49.8	-70.3	-77.7	-67.9	-75.8
479	67.00	34.08	28.23	26.44	28.23	26.44	-18.7	-22.0	-23.0	-22.0	-23.0
480	78.00	38.39	34.58	32.26	34.58	32.26	-28.4	-31.1	-32.8	-31.1	-32.8

Table D.1b
Splice lengths and material savings for beams in lateral load resisting frame system (continued)

Spl. No.	Orig. l_s (in.)	ACI '95 l_s (in.)	l_s (Eq. 3.13^{+}) Conv. (in.)	l_s (Eq. 3.13^{+}) New* (in.)	l_s (Eq. 3.14^{++}) Conv. (in.)	l_s (Eq. 3.14^{++}) New* (in.)	Change in weight of steel (lb) ACI '95	Eq. 3.13^{+} Conv.*	Eq. 3.13^{+} New**	Eq. 3.14^{++} Conv.*	Eq. 3.14^{++} New**
481	78.00	49.88	38.32	34.10	39.65	35.20	-49.8	-70.3	-77.7	-67.9	-75.8
482	67.00	34.08	28.23	26.44	28.23	26.44	-18.7	-22.0	-23.0	-22.0	-23.0
483	78.00	38.39	34.58	32.26	34.58	32.26	-28.4	-31.1	-32.8	-31.1	-32.8
484	96.00	87.85	62.96	55.19	76.86	65.91	-21.7	-87.8	-108.4	-50.8	-79.9
485	78.00	38.37	29.43	25.80	29.43	25.80	-70.2	-86.0	-92.4	-86.0	-92.4
486	96.00	89.68	64.17	56.62	78.60	67.89	-16.8	-84.6	-104.6	-46.2	-74.7
487	78.00	38.37	29.99	26.47	29.99	26.47	-56.8	-68.9	-73.9	-68.9	-73.9
488	96.00	89.68	64.17	56.62	78.60	67.89	-16.8	-84.6	-104.6	-46.2	-74.7
489	78.00	38.37	29.99	26.47	29.99	26.47	-56.8	-68.9	-73.9	-68.9	-73.9
490	96.00	89.68	64.17	56.62	78.60	67.89	-16.8	-84.6	-104.6	-46.2	-74.7
491	78.00	38.37	29.99	26.47	29.99	26.47	-70.2	-85.0	-91.3	-85.0	-91.3
492	96.00	87.85	62.96	55.19	76.86	65.91	-21.7	-87.8	-108.4	-50.8	-79.9
493	78.00	38.37	29.43	25.80	29.43	25.80	-70.2	-86.0	-92.4	-86.0	-92.4
494	96.00	89.68	64.17	56.62	78.60	67.89	-16.8	-84.6	-104.6	-46.2	-74.7
495	78.00	38.37	29.99	26.47	29.99	26.47	-56.8	-68.9	-73.9	-68.9	-73.9
496	96.00	89.68	64.17	56.62	78.60	67.89	-16.8	-84.6	-104.6	-46.2	-74.7
497	78.00	38.37	29.99	26.47	29.99	26.47	-56.8	-68.9	-73.9	-68.9	-73.9
498	96.00	89.68	64.17	56.62	78.60	67.89	-16.8	-84.6	-104.6	-46.2	-74.7
499	78.00	38.37	29.99	26.47	29.99	26.47	-70.2	-85.0	-91.3	-85.0	-91.3
500	96.00	56.22	46.86	41.41	49.46	43.44	-105.7	-130.5	-145.0	-123.6	-139.6
501	96.00	42.60	36.17	31.96	36.17	31.96	-94.6	-106.0	-113.4	-106.0	-113.4
502	96.00	91.34	65.25	57.92	80.17	69.70	-12.4	-81.7	-101.2	-42.0	-69.9
503	96.00	42.60	36.17	31.96	36.17	31.96	-94.6	-106.0	-113.4	-106.0	-113.4
504	96.00	91.34	65.25	57.92	80.17	69.70	-12.4	-81.7	-101.2	-42.0	-69.9
505	96.00	42.60	36.17	31.96	36.17	31.96	-94.6	-106.0	-113.4	-106.0	-113.4
506	96.00	57.07	47.59	42.29	50.28	44.41	-103.4	-128.6	-142.7	-121.5	-137.1
507	96.00	42.60	36.74	32.64	36.74	32.64	-94.6	-105.0	-112.2	-105.0	-112.2
508	96.00	56.22	46.86	41.41	49.46	43.44	-105.7	-130.5	-145.0	-123.6	-139.6
509	96.00	42.60	36.17	31.96	36.17	31.96	-94.6	-106.0	-113.4	-106.0	-113.4
510	96.00	91.34	65.25	57.92	80.17	69.70	-12.4	-81.7	-101.2	-42.0	-69.9
511	96.00	42.60	36.17	31.96	36.17	31.96	-94.6	-106.0	-113.4	-106.0	-113.4
512	96.00	91.34	65.25	57.92	80.17	69.70	-12.4	-81.7	-101.2	-42.0	-69.9
513	96.00	42.60	36.17	31.96	36.17	31.96	-94.6	-106.0	-113.4	-106.0	-113.4
514	96.00	57.07	47.59	42.29	50.28	44.41	-103.4	-128.6	-142.7	-121.5	-137.1
515	96.00	42.60	36.74	32.64	36.74	32.64	-94.6	-105.0	-112.2	-105.0	-112.2
516	96.00	56.22	46.86	41.41	49.46	43.44	-105.7	-130.5	-145.0	-123.6	-139.6
517	96.00	42.60	36.17	31.96	36.17	31.96	-94.6	-106.0	-113.4	-106.0	-113.4
518	96.00	91.34	65.25	57.92	80.17	69.70	-12.4	-81.7	-101.2	-42.0	-69.9
519	96.00	42.60	36.17	31.96	36.17	31.96	-94.6	-106.0	-113.4	-106.0	-113.4
520	96.00	56.22	46.86	41.41	49.46	43.44	-105.7	-130.5	-145.0	-123.6	-139.6

Table D.1b
Splice lengths and material savings for beams in lateral load resisting frame system (continued)

Spl. No.	Orig. l_s (in.)	ACI '95 l_s (in.)	l_s (Eq. 3.13^{+}) Conv. (in.)	l_s (Eq. 3.13^{+}) New* (in.)	l_s (Eq. 3.14^{++}) Conv. (in.)	l_s (Eq. 3.14^{++}) New* (in.)	Change in weight of steel (lb) ACI '95	Eq. 3.13^{+} Conv.*	Eq. 3.13^{+} New**	Eq. 3.14^{++} Conv.*	Eq. 3.14^{++} New**
521	96.00	42.60	36.17	31.96	36.17	31.96	-94.6	-106.0	-113.4	-106.0	-113.4
522	96.00	55.37	37.73	31.43	38.70	32.15	-71.9	-103.2	-114.4	-101.5	-113.1
523	96.00	42.60	36.74	32.64	36.74	32.64	-94.6	-105.0	-112.2	-105.0	-112.2
524	96.00	80.89	58.36	49.89	70.32	58.72	-40.1	-100.0	-122.5	-68.2	-99.0
525	78.00	38.37	27.28	23.33	27.87	23.75	-105.3	-134.7	-145.2	-133.2	-144.1
526	96.00	80.89	58.36	49.89	70.32	58.72	-40.1	-100.0	-122.5	-68.2	-99.0
527	96.00	62.22	44.89	38.38	54.10	45.17	-89.7	-135.8	-153.1	-111.3	-135.0
528	96.00	80.89	58.36	49.89	70.32	58.72	-40.1	-100.0	-122.5	-68.2	-99.0
529	96.00	62.22	44.89	38.38	54.10	45.17	-89.7	-135.8	-153.1	-111.3	-135.0
530	96.00	80.89	58.36	49.89	70.32	58.72	-40.1	-100.0	-122.5	-68.2	-99.0
531	78.00	38.37	27.28	23.33	27.87	23.75	-105.3	-134.7	-145.2	-133.2	-144.1
532	96.00	88.61	62.27	53.23	74.87	62.52	-19.6	-89.6	-113.6	-56.1	-88.9
533	78.00	42.03	29.05	24.83	29.67	25.29	-95.6	-130.0	-141.2	-128.4	-140.0
534	96.00	88.61	62.27	53.23	74.87	62.52	-19.6	-89.6	-113.6	-56.1	-88.9
535	96.00	68.16	47.90	40.95	57.59	48.09	-73.9	-127.8	-146.2	-102.0	-127.3
536	96.00	88.61	62.27	53.23	74.87	62.52	-19.6	-89.6	-113.6	-56.1	-88.9
537	96.00	68.16	47.90	40.95	57.59	48.09	-73.9	-127.8	-146.2	-102.0	-127.3
538	96.00	88.61	62.27	53.23	74.87	62.52	-19.6	-89.6	-113.6	-56.1	-88.9
539	78.00	42.03	29.05	24.83	29.67	25.29	-95.6	-130.0	-141.2	-128.4	-140.0
540	96.00	88.61	62.27	53.23	74.87	62.52	-19.6	-89.6	-113.6	-56.1	-88.9
541	78.00	42.03	29.05	24.83	29.05	24.83	-77.4	-105.3	-114.4	-105.3	-114.4
542	96.00	88.61	62.27	53.23	74.87	62.52	-19.6	-89.6	-113.6	-56.1	-88.9
543	78.00	54.84	40.10	34.55	47.71	40.23	-61.5	-100.7	-115.4	-80.5	-100.3
544	96.00	88.61	62.27	53.23	74.87	62.52	-19.6	-89.6	-113.6	-56.1	-88.9
545	96.00	68.16	47.90	40.95	57.59	48.09	-73.9	-127.8	-146.2	-102.0	-127.3
546	96.00	88.61	62.27	53.23	74.87	62.52	-19.6	-89.6	-113.6	-56.1	-88.9
547	78.00	42.03	29.05	24.83	29.67	25.29	-95.6	-130.0	-141.2	-128.4	-140.0
548	96.00	91.47	64.11	55.32	77.47	65.32	-12.0	-84.7	-108.1	-49.2	-81.5
549	78.00	42.03	29.91	25.81	29.91	25.81	-63.7	-85.2	-92.4	-85.2	-92.4
550	96.00	93.99	65.74	57.19	79.77	67.86	-5.3	-80.4	-103.1	-43.1	-74.7
551	96.00	46.66	36.28	31.40	36.28	31.40	-87.4	-105.8	-114.4	-105.8	-114.4
552	96.00	93.99	65.74	57.19	79.77	67.86	-5.3	-80.4	-103.1	-43.1	-74.7
553	96.00	46.66	36.28	31.40	36.28	31.40	-87.4	-105.8	-114.4	-105.8	-114.4
554	96.00	96.23	67.18	58.88	81.83	70.17	0.6	-76.6	-98.6	-37.6	-68.6
555	96.00	46.66	37.11	32.36	37.11	32.36	-87.4	-104.3	-112.7	-104.3	-112.7
556	96.00	96.23	67.18	58.88	81.83	70.17	0.6	-76.6	-98.6	-37.6	-68.6
557	67.00	37.33	25.79	22.74	25.79	22.74	-52.5	-73.0	-78.4	-73.0	-78.4
558	96.00	98.24	68.46	60.41	83.68	72.28	6.0	-73.2	-94.6	-32.7	-63.0
559	96.00	46.66	37.85	33.23	37.85	33.23	-87.4	-103.0	-111.2	-103.0	-111.2
560	96.00	98.24	68.46	60.41	83.68	72.28	6.0	-73.2	-94.6	-32.7	-63.0

Table D.1b
Splice lengths and material savings for beams in lateral load resisting frame system (continued)

Spl. No.	Orig. l_s (in.)	ACI '95 l_s (in.)	l_s (Eq. 3.13^{+}) Conv. (in.)	l_s (Eq. 3.13^{+}) New* (in.)	l_s (Eq. 3.14^{++}) Conv. (in.)	l_s (Eq. 3.14^{++}) New* (in.)	Change in weight of steel (lb) ACI '95	Eq. 3.13^{+} Conv.*	Eq. 3.13^{+} New**	Eq. 3.14^{++} Conv.*	Eq. 3.14^{++} New**
561	96.00	46.66	37.85	33.23	37.85	33.23	-87.4	-103.0	-111.2	-103.0	-111.2
562	96.00	61.59	49.90	44.09	52.66	46.25	-91.4	-122.5	-137.9	-115.1	-132.2
563	67.00	37.33	26.68	23.81	26.68	23.81	-52.5	-71.4	-76.5	-71.4	-76.5
564	78.00	54.64	36.60	31.39	37.76	32.28	-41.4	-73.3	-82.6	-71.3	-81.0
565	67.00	37.33	28.27	25.80	28.27	25.80	-21.3	-27.8	-29.5	-27.8	-29.5
566	78.00	42.03	34.51	31.35	34.51	31.35	-25.8	-31.2	-33.5	-31.2	-33.5
567	96.00	60.66	41.94	35.36	43.01	36.18	-62.6	-95.7	-107.4	-93.8	-105.9
568	78.00	42.03	33.80	30.46	33.80	30.46	-51.6	-63.4	-68.2	-63.4	-68.2
569	96.00	60.66	41.94	35.36	43.01	36.18	-62.6	-95.7	-107.4	-93.8	-105.9
570	78.00	42.03	33.80	30.46	33.80	30.46	-51.6	-63.4	-68.2	-63.4	-68.2
571	78.00	54.64	36.60	31.39	37.76	32.28	-41.4	-73.3	-82.6	-71.3	-81.0
572	67.00	37.33	28.27	25.80	28.27	25.80	-21.3	-27.8	-29.5	-27.8	-29.5
573	78.00	42.03	34.51	31.35	34.51	31.35	-25.8	-31.2	-33.5	-31.2	-33.5
574	67.00	48.53	33.37	29.87	34.68	30.96	-32.7	-59.6	-65.8	-57.2	-63.8
575	67.00	37.33	30.05	28.15	30.05	28.15	-16.8	-20.9	-22.0	-20.9	-22.0
576	78.00	42.05	36.81	34.35	36.81	34.35	-25.8	-29.5	-31.3	-29.5	-31.3
577	96.00	60.66	48.69	43.10	50.07	44.23	-62.6	-83.8	-93.7	-81.3	-91.7
578	67.00	37.33	30.05	28.15	30.05	28.15	-16.8	-20.9	-22.0	-20.9	-22.0
579	78.00	42.05	36.81	34.35	36.81	34.35	-25.8	-29.5	-31.3	-29.5	-31.3
580	67.00	48.53	33.37	29.87	34.68	30.96	-32.7	-59.6	-65.8	-57.2	-63.8
581	67.00	37.33	30.05	28.15	30.05	28.15	-16.8	-20.9	-22.0	-20.9	-22.0
582	78.00	42.05	36.81	34.35	36.81	34.35	-25.8	-29.5	-31.3	-29.5	-31.3
583	67.00	44.30	34.51	31.84	36.84	33.87	-25.7	-36.8	-39.9	-34.2	-37.6
584	67.00	34.08	30.87	29.46	30.87	29.46	-18.7	-20.5	-21.3	-20.5	-21.3
585	78.00	41.98	37.86	36.03	37.86	36.03	-25.8	-28.8	-30.1	-28.8	-30.1
586	67.00	44.30	34.51	31.84	36.84	33.87	-25.7	-36.8	-39.9	-34.2	-37.6
587	67.00	34.08	30.87	29.46	30.87	29.46	-18.7	-20.5	-21.3	-20.5	-21.3
588	78.00	41.98	37.86	36.03	37.86	36.03	-25.8	-28.8	-30.1	-28.8	-30.1
589	67.00	44.30	34.51	31.84	36.84	33.87	-25.7	-36.8	-39.9	-34.2	-37.6
590	67.00	34.08	30.87	29.46	30.87	29.46	-18.7	-20.5	-21.3	-20.5	-21.3
591	78.00	41.98	37.86	36.03	37.86	36.03	-25.8	-28.8	-30.1	-28.8	-30.1
592	96.00	56.22	46.86	41.41	49.46	43.44	-105.7	-130.5	-145.0	-123.6	-139.6
593	96.00	42.60	36.17	31.96	36.17	31.96	-94.6	-106.0	-113.4	-106.0	-113.4
594	96.00	55.37	45.70	40.46	47.03	41.55	-71.9	-89.1	-98.4	-86.7	-96.4
595	96.00	42.60	36.17	31.96	36.17	31.96	-94.6	-106.0	-113.4	-106.0	-113.4
596	96.00	56.22	46.86	41.41	49.46	43.44	-105.7	-130.5	-145.0	-123.6	-139.6
597	96.00	42.60	36.17	31.96	36.17	31.96	-94.6	-106.0	-113.4	-106.0	-113.4
598	96.00	92.95	66.30	59.20	81.71	71.50	-8.1	-78.9	-97.8	-38.0	-65.1
599	96.00	42.60	36.74	32.64	36.74	32.64	-94.6	-105.0	-112.2	-105.0	-112.2
600	96.00	92.95	66.30	59.20	81.71	71.50	-8.1	-78.9	-97.8	-38.0	-65.1

Table D.1b
Splice lengths and material savings for beams in lateral load resisting frame system (continued)

Spl. No.	Orig. l_s (in.)	ACI '95 l_s (in.)	l_s (Eq. 3.13^{+}) Conv. (in.)	l_s (Eq. 3.13^{+}) New* (in.)	l_s (Eq. 3.14^{++}) Conv. (in.)	l_s (Eq. 3.14^{++}) New* (in.)	Change in weight of steel (lb) ACI '95	Eq. 3.13^{+} Conv.*	Eq. 3.13^{+} New**	Eq. 3.14^{++} Conv.*	Eq. 3.14^{++} New**
601	96.00	42.60	36.74	32.64	36.74	32.64	-94.6	-105.0	-112.2	-105.0	-112.2
602	96.00	92.95	66.30	59.20	81.71	71.50	-8.1	-78.9	-97.8	-38.0	-65.1
603	96.00	42.60	36.74	32.64	36.74	32.64	-94.6	-105.0	-112.2	-105.0	-112.2
604	96.00	57.07	47.59	42.29	50.28	44.41	-103.4	-128.6	-142.7	-121.5	-137.1
605	67.00	34.08	25.42	22.81	25.42	22.81	-47.2	-59.6	-63.4	-59.6	-63.4
606	96.00	55.37	39.37	33.20	40.40	33.98	-71.9	-100.3	-111.2	-98.5	-109.8
607	78.00	38.37	31.75	28.61	31.75	28.61	-56.8	-66.3	-70.8	-66.3	-70.8
608	96.00	57.07	47.59	42.29	50.28	44.41	-103.4	-128.6	-142.7	-121.5	-137.1
609	67.00	34.08	25.42	22.81	25.42	22.81	-47.2	-59.6	-63.4	-59.6	-63.4
610	96.00	57.07	47.59	42.29	50.28	44.41	-103.4	-128.6	-142.7	-121.5	-137.1
611	67.00	34.08	25.42	22.81	25.42	22.81	-47.2	-59.6	-63.4	-59.6	-63.4
612	96.00	55.37	39.37	33.20	40.40	33.98	-71.9	-100.3	-111.2	-98.5	-109.8
613	78.00	38.37	31.75	28.61	31.75	28.61	-56.8	-66.3	-70.8	-66.3	-70.8
614	96.00	57.07	47.59	42.29	50.28	44.41	-103.4	-128.6	-142.7	-121.5	-137.1
615	67.00	34.08	25.42	22.81	25.42	22.81	-47.2	-59.6	-63.4	-59.6	-63.4
616	78.00	49.88	37.70	33.35	38.99	34.41	-49.8	-71.4	-79.1	-69.1	-77.2
617	67.00	34.08	26.77	24.51	26.77	24.51	-37.3	-45.6	-48.2	-45.6	-48.2
618	96.00	55.37	44.93	39.54	46.21	40.58	-71.9	-90.5	-100.0	-88.2	-98.2
619	67.00	34.08	26.77	24.51	26.77	24.51	-28.0	-34.2	-36.1	-34.2	-36.1
620	78.00	49.88	37.70	33.35	38.99	34.41	-49.8	-71.4	-79.1	-69.1	-77.2
621	67.00	34.08	26.77	24.51	26.77	24.51	-37.3	-45.6	-48.2	-45.6	-48.2
622	78.00	49.88	36.23	31.61	37.44	32.58	-49.8	-74.0	-82.2	-71.8	-80.4
623	67.00	34.08	27.36	25.29	27.36	25.29	-18.7	-22.5	-23.6	-22.5	-23.6
624	78.00	38.37	33.46	30.79	33.46	30.79	-28.4	-31.9	-33.9	-31.9	-33.9
625	96.00	55.37	43.10	37.39	44.30	38.34	-71.9	-93.7	-103.8	-91.6	-102.1
626	67.00	34.08	27.36	25.29	27.36	25.29	-18.7	-22.5	-23.6	-22.5	-23.6
627	78.00	38.37	33.46	30.79	33.46	30.79	-28.4	-31.9	-33.9	-31.9	-33.9
628	96.00	55.37	43.10	37.39	44.30	38.34	-71.9	-93.7	-103.8	-91.6	-102.1
629	67.00	34.08	27.36	25.29	27.36	25.29	-18.7	-22.5	-23.6	-22.5	-23.6
630	78.00	38.37	33.46	30.79	33.46	30.79	-28.4	-31.9	-33.9	-31.9	-33.9
631	78.00	49.88	36.23	31.61	37.44	32.58	-49.8	-74.0	-82.2	-71.8	-80.4
632	67.00	34.08	27.36	25.29	27.36	25.29	-18.7	-22.5	-23.6	-22.5	-23.6
633	78.00	38.37	33.46	30.79	33.46	30.79	-28.4	-31.9	-33.9	-31.9	-33.9
634	96.00	87.85	62.96	55.19	76.86	65.91	-21.7	-87.8	-108.4	-50.8	-79.9
635	78.00	38.37	29.43	25.80	29.43	25.80	-70.2	-86.0	-92.4	-86.0	-92.4
636	96.00	87.85	62.96	55.19	76.86	65.91	-21.7	-87.8	-108.4	-50.8	-79.9
637	78.00	38.37	29.43	25.80	29.43	25.80	-56.8	-69.7	-74.9	-69.7	-74.9
638	96.00	87.85	62.96	55.19	76.86	65.91	-21.7	-87.8	-108.4	-50.8	-79.9
639	78.00	38.37	29.43	25.80	29.43	25.80	-56.8	-69.7	-74.9	-69.7	-74.9
640	96.00	87.85	62.96	55.19	76.86	65.91	-21.7	-87.8	-108.4	-50.8	-79.9

Table D.1b
Splice lengths and material savings for beams in lateral load resisting frame system (continued)

Spl. No.	Orig. l_s (in.)	ACI '95 l_s (in.)	l_s (Eq. 3.13†) Conv. (in.)	l_s (Eq. 3.13†) New* (in.)	l_s (Eq. 3.14††) Conv. (in.)	l_s (Eq. 3.14††) New* (in.)	Change in weight of steel (lb) ACI '95	Eq. 3.13† Conv.*	Eq. 3.13† New**	Eq. 3.14†† Conv.*	Eq. 3.14†† New**
641	78.00	38.37	29.43	25.80	29.43	25.80	-70.2	-86.0	-92.4	-86.0	-92.4
642	96.00	87.85	62.96	55.19	76.86	65.91	-21.7	-87.8	-108.4	-50.8	-79.9
643	78.00	38.37	29.43	25.80	29.43	25.80	-70.2	-86.0	-92.4	-86.0	-92.4
644	96.00	87.85	62.96	55.19	76.86	65.91	-21.7	-87.8	-108.4	-50.8	-79.9
645	78.00	38.37	29.43	25.80	29.43	25.80	-56.8	-69.7	-74.9	-69.7	-74.9
646	96.00	87.85	62.96	55.19	76.86	65.91	-21.7	-87.8	-108.4	-50.8	-79.9
647	78.00	38.37	29.43	25.80	29.43	25.80	-56.8	-69.7	-74.9	-69.7	-74.9
648	96.00	87.85	62.96	55.19	76.86	65.91	-21.7	-87.8	-108.4	-50.8	-79.9
649	78.00	38.37	29.43	25.80	29.43	25.80	-70.2	-86.0	-92.4	-86.0	-92.4
650	96.00	55.37	39.37	33.20	40.40	33.98	-71.9	-100.3	-111.2	-98.5	-109.8
651	96.00	42.67	37.72	33.84	37.72	33.84	-94.4	-103.2	-110.1	-103.2	-110.1
652	96.00	55.37	39.37	33.20	40.40	33.98	-71.9	-100.3	-111.2	-98.5	-109.8
653	96.00	42.67	37.72	33.84	37.72	33.84	-94.4	-103.2	-110.1	-103.2	-110.1
654	96.00	55.37	39.37	33.20	40.40	33.98	-71.9	-100.3	-111.2	-98.5	-109.8
655	96.00	42.67	37.72	33.84	37.72	33.84	-94.4	-103.2	-110.1	-103.2	-110.1
656	96.00	55.37	39.37	33.20	40.40	33.98	-71.9	-100.3	-111.2	-98.5	-109.8
657	96.00	42.67	37.72	33.84	37.72	33.84	-94.4	-103.2	-110.1	-103.2	-110.1
658	96.00	55.37	39.37	33.20	40.40	33.98	-71.9	-100.3	-111.2	-98.5	-109.8
659	96.00	42.67	37.72	33.84	37.72	33.84	-94.4	-103.2	-110.1	-103.2	-110.1
660	96.00	55.37	39.37	33.20	40.40	33.98	-71.9	-100.3	-111.2	-98.5	-109.8
661	96.00	42.67	37.72	33.84	37.72	33.84	-94.4	-103.2	-110.1	-103.2	-110.1
662	96.00	55.37	39.37	33.20	40.40	33.98	-71.9	-100.3	-111.2	-98.5	-109.8
663	96.00	42.67	37.72	33.84	37.72	33.84	-94.4	-103.2	-110.1	-103.2	-110.1
664	96.00	55.37	39.37	33.20	40.40	33.98	-71.9	-100.3	-111.2	-98.5	-109.8
665	96.00	42.67	37.72	33.84	37.72	33.84	-94.4	-103.2	-110.1	-103.2	-110.1
666	96.00	55.37	44.93	39.54	46.21	40.58	-71.9	-90.5	-100.0	-88.2	-98.2
667	96.00	45.88	40.84	37.82	40.84	37.82	-88.8	-97.7	-103.0	-97.7	-103.0
668	96.00	55.37	44.93	39.54	46.21	40.58	-71.9	-90.5	-100.0	-88.2	-98.2
669	96.00	45.88	40.84	37.82	40.84	37.82	-88.8	-97.7	-103.0	-97.7	-103.0
670	96.00	55.37	44.93	39.54	46.21	40.58	-71.9	-90.5	-100.0	-88.2	-98.2
671	96.00	45.88	40.84	37.82	40.84	37.82	-88.8	-97.7	-103.0	-97.7	-103.0
672	96.00	55.37	44.93	39.54	46.21	40.58	-71.9	-90.5	-100.0	-88.2	-98.2
673	96.00	45.88	40.84	37.82	40.84	37.82	-88.8	-97.7	-103.0	-97.7	-103.0
674	78.00	64.04	50.02	45.35	55.94	50.20	-24.7	-49.6	-57.8	-39.1	-49.2
675	67.00	37.33	29.37	26.93	32.07	29.19	-33.6	-42.7	-45.4	-39.6	-42.9
676	96.00	81.25	61.83	56.06	69.80	62.61	-26.1	-60.5	-70.7	-46.4	-59.1
677	67.00	37.33	29.78	27.47	32.57	29.83	-33.6	-42.2	-44.8	-39.0	-42.1
678	96.00	81.25	61.83	56.06	69.80	62.61	-26.1	-60.5	-70.7	-46.4	-59.1
679	67.00	37.33	29.78	27.47	32.57	29.83	-33.6	-42.2	-44.8	-39.0	-42.1
680	96.00	81.25	61.83	56.06	69.80	62.61	-26.1	-60.5	-70.7	-46.4	-59.1

Table D.1b
Splice lengths and material savings for beams in lateral load resisting frame system (continued)

Spl. No.	Orig. l_s (in.)	ACI '95 l_s (in.)	l_s (Eq. 3.13†) Conv. (in.)	l_s (Eq. 3.13†) New* (in.)	l_s (Eq. 3.14††) Conv. (in.)	l_s (Eq. 3.14††) New* (in.)	Change in weight of steel (lb) ACI '95	Eq. 3.13† Conv.*	Eq. 3.13† New**	Eq. 3.14†† Conv.*	Eq. 3.14†† New**
681	67.00	37.33	29.78	27.47	32.57	29.83	-33.6	-42.2	-44.8	-39.0	-42.1
682	78.00	65.17	50.83	46.38	56.95	51.46	-22.7	-48.1	-56.0	-37.3	-47.0
683	67.00	37.33	29.78	27.47	32.57	29.83	-33.6	-42.2	-44.8	-39.0	-42.1
684	78.00	61.98	48.87	44.42	54.15	48.76	-23.0	-41.8	-48.2	-34.2	-41.9
685	67.00	37.33	29.37	26.93	32.07	29.19	-33.6	-42.7	-45.4	-39.6	-42.9
686	78.00	63.04	49.65	45.41	55.09	49.94	-21.5	-40.7	-46.8	-32.9	-40.2
687	67.00	37.33	29.78	27.47	32.57	29.83	-33.6	-42.2	-44.8	-39.0	-42.1
688	78.00	65.17	50.83	46.38	56.95	51.46	-22.7	-48.1	-56.0	-37.3	-47.0
689	67.00	37.33	29.78	27.47	32.57	29.83	-33.6	-42.2	-44.8	-39.0	-42.1
690	96.00	81.25	61.83	56.06	69.80	62.61	-21.2	-49.0	-57.3	-37.6	-47.9
691	67.00	37.33	29.78	27.47	32.57	29.83	-33.6	-42.2	-44.8	-39.0	-42.1
692	78.00	65.17	50.83	46.38	56.95	51.46	-22.7	-48.1	-56.0	-37.3	-47.0
693	67.00	37.33	29.78	27.47	32.57	29.83	-33.6	-42.2	-44.8	-39.0	-42.1
694	78.00	61.98	48.87	44.42	54.15	48.76	-23.0	-41.8	-48.2	-34.2	-41.9
695	67.00	37.33	29.37	26.93	32.07	29.19	-33.6	-42.7	-45.4	-39.6	-42.9
696	78.00	61.98	48.87	44.42	54.15	48.76	-23.0	-41.8	-48.2	-34.2	-41.9
697	67.00	37.33	29.37	26.93	32.07	29.19	-33.6	-42.7	-45.4	-39.6	-42.9
698	78.00	64.04	50.02	45.35	55.94	50.20	-24.7	-49.6	-57.8	-39.1	-49.2
699	67.00	37.33	29.37	26.93	32.07	29.19	-33.6	-42.7	-45.4	-39.6	-42.9
700	96.00	81.25	61.83	56.06	69.80	62.61	-26.1	-60.5	-70.7	-46.4	-59.1
701	67.00	37.33	29.78	27.47	32.57	29.83	-33.6	-42.2	-44.8	-39.0	-42.1
702	96.00	81.25	61.83	56.06	69.80	62.61	-26.1	-60.5	-70.7	-46.4	-59.1
703	67.00	37.33	29.78	27.47	32.57	29.83	-33.6	-42.2	-44.8	-39.0	-42.1
704	67.00	50.65	41.93	39.77	44.81	42.36	-18.5	-28.4	-30.9	-25.1	-27.9
705	67.00	38.96	32.42	30.74	34.47	32.58	-31.8	-39.2	-41.1	-36.9	-39.0
706	67.00	44.30	29.56	25.96	30.85	27.00	-12.9	-21.2	-23.3	-20.5	-22.7
707	78.00	49.88	35.89	31.34	37.44	32.58	-20.2	-30.2	-33.5	-29.1	-32.6
708	67.00	34.08	27.36	25.29	27.36	25.29	-18.7	-22.5	-23.6	-22.5	-23.6
709	78.00	38.37	33.46	30.79	33.46	30.79	-28.4	-31.9	-33.9	-31.9	-33.9
710	67.00	44.30	29.56	25.96	30.85	27.00	-12.9	-21.2	-23.3	-20.5	-22.7
711	78.00	49.88	35.89	31.34	37.44	32.58	-20.2	-30.2	-33.5	-29.1	-32.6
712	67.00	34.08	27.36	25.29	27.36	25.29	-18.7	-22.5	-23.6	-22.5	-23.6
713	78.00	38.37	33.46	30.79	33.46	30.79	-28.4	-31.9	-33.9	-31.9	-33.9
714	67.00	44.30	29.56	25.96	30.85	27.00	-12.9	-21.2	-23.3	-20.5	-22.7
715	78.00	49.88	35.89	31.34	37.44	32.58	-20.2	-30.2	-33.5	-29.1	-32.6
716	67.00	34.08	27.36	25.29	27.36	25.29	-18.7	-22.5	-23.6	-22.5	-23.6
717	78.00	38.37	33.46	30.79	33.46	30.79	-28.4	-31.9	-33.9	-31.9	-33.9
718	67.00	44.30	29.56	25.96	30.85	27.00	-12.9	-21.2	-23.3	-20.5	-22.7
719	78.00	49.88	35.89	31.34	37.44	32.58	-20.2	-30.2	-33.5	-29.1	-32.6
720	67.00	34.08	27.36	25.29	27.36	25.29	-18.7	-22.5	-23.6	-22.5	-23.6

Table D.1b
Splice lengths and material savings for beams in lateral load resisting frame system (continued)

Spl. No.	Orig. l_s (in.)	ACI '95 l_s (in.)	l_s (Eq. 3.13^{+}) Conv. (in.)	l_s (Eq. 3.13^{+}) New* (in.)	l_s (Eq. 3.14^{++}) Conv. (in.)	l_s (Eq. 3.14^{++}) New* (in.)	Change in weight of steel (lb) ACI '95	Eq. 3.13^{+} Conv.*	Eq. 3.13^{+} New**	Eq. 3.14^{++} Conv.*	Eq. 3.14^{++} New**
721	78.00	38.37	33.46	30.79	33.46	30.79	-28.4	-31.9	-33.9	-31.9	-33.9
722	96.00	87.85	62.96	55.19	76.86	65.91	-21.7	-87.8	-108.4	-50.8	-79.9
723	78.00	38.37	29.43	25.80	29.43	25.80	-70.2	-86.0	-92.4	-86.0	-92.4
724	96.00	87.85	62.96	55.19	76.86	65.91	-21.7	-87.8	-108.4	-50.8	-79.9
725	78.00	38.37	29.43	25.80	29.43	25.80	-56.8	-69.7	-74.9	-69.7	-74.9
726	96.00	87.85	62.96	55.19	76.86	65.91	-21.7	-87.8	-108.4	-50.8	-79.9
727	78.00	38.37	29.43	25.80	29.43	25.80	-56.8	-69.7	-74.9	-69.7	-74.9
728	96.00	87.85	62.96	55.19	76.86	65.91	-21.7	-87.8	-108.4	-50.8	-79.9
729	78.00	38.37	29.43	25.80	29.43	25.80	-70.2	-86.0	-92.4	-86.0	-92.4
730	96.00	87.85	62.96	55.19	76.86	65.91	-21.7	-87.8	-108.4	-50.8	-79.9
731	78.00	38.37	29.43	25.80	29.43	25.80	-70.2	-86.0	-92.4	-86.0	-92.4
732	96.00	87.85	62.96	55.19	76.86	65.91	-21.7	-87.8	-108.4	-50.8	-79.9
733	78.00	38.37	29.43	25.80	29.43	25.80	-56.8	-69.7	-74.9	-69.7	-74.9
734	96.00	87.85	62.96	55.19	76.86	65.91	-21.7	-87.8	-108.4	-50.8	-79.9
735	78.00	38.37	29.43	25.80	29.43	25.80	-56.8	-69.7	-74.9	-69.7	-74.9
736	96.00	87.85	62.96	55.19	76.86	65.91	-21.7	-87.8	-108.4	-50.8	-79.9
737	78.00	38.37	29.43	25.80	29.43	25.80	-70.2	-86.0	-92.4	-86.0	-92.4
738	96.00	55.37	39.37	33.20	40.40	33.98	-71.9	-100.3	-111.2	-98.5	-109.8
739	96.00	42.67	37.72	33.84	37.72	33.84	-94.4	-103.2	-110.1	-103.2	-110.1
740	96.00	55.37	39.37	33.20	40.40	33.98	-71.9	-100.3	-111.2	-98.5	-109.8
741	96.00	42.67	37.72	33.84	37.72	33.84	-94.4	-103.2	-110.1	-103.2	-110.1
742	96.00	55.37	39.37	33.20	40.40	33.98	-71.9	-100.3	-111.2	-98.5	-109.8
743	96.00	42.67	37.72	33.84	37.72	33.84	-94.4	-103.2	-110.1	-103.2	-110.1
744	96.00	55.37	39.37	33.20	40.40	33.98	-71.9	-100.3	-111.2	-98.5	-109.8
745	96.00	42.67	37.72	33.84	37.72	33.84	-94.4	-103.2	-110.1	-103.2	-110.1
746	96.00	55.37	39.37	33.20	40.40	33.98	-71.9	-100.3	-111.2	-98.5	-109.8
747	96.00	42.67	37.72	33.84	37.72	33.84	-94.4	-103.2	-110.1	-103.2	-110.1
748	96.00	55.37	39.37	33.20	40.40	33.98	-71.9	-100.3	-111.2	-98.5	-109.8
749	96.00	42.67	37.72	33.84	37.72	33.84	-94.4	-103.2	-110.1	-103.2	-110.1
750	96.00	55.37	39.37	33.20	40.40	33.98	-71.9	-100.3	-111.2	-98.5	-109.8
751	96.00	42.67	37.72	33.84	37.72	33.84	-94.4	-103.2	-110.1	-103.2	-110.1
752	96.00	55.37	39.37	33.20	40.40	33.98	-71.9	-100.3	-111.2	-98.5	-109.8
753	96.00	42.67	37.72	33.84	37.72	33.84	-94.4	-103.2	-110.1	-103.2	-110.1
754	96.00	55.37	44.93	39.54	46.21	40.58	-71.9	-90.5	-100.0	-88.2	-98.2
755	96.00	45.88	40.84	37.82	40.84	37.82	-88.8	-97.7	-103.0	-97.7	-103.0
756	96.00	55.37	44.93	39.54	46.21	40.58	-71.9	-90.5	-100.0	-88.2	-98.2
757	96.00	45.88	40.84	37.82	40.84	37.82	-88.8	-97.7	-103.0	-97.7	-103.0
758	96.00	55.37	44.93	39.54	46.21	40.58	-71.9	-90.5	-100.0	-88.2	-98.2
759	96.00	45.88	40.84	37.82	40.84	37.82	-88.8	-97.7	-103.0	-97.7	-103.0
760	96.00	55.37	44.93	39.54	46.21	40.58	-71.9	-90.5	-100.0	-88.2	-98.2

Table D.1b
Splice lengths and material savings for beams in lateral load resisting frame system (continued)

Spl. No.	Orig. l_s (in.)	ACI '95 l_s (in.)	l_s (Eq. 3.13^{+}) Conv. (in.)	l_s (Eq. 3.13^{+}) New* (in.)	l_s (Eq. 3.14^{++}) Conv. (in.)	l_s (Eq. 3.14^{++}) New* (in.)	Change in weight of steel (lb) ACI '95	Eq. 3.13^{+} Conv.*	Eq. 3.13^{+} New**	Eq. 3.14^{++} Conv.*	Eq. 3.14^{++} New**
761	96.00	45.88	40.84	37.82	40.84	37.82	-88.8	-97.7	-103.0	-97.7	-103.0
762	67.00	44.30	26.59	23.73	30.85	27.00	-19.3	-34.3	-36.8	-30.7	-34.0
763	67.00	34.08	27.36	25.29	27.36	25.29	-18.7	-22.5	-23.6	-22.5	-23.6
764	78.00	38.37	33.46	30.79	33.46	30.79	-28.4	-31.9	-33.9	-31.9	-33.9
765	67.00	44.30	26.59	23.73	30.85	27.00	-19.3	-34.3	-36.8	-30.7	-34.0
766	67.00	44.30	26.59	23.73	30.85	27.00	-19.3	-34.3	-36.8	-30.7	-34.0
767	96.00	55.37	45.16	39.39	47.57	41.22	-107.9	-135.1	-150.4	-128.7	-145.5
768	78.00	38.37	29.43	25.80	29.43	25.80	-56.8	-69.7	-74.9	-69.7	-74.9
769	96.00	55.37	45.70	40.46	47.03	41.55	-71.9	-89.1	-98.4	-86.7	-96.4
770	78.00	38.37	30.50	27.08	30.50	27.08	-56.8	-68.1	-73.0	-68.1	-73.0
771	96.00	55.37	45.16	39.39	47.57	41.22	-107.9	-135.1	-150.4	-128.7	-145.5
772	78.00	38.37	29.43	25.80	29.43	25.80	-56.8	-69.7	-74.9	-69.7	-74.9
773	96.00	55.37	37.73	31.43	38.70	32.15	-71.9	-103.2	-114.4	-101.5	-113.1
774	78.00	38.37	30.96	27.63	30.96	27.63	-70.2	-83.3	-89.2	-83.3	-89.2
775	96.00	55.37	37.73	31.43	38.70	32.15	-71.9	-103.2	-114.4	-101.5	-113.1
776	78.00	38.37	30.96	27.63	30.96	27.63	-56.8	-67.5	-72.2	-67.5	-72.2
777	96.00	55.37	37.73	31.43	38.70	32.15	-71.9	-103.2	-114.4	-101.5	-113.1
778	78.00	38.37	30.96	27.63	30.96	27.63	-70.2	-83.3	-89.2	-83.3	-89.2
779	96.00	55.37	42.01	36.15	43.16	37.05	-71.9	-95.6	-106.0	-93.6	-104.4
780	78.00	38.37	32.97	30.16	32.97	30.16	-70.2	-79.7	-84.7	-79.7	-84.7
781	96.00	55.37	42.01	36.15	43.16	37.05	-71.9	-95.6	-106.0	-93.6	-104.4
782	78.00	38.37	32.97	30.16	32.97	30.16	-56.8	-64.6	-68.6	-64.6	-68.6
783	96.00	55.37	42.01	36.15	43.16	37.05	-71.9	-95.6	-106.0	-93.6	-104.4
784	78.00	38.37	32.97	30.16	32.97	30.16	-70.2	-79.7	-84.7	-79.7	-84.7
785	78.00	49.88	37.00	32.52	38.26	33.54	-49.8	-72.6	-80.5	-70.4	-78.7
786	67.00	34.08	27.69	25.72	27.69	25.72	-47.2	-56.4	-59.2	-56.4	-59.2
787	96.00	55.37	44.93	39.54	46.21	40.58	-71.9	-90.5	-100.0	-88.2	-98.2
788	78.00	38.37	34.25	31.83	34.25	31.83	-56.8	-62.8	-66.2	-62.8	-66.2
789	78.00	49.88	37.00	32.52	38.26	33.54	-49.8	-72.6	-80.5	-70.4	-78.7
790	67.00	34.08	27.69	25.72	27.69	25.72	-47.2	-56.4	-59.2	-56.4	-59.2
791	67.00	44.30	31.23	28.95	36.84	33.87	-25.7	-40.5	-43.1	-34.2	-37.6
792	67.00	34.08	30.87	29.46	30.87	29.46	-18.7	-20.5	-21.3	-20.5	-21.3
793	78.00	41.98	37.86	36.03	37.86	36.03	-25.8	-28.8	-30.1	-28.8	-30.1
794	67.00	44.30	34.51	31.84	36.84	33.87	-25.7	-36.8	-39.9	-34.2	-37.6
795	67.00	34.08	30.87	29.46	30.87	29.46	-18.7	-20.5	-21.3	-20.5	-21.3
796	78.00	41.98	37.86	36.03	37.86	36.03	-25.8	-28.8	-30.1	-28.8	-30.1
797	67.00	44.30	31.23	28.95	36.84	33.87	-25.7	-40.5	-43.1	-34.2	-37.6
798	67.00	34.08	30.87	29.46	30.87	29.46	-18.7	-20.5	-21.3	-20.5	-21.3
799	78.00	41.98	37.86	36.03	37.86	36.03	-25.8	-28.8	-30.1	-28.8	-30.1
800	96.00	94.40	66.72	58.74	80.39	69.37	-4.2	-77.8	-99.0	-41.5	-70.7

Table D.1b
Splice lengths and material savings for beams in lateral load resisting frame system (continued)

Spl. No.	Orig. l_s (in.)	ACI '95 l_s (in.)	l_s (Eq. 3.13[+]) Conv. (in.)	l_s (Eq. 3.13[+]) New* (in.)	l_s (Eq. 3.14[++]) Conv. (in.)	l_s (Eq. 3.14[++]) New* (in.)	Change in weight of steel (lb) ACI '95	Eq. 3.13[+] Conv.*	Eq. 3.13[+] New**	Eq. 3.14[++] Conv.*	Eq. 3.14[++] New**
801	67.00	37.33	28.88	26.30	31.49	28.46	-33.6	-43.2	-46.1	-40.2	-43.7
802	96.00	94.40	66.72	58.74	80.39	69.37	-4.2	-77.8	-99.0	-41.5	-70.7
803	67.00	65.98	50.01	47.48	58.40	55.02	-1.1	-18.3	-21.0	-9.3	-12.9
804	78.00	80.87	60.94	57.72	70.83	66.56	3.1	-18.3	-21.8	-7.7	-12.3
805	67.00	41.38	33.24	31.80	36.58	34.84	-14.5	-19.1	-19.9	-17.2	-18.2
806	78.00	51.03	40.77	38.91	44.72	42.48	-19.3	-26.7	-28.0	-23.9	-25.5
807	67.00	65.98	50.01	47.48	58.40	55.02	-1.1	-18.3	-21.0	-9.3	-12.9
808	78.00	80.87	60.94	57.72	70.83	66.56	3.1	-18.3	-21.8	-7.7	-12.3
809	67.00	37.33	28.94	25.77	31.97	28.16	-52.5	-67.4	-73.0	-62.0	-68.8
810	96.00	78.18	59.55	53.22	66.93	59.11	-31.6	-64.6	-75.8	-51.5	-65.3
811	67.00	37.33	28.94	25.77	31.97	28.16	-52.5	-67.4	-73.0	-62.0	-68.8
812	67.00	50.80	41.13	38.47	45.03	41.87	-9.2	-14.7	-16.2	-12.4	-14.2
813	78.00	62.74	50.30	46.88	54.90	50.85	-10.9	-19.9	-22.3	-16.6	-19.5
814	67.00	39.07	31.64	29.59	34.64	32.20	-15.8	-20.0	-21.2	-18.3	-19.7
815	78.00	48.26	38.69	36.06	42.23	39.12	-21.3	-28.2	-30.1	-25.7	-27.9
816	67.00	37.75	31.02	28.85	33.49	30.97	-33.1	-40.8	-43.2	-38.0	-40.8
817	78.00	64.85	51.54	47.95	56.74	52.43	-18.9	-38.0	-43.1	-30.5	-36.7
818	67.00	37.75	31.02	28.85	33.49	30.97	-33.1	-40.8	-43.2	-38.0	-40.8
Total change in weight of steel (lb)							-42337	-62480	-69979	-55918	-64904

[+] $$\text{Eq. 3.13} = \frac{l_d}{d_b} = \frac{\frac{f_y}{f_c'^{1/4}} - 1900\left(0.1\frac{c_M}{c_m} + 0.9\right)}{72\left(\frac{c + K_{tr}}{d_b}\right)}$$

[++] $$\text{Eq. 3.14} = \frac{l_d}{d_b} = \frac{\frac{f_y}{f_c'^{1/4}} - 1900}{72\left(\frac{c + K_{tr}}{d_b}\right)}$$

* Conventional reinforcement (avg. $R_r = 0.0727$)

** New reinforcement (avg. $R_r = 0.1275$)

1 in. = 25.4 mm; 1 lb = 0.454 kg

Table D.1c
Splice length ratios for beams in lateral load resisting frame system

Spl. No.	ACI '95 Orig.	Eq. 3.13[+] Orig. Conv.*	Eq. 3.13[+] Orig. New**	Eq. 3.14[++] Orig. Conv.*	Eq. 3.14[++] Orig. New**	Eq. 3.13[+] ACI '95 Conv.*	Eq. 3.13[+] ACI '95 New**	Eq. 3.14[++] ACI '95 Conv.*	Eq. 3.14[++] ACI '95 New**	Eq. 3.13[+] Eq. 3.14[++] Conv.*	Eq. 3.13[+] Eq. 3.14[++] New**	New** Conv.* Eq. 3.13[+]	New** Conv.* Eq. 3.14[++]
1	0.577	0.476	0.421	0.490	0.433	0.825	0.731	0.849	0.750	0.972	0.974	0.885	0.883
2	0.482	0.430	0.400	0.430	0.400	0.891	0.829	0.891	0.829	1.000	1.000	0.930	0.930
3	0.509	0.421	0.395	0.421	0.395	0.828	0.776	0.828	0.776	1.000	1.000	0.936	0.936
4	0.577	0.476	0.421	0.490	0.433	0.825	0.731	0.849	0.750	0.972	0.974	0.885	0.883
5	0.482	0.430	0.400	0.430	0.400	0.891	0.829	0.891	0.829	1.000	1.000	0.930	0.930
6	0.509	0.421	0.395	0.421	0.395	0.828	0.776	0.828	0.776	1.000	1.000	0.936	0.936
7	0.915	0.656	0.575	0.801	0.687	0.717	0.628	0.875	0.750	0.819	0.837	0.877	0.858
8	0.492	0.377	0.331	0.377	0.331	0.767	0.672	0.767	0.672	1.000	1.000	0.877	0.877
9	0.915	0.656	0.575	0.801	0.687	0.717	0.628	0.875	0.750	0.819	0.837	0.877	0.858
10	0.492	0.377	0.331	0.377	0.331	0.767	0.672	0.767	0.672	1.000	1.000	0.877	0.877
11	0.915	0.656	0.575	0.801	0.687	0.717	0.628	0.875	0.750	0.819	0.837	0.877	0.858
12	0.492	0.377	0.331	0.377	0.331	0.767	0.672	0.767	0.672	1.000	1.000	0.877	0.877
13	0.915	0.656	0.575	0.801	0.687	0.717	0.628	0.875	0.750	0.819	0.837	0.877	0.858
14	0.492	0.377	0.331	0.377	0.331	0.767	0.672	0.767	0.672	1.000	1.000	0.877	0.877
15	0.639	0.503	0.447	0.515	0.456	0.786	0.699	0.805	0.714	0.977	0.979	0.888	0.886
16	0.444	0.377	0.333	0.377	0.333	0.849	0.750	0.849	0.750	1.000	1.000	0.883	0.883
17	0.639	0.503	0.447	0.515	0.456	0.786	0.699	0.805	0.714	0.977	0.979	0.888	0.886
18	0.444	0.377	0.333	0.377	0.333	0.849	0.750	0.849	0.750	1.000	1.000	0.883	0.883
19	0.639	0.503	0.447	0.515	0.456	0.786	0.699	0.805	0.714	0.977	0.979	0.888	0.886
20	0.492	0.391	0.347	0.391	0.347	0.795	0.706	0.795	0.706	1.000	1.000	0.888	0.888
21	0.639	0.503	0.447	0.515	0.456	0.786	0.699	0.805	0.714	0.977	0.979	0.888	0.886
22	0.492	0.391	0.347	0.391	0.347	0.795	0.706	0.795	0.706	1.000	1.000	0.888	0.888
23	0.577	0.485	0.428	0.496	0.437	0.840	0.743	0.860	0.758	0.977	0.979	0.884	0.882
24	0.444	0.377	0.333	0.377	0.333	0.849	0.750	0.849	0.750	1.000	1.000	0.883	0.883
25	0.577	0.485	0.428	0.496	0.437	0.840	0.743	0.860	0.758	0.977	0.979	0.884	0.882
26	0.444	0.377	0.333	0.377	0.333	0.849	0.750	0.849	0.750	1.000	1.000	0.883	0.883
27	0.639	0.503	0.447	0.515	0.456	0.786	0.699	0.805	0.714	0.977	0.979	0.888	0.886
28	0.444	0.377	0.333	0.377	0.333	0.849	0.750	0.849	0.750	1.000	1.000	0.883	0.883
29	0.639	0.503	0.447	0.515	0.456	0.786	0.699	0.805	0.714	0.977	0.979	0.888	0.886
30	0.444	0.377	0.333	0.377	0.333	0.849	0.750	0.849	0.750	1.000	1.000	0.883	0.883
31	0.642	0.520	0.459	0.549	0.482	0.810	0.716	0.855	0.751	0.947	0.953	0.884	0.878
32	0.539	0.416	0.370	0.422	0.374	0.773	0.686	0.782	0.694	0.988	0.989	0.888	0.886
33	0.642	0.520	0.459	0.549	0.482	0.810	0.716	0.855	0.751	0.947	0.953	0.884	0.878
34	0.539	0.416	0.370	0.422	0.374	0.773	0.686	0.782	0.694	0.988	0.989	0.888	0.886
35	0.642	0.520	0.459	0.549	0.482	0.810	0.716	0.855	0.751	0.947	0.953	0.884	0.878
36	0.539	0.416	0.370	0.422	0.374	0.773	0.686	0.782	0.694	0.988	0.989	0.888	0.886
37	0.642	0.520	0.459	0.549	0.482	0.810	0.716	0.855	0.751	0.947	0.953	0.884	0.878
38	0.539	0.416	0.370	0.422	0.374	0.773	0.686	0.782	0.694	0.988	0.989	0.888	0.886
39	0.668	0.542	0.486	0.573	0.511	0.811	0.728	0.858	0.766	0.945	0.951	0.897	0.892
40	0.487	0.418	0.375	0.418	0.375	0.859	0.771	0.859	0.771	1.000	1.000	0.897	0.897
41	0.668	0.542	0.486	0.573	0.511	0.811	0.728	0.858	0.766	0.945	0.951	0.897	0.892
42	0.487	0.418	0.375	0.418	0.375	0.859	0.771	0.859	0.771	1.000	1.000	0.897	0.897
43	0.700	0.571	0.519	0.598	0.542	0.815	0.740	0.854	0.773	0.955	0.958	0.908	0.906
44	0.581	0.509	0.482	0.509	0.482	0.876	0.828	0.876	0.828	1.000	1.000	0.946	0.946
45	0.700	0.571	0.519	0.598	0.542	0.815	0.740	0.854	0.773	0.955	0.958	0.908	0.906
46	0.581	0.509	0.482	0.509	0.482	0.876	0.828	0.876	0.828	1.000	1.000	0.946	0.946
47	0.724	0.498	0.446	0.518	0.462	0.688	0.615	0.715	0.638	0.962	0.965	0.895	0.893
48	0.539	0.472	0.440	0.472	0.440	0.875	0.817	0.875	0.817	1.000	1.000	0.933	0.933
49	0.724	0.498	0.446	0.518	0.462	0.688	0.615	0.715	0.638	0.962	0.965	0.895	0.893
50	0.539	0.472	0.440	0.472	0.440	0.875	0.817	0.875	0.817	1.000	1.000	0.933	0.933
51	0.702	0.581	0.533	0.614	0.562	0.827	0.760	0.874	0.800	0.946	0.949	0.918	0.915
52	0.557	0.490	0.468	0.490	0.468	0.880	0.840	0.880	0.840	1.000	1.000	0.954	0.954
53	0.590	0.517	0.492	0.517	0.492	0.876	0.834	0.876	0.834	1.000	1.000	0.952	0.952
54	0.702	0.581	0.533	0.614	0.562	0.827	0.760	0.874	0.800	0.946	0.949	0.918	0.915
55	0.557	0.490	0.468	0.490	0.468	0.880	0.840	0.880	0.840	1.000	1.000	0.954	0.954
56	0.590	0.517	0.492	0.517	0.492	0.876	0.834	0.876	0.834	1.000	1.000	0.952	0.952
57	0.639	0.427	0.362	0.439	0.372	0.668	0.566	0.687	0.581	0.972	0.974	0.848	0.846
58	0.577	0.409	0.345	0.421	0.354	0.709	0.598	0.730	0.614	0.972	0.975	0.843	0.841
59	0.509	0.389	0.352	0.389	0.352	0.764	0.692	0.764	0.692	1.000	1.000	0.906	0.906
60	0.492	0.407	0.367	0.407	0.367	0.828	0.746	0.828	0.746	1.000	1.000	0.901	0.901

Table D.1c
Splice length ratios for beams in lateral load resisting frame system (continued)

Spl. No.	ACI '95 Orig.	Eq. 3.13^{+} Orig. Conv.*	Eq. 3.13^{+} Orig. New**	Eq. 3.14^{++} Orig. Conv.*	Eq. 3.14^{++} Orig. New**	Eq. 3.13^{+} ACI '95 Conv.*	Eq. 3.13^{+} ACI '95 New**	Eq. 3.14^{++} ACI '95 Conv.*	Eq. 3.14^{++} ACI '95 New**	Eq. 3.13^{+} Eq. 3.14^{++} Conv.*	Eq. 3.13^{+} Eq. 3.14^{++} New**	New** Conv.* Eq. 3.13^{+}	New** Conv.* Eq. 3.14^{++}
61	0.577	0.410	0.346	0.421	0.354	0.711	0.599	0.730	0.614	0.974	0.977	0.843	0.841
62	0.509	0.389	0.352	0.389	0.352	0.764	0.692	0.764	0.692	1.000	1.000	0.906	0.906
63	0.492	0.407	0.367	0.407	0.367	0.828	0.746	0.828	0.746	1.000	1.000	0.901	0.901
64	0.577	0.410	0.346	0.421	0.354	0.711	0.599	0.730	0.614	0.974	0.977	0.843	0.841
65	0.509	0.389	0.352	0.389	0.352	0.764	0.692	0.764	0.692	1.000	1.000	0.906	0.906
66	0.492	0.407	0.367	0.407	0.367	0.828	0.746	0.828	0.746	1.000	1.000	0.901	0.901
67	0.577	0.410	0.346	0.421	0.354	0.711	0.599	0.730	0.614	0.974	0.977	0.843	0.841
68	0.509	0.389	0.352	0.389	0.352	0.764	0.692	0.764	0.692	1.000	1.000	0.906	0.906
69	0.492	0.407	0.367	0.407	0.367	0.828	0.746	0.828	0.746	1.000	1.000	0.901	0.901
70	0.577	0.410	0.346	0.421	0.354	0.711	0.599	0.730	0.614	0.974	0.977	0.843	0.841
71	0.509	0.389	0.352	0.389	0.352	0.764	0.692	0.764	0.692	1.000	1.000	0.906	0.906
72	0.492	0.407	0.367	0.407	0.367	0.828	0.746	0.828	0.746	1.000	1.000	0.901	0.901
73	0.639	0.427	0.362	0.439	0.372	0.668	0.566	0.687	0.581	0.972	0.974	0.848	0.846
74	0.577	0.409	0.345	0.421	0.354	0.709	0.598	0.730	0.614	0.972	0.975	0.843	0.841
75	0.509	0.389	0.352	0.389	0.352	0.764	0.692	0.764	0.692	1.000	1.000	0.906	0.906
76	0.492	0.407	0.367	0.407	0.367	0.828	0.746	0.828	0.746	1.000	1.000	0.901	0.901
77	0.857	0.617	0.530	0.746	0.626	0.721	0.619	0.870	0.731	0.828	0.847	0.859	0.839
78	0.444	0.381	0.338	0.381	0.338	0.859	0.762	0.859	0.762	1.000	1.000	0.887	0.887
79	0.894	0.642	0.558	0.780	0.664	0.718	0.625	0.873	0.743	0.822	0.841	0.870	0.851
80	0.444	0.355	0.307	0.355	0.307	0.800	0.692	0.800	0.692	1.000	1.000	0.866	0.866
81	0.894	0.642	0.558	0.780	0.664	0.718	0.625	0.873	0.743	0.822	0.841	0.870	0.851
82	0.444	0.355	0.307	0.355	0.307	0.800	0.692	0.800	0.692	1.000	1.000	0.866	0.866
83	0.894	0.642	0.558	0.780	0.664	0.718	0.625	0.873	0.743	0.822	0.841	0.870	0.851
84	0.444	0.355	0.307	0.355	0.307	0.800	0.692	0.800	0.692	1.000	1.000	0.866	0.866
85	0.894	0.642	0.558	0.780	0.664	0.718	0.625	0.873	0.743	0.822	0.841	0.870	0.851
86	0.444	0.355	0.307	0.355	0.307	0.800	0.692	0.800	0.692	1.000	1.000	0.866	0.866
87	0.857	0.617	0.530	0.746	0.626	0.721	0.619	0.870	0.731	0.828	0.847	0.859	0.839
88	0.444	0.381	0.338	0.381	0.338	0.859	0.762	0.859	0.762	1.000	1.000	0.887	0.887
89	0.870	0.626	0.540	0.758	0.639	0.720	0.621	0.871	0.735	0.826	0.845	0.863	0.843
90	0.444	0.346	0.297	0.346	0.297	0.780	0.669	0.780	0.669	1.000	1.000	0.858	0.858
91	0.870	0.626	0.540	0.758	0.639	0.720	0.621	0.871	0.735	0.826	0.845	0.863	0.843
92	0.444	0.346	0.297	0.346	0.297	0.780	0.669	0.780	0.669	1.000	1.000	0.858	0.858
93	0.870	0.626	0.540	0.758	0.639	0.720	0.621	0.871	0.735	0.826	0.845	0.863	0.843
94	0.444	0.346	0.297	0.346	0.297	0.780	0.669	0.780	0.669	1.000	1.000	0.858	0.858
95	0.870	0.626	0.540	0.758	0.639	0.720	0.621	0.871	0.735	0.826	0.845	0.863	0.843
96	0.444	0.346	0.297	0.346	0.297	0.780	0.669	0.780	0.669	1.000	1.000	0.858	0.858
97	0.870	0.626	0.540	0.758	0.639	0.720	0.621	0.871	0.735	0.826	0.845	0.863	0.843
98	0.444	0.346	0.297	0.346	0.297	0.780	0.669	0.780	0.669	1.000	1.000	0.858	0.858
99	0.870	0.626	0.540	0.758	0.639	0.720	0.621	0.871	0.735	0.826	0.845	0.863	0.843
100	0.444	0.346	0.297	0.346	0.297	0.780	0.669	0.780	0.669	1.000	1.000	0.858	0.858
101	0.915	0.656	0.575	0.801	0.687	0.717	0.628	0.875	0.750	0.819	0.837	0.877	0.858
102	0.444	0.363	0.317	0.363	0.317	0.818	0.714	0.818	0.714	1.000	1.000	0.872	0.872
103	0.915	0.656	0.575	0.801	0.687	0.717	0.628	0.875	0.750	0.819	0.837	0.877	0.858
104	0.444	0.363	0.317	0.363	0.317	0.818	0.714	0.818	0.714	1.000	1.000	0.872	0.872
105	0.915	0.656	0.575	0.801	0.687	0.717	0.628	0.875	0.750	0.819	0.837	0.877	0.858
106	0.444	0.363	0.317	0.363	0.317	0.818	0.714	0.818	0.714	1.000	1.000	0.872	0.872
107	0.915	0.656	0.575	0.801	0.687	0.717	0.628	0.875	0.750	0.819	0.837	0.877	0.858
108	0.444	0.363	0.317	0.363	0.317	0.818	0.714	0.818	0.714	1.000	1.000	0.872	0.872
109	0.915	0.656	0.575	0.801	0.687	0.717	0.628	0.875	0.750	0.819	0.837	0.877	0.858
110	0.444	0.363	0.317	0.363	0.317	0.818	0.714	0.818	0.714	1.000	1.000	0.872	0.872
111	0.915	0.656	0.575	0.801	0.687	0.717	0.628	0.875	0.750	0.819	0.837	0.877	0.858
112	0.444	0.363	0.317	0.363	0.317	0.818	0.714	0.818	0.714	1.000	1.000	0.872	0.872
113	0.915	0.656	0.575	0.801	0.687	0.717	0.628	0.875	0.750	0.819	0.837	0.877	0.858
114	0.444	0.363	0.317	0.363	0.317	0.818	0.714	0.818	0.714	1.000	1.000	0.872	0.872
115	0.915	0.656	0.575	0.801	0.687	0.717	0.628	0.875	0.750	0.819	0.837	0.877	0.858
116	0.444	0.363	0.317	0.363	0.317	0.818	0.714	0.818	0.714	1.000	1.000	0.872	0.872
117	0.915	0.656	0.575	0.801	0.687	0.717	0.628	0.875	0.750	0.819	0.837	0.877	0.858
118	0.444	0.363	0.317	0.363	0.317	0.818	0.714	0.818	0.714	1.000	1.000	0.872	0.872
119	0.915	0.656	0.575	0.801	0.687	0.717	0.628	0.875	0.750	0.819	0.837	0.877	0.858
120	0.444	0.363	0.317	0.363	0.317	0.818	0.714	0.818	0.714	1.000	1.000	0.872	0.872

Table D.1c
Splice length ratios for beams in lateral load resisting frame system (continued)

Spl. No.	ACI '95 Orig.	Eq. 3.13^{+} Orig. Conv.*	Eq. 3.13^{+} Orig. New**	Eq. 3.14^{++} Orig. Conv.*	Eq. 3.14^{++} Orig. New**	Eq. 3.13^{+} ACI '95 Conv.*	Eq. 3.13^{+} ACI '95 New**	Eq. 3.14^{++} ACI '95 Conv.*	Eq. 3.14^{++} ACI '95 New**	Eq. 3.13^{+} Eq. 3.14^{++} Conv.*	Eq. 3.13^{+} Eq. 3.14^{++} New**	New** Conv.* Eq. 3.13^{+}	New** Conv.* Eq. 3.14^{++}
121	0.915	0.656	0.575	0.801	0.687	0.717	0.628	0.875	0.750	0.819	0.837	0.877	0.858
122	0.444	0.363	0.317	0.363	0.317	0.818	0.714	0.818	0.714	1.000	1.000	0.872	0.872
123	0.915	0.656	0.575	0.801	0.687	0.717	0.628	0.875	0.750	0.819	0.837	0.877	0.858
124	0.444	0.363	0.317	0.363	0.317	0.818	0.714	0.818	0.714	1.000	1.000	0.872	0.872
125	0.586	0.488	0.431	0.515	0.452	0.833	0.737	0.880	0.773	0.947	0.953	0.884	0.878
126	0.444	0.377	0.333	0.377	0.333	0.849	0.750	0.849	0.750	1.000	1.000	0.883	0.883
127	0.934	0.668	0.590	0.819	0.707	0.715	0.631	0.876	0.757	0.816	0.834	0.882	0.864
128	0.444	0.370	0.325	0.370	0.325	0.835	0.733	0.835	0.733	1.000	1.000	0.878	0.878
129	0.934	0.668	0.590	0.819	0.707	0.715	0.631	0.876	0.757	0.816	0.834	0.882	0.864
130	0.444	0.370	0.325	0.370	0.325	0.835	0.733	0.835	0.733	1.000	1.000	0.878	0.878
131	0.934	0.668	0.590	0.819	0.707	0.715	0.631	0.876	0.757	0.816	0.834	0.882	0.864
132	0.444	0.370	0.325	0.370	0.325	0.835	0.733	0.835	0.733	1.000	1.000	0.878	0.878
133	0.934	0.668	0.590	0.819	0.707	0.715	0.631	0.876	0.757	0.816	0.834	0.882	0.864
134	0.444	0.370	0.325	0.370	0.325	0.835	0.733	0.835	0.733	1.000	1.000	0.878	0.878
135	0.586	0.488	0.431	0.515	0.452	0.833	0.737	0.880	0.773	0.947	0.953	0.884	0.878
136	0.444	0.377	0.333	0.377	0.333	0.849	0.750	0.849	0.750	1.000	1.000	0.883	0.883
137	0.586	0.488	0.431	0.515	0.452	0.833	0.737	0.880	0.773	0.947	0.953	0.884	0.878
138	0.444	0.377	0.333	0.377	0.333	0.849	0.750	0.849	0.750	1.000	1.000	0.883	0.883
139	0.934	0.668	0.590	0.819	0.707	0.715	0.631	0.876	0.757	0.816	0.834	0.882	0.864
140	0.444	0.370	0.325	0.370	0.325	0.835	0.733	0.835	0.733	1.000	1.000	0.878	0.878
141	0.934	0.668	0.590	0.819	0.707	0.715	0.631	0.876	0.757	0.816	0.834	0.882	0.864
142	0.444	0.370	0.325	0.370	0.325	0.835	0.733	0.835	0.733	1.000	1.000	0.878	0.878
143	0.934	0.668	0.590	0.819	0.707	0.715	0.631	0.876	0.757	0.816	0.834	0.882	0.864
144	0.444	0.370	0.325	0.370	0.325	0.835	0.733	0.835	0.733	1.000	1.000	0.878	0.878
145	0.934	0.668	0.590	0.819	0.707	0.715	0.631	0.876	0.757	0.816	0.834	0.882	0.864
146	0.444	0.370	0.325	0.370	0.325	0.835	0.733	0.835	0.733	1.000	1.000	0.878	0.878
147	0.586	0.488	0.431	0.515	0.452	0.833	0.737	0.880	0.773	0.947	0.953	0.884	0.878
148	0.444	0.377	0.333	0.377	0.333	0.849	0.750	0.849	0.750	1.000	1.000	0.883	0.883
149	0.700	0.535	0.476	0.548	0.486	0.764	0.679	0.782	0.694	0.977	0.979	0.888	0.886
150	0.486	0.401	0.354	0.401	0.354	0.825	0.729	0.825	0.729	1.000	1.000	0.883	0.883
151	0.994	0.727	0.651	0.867	0.764	0.731	0.655	0.872	0.768	0.838	0.853	0.896	0.881
152	0.539	0.416	0.370	0.416	0.370	0.773	0.686	0.773	0.686	1.000	1.000	0.888	0.888
153	0.994	0.727	0.651	0.867	0.764	0.731	0.655	0.872	0.768	0.838	0.853	0.896	0.881
154	0.486	0.401	0.354	0.401	0.354	0.825	0.729	0.825	0.729	1.000	1.000	0.883	0.883
155	0.994	0.727	0.651	0.867	0.764	0.731	0.655	0.872	0.768	0.838	0.853	0.896	0.881
156	0.486	0.401	0.354	0.401	0.354	0.825	0.729	0.825	0.729	1.000	1.000	0.883	0.883
157	0.994	0.727	0.651	0.867	0.764	0.731	0.655	0.872	0.768	0.838	0.853	0.896	0.881
158	0.539	0.416	0.370	0.416	0.370	0.773	0.686	0.773	0.686	1.000	1.000	0.888	0.888
159	0.700	0.535	0.476	0.548	0.486	0.764	0.679	0.782	0.694	0.977	0.979	0.888	0.886
160	0.486	0.401	0.354	0.401	0.354	0.825	0.729	0.825	0.729	1.000	1.000	0.883	0.883
161	0.632	0.419	0.349	0.429	0.357	0.663	0.552	0.679	0.564	0.976	0.978	0.833	0.831
162	0.539	0.423	0.377	0.423	0.377	0.784	0.700	0.784	0.700	1.000	1.000	0.893	0.893
163	0.632	0.419	0.349	0.429	0.357	0.663	0.552	0.679	0.564	0.976	0.978	0.833	0.831
164	0.539	0.423	0.377	0.423	0.377	0.784	0.700	0.784	0.700	1.000	1.000	0.893	0.893
165	0.632	0.419	0.349	0.429	0.357	0.663	0.552	0.679	0.564	0.976	0.978	0.833	0.831
166	0.539	0.423	0.377	0.423	0.377	0.784	0.700	0.784	0.700	1.000	1.000	0.893	0.893
167	0.632	0.419	0.349	0.429	0.357	0.663	0.552	0.679	0.564	0.976	0.978	0.833	0.831
168	0.539	0.423	0.377	0.423	0.377	0.784	0.700	0.784	0.700	1.000	1.000	0.893	0.893
169	0.632	0.419	0.349	0.429	0.357	0.663	0.552	0.679	0.564	0.976	0.978	0.833	0.831
170	0.539	0.423	0.377	0.423	0.377	0.784	0.700	0.784	0.700	1.000	1.000	0.893	0.893
171	0.632	0.419	0.349	0.429	0.357	0.663	0.552	0.679	0.564	0.976	0.978	0.833	0.831
172	0.539	0.423	0.377	0.423	0.377	0.784	0.700	0.784	0.700	1.000	1.000	0.893	0.893
173	0.700	0.469	0.402	0.484	0.414	0.670	0.574	0.691	0.591	0.969	0.972	0.857	0.855
174	0.557	0.422	0.385	0.422	0.385	0.757	0.691	0.757	0.691	1.000	1.000	0.913	0.913
175	0.539	0.442	0.402	0.442	0.402	0.821	0.746	0.821	0.746	1.000	1.000	0.908	0.908
176	0.700	0.467	0.401	0.484	0.414	0.667	0.572	0.691	0.591	0.965	0.968	0.858	0.855
177	0.497	0.427	0.387	0.427	0.387	0.861	0.779	0.861	0.779	1.000	1.000	0.905	0.905
178	0.700	0.467	0.401	0.484	0.414	0.667	0.572	0.691	0.591	0.965	0.968	0.858	0.855
179	0.497	0.427	0.387	0.427	0.387	0.861	0.779	0.861	0.779	1.000	1.000	0.905	0.905
180	0.700	0.467	0.401	0.484	0.414	0.667	0.572	0.691	0.591	0.965	0.968	0.858	0.855

Table D.1c
Splice length ratios for beams in lateral load resisting frame system (continued)

Spl. No.	ACI '95 Orig.	Eq. 3.13^{-} Orig. Conv.*	Eq. 3.13^{+} Orig. New**	Eq. 3.14^{--} Orig. Conv.*	Eq. 3.14^{--} Orig. New**	Eq. 3.13^{-} ACI '95 Conv.*	Eq. 3.13^{+} ACI '95 New**	Eq. 3.14^{--} ACI '95 Conv.*	Eq. 3.14^{--} ACI '95 New**	Eq. 3.13^{-} Eq. 3.14^{--} Conv.*	Eq. 3.13^{-} Eq. 3.14^{--} New**	New** Conv.* Eq. 3.13^{+}	New** Conv.* Eq. 3.14^{--}
181	0.497	0.427	0.387	0.427	0.387	0.861	0.779	0.861	0.779	1.000	1.000	0.905	0.905
182	0.700	0.467	0.401	0.484	0.414	0.667	0.572	0.691	0.591	0.965	0.968	0.858	0.855
183	0.497	0.427	0.387	0.427	0.387	0.861	0.779	0.861	0.779	1.000	1.000	0.905	0.905
184	0.700	0.469	0.402	0.484	0.414	0.670	0.574	0.691	0.591	0.969	0.972	0.857	0.855
185	0.557	0.422	0.385	0.422	0.385	0.757	0.691	0.757	0.691	1.000	1.000	0.913	0.913
186	0.539	0.442	0.402	0.442	0.402	0.821	0.746	0.821	0.746	1.000	1.000	0.908	0.908
187	0.632	0.478	0.415	0.491	0.425	0.757	0.657	0.778	0.673	0.973	0.976	0.868	0.866
188	0.557	0.435	0.402	0.435	0.402	0.780	0.721	0.780	0.721	1.000	1.000	0.924	0.924
189	0.539	0.457	0.420	0.457	0.420	0.848	0.780	0.848	0.780	1.000	1.000	0.920	0.920
190	0.632	0.478	0.415	0.491	0.425	0.757	0.657	0.778	0.673	0.973	0.976	0.868	0.866
191	0.539	0.457	0.420	0.457	0.420	0.848	0.780	0.848	0.780	1.000	1.000	0.920	0.920
192	0.632	0.478	0.415	0.491	0.425	0.757	0.657	0.778	0.673	0.973	0.976	0.868	0.866
193	0.539	0.457	0.420	0.457	0.420	0.848	0.780	0.848	0.780	1.000	1.000	0.920	0.920
194	0.632	0.478	0.415	0.491	0.425	0.757	0.657	0.778	0.673	0.973	0.976	0.868	0.866
195	0.539	0.457	0.420	0.457	0.420	0.848	0.780	0.848	0.780	1.000	1.000	0.920	0.920
196	0.632	0.478	0.415	0.491	0.425	0.757	0.657	0.778	0.673	0.973	0.976	0.868	0.866
197	0.539	0.457	0.420	0.457	0.420	0.848	0.780	0.848	0.780	1.000	1.000	0.920	0.920
198	0.632	0.478	0.415	0.491	0.425	0.757	0.657	0.778	0.673	0.973	0.976	0.868	0.866
199	0.557	0.435	0.402	0.435	0.402	0.780	0.721	0.780	0.721	1.000	1.000	0.924	0.924
200	0.539	0.457	0.420	0.457	0.420	0.848	0.780	0.848	0.780	1.000	1.000	0.920	0.920
201	0.724	0.498	0.462	0.585	0.538	0.688	0.637	0.808	0.743	0.851	0.858	0.927	0.919
202	0.557	0.490	0.468	0.490	0.468	0.880	0.840	0.880	0.840	1.000	1.000	0.954	0.954
203	0.590	0.517	0.492	0.517	0.492	0.876	0.834	0.876	0.834	1.000	1.000	0.952	0.952
204	0.724	0.468	0.411	0.490	0.429	0.646	0.567	0.677	0.592	0.954	0.958	0.879	0.875
205	0.539	0.457	0.420	0.457	0.420	0.848	0.780	0.848	0.780	1.000	1.000	0.920	0.920
206	0.724	0.468	0.411	0.490	0.429	0.646	0.567	0.677	0.592	0.954	0.958	0.879	0.875
207	0.539	0.457	0.420	0.457	0.420	0.848	0.780	0.848	0.780	1.000	1.000	0.920	0.920
208	0.724	0.468	0.411	0.490	0.429	0.646	0.567	0.677	0.592	0.954	0.958	0.879	0.875
209	0.539	0.457	0.420	0.457	0.420	0.848	0.780	0.848	0.780	1.000	1.000	0.920	0.920
210	0.724	0.468	0.411	0.490	0.429	0.646	0.567	0.677	0.592	0.954	0.958	0.879	0.875
211	0.539	0.457	0.420	0.457	0.420	0.848	0.780	0.848	0.780	1.000	1.000	0.920	0.920
212	0.724	0.498	0.462	0.585	0.538	0.688	0.637	0.808	0.743	0.851	0.858	0.927	0.919
213	0.557	0.490	0.468	0.490	0.468	0.880	0.840	0.880	0.840	1.000	1.000	0.954	0.954
214	0.590	0.517	0.492	0.517	0.492	0.876	0.834	0.876	0.834	1.000	1.000	0.952	0.952
215	0.661	0.518	0.478	0.550	0.505	0.784	0.723	0.832	0.764	0.942	0.945	0.922	0.919
216	0.641	0.544	0.499	0.577	0.528	0.848	0.779	0.900	0.824	0.943	0.946	0.918	0.915
217	0.509	0.461	0.440	0.461	0.440	0.906	0.864	0.906	0.864	1.000	1.000	0.954	0.954
218	0.538	0.485	0.462	0.485	0.462	0.902	0.858	0.902	0.858	1.000	1.000	0.952	0.952
219	0.661	0.518	0.478	0.550	0.505	0.784	0.723	0.832	0.764	0.942	0.945	0.922	0.919
220	0.641	0.544	0.499	0.577	0.528	0.848	0.779	0.900	0.824	0.943	0.946	0.918	0.915
221	0.509	0.461	0.440	0.461	0.440	0.906	0.864	0.906	0.864	1.000	1.000	0.954	0.954
222	0.538	0.485	0.462	0.485	0.462	0.902	0.858	0.902	0.858	1.000	1.000	0.952	0.952
223	0.577	0.468	0.412	0.481	0.423	0.811	0.714	0.835	0.733	0.972	0.974	0.880	0.878
224	0.444	0.370	0.325	0.370	0.325	0.835	0.733	0.835	0.733	1.000	1.000	0.878	0.878
225	0.577	0.468	0.412	0.481	0.423	0.811	0.714	0.835	0.733	0.972	0.974	0.880	0.878
226	0.444	0.370	0.325	0.370	0.325	0.835	0.733	0.835	0.733	1.000	1.000	0.878	0.878
227	0.577	0.393	0.327	0.403	0.335	0.681	0.568	0.699	0.581	0.975	0.978	0.833	0.831
228	0.444	0.383	0.340	0.383	0.340	0.863	0.766	0.863	0.766	1.000	1.000	0.888	0.888
229	0.577	0.393	0.327	0.403	0.335	0.681	0.568	0.699	0.581	0.975	0.978	0.833	0.831
230	0.444	0.383	0.340	0.383	0.340	0.863	0.766	0.863	0.766	1.000	1.000	0.888	0.888
231	0.577	0.425	0.362	0.436	0.371	0.736	0.628	0.756	0.643	0.974	0.976	0.852	0.850
232	0.453	0.402	0.363	0.402	0.363	0.886	0.801	0.886	0.801	1.000	1.000	0.905	0.905
233	0.577	0.425	0.362	0.436	0.371	0.736	0.628	0.756	0.643	0.974	0.976	0.852	0.850
234	0.453	0.402	0.363	0.402	0.363	0.886	0.801	0.886	0.801	1.000	1.000	0.905	0.905
235	0.577	0.438	0.377	0.450	0.386	0.759	0.653	0.780	0.669	0.973	0.976	0.860	0.858
236	0.461	0.409	0.372	0.409	0.372	0.887	0.808	0.887	0.808	1.000	1.000	0.911	0.911
237	0.577	0.438	0.377	0.450	0.386	0.759	0.653	0.780	0.669	0.973	0.976	0.860	0.858
238	0.461	0.409	0.372	0.409	0.372	0.887	0.808	0.887	0.808	1.000	1.000	0.911	0.911
239	0.577	0.438	0.377	0.450	0.386	0.759	0.653	0.780	0.669	0.973	0.976	0.860	0.858
240	0.461	0.409	0.372	0.409	0.372	0.887	0.808	0.887	0.808	1.000	1.000	0.911	0.911

Table D.1c
Splice length ratios for beams in lateral load resisting frame system (continued)

Spl. No.	ACI '95 Orig.	Eq. 3.13^{+} Orig. Conv.*	Eq. 3.13^{+} Orig. New**	Eq. 3.14^{++} Orig. Conv.*	Eq. 3.14^{++} Orig. New**	Eq. 3.13^{+} ACI '95 Conv.*	Eq. 3.13^{+} ACI '95 New**	Eq. 3.14^{++} ACI '95 Conv.*	Eq. 3.14^{++} ACI '95 New**	Eq. 3.13^{+} Eq. 3.14^{++} Conv.*	Eq. 3.13^{+} Eq. 3.14^{++} New**	New** Eq. 3.13^{+}	New** Conv.* Eq. 3.14^{++}
241	0.577	0.438	0.377	0.450	0.386	0.759	0.653	0.780	0.669	0.973	0.976	0.860	0.858
242	0.461	0.409	0.372	0.409	0.372	0.887	0.808	0.887	0.808	1.000	1.000	0.911	0.911
243	0.577	0.425	0.362	0.436	0.371	0.736	0.628	0.756	0.643	0.974	0.976	0.852	0.850
244	0.453	0.402	0.363	0.402	0.363	0.886	0.801	0.886	0.801	1.000	1.000	0.905	0.905
245	0.577	0.425	0.362	0.436	0.371	0.736	0.628	0.756	0.643	0.974	0.976	0.852	0.850
246	0.453	0.402	0.363	0.402	0.363	0.886	0.801	0.886	0.801	1.000	1.000	0.905	0.905
247	0.632	0.453	0.386	0.464	0.395	0.716	0.610	0.735	0.625	0.974	0.977	0.852	0.850
248	0.497	0.427	0.387	0.427	0.387	0.861	0.779	0.861	0.779	1.000	1.000	0.905	0.905
249	0.632	0.453	0.386	0.464	0.395	0.716	0.610	0.735	0.625	0.974	0.977	0.852	0.850
250	0.497	0.427	0.387	0.427	0.387	0.861	0.779	0.861	0.779	1.000	1.000	0.905	0.905
251	0.632	0.466	0.401	0.479	0.411	0.738	0.635	0.758	0.650	0.974	0.976	0.860	0.858
252	0.505	0.435	0.397	0.435	0.397	0.862	0.785	0.862	0.785	1.000	1.000	0.911	0.911
253	0.632	0.466	0.401	0.479	0.411	0.738	0.635	0.758	0.650	0.974	0.976	0.860	0.858
254	0.505	0.435	0.397	0.435	0.397	0.862	0.785	0.862	0.785	1.000	1.000	0.911	0.911
255	0.632	0.499	0.439	0.513	0.450	0.789	0.694	0.811	0.712	0.973	0.975	0.880	0.878
256	0.557	0.445	0.415	0.445	0.415	0.798	0.744	0.798	0.744	1.000	1.000	0.933	0.933
257	0.539	0.467	0.434	0.467	0.434	0.868	0.806	0.868	0.806	1.000	1.000	0.929	0.929
258	0.632	0.499	0.439	0.513	0.450	0.789	0.694	0.811	0.712	0.973	0.975	0.880	0.878
259	0.557	0.445	0.415	0.445	0.415	0.798	0.744	0.798	0.744	1.000	1.000	0.933	0.933
260	0.539	0.467	0.434	0.467	0.434	0.868	0.806	0.868	0.806	1.000	1.000	0.929	0.929
261	0.700	0.521	0.464	0.541	0.480	0.744	0.662	0.773	0.686	0.963	0.965	0.890	0.888
262	0.539	0.472	0.440	0.472	0.440	0.875	0.817	0.875	0.817	1.000	1.000	0.933	0.933
263	0.700	0.521	0.464	0.541	0.480	0.744	0.662	0.773	0.686	0.963	0.965	0.890	0.888
264	0.539	0.472	0.440	0.472	0.440	0.875	0.817	0.875	0.817	1.000	1.000	0.933	0.933
265	0.632	0.478	0.415	0.491	0.425	0.757	0.657	0.778	0.673	0.973	0.976	0.868	0.866
266	0.557	0.435	0.402	0.435	0.402	0.780	0.721	0.780	0.721	1.000	1.000	0.924	0.924
267	0.539	0.457	0.420	0.457	0.420	0.848	0.780	0.848	0.780	1.000	1.000	0.920	0.920
268	0.632	0.478	0.415	0.491	0.425	0.757	0.657	0.778	0.673	0.973	0.976	0.868	0.866
269	0.557	0.435	0.402	0.435	0.402	0.780	0.721	0.780	0.721	1.000	1.000	0.924	0.924
270	0.539	0.457	0.420	0.457	0.420	0.848	0.780	0.848	0.780	1.000	1.000	0.920	0.920
271	0.724	0.554	0.511	0.585	0.538	0.764	0.705	0.808	0.743	0.946	0.949	0.922	0.919
272	0.702	0.581	0.533	0.614	0.562	0.827	0.760	0.874	0.800	0.946	0.949	0.918	0.915
273	0.557	0.490	0.468	0.490	0.468	0.880	0.840	0.880	0.840	1.000	1.000	0.954	0.954
274	0.590	0.517	0.492	0.517	0.492	0.876	0.834	0.876	0.834	1.000	1.000	0.952	0.952
275	0.724	0.554	0.511	0.585	0.538	0.764	0.705	0.808	0.743	0.946	0.949	0.922	0.919
276	0.702	0.581	0.533	0.614	0.562	0.827	0.760	0.874	0.800	0.946	0.949	0.918	0.915
277	0.557	0.490	0.468	0.490	0.468	0.880	0.840	0.880	0.840	1.000	1.000	0.954	0.954
278	0.590	0.517	0.492	0.517	0.492	0.876	0.834	0.876	0.834	1.000	1.000	0.952	0.952
279	0.577	0.449	0.390	0.461	0.399	0.778	0.675	0.800	0.692	0.973	0.975	0.868	0.866
280	0.509	0.408	0.377	0.408	0.377	0.803	0.742	0.803	0.742	1.000	1.000	0.924	0.924
281	0.492	0.429	0.395	0.429	0.395	0.872	0.803	0.872	0.803	1.000	1.000	0.920	0.920
282	0.577	0.449	0.390	0.461	0.399	0.778	0.675	0.800	0.692	0.973	0.975	0.868	0.866
283	0.509	0.408	0.377	0.408	0.377	0.803	0.742	0.803	0.742	1.000	1.000	0.924	0.924
284	0.492	0.429	0.395	0.429	0.395	0.872	0.803	0.872	0.803	1.000	1.000	0.920	0.920
285	0.577	0.449	0.390	0.461	0.399	0.778	0.675	0.800	0.692	0.973	0.975	0.868	0.866
286	0.509	0.408	0.377	0.408	0.377	0.803	0.742	0.803	0.742	1.000	1.000	0.924	0.924
287	0.492	0.429	0.395	0.429	0.395	0.872	0.803	0.872	0.803	1.000	1.000	0.920	0.920
288	0.655	0.518	0.448	0.572	0.489	0.791	0.684	0.874	0.746	0.905	0.917	0.865	0.854
289	0.504	0.398	0.344	0.440	0.376	0.791	0.684	0.874	0.746	0.905	0.917	0.865	0.854
290	0.655	0.518	0.448	0.572	0.489	0.791	0.684	0.874	0.746	0.905	0.917	0.865	0.854
291	0.504	0.398	0.344	0.440	0.376	0.791	0.684	0.874	0.746	0.905	0.917	0.865	0.854
292	0.655	0.518	0.448	0.572	0.489	0.791	0.684	0.874	0.746	0.905	0.917	0.865	0.854
293	0.504	0.398	0.344	0.440	0.376	0.791	0.684	0.874	0.746	0.905	0.917	0.865	0.854
294	0.843	0.608	0.520	0.733	0.612	0.721	0.617	0.869	0.726	0.830	0.850	0.855	0.835
295	0.444	0.336	0.285	0.351	0.296	0.756	0.643	0.791	0.668	0.956	0.963	0.850	0.844
296	0.843	0.608	0.520	0.733	0.612	0.721	0.617	0.869	0.726	0.830	0.850	0.855	0.835
297	0.648	0.468	0.400	0.564	0.471	0.721	0.617	0.869	0.726	0.830	0.850	0.855	0.835
298	0.843	0.608	0.520	0.733	0.612	0.721	0.617	0.869	0.726	0.830	0.850	0.855	0.835
299	0.444	0.336	0.285	0.351	0.296	0.756	0.643	0.791	0.668	0.956	0.963	0.850	0.844
300	0.857	0.617	0.530	0.746	0.626	0.721	0.619	0.870	0.731	0.828	0.847	0.859	0.839

Table D.1c
Splice length ratios for beams in lateral load resisting frame system (continued)

Spl. No.	ACI '95 Orig.	Eq. 3.13^{+} Orig. Conv.*	Eq. 3.13^{-} Orig. New**	Eq. 3.14^{--} Orig. Conv.*	Eq. 3.14^{++} Orig. New**	Eq. 3.13^{+} ACI '95 Conv.*	Eq. 3.13^{+} ACI '95 New**	Eq. 3.14^{++} ACI '95 Conv.*	Eq. 3.14^{++} ACI '95 New**	Eq. 3.13^{-} Eq. 3.14^{--} Conv.*	Eq. 3.13^{+} Eq. 3.14^{++} New**	New** Conv.* Eq. 3.13^{+}	New** Conv.* Eq. 3.14^{++}
301	0.444	0.341	0.291	0.341	0.291	0.768	0.656	0.768	0.656	1.000	1.000	0.854	0.854
302	0.857	0.617	0.530	0.746	0.626	0.721	0.619	0.870	0.731	0.828	0.847	0.859	0.839
303	0.444	0.341	0.291	0.341	0.291	0.768	0.656	0.768	0.656	1.000	1.000	0.854	0.854
304	0.857	0.617	0.530	0.746	0.626	0.721	0.619	0.870	0.731	0.828	0.847	0.859	0.839
305	0.444	0.341	0.291	0.341	0.291	0.768	0.656	0.768	0.656	1.000	1.000	0.854	0.854
306	0.915	0.656	0.575	0.801	0.687	0.717	0.628	0.875	0.750	0.819	0.837	0.877	0.858
307	0.444	0.363	0.317	0.363	0.317	0.818	0.714	0.818	0.714	1.000	1.000	0.872	0.872
308	0.915	0.656	0.575	0.801	0.687	0.717	0.628	0.875	0.750	0.819	0.837	0.877	0.858
309	0.444	0.363	0.317	0.363	0.317	0.818	0.714	0.818	0.714	1.000	1.000	0.872	0.872
310	0.915	0.656	0.575	0.801	0.687	0.717	0.628	0.875	0.750	0.819	0.837	0.877	0.858
311	0.444	0.363	0.317	0.363	0.317	0.818	0.714	0.818	0.714	1.000	1.000	0.872	0.872
312	0.915	0.656	0.575	0.801	0.687	0.717	0.628	0.875	0.750	0.819	0.837	0.877	0.858
313	0.492	0.377	0.331	0.377	0.331	0.767	0.672	0.767	0.672	1.000	1.000	0.877	0.877
314	0.934	0.668	0.590	0.819	0.707	0.715	0.631	0.876	0.757	0.816	0.834	0.882	0.864
315	0.444	0.370	0.325	0.370	0.325	0.835	0.733	0.835	0.733	1.000	1.000	0.878	0.878
316	0.915	0.656	0.575	0.801	0.687	0.717	0.628	0.875	0.750	0.819	0.837	0.877	0.858
317	0.492	0.377	0.331	0.377	0.331	0.767	0.672	0.767	0.672	1.000	1.000	0.877	0.877
318	0.857	0.617	0.530	0.746	0.626	0.721	0.619	0.870	0.731	0.828	0.847	0.859	0.839
319	0.444	0.341	0.291	0.341	0.291	0.768	0.656	0.768	0.656	1.000	1.000	0.854	0.854
320	0.857	0.617	0.530	0.746	0.626	0.721	0.619	0.870	0.731	0.828	0.847	0.859	0.839
321	0.444	0.341	0.291	0.341	0.291	0.768	0.656	0.768	0.656	1.000	1.000	0.854	0.854
322	0.857	0.617	0.530	0.746	0.626	0.721	0.619	0.870	0.731	0.828	0.847	0.859	0.839
323	0.444	0.341	0.291	0.341	0.291	0.768	0.656	0.768	0.656	1.000	1.000	0.854	0.854
324	1.002	0.700	0.613	0.852	0.731	0.698	0.612	0.850	0.729	0.821	0.839	0.877	0.858
325	0.539	0.402	0.352	0.402	0.352	0.746	0.654	0.746	0.654	1.000	1.000	0.877	0.877
326	1.002	0.700	0.613	0.852	0.731	0.698	0.612	0.850	0.729	0.821	0.839	0.877	0.858
327	0.486	0.387	0.337	0.387	0.337	0.795	0.694	0.795	0.694	1.000	1.000	0.872	0.872
328	1.002	0.700	0.613	0.852	0.731	0.698	0.612	0.850	0.729	0.821	0.839	0.877	0.858
329	0.539	0.402	0.352	0.402	0.352	0.746	0.654	0.746	0.654	1.000	1.000	0.877	0.877
330	1.002	0.700	0.613	0.852	0.731	0.698	0.612	0.850	0.729	0.821	0.839	0.877	0.858
331	0.539	0.402	0.352	0.402	0.352	0.746	0.654	0.746	0.654	1.000	1.000	0.877	0.877
332	1.002	0.700	0.613	0.852	0.731	0.698	0.612	0.850	0.729	0.821	0.839	0.877	0.858
333	0.486	0.387	0.337	0.387	0.337	0.795	0.694	0.795	0.694	1.000	1.000	0.872	0.872
334	1.002	0.700	0.613	0.852	0.731	0.698	0.612	0.850	0.729	0.821	0.839	0.877	0.858
335	0.539	0.402	0.352	0.402	0.352	0.746	0.654	0.746	0.654	1.000	1.000	0.877	0.877
336	0.632	0.507	0.449	0.522	0.461	0.803	0.711	0.825	0.729	0.972	0.975	0.885	0.883
337	0.539	0.416	0.370	0.416	0.370	0.773	0.686	0.773	0.686	1.000	1.000	0.888	0.888
338	0.632	0.507	0.449	0.522	0.461	0.803	0.711	0.825	0.729	0.972	0.975	0.885	0.883
339	0.539	0.416	0.370	0.416	0.370	0.773	0.686	0.773	0.686	1.000	1.000	0.888	0.888
340	0.632	0.507	0.449	0.522	0.461	0.803	0.711	0.825	0.729	0.972	0.975	0.885	0.883
341	0.539	0.416	0.370	0.416	0.370	0.773	0.686	0.773	0.686	1.000	1.000	0.888	0.888
342	0.632	0.507	0.449	0.522	0.461	0.803	0.711	0.825	0.729	0.972	0.975	0.885	0.883
343	0.557	0.398	0.355	0.398	0.355	0.715	0.638	0.715	0.638	1.000	1.000	0.893	0.893
344	0.539	0.416	0.370	0.416	0.370	0.773	0.686	0.773	0.686	1.000	1.000	0.888	0.888
345	0.632	0.507	0.449	0.522	0.461	0.803	0.711	0.825	0.729	0.972	0.975	0.885	0.883
346	0.539	0.416	0.370	0.416	0.370	0.773	0.686	0.773	0.686	1.000	1.000	0.888	0.888
347	0.632	0.507	0.449	0.522	0.461	0.803	0.711	0.825	0.729	0.972	0.975	0.885	0.883
348	0.557	0.398	0.355	0.398	0.355	0.715	0.638	0.715	0.638	1.000	1.000	0.893	0.893
349	0.539	0.416	0.370	0.416	0.370	0.773	0.686	0.773	0.686	1.000	1.000	0.888	0.888
350	0.700	0.505	0.444	0.522	0.458	0.722	0.634	0.746	0.654	0.968	0.970	0.879	0.877
351	0.557	0.440	0.409	0.440	0.409	0.790	0.733	0.790	0.733	1.000	1.000	0.929	0.929
352	0.632	0.499	0.439	0.513	0.450	0.789	0.694	0.811	0.712	0.973	0.975	0.880	0.878
353	0.557	0.445	0.415	0.445	0.415	0.798	0.744	0.798	0.744	1.000	1.000	0.933	0.933
354	0.700	0.505	0.444	0.522	0.458	0.722	0.634	0.746	0.654	0.968	0.970	0.879	0.877
355	0.557	0.440	0.409	0.440	0.409	0.790	0.733	0.790	0.733	1.000	1.000	0.929	0.929
356	0.632	0.507	0.449	0.522	0.461	0.803	0.711	0.825	0.729	0.972	0.975	0.885	0.883
357	0.557	0.449	0.420	0.449	0.420	0.805	0.754	0.805	0.754	1.000	1.000	0.936	0.936
358	0.539	0.472	0.440	0.472	0.440	0.875	0.817	0.875	0.817	1.000	1.000	0.933	0.933
359	0.632	0.507	0.449	0.522	0.461	0.803	0.711	0.825	0.729	0.972	0.975	0.885	0.883
360	0.557	0.449	0.420	0.449	0.420	0.805	0.754	0.805	0.754	1.000	1.000	0.936	0.936

Table D.1c
Splice length ratios for beams in lateral load resisting frame system (continued)

Spl. No.	ACI '95 Orig.	Eq. 3.13^{+} Orig. Conv.*	Eq. 3.13^{+} Orig. New**	Eq. 3.14^{++} Orig. Conv.*	Eq. 3.14^{++} Orig. New**	Eq. 3.13^{+} ACI '95 Conv.*	Eq. 3.13^{+} ACI '95 New**	Eq. 3.14^{++} ACI '95 Conv.*	Eq. 3.14^{++} ACI '95 New**	Eq. 3.13^{-} Eq. 3.14^{--} Conv.*	Eq. 3.13^{+} Eq. 3.14^{++} New**	New** Conv.* Eq. 3.13^{+}	New** Conv.* Eq. 3.14^{++}
361	0.539	0.472	0.440	0.472	0.440	0.875	0.817	0.875	0.817	1.000	1.000	0.933	0.933
362	0.632	0.507	0.449	0.522	0.461	0.803	0.711	0.825	0.729	0.972	0.975	0.885	0.883
363	0.557	0.449	0.420	0.449	0.420	0.805	0.754	0.805	0.754	1.000	1.000	0.936	0.936
364	0.539	0.472	0.440	0.472	0.440	0.875	0.817	0.875	0.817	1.000	1.000	0.933	0.933
365	0.577	0.449	0.390	0.461	0.399	0.778	0.675	0.800	0.692	0.973	0.975	0.868	0.866
366	0.509	0.408	0.377	0.408	0.377	0.803	0.742	0.803	0.742	1.000	1.000	0.924	0.924
367	0.492	0.429	0.395	0.429	0.395	0.872	0.803	0.872	0.803	1.000	1.000	0.920	0.920
368	0.577	0.449	0.390	0.461	0.399	0.778	0.675	0.800	0.692	0.973	0.975	0.868	0.866
369	0.509	0.408	0.377	0.408	0.377	0.803	0.742	0.803	0.742	1.000	1.000	0.924	0.924
370	0.492	0.429	0.395	0.429	0.395	0.872	0.803	0.872	0.803	1.000	1.000	0.920	0.920
371	0.577	0.449	0.390	0.461	0.399	0.778	0.675	0.800	0.692	0.973	0.975	0.868	0.866
372	0.509	0.408	0.377	0.408	0.377	0.803	0.742	0.803	0.742	1.000	1.000	0.924	0.924
373	0.492	0.429	0.395	0.429	0.395	0.872	0.803	0.872	0.803	1.000	1.000	0.920	0.920
374	0.577	0.449	0.390	0.461	0.399	0.778	0.675	0.800	0.692	0.973	0.975	0.868	0.866
375	0.509	0.408	0.377	0.408	0.377	0.803	0.742	0.803	0.742	1.000	1.000	0.924	0.924
376	0.492	0.429	0.395	0.429	0.395	0.872	0.803	0.872	0.803	1.000	1.000	0.920	0.920
377	0.894	0.642	0.558	0.780	0.664	0.718	0.625	0.873	0.743	0.822	0.841	0.870	0.851
378	0.492	0.369	0.321	0.374	0.325	0.751	0.653	0.760	0.660	0.988	0.990	0.870	0.869
379	0.894	0.642	0.558	0.780	0.664	0.718	0.625	0.873	0.743	0.822	0.841	0.870	0.851
380	0.658	0.498	0.437	0.589	0.509	0.757	0.665	0.896	0.773	0.844	0.860	0.879	0.863
381	0.894	0.642	0.558	0.780	0.664	0.718	0.625	0.873	0.743	0.822	0.841	0.870	0.851
382	0.658	0.498	0.437	0.589	0.509	0.757	0.665	0.896	0.773	0.844	0.860	0.879	0.863
383	0.968	0.691	0.617	0.851	0.745	0.713	0.637	0.879	0.769	0.811	0.828	0.893	0.875
384	0.492	0.397	0.354	0.402	0.358	0.807	0.720	0.817	0.728	0.987	0.989	0.893	0.891
385	0.843	0.608	0.520	0.733	0.612	0.721	0.617	0.869	0.726	0.830	0.850	0.855	0.835
386	0.492	0.350	0.299	0.354	0.302	0.711	0.608	0.719	0.614	0.989	0.990	0.855	0.854
387	0.843	0.608	0.520	0.733	0.612	0.721	0.617	0.869	0.726	0.830	0.850	0.855	0.835
388	0.621	0.473	0.409	0.556	0.471	0.762	0.658	0.895	0.759	0.851	0.868	0.864	0.847
389	0.843	0.608	0.520	0.733	0.612	0.721	0.617	0.869	0.726	0.830	0.850	0.855	0.835
390	0.621	0.473	0.409	0.556	0.471	0.762	0.658	0.895	0.759	0.851	0.868	0.864	0.847
391	0.968	0.691	0.617	0.851	0.745	0.713	0.637	0.879	0.769	0.811	0.828	0.893	0.875
392	0.492	0.397	0.354	0.402	0.358	0.807	0.720	0.817	0.728	0.987	0.989	0.893	0.891
393	0.915	0.656	0.575	0.801	0.687	0.717	0.628	0.875	0.750	0.819	0.837	0.877	0.858
394	0.444	0.363	0.317	0.363	0.317	0.818	0.714	0.818	0.714	1.000	1.000	0.872	0.872
395	0.915	0.656	0.575	0.801	0.687	0.717	0.628	0.875	0.750	0.819	0.837	0.877	0.858
396	0.444	0.363	0.317	0.363	0.317	0.818	0.714	0.818	0.714	1.000	1.000	0.872	0.872
397	0.915	0.656	0.575	0.801	0.687	0.717	0.628	0.875	0.750	0.819	0.837	0.877	0.858
398	0.444	0.363	0.317	0.363	0.317	0.818	0.714	0.818	0.714	1.000	1.000	0.872	0.872
399	0.968	0.691	0.617	0.851	0.745	0.713	0.637	0.879	0.769	0.811	0.828	0.893	0.875
400	0.444	0.383	0.340	0.383	0.340	0.863	0.766	0.863	0.766	1.000	1.000	0.888	0.888
401	0.915	0.656	0.575	0.801	0.687	0.717	0.628	0.875	0.750	0.819	0.837	0.877	0.858
402	0.444	0.363	0.317	0.363	0.317	0.818	0.714	0.818	0.714	1.000	1.000	0.872	0.872
403	0.915	0.656	0.575	0.801	0.687	0.717	0.628	0.875	0.750	0.819	0.837	0.877	0.858
404	0.444	0.363	0.317	0.363	0.317	0.818	0.714	0.818	0.714	1.000	1.000	0.872	0.872
405	0.915	0.656	0.575	0.801	0.687	0.717	0.628	0.875	0.750	0.819	0.837	0.877	0.858
406	0.444	0.363	0.317	0.363	0.317	0.818	0.714	0.818	0.714	1.000	1.000	0.872	0.872
407	0.968	0.691	0.617	0.851	0.745	0.713	0.637	0.879	0.769	0.811	0.828	0.893	0.875
408	0.444	0.383	0.340	0.383	0.340	0.863	0.766	0.863	0.766	1.000	1.000	0.888	0.888
409	0.915	0.656	0.575	0.801	0.687	0.717	0.628	0.875	0.750	0.819	0.837	0.877	0.858
410	0.444	0.363	0.317	0.363	0.317	0.818	0.714	0.818	0.714	1.000	1.000	0.872	0.872
411	0.915	0.656	0.575	0.801	0.687	0.717	0.628	0.875	0.750	0.819	0.837	0.877	0.858
412	0.444	0.363	0.317	0.363	0.317	0.818	0.714	0.818	0.714	1.000	1.000	0.872	0.872
413	0.915	0.656	0.575	0.801	0.687	0.717	0.628	0.875	0.750	0.819	0.837	0.877	0.858
414	0.444	0.363	0.317	0.363	0.317	0.818	0.714	0.818	0.714	1.000	1.000	0.872	0.872
415	0.968	0.691	0.617	0.851	0.745	0.713	0.637	0.879	0.769	0.811	0.828	0.893	0.875
416	0.444	0.383	0.340	0.383	0.340	0.863	0.766	0.863	0.766	1.000	1.000	0.888	0.888
417	0.843	0.608	0.520	0.733	0.612	0.721	0.617	0.869	0.726	0.830	0.850	0.855	0.835
418	0.492	0.350	0.299	0.354	0.302	0.711	0.608	0.719	0.614	0.989	0.990	0.855	0.854
419	0.843	0.608	0.520	0.733	0.612	0.721	0.617	0.869	0.726	0.830	0.850	0.855	0.835
420	0.621	0.473	0.409	0.556	0.471	0.762	0.658	0.895	0.759	0.851	0.868	0.864	0.847

Table D.1c
Splice length ratios for beams in lateral load resisting frame system (continued)

Spl. No.	ACI '95 Orig.	Eq. 3.13^{+} Orig. Conv.*	Eq. 3.13^{-} Orig. New**	Eq. 3.14^{--} Orig. Conv.*	Eq. 3.14^{++} Orig. New**	Eq. 3.13^{+} ACI '95 Conv.*	Eq. 3.13^{-} ACI '95 New**	Eq. 3.14^{--} ACI '95 Conv.*	Eq. 3.14^{++} ACI '95 New**	Eq. 3.13^{+} Eq. 3.14^{++} Conv.*	Eq. 3.13^{-} Eq. 3.14^{--} New**	New** Conv.* Eq. 3.13^{+}	New** Conv.* Eq. 3.14^{++}
421	0.843	0.608	0.520	0.753	0.612	0.721	0.617	0.869	0.726	0.830	0.850	0.855	0.835
422	0.621	0.473	0.409	0.556	0.471	0.762	0.658	0.895	0.759	0.851	0.868	0.864	0.847
423	0.968	0.691	0.617	0.851	0.745	0.713	0.637	0.879	0.769	0.811	0.828	0.893	0.875
424	0.492	0.397	0.354	0.402	0.358	0.807	0.720	0.817	0.728	0.987	0.989	0.893	0.891
425	0.953	0.668	0.576	0.807	0.680	0.701	0.605	0.847	0.714	0.828	0.847	0.863	0.843
426	0.486	0.368	0.316	0.368	0.316	0.758	0.650	0.758	0.650	1.000	1.000	0.858	0.858
427	0.979	0.685	0.596	0.831	0.707	0.699	0.609	0.849	0.722	0.824	0.843	0.870	0.851
428	0.486	0.378	0.327	0.378	0.327	0.778	0.673	0.778	0.673	1.000	1.000	0.866	0.866
429	0.979	0.685	0.596	0.831	0.707	0.699	0.609	0.849	0.722	0.824	0.843	0.870	0.851
430	0.486	0.378	0.327	0.378	0.327	0.778	0.673	0.778	0.673	1.000	1.000	0.866	0.866
431	1.061	0.737	0.658	0.906	0.793	0.695	0.620	0.854	0.748	0.813	0.830	0.893	0.875
432	0.486	0.407	0.362	0.407	0.362	0.838	0.745	0.838	0.745	1.000	1.000	0.888	0.888
433	0.979	0.685	0.596	0.831	0.707	0.699	0.609	0.849	0.722	0.824	0.843	0.870	0.851
434	0.486	0.378	0.327	0.378	0.327	0.778	0.673	0.778	0.673	1.000	1.000	0.866	0.866
435	0.979	0.685	0.596	0.831	0.707	0.699	0.609	0.849	0.722	0.824	0.843	0.870	0.851
436	0.486	0.378	0.327	0.378	0.327	0.778	0.673	0.778	0.673	1.000	1.000	0.866	0.866
437	0.979	0.685	0.596	0.831	0.707	0.699	0.609	0.849	0.722	0.824	0.843	0.870	0.851
438	0.486	0.378	0.327	0.378	0.327	0.778	0.673	0.778	0.673	1.000	1.000	0.866	0.866
439	1.090	0.756	0.681	0.934	0.826	0.693	0.625	0.856	0.757	0.809	0.825	0.901	0.884
440	0.487	0.418	0.375	0.418	0.375	0.859	0.771	0.859	0.771	1.000	1.000	0.897	0.897
441	0.642	0.520	0.459	0.549	0.482	0.810	0.716	0.855	0.751	0.947	0.953	0.884	0.878
442	0.539	0.416	0.370	0.416	0.370	0.773	0.686	0.773	0.686	1.000	1.000	0.888	0.888
443	0.632	0.507	0.449	0.522	0.461	0.803	0.711	0.825	0.729	0.972	0.975	0.885	0.883
444	0.539	0.416	0.370	0.416	0.370	0.773	0.686	0.773	0.686	1.000	1.000	0.888	0.888
445	0.632	0.507	0.449	0.522	0.461	0.803	0.711	0.825	0.729	0.972	0.975	0.885	0.883
446	0.539	0.416	0.370	0.416	0.370	0.773	0.686	0.773	0.686	1.000	1.000	0.888	0.888
447	0.738	0.600	0.562	0.639	0.595	0.814	0.761	0.866	0.807	0.939	0.943	0.936	0.932
448	0.539	0.450	0.412	0.450	0.412	0.835	0.764	0.835	0.764	1.000	1.000	0.915	0.915
449	0.642	0.520	0.459	0.549	0.482	0.810	0.716	0.855	0.751	0.947	0.953	0.884	0.878
450	0.539	0.416	0.370	0.416	0.370	0.773	0.686	0.773	0.686	1.000	1.000	0.888	0.888
451	0.632	0.507	0.449	0.522	0.461	0.803	0.711	0.825	0.729	0.972	0.975	0.885	0.883
452	0.539	0.416	0.370	0.416	0.370	0.773	0.686	0.773	0.686	1.000	1.000	0.888	0.888
453	0.632	0.507	0.449	0.522	0.461	0.803	0.711	0.825	0.729	0.972	0.975	0.885	0.883
454	0.539	0.416	0.370	0.416	0.370	0.773	0.686	0.773	0.686	1.000	1.000	0.888	0.888
455	0.738	0.600	0.562	0.639	0.595	0.814	0.761	0.866	0.807	0.939	0.943	0.936	0.932
456	0.539	0.450	0.412	0.450	0.412	0.835	0.764	0.835	0.764	1.000	1.000	0.915	0.915
457	0.632	0.437	0.368	0.448	0.377	0.691	0.583	0.709	0.596	0.975	0.977	0.843	0.841
458	0.557	0.414	0.375	0.414	0.375	0.743	0.672	0.743	0.672	1.000	1.000	0.906	0.906
459	0.539	0.433	0.391	0.433	0.391	0.804	0.725	0.804	0.725	1.000	1.000	0.901	0.901
460	0.632	0.437	0.368	0.448	0.377	0.691	0.583	0.709	0.596	0.975	0.977	0.843	0.841
461	0.539	0.433	0.391	0.433	0.391	0.804	0.725	0.804	0.725	1.000	1.000	0.901	0.901
462	0.632	0.437	0.368	0.448	0.377	0.691	0.583	0.709	0.596	0.975	0.977	0.843	0.841
463	0.539	0.433	0.391	0.433	0.391	0.804	0.725	0.804	0.725	1.000	1.000	0.901	0.901
464	0.632	0.507	0.449	0.522	0.461	0.803	0.711	0.825	0.729	0.972	0.975	0.885	0.883
465	0.557	0.449	0.420	0.449	0.420	0.805	0.754	0.805	0.754	1.000	1.000	0.936	0.936
466	0.539	0.472	0.440	0.472	0.440	0.875	0.817	0.875	0.817	1.000	1.000	0.933	0.933
467	0.632	0.478	0.415	0.491	0.425	0.757	0.657	0.778	0.673	0.973	0.976	0.868	0.866
468	0.557	0.435	0.402	0.435	0.402	0.780	0.721	0.780	0.721	1.000	1.000	0.924	0.924
469	0.539	0.457	0.420	0.457	0.420	0.848	0.780	0.848	0.780	1.000	1.000	0.920	0.920
470	0.768	0.634	0.606	0.679	0.646	0.826	0.789	0.884	0.841	0.935	0.938	0.954	0.952
471	0.591	0.490	0.468	0.522	0.497	0.831	0.793	0.884	0.841	0.940	0.942	0.954	0.952
472	0.577	0.476	0.421	0.490	0.433	0.825	0.731	0.849	0.750	0.972	0.974	0.885	0.883
473	0.509	0.421	0.395	0.421	0.395	0.828	0.776	0.828	0.776	1.000	1.000	0.936	0.936
474	0.492	0.443	0.414	0.443	0.414	0.901	0.841	0.901	0.841	1.000	1.000	0.933	0.933
475	0.577	0.476	0.421	0.490	0.433	0.825	0.731	0.849	0.750	0.972	0.974	0.885	0.883
476	0.509	0.421	0.395	0.421	0.395	0.828	0.776	0.828	0.776	1.000	1.000	0.936	0.936
477	0.492	0.443	0.414	0.443	0.414	0.901	0.841	0.901	0.841	1.000	1.000	0.933	0.933
478	0.639	0.491	0.437	0.508	0.451	0.768	0.684	0.795	0.706	0.966	0.969	0.890	0.888
479	0.509	0.421	0.395	0.421	0.395	0.828	0.776	0.828	0.776	1.000	1.000	0.936	0.936
480	0.492	0.443	0.414	0.443	0.414	0.901	0.841	0.901	0.841	1.000	1.000	0.933	0.933

Table D.1c
Splice length ratios for beams in lateral load resisting frame system (continued)

Spl. No.	ACI '95 Orig.	Eq. 3.13^{+} Orig. Conv.*	Eq. 3.13^{+} Orig. New**	Eq. 3.14^{++} Orig. Conv.*	Eq. 3.14^{++} Orig. New**	Eq. 3.13^{-} ACI '95 Conv.*	Eq. 3.13^{+} ACI '95 New**	Eq. 3.14^{++} ACI '95 Conv.*	Eq. 3.14^{++} ACI '95 New**	Eq. 3.13^{+} Eq. 3.14^{--} Conv.*	Eq. 3.13^{+} Eq. 3.14^{++} New**	New** Conv.* Eq. 3.13^{+}	New** Conv.* Eq. 3.14^{++}
481	0.639	0.491	0.457	0.508	0.451	0.768	0.684	0.795	0.706	0.966	0.969	0.890	0.888
482	0.509	0.421	0.395	0.421	0.395	0.828	0.776	0.828	0.776	1.000	1.000	0.936	0.936
483	0.492	0.443	0.414	0.443	0.414	0.901	0.841	0.901	0.841	1.000	1.000	0.933	0.933
484	0.915	0.656	0.575	0.801	0.687	0.717	0.628	0.875	0.750	0.819	0.837	0.877	0.858
485	0.492	0.377	0.331	0.377	0.331	0.767	0.672	0.767	0.672	1.000	1.000	0.877	0.877
486	0.934	0.668	0.590	0.819	0.707	0.715	0.631	0.876	0.757	0.816	0.834	0.882	0.864
487	0.492	0.385	0.339	0.385	0.339	0.782	0.690	0.782	0.690	1.000	1.000	0.882	0.882
488	0.934	0.668	0.590	0.819	0.707	0.715	0.631	0.876	0.757	0.816	0.834	0.882	0.864
489	0.492	0.385	0.339	0.385	0.339	0.782	0.690	0.782	0.690	1.000	1.000	0.882	0.882
490	0.934	0.668	0.590	0.819	0.707	0.715	0.631	0.876	0.757	0.816	0.834	0.882	0.864
491	0.492	0.385	0.339	0.385	0.339	0.782	0.690	0.782	0.690	1.000	1.000	0.882	0.882
492	0.915	0.656	0.575	0.801	0.687	0.717	0.628	0.875	0.750	0.819	0.837	0.877	0.858
493	0.492	0.377	0.331	0.377	0.331	0.767	0.672	0.767	0.672	1.000	1.000	0.877	0.877
494	0.934	0.668	0.590	0.819	0.707	0.715	0.631	0.876	0.757	0.816	0.834	0.882	0.864
495	0.492	0.385	0.339	0.385	0.339	0.782	0.690	0.782	0.690	1.000	1.000	0.882	0.882
496	0.934	0.668	0.590	0.819	0.707	0.715	0.631	0.876	0.757	0.816	0.834	0.882	0.864
497	0.492	0.385	0.339	0.385	0.339	0.782	0.690	0.782	0.690	1.000	1.000	0.882	0.882
498	0.934	0.668	0.590	0.819	0.707	0.715	0.631	0.876	0.757	0.816	0.834	0.882	0.864
499	0.492	0.385	0.339	0.385	0.339	0.782	0.690	0.782	0.690	1.000	1.000	0.882	0.882
500	0.586	0.488	0.431	0.515	0.452	0.833	0.737	0.880	0.773	0.947	0.953	0.884	0.878
501	0.444	0.377	0.333	0.377	0.333	0.849	0.750	0.849	0.750	1.000	1.000	0.883	0.883
502	0.951	0.680	0.603	0.835	0.726	0.714	0.634	0.878	0.763	0.814	0.831	0.888	0.869
503	0.444	0.377	0.333	0.377	0.333	0.849	0.750	0.849	0.750	1.000	1.000	0.883	0.883
504	0.951	0.680	0.603	0.835	0.726	0.714	0.634	0.878	0.763	0.814	0.831	0.888	0.869
505	0.444	0.377	0.333	0.377	0.333	0.849	0.750	0.849	0.750	1.000	1.000	0.883	0.883
506	0.595	0.496	0.441	0.524	0.463	0.834	0.741	0.881	0.778	0.947	0.952	0.889	0.883
507	0.444	0.383	0.340	0.383	0.340	0.863	0.766	0.863	0.766	1.000	1.000	0.888	0.888
508	0.586	0.488	0.431	0.515	0.452	0.833	0.737	0.880	0.773	0.947	0.953	0.884	0.878
509	0.444	0.377	0.333	0.377	0.333	0.849	0.750	0.849	0.750	1.000	1.000	0.883	0.883
510	0.951	0.680	0.603	0.835	0.726	0.714	0.634	0.878	0.763	0.814	0.831	0.888	0.869
511	0.444	0.377	0.333	0.377	0.333	0.849	0.750	0.849	0.750	1.000	1.000	0.883	0.883
512	0.951	0.680	0.603	0.835	0.726	0.714	0.634	0.878	0.763	0.814	0.831	0.888	0.869
513	0.444	0.377	0.333	0.377	0.333	0.849	0.750	0.849	0.750	1.000	1.000	0.883	0.883
514	0.595	0.496	0.441	0.524	0.463	0.834	0.741	0.881	0.778	0.947	0.952	0.889	0.883
515	0.444	0.383	0.340	0.383	0.340	0.863	0.766	0.863	0.766	1.000	1.000	0.888	0.888
516	0.586	0.488	0.431	0.515	0.452	0.833	0.737	0.880	0.773	0.947	0.953	0.884	0.878
517	0.444	0.377	0.333	0.377	0.333	0.849	0.750	0.849	0.750	1.000	1.000	0.883	0.883
518	0.951	0.680	0.603	0.835	0.726	0.714	0.634	0.878	0.763	0.814	0.831	0.888	0.869
519	0.444	0.377	0.333	0.377	0.333	0.849	0.750	0.849	0.750	1.000	1.000	0.883	0.883
520	0.586	0.488	0.431	0.515	0.452	0.833	0.737	0.880	0.773	0.947	0.953	0.884	0.878
521	0.444	0.377	0.333	0.377	0.333	0.849	0.750	0.849	0.750	1.000	1.000	0.883	0.883
522	0.577	0.393	0.327	0.403	0.335	0.681	0.568	0.699	0.581	0.975	0.978	0.833	0.831
523	0.444	0.383	0.340	0.383	0.340	0.863	0.766	0.863	0.766	1.000	1.000	0.888	0.888
524	0.843	0.608	0.520	0.733	0.612	0.721	0.617	0.869	0.726	0.830	0.850	0.855	0.835
525	0.492	0.350	0.299	0.357	0.305	0.711	0.608	0.726	0.619	0.979	0.982	0.855	0.852
526	0.843	0.608	0.520	0.733	0.612	0.721	0.617	0.869	0.726	0.830	0.850	0.855	0.835
527	0.648	0.468	0.400	0.564	0.471	0.721	0.617	0.869	0.726	0.830	0.850	0.855	0.835
528	0.843	0.608	0.520	0.733	0.612	0.721	0.617	0.869	0.726	0.830	0.850	0.855	0.835
529	0.648	0.468	0.400	0.564	0.471	0.721	0.617	0.869	0.726	0.830	0.850	0.855	0.835
530	0.843	0.608	0.520	0.733	0.612	0.721	0.617	0.869	0.726	0.830	0.850	0.855	0.835
531	0.492	0.350	0.299	0.357	0.305	0.711	0.608	0.726	0.619	0.979	0.982	0.855	0.852
532	0.923	0.649	0.554	0.780	0.651	0.703	0.601	0.845	0.706	0.832	0.851	0.855	0.835
533	0.539	0.372	0.318	0.380	0.324	0.691	0.591	0.706	0.602	0.979	0.982	0.855	0.852
534	0.923	0.649	0.554	0.780	0.651	0.703	0.601	0.845	0.706	0.832	0.851	0.855	0.835
535	0.710	0.499	0.427	0.600	0.501	0.703	0.601	0.845	0.706	0.832	0.851	0.855	0.835
536	0.923	0.649	0.554	0.780	0.651	0.703	0.601	0.845	0.706	0.832	0.851	0.855	0.835
537	0.710	0.499	0.427	0.600	0.501	0.703	0.601	0.845	0.706	0.832	0.851	0.855	0.835
538	0.923	0.649	0.554	0.780	0.651	0.703	0.601	0.845	0.706	0.832	0.851	0.855	0.835
539	0.539	0.372	0.318	0.380	0.324	0.691	0.591	0.706	0.602	0.979	0.982	0.855	0.852
540	0.923	0.649	0.554	0.780	0.651	0.703	0.601	0.845	0.706	0.832	0.851	0.855	0.835

Table D.1c
Splice length ratios for beams in lateral load resisting frame system (continued)

Spl. No.	ACI '95 Orig.	Eq. 3.13^{-} Orig. Conv.*	Eq. 3.13^{-} Orig. New**	Eq. 3.14^{--} Orig. Conv.*	Eq. 3.14^{++} Orig. New**	Eq. 3.13^{+} ACI '95 Conv.*	Eq. 3.13^{+} ACI '95 New**	Eq. 3.14^{--} ACI '95 Conv.*	Eq. 3.14^{++} ACI '95 New**	Eq. 3.13^{-} Eq. 3.14^{--} Conv.*	Eq. 3.13^{+} Eq. 3.14^{++} New**	New** Conv.* Eq. 3.13^{+}	New** Conv.* Eq. 3.14^{++}
541	0.539	0.372	0.318	0.372	0.318	0.691	0.591	0.691	0.591	1.000	1.000	0.855	0.855
542	0.923	0.649	0.554	0.780	0.651	0.703	0.601	0.845	0.706	0.832	0.851	0.855	0.835
543	0.703	0.514	0.443	0.612	0.516	0.731	0.630	0.870	0.733	0.841	0.859	0.862	0.843
544	0.923	0.649	0.554	0.780	0.651	0.703	0.601	0.845	0.706	0.832	0.851	0.855	0.835
545	0.710	0.499	0.427	0.600	0.501	0.703	0.601	0.845	0.706	0.832	0.851	0.855	0.835
546	0.923	0.649	0.554	0.780	0.651	0.703	0.601	0.845	0.706	0.832	0.851	0.855	0.835
547	0.539	0.372	0.318	0.380	0.324	0.691	0.591	0.706	0.602	0.979	0.982	0.855	0.852
548	0.953	0.668	0.576	0.807	0.680	0.701	0.605	0.847	0.714	0.828	0.847	0.863	0.843
549	0.539	0.383	0.331	0.383	0.331	0.712	0.614	0.712	0.614	1.000	1.000	0.863	0.863
550	0.979	0.685	0.596	0.831	0.707	0.699	0.609	0.849	0.722	0.824	0.843	0.870	0.851
551	0.486	0.378	0.327	0.378	0.327	0.778	0.673	0.778	0.673	1.000	1.000	0.866	0.866
552	0.979	0.685	0.596	0.831	0.707	0.699	0.609	0.849	0.722	0.824	0.843	0.870	0.851
553	0.486	0.378	0.327	0.378	0.327	0.778	0.673	0.778	0.673	1.000	1.000	0.866	0.866
554	1.002	0.700	0.613	0.852	0.731	0.698	0.612	0.850	0.729	0.821	0.839	0.877	0.858
555	0.486	0.387	0.337	0.387	0.337	0.795	0.694	0.795	0.694	1.000	1.000	0.872	0.872
556	1.002	0.700	0.613	0.852	0.731	0.698	0.612	0.850	0.729	0.821	0.839	0.877	0.858
557	0.557	0.385	0.339	0.385	0.339	0.691	0.609	0.691	0.609	1.000	1.000	0.882	0.882
558	1.023	0.713	0.629	0.872	0.753	0.697	0.615	0.852	0.736	0.818	0.836	0.882	0.864
559	0.486	0.394	0.346	0.394	0.346	0.811	0.712	0.811	0.712	1.000	1.000	0.878	0.878
560	1.023	0.713	0.629	0.872	0.753	0.697	0.615	0.852	0.736	0.818	0.836	0.882	0.864
561	0.486	0.394	0.346	0.394	0.346	0.811	0.712	0.811	0.712	1.000	1.000	0.878	0.878
562	0.642	0.520	0.459	0.549	0.482	0.810	0.716	0.855	0.751	0.947	0.953	0.884	0.878
563	0.557	0.398	0.355	0.398	0.355	0.715	0.638	0.715	0.638	1.000	1.000	0.893	0.893
564	0.700	0.469	0.402	0.484	0.414	0.670	0.574	0.691	0.591	0.969	0.972	0.857	0.855
565	0.557	0.422	0.385	0.422	0.385	0.757	0.691	0.757	0.691	1.000	1.000	0.913	0.913
566	0.539	0.442	0.402	0.442	0.402	0.821	0.746	0.821	0.746	1.000	1.000	0.908	0.908
567	0.632	0.437	0.368	0.448	0.377	0.691	0.583	0.709	0.596	0.975	0.977	0.843	0.841
568	0.539	0.433	0.391	0.433	0.391	0.804	0.725	0.804	0.725	1.000	1.000	0.901	0.901
569	0.632	0.437	0.368	0.448	0.377	0.691	0.583	0.709	0.596	0.975	0.977	0.843	0.841
570	0.539	0.433	0.391	0.433	0.391	0.804	0.725	0.804	0.725	1.000	1.000	0.901	0.901
571	0.700	0.469	0.402	0.484	0.414	0.670	0.574	0.691	0.591	0.969	0.972	0.857	0.855
572	0.557	0.422	0.385	0.422	0.385	0.757	0.691	0.757	0.691	1.000	1.000	0.913	0.913
573	0.539	0.442	0.402	0.442	0.402	0.821	0.746	0.821	0.746	1.000	1.000	0.908	0.908
574	0.724	0.498	0.446	0.518	0.462	0.688	0.615	0.715	0.638	0.962	0.965	0.895	0.893
575	0.557	0.449	0.420	0.449	0.420	0.805	0.754	0.805	0.754	1.000	1.000	0.936	0.936
576	0.539	0.472	0.440	0.472	0.440	0.875	0.817	0.875	0.817	1.000	1.000	0.933	0.933
577	0.632	0.507	0.449	0.522	0.461	0.803	0.711	0.825	0.729	0.972	0.975	0.885	0.883
578	0.557	0.449	0.420	0.449	0.420	0.805	0.754	0.805	0.754	1.000	1.000	0.936	0.936
579	0.539	0.472	0.440	0.472	0.440	0.875	0.817	0.875	0.817	1.000	1.000	0.933	0.933
580	0.724	0.498	0.446	0.518	0.462	0.688	0.615	0.715	0.638	0.962	0.965	0.895	0.893
581	0.557	0.449	0.420	0.449	0.420	0.805	0.754	0.805	0.754	1.000	1.000	0.936	0.936
582	0.539	0.472	0.440	0.472	0.440	0.875	0.817	0.875	0.817	1.000	1.000	0.933	0.933
583	0.661	0.515	0.475	0.550	0.505	0.779	0.719	0.832	0.764	0.937	0.940	0.922	0.919
584	0.509	0.461	0.440	0.461	0.440	0.906	0.864	0.906	0.864	1.000	1.000	0.954	0.954
585	0.538	0.485	0.462	0.485	0.462	0.902	0.858	0.902	0.858	1.000	1.000	0.952	0.952
586	0.661	0.515	0.475	0.550	0.505	0.779	0.719	0.832	0.764	0.937	0.940	0.922	0.919
587	0.509	0.461	0.440	0.461	0.440	0.906	0.864	0.906	0.864	1.000	1.000	0.954	0.954
588	0.538	0.485	0.462	0.485	0.462	0.902	0.858	0.902	0.858	1.000	1.000	0.952	0.952
589	0.661	0.515	0.475	0.550	0.505	0.779	0.719	0.832	0.764	0.937	0.940	0.922	0.919
590	0.509	0.461	0.440	0.461	0.440	0.906	0.864	0.906	0.864	1.000	1.000	0.954	0.954
591	0.538	0.485	0.462	0.485	0.462	0.902	0.858	0.902	0.858	1.000	1.000	0.952	0.952
592	0.586	0.488	0.431	0.515	0.452	0.833	0.737	0.880	0.773	0.947	0.953	0.884	0.878
593	0.444	0.377	0.333	0.377	0.333	0.849	0.750	0.849	0.750	1.000	1.000	0.883	0.883
594	0.577	0.476	0.421	0.490	0.433	0.825	0.731	0.849	0.750	0.972	0.974	0.885	0.883
595	0.444	0.377	0.333	0.377	0.333	0.849	0.750	0.849	0.750	1.000	1.000	0.883	0.883
596	0.586	0.488	0.431	0.515	0.452	0.833	0.737	0.880	0.773	0.947	0.953	0.884	0.878
597	0.444	0.377	0.333	0.377	0.333	0.849	0.750	0.849	0.750	1.000	1.000	0.883	0.883
598	0.968	0.691	0.617	0.851	0.745	0.713	0.637	0.879	0.769	0.811	0.828	0.893	0.875
599	0.444	0.383	0.340	0.383	0.340	0.863	0.766	0.863	0.766	1.000	1.000	0.888	0.888
600	0.968	0.691	0.617	0.851	0.745	0.713	0.637	0.879	0.769	0.811	0.828	0.893	0.875

Table D.1c
Splice length ratios for beams in lateral load resisting frame system (continued)

Spl. No.	ACI '95 Orig.	Eq. 3.13^{+} Orig. Conv.*	Eq. 3.13^{+} Orig. New**	Eq. 3.14^{++} Orig. Conv.*	Eq. 3.14^{++} Orig. New**	Eq. 3.13^{+} ACI '95 Conv.*	Eq. 3.13^{+} ACI '95 New**	Eq. 3.14^{++} ACI '95 Conv.*	Eq. 3.14^{++} ACI '95 New**	Eq. 3.13^{+} Eq. 3.14^{++} Conv.*	Eq. 3.13^{+} Eq. 3.14^{++} New**	New** Conv.* Eq. 3.13^{+}	New** Conv.* Eq. 3.14^{++}
601	0.444	0.383	0.340	0.383	0.340	0.863	0.766	0.863	0.766	1.000	1.000	0.888	0.888
602	0.968	0.691	0.617	0.851	0.745	0.713	0.637	0.879	0.769	0.811	0.828	0.893	0.875
603	0.444	0.383	0.340	0.383	0.340	0.863	0.766	0.863	0.766	1.000	1.000	0.888	0.888
604	0.595	0.496	0.441	0.524	0.463	0.834	0.741	0.881	0.778	0.947	0.952	0.889	0.883
605	0.509	0.379	0.340	0.379	0.340	0.746	0.669	0.746	0.669	1.000	1.000	0.897	0.897
606	0.577	0.410	0.346	0.421	0.354	0.711	0.599	0.730	0.614	0.974	0.977	0.843	0.841
607	0.492	0.407	0.367	0.407	0.367	0.828	0.746	0.828	0.746	1.000	1.000	0.901	0.901
608	0.595	0.496	0.441	0.524	0.463	0.834	0.741	0.881	0.778	0.947	0.952	0.889	0.883
609	0.509	0.379	0.340	0.379	0.340	0.746	0.669	0.746	0.669	1.000	1.000	0.897	0.897
610	0.595	0.496	0.441	0.524	0.463	0.834	0.741	0.881	0.778	0.947	0.952	0.889	0.883
611	0.509	0.379	0.340	0.379	0.340	0.746	0.669	0.746	0.669	1.000	1.000	0.897	0.897
612	0.577	0.410	0.346	0.421	0.354	0.711	0.599	0.730	0.614	0.974	0.977	0.843	0.841
613	0.492	0.407	0.367	0.407	0.367	0.828	0.746	0.828	0.746	1.000	1.000	0.901	0.901
614	0.595	0.496	0.441	0.524	0.463	0.834	0.741	0.881	0.778	0.947	0.952	0.889	0.883
615	0.509	0.379	0.340	0.379	0.340	0.746	0.669	0.746	0.669	1.000	1.000	0.897	0.897
616	0.639	0.483	0.428	0.500	0.441	0.756	0.669	0.782	0.690	0.967	0.969	0.885	0.882
617	0.509	0.400	0.366	0.400	0.366	0.786	0.719	0.786	0.719	1.000	1.000	0.916	0.916
618	0.577	0.468	0.412	0.481	0.423	0.811	0.714	0.835	0.733	0.972	0.974	0.880	0.878
619	0.509	0.400	0.366	0.400	0.366	0.786	0.719	0.786	0.719	1.000	1.000	0.916	0.916
620	0.639	0.483	0.428	0.500	0.441	0.756	0.669	0.782	0.690	0.967	0.969	0.885	0.882
621	0.509	0.400	0.366	0.400	0.366	0.786	0.719	0.786	0.719	1.000	1.000	0.916	0.916
622	0.639	0.464	0.405	0.480	0.418	0.726	0.634	0.751	0.653	0.968	0.970	0.873	0.870
623	0.509	0.408	0.377	0.408	0.377	0.803	0.742	0.803	0.742	1.000	1.000	0.924	0.924
624	0.492	0.429	0.395	0.429	0.395	0.872	0.803	0.872	0.803	1.000	1.000	0.920	0.920
625	0.577	0.449	0.390	0.461	0.399	0.778	0.675	0.800	0.692	0.973	0.975	0.868	0.866
626	0.509	0.408	0.377	0.408	0.377	0.803	0.742	0.803	0.742	1.000	1.000	0.924	0.924
627	0.492	0.429	0.395	0.429	0.395	0.872	0.803	0.872	0.803	1.000	1.000	0.920	0.920
628	0.577	0.449	0.390	0.461	0.399	0.778	0.675	0.800	0.692	0.973	0.975	0.868	0.866
629	0.509	0.408	0.377	0.408	0.377	0.803	0.742	0.803	0.742	1.000	1.000	0.924	0.924
630	0.492	0.429	0.395	0.429	0.395	0.872	0.803	0.872	0.803	1.000	1.000	0.920	0.920
631	0.639	0.464	0.405	0.480	0.418	0.726	0.634	0.751	0.653	0.968	0.970	0.873	0.870
632	0.509	0.408	0.377	0.408	0.377	0.803	0.742	0.803	0.742	1.000	1.000	0.924	0.924
633	0.492	0.429	0.395	0.429	0.395	0.872	0.803	0.872	0.803	1.000	1.000	0.920	0.920
634	0.915	0.656	0.575	0.801	0.687	0.717	0.628	0.875	0.750	0.819	0.837	0.877	0.858
635	0.492	0.377	0.331	0.377	0.331	0.767	0.672	0.767	0.672	1.000	1.000	0.877	0.877
636	0.915	0.656	0.575	0.801	0.687	0.717	0.628	0.875	0.750	0.819	0.837	0.877	0.858
637	0.492	0.377	0.331	0.377	0.331	0.767	0.672	0.767	0.672	1.000	1.000	0.877	0.877
638	0.915	0.656	0.575	0.801	0.687	0.717	0.628	0.875	0.750	0.819	0.837	0.877	0.858
639	0.492	0.377	0.331	0.377	0.331	0.767	0.672	0.767	0.672	1.000	1.000	0.877	0.877
640	0.915	0.656	0.575	0.801	0.687	0.717	0.628	0.875	0.750	0.819	0.837	0.877	0.858
641	0.492	0.377	0.331	0.377	0.331	0.767	0.672	0.767	0.672	1.000	1.000	0.877	0.877
642	0.915	0.656	0.575	0.801	0.687	0.717	0.628	0.875	0.750	0.819	0.837	0.877	0.858
643	0.492	0.377	0.331	0.377	0.331	0.767	0.672	0.767	0.672	1.000	1.000	0.877	0.877
644	0.915	0.656	0.575	0.801	0.687	0.717	0.628	0.875	0.750	0.819	0.837	0.877	0.858
645	0.492	0.377	0.331	0.377	0.331	0.767	0.672	0.767	0.672	1.000	1.000	0.877	0.877
646	0.915	0.656	0.575	0.801	0.687	0.717	0.628	0.875	0.750	0.819	0.837	0.877	0.858
647	0.492	0.377	0.331	0.377	0.331	0.767	0.672	0.767	0.672	1.000	1.000	0.877	0.877
648	0.915	0.656	0.575	0.801	0.687	0.717	0.628	0.875	0.750	0.819	0.837	0.877	0.858
649	0.492	0.377	0.331	0.377	0.331	0.767	0.672	0.767	0.672	1.000	1.000	0.877	0.877
650	0.577	0.410	0.346	0.421	0.354	0.711	0.599	0.730	0.614	0.974	0.977	0.843	0.841
651	0.444	0.393	0.353	0.393	0.353	0.884	0.793	0.884	0.793	1.000	1.000	0.897	0.897
652	0.577	0.410	0.346	0.421	0.354	0.711	0.599	0.730	0.614	0.974	0.977	0.843	0.841
653	0.444	0.393	0.353	0.393	0.353	0.884	0.793	0.884	0.793	1.000	1.000	0.897	0.897
654	0.577	0.410	0.346	0.421	0.354	0.711	0.599	0.730	0.614	0.974	0.977	0.843	0.841
655	0.444	0.393	0.353	0.393	0.353	0.884	0.793	0.884	0.793	1.000	1.000	0.897	0.897
656	0.577	0.410	0.346	0.421	0.354	0.711	0.599	0.730	0.614	0.974	0.977	0.843	0.841
657	0.444	0.393	0.353	0.393	0.353	0.884	0.793	0.884	0.793	1.000	1.000	0.897	0.897
658	0.577	0.410	0.346	0.421	0.354	0.711	0.599	0.730	0.614	0.974	0.977	0.843	0.841
659	0.444	0.393	0.353	0.393	0.353	0.884	0.793	0.884	0.793	1.000	1.000	0.897	0.897
660	0.577	0.410	0.346	0.421	0.354	0.711	0.599	0.730	0.614	0.974	0.977	0.843	0.841

Table D.1c
Splice length ratios for beams in lateral load resisting frame system (continued)

Spl. No.	ACI '95 Orig.	Eq. 3.13* Orig. Conv.*	Eq. 3.13* Orig. New**	Eq. 3.14** Orig. Conv.*	Eq. 3.14** Orig. New**	Eq. 3.13* ACI '95 Conv.*	Eq. 3.13* ACI '95 New**	Eq. 3.14** ACI '95 Conv.*	Eq. 3.14** ACI '95 New**	Eq. 3.13* Eq. 3.14** Conv.*	Eq. 3.13* Eq. 3.14** New**	New** Conv.* Eq. 3.13*	New** Conv.* Eq. 3.14**
661	0.444	0.395	0.353	0.395	0.353	0.884	0.793	0.884	0.793	1.000	1.000	0.897	0.897
662	0.577	0.410	0.346	0.421	0.354	0.711	0.599	0.730	0.614	0.974	0.977	0.843	0.841
663	0.444	0.393	0.353	0.393	0.353	0.884	0.793	0.884	0.793	1.000	1.000	0.897	0.897
664	0.577	0.410	0.346	0.421	0.354	0.711	0.599	0.730	0.614	0.974	0.977	0.843	0.841
665	0.444	0.393	0.353	0.393	0.353	0.884	0.793	0.884	0.793	1.000	1.000	0.897	0.897
666	0.577	0.468	0.412	0.481	0.423	0.811	0.714	0.835	0.733	0.972	0.974	0.880	0.878
667	0.478	0.425	0.394	0.425	0.394	0.890	0.824	0.890	0.824	1.000	1.000	0.926	0.926
668	0.577	0.468	0.412	0.481	0.423	0.811	0.714	0.835	0.733	0.972	0.974	0.880	0.878
669	0.478	0.425	0.394	0.425	0.394	0.890	0.824	0.890	0.824	1.000	1.000	0.926	0.926
670	0.577	0.468	0.412	0.481	0.423	0.811	0.714	0.835	0.733	0.972	0.974	0.880	0.878
671	0.478	0.425	0.394	0.425	0.394	0.890	0.824	0.890	0.824	1.000	1.000	0.926	0.926
672	0.577	0.468	0.412	0.481	0.423	0.811	0.714	0.835	0.733	0.972	0.974	0.880	0.878
673	0.478	0.425	0.394	0.425	0.394	0.890	0.824	0.890	0.824	1.000	1.000	0.926	0.926
674	0.821	0.641	0.581	0.717	0.644	0.781	0.708	0.873	0.784	0.894	0.903	0.907	0.897
675	0.557	0.438	0.402	0.479	0.436	0.787	0.721	0.859	0.782	0.916	0.923	0.917	0.910
676	0.846	0.644	0.584	0.727	0.652	0.761	0.690	0.859	0.771	0.886	0.895	0.907	0.897
677	0.557	0.445	0.410	0.486	0.445	0.798	0.736	0.872	0.799	0.915	0.921	0.922	0.916
678	0.846	0.644	0.584	0.727	0.652	0.761	0.690	0.859	0.771	0.886	0.895	0.907	0.897
679	0.557	0.445	0.410	0.486	0.445	0.798	0.736	0.872	0.799	0.915	0.921	0.922	0.916
680	0.846	0.644	0.584	0.727	0.652	0.761	0.690	0.859	0.771	0.886	0.895	0.907	0.897
681	0.557	0.445	0.410	0.486	0.445	0.798	0.736	0.872	0.799	0.915	0.921	0.922	0.916
682	0.836	0.652	0.595	0.730	0.660	0.780	0.712	0.874	0.790	0.893	0.901	0.913	0.904
683	0.557	0.445	0.410	0.486	0.445	0.798	0.736	0.872	0.799	0.915	0.921	0.922	0.916
684	0.795	0.627	0.569	0.694	0.625	0.789	0.717	0.874	0.787	0.903	0.911	0.909	0.900
685	0.557	0.438	0.402	0.479	0.436	0.787	0.721	0.859	0.782	0.916	0.923	0.917	0.910
686	0.808	0.637	0.582	0.706	0.640	0.788	0.720	0.874	0.792	0.901	0.909	0.915	0.907
687	0.557	0.445	0.410	0.486	0.445	0.798	0.736	0.872	0.799	0.915	0.921	0.922	0.916
688	0.836	0.652	0.595	0.730	0.660	0.780	0.712	0.874	0.790	0.893	0.901	0.913	0.904
689	0.557	0.445	0.410	0.486	0.445	0.798	0.736	0.872	0.799	0.915	0.921	0.922	0.916
690	0.846	0.644	0.584	0.727	0.652	0.761	0.690	0.859	0.771	0.886	0.895	0.907	0.897
691	0.557	0.445	0.410	0.486	0.445	0.798	0.736	0.872	0.799	0.915	0.921	0.922	0.916
692	0.836	0.652	0.595	0.730	0.660	0.780	0.712	0.874	0.790	0.893	0.901	0.913	0.904
693	0.557	0.445	0.410	0.486	0.445	0.798	0.736	0.872	0.799	0.915	0.921	0.922	0.916
694	0.795	0.627	0.569	0.694	0.625	0.789	0.717	0.874	0.787	0.903	0.911	0.909	0.900
695	0.557	0.438	0.402	0.479	0.436	0.787	0.721	0.859	0.782	0.916	0.923	0.917	0.910
696	0.795	0.627	0.569	0.694	0.625	0.789	0.717	0.874	0.787	0.903	0.911	0.909	0.900
697	0.557	0.438	0.402	0.479	0.436	0.787	0.721	0.859	0.782	0.916	0.923	0.917	0.910
698	0.821	0.641	0.581	0.717	0.644	0.781	0.708	0.873	0.784	0.894	0.903	0.907	0.897
699	0.557	0.438	0.402	0.479	0.436	0.787	0.721	0.859	0.782	0.916	0.923	0.917	0.910
700	0.846	0.644	0.584	0.727	0.652	0.761	0.690	0.859	0.771	0.886	0.895	0.907	0.897
701	0.557	0.445	0.410	0.486	0.445	0.798	0.736	0.872	0.799	0.915	0.921	0.922	0.916
702	0.846	0.644	0.584	0.727	0.652	0.761	0.690	0.859	0.771	0.886	0.895	0.907	0.897
703	0.557	0.445	0.410	0.486	0.445	0.798	0.736	0.872	0.799	0.915	0.921	0.922	0.916
704	0.756	0.626	0.594	0.669	0.632	0.828	0.785	0.885	0.836	0.936	0.939	0.949	0.945
705	0.582	0.484	0.459	0.515	0.486	0.832	0.789	0.885	0.836	0.940	0.944	0.948	0.945
706	0.661	0.441	0.387	0.460	0.403	0.667	0.586	0.696	0.609	0.958	0.961	0.878	0.875
707	0.639	0.460	0.402	0.480	0.418	0.720	0.628	0.751	0.653	0.959	0.962	0.873	0.870
708	0.509	0.408	0.377	0.408	0.377	0.803	0.742	0.803	0.742	1.000	1.000	0.924	0.924
709	0.492	0.429	0.395	0.429	0.395	0.872	0.803	0.872	0.803	1.000	1.000	0.920	0.920
710	0.661	0.441	0.387	0.460	0.403	0.667	0.586	0.696	0.609	0.958	0.961	0.878	0.875
711	0.639	0.460	0.402	0.480	0.418	0.720	0.628	0.751	0.653	0.959	0.962	0.873	0.870
712	0.509	0.408	0.377	0.408	0.377	0.803	0.742	0.803	0.742	1.000	1.000	0.924	0.924
713	0.492	0.429	0.395	0.429	0.395	0.872	0.803	0.872	0.803	1.000	1.000	0.920	0.920
714	0.661	0.441	0.387	0.460	0.403	0.667	0.586	0.696	0.609	0.958	0.961	0.878	0.875
715	0.639	0.460	0.402	0.480	0.418	0.720	0.628	0.751	0.653	0.959	0.962	0.873	0.870
716	0.509	0.408	0.377	0.408	0.377	0.803	0.742	0.803	0.742	1.000	1.000	0.924	0.924
717	0.492	0.429	0.395	0.429	0.395	0.872	0.803	0.872	0.803	1.000	1.000	0.920	0.920
718	0.661	0.441	0.387	0.460	0.403	0.667	0.586	0.696	0.609	0.958	0.961	0.878	0.875
719	0.639	0.460	0.402	0.480	0.418	0.720	0.628	0.751	0.653	0.959	0.962	0.873	0.870
720	0.509	0.408	0.377	0.408	0.377	0.803	0.742	0.803	0.742	1.000	1.000	0.924	0.924

Table D.1c
Splice length ratios for beams in lateral load resisting frame system (continued)

Spl. No.	ACI '95 Orig.	Eq. 3.13+ Orig. Conv.*	Eq. 3.13+ Orig. New**	Eq. 3.14++ Orig. Conv.*	Eq. 3.14++ Orig. New**	Eq. 3.13+ ACI '95 Conv.*	Eq. 3.13+ ACI '95 New**	Eq. 3.14++ ACI '95 Conv.*	Eq. 3.14++ ACI '95 New**	Eq. 3.13+ Eq. 3.14++ Conv.*	Eq. 3.13+ Eq. 3.14++ New**	New** Conv.* Eq. 3.13+	New** Conv.* Eq. 3.14++
721	0.492	0.429	0.395	0.429	0.395	0.872	0.803	0.872	0.803	1.000	1.000	0.920	0.920
722	0.915	0.656	0.575	0.801	0.687	0.717	0.628	0.875	0.750	0.819	0.837	0.877	0.858
723	0.492	0.377	0.331	0.377	0.331	0.767	0.672	0.767	0.672	1.000	1.000	0.877	0.877
724	0.915	0.656	0.575	0.801	0.687	0.717	0.628	0.875	0.750	0.819	0.837	0.877	0.858
725	0.492	0.377	0.331	0.377	0.331	0.767	0.672	0.767	0.672	1.000	1.000	0.877	0.877
726	0.915	0.656	0.575	0.801	0.687	0.717	0.628	0.875	0.750	0.819	0.837	0.877	0.858
727	0.492	0.377	0.331	0.377	0.331	0.767	0.672	0.767	0.672	1.000	1.000	0.877	0.877
728	0.915	0.656	0.575	0.801	0.687	0.717	0.628	0.875	0.750	0.819	0.837	0.877	0.858
729	0.492	0.377	0.331	0.377	0.331	0.767	0.672	0.767	0.672	1.000	1.000	0.877	0.877
730	0.915	0.656	0.575	0.801	0.687	0.717	0.628	0.875	0.750	0.819	0.837	0.877	0.858
731	0.492	0.377	0.331	0.377	0.331	0.767	0.672	0.767	0.672	1.000	1.000	0.877	0.877
732	0.915	0.656	0.575	0.801	0.687	0.717	0.628	0.875	0.750	0.819	0.837	0.877	0.858
733	0.492	0.377	0.331	0.377	0.331	0.767	0.672	0.767	0.672	1.000	1.000	0.877	0.877
734	0.915	0.656	0.575	0.801	0.687	0.717	0.628	0.875	0.750	0.819	0.837	0.877	0.858
735	0.492	0.377	0.331	0.377	0.331	0.767	0.672	0.767	0.672	1.000	1.000	0.877	0.877
736	0.915	0.656	0.575	0.801	0.687	0.717	0.628	0.875	0.750	0.819	0.837	0.877	0.858
737	0.492	0.377	0.331	0.377	0.331	0.767	0.672	0.767	0.672	1.000	1.000	0.877	0.877
738	0.577	0.410	0.346	0.421	0.354	0.711	0.599	0.730	0.614	0.974	0.977	0.843	0.841
739	0.444	0.393	0.353	0.393	0.353	0.884	0.793	0.884	0.793	1.000	1.000	0.897	0.897
740	0.577	0.410	0.346	0.421	0.354	0.711	0.599	0.730	0.614	0.974	0.977	0.843	0.841
741	0.444	0.393	0.353	0.393	0.353	0.884	0.793	0.884	0.793	1.000	1.000	0.897	0.897
742	0.577	0.410	0.346	0.421	0.354	0.711	0.599	0.730	0.614	0.974	0.977	0.843	0.841
743	0.444	0.393	0.353	0.393	0.353	0.884	0.793	0.884	0.793	1.000	1.000	0.897	0.897
744	0.577	0.410	0.346	0.421	0.354	0.711	0.599	0.730	0.614	0.974	0.977	0.843	0.841
745	0.444	0.393	0.353	0.393	0.353	0.884	0.793	0.884	0.793	1.000	1.000	0.897	0.897
746	0.577	0.410	0.346	0.421	0.354	0.711	0.599	0.730	0.614	0.974	0.977	0.843	0.841
747	0.444	0.393	0.353	0.393	0.353	0.884	0.793	0.884	0.793	1.000	1.000	0.897	0.897
748	0.577	0.410	0.346	0.421	0.354	0.711	0.599	0.730	0.614	0.974	0.977	0.843	0.841
749	0.444	0.393	0.353	0.393	0.353	0.884	0.793	0.884	0.793	1.000	1.000	0.897	0.897
750	0.577	0.410	0.346	0.421	0.354	0.711	0.599	0.730	0.614	0.974	0.977	0.843	0.841
751	0.444	0.393	0.353	0.393	0.353	0.884	0.793	0.884	0.793	1.000	1.000	0.897	0.897
752	0.577	0.410	0.346	0.421	0.354	0.711	0.599	0.730	0.614	0.974	0.977	0.843	0.841
753	0.444	0.393	0.353	0.393	0.353	0.884	0.793	0.884	0.793	1.000	1.000	0.897	0.897
754	0.577	0.468	0.412	0.481	0.423	0.811	0.714	0.835	0.733	0.972	0.974	0.880	0.878
755	0.478	0.425	0.394	0.425	0.394	0.890	0.824	0.890	0.824	1.000	1.000	0.926	0.926
756	0.577	0.468	0.412	0.481	0.423	0.811	0.714	0.835	0.733	0.972	0.974	0.880	0.878
757	0.478	0.425	0.394	0.425	0.394	0.890	0.824	0.890	0.824	1.000	1.000	0.926	0.926
758	0.577	0.468	0.412	0.481	0.423	0.811	0.714	0.835	0.733	0.972	0.974	0.880	0.878
759	0.478	0.425	0.394	0.425	0.394	0.890	0.824	0.890	0.824	1.000	1.000	0.926	0.926
760	0.577	0.468	0.412	0.481	0.423	0.811	0.714	0.835	0.733	0.972	0.974	0.880	0.878
761	0.478	0.425	0.394	0.425	0.394	0.890	0.824	0.890	0.824	1.000	1.000	0.926	0.926
762	0.661	0.397	0.354	0.460	0.403	0.600	0.536	0.696	0.609	0.862	0.879	0.892	0.875
763	0.509	0.408	0.377	0.408	0.377	0.803	0.742	0.803	0.742	1.000	1.000	0.924	0.924
764	0.492	0.429	0.395	0.429	0.395	0.872	0.803	0.872	0.803	1.000	1.000	0.920	0.920
765	0.661	0.397	0.354	0.460	0.403	0.600	0.536	0.696	0.609	0.862	0.879	0.892	0.875
766	0.661	0.397	0.354	0.460	0.403	0.600	0.536	0.696	0.609	0.862	0.879	0.892	0.875
767	0.577	0.470	0.410	0.496	0.429	0.816	0.711	0.859	0.744	0.949	0.956	0.872	0.867
768	0.492	0.377	0.331	0.377	0.331	0.767	0.672	0.767	0.672	1.000	1.000	0.877	0.877
769	0.577	0.476	0.421	0.490	0.433	0.825	0.731	0.849	0.750	0.972	0.974	0.885	0.883
770	0.492	0.391	0.347	0.391	0.347	0.795	0.706	0.795	0.706	1.000	1.000	0.888	0.888
771	0.577	0.470	0.410	0.496	0.429	0.816	0.711	0.859	0.744	0.949	0.956	0.872	0.867
772	0.492	0.377	0.331	0.377	0.331	0.767	0.672	0.767	0.672	1.000	1.000	0.877	0.877
773	0.577	0.393	0.327	0.403	0.335	0.681	0.568	0.699	0.581	0.975	0.978	0.833	0.831
774	0.492	0.397	0.354	0.397	0.354	0.807	0.720	0.807	0.720	1.000	1.000	0.893	0.893
775	0.577	0.393	0.327	0.403	0.335	0.681	0.568	0.699	0.581	0.975	0.978	0.833	0.831
776	0.492	0.397	0.354	0.397	0.354	0.807	0.720	0.807	0.720	1.000	1.000	0.893	0.893
777	0.577	0.393	0.327	0.403	0.335	0.681	0.568	0.699	0.581	0.975	0.978	0.833	0.831
778	0.492	0.397	0.354	0.397	0.354	0.807	0.720	0.807	0.720	1.000	1.000	0.893	0.893
779	0.577	0.438	0.377	0.450	0.386	0.759	0.653	0.780	0.669	0.973	0.976	0.860	0.858
780	0.492	0.423	0.387	0.423	0.387	0.859	0.786	0.859	0.786	1.000	1.000	0.915	0.915

Table D.1c
Splice length ratios for beams in lateral load resisting frame system (continued)

Spl. No.	ACI '95 Orig.	Eq. 3.13+ Orig. Conv.*	Eq. 3.13+ Orig. New**	Eq. 3.14++ Orig. Conv.*	Eq. 3.14++ Orig. New**	Eq. 3.13+ ACI '95 Conv.*	Eq. 3.13+ ACI '95 New**	Eq. 3.14++ ACI '95 Conv.*	Eq. 3.14++ ACI '95 New**	Eq. 3.13+ Eq. 3.14++ Conv.*	Eq. 3.13+ Eq. 3.14++ New**	New** Conv.* Eq. 3.13+	New** Conv.* Eq. 3.14++
781	0.577	0.438	0.377	0.450	0.386	0.759	0.653	0.780	0.669	0.973	0.976	0.860	0.858
782	0.492	0.423	0.387	0.423	0.387	0.859	0.786	0.859	0.786	1.000	1.000	0.915	0.915
783	0.577	0.438	0.377	0.450	0.386	0.759	0.653	0.780	0.669	0.973	0.976	0.860	0.858
784	0.492	0.423	0.387	0.423	0.387	0.859	0.786	0.859	0.786	1.000	1.000	0.915	0.915
785	0.639	0.474	0.417	0.491	0.430	0.742	0.652	0.767	0.672	0.967	0.970	0.879	0.877
786	0.509	0.413	0.384	0.413	0.384	0.813	0.755	0.813	0.755	1.000	1.000	0.929	0.929
787	0.577	0.468	0.412	0.481	0.423	0.811	0.714	0.835	0.733	0.972	0.974	0.880	0.878
788	0.492	0.439	0.408	0.439	0.408	0.893	0.830	0.893	0.830	1.000	1.000	0.929	0.929
789	0.639	0.474	0.417	0.491	0.430	0.742	0.652	0.767	0.672	0.967	0.970	0.879	0.877
790	0.509	0.413	0.384	0.413	0.384	0.813	0.755	0.813	0.755	1.000	1.000	0.929	0.929
791	0.661	0.466	0.432	0.550	0.505	0.705	0.654	0.832	0.764	0.848	0.855	0.927	0.919
792	0.509	0.461	0.440	0.461	0.440	0.906	0.864	0.906	0.864	1.000	1.000	0.954	0.954
793	0.538	0.485	0.462	0.485	0.462	0.902	0.858	0.902	0.858	1.000	1.000	0.952	0.952
794	0.661	0.515	0.475	0.550	0.505	0.779	0.719	0.832	0.764	0.937	0.940	0.922	0.919
795	0.509	0.461	0.440	0.461	0.440	0.906	0.864	0.906	0.864	1.000	1.000	0.954	0.954
796	0.538	0.485	0.462	0.485	0.462	0.902	0.858	0.902	0.858	1.000	1.000	0.952	0.952
797	0.661	0.466	0.432	0.550	0.505	0.705	0.654	0.832	0.764	0.848	0.855	0.927	0.919
798	0.509	0.461	0.440	0.461	0.440	0.906	0.864	0.906	0.864	1.000	1.000	0.954	0.954
799	0.538	0.485	0.462	0.485	0.462	0.902	0.858	0.902	0.858	1.000	1.000	0.952	0.952
800	0.983	0.695	0.612	0.837	0.723	0.707	0.622	0.852	0.735	0.830	0.847	0.880	0.863
801	0.557	0.431	0.393	0.470	0.425	0.774	0.705	0.844	0.762	0.917	0.924	0.911	0.904
802	0.983	0.695	0.612	0.837	0.723	0.707	0.622	0.852	0.735	0.830	0.847	0.880	0.863
803	0.985	0.746	0.709	0.872	0.821	0.758	0.720	0.885	0.834	0.856	0.863	0.950	0.942
804	1.037	0.781	0.740	0.908	0.853	0.754	0.714	0.876	0.823	0.860	0.867	0.947	0.940
805	0.618	0.496	0.475	0.546	0.520	0.803	0.769	0.884	0.842	0.909	0.913	0.957	0.952
806	0.654	0.523	0.499	0.573	0.545	0.799	0.762	0.876	0.833	0.912	0.916	0.954	0.950
807	0.985	0.746	0.709	0.872	0.821	0.758	0.720	0.885	0.834	0.856	0.863	0.950	0.942
808	1.037	0.781	0.740	0.908	0.853	0.754	0.714	0.876	0.823	0.860	0.867	0.947	0.940
809	0.557	0.432	0.385	0.477	0.420	0.775	0.690	0.856	0.754	0.905	0.915	0.890	0.881
810	0.814	0.620	0.554	0.697	0.616	0.762	0.681	0.856	0.756	0.890	0.900	0.894	0.883
811	0.557	0.432	0.385	0.477	0.420	0.775	0.690	0.856	0.754	0.905	0.915	0.890	0.881
812	0.758	0.614	0.574	0.672	0.625	0.810	0.757	0.887	0.824	0.913	0.919	0.935	0.930
813	0.804	0.645	0.601	0.704	0.652	0.802	0.747	0.875	0.811	0.916	0.922	0.932	0.926
814	0.583	0.472	0.442	0.517	0.481	0.810	0.757	0.887	0.824	0.913	0.919	0.935	0.930
815	0.619	0.496	0.462	0.541	0.502	0.802	0.747	0.875	0.811	0.916	0.922	0.932	0.926
816	0.563	0.463	0.431	0.500	0.462	0.822	0.764	0.887	0.820	0.926	0.931	0.930	0.925
817	0.831	0.661	0.615	0.727	0.672	0.795	0.739	0.875	0.808	0.908	0.915	0.930	0.924
818	0.563	0.463	0.431	0.500	0.462	0.822	0.764	0.887	0.820	0.926	0.931	0.930	0.925
Max.	1.090	0.781	0.740	0.934	0.853	0.906	0.864	0.906	0.864	1.000	1.000	0.957	0.954
Min.	0.444	0.336	0.285	0.341	0.291	0.600	0.536	0.677	0.564	0.809	0.825	0.833	0.831
Avg.	0.622	0.480	0.427	0.516	0.455	0.782	0.697	0.826	0.731	0.949	0.954	0.890	0.885

$$+ \quad \text{Eq. 3.13} = \frac{l_d}{d_b} = \frac{\dfrac{f_y}{f_c'^{1/4}} - 1900\left(0.1\dfrac{c_M}{c_m} + 0.9\right)}{72\left(\dfrac{c + K_{tr}}{d_b}\right)}$$

$$++ \quad \text{Eq. 3.14} = \frac{l_d}{d_b} = \frac{\dfrac{f_y}{f_c'^{1/4}} - 1900}{72\left(\dfrac{c + K_{tr}}{d_b}\right)}$$

* Conventional reinforcement (avg. $R_r = 0.0727$)

** New reinforcement (avg. $R_r = 0.1275$)

Table D.2a
Splice data for columns in lateral load resisting frame system

Splice	Spliced Bars* A Bars		Spliced Bars* B Bars		Cover			Transverse Reinf.		
					c_b	c_{so}	c_{si}	A_{tr}/n	s	f'_c
No.	# bars	d_b (in.)	# bars	d_b (in.)	(in.)	(in.)	(in.)	($in.^2$)	(in.)	(psi)
1	4	1.41	4	1.41	2.00	2.00	7.59	0.200	6.00	5000
2	12	1.41	12	1.41	2.25	2.25	3.98	0.375	3.75	5000
3	12	1.41	16	1.41	2.13	2.13	3.78	0.305	3.50	5000
4	28	1.41	24	1.41	2.13	2.13	1.77	0.237	4.00	5000
5	24	1.41	16	1.41	2.25	2.25	2.53	0.336	3.75	6000
6	16	1.41	24	1.41	2.25	2.25	2.53	0.336	3.75	6000
7	24	1.41	24	1.41	2.25	2.25	2.02	0.280	3.75	6000
8	24	1.41	20	1.41	2.25	2.25	2.02	0.280	3.75	6000
9	4	1.41	4	1.41	2.00	2.00	7.59	0.200	6.00	5000
10	16	1.41	16	1.41	2.13	2.13	2.84	0.244	3.50	5000
11	16	1.41	20	1.41	2.13	2.13	2.66	0.284	4.00	5000
12	20	1.41	24	1.41	2.13	2.13	2.05	0.237	4.00	5000
13	24	1.41	24	1.41	2.25	2.25	2.02	0.280	3.75	6000
14	20	1.41	24	1.41	2.25	2.25	2.02	0.280	3.75	6000
15	24	1.41	24	1.41	2.25	2.25	2.02	0.280	3.75	6000
16	24	1.41	20	1.41	2.25	2.25	2.02	0.280	3.75	6000
17	4	1.41	4	1.41	2.00	2.00	7.59	0.200	6.00	5000
18	16	1.41	16	1.41	2.13	2.13	2.84	0.244	3.50	5000
19	16	1.41	20	1.41	2.13	2.13	2.66	0.284	4.00	5000
20	20	1.41	24	1.41	2.13	2.13	2.05	0.237	4.00	5000
21	24	1.41	24	1.41	2.25	2.25	2.02	0.280	3.75	6000
22	20	1.41	24	1.41	2.25	2.25	2.02	0.280	3.75	6000
23	24	1.41	24	1.41	2.25	2.25	2.02	0.280	3.75	6000
24	24	1.41	20	1.41	2.25	2.25	2.02	0.280	3.75	6000
25	4	1.41	4	1.41	2.00	2.00	7.59	0.200	6.00	5000
26	16	1.41	16	1.41	2.13	2.13	2.84	0.244	3.50	5000
27	16	1.41	20	1.41	2.13	2.13	2.66	0.284	4.00	5000
28	20	1.41	24	1.41	2.13	2.13	2.05	0.237	4.00	5000
29	24	1.41	24	1.41	2.25	2.25	2.02	0.280	3.75	6000
30	20	1.41	24	1.41	2.25	2.25	2.02	0.280	3.75	6000
31	24	1.41	24	1.41	2.25	2.25	2.02	0.280	3.75	6000
32	24	1.41	20	1.41	2.25	2.25	2.02	0.280	3.75	6000
33	16	1.41	16	1.41	2.13	2.13	2.84	0.244	3.50	5000
34	16	1.41	20	1.41	2.13	2.13	2.66	0.284	4.00	5000
35	20	1.41	24	1.41	2.13	2.13	2.05	0.237	4.00	5000
36	24	1.41	24	1.41	2.25	2.25	2.02	0.280	3.75	6000
37	20	1.41	24	1.41	2.25	2.25	2.02	0.280	3.75	6000
38	24	1.41	24	1.41	2.25	2.25	2.02	0.280	3.75	6000
39	24	1.41	20	1.41	2.25	2.25	2.02	0.280	3.75	6000
40	12	1.41	12	1.41	2.25	2.25	3.98	0.375	3.75	5000

Table D.2a
Splice data for columns in lateral load resisting frame system (continued)

Splice	Spliced Bars* A Bars		Spliced Bars* B Bars		Cover			Transverse Reinf.		
					c_b	c_{so}	c_{si}	A_{tr}/n	s	f'_c
No.	# bars	d_b (in.)	# bars	d_b (in.)	(in.)	(in.)	(in.)	($in.^2$)	(in.)	(psi)
41	12	1.41	16	1.41	2.13	2.13	3.78	0.305	3.50	5000
42	20	1.41	24	1.41	2.13	2.13	2.05	0.237	4.00	5000
43	24	1.41	16	1.41	2.25	2.25	2.53	0.336	3.75	6000
44	16	1.41	24	1.41	2.25	2.25	2.53	0.336	3.75	6000
45	24	1.41	24	1.41	2.25	2.25	2.02	0.280	3.75	6000
46	24	1.41	20	1.41	2.25	2.25	2.02	0.280	3.75	6000
47	12	1.41	16	1.41	2.13	2.13	3.78	0.305	3.50	5000
48	20	1.41	24	1.41	2.13	2.13	2.05	0.237	4.00	5000
49	24	1.41	16	1.41	2.25	2.25	2.53	0.336	3.75	6000
50	16	1.41	24	1.41	2.25	2.25	2.53	0.336	3.75	6000
51	24	1.41	24	1.41	2.25	2.25	2.02	0.280	3.75	6000
52	24	1.41	20	1.41	2.25	2.25	2.02	0.280	3.75	6000
53	16	1.41	20	1.41	2.13	2.13	2.66	0.284	4.00	5000
54	20	1.41	24	1.41	2.13	2.13	2.05	0.237	4.00	5000
55	24	1.41	24	1.41	2.25	2.25	2.02	0.280	3.75	6000
56	20	1.41	24	1.41	2.25	2.25	2.02	0.280	3.75	6000
57	24	1.41	24	1.41	2.25	2.25	2.02	0.280	3.75	6000
58	24	1.41	20	1.41	2.25	2.25	2.02	0.280	3.75	6000
59	16	1.41	20	1.41	2.13	2.13	2.66	0.284	4.00	5000
60	20	1.41	24	1.41	2.13	2.13	2.05	0.237	4.00	5000
61	24	1.41	24	1.41	2.25	2.25	2.02	0.280	3.75	6000
62	20	1.41	24	1.41	2.25	2.25	2.02	0.280	3.75	6000
63	24	1.41	24	1.41	2.25	2.25	2.02	0.280	3.75	6000
64	24	1.41	20	1.41	2.25	2.25	2.02	0.280	3.75	6000
65	16	1.41	20	1.41	2.13	2.13	2.66	0.284	4.00	5000
66	20	1.41	24	1.41	2.13	2.13	2.05	0.237	4.00	5000
67	24	1.41	24	1.41	2.25	2.25	2.02	0.280	3.75	6000
68	20	1.41	24	1.41	2.25	2.25	2.02	0.280	3.75	6000
69	24	1.41	24	1.41	2.25	2.25	2.02	0.280	3.75	6000
70	24	1.41	20	1.41	2.25	2.25	2.02	0.280	3.75	6000
71	16	1.41	20	1.41	2.13	2.13	2.66	0.284	4.00	5000
72	20	1.41	24	1.41	2.13	2.13	2.05	0.237	4.00	5000
73	24	1.41	24	1.41	2.25	2.25	2.02	0.280	3.75	6000
74	20	1.41	24	1.41	2.25	2.25	2.02	0.280	3.75	6000
75	24	1.41	24	1.41	2.25	2.25	2.02	0.280	3.75	6000
76	24	1.41	20	1.41	2.25	2.25	2.02	0.280	3.75	6000
77	16	1.41	20	1.41	2.13	2.13	2.66	0.284	4.00	5000
78	20	1.41	24	1.41	2.13	2.13	2.05	0.237	4.00	5000
79	24	1.41	24	1.41	2.25	2.25	2.02	0.280	3.75	6000
80	20	1.41	24	1.41	2.25	2.25	2.02	0.280	3.75	6000

Table D.2a
Splice data for columns in lateral load resisting frame system (continued)

Splice	Spliced Bars*				Cover			Transverse Reinf.		
	A Bars		B Bars		c_b	c_{so}	c_{si}	A_{tr}/n	s	f'_c
No.	# bars	d_b (in.)	# bars	d_b (in.)	(in.)	(in.)	(in.)	($in.^2$)	(in.)	(psi)
81	24	1.41	24	1.41	2.25	2.25	2.02	0.280	3.75	6000
82	24	1.41	20	1.41	2.25	2.25	2.02	0.280	3.75	6000
83	12	1.41	16	1.41	2.13	2.13	3.78	0.305	3.50	5000
84	20	1.41	24	1.41	2.13	2.13	2.05	0.237	4.00	5000
85	24	1.41	16	1.41	2.25	2.25	2.53	0.336	3.75	6000
86	16	1.41	24	1.41	2.25	2.25	2.53	0.336	3.75	6000
87	24	1.41	24	1.41	2.25	2.25	2.02	0.280	3.75	6000
88	24	1.41	20	1.41	2.25	2.25	2.02	0.280	3.75	6000
89	12	1.41	12	1.41	2.25	2.25	3.98	0.375	3.75	5000
90	12	1.41	16	1.41	2.13	2.13	3.78	0.305	3.50	5000
91	20	1.41	24	1.41	2.13	2.13	2.05	0.237	4.00	5000
92	24	1.41	16	1.41	2.25	2.25	2.53	0.336	3.75	6000
93	16	1.41	24	1.41	2.25	2.25	2.53	0.336	3.75	6000
94	24	1.41	24	1.41	2.25	2.25	2.02	0.280	3.75	6000
95	24	1.41	20	1.41	2.25	2.25	2.02	0.280	3.75	6000
96	16	1.41	16	1.41	2.13	2.13	2.84	0.244	3.50	5000
97	16	1.41	20	1.41	2.13	2.13	2.66	0.284	4.00	5000
98	20	1.41	24	1.41	2.13	2.13	2.05	0.237	4.00	5000
99	24	1.41	24	1.41	2.25	2.25	2.02	0.280	3.75	6000
100	20	1.41	24	1.41	2.25	2.25	2.02	0.280	3.75	6000
101	24	1.41	24	1.41	2.25	2.25	2.02	0.280	3.75	6000
102	24	1.41	20	1.41	2.25	2.25	2.02	0.280	3.75	6000
103	12	1.41	12	1.41	2.25	2.25	3.98	0.375	3.75	5000
104	12	1.41	16	1.41	2.13	2.13	3.78	0.305	3.50	5000
105	20	1.41	24	1.41	2.13	2.13	2.05	0.237	4.00	5000
106	24	1.41	16	1.41	2.25	2.25	2.53	0.336	3.75	6000
107	16	1.41	24	1.41	2.25	2.25	2.53	0.336	3.75	6000
108	24	1.41	24	1.41	2.25	2.25	2.02	0.280	3.75	6000
109	24	1.41	20	1.41	2.25	2.25	2.02	0.280	3.75	6000
110	12	1.41	12	1.41	2.25	2.25	3.98	0.375	3.75	5000
111	12	1.41	16	1.41	2.13	2.13	3.78	0.305	3.50	5000
112	20	1.41	24	1.41	2.13	2.13	2.05	0.237	4.00	5000
113	24	1.41	16	1.41	2.25	2.25	2.53	0.336	3.75	6000
114	16	1.41	24	1.41	2.25	2.25	2.53	0.336	3.75	6000
115	24	1.41	24	1.41	2.25	2.25	2.02	0.280	3.75	6000
116	24	1.41	20	1.41	2.25	2.25	2.02	0.280	3.75	6000
117	12	1.41	12	1.41	2.25	2.25	3.98	0.375	3.75	5000
118	12	1.41	16	1.41	2.13	2.13	3.78	0.305	3.50	5000
119	20	1.41	24	1.41	2.13	2.13	2.05	0.237	4.00	5000
120	24	1.41	16	1.41	2.25	2.25	2.53	0.336	3.75	6000

Table D.2a
Splice data for columns in lateral load resisting frame system (continued)

Splice	Spliced Bars*				Cover			Transverse Reinf.		
	A Bars		B Bars		c_b	c_{so}	c_{si}	A_{tr}/n	s	f'_c
No.	# bars	d_b (in.)	# bars	d_b (in.)	(in.)	(in.)	(in.)	($in.^2$)	(in.)	(psi)
121	16	1.41	24	1.41	2.25	2.25	2.53	0.336	3.75	6000
122	24	1.41	24	1.41	2.25	2.25	2.02	0.280	3.75	6000
123	24	1.41	20	1.41	2.25	2.25	2.02	0.280	3.75	6000
124	16	1.41	16	1.41	2.13	2.13	2.84	0.244	3.50	5000
125	16	1.41	20	1.41	2.13	2.13	2.66	0.284	4.00	5000
126	24	1.41	24	1.41	2.13	2.13	2.05	0.237	4.00	5000
127	24	1.41	24	1.41	2.25	2.25	2.02	0.280	3.75	6000
128	20	1.41	24	1.41	2.25	2.25	2.02	0.280	3.75	6000
129	24	1.41	24	1.41	2.25	2.25	2.02	0.280	3.75	6000
130	24	1.41	20	1.41	2.25	2.25	2.02	0.280	3.75	6000
131	16	1.41	16	1.41	2.13	2.13	2.84	0.244	3.50	5000
132	16	1.41	20	1.41	2.13	2.13	2.66	0.284	4.00	5000
133	24	1.41	24	1.41	2.13	2.13	2.05	0.237	4.00	5000
134	24	1.41	24	1.41	2.25	2.25	2.02	0.280	3.75	6000
135	20	1.41	24	1.41	2.25	2.25	2.02	0.280	3.75	6000
136	24	1.41	24	1.41	2.25	2.25	2.02	0.280	3.75	6000
137	24	1.41	20	1.41	2.25	2.25	2.02	0.280	3.75	6000
138	16	1.41	16	1.41	2.13	2.13	2.84	0.244	3.50	5000
139	16	1.41	20	1.41	2.13	2.13	2.66	0.284	4.00	5000
140	20	1.41	24	1.41	2.13	2.13	2.05	0.237	4.00	5000
141	24	1.41	24	1.41	2.25	2.25	2.02	0.280	3.75	6000
142	20	1.41	24	1.41	2.25	2.25	2.02	0.280	3.75	6000
143	24	1.41	24	1.41	2.25	2.25	2.02	0.280	3.75	6000
144	24	1.41	20	1.41	2.25	2.25	2.02	0.280	3.75	6000
145	16	1.41	16	1.41	2.13	2.13	2.84	0.244	3.50	5000
146	16	1.41	20	1.41	2.13	2.13	2.66	0.284	4.00	5000
147	20	1.41	24	1.41	2.13	2.13	2.05	0.237	4.00	5000
148	24	1.41	24	1.41	2.25	2.25	2.02	0.280	3.75	6000
149	20	1.41	24	1.41	2.25	2.25	2.02	0.280	3.75	6000
150	24	1.41	24	1.41	2.25	2.25	2.02	0.280	3.75	6000
151	24	1.41	20	1.41	2.25	2.25	2.02	0.280	3.75	6000
152	16	1.41	16	1.41	2.13	2.13	2.84	0.244	3.50	5000
153	16	1.41	20	1.41	2.13	2.13	2.66	0.284	4.00	5000
154	20	1.41	24	1.41	2.13	2.13	2.05	0.237	4.00	5000
155	24	1.41	24	1.41	2.25	2.25	2.02	0.280	3.75	6000
156	20	1.41	24	1.41	2.25	2.25	2.02	0.280	3.75	6000
157	24	1.41	24	1.41	2.25	2.25	2.02	0.280	3.75	6000
158	24	1.41	20	1.41	2.25	2.25	2.02	0.280	3.75	6000
159	24	1.41	16	1.41	2.13	2.13	2.56	0.284	4.00	5000
160	16	1.41	20	1.41	2.13	2.13	2.66	0.284	4.00	5000

Table D.2a
Splice data for columns in lateral load resisting frame system (continued)

Splice	Spliced Bars*				Cover			Transverse Reinf.		f'_c
	A Bars		B Bars		c_b	c_{so}	c_{si}	A_{tr}/n	s	
No.	# bars	d_b (in.)	# bars	d_b (in.)	(in.)	(in.)	(in.)	($in.^2$)	(in.)	(psi)
161	20	1.41	24	1.41	2.13	2.13	2.05	0.237	4.00	5000
162	24	1.41	24	1.41	2.25	2.25	2.02	0.280	3.75	6000
163	20	1.41	24	1.41	2.25	2.25	2.02	0.280	3.75	6000
164	24	1.41	24	1.41	2.25	2.25	2.02	0.280	3.75	6000
165	24	1.41	20	1.41	2.25	2.25	2.02	0.280	3.75	6000
166	16	1.41	16	1.41	2.13	2.13	2.84	0.244	3.50	5000
167	16	1.41	20	1.41	2.13	2.13	2.66	0.284	4.00	5000
168	20	1.41	24	1.41	2.13	2.13	2.05	0.237	4.00	5000
169	24	1.41	24	1.41	2.25	2.25	2.02	0.280	3.75	6000
170	20	1.41	24	1.41	2.25	2.25	2.02	0.280	3.75	6000
171	24	1.41	24	1.41	2.25	2.25	2.02	0.280	3.75	6000
172	24	1.41	20	1.41	2.25	2.25	2.02	0.280	3.75	6000
173	16	1.41	16	1.41	2.13	2.13	2.84	0.244	3.50	5000
174	16	1.41	20	1.41	2.13	2.13	2.66	0.284	4.00	5000
175	20	1.41	24	1.41	2.13	2.13	2.05	0.237	4.00	5000
176	24	1.41	24	1.41	2.25	2.25	2.02	0.280	3.75	6000
177	20	1.41	24	1.41	2.25	2.25	2.02	0.280	3.75	6000
178	24	1.41	24	1.41	2.25	2.25	2.02	0.280	3.75	6000
179	24	1.41	20	1.41	2.25	2.25	2.02	0.280	3.75	6000
180	16	1.41	24	1.41	2.25	2.25	2.53	0.336	3.75	6000
181	28	1.41	28	1.41	2.25	2.25	1.24	0.210	3.75	6000
182	28	1.41	20	1.41	2.25	2.25	1.74	0.280	3.75	6000
183	20	1.41	24	1.41	2.25	2.25	2.02	0.280	3.75	6000
184	32	1.41	32	1.41	2.25	2.25	1.24	0.210	3.75	6000
185	32	1.41	20	1.41	2.25	2.25	1.74	0.280	3.75	6000
186	20	1.41	24	1.41	2.25	2.25	2.02	0.280	3.75	6000
187	32	1.41	32	1.41	2.25	2.25	1.24	0.210	3.75	6000
188	32	1.41	20	1.41	2.25	2.25	1.74	0.280	3.75	6000
189	16	1.41	24	1.41	2.25	2.25	2.53	0.336	3.75	6000
190	28	1.41	28	1.41	2.25	2.25	1.24	0.210	3.75	6000
191	28	1.41	20	1.41	2.25	2.25	1.74	0.280	3.75	6000
192	16	1.41	24	1.41	2.25	2.25	2.53	0.336	3.75	6000
193	28	1.41	28	1.41	2.25	2.25	1.24	0.210	3.75	6000
194	28	1.41	20	1.41	2.25	2.25	1.74	0.280	3.75	6000
195	20	1.41	24	1.41	2.25	2.25	2.02	0.280	3.75	6000
196	32	1.41	32	1.41	2.25	2.25	1.24	0.210	3.75	6000
197	32	1.41	20	1.41	2.25	2.25	1.74	0.280	3.75	6000
198	20	1.41	24	1.41	2.25	2.25	2.02	0.280	3.75	6000
199	32	1.41	32	1.41	2.25	2.25	1.24	0.210	3.75	6000
200	32	1.41	20	1.41	2.25	2.25	1.74	0.280	3.75	6000

Table D.2a
Splice data for columns in lateral load resisting frame system (continued)

Splice	Spliced Bars*				Cover			Transverse Reinf.		f'_c
	A Bars		B Bars		c_b	c_{so}	c_{si}	A_{tr}/n	s	
No.	# bars	d_b (in.)	# bars	d_b (in.)	(in.)	(in.)	(in.)	($in.^2$)	(in.)	(psi)
201	20	1.41	24	1.41	2.25	2.25	2.02	0.280	3.75	6000
202	32	1.41	32	1.41	2.25	2.25	1.24	0.210	3.75	6000
203	32	1.41	20	1.41	2.25	2.25	1.74	0.280	3.75	6000
204	16	1.41	16	1.41	2.13	2.13	2.84	0.244	3.50	5000
205	16	1.41	16	1.41	2.13	2.13	2.84	0.244	3.50	5000
206	16	1.41	16	1.41	2.13	2.13	2.84	0.244	3.50	5000
207	16	1.41	16	1.41	2.13	2.13	2.84	0.244	3.50	5000
208	16	1.41	24	1.41	2.25	2.25	2.53	0.336	3.75	6000
209	28	1.41	28	1.41	2.25	2.25	1.24	0.210	3.75	6000
210	28	1.41	20	1.41	2.25	2.25	1.74	0.280	3.75	6000
211	20	1.41	24	1.41	2.25	2.25	2.02	0.280	3.75	6000
212	32	1.41	32	1.41	2.25	2.25	1.24	0.210	3.75	6000
213	32	1.41	20	1.41	2.25	2.25	1.74	0.280	3.75	6000
214	20	1.41	24	1.41	2.25	2.25	2.02	0.280	3.75	6000
215	32	1.41	32	1.41	2.25	2.25	1.24	0.210	3.75	6000
216	32	1.41	20	1.41	2.25	2.25	1.74	0.280	3.75	6000
217	20	1.41	24	1.41	2.25	2.25	2.02	0.280	3.75	6000
218	32	1.41	32	1.41	2.25	2.25	1.24	0.210	3.75	6000
219	32	1.41	20	1.41	2.25	2.25	1.74	0.280	3.75	6000
220	16	1.41	24	1.41	2.25	2.25	2.53	0.336	3.75	6000
221	28	1.41	28	1.41	2.25	2.25	1.24	0.210	3.75	6000
222	28	1.41	20	1.41	2.25	2.25	1.74	0.280	3.75	6000
223	16	1.41	24	1.41	2.25	2.25	2.53	0.336	3.75	6000
224	28	1.41	28	1.41	2.25	2.25	1.24	0.210	3.75	6000
225	28	1.41	20	1.41	2.25	2.25	1.74	0.280	3.75	6000
226	20	1.41	24	1.41	2.25	2.25	2.02	0.280	3.75	6000
227	32	1.41	32	1.41	2.25	2.25	1.24	0.210	3.75	6000
228	32	1.41	20	1.41	2.25	2.25	1.74	0.280	3.75	6000
229	20	1.41	24	1.41	2.25	2.25	2.02	0.280	3.75	6000
230	32	1.41	32	1.41	2.25	2.25	1.24	0.210	3.75	6000
231	32	1.41	20	1.41	2.25	2.25	1.74	0.280	3.75	6000

* A bars spliced to B bars

1 in. = 25.4 mm; 1 psi = 6.89 kPa

Table D.2c
Splice length ratios for columns in lateral load resisting frame system

Spl. No.	ACI '95 Orig.	Eq. 3.13+ Orig. Conv.*	Eq. 3.13+ Orig. New**	Eq. 3.14++ Orig. Conv.*	Eq. 3.14++ Orig. New**	Eq. 3.13+ ACI '95 Conv.*	Eq. 3.13+ ACI '95 New**	Eq. 3.14++ ACI '95 Conv.*	Eq. 3.14++ ACI '95 New**	Eq. 3.13+ Eq. 3.14++ Conv.*	Eq. 3.13+ Eq. 3.14++ New**	New** Conv.* Eq. 3.13+	New** Conv.* Eq. 3.14++
1	0.598	0.450	0.450	0.450	0.450	0.752	0.752	0.752	0.752	1.000	1.000	1.000	1.000
2	0.598	0.450	0.450	0.450	0.450	0.752	0.752	0.752	0.752	1.000	1.000	1.000	1.000
3	0.598	0.450	0.450	0.450	0.450	0.752	0.752	0.752	0.752	1.000	1.000	1.000	1.000
4	0.598	0.450	0.450	0.450	0.450	0.752	0.752	0.752	0.752	1.000	1.000	1.000	1.000
5	0.546	0.450	0.450	0.450	0.450	0.824	0.824	0.824	0.824	1.000	1.000	1.000	1.000
6	0.546	0.450	0.450	0.450	0.450	0.824	0.824	0.824	0.824	1.000	1.000	1.000	1.000
7	0.546	0.450	0.450	0.450	0.450	0.824	0.824	0.824	0.824	1.000	1.000	1.000	1.000
8	0.546	0.450	0.450	0.450	0.450	0.824	0.824	0.824	0.824	1.000	1.000	1.000	1.000
9	0.598	0.450	0.450	0.450	0.450	0.752	0.752	0.752	0.752	1.000	1.000	1.000	1.000
10	0.598	0.450	0.450	0.450	0.450	0.752	0.752	0.752	0.752	1.000	1.000	1.000	1.000
11	0.598	0.450	0.450	0.450	0.450	0.752	0.752	0.752	0.752	1.000	1.000	1.000	1.000
12	0.598	0.450	0.450	0.450	0.450	0.752	0.752	0.752	0.752	1.000	1.000	1.000	1.000
13	0.546	0.450	0.450	0.450	0.450	0.824	0.824	0.824	0.824	1.000	1.000	1.000	1.000
14	0.546	0.450	0.450	0.450	0.450	0.824	0.824	0.824	0.824	1.000	1.000	1.000	1.000
15	0.546	0.450	0.450	0.450	0.450	0.824	0.824	0.824	0.824	1.000	1.000	1.000	1.000
16	0.546	0.450	0.450	0.450	0.450	0.824	0.824	0.824	0.824	1.000	1.000	1.000	1.000
17	0.598	0.450	0.450	0.450	0.450	0.752	0.752	0.752	0.752	1.000	1.000	1.000	1.000
18	0.598	0.450	0.450	0.450	0.450	0.752	0.752	0.752	0.752	1.000	1.000	1.000	1.000
19	0.598	0.450	0.450	0.450	0.450	0.752	0.752	0.752	0.752	1.000	1.000	1.000	1.000
20	0.598	0.450	0.450	0.450	0.450	0.752	0.752	0.752	0.752	1.000	1.000	1.000	1.000
21	0.546	0.450	0.450	0.450	0.450	0.824	0.824	0.824	0.824	1.000	1.000	1.000	1.000
22	0.546	0.450	0.450	0.450	0.450	0.824	0.824	0.824	0.824	1.000	1.000	1.000	1.000
23	0.546	0.450	0.450	0.450	0.450	0.824	0.824	0.824	0.824	1.000	1.000	1.000	1.000
24	0.546	0.450	0.450	0.450	0.450	0.824	0.824	0.824	0.824	1.000	1.000	1.000	1.000
25	0.598	0.450	0.450	0.450	0.450	0.752	0.752	0.752	0.752	1.000	1.000	1.000	1.000
26	0.598	0.450	0.450	0.450	0.450	0.752	0.752	0.752	0.752	1.000	1.000	1.000	1.000
27	0.598	0.450	0.450	0.450	0.450	0.752	0.752	0.752	0.752	1.000	1.000	1.000	1.000
28	0.598	0.450	0.450	0.450	0.450	0.752	0.752	0.752	0.752	1.000	1.000	1.000	1.000
29	0.546	0.450	0.450	0.450	0.450	0.824	0.824	0.824	0.824	1.000	1.000	1.000	1.000
30	0.546	0.450	0.450	0.450	0.450	0.824	0.824	0.824	0.824	1.000	1.000	1.000	1.000
31	0.546	0.450	0.450	0.450	0.450	0.824	0.824	0.824	0.824	1.000	1.000	1.000	1.000
32	0.546	0.450	0.450	0.450	0.450	0.824	0.824	0.824	0.824	1.000	1.000	1.000	1.000
33	0.598	0.450	0.450	0.450	0.450	0.752	0.752	0.752	0.752	1.000	1.000	1.000	1.000
34	0.598	0.450	0.450	0.450	0.450	0.752	0.752	0.752	0.752	1.000	1.000	1.000	1.000
35	0.598	0.450	0.450	0.450	0.450	0.752	0.752	0.752	0.752	1.000	1.000	1.000	1.000
36	0.546	0.450	0.450	0.450	0.450	0.824	0.824	0.824	0.824	1.000	1.000	1.000	1.000
37	0.546	0.450	0.450	0.450	0.450	0.824	0.824	0.824	0.824	1.000	1.000	1.000	1.000
38	0.546	0.450	0.450	0.450	0.450	0.824	0.824	0.824	0.824	1.000	1.000	1.000	1.000
39	0.546	0.450	0.450	0.450	0.450	0.824	0.824	0.824	0.824	1.000	1.000	1.000	1.000
40	0.598	0.450	0.450	0.450	0.450	0.752	0.752	0.752	0.752	1.000	1.000	1.000	1.000
41	0.598	0.450	0.450	0.450	0.450	0.752	0.752	0.752	0.752	1.000	1.000	1.000	1.000
42	0.598	0.450	0.450	0.450	0.450	0.752	0.752	0.752	0.752	1.000	1.000	1.000	1.000
43	0.546	0.450	0.450	0.450	0.450	0.824	0.824	0.824	0.824	1.000	1.000	1.000	1.000
44	0.546	0.450	0.450	0.450	0.450	0.824	0.824	0.824	0.824	1.000	1.000	1.000	1.000
45	0.546	0.450	0.450	0.450	0.450	0.824	0.824	0.824	0.824	1.000	1.000	1.000	1.000
46	0.546	0.450	0.450	0.450	0.450	0.824	0.824	0.824	0.824	1.000	1.000	1.000	1.000
47	0.598	0.450	0.450	0.450	0.450	0.752	0.752	0.752	0.752	1.000	1.000	1.000	1.000
48	0.598	0.450	0.450	0.450	0.450	0.752	0.752	0.752	0.752	1.000	1.000	1.000	1.000
49	0.546	0.450	0.450	0.450	0.450	0.824	0.824	0.824	0.824	1.000	1.000	1.000	1.000
50	0.546	0.450	0.450	0.450	0.450	0.824	0.824	0.824	0.824	1.000	1.000	1.000	1.000
51	0.546	0.450	0.450	0.450	0.450	0.824	0.824	0.824	0.824	1.000	1.000	1.000	1.000
52	0.546	0.450	0.450	0.450	0.450	0.824	0.824	0.824	0.824	1.000	1.000	1.000	1.000
53	0.598	0.450	0.450	0.450	0.450	0.752	0.752	0.752	0.752	1.000	1.000	1.000	1.000
54	0.598	0.450	0.450	0.450	0.450	0.752	0.752	0.752	0.752	1.000	1.000	1.000	1.000
55	0.546	0.450	0.450	0.450	0.450	0.824	0.824	0.824	0.824	1.000	1.000	1.000	1.000
56	0.546	0.450	0.450	0.450	0.450	0.824	0.824	0.824	0.824	1.000	1.000	1.000	1.000
57	0.546	0.450	0.450	0.450	0.450	0.824	0.824	0.824	0.824	1.000	1.000	1.000	1.000
58	0.546	0.450	0.450	0.450	0.450	0.824	0.824	0.824	0.824	1.000	1.000	1.000	1.000
59	0.598	0.450	0.450	0.450	0.450	0.752	0.752	0.752	0.752	1.000	1.000	1.000	1.000
60	0.598	0.450	0.450	0.450	0.450	0.752	0.752	0.752	0.752	1.000	1.000	1.000	1.000
61	0.546	0.450	0.450	0.450	0.450	0.824	0.824	0.824	0.824	1.000	1.000	1.000	1.000
62	0.546	0.450	0.450	0.450	0.450	0.824	0.824	0.824	0.824	1.000	1.000	1.000	1.000
63	0.546	0.450	0.450	0.450	0.450	0.824	0.824	0.824	0.824	1.000	1.000	1.000	1.000
64	0.546	0.450	0.450	0.450	0.450	0.824	0.824	0.824	0.824	1.000	1.000	1.000	1.000
65	0.598	0.450	0.450	0.450	0.450	0.752	0.752	0.752	0.752	1.000	1.000	1.000	1.000

Table D.2c
Splice length ratios for columns in lateral load resisting frame system (continued)

Spl. No.	ACI '95 Orig.	Eq. 3.13^{+} Orig. Conv.*	Eq. 3.13^{-} Orig. New**	Eq. 3.14^{+-} Orig. Conv.*	Eq. 3.14^{-+} Orig. New**	Eq. 3.13^{+} ACI '95 Conv.*	Eq. 3.13^{-} ACI '95 New**	Eq. 3.14^{+-} ACI '95 Conv.*	Eq. 3.14^{-+} ACI '95 New**	Eq. 3.13^{-} Eq. 3.14^{+-} Conv.*	Eq. 3.13^{+} Eq. 3.14^{-+} New**	New** Conv.* Eq. 3.13^{+}	New** Conv.* Eq. 3.14^{++}
66	0.598	0.450	0.450	0.450	0.450	0.752	0.752	0.752	0.752	1.000	1.000	1.000	1.000
67	0.546	0.450	0.450	0.450	0.450	0.824	0.824	0.824	0.824	1.000	1.000	1.000	1.000
68	0.546	0.450	0.450	0.450	0.450	0.824	0.824	0.824	0.824	1.000	1.000	1.000	1.000
69	0.546	0.450	0.450	0.450	0.450	0.824	0.824	0.824	0.824	1.000	1.000	1.000	1.000
70	0.546	0.450	0.450	0.450	0.450	0.824	0.824	0.824	0.824	1.000	1.000	1.000	1.000
71	0.598	0.450	0.450	0.450	0.450	0.752	0.752	0.752	0.752	1.000	1.000	1.000	1.000
72	0.598	0.450	0.450	0.450	0.450	0.752	0.752	0.752	0.752	1.000	1.000	1.000	1.000
73	0.546	0.450	0.450	0.450	0.450	0.824	0.824	0.824	0.824	1.000	1.000	1.000	1.000
74	0.546	0.450	0.450	0.450	0.450	0.824	0.824	0.824	0.824	1.000	1.000	1.000	1.000
75	0.546	0.450	0.450	0.450	0.450	0.824	0.824	0.824	0.824	1.000	1.000	1.000	1.000
76	0.546	0.450	0.450	0.450	0.450	0.824	0.824	0.824	0.824	1.000	1.000	1.000	1.000
77	0.598	0.450	0.450	0.450	0.450	0.752	0.752	0.752	0.752	1.000	1.000	1.000	1.000
78	0.598	0.450	0.450	0.450	0.450	0.752	0.752	0.752	0.752	1.000	1.000	1.000	1.000
79	0.546	0.450	0.450	0.450	0.450	0.824	0.824	0.824	0.824	1.000	1.000	1.000	1.000
80	0.546	0.450	0.450	0.450	0.450	0.824	0.824	0.824	0.824	1.000	1.000	1.000	1.000
81	0.546	0.450	0.450	0.450	0.450	0.824	0.824	0.824	0.824	1.000	1.000	1.000	1.000
82	0.546	0.450	0.450	0.450	0.450	0.824	0.824	0.824	0.824	1.000	1.000	1.000	1.000
83	0.598	0.450	0.450	0.450	0.450	0.752	0.752	0.752	0.752	1.000	1.000	1.000	1.000
84	0.598	0.450	0.450	0.450	0.450	0.752	0.752	0.752	0.752	1.000	1.000	1.000	1.000
85	0.546	0.450	0.450	0.450	0.450	0.824	0.824	0.824	0.824	1.000	1.000	1.000	1.000
86	0.546	0.450	0.450	0.450	0.450	0.824	0.824	0.824	0.824	1.000	1.000	1.000	1.000
87	0.546	0.450	0.450	0.450	0.450	0.824	0.824	0.824	0.824	1.000	1.000	1.000	1.000
88	0.546	0.450	0.450	0.450	0.450	0.824	0.824	0.824	0.824	1.000	1.000	1.000	1.000
89	0.598	0.450	0.450	0.450	0.450	0.752	0.752	0.752	0.752	1.000	1.000	1.000	1.000
90	0.598	0.450	0.450	0.450	0.450	0.752	0.752	0.752	0.752	1.000	1.000	1.000	1.000
91	0.598	0.450	0.450	0.450	0.450	0.752	0.752	0.752	0.752	1.000	1.000	1.000	1.000
92	0.546	0.450	0.450	0.450	0.450	0.824	0.824	0.824	0.824	1.000	1.000	1.000	1.000
93	0.546	0.450	0.450	0.450	0.450	0.824	0.824	0.824	0.824	1.000	1.000	1.000	1.000
94	0.546	0.450	0.450	0.450	0.450	0.824	0.824	0.824	0.824	1.000	1.000	1.000	1.000
95	0.546	0.450	0.450	0.450	0.450	0.824	0.824	0.824	0.824	1.000	1.000	1.000	1.000
96	0.598	0.450	0.450	0.450	0.450	0.752	0.752	0.752	0.752	1.000	1.000	1.000	1.000
97	0.598	0.450	0.450	0.450	0.450	0.752	0.752	0.752	0.752	1.000	1.000	1.000	1.000
98	0.598	0.450	0.450	0.450	0.450	0.752	0.752	0.752	0.752	1.000	1.000	1.000	1.000
99	0.546	0.450	0.450	0.450	0.450	0.824	0.824	0.824	0.824	1.000	1.000	1.000	1.000
100	0.546	0.450	0.450	0.450	0.450	0.824	0.824	0.824	0.824	1.000	1.000	1.000	1.000
101	0.546	0.450	0.450	0.450	0.450	0.824	0.824	0.824	0.824	1.000	1.000	1.000	1.000
102	0.546	0.450	0.450	0.450	0.450	0.824	0.824	0.824	0.824	1.000	1.000	1.000	1.000
103	0.598	0.450	0.450	0.450	0.450	0.752	0.752	0.752	0.752	1.000	1.000	1.000	1.000
104	0.598	0.450	0.450	0.450	0.450	0.752	0.752	0.752	0.752	1.000	1.000	1.000	1.000
105	0.598	0.450	0.450	0.450	0.450	0.752	0.752	0.752	0.752	1.000	1.000	1.000	1.000
106	0.546	0.450	0.450	0.450	0.450	0.824	0.824	0.824	0.824	1.000	1.000	1.000	1.000
107	0.546	0.450	0.450	0.450	0.450	0.824	0.824	0.824	0.824	1.000	1.000	1.000	1.000
108	0.546	0.450	0.450	0.450	0.450	0.824	0.824	0.824	0.824	1.000	1.000	1.000	1.000
109	0.546	0.450	0.450	0.450	0.450	0.824	0.824	0.824	0.824	1.000	1.000	1.000	1.000
110	0.598	0.450	0.450	0.450	0.450	0.752	0.752	0.752	0.752	1.000	1.000	1.000	1.000
111	0.598	0.450	0.450	0.450	0.450	0.752	0.752	0.752	0.752	1.000	1.000	1.000	1.000
112	0.598	0.450	0.450	0.450	0.450	0.752	0.752	0.752	0.752	1.000	1.000	1.000	1.000
113	0.546	0.450	0.450	0.450	0.450	0.824	0.824	0.824	0.824	1.000	1.000	1.000	1.000
114	0.546	0.450	0.450	0.450	0.450	0.824	0.824	0.824	0.824	1.000	1.000	1.000	1.000
115	0.546	0.450	0.450	0.450	0.450	0.824	0.824	0.824	0.824	1.000	1.000	1.000	1.000
116	0.546	0.450	0.450	0.450	0.450	0.824	0.824	0.824	0.824	1.000	1.000	1.000	1.000
117	0.598	0.450	0.450	0.450	0.450	0.752	0.752	0.752	0.752	1.000	1.000	1.000	1.000
118	0.598	0.450	0.450	0.450	0.450	0.752	0.752	0.752	0.752	1.000	1.000	1.000	1.000
119	0.598	0.450	0.450	0.450	0.450	0.752	0.752	0.752	0.752	1.000	1.000	1.000	1.000
120	0.546	0.450	0.450	0.450	0.450	0.824	0.824	0.824	0.824	1.000	1.000	1.000	1.000
121	0.546	0.450	0.450	0.450	0.450	0.824	0.824	0.824	0.824	1.000	1.000	1.000	1.000
122	0.546	0.450	0.450	0.450	0.450	0.824	0.824	0.824	0.824	1.000	1.000	1.000	1.000
123	0.546	0.450	0.450	0.450	0.450	0.824	0.824	0.824	0.824	1.000	1.000	1.000	1.000
124	0.598	0.450	0.450	0.450	0.450	0.752	0.752	0.752	0.752	1.000	1.000	1.000	1.000
125	0.598	0.450	0.450	0.450	0.450	0.752	0.752	0.752	0.752	1.000	1.000	1.000	1.000
126	0.598	0.450	0.450	0.450	0.450	0.752	0.752	0.752	0.752	1.000	1.000	1.000	1.000
127	0.546	0.450	0.450	0.450	0.450	0.824	0.824	0.824	0.824	1.000	1.000	1.000	1.000
128	0.546	0.450	0.450	0.450	0.450	0.824	0.824	0.824	0.824	1.000	1.000	1.000	1.000
129	0.546	0.450	0.450	0.450	0.450	0.824	0.824	0.824	0.824	1.000	1.000	1.000	1.000
130	0.546	0.450	0.450	0.450	0.450	0.824	0.824	0.824	0.824	1.000	1.000	1.000	1.000

Table D.2c
Splice length ratios for columns in lateral load resisting frame system (continued)

Spl. No.	ACI '95 Orig.	Eq. 3.13† Orig. Conv.*	Eq. 3.13† Orig. New**	Eq. 3.14†† Orig. Conv.*	Eq. 3.14†† Orig. New**	Eq. 3.13† ACI '95 Conv.*	Eq. 3.13† ACI '95 New**	Eq. 3.14†† ACI '95 Conv.*	Eq. 3.14†† ACI '95 New**	Eq. 3.13† Eq. 3.14†† Conv.*	Eq. 3.13† Eq. 3.14†† New**	New** Conv.* Eq. 3.13†	New** Conv.* Eq. 3.14††
131	0.598	0.450	0.450	0.450	0.450	0.752	0.752	0.752	0.752	1.000	1.000	1.000	1.000
132	0.598	0.450	0.450	0.450	0.450	0.752	0.752	0.752	0.752	1.000	1.000	1.000	1.000
133	0.598	0.450	0.450	0.450	0.450	0.752	0.752	0.752	0.752	1.000	1.000	1.000	1.000
134	0.546	0.450	0.450	0.450	0.450	0.824	0.824	0.824	0.824	1.000	1.000	1.000	1.000
135	0.546	0.450	0.450	0.450	0.450	0.824	0.824	0.824	0.824	1.000	1.000	1.000	1.000
136	0.546	0.450	0.450	0.450	0.450	0.824	0.824	0.824	0.824	1.000	1.000	1.000	1.000
137	0.546	0.450	0.450	0.450	0.450	0.824	0.824	0.824	0.824	1.000	1.000	1.000	1.000
138	0.598	0.450	0.450	0.450	0.450	0.752	0.752	0.752	0.752	1.000	1.000	1.000	1.000
139	0.598	0.450	0.450	0.450	0.450	0.752	0.752	0.752	0.752	1.000	1.000	1.000	1.000
140	0.598	0.450	0.450	0.450	0.450	0.752	0.752	0.752	0.752	1.000	1.000	1.000	1.000
141	0.546	0.450	0.450	0.450	0.450	0.824	0.824	0.824	0.824	1.000	1.000	1.000	1.000
142	0.546	0.450	0.450	0.450	0.450	0.824	0.824	0.824	0.824	1.000	1.000	1.000	1.000
143	0.546	0.450	0.450	0.450	0.450	0.824	0.824	0.824	0.824	1.000	1.000	1.000	1.000
144	0.546	0.450	0.450	0.450	0.450	0.824	0.824	0.824	0.824	1.000	1.000	1.000	1.000
145	0.598	0.450	0.450	0.450	0.450	0.752	0.752	0.752	0.752	1.000	1.000	1.000	1.000
146	0.598	0.450	0.450	0.450	0.450	0.752	0.752	0.752	0.752	1.000	1.000	1.000	1.000
147	0.598	0.450	0.450	0.450	0.450	0.752	0.752	0.752	0.752	1.000	1.000	1.000	1.000
148	0.546	0.450	0.450	0.450	0.450	0.824	0.824	0.824	0.824	1.000	1.000	1.000	1.000
149	0.546	0.450	0.450	0.450	0.450	0.824	0.824	0.824	0.824	1.000	1.000	1.000	1.000
150	0.546	0.450	0.450	0.450	0.450	0.824	0.824	0.824	0.824	1.000	1.000	1.000	1.000
151	0.546	0.450	0.450	0.450	0.450	0.824	0.824	0.824	0.824	1.000	1.000	1.000	1.000
152	0.598	0.450	0.450	0.450	0.450	0.752	0.752	0.752	0.752	1.000	1.000	1.000	1.000
153	0.598	0.450	0.450	0.450	0.450	0.752	0.752	0.752	0.752	1.000	1.000	1.000	1.000
154	0.598	0.450	0.450	0.450	0.450	0.752	0.752	0.752	0.752	1.000	1.000	1.000	1.000
155	0.546	0.450	0.450	0.450	0.450	0.824	0.824	0.824	0.824	1.000	1.000	1.000	1.000
156	0.546	0.450	0.450	0.450	0.450	0.824	0.824	0.824	0.824	1.000	1.000	1.000	1.000
157	0.546	0.450	0.450	0.450	0.450	0.824	0.824	0.824	0.824	1.000	1.000	1.000	1.000
158	0.546	0.450	0.450	0.450	0.450	0.824	0.824	0.824	0.824	1.000	1.000	1.000	1.000
159	0.598	0.450	0.450	0.450	0.450	0.752	0.752	0.752	0.752	1.000	1.000	1.000	1.000
160	0.598	0.450	0.450	0.450	0.450	0.752	0.752	0.752	0.752	1.000	1.000	1.000	1.000
161	0.598	0.450	0.450	0.450	0.450	0.752	0.752	0.752	0.752	1.000	1.000	1.000	1.000
162	0.546	0.450	0.450	0.450	0.450	0.824	0.824	0.824	0.824	1.000	1.000	1.000	1.000
163	0.546	0.450	0.450	0.450	0.450	0.824	0.824	0.824	0.824	1.000	1.000	1.000	1.000
164	0.546	0.450	0.450	0.450	0.450	0.824	0.824	0.824	0.824	1.000	1.000	1.000	1.000
165	0.546	0.450	0.450	0.450	0.450	0.824	0.824	0.824	0.824	1.000	1.000	1.000	1.000
166	0.598	0.450	0.450	0.450	0.450	0.752	0.752	0.752	0.752	1.000	1.000	1.000	1.000
167	0.598	0.450	0.450	0.450	0.450	0.752	0.752	0.752	0.752	1.000	1.000	1.000	1.000
168	0.598	0.450	0.450	0.450	0.450	0.752	0.752	0.752	0.752	1.000	1.000	1.000	1.000
169	0.546	0.450	0.450	0.450	0.450	0.824	0.824	0.824	0.824	1.000	1.000	1.000	1.000
170	0.546	0.450	0.450	0.450	0.450	0.824	0.824	0.824	0.824	1.000	1.000	1.000	1.000
171	0.546	0.450	0.450	0.450	0.450	0.824	0.824	0.824	0.824	1.000	1.000	1.000	1.000
172	0.546	0.450	0.450	0.450	0.450	0.824	0.824	0.824	0.824	1.000	1.000	1.000	1.000
173	0.598	0.450	0.450	0.450	0.450	0.752	0.752	0.752	0.752	1.000	1.000	1.000	1.000
174	0.598	0.450	0.450	0.450	0.450	0.752	0.752	0.752	0.752	1.000	1.000	1.000	1.000
175	0.598	0.450	0.450	0.450	0.450	0.752	0.752	0.752	0.752	1.000	1.000	1.000	1.000
176	0.546	0.450	0.450	0.450	0.450	0.824	0.824	0.824	0.824	1.000	1.000	1.000	1.000
177	0.546	0.450	0.450	0.450	0.450	0.824	0.824	0.824	0.824	1.000	1.000	1.000	1.000
178	0.546	0.450	0.450	0.450	0.450	0.824	0.824	0.824	0.824	1.000	1.000	1.000	1.000
179	0.546	0.450	0.450	0.450	0.450	0.824	0.824	0.824	0.824	1.000	1.000	1.000	1.000
180	0.546	0.450	0.450	0.450	0.450	0.824	0.824	0.824	0.824	1.000	1.000	1.000	1.000
181	0.546	0.450	0.450	0.450	0.450	0.824	0.824	0.824	0.824	1.000	1.000	1.000	1.000
182	0.546	0.450	0.450	0.450	0.450	0.824	0.824	0.824	0.824	1.000	1.000	1.000	1.000
183	0.546	0.450	0.450	0.450	0.450	0.824	0.824	0.824	0.824	1.000	1.000	1.000	1.000
184	0.546	0.450	0.450	0.450	0.450	0.824	0.824	0.824	0.824	1.000	1.000	1.000	1.000
185	0.546	0.450	0.450	0.450	0.450	0.824	0.824	0.824	0.824	1.000	1.000	1.000	1.000
186	0.546	0.450	0.450	0.450	0.450	0.824	0.824	0.824	0.824	1.000	1.000	1.000	1.000
187	0.546	0.450	0.450	0.450	0.450	0.824	0.824	0.824	0.824	1.000	1.000	1.000	1.000
188	0.546	0.450	0.450	0.450	0.450	0.824	0.824	0.824	0.824	1.000	1.000	1.000	1.000
189	0.546	0.450	0.450	0.450	0.450	0.824	0.824	0.824	0.824	1.000	1.000	1.000	1.000
190	0.546	0.450	0.450	0.450	0.450	0.824	0.824	0.824	0.824	1.000	1.000	1.000	1.000
191	0.546	0.450	0.450	0.450	0.450	0.824	0.824	0.824	0.824	1.000	1.000	1.000	1.000
192	0.546	0.450	0.450	0.450	0.450	0.824	0.824	0.824	0.824	1.000	1.000	1.000	1.000
193	0.546	0.450	0.450	0.450	0.450	0.824	0.824	0.824	0.824	1.000	1.000	1.000	1.000
194	0.546	0.450	0.450	0.450	0.450	0.824	0.824	0.824	0.824	1.000	1.000	1.000	1.000
195	0.546	0.450	0.450	0.450	0.450	0.824	0.824	0.824	0.824	1.000	1.000	1.000	1.000

Table D.2c
Splice length ratios for columns in lateral load resisting frame system (continued)

Spl. No.	ACI '95 Orig.	Eq. 3.13[+] Orig. Conv.*	Eq. 3.13[+] Orig. New**	Eq. 3.14[++] Orig. Conv.*	Eq. 3.14[++] Orig. New**	Eq. 3.13[+] ACI '95 Conv.*	Eq. 3.13[+] ACI '95 New**	Eq. 3.14[++] ACI '95 Conv.*	Eq. 3.14[++] ACI '95 New**	Eq. 3.13[+] Eq. 3.14[++] Conv.*	Eq. 3.13[+] Eq. 3.14[++] New**	New** Conv.* Eq. 3.13[+]	New** Conv.* Eq. 3.14[++]
196	0.546	0.450	0.450	0.450	0.450	0.824	0.824	0.824	0.824	1.000	1.000	1.000	1.000
197	0.546	0.450	0.450	0.450	0.450	0.824	0.824	0.824	0.824	1.000	1.000	1.000	1.000
198	0.546	0.450	0.450	0.450	0.450	0.824	0.824	0.824	0.824	1.000	1.000	1.000	1.000
199	0.546	0.450	0.450	0.450	0.450	0.824	0.824	0.824	0.824	1.000	1.000	1.000	1.000
200	0.546	0.450	0.450	0.450	0.450	0.824	0.824	0.824	0.824	1.000	1.000	1.000	1.000
201	0.546	0.450	0.450	0.450	0.450	0.824	0.824	0.824	0.824	1.000	1.000	1.000	1.000
202	0.546	0.450	0.450	0.450	0.450	0.824	0.824	0.824	0.824	1.000	1.000	1.000	1.000
203	0.546	0.450	0.450	0.450	0.450	0.824	0.824	0.824	0.824	1.000	1.000	1.000	1.000
204	0.598	0.450	0.450	0.450	0.450	0.752	0.752	0.752	0.752	1.000	1.000	1.000	1.000
205	0.598	0.450	0.450	0.450	0.450	0.752	0.752	0.752	0.752	1.000	1.000	1.000	1.000
206	0.598	0.450	0.450	0.450	0.450	0.752	0.752	0.752	0.752	1.000	1.000	1.000	1.000
207	0.598	0.450	0.450	0.450	0.450	0.752	0.752	0.752	0.752	1.000	1.000	1.000	1.000
208	0.546	0.450	0.450	0.450	0.450	0.824	0.824	0.824	0.824	1.000	1.000	1.000	1.000
209	0.546	0.450	0.450	0.450	0.450	0.824	0.824	0.824	0.824	1.000	1.000	1.000	1.000
210	0.546	0.450	0.450	0.450	0.450	0.824	0.824	0.824	0.824	1.000	1.000	1.000	1.000
211	0.546	0.450	0.450	0.450	0.450	0.824	0.824	0.824	0.824	1.000	1.000	1.000	1.000
212	0.546	0.450	0.450	0.450	0.450	0.824	0.824	0.824	0.824	1.000	1.000	1.000	1.000
213	0.546	0.450	0.450	0.450	0.450	0.824	0.824	0.824	0.824	1.000	1.000	1.000	1.000
214	0.546	0.450	0.450	0.450	0.450	0.824	0.824	0.824	0.824	1.000	1.000	1.000	1.000
215	0.546	0.450	0.450	0.450	0.450	0.824	0.824	0.824	0.824	1.000	1.000	1.000	1.000
216	0.546	0.450	0.450	0.450	0.450	0.824	0.824	0.824	0.824	1.000	1.000	1.000	1.000
217	0.546	0.450	0.450	0.450	0.450	0.824	0.824	0.824	0.824	1.000	1.000	1.000	1.000
218	0.546	0.450	0.450	0.450	0.450	0.824	0.824	0.824	0.824	1.000	1.000	1.000	1.000
219	0.546	0.450	0.450	0.450	0.450	0.824	0.824	0.824	0.824	1.000	1.000	1.000	1.000
220	0.546	0.450	0.450	0.450	0.450	0.824	0.824	0.824	0.824	1.000	1.000	1.000	1.000
221	0.546	0.450	0.450	0.450	0.450	0.824	0.824	0.824	0.824	1.000	1.000	1.000	1.000
222	0.546	0.450	0.450	0.450	0.450	0.824	0.824	0.824	0.824	1.000	1.000	1.000	1.000
223	0.546	0.450	0.450	0.450	0.450	0.824	0.824	0.824	0.824	1.000	1.000	1.000	1.000
224	0.546	0.450	0.450	0.450	0.450	0.824	0.824	0.824	0.824	1.000	1.000	1.000	1.000
225	0.546	0.450	0.450	0.450	0.450	0.824	0.824	0.824	0.824	1.000	1.000	1.000	1.000
226	0.546	0.450	0.450	0.450	0.450	0.824	0.824	0.824	0.824	1.000	1.000	1.000	1.000
227	0.546	0.450	0.450	0.450	0.450	0.824	0.824	0.824	0.824	1.000	1.000	1.000	1.000
228	0.546	0.450	0.450	0.450	0.450	0.824	0.824	0.824	0.824	1.000	1.000	1.000	1.000
229	0.546	0.450	0.450	0.450	0.450	0.824	0.824	0.824	0.824	1.000	1.000	1.000	1.000
230	0.546	0.450	0.450	0.450	0.450	0.824	0.824	0.824	0.824	1.000	1.000	1.000	1.000
231	0.546	0.450	0.450	0.450	0.450	0.824	0.824	0.824	0.824	1.000	1.000	1.000	1.000
Max.	0.598	0.450	0.450	0.450	0.450	0.824	0.824	0.824	0.824	1.000	1.000	1.000	1.000
Min.	0.546	0.450	0.450	0.450	0.450	0.752	0.752	0.752	0.752	1.000	1.000	1.000	1.000
Avg.	0.564	0.450	0.450	0.450	0.450	0.800	0.800	0.800	0.800	1.000	1.000	1.000	1.000

[+] $$\text{Eq. 3.13} = \frac{l_d}{d_b} = \frac{\dfrac{f_y}{f_c'^{1/4}} - 1900\left(0.1\dfrac{c_M}{c_m} + 0.9\right)}{72\left(\dfrac{c + K_{tr}}{d_b}\right)}$$

[++] $$\text{Eq. 3.14} = \frac{l_d}{d_b} = \frac{\dfrac{f_y}{f_c'^{1/4}} - 1900}{72\left(\dfrac{c + K_{tr}}{d_b}\right)}$$

* Conventional reinforcement (avg. $R_r = 0.0727$)

** New reinforcement (avg. $R_r = 0.1275$)